USGS
science for a changing world

Water Availability and Use Science Program

Prepared in cooperation with the Sonoma County Water Agency and the City of Petaluma

Hydrologic and Geochemical Characterization of the Petaluma River Watershed, Sonoma County, California

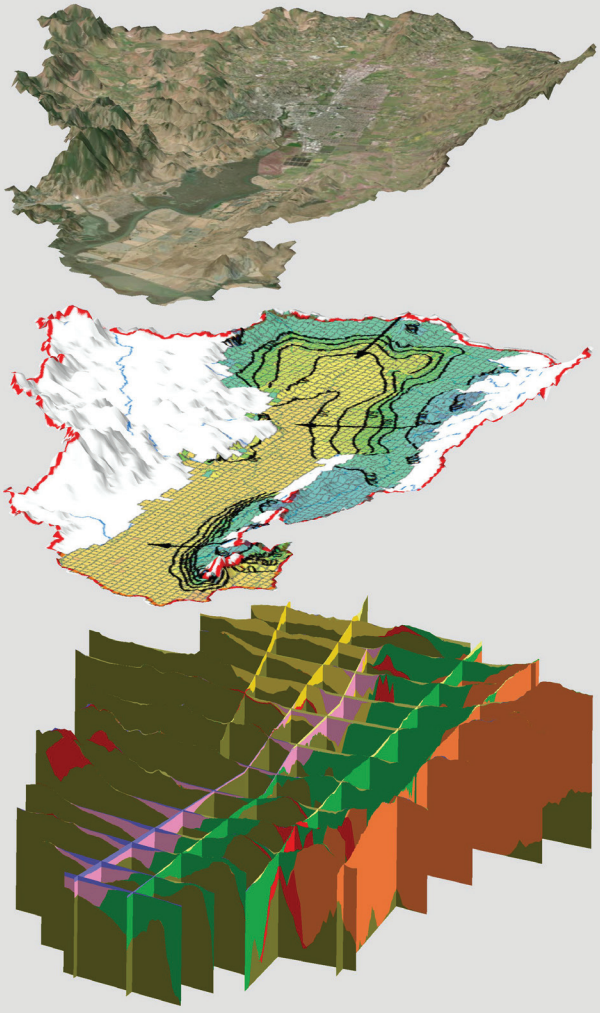

Scientific Investigations Report 2022–5009

U.S. Department of the Interior
U.S. Geological Survey

Cover: Visualization of the 3D geology (bottom), simulated groundwater altitude (middle), and airphoto (top) of the Petaluma River Watershed, Sonoma County, California.

Hydrologic and Geochemical Characterization of the Petaluma River Watershed, Sonoma County, California

By Jonathan A. Traum, Nick F. Teague, Donald S. Sweetkind, Tracy Nishikawa

Water Availability and Use Science Program

Prepared in cooperation with the Sonoma County Water Agency and the City of Petaluma

Scientific Investigations Report 2022–5009

U.S. Geological Survey, Reston, Virginia: 2022

For more information on the USGS—the Federal source for science about the Earth, its natural and living resources, natural hazards, and the environment—visit https://www.usgs.gov or call 1–888–ASK–USGS.

For an overview of USGS information products, including maps, imagery, and publications, visit https://store.usgs.gov/.

Suggested citation:
Traum, J.A., Teague, N.F., Sweetkind, D.S., and Nishikawa, T., 2022, Hydrologic and geochemical characterization of the Petaluma River watershed, Sonoma County, California: U.S. Geological Survey Scientific Investigations Report 2022–5009, 217 p., https://doi.org/10.3133/sir20225009.

Associated data for this publication:
Seymour, W.A., and Traum, J.A., 2021, Petaluma Model GIS Data: U.S. Geological Survey data release, https://doi.org/10.5066/P9IQDHIT.

Sweetkind, D.S., 2019, Data release of three-dimensional hydrogeologic framework model of the Petaluma Valley watershed, Sonoma County, California: U.S. Geological Survey data release, https://doi.org/10.5066/P9NL90P8.

Teague, N.F., 2022, Selected chemical and physical properties and inorganic constituents and time-series nitrate in samples from selected wells and/or springs, Petaluma Valley watershed, Sonoma County, California, 1959–2015: U.S. Geological Survey data release, https://doi.org/10.5066/P9IRYFMB.

Traum, J.A., 2022, MODFLOW-OWHM used to characterize the flow system of the Petaluma River watershed, Sonoma County, California: U.S. Geological Survey data release, https://doi.org/10.5066/P965IDQZ.

ISSN 2328-0328 (online)

Acknowledgments

The authors acknowledge the support of Sonoma County Water Agency and the City of Petaluma and their respective personnel for providing datasets used in this study. The authors thank Scott Boyce for his guidance in the theory and application of MODFLOW-OWHM.

Contents

Figures

Tables

Conversion Factors

U.S. customary units to International System of Units

Multiply	By	To obtain
	Length	
inch (in.)	2.54	centimeter (cm)
inch (in.)	25.4	millimeter (mm)
foot (ft)	0.3048	meter (m)
mile (mi)	1.609	kilometer (km)
	Area	
acre	4,047	square meter (m^2)
acre	0.4047	hectare (ha)
acre	0.4047	square hectometer (hm^2)
acre	0.004047	square kilometer (km^2)
square foot (ft^2)	929.0	square centimeter (cm^2)
square foot (ft^2)	0.09290	square meter (m^2)
square mile (mi^2)	259.0	hectare (ha)
square mile (mi^2)	2.590	square kilometer (km^2)
	Volume	
acre-foot (acre-ft)	1,233	cubic meter (m^3)
acre-foot (acre-ft)	0.001233	cubic hectometer (hm^3)
	Flow rate	
acre-foot per day (acre-ft/d)	0.01427	cubic meter per second (m^3/s)
acre-foot per year (acre-ft/yr)	1,233	cubic meter per year (m^3/yr)
acre-foot per year (acre-ft/yr)	0.001233	cubic hectometer per year (hm^3/yr)
foot per day (ft/d)	0.3048	meter per day (m/d)
cubic foot per second (ft^3/s)	0.02832	cubic meter per second (m^3/s)
gallon per minute (gal/min)	0.06309	liter per second (L/s)
inch per hour (in/h)	0.0254	meter per hour (m/h)
inch per year (in/yr)	25.4	millimeter per year (mm/yr)
	Radioactivity	
picocurie per liter (pCi/L)	0.037	becquerel per liter (Bq/L)
	Specific capacity	
gallon per minute per foot ([gal/min]/ft)	0.2070	liter per second per meter ([L/s]/m)
	Hydraulic conductivity	
foot per day (ft/d)	0.3048	meter per day (m/d)
	Transmissivity	
foot squared per day (ft^2/d)	0.09290	meter squared per day (m^2/d)

International System of Units to U.S. customary units

Multiply	By	To obtain
	Length	
meter (m)	3.281	foot (ft)
	Flow rate	
cubic meter per day (m^3/d)	0.0008107	acre-foot per day (ft^3/d)

Temperature in degrees Fahrenheit (°F) may be converted to degrees Celsius (°C) as follows:

$$°C = (°F – 32) / 1.8.$$

Datum

Vertical coordinate information is referenced to the North American Vertical Datum of 1988 (NAVD 88).

Horizontal coordinate information is referenced to the North American Datum of 1983 (NAD 83).

Altitude, as used in this report, refers to distance above or below the North American Vertical Datum of 1988 (NAVD 88).

Supplemental Information

Specific conductance is given in microsiemens per centimeter at 25 degrees Celsius (µS/cm at 25 °C).

Concentrations of chemical constituents in water are given in either milligrams per liter (mg/L) or micrograms per liter (µg/L).

Activities for radioactive constituents in water are given in picocuries per liter (pCi/L).

Groundwater ages measured with tritium or carbon-14 dating methods are given as “years before present”(ybp).

Carbon-14 data are expressed as percent modern carbon (pMC) by comparing carbon-14 activities to the specific activity of National Bureau of Standards oxalic acid.

Percentage of total cations or anions is measured in milliequivalents per liter (meq/L)

Below land surface (bls) is used to express well screen depths (rather than altitudes).

The aquifer specific storage parameter is expressed in units of one per foot (1/ft).

Differences in the ratios of Oxygen-18/Oxygen-16 and Hydrogen-2/Hydrogen-1 in samples relative to a standard known as Vienna Standard Mean Ocean Water are expressed in per mil, which is also referred to as parts per thousand (‰)”.

Vienna Standard Mean Ocean Water (VSMOW) is an isotopic standard for water (pure water with no salt or other chemicals found in the oceans).

Abbreviations

^{14}C	carbon-14
^{13}C	Carbon-13
^{18}O	Oxygen-18
^{2}H	Deuterium
3D	three-dimensional
^{3}H	tritium
CaCO3	Calcium carbonate
CaMg(CaCO3)2	Dolomite
CASGEM	California Statewide Groundwater Elevation Monitoring
CDPH	California Department of Public Health
CDWR	California Department of Water Resources
Cl	Chloride
CO2	Carbon dioxide
CO3	Carbonate
DDW	Division of Drinking Water
DEM	digital elevation model
DIC	dissolved inorganic carbon
DRT	Drain Return Flow Package
ECWRF	Ellis Creek Water Recycling Facility
ELAP	Environmental Laboratory Accreditation Program
EPA	U.S. Environmental Protection Agency
ET	evapotranspiration
ET_o	reference evapotranspiration
eWRIMS	enhanced Water Right Information Management System
FEI	fraction of evaporation of irrigation
FMP	farm process
FTR	fraction of transpiration
GAMA	Groundwater Ambient Monitoring and Assessment
GFM	geologic framework model
GHB	general-head boundary
GIDS	gradient-plus-inverse-distance squared
GIS	geographic information system
GMWL	Global Meteoric Water Line
GSA	Groundwater Sustainability Agency

GSP	Groundwater Sustainability Plan
HANI	horizontal anisotropy parameter
HCO3	Bicarbonate
HFB	Horizontal Flow Boundary Package
HK	horizontal hydraulic conductivity
HYD	Hydmod Package
ICP-AES	inductively coupled plasma with atomic-emission spectrometry
ICP-MS	inductively coupled plasma with mass spectrometry
KC	Crop Coefficient
LAK	Lake Package
LLNL	Lawrence Livermore National Laboratory
Ma	one-million years
MCL	maximum contaminant level
MHW	mean high water
MNW2	Multi-Node Well Package
MTL	mean tide level
Na-HCO3	sodium-bicarbonate
NO3-N	Nitrate as nitrogen
NOSAMS	National Ocean Sciences Accelerator Mass Spectrometry
NPDES	National Pollution Discharge Elimination System
NSF	north San Francisco Bay
NWIS	National Water Information System
NWQL	National Water-Quality Laboratory
OBS	Observation Package
PRISM	Parameter-elevation Regressions on Independent Slopes Model
PRW	Petaluma River watershed
PVIHM	Petaluma Valley Integrated Hydrologic Model
PVW	Petaluma valley watershed
RCH	Recharge Package
SC	specific conductance
SCWA	Sonoma County Water Agency
SFR	Streamflow Routing Package
SGMA	Sustainable Groundwater Management Act
SMCL	secondary maximum contaminant level
SRP	Santa Rosa Plain

STATSGO2	State Soil Geographic
SSURGO	Soil Survey Geographic
SWRCB	State Water Resources Control Board
TDS	total dissolved solids
TRS	township–range section
UGB	urban-growth boundary
UPW	Upstream Weighting Package
USGS	U.S. Geological Survey
VANI	vertical anisotropy parameter
VK	vertical hydraulic conductivity
VOC	volatile organic compounds
VSMOW	Vienna Standard Mean Ocean Water
WDL	Water data library
WEL	Well Package
WGFH	Wilson Grove Formation Highlands
WRCC	Western Regional Climate Center
WY	water year

Hydrologic and Geochemical Characterization of the Petaluma River Watershed, Sonoma County, California

By Jonathan A. Traum, Nick F. Teague, Donald S. Sweetkind, Tracy Nishikawa

Executive Summary

Principal water agencies in the Petaluma Valley groundwater basin seek to understand the availability of groundwater to meet increasing regional water supply demand caused by increasing agricultural and urban water demands. Surface water from the Russian River is the primary water supply in the basin, but the future availability of this surface-water supply is uncertain. Groundwater is an important supplemental source of water for the City of Petaluma and the primary supply for agriculture and domestic use by rural property owners. Furthermore, supplies of recycled water are becoming more available. Water managers face the challenge of meeting increasing water demand with a combination of surface water, local groundwater resources, and use of recycled wastewater.

In 2014, California adopted legislation to manage groundwater: the Sustainable Groundwater Management Act (SGMA). The SGMA requires the development and implementation of Groundwater Sustainability Plans (GSPs) in 127 medium- or high-priority groundwater basins, and the Petaluma Valley groundwater basin was designated as a high-priority basin. Sustainability is defined within the SGMA in terms of avoiding undesirable results: significant and unreasonable groundwater-level declines, reduction in groundwater storage, seawater intrusion, water-quality degradation, land subsidence, and surface-water depletion. The U.S. Geological Survey (USGS), in cooperation with the Sonoma County Water Agency (SCWA) and the City of Petaluma, characterized the hydrology of the Petaluma valley watershed (PVW) and developed an integrated hydrologic model that can be used to improve understanding and management of the groundwater system and develop a GSP.

The objectives of the study are to (1) develop an updated assessment of the hydrogeology and geochemistry of the PVW and (2) develop an integrated hydrologic model for the PVW. The purpose of this report is to describe the conceptual model of the hydrologic, hydrogeologic, and water-quality characteristics of the PVW and a numerical groundwater-flow model of PVW.

Study Area

The PVW includes the Petaluma River watershed (PRW) as defined by the California Interagency Watershed Map of 1999 (California Interagency Watershed Mapping Committee, 2004), Petaluma Valley groundwater basin, and parts of the Novato Valley and Wilson Grove Formation Highlands groundwater basins (California Department of Water Resources, 2020).

- The population center is the City of Petaluma.
- Agricultural land use is the primary land-use type.
- About 77,400 acres of the 99,200-acre PVW is in Sonoma County, and the remaining 21,800 acres are in northern Marin County.
- The primary source of water supply to the City of Petaluma is imported surface water from the Russian River.

Geohydrology

The geohydrology of the study area was refined through the incorporation of recently published surface-geologic mapping and geophysical and subsurface geologic studies. The specific goals of this study were to identify the surface and subsurface configuration of the water-bearing units, the aquifer properties of these units, the major structures in the study area, and the three-dimensional shape of the basin.

Major findings regarding the geohydrology from this study are the following:

- The spatial extent of water-bearing units at the surface and in the subsurface is limited to specific parts of the PVW.
- Well lithologic data confirm the presence of a northwest-trending Petaluma valley fault beneath the valley axis that is separate from the Meacham Hill and Tolay faults.
- A lithologically heterogeneous unit was identified in the subsurface beneath the axis of the valley based on well data. This unit is referred to as the Quaternary mixed unit in this report and may broadly correlate with the Glen Ellen Formation exposed in nearby basins.

Surface-Water Hydrology

Surface-water hydrology in the PVW is dominated by the Petaluma River and tributary streams. Flow throughout the Petaluma River is controlled by precipitation runoff, and tidal effects also control flows in the lower reaches of the Petaluma River. The lower reach of the Petaluma River is a 13-mile (mi) long tidal slough that empties into San Pablo Bay and has been dredged to create a navigable channel. Petaluma River water is not a primary source of water supply to the City of Petaluma but may influence groundwater quality and supply. Major findings regarding surface-water hydrology from this study are the following:

- Major tributaries to the Petaluma River addressed in this study include Adobe Creek, Lichau Creek, Lynch Creek, Black John Slough, Willow Brook, and San Antonio Creek. Minor tributaries, such as Liberty Creek and Wiggins Creek, are also simulated.
- Tidal influence extends from San Pablo Bay to north of downtown Petaluma, near the confluence of Lynch Creek.
- The lower 13 miles of the Petaluma River flow through the Petaluma marsh.
- Monthly mean discharge was highest in December and lowest in August, with tidally filtered discharge values of 274 and 8.9 acre-feet per day (acre-ft/d), respectively. The median monthly discharge was 20.4 acre-ft/d.
- High discharge values seen in December through March were associated with the high precipitation season from November through March and include some lag time between precipitation and streamflow. The decreases in discharge seen from May through September were directly associated with the dry season.

Aquifer System and Groundwater Movement

The aquifer system in the study area includes the saturated sedimentary rocks and sediments underlying the floor of the PVW and neighboring lowlands. Volcanic rocks underlying the mountains to the east and west of the PVW are sufficiently permeable to yield water. Beneath the floor of the PVW, the principal aquifer system is lithologically heterogeneous but consists of one continuous body of saturated material. This reservoir is typically in hydraulic communication laterally with permeable consolidated rocks that underlie the uplands surrounding the PVW and interfinger with the basin-fill deposits. Groundwater in the principal aquifer is contained in the pore spaces of the Quaternary alluvial materials and Tertiary sedimentary material, including the Wilson Grove Formation, the Petaluma Formation, a Quaternary mixed unit, and bay mud deposits. Groundwater is also contained in locally permeable areas within the Franciscan Complex and the Sonoma Volcanics. Major findings regarding groundwater movement and levels from this study are the following:

- Sources of groundwater recharge in the PVW include percolation of precipitation and excess irrigation water, infiltration from streams, and boundary inflow from neighboring groundwater basins.
- Groundwater discharge sinks include groundwater pumpage, evapotranspiration, root uptake of shallow groundwater, boundary outflow to San Pablo Bay, and base flow to streams.
- Groundwater levels indicate that, on a larger scale, groundwater in the southwest side of the PVW flows eastward from the hills in the Wilson Grove Formation and the Franciscan Complex hydrogeologic units. Groundwater in the northeast side of the PVW, from the Sonoma Mountains westward, flows toward the Petaluma River in the axis of the Petaluma valley watershed. In the center of the PVW, groundwater flows northwest to southeast following the path of the Petaluma River.
- Hydrographs of measured groundwater levels indicate that long-term groundwater levels were generally stable, with some local drawdown possibly resulting from pumping.
- Groundwater elevations adjacent to the tidally influenced reach of the Petaluma River were below the stage in the river during high tides.

- Hydraulic gradients indicate that some groundwater moves south from the Santa Rosa Plain groundwater subbasin into the PVW. Model results indicated that there was a net inflow of about 880 acre-feet per year (acre-ft/yr) from the Santa Rosa Plain into the PVW. Previous studies estimated that less than 50 acre-ft/yr of groundwater flows from the Santa Rosa Plain to the PVW.
- Groundwater levels indicate that the Petaluma River gained groundwater from its terminus at San Pablo Bay upstream to just downstream from the confluence with Lichau Creek. Lichau Creek lost water upstream from Penngrove, California, and gained groundwater downstream from Penngrove. Willow Brook may have lost water upstream from the confluence with Lichau Creek, and Wiggins Creek gained groundwater along its entire reach. The upstream portions of Lynch Creek gained groundwater and may have lost water near the confluence with the Petaluma River, and Adobe Creek gained groundwater upstream from State Route 116.

Groundwater Quality

Groundwater quality was characterized in the PVW using data for selected physical properties and inorganic constituents compiled from previous investigations and databases maintained by the USGS, the California State Water Resources Control Board, Division of Drinking Water, California Department of Water Resources, and public-supply purveyors for 1959–2016. Data were used to characterize the areal, vertical, and temporal variations in groundwater quality and to identify constituents of potential concern. Stable and radioactive isotopes analyzed from groundwater samples collected in 2004 and 2012 as part of the USGS Groundwater Ambient Monitoring and Assessment Program, or analyzed from surface-water and groundwater samples collected from 2015 to 2016 as part of this study, were used to identify recharge sources and ages of groundwater in the study area.

Major findings from this study about groundwater quality are the following:

- Based on major-ion and stable-isotope data, the primary source of groundwater in the PVW is infiltration of precipitation in the higher elevations within, and to a limited extent just outside of, the watershed boundary.
- The tritium (^{3}H) and carbon-14 (^{14}C) data indicate that modern (post-1950s) groundwater is generally constrained to wells screened near land surface.
- The ^{3}H and ^{14}C data indicate that groundwater sampled from deep wells along the axis of Petaluma valley is pre-modern water representing groundwater at the end of regional groundwater.
- Groundwater samples in the Wilson Grove Formation were mostly composed of pre-modern groundwater, indicating that groundwater does not mix with surface-water sources after infiltrating as precipitation in higher elevations.
- Groundwater movement through the Wilson Grove Formation, from the PVW boundary to the Petaluma River, is inferred from an increase in groundwater age along groundwater flow paths, as determined from ^{3}H and ^{14}C data.
- Major-ion data indicate that groundwater from the Wilson Grove Formation is a substantial input to streamflow in the upper reach of the Petaluma Formation.
- Major-ion data indicate that groundwater moves through the Sonoma Volcanics with minimal change in chemistry from reactions with the aquifer material before entering the Petaluma Formation.
- In the Petaluma Formation, the ^{3}H and ^{14}C data indicate that groundwater in shallow and mixed-depth wells is a mixture of modern and pre-modern waters, demonstrating that pre-modern groundwater is mixing with modern water infiltrating from land surface.
- As groundwater moves into greater depths in the Petaluma formation and toward the axis of the valley, water-rock reactions with aquifer material lead to an increase in specific conductance, total dissolved solids, major-ion concentrations, and evolution into sodium-bicarbonate ($Na\text{-}HCO_3$) type water.
- Groundwater in the northern and southern parts of the Petaluma Formation has moved along different flow paths from those of groundwater sampled by the wells in the central part of the formation, leading to different major-ion compositions as a result of different groundwater evolution.
- Modern water sampled from wells perforated in the Quaternary mixed unit is a mixture of infiltration of precipitation and infiltration of agricultural return and urban runoff.
- Major-ion data indicate that pre-modern groundwater in deep wells perforated in the Quaternary mixed unit is a mixture of groundwater from the Wilson Grove and Petaluma Formations, which in some places may be mixing with a deeper, relatively saline source of groundwater.
- Isotopically light water, with ^{14}C ages greater than 17,000 years before present sampled from wells perforated in the Quaternary mixed unit near the axis

of the valley, indicates a deep source of water that infiltrated under a cooler climatic environment, tens of thousands of years before present.

- Concentrations of nitrate as nitrogen (NO_3-N) were generally detected in shallow and mixed depth wells in urban and agricultural areas.
- The general absence of high NO_3-N concentrations in groundwater samples in this study indicates that NO_3 contamination has not moved into the deep parts of the aquifer. This lack of movement, however, should not be interpreted as evidence that historical NO_3 contamination in the shallow part of the Wilson Grove Formation has been resolved.

Integrated Hydrologic Model

The Petaluma Valley Integrated Hydrologic Model (PVIHM) is an integrated hydrologic model that simulates the groundwater-flow system, the surface-water flow system, and landscape processes in a single model. Key features of the PVIHM spatially and temporally calibrated simulations include the following:

- A simulation using the MODFLOW-OWHM code that incorporates groundwater flow, surface-water flow, and landscape processes.
- Simulation of the entire 99,200-acre PVW, including 54,000 acres in which groundwater flow is simulated.
- Simulation of historical conditions from water year 1960 to 2015 that includes a range of wet and dry climatic conditions.
- Incorporation of data collected as part of this study, as well as other datasets from local, State, and Federal sources.

The PVIHM was calibrated using measured groundwater levels and changes in groundwater levels from 41 groundwater monitoring wells and measured streamflow data from three USGS streamgages. The model was calibrated using a combination of public-domain model-independent parameter-estimation software and trial-and-error.

Key model results are listed here:

- Variability in annual water budgets indicated storage losses during dry climatic periods and storage gains during wet climatic periods.
- Groundwater recharge from percolation ranged from about 6,000 acre-ft/yr in dry conditions (water year [WY] 1976) to about 25,000 acre-ft/yr in wet conditions (WY 1978).
- Runoff was the predominant source of water into the Petaluma River.
- The average net outflow of groundwater to San Pablo Bay was about 500 acre-feet per year.
- Average annual water budgets indicated that stream seepage to groundwater was the predominate inflow to the groundwater system (78 percent). Other sources of inflow included recharge of precipitation, excess irrigation water (12 percent), and boundary inflow (10 percent). Groundwater discharge to streams s the predominate outflow from the groundwater system (80 percent). Other sources of outflow included root uptake of shallow groundwater (11 percent), agricultural groundwater pumping (5 percent), and rural groundwater pumping (4 percent). Municipal groundwater pumping accounted for less than 1 percent of total groundwater outflow.
- The long-term, average decline in groundwater storage over the entire study area is 76 acre-ft/yr (only 0.4 percent of the average recharge).
- The calibrated model provides a tool for the City of Petaluma and SCWA to evaluate hydrologic effects related to conjunctive use of surface water, recycled water, and groundwater. The model can also be used to help the Petaluma Valley Groundwater Sustainability Agency develop a GSP for the Petaluma Valley groundwater basin.

Data Gaps

The datasets used in this study represent the best information available at the time of the study; however, some datasets were limited or incomplete, resulting in data gaps. Key data gaps include the following:

- Streamgages were not active and consistent streamflow data were not collected along the Petaluma River from October 1963 through January 1999.
- Increased water-quality coverage in areas outside of the axis of Petaluma valley, particularly in the eastern part of the Petaluma Formation, could improve model calibrations.
- Only annual totals of groundwater production for the City of Petaluma were available before 1994.
- Groundwater production data for rural or agricultural use were not available.
- Local-scale crop related data were not available (for example, irrigation efficiencies and crop coefficients).

Major Findings

This study resulted in several major findings about the hydrology of the PVW:

- Stable-isotope data indicate that the primary source of water in the PVW is infiltration of precipitation.
- Groundwater moves from the Wilson Grove Formation Highlands groundwater basin to the west and from the Sonoma Mountains to the east, through the Wilson Grove and Petaluma Formations, respectively, toward the Petaluma River and the Quaternary alluvium and Quaternary mixed unit that fill the axis of the Petaluma valley. Groundwater also moves north to south through the Petaluma Formation, the Quaternary mixed unit, and the Quaternary alluvium, following the trace of the river.
- Long-term measured groundwater levels indicate that levels are generally stable, but some localized drawdown was observed.
- The Petaluma River gains groundwater along the non-tidally influenced reach, north of the City of Petaluma. The tidally influenced reach of the Petaluma River can gain or lose groundwater depending on streamflow and tidal cycle.
- Age data indicate a long flow path from the Sonoma Mountains to the east to the Quaternary mixed unit in the northern part of the PVW.

Simulated results indicated the following about the groundwater system:

- Groundwater pumping caused only minor decreases in groundwater storage; pumped groundwater resulted primarily in loss of streamflow.
- Runoff was the predominant source of water into the Petaluma River.
- Little hydraulic communication was observed among neighboring groundwater basins.
- Groundwater recharge from precipitation varied with climate variability.

Chapter A. Introduction to the Study Area

By Nick F. Teague, Donald S. Sweetkind, Tracy Nishikawa, and Jonathan A. Traum

Introduction

The Petaluma River watershed (PRW; fig. A1; California Interagency Watershed Mapping Committee, 2004) has about 60,500 residents (U.S. Census Bureau, 2017), corresponding to approximately 12 percent of the population of Sonoma County, California. Water supply to the urban areas of the PRW is provided primarily by surface water imported by an aqueduct from the Russian River (not shown), but groundwater is an important supplemental source of water for the City of Petaluma and is a source of supply for agriculture and domestic use by rural property owners. Water managers face the challenge of meeting population growth and the increasing water demand from local groundwater resources, recycled wastewater, and Russian River water.

Historically, agricultural and domestic groundwater users in the PRW have used private wells and have operated independently from each other based on local supply needs. The City of Petaluma has operated several municipal wells to supplement imported surface-water supplies, but historically, surface water from the Russian River and groundwater have been managed as separate supplies. Increasing water demand, reliance on imported Russian River water, and increasing awareness of drought conditions have increased the attention to management of surface-water and groundwater supplies. Groundwater flow in the PRW has not been studied since 1982 (Herbst, 1982); therefore, an improved and updated understanding of groundwater sustainability in the PRW would allow for better management of this resource as the need for groundwater-production withdrawals increases. The U.S. Geological Survey (USGS), in cooperation with Sonoma County Water Agency (SCWA) and the City of Petaluma, undertook this study to characterize the hydrology of the PRW and to develop tools to help improve understanding and management of the groundwater system.

Previous Work

Previous groundwater studies of Petaluma valley and the Petaluma Valley groundwater basin were done by Cardwell (1958), Herbst (1982), and Kulongoski and others (2010). Additionally, water-level and water-quality data have been regularly collected in the Petaluma valley watershed (PVW) by the California Department of Water Resources (CDWR) since 1950, and the California drinking water regulatory program has collected water-quality data since 1941.

Cardwell (1958) described the extent, composition, and hydrologic properties of the major geologic formations in the PVW, including sources of recharge and discharge and movement of groundwater and surface water. The most important aquifers in the area are the Wilson Grove Formation Highlands groundwater basin, the older Pleistocene alluvium and terrace deposits, and younger alluvium of recent age (Cardwell, 1958). The Petaluma Formation was recognized as a source of groundwater generally yielding less than the other formations or deposits. Infiltration of precipitation and seepage from streams were described as the primary source of groundwater recharge. The primary groundwater discharges were flows to streams and springs, evapotranspiration, and pumping. There were an estimated 1,500 domestic, public-supply, and irrigation wells active in the area in 1950, and the total pumpage for the Petaluma Valley groundwater basin in 1949 was 1,800 acre-feet (acre-ft; Cardwell, 1958). Movement of groundwater in the Petaluma Valley groundwater basin was described as generally northeastward and southwestward toward what is now the Petaluma River and downgradient toward tidal sloughs near San Pablo Bay. Exchange of water between the Petaluma River and groundwater was noted within a few hundred feet of the tidal channel in the southern part of the valley and near the City of Petaluma.

Herbst (1982) described the groundwater in the Petaluma Valley groundwater basin as compartmentalized because of the discontinuous nature of the water-bearing deposits and extensive faulting in the area. The Wilson Grove Formation Highlands groundwater basin, however, was described as having a high degree of vertical and horizontal continuity. The storage capacity of the basin was estimated at 1,697,000 acre-ft, and the total volume of groundwater in storage was estimated at 1,420,000 acre-ft. Average annual recharge was estimated at 40,000 acre-ft. The water quality in the Petaluma valley was classified as generally poor, with nitrate contamination northwest of the City of Petaluma and seawater intrusion in the southern part of the valley (Herbst, 1982). The total volume of potable groundwater in storage was estimated at 1,332,000 acre-ft, or 94 percent of the total volume of groundwater in storage.

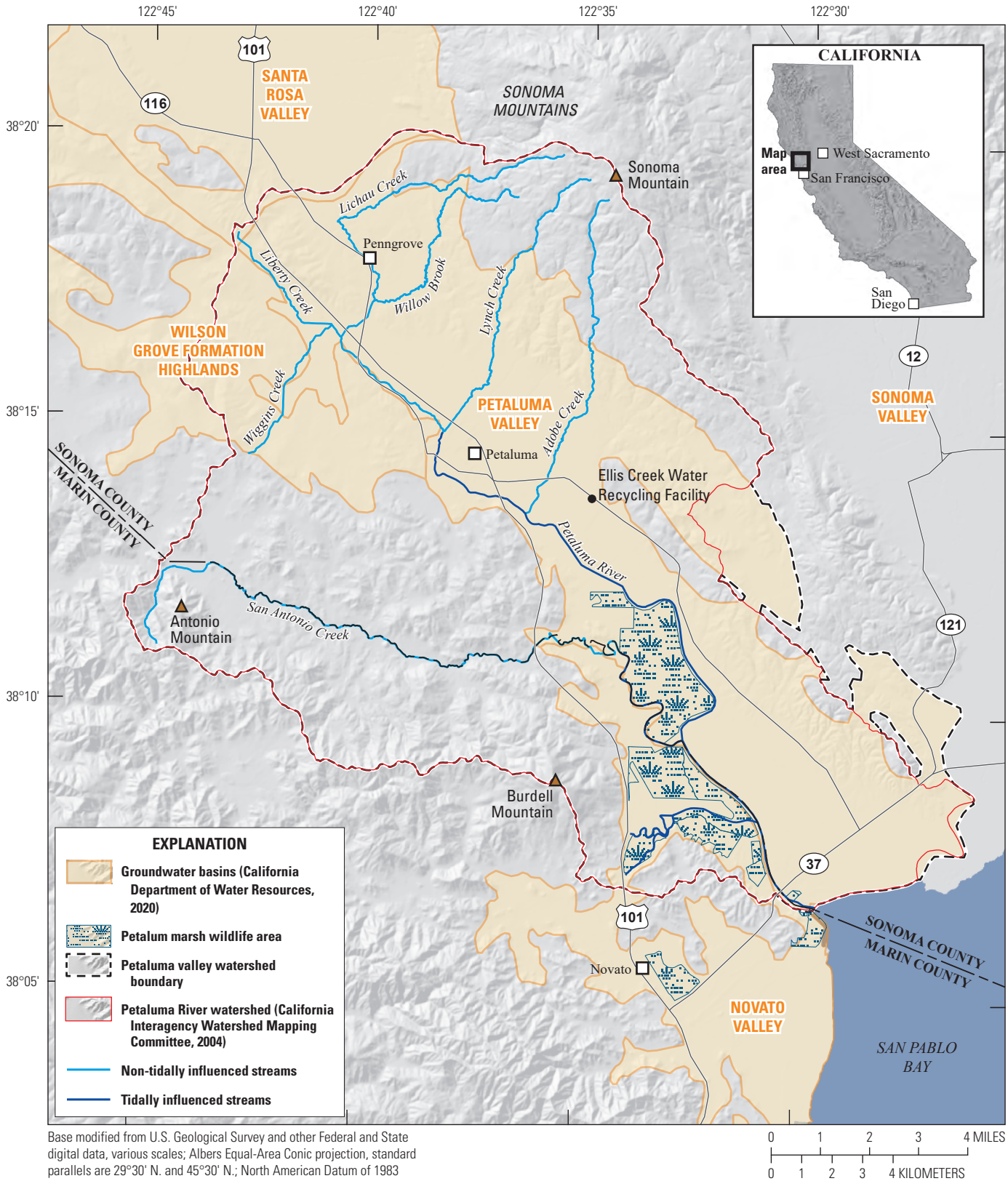

Figure A1. Petaluma River watershed study area, Sonoma County, California.

Kulongoski and others (2010) investigated groundwater quality in the Petaluma Valley groundwater basin as part of the USGS Priority Basin Project of the Groundwater Ambient Monitoring and Assessment (GAMA) Program. The Petaluma Valley groundwater basin is part of a larger study area that included Marin, Napa (not shown), and Sonoma Counties. The study consisted of two components: (1) characterization of the current quality of the groundwater resources within the primary aquifers using data from samples analyzed for volatile organic compounds (VOC), pesticides, and naturally present inorganic constituents such as major ions and trace elements and (2) identification of the natural and human factors that affect groundwater quality by evaluating land use, physical characteristics of the wells, geochemical conditions of the aquifer, and water temperature. Although data for wells in the Petaluma Valley groundwater basin are presented in this GAMA study, the results focused on the larger region, and conclusions were not drawn specifically to the local geohydrology of the Petaluma Valley groundwater basin.

Purpose and Scope

The purpose of this report is to synthesize available data for the City of Petaluma and the SCWA to use to evaluate the sustainability of groundwater supplies in the PVW. In 2014, California adopted legislation to manage its groundwater, the Sustainable Groundwater Management Act (SGMA; California Department of Water Resources, 2018), which requires the development and implementation of Groundwater Sustainability Plans in priority groundwater basins; the Petaluma Valley groundwater basin was designated as a medium-priority basin (potentially increasing to high priority based on the California Department of Water Resources, 2018, draft "Basin Prioritization" report) and is subject to SGMA requirements. Sustainability is defined in the SGMA as avoiding undesirable results that are significant and unreasonable, including groundwater-level declines, reduction in groundwater storage, seawater intrusion, water-quality degradation, land subsidence, and surface-water depletion.

The scope of the project included (1) an updated assessment of the geohydrology and geochemistry of the PVW using available data and collection of new data from existing wells, (2) the development of an integrated hydrologic model, and (3) identification of data that could fill gaps (for example, locations where depth-dependent water-quality or additional geologic data are needed) to improve the current understanding of the geochemistry and groundwater flow in the PVW.

This report comprises four chapters. Chapter A includes the purpose and scope of the study, describes the study area, and presents an overview of previous work. Chapter B describes the geology in detail, outlines the development of a geologic framework model, and discusses the surface and groundwater hydrology of the study area. The "Geology" section includes descriptions of the geologic setting, stratigraphic units, major faults, and basin depth and geometry. Chapter B also includes a description of a three-dimensional geologic model that represents the subsurface geometry of stratigraphic units on top of the Franciscan Complex. The "Surface-Water Hydrology" section provides a detailed description of the hydrography of the study area. The "Groundwater Hydrology" section describes the aquifer system, groundwater recharge and discharge, and groundwater flow. Chapter C describes groundwater-quality conditions, sources and ages of groundwater, and a conceptual model of groundwater flow based on results from chapters B and C. Chapter D describes the development of the integrated hydrologic model of the PVW and simulation results.

Study Area Description

The PRW is in Sonoma County, about 30 miles (mi) north of San Francisco, California, and the City of Petaluma is the population center of the PRW (fig. A1). The boundary of the study area described herein, referred to as the Petaluma valley watershed (PVW; fig. A1), extends slightly beyond the PRW (California Interagency Watershed Mapping Committee, 2004), primarily along the southeast section of the boundary, to represent the complete area of the Petaluma Valley groundwater basin as defined by the California Department of Water Resources (CDWR, 2020; fig. A1). The study area also includes parts of the Novato Valley groundwater basin and parts of the Wilson Grove Formation Highlands groundwater basin (formerly referred to as the Merced Formation; fig. A1).

The forthcoming description of the study area provides an overview of the physiography, soils, climate, and land use of the PVW. The description of the physiography includes an overview of the geologic controls on landforms in and around the study area. The description of land use provides a brief history of land-use changes and includes an overview of the effect of land-use change on the hydrology of the PVW.

Physiography

The PVW covers about 155 square miles (mi^2; 99,200 acres) of the Petaluma valley and the slopes of surrounding mountains and hills. About 121 mi^2 of the PVW is in Sonoma County; the remaining 34 mi^2 are in northern Marin County. The Petaluma valley is a structurally controlled, northwest-trending depression in the Coast Ranges of northern California (not shown) making up about 45 mi^2 of alluvial plains, of which about 10 mi^2 is tidal marsh (Cardwell, 1958). The PVW is bounded by the Santa Rosa Plain groundwater subbasin (not shown; part of the Santa Rosa Valley groundwater basin; fig. A1) to the north, the San Pablo Bay to the south, the Sonoma Mountains to the east, and the ridges connecting Burdell Mountain and Antonio Mountain to the south (fig. A1).

Altitudes in the PVW range from 3 feet (ft) below sea level to 2,295 ft above sea level, and all presented altitudes are referenced to the North American Vertical Datum of 1988 (NAVD 88). The altitude of most of the upper PVW is between sea level and 50 ft, and the altitude of the lower PVW is at or below sea level by as much as 3 ft (Cardwell, 1958). In the PVW, Sonoma Mountain (fig. A1), along the northeastern edge of the study boundary, has the maximum altitude of 2,295 ft above NAVD 88. In the southwestern part of the study area, Burdell Mountain (fig. A1) has the highest altitude at 1,558 ft. The PVW and the Santa Rosa Plain are topographically connected through a gap in the hills about 2 mi northwest of Penngrove (Cardwell, 1958). Ground-surface altitude data used for this study were obtained from a digital elevation model (DEM) provided by the USGS National Elevation Dataset (Gesch and others, 2009), and lidar data were provided by Sonoma County (2018).

Soils

Soil data used for the study were obtained from the Soil Survey Geographic (SSURGO) Database and State Soil Geographic (STATSGO2) Database (U.S. Department of Agriculture, Natural Resource Conservation Service, 2005). Soil properties were classified into three categories based on their hydrologic soil groups: silty clay (50 percent), silt (42 percent), and sandy loam (8 percent; fig. A2).

Climate

The climate for the PVW is Mediterranean, with cool, wet winters; warm, dry summers; and a strong coastal influence on climate that moderates temperature extremes (Sonoma Resource Conservation District, 2015). Climate in the area varies with topography.

Precipitation

The spatial distribution of mean annual precipitation is strongly affected by topography and varies considerably in the PVW (fig. A3). Temporal variability in precipitation is primarily controlled by seasonal patterns. Mean annual precipitation calculated for the Western Regional Climate Center (WRCC) climate station in the City of Petaluma (046826) for 1913–2015 was 23.12 inches (in.; Western Regional Climate Center, 2016). About 98 percent of the annual precipitation falls from November through March. At the Petaluma climate station, the wettest month has been December, with an average precipitation of about 5 in. 1913–2015 (fig. A4). March is the next wettest month. The months of May through September all have less than 1 in. average monthly precipitation; July is the driest month, at 0.02 in., for the 1913–2015 period.

In addition to seasonal variation, there is also strong year-to-year variability in precipitation caused by natural cycles and trends in global circulation patterns that affect climate (fig. A5). The California Department of Water Resources (2015) stated that the droughts of 1928–34, 1976–77, 1987–92, 2007–09, and 2012–15 were important from a water-supply standpoint. Wetter-than-normal periods generally result from an increase in the frequency and duration of storms. For example, Dettinger and others (2011) stated that atmospheric rivers contribute 20–50 percent of precipitation in California.

Air Temperature

As with precipitation, the spatial and temporal distributions of air temperature are also strongly affected by topography and season. Mean monthly air temperatures between 1983 and 2012 for WRCC climate station 046826 varied from a minimum of 47 degrees Fahrenheit (°F) during January to a maximum of 67 °F during August, with a mean temperature of 58 °F (Western Regional Climate Center, 2016).

Modern (post-1950) Changes in Land Use and Effects on Hydrology

The earliest record of land use in the area (Adams, 1913) reports that 60 acres of the 90,000 acres of available agricultural land in Santa Rosa and Petaluma valleys were irrigated. Beginning in the late 1940s, there was a shift in agricultural land use from poultry to dairy (Cardwell, 1958). In 1960, about 20 percent of land in the area was used for dairies, poultry, and egg production; by 1982, only about 6 percent of the land was used for dairies and poultry (Herbst, 1982). In 2006, agriculture remained the primary land-use type (87.4 percent); other types included residential (8.7 percent), commercial (1.5 percent), public/quasi-public (2 percent), resources and rural development (0.3 percent), and industrial (0.1 percent; Sonoma County, 2006).

The population of Petaluma valley grew substantially during the middle of the 20th century. In 1950, the population of the City of Petaluma was 10,315 (Bay Area Census, 2021), which increased to about 58,000 by 2010 (Bay Area Census, 2021), and there were corresponding increases in urban and residential land use. In 1998, the City of Petaluma created a 20-year urban growth boundary (UGB) to separate urban growth from surrounding farms, ranches, open lands, and parks. The goal of the UGB was to protect productive farmlands from development, provide habitat for wildlife, and secure healthy watersheds (Sonoma Resource Conservation District, 2015). The city renewed the measure in 2010 to extend the UGB timeline through the year 2025 (Sonoma Resource Conservation District, 2015).

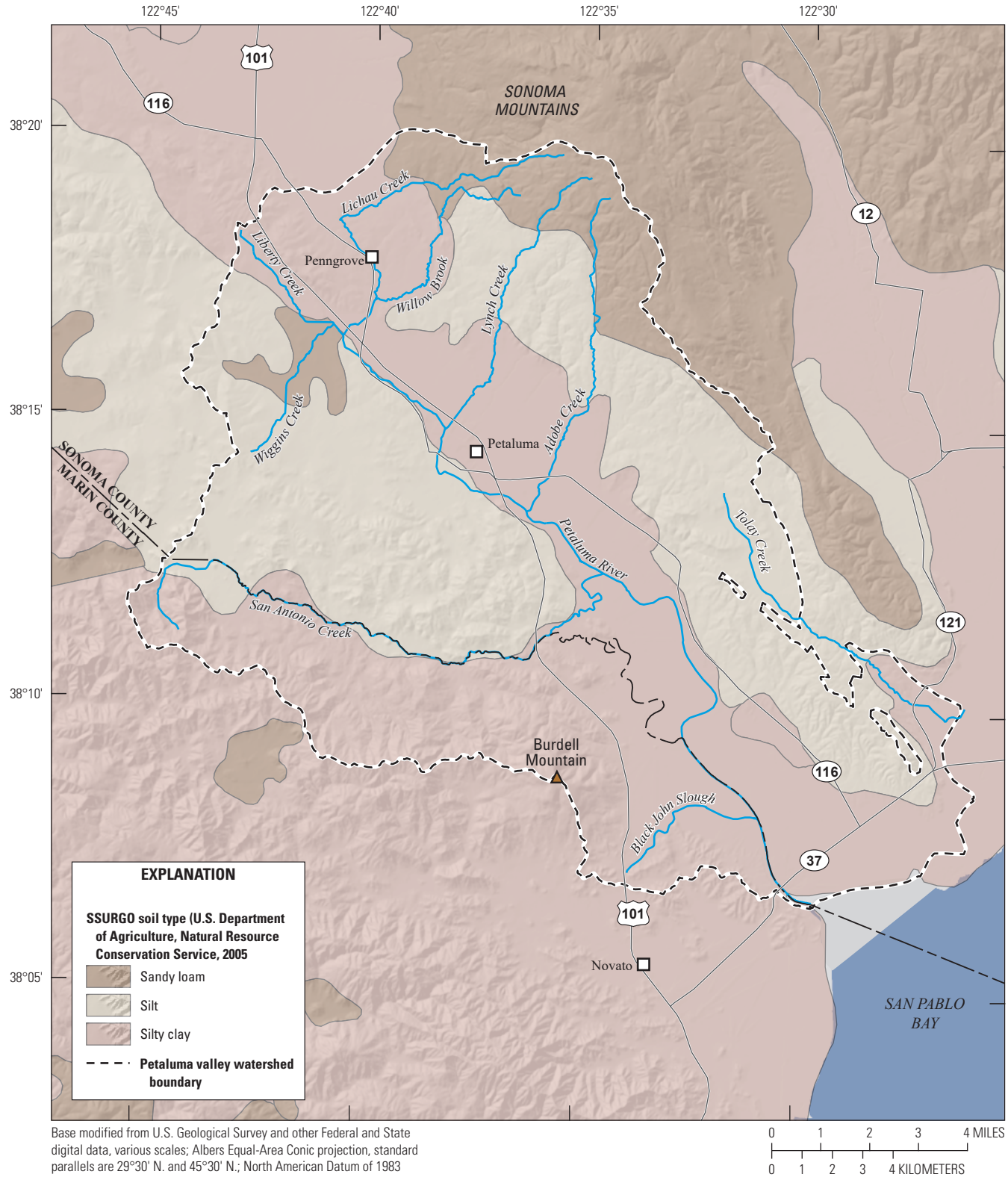

Figure A2. Distribution of soil types, Petaluma valley watershed, Sonoma County, California.

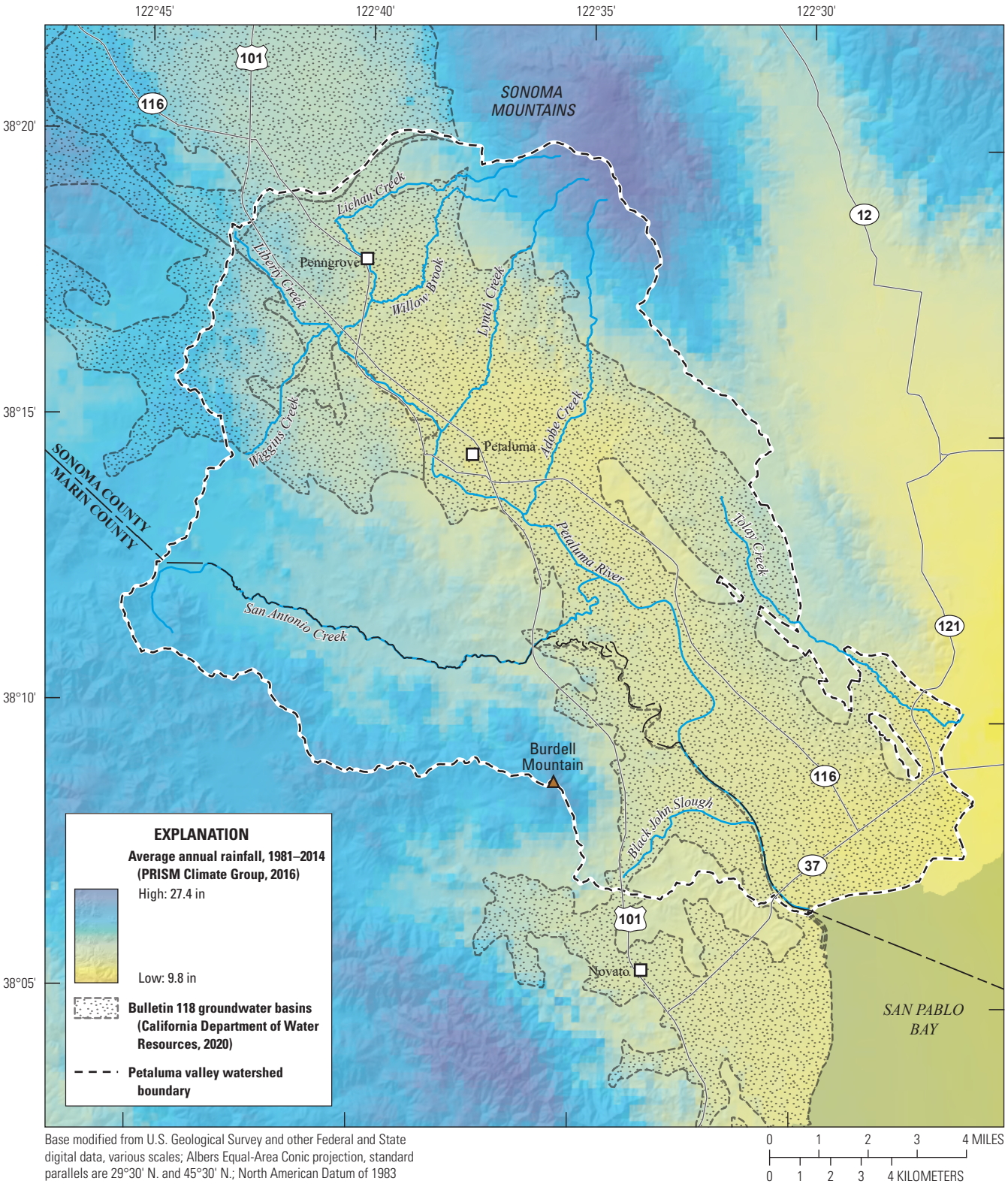

Figure A3. Spatial distribution of average annual precipitation in the Petaluma valley watershed, Sonoma County, California, 1981–2010 (PRISM Climate Group, 2016).

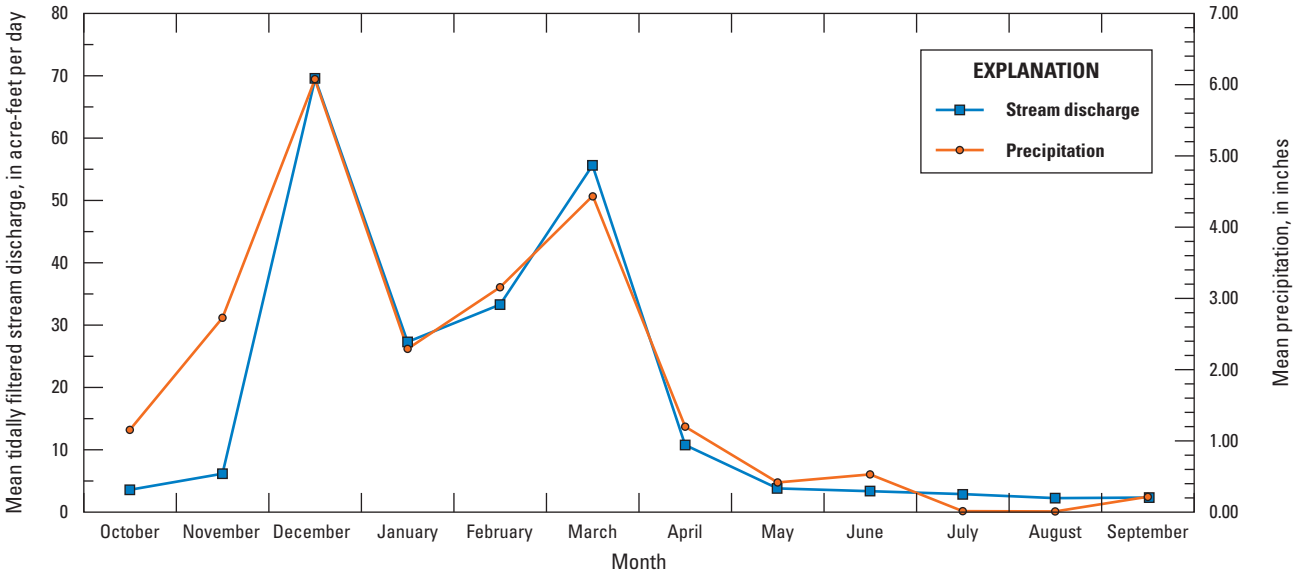

Figure A4. Average monthly precipitation data measured at the Western Regional Climate Center climate station in the City of Petaluma (046826); Western Regional Climate Center, 2016), Petaluma valley watershed, California, water years 2011–16.

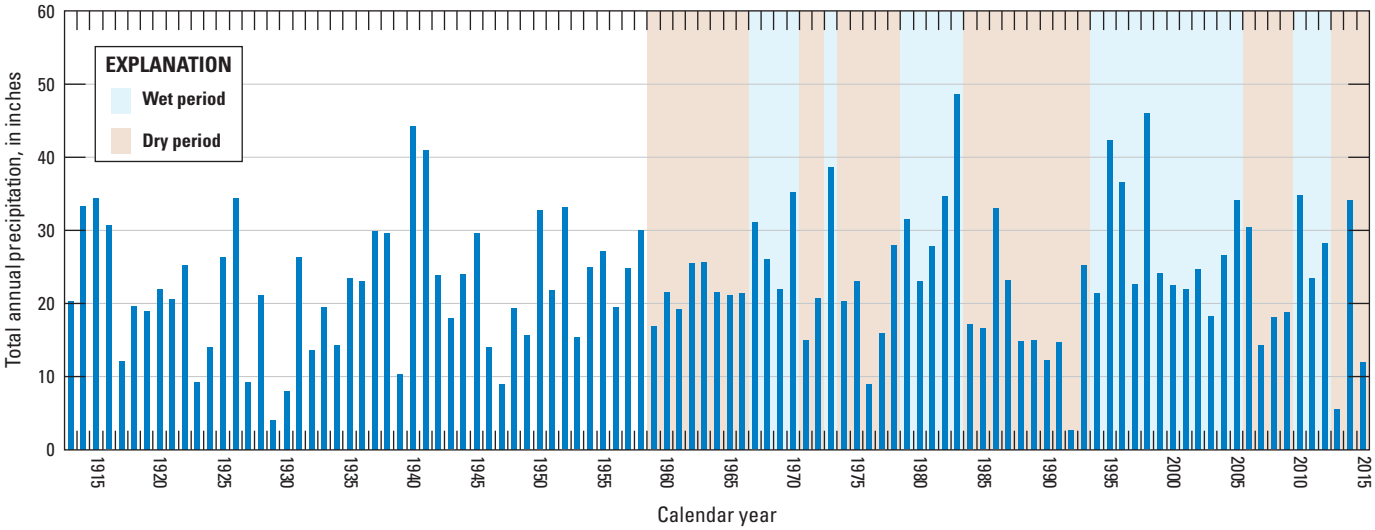

Figure A5. Annual total precipitation data measured at the Western Regional Climate Center climate station in the City of Petaluma (046826; Western Regional Climate Center, 2016) from 1913 to 2015, Petaluma, California.

Land-use data for the PVW in Sonoma County were available from CDWR for 1959 (California Department of Water Resources, 1959; Seymour and Traum, 2021), 1979 (California Department of Water Resources, 1979; Seymour and Traum, 2021), 1986 (California Department of Water Resources, 1986; Seymour and Traum, 2021), 1999, and 2012 (California Department of Water Resources, 2016). Land-use data were available for Marin County for 1999 and 2011 (California Department of Water Resources, 2016; figs. A6–A10). For the study, the 1999 Marin County survey and the 1999 Sonoma County survey were merged into a single dataset, referred to as the 1999 survey. Similarly, the 2011 Marin County survey and the Sonoma County 2012 survey were merged into a single dataset, referred to as the 2011–12 survey. The land-use data for 1959, 1979, and 1986 are from partial coverages of the study area based on digitized CDWR land-use surveys.

The CDWR land-use surveys have more than 80 land-use categories; these were consolidated to 12 land-use types for this study based on the CDWR "class" symbol, which is the minimum division of land use provided in their surveys. For this study, the urban class was further divided into rural and urban because each subclass has different water-use characteristics. This division was based on a combination of analyses using the subclasses of urban (if provided in the CDWR survey), the secondary land uses (if provided in the CDWR survey), and aerial photography.

Areas covered by each land-use type are compiled in table A1. Based on the 2011–12 survey, the study area is predominantly native vegetation, which covers 72 percent of the study area (64 percent upland native vegetation and 8 percent riparian vegetation). Agriculture is the second largest land-use type by area, covering 16 percent of the study area. The major crop types in the study area are grain and hay (8 percent) and vineyards (3 percent). Urban land use makes up the remaining 12 percent of the study area (9 percent city urban and 3 percent rural urban).

Population growth can cause increases in water demand and subsequent increases in groundwater pumping. Additionally, changes in agricultural practices may increase or decrease the demand for groundwater production, depending on the water needs for the new crop or livestock compared to the previous crop or livestock. In 1951, about 1,500 wells were in use in Petaluma valley, of which about 95 percent were used for domestic purposes, and groundwater supplied 48 percent of the water supply for the city (Cardwell, 1958). As a result, groundwater levels in wells near the City of Petaluma dropped from the mid-1950s until the early 1960s (Herbst, 1982). Beginning in 1962, the City of Petaluma began importing Russian River (not shown) water to supplement water supply (Herbst, 1982). By 1980, groundwater only provided 15 percent of the water supply for the City of Petaluma, and water levels began to recover (Herbst, 1982). Groundwater pumping for municipal supply was near zero in 1997 but increased to provide 10 percent of the city water supply by 2002 (Kenneth Loy, West Yost Associates, written commun., 2004). In 2000, the City of Petaluma used groundwater only for meeting peak water demands. In 2015, 6 of the existing 12 active wells were used for production, and the volume of groundwater pumped by city water-supply wells was 375 acre-ft, or 5 percent of the total water supply (City of Petaluma, 2016).

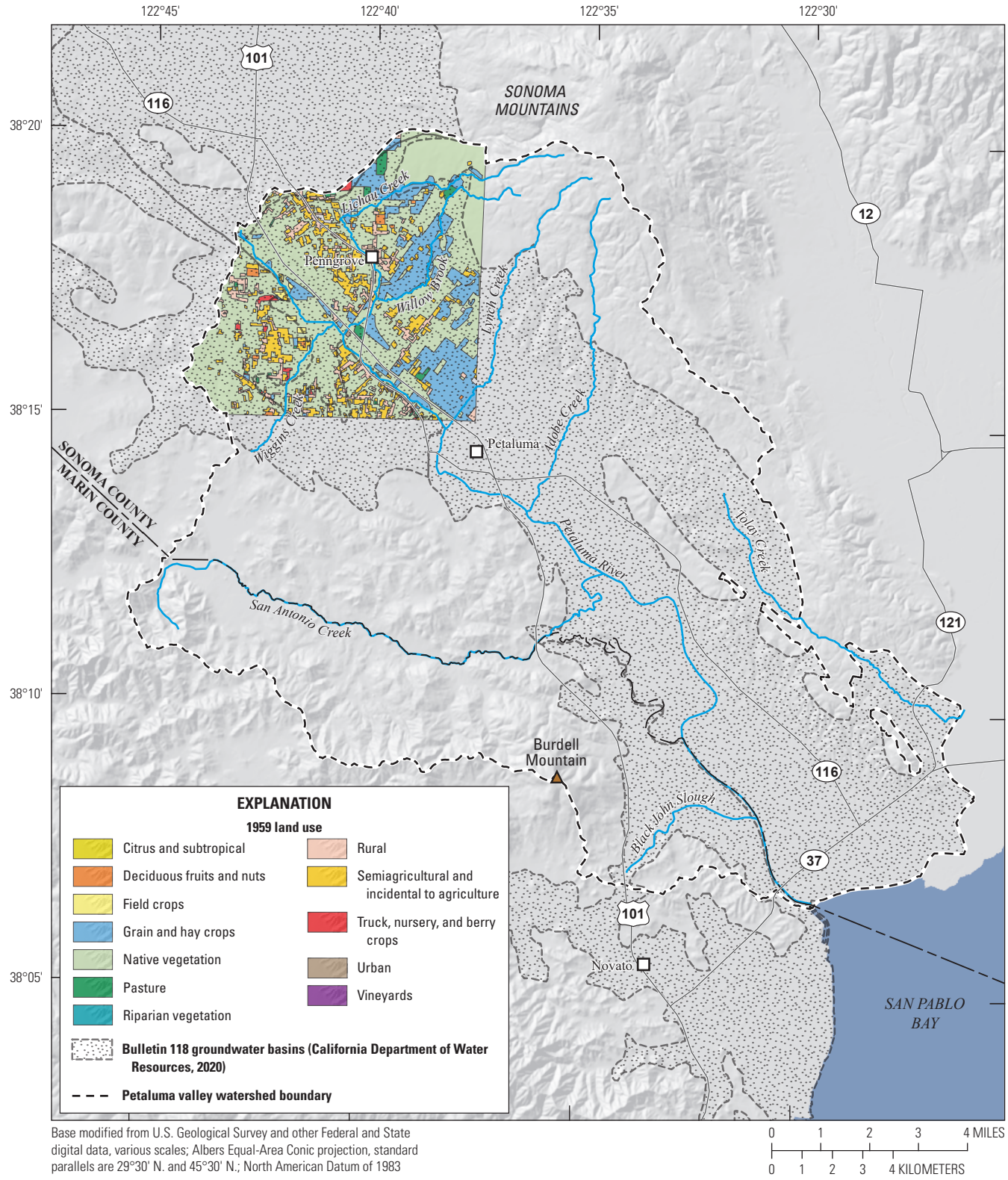

Figure A6. The 1959 distribution of land use, Petaluma valley watershed, Sonoma County, California (California Department of Water Resources, 1959; Seymour and Traum, 2021).

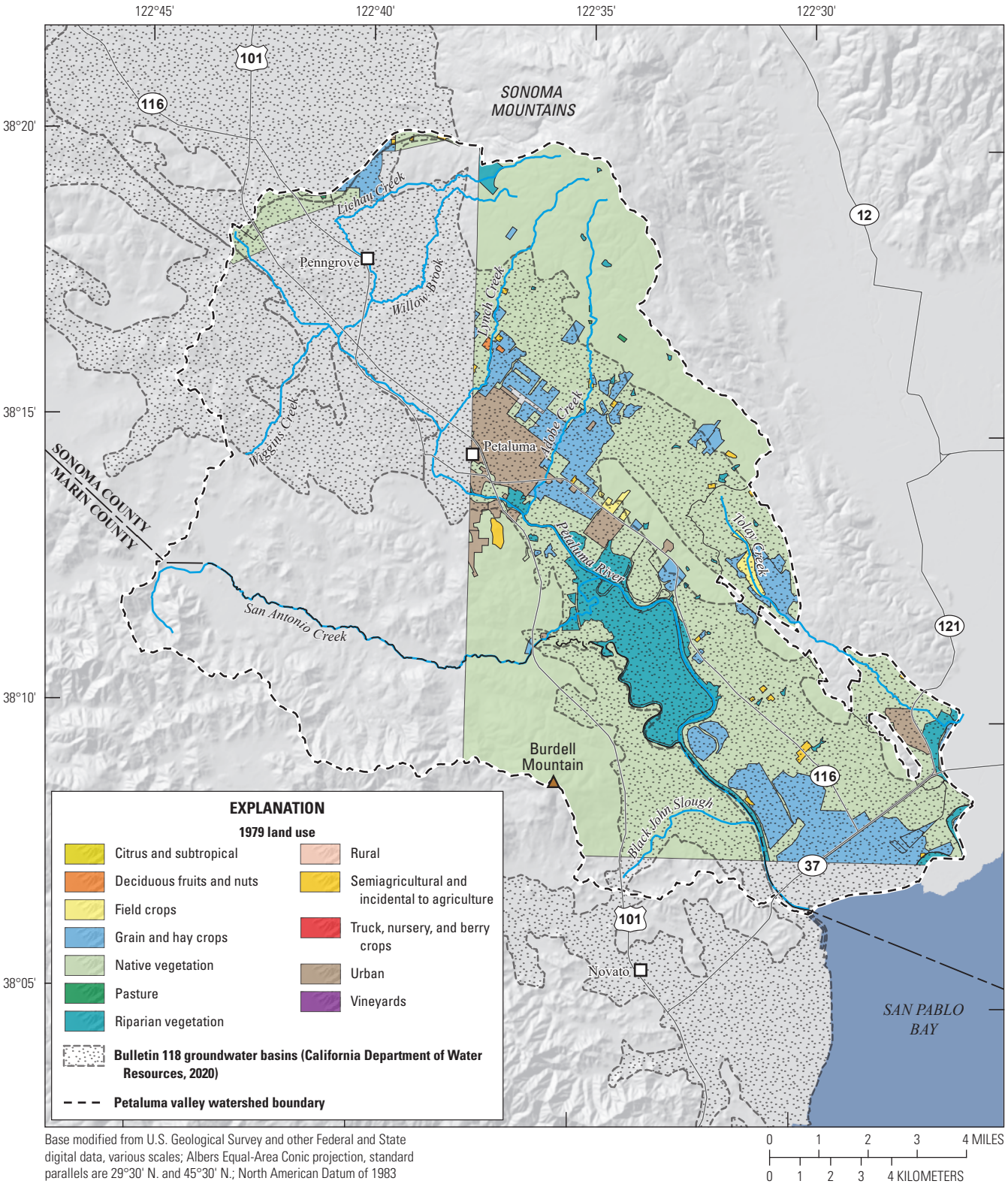

Figure A7. The 1979 distribution of land use, Petaluma valley watershed, Sonoma County, California (California Department of Water Resources, 1979; Seymour and Traum, 2021).

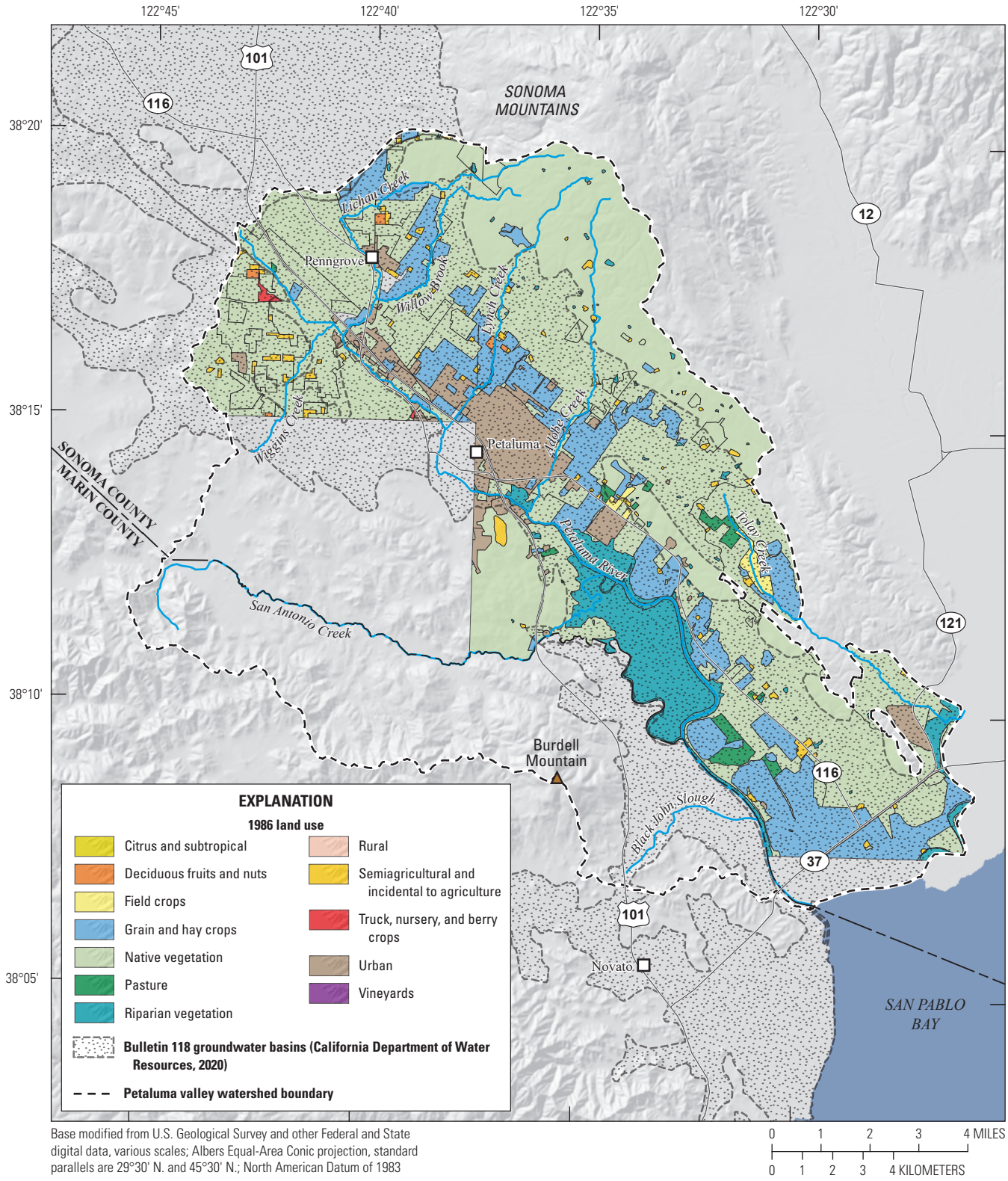

Figure A8. The 1986 distribution of land use, Petaluma valley watershed, Sonoma County, California (California Department of Water Resources, 1986; Seymour and Traum, 2021).

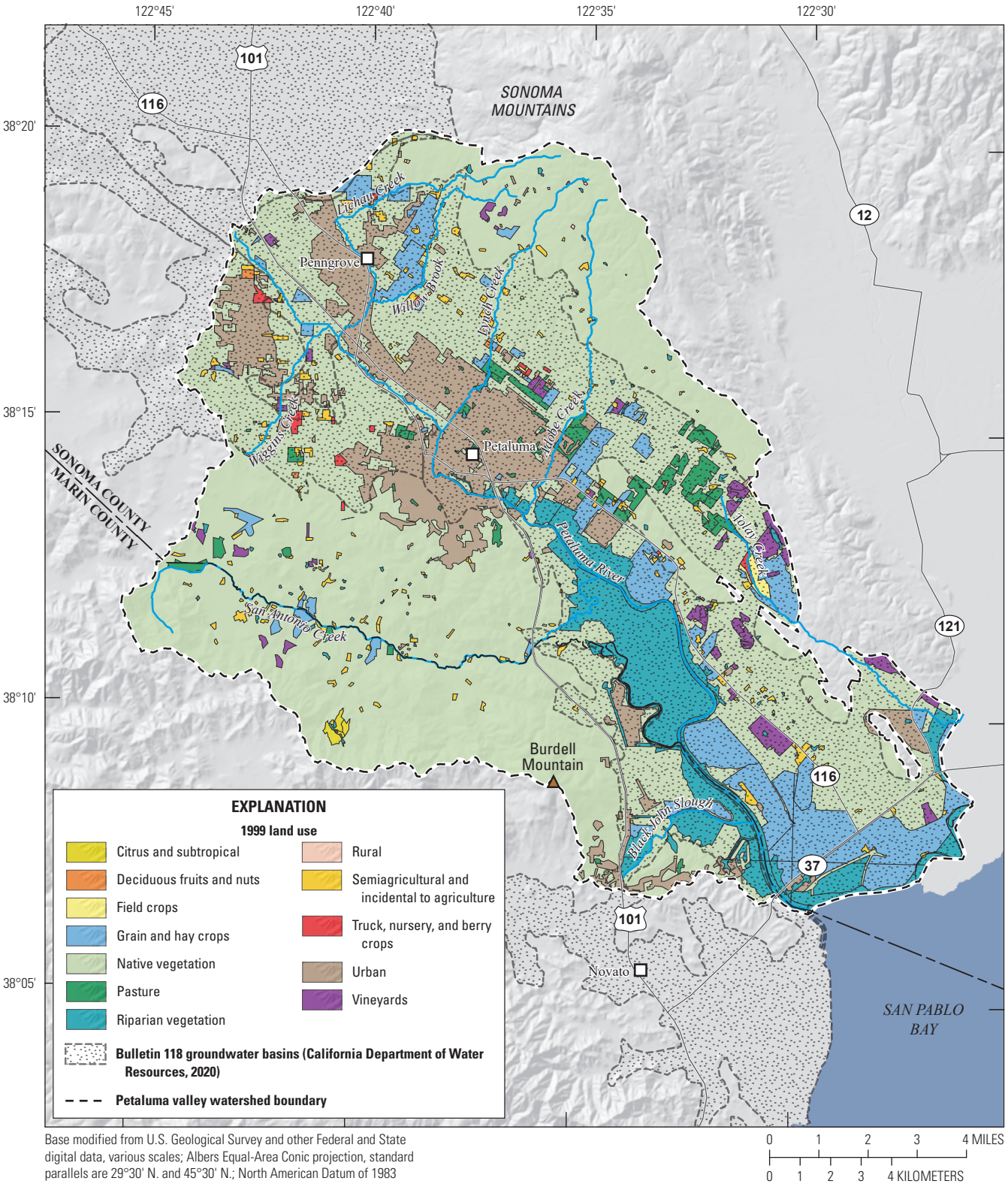

Figure A9. The 1999 distribution of land use, Petaluma valley watershed, Sonoma County, California (California Department of Water Resources, 2016).

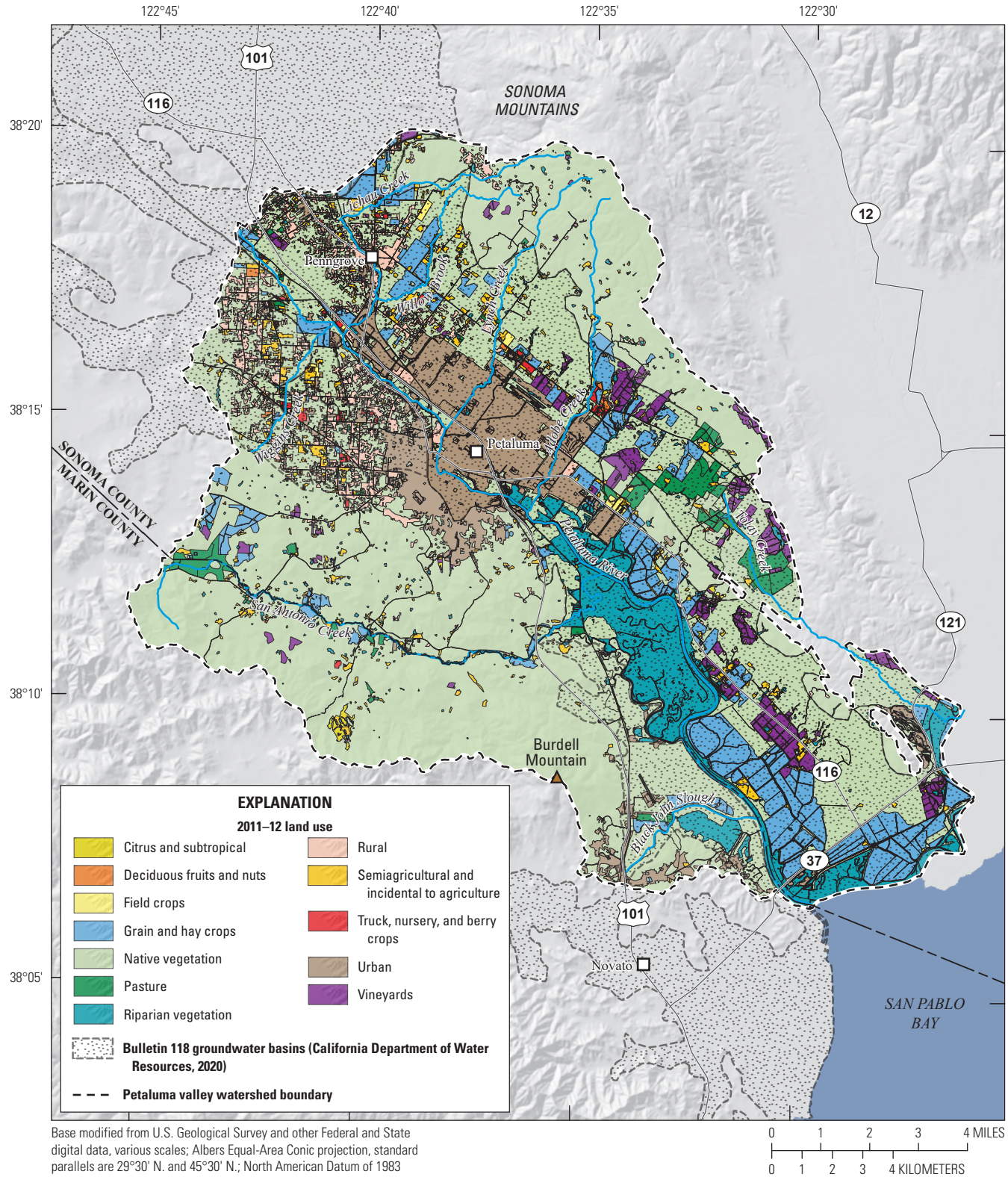

Figure A10. The 2011–12 distribution of land use, Petaluma valley watershed, Sonoma County, California (California Department of Water Resources, 2016).

Table A1. Land-use data for the Petaluma valley watershed for years 1979, 1986, 1999, and 2011–12, Petaluma valley watershed, California.

[—, no data available]

Land-use type	1979		1986		1999		2011–12	
	Area (acres)	Percent	Area (acres)	Percent	Area (acres)	Percent	Area (acres)	Percent
Citrus and subtropical	—	—	—	—	114	0.1	115	0.1
Deciduous fruits and nuts	28	0.1	90	0.1	60	0.1	128	0.1
Field crops	421	0.8	101	0.1	8	0.0	313	0.3
Grain and hay crops	5,657	10.8	9,296	13.7	7,316	7.7	13,729	12.0
Native vegetation	39,529	75.8	39,130	57.5	65,445	69.2	60,931	53.1
Pasture	16	0.0	448	0.7	956	1.0	1,604	1.4
Riparian vegetation	4,167	8.0	4,251	6.2	5,983	6.3	12,403	10.8
Semiagricultural and incidental to agriculture	231	0.4	720	1.1	1,626	1.7	3,290	2.9
Truck, nursery, and berry crops	—	—	62	0.1	206	0.2	411	0.4
Urban	2,064	4.0	3,979	5.8	11,912	12.6	18,428	16.0
Vineyards	—	—	2	0.0	908	1.0	3,481	3.0
Unknown	54	0.1	9,949	14.6	1	0.0	—	—
Total area	52,166	100.0	68,028	100.0	94,535	100.0	114,834	100.0

References Cited

Adams, F.D., 1913, Irrigation resources of California and their utilization: U.S. Department of Agriculture Office of Experiment Stations Bulletin, v. 254, 95 p.

Bay Area Census, 2021, City of Petaluma: Bay Area Census, accessed February 1, 2021, at http://www.bayareacensus.ca.gov/cities/Petaluma50.htm.

California Department of Water Resources, 1959, 1959 Sonoma County land use survey data: Unpublished data located at Division of Integrated Regional Water Management, North-Central Region, West Sacramento, California, 1:24,000 scale.

California Department of Water Resources, 1979, 1979 Sonoma County land use survey data: Unpublished data located at Division of Integrated Regional Water Management, North-Central Region, West Sacramento, California, 1:24,000 scale.

California Department of Water Resources, 1986, 1986 Sonoma County land use survey data: Unpublished data located at Division of Integrated Regional Water Management, North-Central Region, West Sacramento, California, 1:24,000 scale.

California Department of Water Resources, 2015, Drought in California, accessed July 15, 2016, at https://water.ca.gov/-/media/DWR-Website/Web-Pages/Water-Basics/Drought/Files/Publications-And-Reports/DroughtBrochure2021update_ay11.pdf.

California Department of Water Resources, 2016, California Land and Water Use - Land Use Surveys, accessed July 18, 2016, at https://water.ca.gov/programs/water-use-and-efficiency/land-and-water-use/land-use-surveys.

California Department of Water Resources, 2018, Sustainable Groundwater Management Act (SGMA): California Department of Water Resources, accessed July 20, 2018, at https://water.ca.gov/sgma.

California Department of Water Resources, 2020, Bulletin 118-Groundwater basins: California Department of Water Resources, accessed November 4, 2020, at https://gis.water.ca.gov/arcgis/rest/services/Geoscientific/i08_B118_CA_GroundwaterBasins/FeatureServer/0.

California Interagency Watershed Mapping Committee, 2004, California Interagency Watershed Map of 1999 (updated May 2004), Calwater 2.2.1: Sacramento, Calif., State of California, California Resources Agency, accessed August 28, 2017, at https://www.calfish.org/programsdata/referencelayershydrography/californiainteragencywatershedmapof1999.aspx.

Cardwell, G.T., 1958, Geology and ground water in the Santa Rosa and Petaluma valley areas, Sonoma County, California: U.S. Geological Survey Water-Supply Paper 1427, 273 p. [Available at https://doi.org/10.3133/wsp1427.]

City of Petaluma, 2016, 2015 Urban Water Management Plan, accessed February 16, 2017, at https://storage.googleapis.com/proudcity/petalumaca/uploads/2020/02/FINAL-2015-UWMP-1.pdf.

Dettinger, M.D., Ralph, F.M., Das, T., Neiman, P.J., and Cayan, D.R., 2011, Atmospheric rivers, floods and the water resources of California: Water (Basel), v. 3, no. 2, p. 445–478. [Available at https://doi.org/10.3390/w3020445.]

Gesch, D., Evans, G., Mauck, J., Hutchinson, J., and Carswell, W.J., Jr., 2009, The National Map—Elevation: U.S. Geological Survey Fact Sheet 2009–3053, 4 p. [Available at https://pubs.usgs.gov/fs/2009/3053/pdf/fs2009_3053.pdf.]

Herbst, C.M., 1982, Evaluation of ground water resources, Sonoma County, volume 3: Petaluma valley, California Department of Water Resources, Bulletin 118-4, 94 p.

Kulongoski, J.T., Belitz, K., Landon, M.K., and Farrar, C.D., 2010, Status and understanding of groundwater quality in the North San Francisco Bay groundwater basins, 2004—California GAMA Priority Basin Project: U.S. Geological Survey Scientific Investigations Report 2010–5089, 88 p. [Available at https://pubs.usgs.gov/sir/2010/5089/.]

PRISM Climate Group, 2016, Data Explorer: Time Series Values for Individual Locations, accessed July 19, 2016, at https://prism.oregonstate.edu/.

Seymour, W.A., and Traum, J.A., 2021, Petaluma Model GIS Data: U.S. Geological Survey data release. [Available at https://doi.org/10.5066/P9IQDHIT.]

Sonoma County, 2006, Sonoma County general plan 2020—Draft Environmental Impact Report, Sonoma County Permit and Resource Management Department, January 2006, accessed July 18, 2016, at https://sonomacounty.ca.gov/PRMD/Planning/Significant-EIRs/#GP2020.

Sonoma County, 2018, Sonoma County vegetation mapping and lidar program, accessed August 17, 2018, at http://sonomavegmap.org/data-downloads/.

Sonoma Resource Conservation District, 2015, Draft Petaluma Watershed Enhancement Plan, accessed July 19, 2016, at https://sonomarcd.org/wp-content/uploads/2017/06/Petaluma-Watershed-Enhancement-Plan-2015.pdf.

U.S. Census Bureau, 2017, State and County QuickFacts—Population estimates, July 1, 2016, for Petaluma, California: U.S. Census Bureau database, accessed August 28, 2017, at https://www.census.gov/quickfacts/fact/table/petalumacitycalifornia/HSG030210.

U.S. Department of Agriculture, Natural Resource Conservation Service, 2005, Soil Survey Geographic (*SSURGO*) Database and State Soil Geographic (STATSGO2) Database, accessed October 2, 2016, at https://websoilsurvey.sc.egov.usda.gov/App/HomePage.htm.

Western Regional Climate Center, 2016, Cooperative Climatological Data Summaries—NOAA Cooperative Stations—Temperature and Precipitation: Western Regional Climate Center database, accessed July 18, 2016, at http://wrcc.dri.edu/cgi-bin/cliMAIN.pl?ca6826.

Chapter B. Hydrogeology of the Petaluma Valley Watershed, Sonoma County, California

By Donald S. Sweetkind and Nick F. Teague

Introduction

The Petaluma valley watershed (PVW) is geologically and hydrologically complex, with multiple geologic units and cross-cutting structures affecting a variety of surface-water and groundwater processes (fig. B1). The U.S. Geological Survey (USGS), in cooperation with the Sonoma County Water Agency (SCWA) and the City of Petaluma, described and analyzed the geology, surface-water hydrology, and groundwater hydrology of the PVW for the purpose of evaluating regional groundwater availability. Aspects of the PVW described in this chapter include the delineation of hydrogeologic units based on lithology and hydraulic properties, construction of a detailed three-dimensional geologic framework, description of the surface-water and groundwater systems, and an analysis of predevelopment and modern-day groundwater recharge and discharge.

Geology

The PVW includes Petaluma valley, a relatively narrow alluvial valley that opens southeastward to San Pablo Bay (fig. B1). The valley-filling sediments and surrounding consolidated rocks are offset and folded by several predominantly strike-slip faults, including the Rodgers Creek and Burdell Mountain faults, (fig. B1). Previous groundwater-resource investigations of the PVW (Cardwell, 1958; Ford, 1975; Herbst, 1982) defined the geology of the groundwater-flow system. Recent geologic mapping and stratigraphic studies have refined the understanding of the age and stratigraphic relations of the basin-filling rocks and deposits (Allen, 2003; Davies, 1986; Powell and others, 2004; Graymer and others, 2007; Wagner and Gutierrez, 2010; Wagner and others, 2011), and new tectonic interpretations and geophysical data have refined the understanding of the locations and influence of faults that cut the basin (Graymer and others, 2002; Langenheim and others, 2010; Watt and others, 2016). Data from these studies were integrated with digital geologic map, borehole, and geophysical data to create a three-dimensional (3D) geologic framework model (GFM) of the PVW that defines the subsurface stratigraphic and structural architecture of the study area.

Consolidated rocks and unconsolidated deposits of the PVW display a great deal of stratigraphic complexity (fig. B2), which has resulted from the changing depositional environments through time, the presence of local volcanic eruptive centers, and the evolution of structures along the California continental margin (Nilsen and Clarke, 1989; McLaughlin and others, 1996; Wagner and others, 2011). To create a stacked sequence of stratigraphic units amenable to 3D geologic framework modeling, the stratigraphy of the PVW was generalized to the following geologic units, from oldest to youngest: (1) Franciscan Complex, (2) Tolay Volcanics, (3) Sonoma Volcanics, (4) Petaluma Formation, (5) Wilson Grove Formation, (6) Quaternary mixed unit, (7) bay mud deposits, and (8) Quaternary alluvium.

Mesozoic basement rocks that surround (and are inferred to underlie) the PVW are shown on geologic maps of the area as rocks of the Franciscan Complex, overlain by, or tectonically imbricated with, rocks of the Great Valley Sequence (Wagner and Gutierrez, 2010; Wagner and others, 2011). These rocks are characterized by a variety of consolidated and deformed rock types, including shale, graywacke, mélange with blocks of chert and greenstone, and thinly interbedded shale and sandstone. The Franciscan Complex is widely exposed in the uplands south and west of the Petaluma River and are uplifted on the west side of the Tolay fault in the southeastern part of the PVW (fig. B1). Overlying the Franciscan Complex are local accumulations of Miocene, predominantly mafic volcanic rocks that, for the purposes of this report, are referred to as Tolay Volcanics (Fox and others, 1985; Wagner and others, 2011; figs. B1, B2). These rocks are exposed on Burdell Mountain (southwest of the City of Petaluma), on Meacham Hill (north of the City of Petaluma), and to the east of the Tolay fault (fig. B1). Tolay Volcanics are up to 650 feet (ft) thick on Burdell Mountain (Ford, 2007); only about 160 ft of volcanic rocks are exposed in outcrops to the west of the City of Petaluma.

Neogene sedimentary rocks in the PVW were deposited in fault-related basins that formed in response to the development of the San Andreas fault zone (Fox, 1983; Nilsen and Clarke, 1989). These sedimentary rocks are assigned to two formations: the fine-grained marine sandstone of the Wilson Grove Formation, exposed in the northwest part of the PVW, and the fluvial, estuarine, and lacustrine Petaluma Formation, exposed on the northeast and east side of the PVW along the east flank of Petaluma valley (figs. B1, B2). The Wilson Grove Formation consists of fine- to medium-grained, thick-bedded to massively bedded, moderate- to well-sorted, uncemented to weakly cemented, fossiliferous marine sandstone (Powell and others, 2004). Wilson Grove Formation is generally 650–950 ft thick based on outcrop exposures and well intercepts in the northwest part of the PVW but may be as thick as 3,000 ft to the northwest of the PVW (Powell and others, 2004).

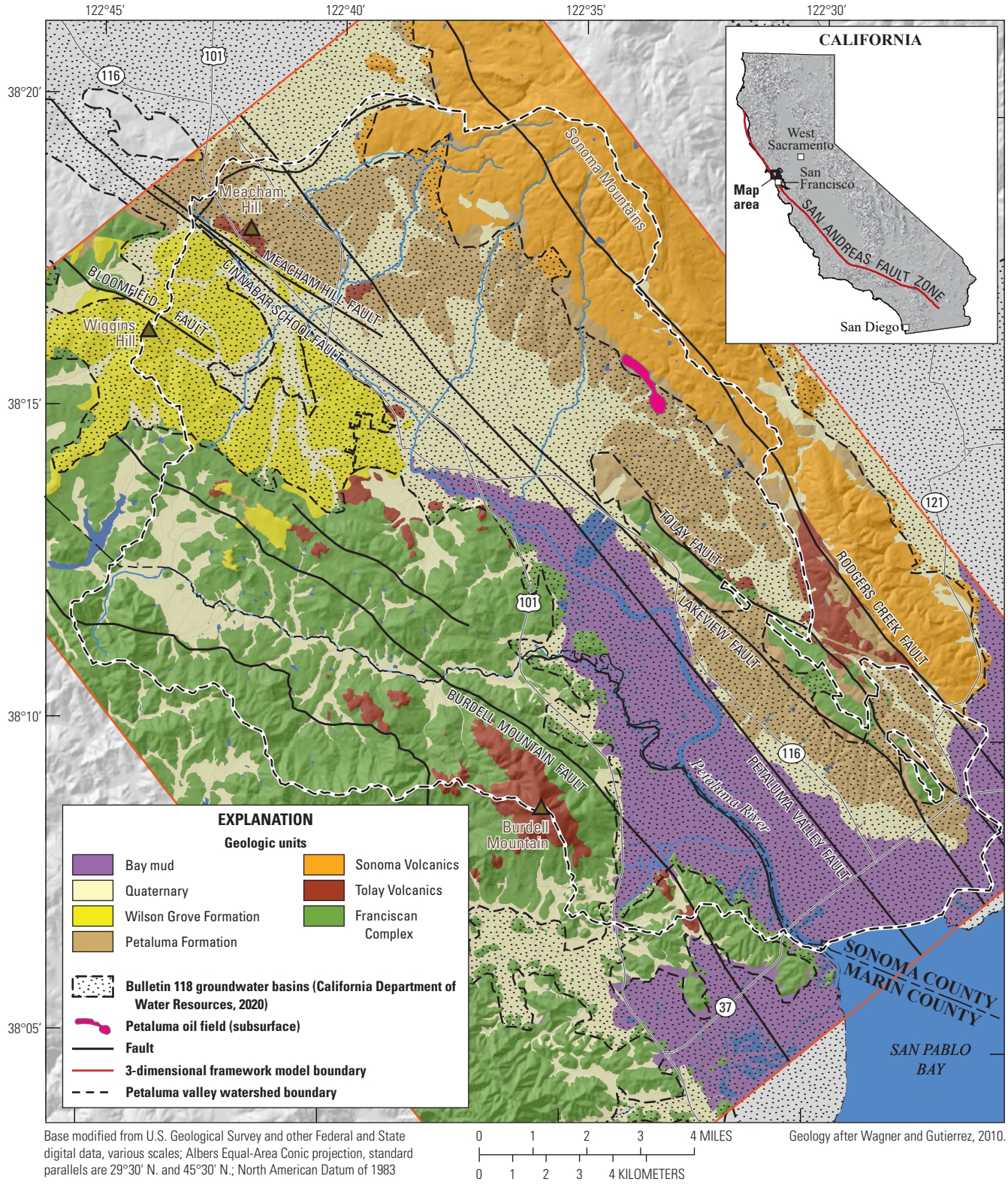

Figure B1. Generalized geologic map of the Petaluma valley watershed, Sonoma County, California.

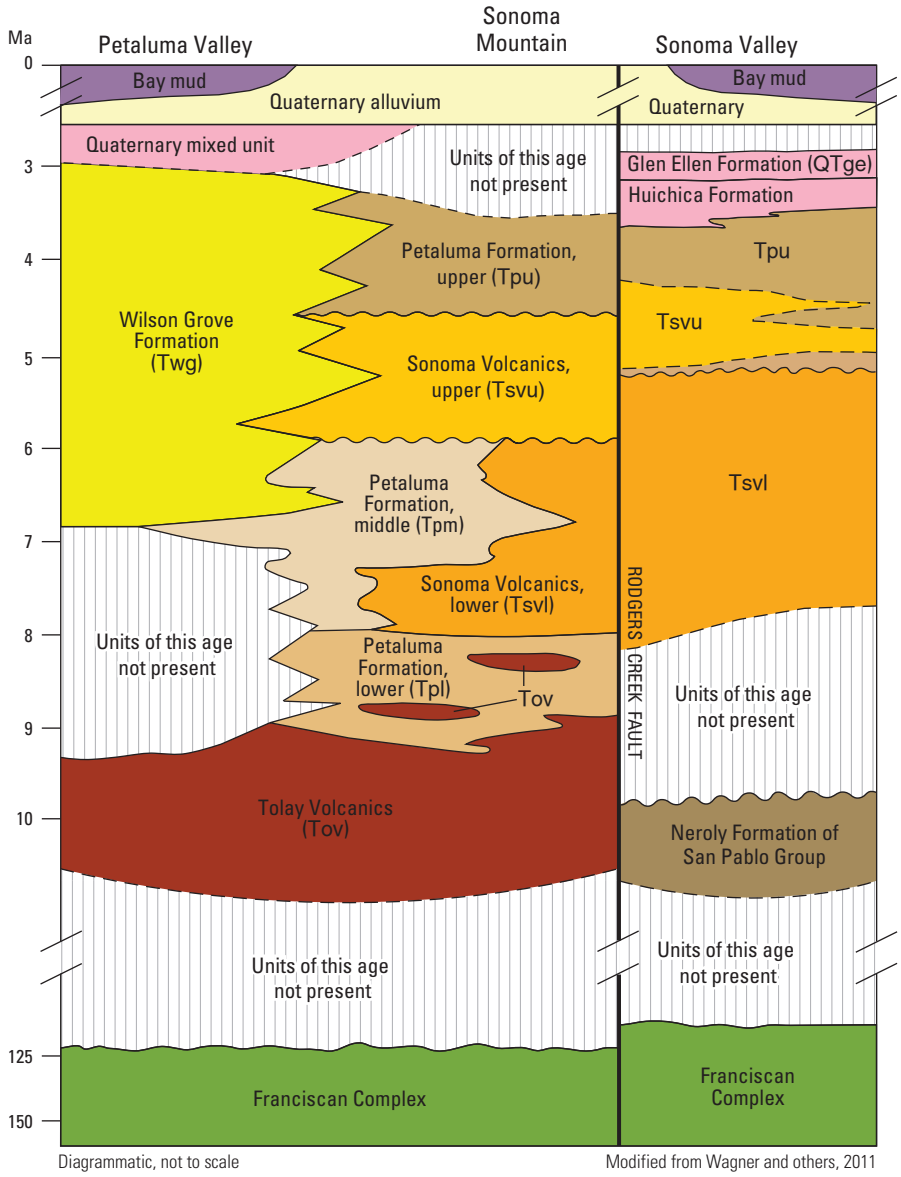

Figure B2. Generalized stratigraphic column of the Petaluma valley watershed, Sonoma County, California.

The late Miocene to Pliocene Petaluma Formation is dominated by deposits of moderately to weakly consolidated, silty to clayey mudstone with local beds and lenses of poorly sorted sandstone and minor beds of nodular limestone and conglomerate (Davies, 1986; Allen, 2003; Sweetkind and others, 2010). Regionally, the Petaluma Formation has been subdivided into lower, middle, and upper members based on detailed stratigraphic analysis using the coarser grained materials and fossils (fig. B2; Allen, 2003; Wagner and others, 2011), but the Petaluma Formation is treated as a single unit in the GFM. The formation is at least 4,200-ft thick in the Petaluma oil field, near the eastern edge of the PVW (fig. B1; Wright, 1992).

Neogene volcanic rocks of the Sonoma Volcanics are exposed on both sides of the Rodgers Creek fault on the east side of the PVW (fig. B1). The Sonoma Volcanics include a thick accumulation of andesitic and basaltic tuffs containing interbedded lavas and volcaniclastic rocks (Wagner and others, 2011). These volcanic rocks interfinger with the Petaluma Formation in the PVW (fig. B2; Wagner and Gutierrez, 2010; Wagner and others, 2011). The total thickness of Sonoma Volcanics ranges up to at least a few thousand feet; however, volcanic-rock thickness is highly variable.

Quaternary alluvium unconformably overlies the Wilson Grove and Petaluma Formations (figs. B1, B2; Wagner and Gutierrez, 2010); these deposits include alluvial fan deposits that blanket the northeastern part of Petaluma valley and channel alluvial deposits along the Petaluma River and smaller drainages in the Petaluma valley. Quaternary alluvium consists of poorly sorted coarse sand and gravel interbedded with moderately sorted fine sand, silt, and silty clay. A lithologically heterogeneous unit of alternating thin beds of conglomerate, sand, and mudstone was identified beneath the Quaternary alluvium on the basis of well lithologic data; this unit is not mapped at the surface and is lithologically unlike the Wilson Grove and Petaluma Formations (figs. B2, B3). This unit may be broadly correlative with the Pliocene–Pleistocene terrestrial deposits mapped as Huichica Formation and Glen Ellen Formation that are exposed in nearby basins (fig. B2; Weaver, 1949; Fox, 1983; Wagner and Gutierrez, 2010; Wagner and others, 2011). This unit is referred to as the Quaternary mixed unit in this report (figs. B2, B3).

Holocene bay mud deposits cover the southeastern part of the PVW, flanking the trace of the Petaluma River to San Pablo Bay (fig. B1). The muds consist of mud, silty mud, and silt (Goldman, 1969; McDonald and others, 1978).

The study area is transected by several large-offset, northwest-trending, right-lateral strike-slip faults that are part of the San Andreas fault zone, including the Rodgers Creek, the Burdell Mountain, and the Petaluma valley faults (fig. B1; McLaughlin and others, 1996; Graymer and others, 2002; Wagner and Gutierrez, 2010; Wagner and others, 2011; Watt and others, 2016). Bends in the fault trace result in local basin opening or local compression and uplift, such that adjacent to faults large variations in stratigraphic thickness are possible. The Rodgers Creek and Burdell Mountain faults are mapped at the surface as wide, steeply dipping zones with multiple fault strands, rather than single fault planes (Randolph-Loar, 2002; Ford, 2007). Although buried beneath the alluvium of Petaluma valley and not observable at the surface, the Petaluma valley fault was proposed by Graymer and others (2002) through interpretation of offset parts of basalts dated at 10–9.2 millions of years (Ma) and tuff dated at 6 Ma exposed on opposite sides of the fault. Analysis of well-lithologic data for this study confirms the presence of a northwest-trending fault beneath the valley axis, based on observed sharp truncations of rocks interpreted as Wilson Grove and Petaluma Formations.

The Meacham Hill and Tolay faults are steeply dipping, northeast- or southwest-vergent reverse thrusts that bound structurally uplifted older rocks (fig. B1). Cardwell (1958) connected these two faults as a single Tolay fault trace, which was interpreted to be the major through-going fault in the basin. These faults, however, have no obvious dextral displacement required by offset geologic features (Graymer and others, 2002) and have more recently been interpreted as localized compressional features associated with left-lateral strike-slip offset along Rodgers Creek fault, rather than a single connected fault (Wagner and others, 2011). In the northwest part of the PVW are several northwest-trending reverse faults of relatively small displacement, including the Bloomfield fault (Hitchcock and Kelson, 1998; Wagner and Gutierrez, 2010) and the Cinnabar School fault (Herbst, 1982).

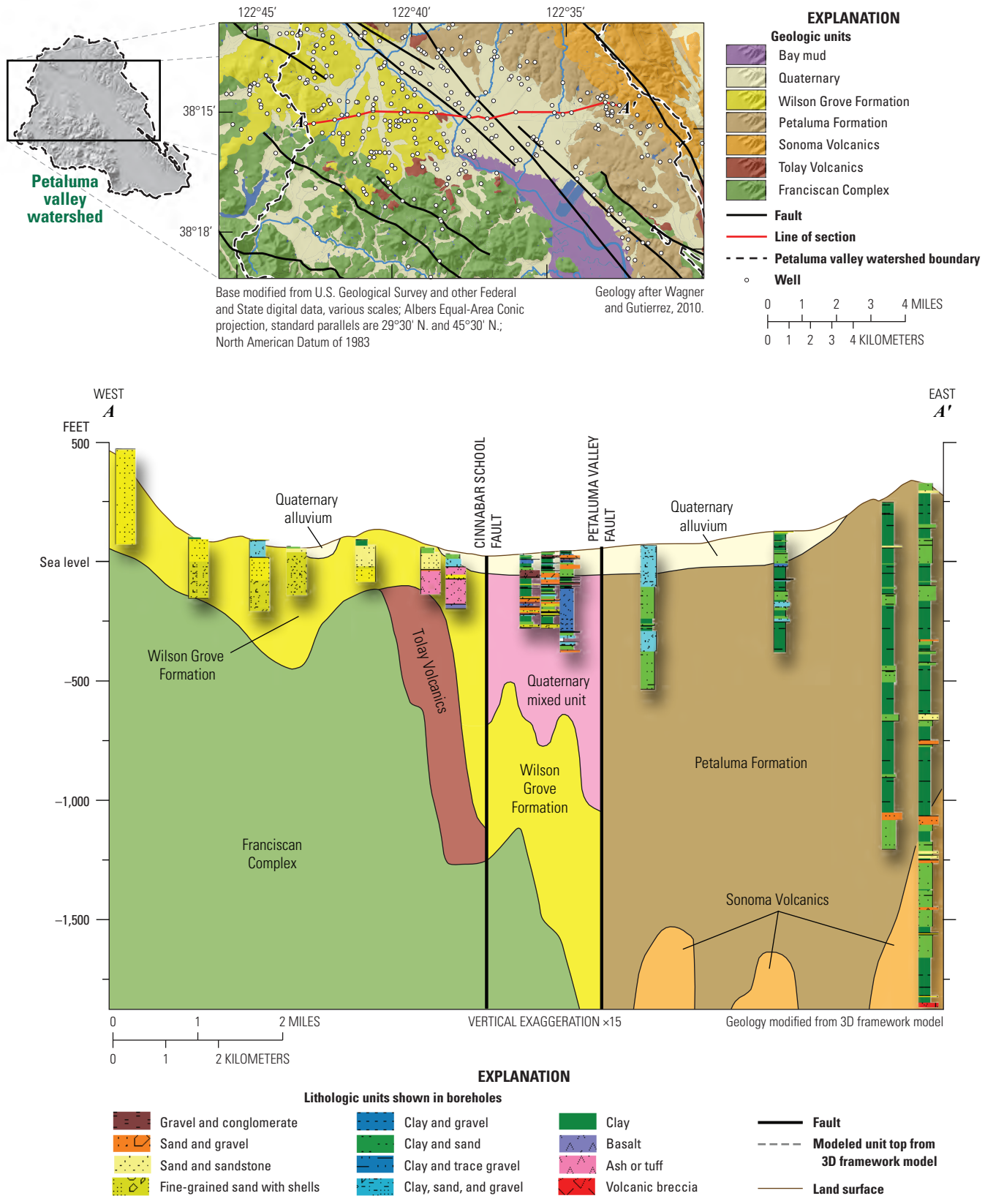

Figure B3. Borehole lithologic logs and interpreted subsurface stratigraphy, Petaluma valley watershed, Sonoma County, California.

Three-Dimensional Geologic Framework Model

A 3D geologic framework model (GFM) was constructed to represent the subsurface geometry of top of Franciscan Complex and seven basin-filling stratigraphic units, from deepest to shallowest: Tolay Volcanics, Sonoma Volcanics, Petaluma Formation, Wilson Grove Formation, Quaternary mixed unit, bay mud deposits, and Quaternary alluvium. Although some of these units are lithologically variable and some units interfinger with each other (fig. B2), in general, the mapped formations described here are sufficiently distinct from each other that they were selected as the model units for the GFM. The framework model was built by integrating digital information from well data, surface-geologic maps, and geophysical data to construct subsurface maps of each stratigraphic unit in the PVW, which were then stacked in 3D space. The framework model defines the location of structures within the basin and the extent, altitude, and thickness of each stratigraphic unit. This digital model provides the geologic framework for the subsequent development of the finite difference, integrated hydrologic model of the PVW.

Geologic and Geophysical Data for Framework Modeling

Construction of the 3D GFM used surface and subsurface data from multiple sources to define the top surface and extent of each stratigraphic unit. Data sources include topographic data, geologic maps, stratigraphic tops interpreted from water- and oil-well data, and geophysical data. The various geologic datasets were compiled in a geographic information system (GIS) as the initial step in the construction of the 3D GFM. Surface geology was extracted from a digital geologic map of the south half Napa 30×60′ quadrangle (Wagner and Gutierrez, 2010). Fault-surface traces were generalized from published geologic maps (Blake and others, 2000; Graymer and others, 2007; Wagner and Gutierrez, 2010) and modified based on geophysical (Langenheim and others, 2010) and well data. Cardwell (1958) interpreted the Tolay fault to bisect the basin; however, the more recent interpretation of Graymer and others (2002), where the Petaluma valley fault is the major through-going fault in the basin (fig. B1), is used in the 3D GFM. For numerical simplicity in the geologic framework model, all faults were assumed to be vertical features.

Well data were compiled from a variety of sources, including U.S. Geological Survey (USGS) reports (Cardwell, 1958; Sweetkind and Taylor, 2010), oil and gas exploration holes (Brabb and others, 2001; California Department of Conservation, Division of Oil, Gas, and Geothermal Resources, 2014), data provided by local water agencies, and water wells drilled by independent entities and compiled by the California Department of Water Resources (CDWR; fig. B4). Lithologic descriptions from drillers were standardized to a limited number of lithologic classes through interpretation of lithology, grain size, and bedding characteristics and comparisons with observations of the stratigraphic units in outcrop following the methodology described by Sweetkind and others (2010).

The surface inferred to represent the altitude of the top of Franciscan Complex is extracted from the top of the geophysically modeled high-density basement rocks as derived from inversion of regional gravity measurements (Langenheim and others, 2010). Altitudes in the originally modeled surface were locally modified using well data not used in the original gravity analysis, revising the altitude of the Franciscan Complex to honor well intercepts and forcing the altitude of the Franciscan Complex to be deeper than the drilled depth of wells that did not report the Franciscan Complex. Abrupt changes in altitude of the Franciscan Complex surface were used to infer the location of basin-bounding or intrabasinal faults. Aeromagnetic data were extracted from a regional aeromagnetic dataset (Langenheim and others, 2010). Aeromagnetic anomalies reflect magnetic variation in Franciscan Complex rocks and Neogene volcanic rocks, either exposed or in the subsurface (Langenheim and others, 2010). Anomaly patterns were used to help locate faults in the basin and define the extent of the Sonoma Volcanics.

Interpretation of Stratigraphy from Well Data

Driller descriptions were simplified to a small number of internally consistent lithologic classes for the available 685 driller lithologic logs. The locations of the 685 wells with driller logs are shown in figure B4. Each of the stratigraphic units are generally lithologically distinct, and when numerous driller lithologic logs were viewed and interpreted together, the principal stratigraphic units were mappable in the subsurface (fig. B3). Mappable lithologic sequences were identified in well data by analyzing numerous serial geologic sections across the PVW and making stratigraphic interpretations based on rock type, bedding and sorting characteristics, stratigraphic succession, and an understanding of the relation between the mapped geologic units and their lithologic characteristics (fig. B3; Sweetkind and others, 2010). Stratigraphic tops were picked interactively by viewing lithologic logs from 10 to 20 wells in a profile. Contacts were picked in an iterative fashion from numerous geologic sections of varying orientations, with combinations of wells examined to eliminate spurious picks and to maximize the consistency of the stratigraphic interpretation. Subsurface interpretation began with those wells located directly on outcrops of a specific stratigraphic unit or using wells with the most detailed lithologic descriptions to condition the rest of the dataset.

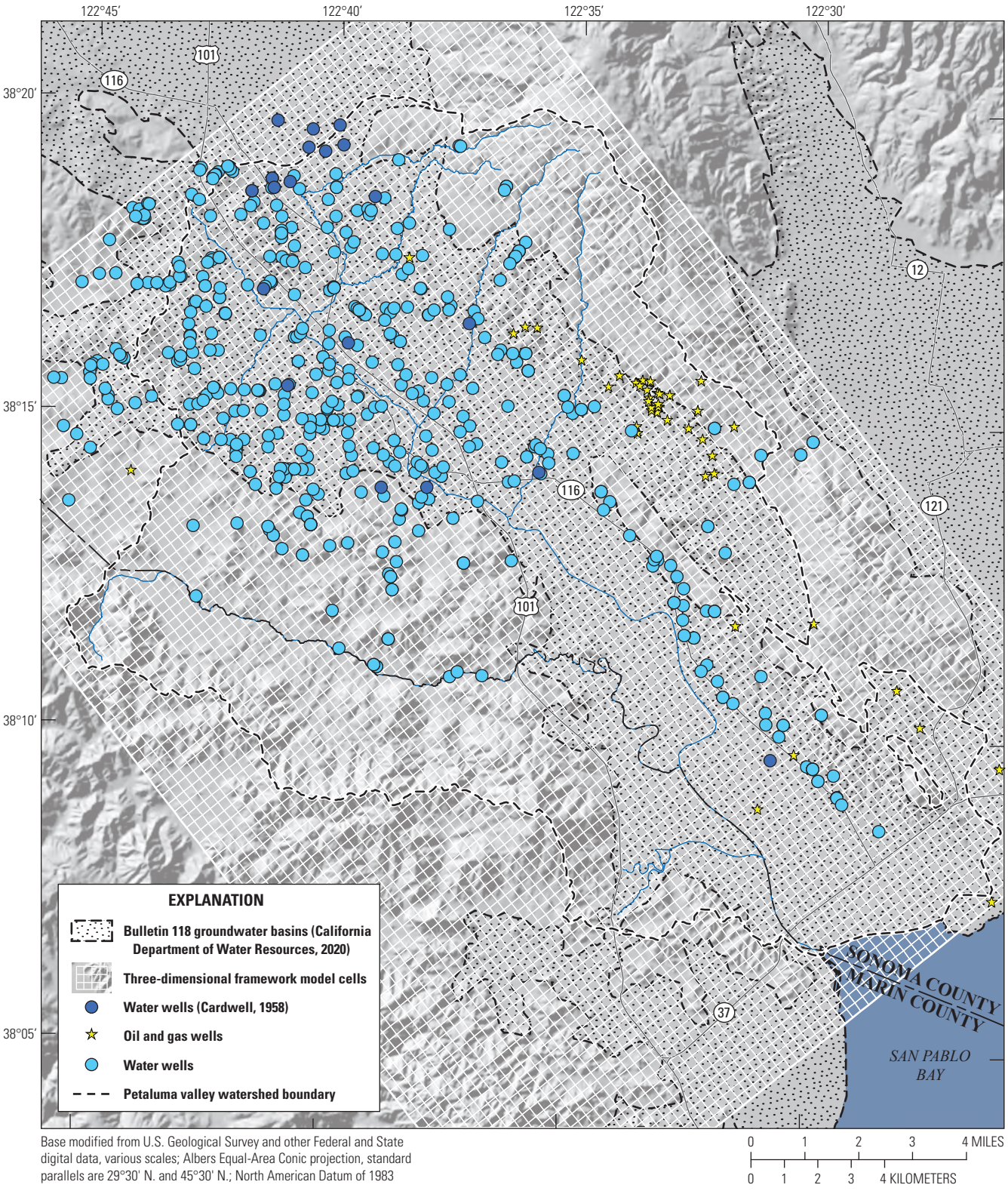

Figure B4. Distribution of wells used in geologic interpretation and the three-dimensional geologic framework model grid of the study area (Sweetkind, 2019), Petaluma valley watershed, Sonoma County, California.

Construction of Gridded Surfaces

Construction of the 3D GFM began with the creation of gridded surfaces representing the altitudes of the top of each stratigraphic unit. Surfaces representing the altitudes of the top of each stratigraphic unit were created through interpolation of data points into grids using two-dimensional horizon-gridding software. The 3D GFM is created using a modified geocellular modeling approach, where x, y, and z coordinates for the top of each geologic unit are stored in a regular array of grid cells (fig. B4; Shepherd, 2009). Gridded horizons representing the stratigraphic top of each unit were mapped to an x-y array of nodes representing the centroids of cells in the finite difference hydrologic model. The rectangular array of nodes was rotated to the northwest and represents a uniform grid with a cell spacing of 980 ft to match the numerical model (fig. B4). Resultant dimensions of the array used in the 3D GFM were 75,800 ft (77 grid cells) in the northeast-southwest direction and 106,300 ft (108 cells) in the northwest–southeast direction.

Geologic map data for input to the 3D GFM were created from the digital geologic map of the south half Napa 30×60′ quadrangle (Wagner and Gutierrez, 2010). Areas where a stratigraphic unit cropped out at land surface were defined by querying the digital geologic map in a GIS. Grid nodes within each map polygon were assigned *z* values equal to land surface from a 10-meter (m) DEM.

Interpreted subsurface stratigraphic contacts at each borehole were assigned x, y, and z coordinate locations for use in the geologic framework model. All boreholes were assumed to be vertical, so that all contacts from a well were assigned the x, y coordinates of the well's surface location. Stratigraphic unit contacts, originally compiled as depth below land surface from the source data, were converted to altitude values by subtracting measured depth from the land-surface altitude at the well using 10-m DEM data. A series of files were exported that contained x, y, and z coordinates for the top of each geologic unit.

The upper surfaces of all geologic units were gridded using Rockware Rockworks17® 3D-modeling software. Input data points were interpolated using the ordinary kriging algorithm in Rockworks17®. This geostatistical interpolation method is a distance-weighted estimation algorithm that characterizes the variability between individual data points across a study area and fits a surface to the observed spatial-correlation structure (Isaaks and Srivastava 1989; Journel and Huijbregts, 1978). Kriging was done with Rockworks17® using automatic settings, allowing the program to determine the variability versus distance variogram type, based on the highest spatial correlation in the data.

Surfaces for the Quaternary alluvium and bay muds were created assuming no influence from faulting. For all other units, faults served as two-dimensional boundaries that delineated the areal extent during gridding. The upper surfaces of the Quaternary mixed unit, the Wilson Grove and Petaluma Formations, Tolay Volcanics, and the Franciscan Complex were gridded using surface and subsurface geologic data. Gridding of the bay muds and Sonoma Volcanics required additional data, as discussed next.

Thicknesses of bay mud deposits are uncertain because a very small number of wells are drilled into, or fully penetrate, this unit. Contours of mud thickness were hand-drawn based on published maps and interpretations to create a spatially distributed array of points for the 3D GFM, with the assumption that the muds fill preexisting topography of eroded stream valleys (Goldman, 1969; McDonald and others, 1978). Isopach contours were digitized in a GIS and converted to a series of regularly spaced points, which were assigned horizontal coordinate locations from the map base and altitudes from the contour altitude. A file was exported that contained x, y, and z coordinates for the thickness of the bay mud deposits.

The altitude of Sonoma Volcanics in the subsurface in the eastern part of the PVW is uncertain because relatively few water wells fully penetrate the entire thickness of the Petaluma Formation to intercept the interfingered but generally underlying Sonoma Volcanics at depth. A hand-drawn structure contour map of the top of the Sonoma Volcanics was created using data from a small number of deep wells (including 41 oil and gas wells primarily from the Petaluma oil field) and by forcing the contours to be deeper than the drilled depths of wells where volcanic rocks were not encountered. Structure contours were converted to a series of regularly spaced points, which were assigned coordinate locations and given the contoured altitude value. These points became part of the data for gridding the top of the Sonoma Volcanics.

Final gridded surfaces representing the tops of the stratigraphic units (fig. B5) were developed through an iterative process involving multiple cycles of grid creation, evaluation, and editing. Locally, specific grid nodes were hand-edited to remove gridding artifacts, to eliminate grid overextrapolation, and to explicitly honor fault locations. Grids were edited to force unit tops to be at or below land-surface altitude and to ensure that the altitude of the top of each stratigraphic unit was not higher than that of an overlying unit grid nor lower than the tops of underlying units. The final altitude of each geologic unit, and the thickness of bay mud, is shown in figure B5. Except for the Franciscan Complex, none of the units are continuous throughout the entire study area. Altitude maps are not colored where the geologic unit is absent.

Altitude of the Franciscan Complex is variable within the PVW (fig. B5*H*). Geophysical studies and well data indicate that the Franciscan Complex is shallowest in the west and southwest parts of the PVW, where the Franciscan Complex is as shallow as 100 ft beneath surface outcrops of the Wilson Grove Formation (Langenheim and others, 2010). Basin depth increases rapidly to the east and the northeast, where the Franciscan Complex altitude is, in places, deeper than 3,000 ft below the North American Vertical Datum of 1988 (NAVD 88; fig. B5*H*).

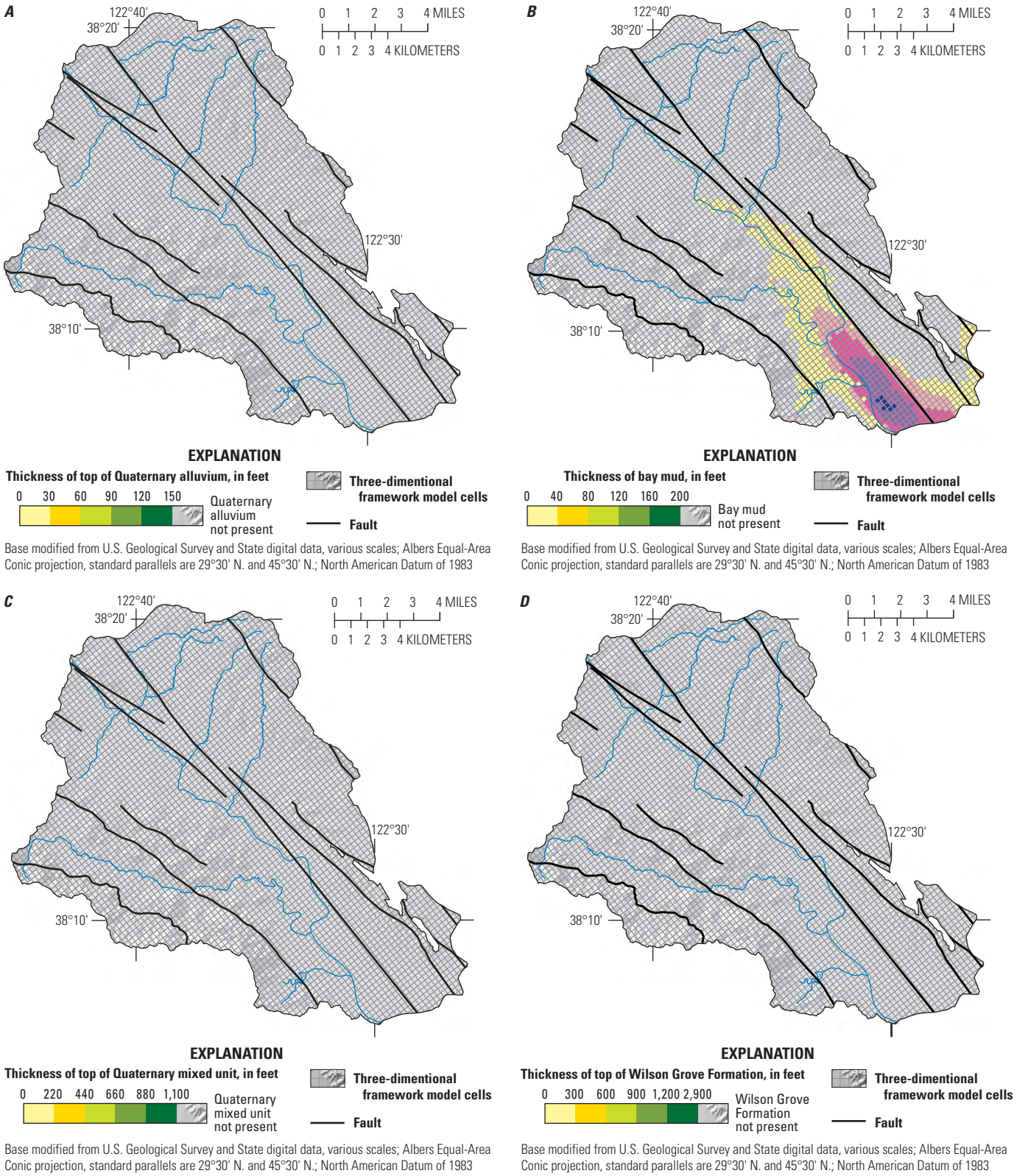

Figure B5. Final grids of thickness of geologic units used in three-dimensional (3D) geologic framework model, Petaluma valley watershed, Sonoma County, California: *A*, Quaternary alluvium; *B*, Bay mud; *C*, Quaternary mixed unit; *D*, Wilson Grove Formation; *E*, Petaluma Formation; *F*, Sonoma Volcanics; and *G*, Tolay Volcanics or altitude; *H*, Franciscan Complex.

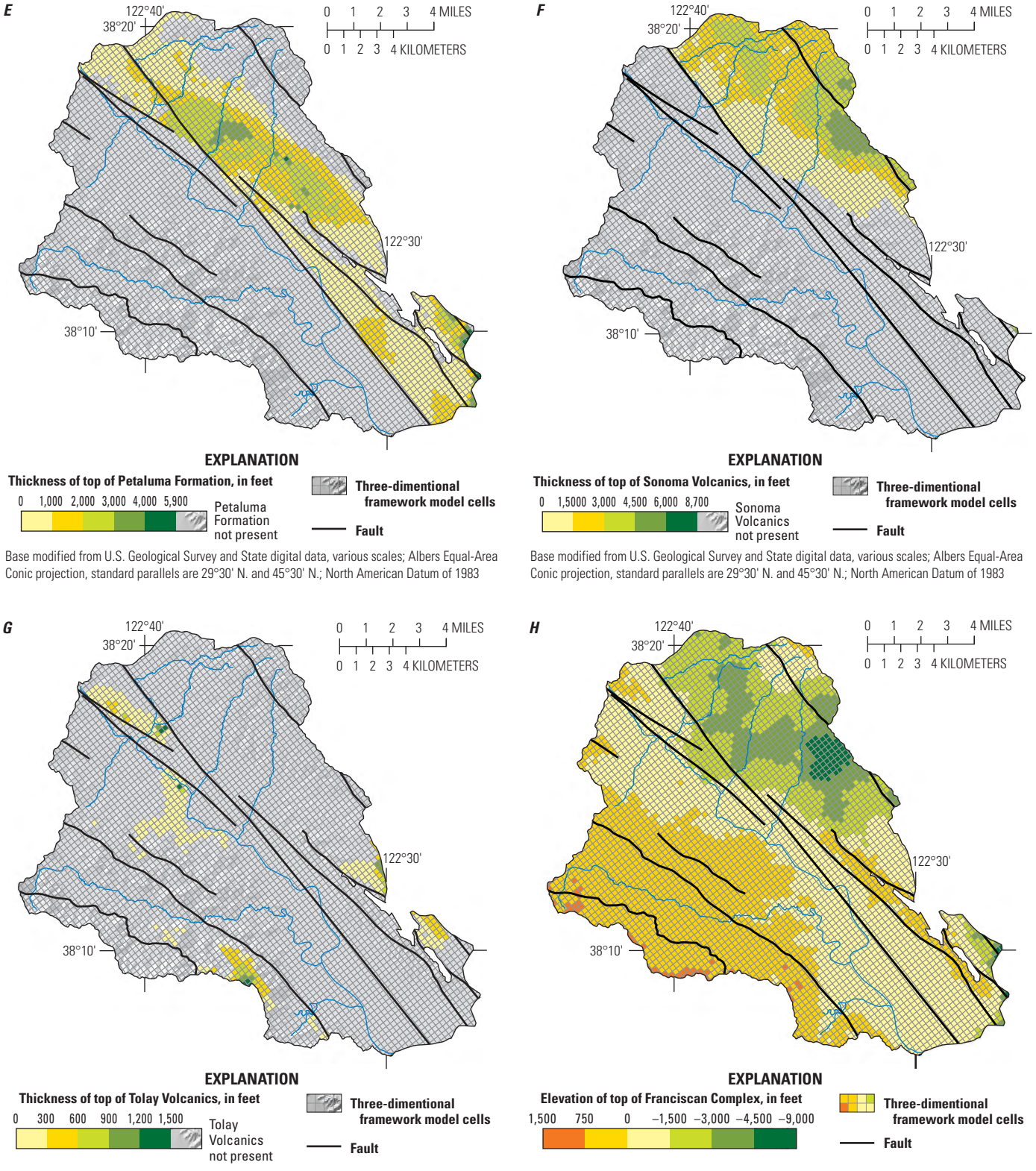

Figure B5.—Continued

Three-Dimensional Geologic Framework Model Results

The final 3D GFM was compiled from the gridded surfaces of geologic unit tops by stacking the individual surfaces in stratigraphic order using Rockware Rockworks17® 3D-modeling software (fig. B6). Unit thickness is represented by the difference between altitudes of successive stratigraphic tops, such that the altitude of the base of a unit is always equal to the altitude of the top of the unit directly below it in the stacking order.

A series of vertical sections show the stacked gridded surfaces as an interpolated stratigraphic fence diagram (fig. B6). In this perspective view, section panels showing the upper and lower surfaces of all stratigraphic units in the GFM are symbolized with colors representing the volume occupied by each geologic unit. Section panels extend down to –3,281 ft below NAVD 88; the top edge of each panel represents the topographic profile at land surface. For spatial reference, an index map is hung at an arbitrary altitude of –3,281 ft below NAVD 88, such that the sections appear to be extruded above the surface of the map (fig. B6).

In this perspective view, Franciscan Complex rocks dominate the subsurface on the southwest side of the basin, capped locally by Tolay Volcanics and a relatively uniform thickness of Wilson Grove Formation in the northwestern part of the PVW. Depth to Franciscan Complex and aggregate thickness of post-Mesozoic basin fill dramatically increase to the north and east, where the basin is filled by a thick sequence of Petaluma Formation and Sonoma Volcanics. In this view, looking to the northwest, the axis of topographic Petaluma valley extends from the center of the diagram to the upper center, and downfolded, locally thick accumulations of the Wilson Grove Formation and the Quaternary mixed unit are present in the subsurface. San Pablo Bay at the southeast end of the study area appears at the bottom front edge of the figure, where the Quaternary mixed unit and Petaluma Formation are capped by a relatively thin veneer of bay muds (fig. B6).

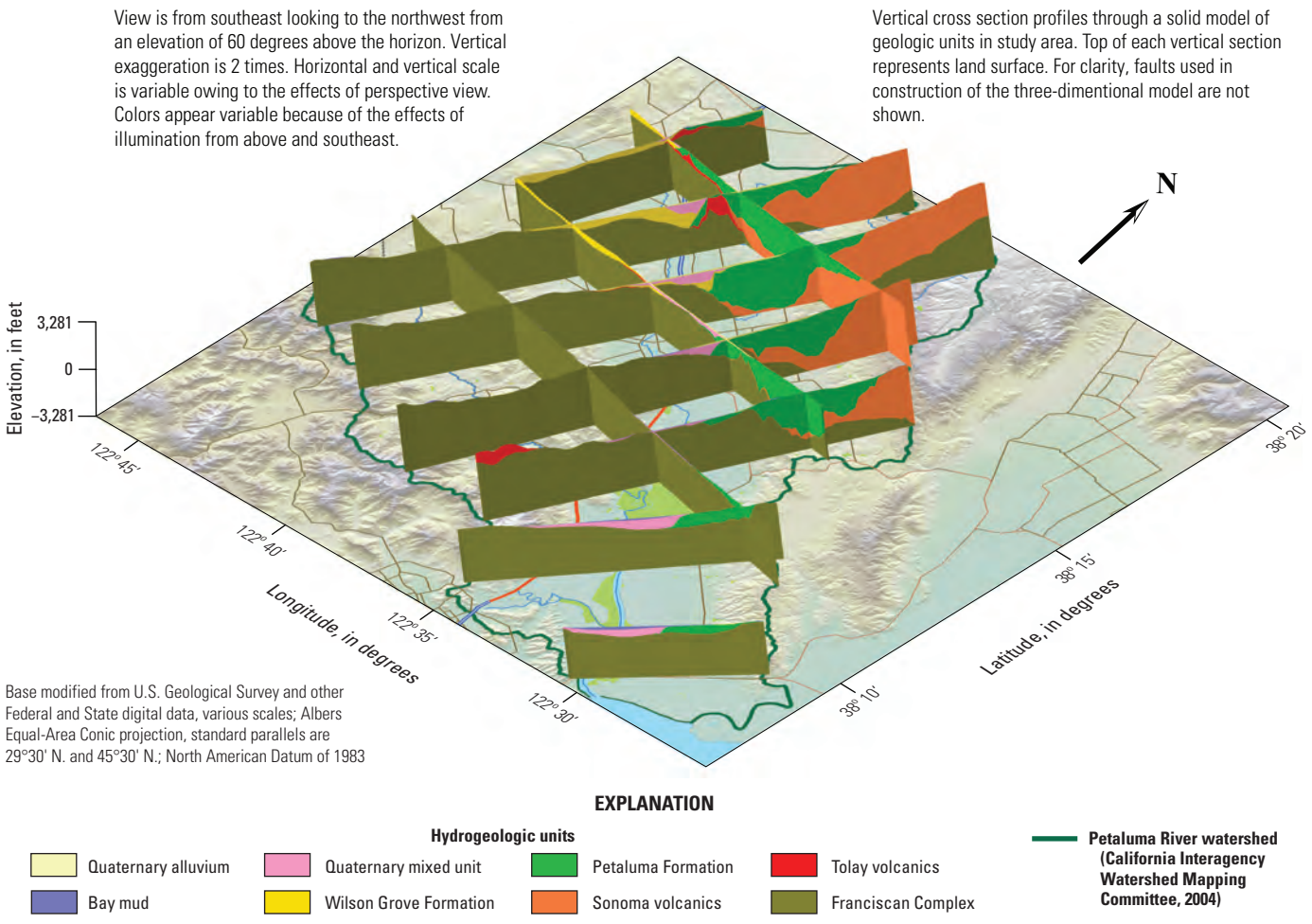

Figure B6. Perspective view of vertical cross sections cut through three-dimensional (3D) solid model, Petaluma valley watershed, Sonoma County, California.

Surface-Water Hydrology

The characteristics of streamflow generally provide an indication of the integrated hydrologic response of the upstream drainage to precipitation. Available streamflow records from streamgages in the PVW were analyzed to develop a better understanding of the seasonal distribution of streamflow, along with the response of streamflow to variability in climate.

Surface-Water Drainage Pattern

The Petaluma River is the largest surface-water body in the PVW. The river flows from the confluence of Lichau Creek southeast through Denman Flat, a natural detention basin hydraulically connected to the Petaluma River, and the City of Petaluma before flowing through the Petaluma marsh and into San Pablo Bay (fig. B7; Sonoma Resource Conservation District, 2015). The headwaters of the tributaries of Petaluma River are along the southwest slopes of Sonoma Mountain (Lichau Creek, Lynch Creek, and Adobe Creek), the southern slopes of Meacham Hill (Petaluma River), and the eastern slopes of Wiggins Creek and Burdell Mountain (San Antonio Creek and Black John Slough; fig. B7). Flow in the stream channels is seasonal; when winters are drier-than-normal, the main-stream channels often go dry during the summer. For example, water year 2014 was a dry year (total annual precipitation of 15.97 inches [in.]), and the average annual stream discharge in Petaluma River at streamgage 11459150 (Petaluma River at Copland Pumping Station at Petaluma, California; U.S. Geological Survey, 2016a) was about 35 percent of the mean annual mean discharge for water years 2011–16. The upper reach of the Petaluma River, north of the confluence with Lynch Creek, is seasonally ephemeral (often dry), whereas the lower reach of the river is tidally influenced and can flood during periods of high flow (Cardwell, 1958). Based on the location of Adobe Creek relative to the upper limit of the tidally influenced reach of the Petaluma River, the lower reach of Adobe Creek may also be tidally influenced (fig. B7). The PVW also includes Tolay Creek (fig. B7), which is part of the Sonoma Creek watershed (not shown) in Sonoma Valley, to the east of the study area (fig. B7); Tolay Creek is included in the study area because it overlies part of the Petaluma Valley groundwater basin.

Stream-discharge data collected along the Petaluma River by the USGS for this study were used to evaluate streamflow gains and losses along the Petaluma River and San Antonio Creek (fig. B7). The streamflow data are representative of the seasonally intermittent nature of surface-water flows in the PVW; streamflows in the Petaluma River and San Antonio Creek were negligible during the October 2014 measurement period (table B1). The upper reach of the Petaluma River (seepage sites PT1 to PT5; fig. B7) was consistently dry. The river gained flow from the confluence with Wiggins Creek (seepage site PT6; fig. B7) downstream to just north of the confluence with Lynch Creek (seepage site PT12; fig. B7), where streamflow became tidally affected. San Antonio Creek generally gained flow moving downstream; however, the area between seepage sites SA4 and SA6 might have lost flows at times (table B1). Flooding in the PVW is strongly influenced by tidal action in the San Pablo Bay, particularly in the area between Denman Flat and the Lynch Creek confluence and in the Payran floodplain, just south of the Lynch Creek confluence (fig. B7; Sonoma County, 2006).

The City of Petaluma operates a wastewater collection and treatment system, the Ellis Creek Water Recycling Facility (ECWRF), south of the city (fig. B7). A permit from the National Pollution Discharge Elimination System (NPDES) allows for discharge from ECWRF to the Petaluma River from October 21 through April 30 of each year (City of Petaluma, 2016). The volume of discharge of disinfected, secondary effluent to the river was 4,737 acre-feet (acre-ft) in 2015 (City of Petaluma, 2016).

Streamgages

The USGS previously maintained two streamgages on the Petaluma River and one on San Antonio Creek (fig. B7). The hydrographs for the three streamgages are shown in figure B8. Streamgage 11459150 (Petaluma River at Copland Pumping Station at Petaluma, California) is near the City of Petaluma, along the northern end of the tidally influenced reach of the river (fig. B7). Data collection at this streamgage began in November 1998 and ended in November 2016 (U.S. Geological Survey, 2016a). Water-surface altitude in the Petaluma River fluctuates with the tides and can be as much as 6 ft above NAVD 88 during high tide (U.S. Geological Survey, 2018). Beginning in 2011, streamflow data for streamgage 11459150 were tidally filtered (for an explanation of tidally filtering streamflow data, see Ruhl and Simpson, 2005) to provide a better understanding of streamflows at the streamgage. Using unfiltered flow data, the average annual discharge measured at streamgage 11459150 from water years 1999 to 2010 was about 547.7 acre-feet per day (acre-ft/d). In contrast, the average annual tidally filtered discharge measured at streamgage 11459150 from water years 2011 to 2017 was about 83.2 acre-ft/d.

Mean monthly tidally filtered streamflow for water years 2010–16 was greatest in December and lowest in August, at discharge values of 274 and 8.9 acre-ft/d, respectively. The mean monthly tidally filtered discharge was 68.5 acre-ft/d. High streamflows recorded in December through March are associated with the high precipitation season from November through March (see chapter A; fig. B5; Western Regional Climate Center, 2016), with some lag time between precipitation and streamflow. The decreases in discharge from May through September could be related to the dry season and the increased groundwater pumping during this season.

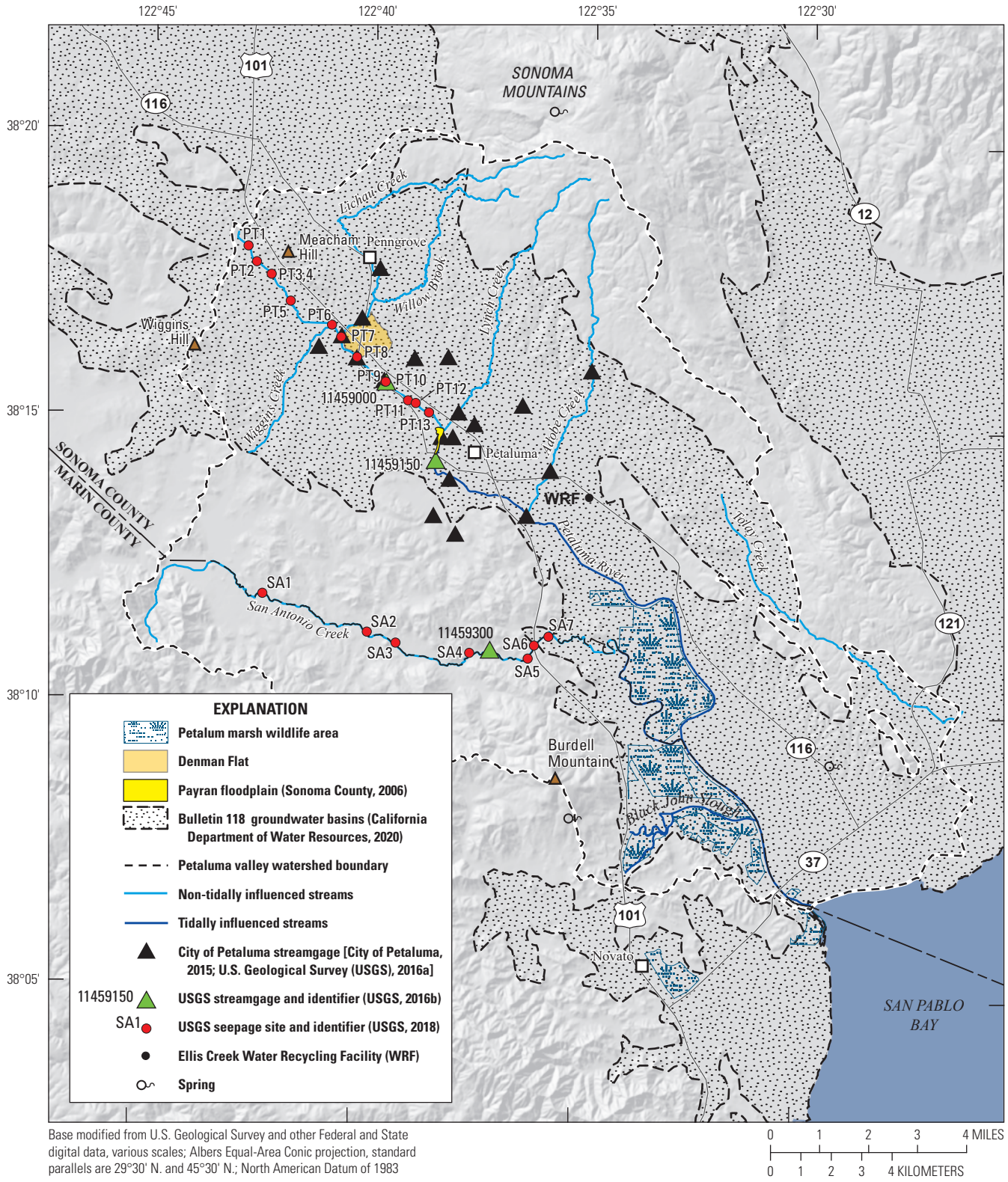

Figure B7. Surface-water features, streamgages, and U.S. Geological Survey (USGS) seepage sites in the Petaluma valley watershed, Sonoma County, California.

Table B1. Streamflow data collected along the Petaluma River and San Antonio Creek, Sonoma County, California, 2014–15.

[—, no data; ft³/s, cubic foot per second; acre-ft/d, acre-foot per day]

Site	October 24, 2014			April 29, 2015			May 4, 2016		
	Discharge (ft³/s)	Discharge (acre-ft/d)	Notes	Discharge (ft³/s)	Discharge (acre-ft/d)	Notes	Discharge (ft³/s)	Discharge (acre-ft/d)	Notes
Petaluma River									
PT1	0	0	Dry	Dry	Dry	—	Dry	Dry	—
PT2	0	0	Dry	Dry	Dry	—	Dry	Dry	—
PT3	0	0	Dry	0.0007	0.001	Possible Ag runoff	Dry	Dry	—
PT4	0	0	Dry	Dry	Dry	—	Dry	Dry	—
PT5	0	0	Dry	Dry	Dry	—	Dry	Dry	—
PT6	0	0	Dry	0.0067	0.0133	—	—	—	Access denied
PT trib	—	—	—	—	—	—	0.038	0.075	Flume; gaining between PT6 and PT7 from inflow from tributary
PT7	0	0	Isolated pool	0.049	0.097	—	—	—	Access denied
PT8	0	0	Isolated pools downstream	0.2	0.4	—	0.273	0.541	—
PT9	0	0	Dry	0.31	0.61	—	0.296	0.586	—
PT10	0.013	0.026	From culvert	0.33	0.65		0.394	0.780	—
PT11	0	0	Isolated pools	0.47	0.93	Possible tide affect, –0.04 ft stage drop	0.451	0.893	—
PT12	—	—	Tidally affected	—	—	Tidally affected	—	—	Tidally affected
PT13	—	—	Tidally affected	—	—	Tidally affected	—	—	Tidally affected
San Antonio Creek									
SA1	0	0	Dry	0.04	0.08	—	0.253	0.501	—
SA2	0	0	Dry	0.09	0.18	—	0.448	0.887	—
SA3	0	0	Isolated pool downstream	0.26	0.51	—	0.773	1.53	—
SA4	0	0	Dry	0.36	0.71	—	1.16	2.30	—
SA5	0	0	Dry	0.38	0.75	—	1.03	2.04	—
SA6	0	0	Dry	0.19	0.38	—	1.21	2.40	—
SA7	0	0	Dry	0.3	0.6	—	1.21	2.40	—

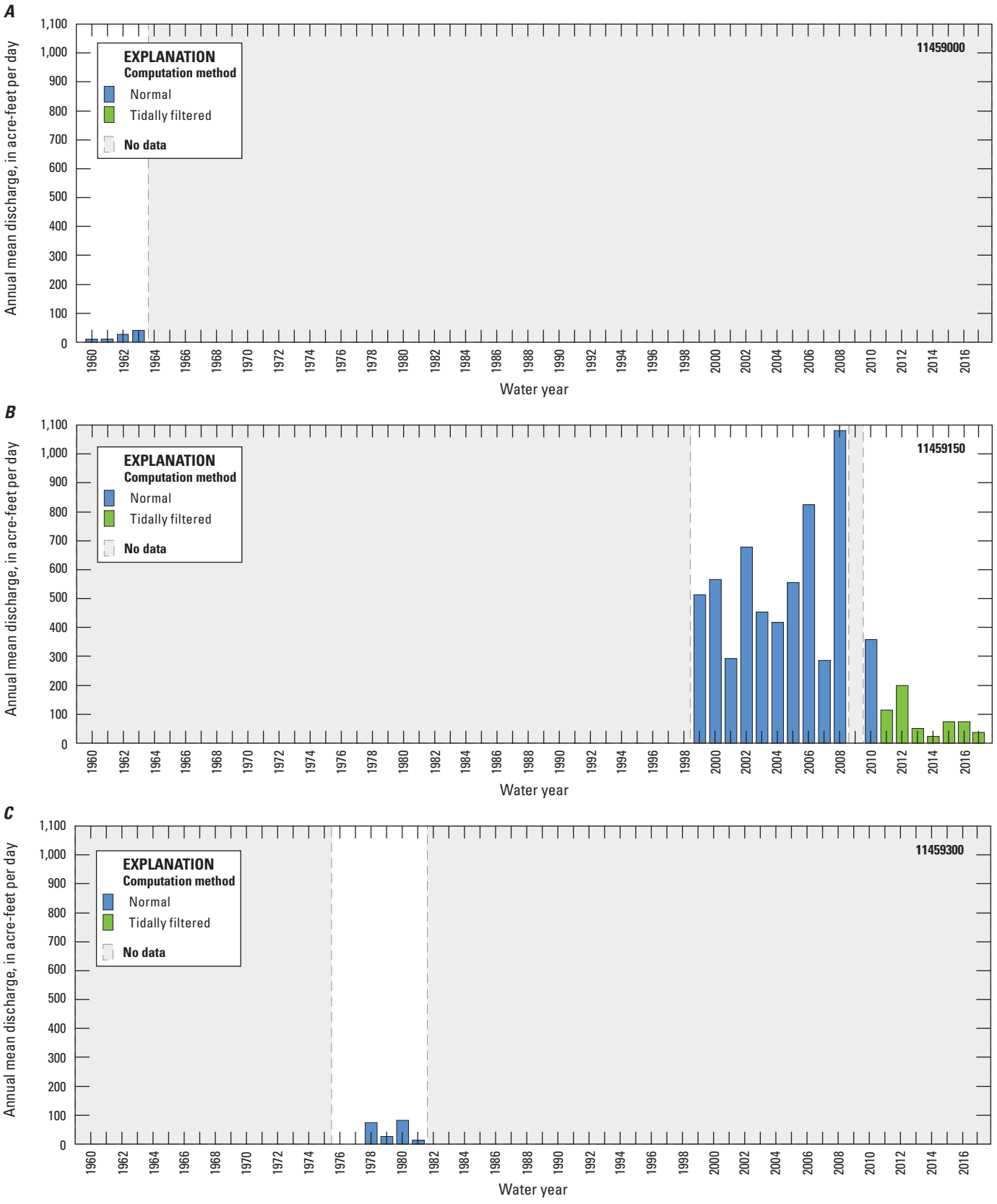

Figure B8. Annual mean streamflow for the Petaluma valley watershed, Sonoma County, California: *A*, streamgage 11459150 Petaluma River at Copland Pumping Station, 1960–63; *B*, streamgage 11459000 Petaluma River at Petaluma, 1999–2017; and *C*, streamgage 11459300 San Antonio Creek near Petaluma, 1978–81.

Streamgage 11459000 (Petaluma River at Petaluma, California) is north of the City of Petaluma, along the non-tidally influenced reach of the river. Data collection at this streamgage began in October 1948 and ended in September 1963 (U.S. Geological Survey, 2016b).

The USGS also historically operated streamgage 11459300 (San Antonio Creek near Petaluma, California) located on San Antonio Creek about 3 mi upstream from the confluence with the Petaluma River at the Petaluma marsh. Data collection at this streamgage began in August 1975 and ended in September 1981 (U.S. Geological Survey, 2016c).

In addition to the USGS streamgages, the City of Petaluma manages five streamgages on the Petaluma River (City of Petaluma, 2015; fig. B7). The City of Petaluma also manages 14 streamgages on tributaries of the Petaluma River (fig. B7). Long-term data for city-operated streamgages were not available (Kent Carothers, City of Petaluma, written commun., 2018).

Groundwater Hydrology

Groundwater in the study area is found in the saturated sedimentary rocks and unconsolidated deposits underlying the floor of Petaluma valley and surrounding lowlands as well as in the volcanic rocks underlying the mountains in the eastern PVW, where such rocks are sufficiently permeable to yield water. Beneath Petaluma valley, groundwater flows through the Quaternary alluvium, the Quaternary mixed unit, and the Neogene sedimentary rocks of the Wilson Grove and Petaluma Formations. Groundwater also flows through locally permeable intervals within the Sonoma Volcanics and, to a much lesser extent, in fractured Franciscan Complex. The aquifer system in the PVW could be hydraulically connected to four neighboring groundwater basins: the Santa Rosa valley, Sonoma Valley, Wilson Grove Formation Highlands, and Novato Valley (fig. A1). Data compiled largely from previous studies (Cardwell, 1958; Ford, 1975; Herbst, 1982) were used to describe the aquifer system, aquifer hydraulic properties, recharge and discharge, and groundwater flow in the PVW.

Definition of Aquifer System

The Quaternary alluvium, the Quaternary mixed unit, Wilson Grove and Petaluma Formations, and the Sonoma Volcanics have distinct lithologic and aquifer properties and constitute the principal aquifers in the PVW. The subsurface extent, thickness, and structural and stratigraphic boundaries between these aquifers are defined in the 3D GFM, which was used in this study to define the PVW aquifer system.

Groundwater flow between aquifers in the PVW is controlled by the areal extent of each aquifer, degree of hydraulic connection to underlying or adjacent aquifers, and permeability of fault zones that separate aquifers. The aquifer system is conceptualized as a set of distinct aquifers occupying fault-bounded domains (fig. B9). Subsurface unit extents from the 3D GFM are shown in map view for each domain; when shallow Quaternary alluvium are removed, the extent of underlying aquifers in the subsurface is evident (fig. B9). Figure B9 emphasizes the fragmented nature of the aquifer system and is an example of the utility of the 3D GFM as a tool for predicting where specific aquifers could be expected in the subsurface.

Previously reported estimates of specific yield of various geologic formations in the PVW ranged from 0 to 25 percent (Cardwell, 1958; Herbst, 1982). For this study, data from 125 wells were compiled from throughout the basin to determine the range and distribution of well productivity. Driller reports provided information on well tests, including discharge rate, water-level drawdown, and the length of test. Productivity was computed as specific capacity, given in terms of gallons per minute per foot [(gal/min)/ft] of drawdown. Coarse-grained, well-sorted sedimentary materials have high specific yields and specific capacities because of the large amount of connected pore volume in the material. Conversely, cemented deposits and clay-rich deposits have limited or very small pore spaces and correspondingly lower specific yields and specific capacities.

Quaternary alluvium are minor aquifers of limited areal extent along major streams and beneath the alluvial fans on the eastern side of the PVW (fig. B1). Previous work indicates these alluvial aquifers are vertically continuous, lacking notable internal lithologic heterogeneity (Herbst, 1982). These alluvial deposits may be hydraulically connected with underlying permeable formations, such as to the northwest of the City of Petaluma where alluvial deposits overlie the Wilson Grove Formation (Herbst, 1982). Reported specific yields of the Quaternary alluvium ranged from 8 to 17 percent (Herbst, 1982); specific capacities were not computed because of uncertainty identifying wells open only to this unit.

The Quaternary mixed unit aquifer is only present along the axis of Petaluma valley (figs. B5*C*, B9) and is likely hydraulically connected with overlying Quaternary alluvium and with the Wilson Grove Formation. This aquifer is lithologically heterogeneous, consisting of alternating thin beds of conglomerate, sand, and mudstone. Although previous studies of the PVW did not report aquifer properties for the Quaternary mixed unit, this unit is lithologically similar to the Glen Ellen Formation (fig. B2) in the Santa Rosa valley to the north of the PVW (chapter A, fig. A1); therefore, reported specific yields of 3 and 7 percent may be applicable (Herbst and others, 1982).

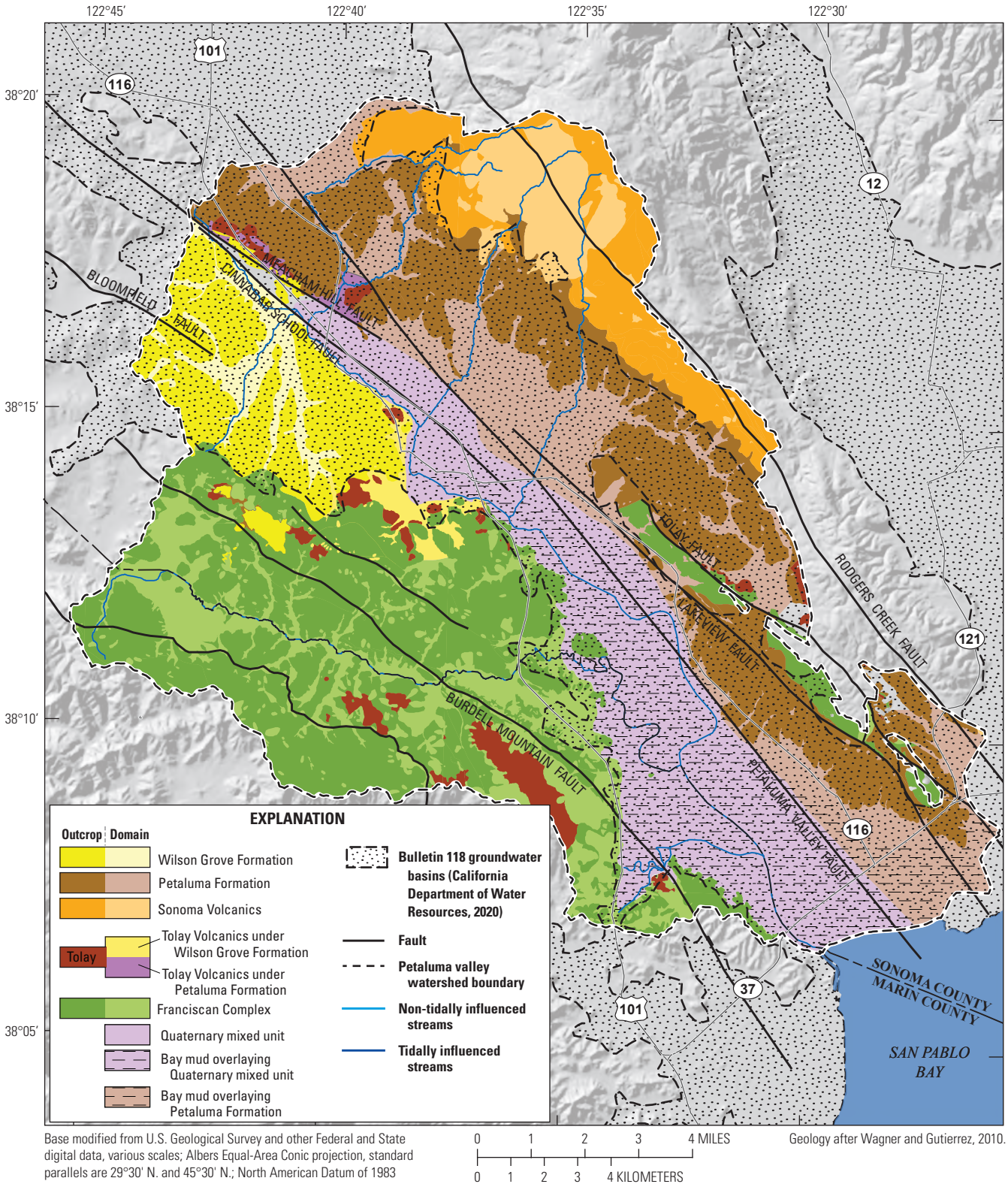

Figure B9. Hydrogeologic unit domains of the Petaluma valley watershed, Sonoma County, California.

The fine-grained marine sandstone of the Wilson Grove Formation forms a single, continuous aquifer because of lithologic homogeneity and the absence of faults. This aquifer is present only in the northwest part of the PVW (figs. B5*D*, B9). The sand and sandstones of the Wilson Grove Formation are generally productive aquifers, with reported specific yields of 10 to 20 percent (Herbst, 1982) and a range in specific capacities of 0.05 to 0.5 (gal/min)/ft. The specific capacities for the Wilson Grove Formation are approximately equivalent to transmissivities of 13.0 to 134 foot squared per day (ft^2/d) for confined aquifers and 10.0 to 100 ft^2/d for unconfined aquifers.

The Petaluma Formation has the greatest extent of any aquifer in the PVW, occupying much of the eastern part of the PVW (figs. B5*E*, B9). The Petaluma Formation aquifer is composed of discontinuous lenses of sands and gravels, and hydraulic connections with overlying and adjacent aquifers only exist where these lenses are juxtaposed with other aquifers. Wells in the Petaluma Formation produce moderate amounts of water when they intercept the sand and gravel lenses, but well productivity can be low because of the clay-dominated lithology of the Petaluma Formation. Estimated specific yields for the Petaluma Formation from previous studies range from 3 to 7 percent (Herbst, 1982), and specific capacities range from 0.015 to 7.5 (gal/min)/ft. The specific capacities for the Petaluma Formation are approximately equivalent to transmissivities of 4.0 to 2,005 ft^2/d for confined aquifers and 3.7 to 1,504 ft^2/d for unconfined aquifers.

The Sonoma Volcanics are present only at the northeast edge of the PVW (figs. B5*F*, B9), whereas Tolay Volcanics are only in relatively isolated regions in the PVW (figs. B5*G*, B9). Water production from the Sonoma Volcanics is highly variable; specific yield is estimated to range from 0 to 15 percent (Herbst, 1982) and specific capacity ranges from 0.03 to 0.5 (gal/min)/ft. The specific capacities for the Sonoma Volcanics are approximately equivalent to transmissivities of 8.0 to 133.7 ft^2/d for confined aquifers and 6.0 to 100.2 ft^2/d for unconfined aquifers.

Groundwater Recharge and Discharge

Sources of groundwater recharge in the PVW are infiltration from precipitation, seepage from the Petaluma River and its tributaries, irrigation return flow, and intrusion from San Pablo Bay and adjacent saltwater marshes. Leakage from water-supply infrastructure is another possible source; however, the city estimates that losses are minimal and are not considered to be important sources (Leah Walker, City of Petaluma, written commun., 2018). Groundwater discharges as base flow to streams, spring flow, evapotranspiration (ET), and groundwater pumpage. Groundwater can also recharge to and discharge from the PVW as underflows across the PVW boundary into or out of neighboring groundwater basins.

Groundwater Recharge

Using criteria based on measured infiltration rates (greater than 0.6 inches per hour, or in/h) and land slopes (less than 15 percent), Herbst (1982) concluded that approximately 20 percent of the Petaluma Valley groundwater basin could contribute to groundwater recharge, primarily in and northwest of the City of Petaluma and along the crest of Sonoma Mountain (chapter A, fig. A1). Groundwater also recharges through infiltration along stream channels where erosion has exposed permeable beds within the Petaluma and Wilson Grove Formations (West Yost, 2004); however, this flux has not been estimated. Herbst (1982) estimated the average total annual natural recharge in the Petaluma Valley groundwater basin to be about 40,000 acre-ft (8 in.). Using a basin characterization model (BCM; Flint and Flint, 2007), Micheli and others (2012) estimated an annual average of 29 in. (230,000 acre-ft) of precipitation and 25,000 acre-ft of natural recharge in the PVW for 1981–2010.

Groundwater Discharge

Groundwater discharges to streams as base flow during the wet season along the Petaluma River and its tributaries north of the tidally influenced reach; however, base flow in the PVW has not been estimated. Groundwater discharges through springs in areas of the Sonoma Mountains and near the summit of Burdell Mountain (fig. B7) where stratigraphic contacts between fractured volcanic rocks and the underlying Franciscan Complex forces water to land surface. Micheli and others (2012) estimated the actual ET rate for 1981–2010 was about 20 in/yr. Assuming a total area for the PVW of about 99,060 acres, the total actual ET was 165,100 acre-ft/year (acre-ft/yr). Most of the groundwater discharge through ET occurs where depth to groundwater is shallow, such as in the Petaluma marsh (fig. B7).

Groundwater pumped from wells in Petaluma valley is used for residential, agricultural, and industrial purposes. Historically (pre-1950), groundwater pumped from wells was the primary source of water supply in the PVW (Herbst, 1982) and was mainly used for agricultural purposes (Cardwell, 1958). Cardwell (1958) estimated the total average annual pumpage of 1,600 acre-ft/yr from the Petaluma Valley groundwater basin between 1945 and 1949. The CDWR has identified well-completion reports for about 463 domestic wells and 78 municipal or irrigation wells in the Petaluma Valley groundwater basin (California Department of Water Resources, 2014). The average well yield was 38 gal/min for domestic wells and 140 gal/min for municipal or irrigation wells (California Department of Water Resources, 2014).

As of 2015, the City of Petaluma had 12 production wells, six of which are active and are permitted by the State Water Resources Control Board, Division of Drinking Water (DDW), for drinking water supply (City of Petaluma, 2016). Withdrawal rates from the wells range from 100 to 600 gal/min (City of Petaluma, 2015) but are limited to 60 to 180 gal/min during summer months to prevent large drawdowns (West Yost, 2004). Annual groundwater pumpage for the City of Petaluma for 1959 through 2002 ranged from 0 to about 1,400 acre-ft (fig. B10; West Yost, 2004). Reported annual values for groundwater pumped by the City of Petaluma for 2006 through 2015 ranged from a minimum of 0 acre-ft in 2006 to a maximum of 1,073 acre-ft in 2009, with a median value of 375 acre-ft (City of Petaluma, 2016).

Underflow

Woolfenden and Hevesi (2014) used a coupled watershed and groundwater model to simulate groundwater flow in the Santa Rosa Valley groundwater basin and surrounding areas to the north of the PVW (chapter A, fig. A1). Model results indicated very little underflow (50 acre-ft/yr) between the Santa Rosa Valley groundwater basin and the PVW (Woolfenden and Hevesi, 2014). Intrusion of water from San Pablo Bay to the PVW has been mentioned by previous reports (Cardwell, 1958; Herbst, 1982; West Yost, 2004); however, estimates of this underflow are not available. Underflow from the Wilson Grove Formation Highlands groundwater basin through the northwestern boundary of the PVW is also possible but has not been estimated.

Groundwater Levels and Movement

Mapping the spatial and temporal variation of groundwater levels provides information about groundwater flow through aquifer systems. Examination of the water table and potentiometric surfaces reveals hydrogeologic characteristics of the watershed, such as the areas of recharge and discharge, gaining and losing sections of streams, and effects of geologic structure on groundwater flow. Declining water-level hydrographs over time indicate where groundwater discharge is in excess of recharge.

Groundwater Levels

Groundwater levels in the PVW have been measured by the USGS since 1949 (Cardwell, 1958). Additional groundwater-level data were collected by the CDWR and the DDW since the 1950s. Using groundwater-level data, Cardwell (1958) identified a groundwater divide in the Santa Rosa Valley groundwater basin (chapter A, fig. A1), north of which water moves northward, away from the PVW, and south of which water moves into the PVW. This groundwater divide is likely caused by uplift of low permeability rocks on the northeast side of the Meacham Hill fault (fig. B1).

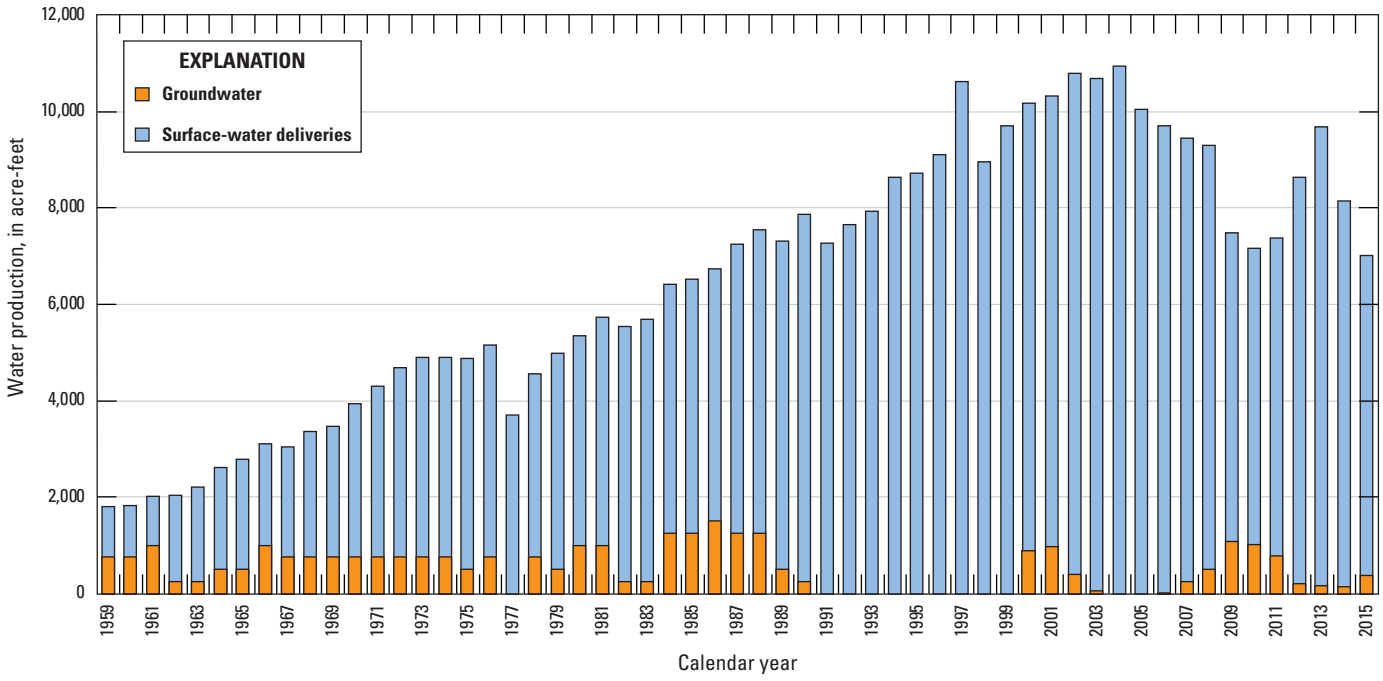

Figure B10. Historical water production for the City of Petaluma, Sonoma County, California, 1959–2015; data for the 1959–2000 period from West Yost (2004); data for 2001–15 provided by the City of Petaluma.

The groundwater-level contours constructed for the PVW in 1951 by Cardwell (1958) and in 1980 by Herbst (1982; figs. B11*A*–*B*, respectively) used a comprehensive set of water-level data and were compared with the groundwater-level altitude contours constructed for this study using data collected primarily in 2015 (table B2; fig B11*C*; California Department of Water Resources, 2018a; California Department of Water Resources, 2018b). This comparison provided information about changes in the direction of groundwater movement and the quantity groundwater in storage over period of record.

A comparison of groundwater-level altitude contours in figure B11 shows little overall change from 1951 through 2015. Minor differences between the mapped contours are attributed to differences in available data. Groundwater-flow patterns have not changed substantially, and groundwater still moves from the higher altitudes in the east and west of the watershed, toward the Petaluma River (fig. B11). Contours indicate that groundwater in the western part of the watershed moves from an area just outside of the watershed boundary (fig. B11*B*). South of the City of Petaluma, contours indicate that groundwater adjacent to the Petaluma River may move southeast along the trace of the river (figs. B11*A*, B11*C*). Groundwater may also flow into the watershed from the groundwater divide underlying the boundary with the Santa Rosa Valley groundwater basin to the north, in the area to the northwest of the town of Penngrove, Calif. (figs. B11*A*, B11*C*).

Table B2. Groundwater-level altitudes for the Petaluma valley watershed, Sonoma County, California, Spring 2014–15 (California Department of Water Resources, 2018a, b).

[All data from California Department of Water Resources. **Abbreviations**: NAD 83, North American Datum of 1983; NAVD 88, North American Vertical Datum of 1988; mm/dd/yyyy, month/day/year; —, no data]

Well number	State well number	Local well designation	Latitude (NAD 83)	Longitude (NAD 83)	Groundwater-level altitude (feet above NAVD 88)	Date (mm/dd/yyyy)
WL-1	—	Cardinaux	38.234200	–122.552500	205	05/05/2015
WL-2	04N06W07A001M	—	38.211700	–122.555600	–20	03/26/2015
WL-3	05N07W36R001M	—	38.227600	–122.576300	11	03/26/2015
WL-4	—	5/7-25 PG&E	38.251400	–122.579100	34	05/11/2015
WL-5	05N07W11F001M	—	38.293400	–122.601600	479	03/26/2015
WL-6	—	Casa De Arroyo	38.234099	–122.603065	–14	05/11/2015
WL-7	—	Miwok	38.235736	–122.609359	12	05/11/2015
WL-8	05N07W11N001M	—	38.286700	–122.609500	243	03/20/2014
WL-9	—	Garfield	38.258046	–122.616797	47	05/11/2015
WL-10	05N07W15K002M	—	38.276600	–122.617900	128	03/26/2015
WL-11	—	Tahola	38.256218	–122.625931	33	05/11/2015
WL-12	—	Station 1401	38.264787	–122.644282	29	05/11/2015
WL-13	05N07W20B002M	—	38.267200	–122.654100	6	03/26/2015
WL-14	05N07W31R002M	—	38.230500	–122.665400	122	03/26/2015
WL-15	06N07W31J001M	—	38.318200	–122.671000	123	03/18/2015
WL-16	05N07W30K014M	—	38.248300	–122.672600	67	03/26/2015
WL-17	05N07W31P003M	—	38.227700	–122.674000	147	03/26/2015
WL-18	05N07W19N001M	—	38.256400	–122.681000	42	05/12/2015
WL-19	05N08W13Q001M	—	38.271100	–122.690700	31	03/26/2015
WL-20	05N08W01L002M	—	38.304700	–122.698100	244	03/18/2015
WL-21	05N08W02H001M	—	38.307600	–122.704100	91	03/18/2015
WL-22	05N08W14K002M	—	38.274900	–122.707100	107	03/26/2015
WL-23	—	St. John	38.309600	–122.709800	171	06/12/2015
WL-24	05N08W14P001M	—	38.271500	–122.715100	135	03/26/2015
WL-25	05N08W23M001M	—	38.262300	–122.721800	59	03/26/2015

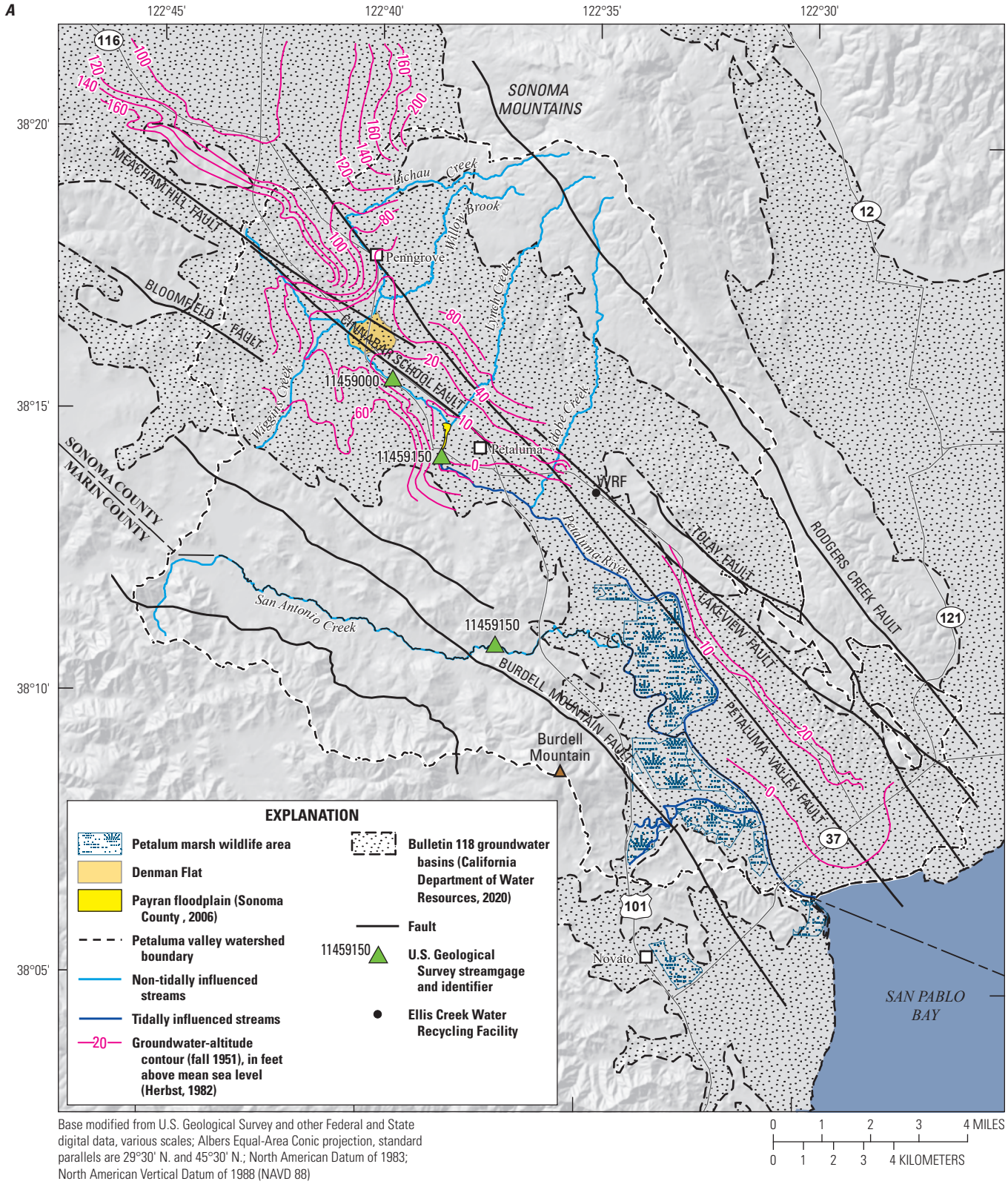

Figure B11. Groundwater-level altitude contours for the Petaluma valley watershed, Sonoma County, California, *A*, April 10–18, 1951 (modified from Cardwell, 1958); *B*, fall 1980 (modified from Herbst, 1982); and *C*, this study, spring of 2014 or 15 (date for contours is provided in table B2).

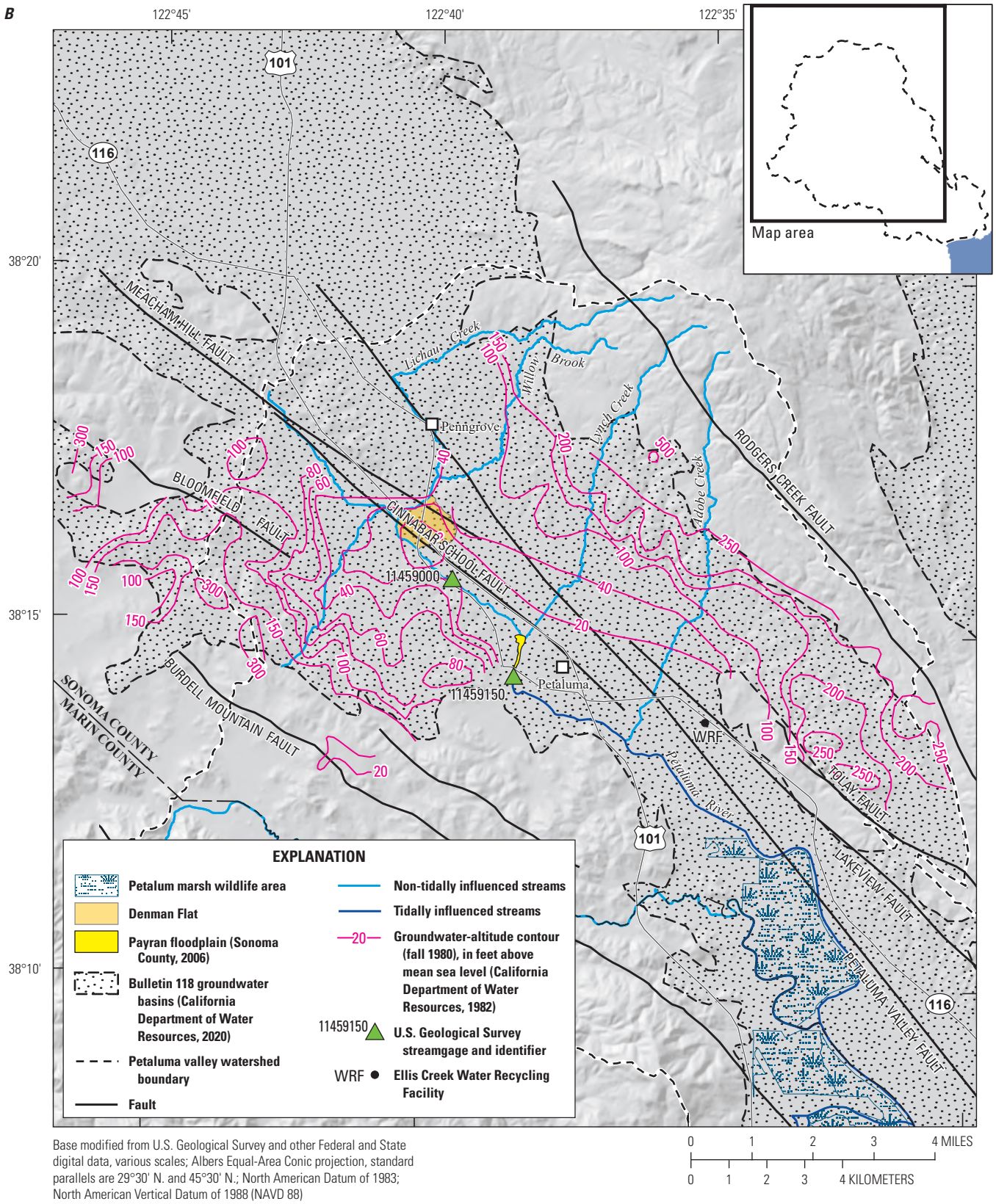

Base modified from U.S. Geological Survey and other Federal and State digital data, various scales; Albers Equal-Area Conic projection, standard parallels are 29°30' N. and 45°30' N.; North American Datum of 1983; North American Vertical Datum of 1988 (NAVD 88)

Figure B11.—Continued

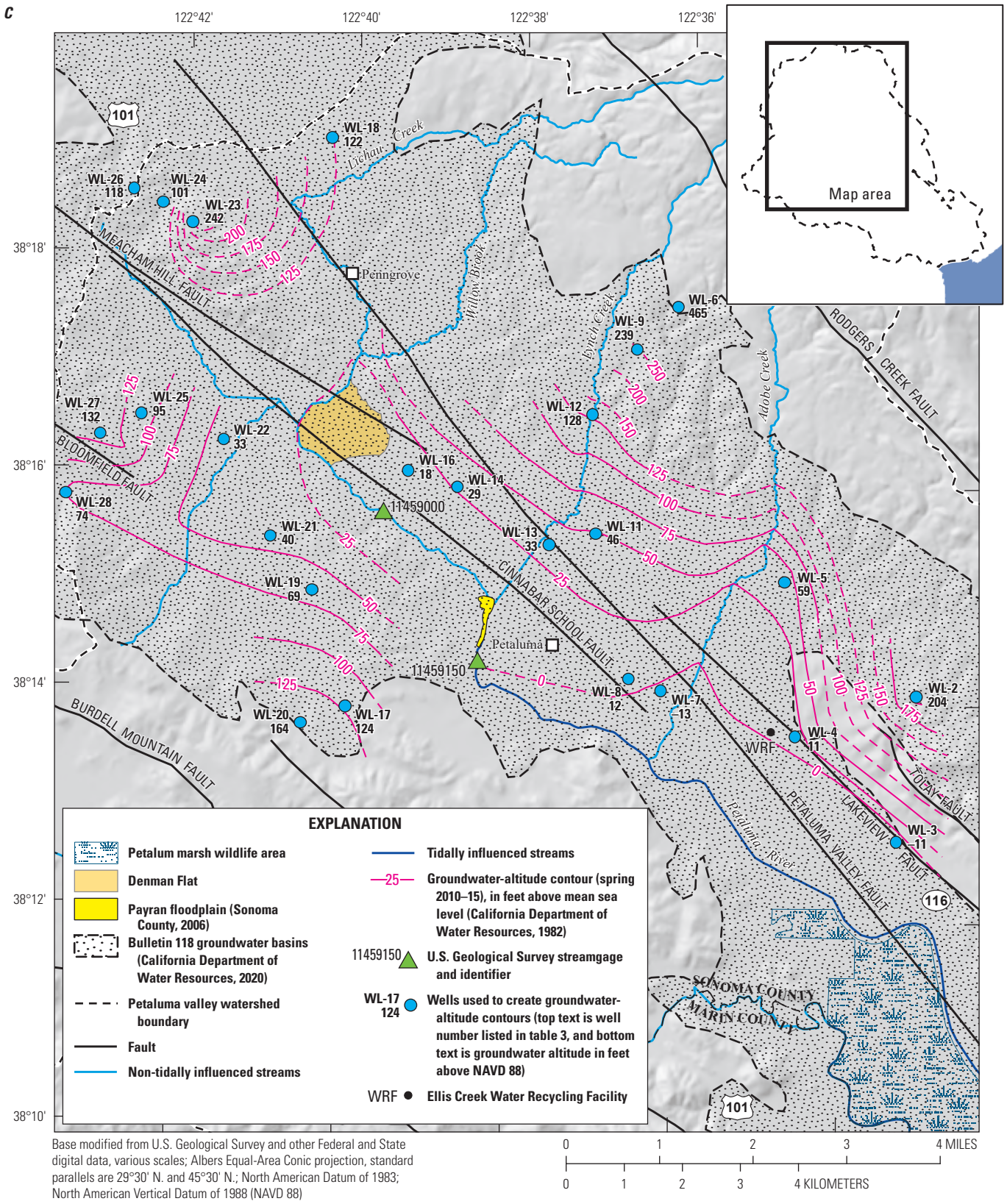

Figure B11.—Continued

Groundwater levels were 10 ft above NAVD 88 in the City of Petaluma and at or below NAVD 88 near the Petaluma River, from the ECWRF to San Pablo Bay, and in the southern part of the PVW. Groundwater levels in Denman Flat, a natural detention basin hydraulically connected to the Petaluma River, were also at or below NAVD 88. Much of the groundwater in the southern part of the study area was near the sea-level altitude of NAVD 88. In this area of low water levels, the river may be gaining or losing flow depending on the tidal cycle and the resultant water surface altitude in the river in relation to groundwater altitudes (generally gaining flow during low tides and losing flow during high tides).

Gaining and losing reaches of the Petaluma River and its tributaries can be identified on water-level contour maps (fig. B11). The 1951 and 1980 groundwater levels indicated that the Petaluma River gained groundwater upstream from the confluence with Lichau Creek (figs. B11A–*B*). In 1951, the lower reach of Lichau Creek gained water upstream from the confluence with Willow Brook (fig. B11*A*). Wiggins Creek gained groundwater in 1980. Willow Brook lost water upstream from the confluence with Lichau Creek in 1980 and during the 2010s. The middle parts of Lynch Creek gained groundwater in 1980 (fig. B11*B*) and may have lost water as it neared the Petaluma River in 1951 and the 2010s (figs. B11*A*, B11*C*). In 1980, Adobe Creek gained and lost groundwater in the middle part (fig. B11*B*) and was neutral or lost water groundwater in the middle part during the 2010s (fig. B11*C*).

Groundwater Hydrographs

In general, groundwater levels, and therefore groundwater storage, have remained consistent throughout the PVW for the period of record. Groundwater hydrographs measured in wells also can be used to identify saltwater intrusion through time. Although groundwater levels generally indicate little to no trend, there are temporal variations in groundwater levels and also variability in groundwater hydrographs between principal aquifers. Groundwater levels have decreased slightly in some wells in the northeastern part of the study area, particularly in wells completed in the Petaluma Formation. Changes in groundwater levels measured in select wells by CDWR (fig. B12) are shown in hydrographs. Declines in groundwater levels indicate areas where groundwater storage has declined.

Groundwater hydrographs from wells in the Wilson Grove Formation (fig. B12, wells 05N/08W-13Q01, -14K02, -14P01, 05N/07W-19N01, -30K14, -31P03, and -31R02) indicate that groundwater levels fluctuated seasonally in response to precipitation and pumping. In general, groundwater levels in this area were higher in the spring and lower in the fall, with little trend in groundwater levels during the period of record (fig. B13*A*). Water-level differences between neighboring wells (for example, wells 31P03 and 31R02) could be the result of differences in land-surface altitude, because the water-table generally resembles the land surface; however, wells 14K02 and 14P01 have similar land-surface altitudes (170 and 165 ft relative to NAVD 88, respectively), and the water levels for well 14P01 were generally 25 ft higher than those for 14K02. The difference in water-level altitudes in wells 14K02 and 14P01 could be associated with several factors, including differences in well construction (well 14K02 is about 44 ft deeper than well 14P01).

Groundwater hydrographs from wells in the northern part of the area where the Petaluma Formation crops out (fig. B12, wells 05N/07W-11F01, -11N01, -15K02, -15Q01, -18B01, and -25G01) indicate large, irregular fluctuations in groundwater levels with drawdowns ranging from about 8 ft (well 18B01) to almost 110 ft (well 11F01; fig. B13*B*). The large fluctuations are likely the result of groundwater pumping. Increases in groundwater levels appear to correspond to periods of increased precipitation (fig. B14) and associated decreases in groundwater pumping and increases in streamflow. There generally is a trend of decreasing groundwater levels in this area during the period of record, which may be caused by discharge, such as groundwater pumping, in excess of recharge. For example, the decrease in groundwater levels in well 15Q01 beginning in the mid- to late-1990s may be caused by pumping from nearby agricultural or rural domestic wells. Groundwater hydrographs from wells in the southern part of the area where the Petaluma Formation crops out (fig. B12, wells 03N/06W-01Q01, 04N/06W-07A01, -21A01, and 05N/07W-36R01) generally indicate little seasonal variation; however, well data indicate potentially large multi-year variation. Water-level fluctuations of as much 95 ft in the hydrograph for well 04N/06W-07A01 (fig. B13*C*) may be caused by groundwater pumping.

Groundwater hydrographs from wells in the Quaternary mixed unit (fig. B12; wells 05N/07W-20B02 and -34L01) indicate seasonal variation. A gradual increase of about 5 ft for the period of record was observed in well 20B02 (fig. B13*D*). In contrast, a discernable trend was not observed in well 34L01, and seasonal variation was less in well 34L01 compared to well 20N02 (fig. B13*D*).

Groundwater hydrographs from wells can be used to identify saltwater intrusion through time in the southeastern part of the PVW. In areas of the PVW where groundwater levels are near sea level, levels fluctuate in response to tidal fluctuations (Cardwell, 1958). Wells 04N/06W-07A01 and 05N/07W-34L01 are by the tidally influenced reach of the Petaluma River, and well 03N/06W-01Q01 is by San Pablo Bay (fig. B12). The hydrograph for well 7A01 (fig. B13*C*) indicates that the groundwater level is generally well below NAVD 88, whereas the hydrographs for wells 01Q01 and 34L01 (figs. B13*C*, B13*D*, respectively) indicate that the groundwater levels are at about NAVD 88 (2.94 ft below NAVD 88). Groundwater hydrographs near NAVD 88 indicate that groundwater in this area may be subject to intrusion of salt water from the Petaluma River or San Pablo Bay during high tides (figs. B13*C*, B13*D*). Fluctuations in river stage and groundwater level caused by tidal influences can cause reversals in the exchange between the groundwater system and (1) the tidally influenced, potentially saline reach of the Petaluma River and (2) San Pablo Bay.

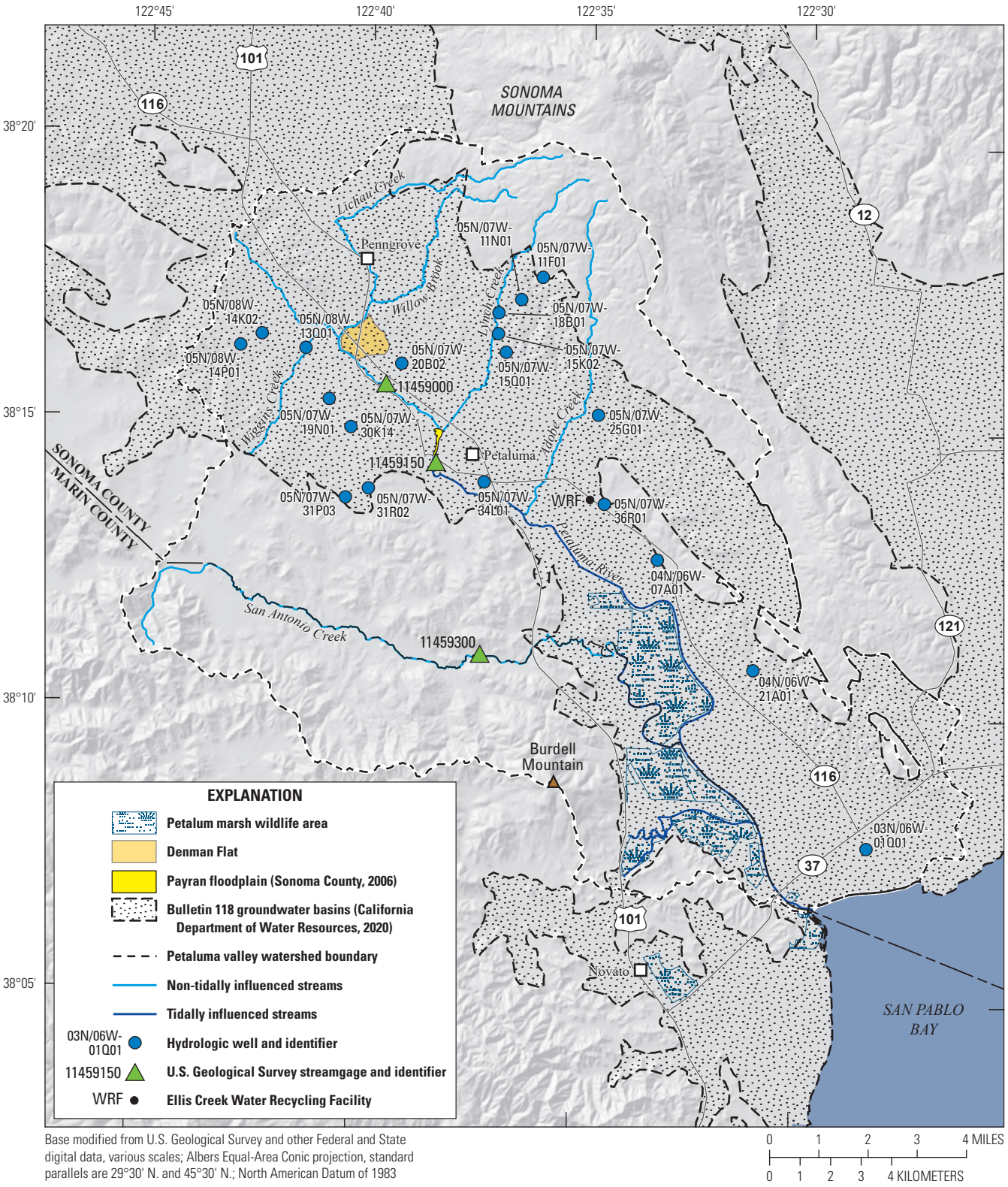

Figure B12. Locations of select wells with historical groundwater-level altitudes, Petaluma valley watershed, Sonoma County, California, 1949–2015 (California Department of Water Resources, 2018a; California Department of Water Resources, 2018b).

A

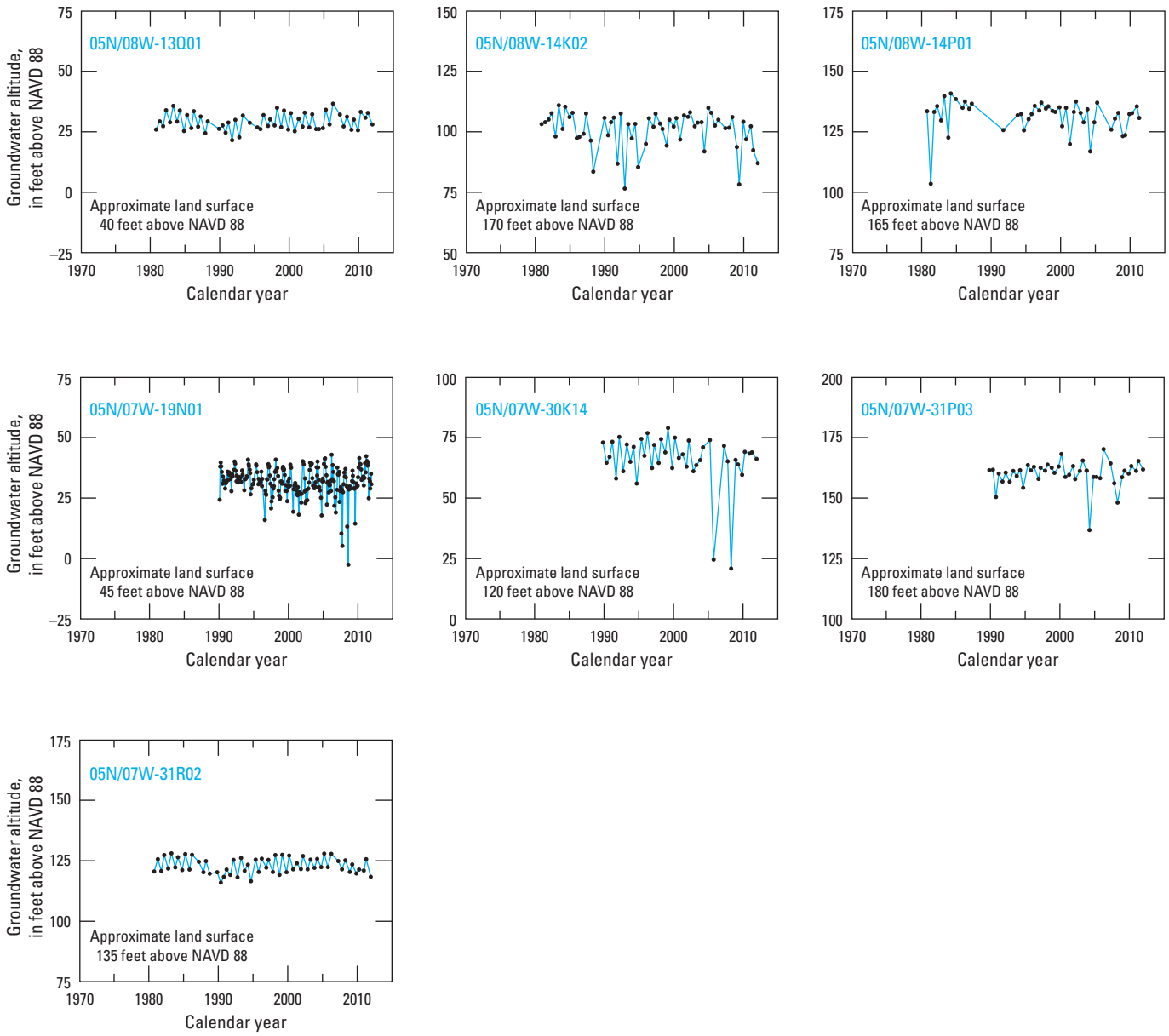

Figure B13. Groundwater levels relative to North American Vertical Datum of 1988 (NAVD 88) during varying periods for selected wells perforated in the following geologic units in the Petaluma valley watershed, Sonoma County, California (California Department of Water Resources, 2018a; California Department of Water Resources, 2018b): *A*, Wilson Grove Formation (05N/08W-13Q01, -14K02, -14P01, 5N/7W-19N01, -30K14, -31P03, and -31R02); *B*, northern Petaluma Formation (05N/07W-11F01, -11N01, -15K02, -15Q01, 18B01, and -25G01); *C*, southern Petaluma Formation (03N/06W-01Q01, 04N/06W-07A01, -21A01, and 05N/07W-36R01); and *D*, Quaternary mixed unit (05N/07W-20B02 and 34L01) .

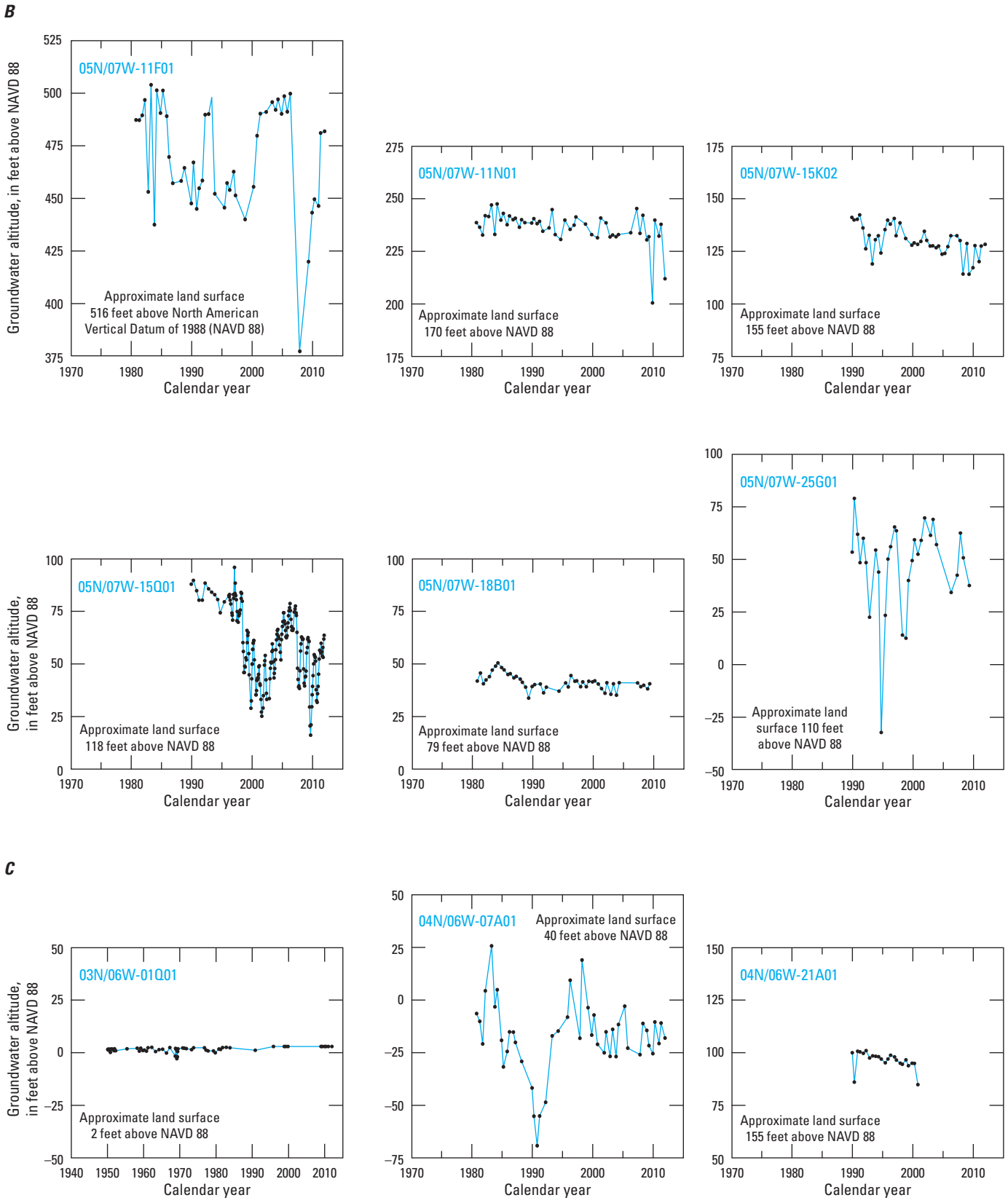

Figure B13.—Continued

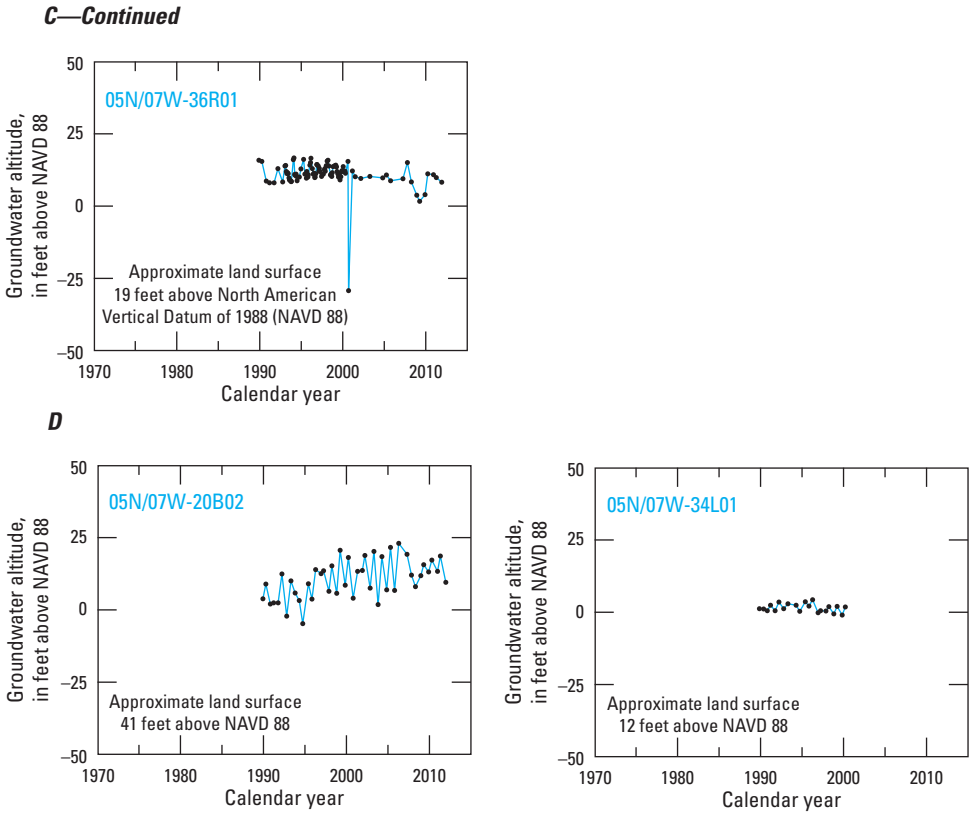

Figure B13.—Continued

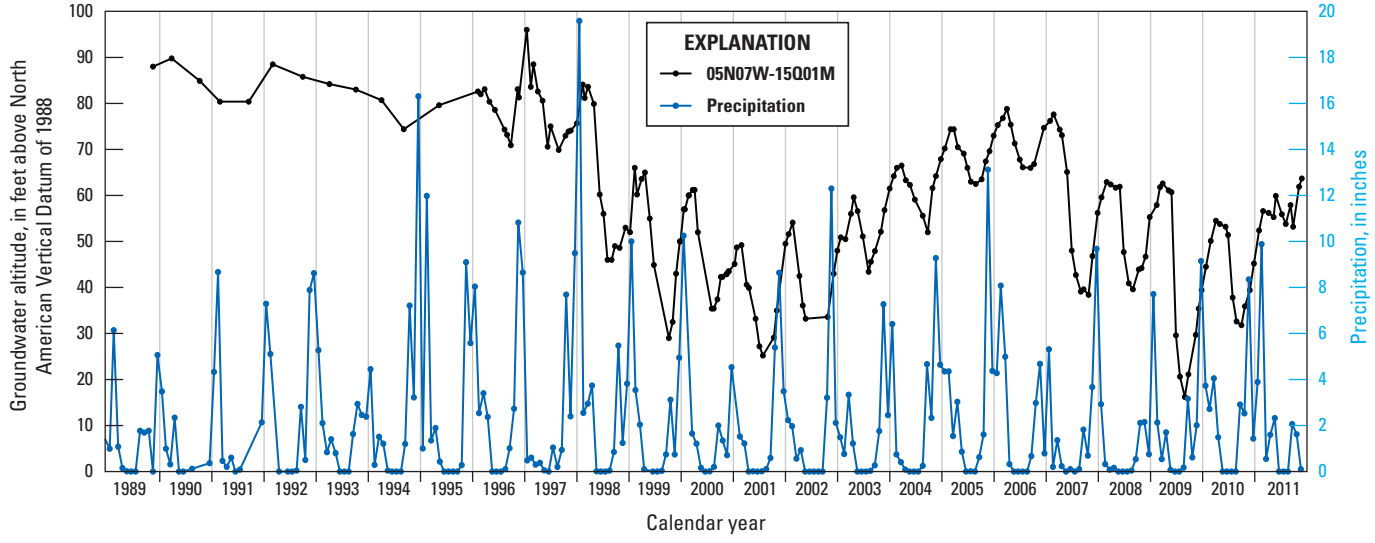

Figure B14. Water-level altitudes for well 05N/07W-15Q01 (California Department of Water Resources, 2018a) and precipitation data from the Western Regional Climate Center in the City of Petaluma (046826; Western Regional Climate Center, 2016), Petaluma valley watershed, Sonoma County, California, 1989–2011.

Faults and Groundwater Flow

The effect of faults on groundwater flow is difficult to determine in the PVW because of the lack of aquifer-test data near faults and because the northwest-trending faults in the basin run parallel to the predominant direction of groundwater flow along the axis of the valley. Previously published groundwater-level maps (Cardwell, 1958; Herbst, 1982) do not indicate potential effects of the Burdell Mountain and Rodgers Creek faults on groundwater flow, and data to determine the effect of these faults on groundwater levels and flows are insufficient. In the northwest part of the PVW, where the Wilson Grove Formation crops out (fig. B9), the shapes of groundwater-level contours (Cardwell, 1958; Herbst, 1982) generally mimic surface topography and do not indicate substantial changes in gradient. This lack of gradient changes indicates that the Bloomfield and Cinnabar School faults do not influence groundwater levels in this area (figs. B11*A*, B11*B*). Groundwater-level contours steepen in the vicinity of the Meacham Hill and Tolay fault traces (fig. B11*B*; Herbst, 1982). Steepening contours probably result from the fault-related juxtaposition of low-permeability rocks (Franciscan Complex or Tolay Volcanics) with more permeable units rather than the result of any special hydraulic properties of the fault zones (Herbst, 1982). Groundwater-level contours indicate the Petaluma valley fault may not influence groundwater flow (figs. B11*A*, B11*C*). The potential effect of the Lakeville fault (Wagner and others, 2005) on water levels could not be determined because of a lack of water-level data on the east side of the fault.

Summary

The U.S. Geological Survey (USGS), in cooperation with the Sonoma County Water Agency (SCWA) and the City of Petaluma, constructed a three-dimensional geologic framework model of the Petaluma valley watershed (PVW) to represent the subsurface geometry of the basin-filling geologic units and the top of Franciscan Complex. The framework model was built by integrating digital information from well data, surface geologic maps, and geophysical data to construct subsurface maps of each geologic unit in the PVW. The geologic framework model defines the location of structures in the basin; defines the extent, altitude, and thickness of each geologic unit; and provides the fundamental geologic framework for the subsequent development of a transient numerical groundwater-flow model of the PVW.

The principal water-bearing strata in the study area include Quaternary alluvium and Neogene sedimentary rocks underlying the floor of Petaluma valley and surrounding lowlands, as well as permeable zones in Miocene and Pliocene volcanic rocks in contact with the sedimentary section in the eastern part of the PVW. Various rocks underlie Quaternary alluvium and include, in generally descending order, the Quaternary mixed unit, a heterogeneous sequence possibly correlative with the Glen Ellen Formation; the Wilson Grove and Petaluma Formations; and the Sonoma Volcanics. Geophysical investigations and well data indicate that the Franciscan Complex is shallowest in the west and southwest parts of the PVW, where the Franciscan Complex is as shallow as 100–330 feet (ft) beneath surface outcrops of the Wilson Grove Formation. Basin depth increases rapidly to the east, and the northeast Franciscan Complex altitude is deeper than 3,000 ft below the North American Vertical Datum of 1988. The principal aquifers occupy fault-bounded domains where distinct stratigraphic packages are present in specific fault blocks because of the combined effects of extent of original deposition, structural disruption, and subsequent erosion.

Geologic materials within the depth range perforated by wells vary with location in the PVW. In the northwest part of the watershed, wells that penetrate Wilson Grove Formation commonly penetrate fine-grained sand that have relatively high specific capacities and specific yields that result in good well yields and small drawdowns. Beneath the valley axis and in the eastern part of the PVW, wells commonly penetrate layered sequences of heterogeneous, fine-grained or poorly sorted sediments that have generally low specific capacities and specific yields that result in low-to-modest well yields and large drawdowns. Well productivity is generally higher where wells are open to gravel or sand intervals in these layered sequences. In most parts of the study area, shallow groundwater flow is unconfined; groundwater may be confined at depth where aquifers are sand and gravel lenses in dominantly clay sequences. Fine-grained material either interbeds within coarser-grained materials or is in thick, but not laterally extensive, beds.

Surface water in the PVW originates along the southwest slopes of Sonoma Mountain, the southern slopes of Meacham Hill, the eastern slopes of Wiggins Hill, and Burdell Mountain. Flow in the upper reach of the Petaluma River and its tributaries is seasonal; when there are drier-than-normal winters, the main-stream channels will often go dry during the summer. The Petaluma River flows from the confluence of Willow Brook, Lichau Creek, and Wiggins Creek southeast through Denman Flat and the City of Petaluma before flowing through the Petaluma marsh and into San Pablo Bay. The lower reach of the Petaluma River is tidally influenced and can flood during periods of high flow. Streamflow in the Petaluma River is monitored using two streamgages operated by the U.S. Geological Survey (USGS) and five streamgages operated by the City of Petaluma. The city also manages 14 streamgages on tributaries to the Petaluma River.

Measured streamflows at USGS streamgage 11459150 indicate that streamflow is influenced by seasonal and annual variations in precipitation and runoff. Additionally, the data indicate that streamflow can sometimes be less than the magnitude of flow in response to tidal fluctuations. Streamflow data collected along the Petaluma River by the USGS indicated that (1) the upper reach of the Petaluma River was consistently dry; (2) the river gains flow from the confluence with Willow Brook to just north of the confluence with Lynch Creek, where streamflow becomes tidally affected; and (3) San Antonio Creek generally gains flow.

Sources of groundwater recharge in the PVW are infiltration from precipitation, seepage from the Petaluma River and its tributaries, irrigation return flow, and intrusion from San Pablo Bay and adjacent saltwater marshes. Estimates of average annual natural recharge in the PVW range from 25,000 to 40,000 acre-ft. Groundwater discharges as base flow to streams, spring flow, evapotranspiration (ET), and groundwater pumpage, but base flows and spring flows have not been estimated. Total ET may equal 165,100 acre-ft/yr. The median annual pumpage by the City of Petaluma was about 375 acre-feet (acre-ft), but agricultural and rural pumpage have not been estimated. Groundwater recharge to and discharge from the PVW also can be underflow across the PVW boundary into or out of neighboring groundwater basins.

A comparison of groundwater-level contour maps from 1951 through the 2010s shows little change in direction of groundwater movement during the period, with minor changes in groundwater levels next to the non-tidally influenced reach of the Petaluma River. Groundwater-level contour maps indicate that groundwater flows from the east and west boundaries of the watershed toward the Petaluma River along the axis of the valley. The effects of faults on the groundwater system have not been determined, but maps indicate that the Bloomfield, Cinnabar School, Meacham Hill, and Tolay faults likely do not influence groundwater flow, whereas the Petaluma valley fault could influence groundwater flow. Groundwater also discharges to the northern, non-tidally influenced reach of the Petaluma River. Along the southern, tidally influenced reach of the Petaluma River, changes in river water-surface altitude result in either gaining or losing conditions in response to tidal fluctuations, allowing infiltrating river water to mix with groundwater in areas near the river. Hydrographs indicate groundwater levels have remained consistent throughout the watershed for the respective periods of record for the groundwater wells, except for slight decreases in the northern part of the Petaluma Formation that respond to seasonal pumping and precipitation events.

References Cited

Allen, J.R., 2003, Stratigraphy and tectonics of Neogene strata, northern San Francisco Bay Area: San Jose State University, M.S. thesis, 183 p.

Blake, M.C., Jr., Graymer, R.W., and Jones, D.L., 2000, Geologic map and map database of parts of Marin, San Francisco, Alameda, Contra Costa, and Sonoma Counties, California: U.S. Geological Survey Miscellaneous Field Studies MF 2337, scale 1:62,500.

Brabb, E.E., Powell, C.L., II, and Brocher, T.M., 2001, Preliminary compilation of data for selected oil test wells in northern California: U.S. Geological Survey Open-File Report 01–152, 310 p. [Available at https://doi.org/10.3133/ofr01152.]

California Department of Conservation, Division of Oil, Gas, and Geothermal Resources, 2014, Division of oil, gas, and geothermal resources: Sacramento, Calif., State of California, accessed July 2014 at https://www.conservation.ca.gov/dog.

California Department of Water Resources, 2014, Petaluma Valley groundwater basin: Bulletin 118 groundwater basin descriptions–Update June 30, 2014: Sacramento, Calif., State of California, 5 p. [Available at https://water.ca.gov/-/media/DWR-Website/Web-Pages/Programs/Groundwater-Management/Bulletin-118/Files/2003-Basin-Descriptions/2_001_PetalumaValley.pdf.]

California Department of Water Resources, 2018a, California Water Data Library (WDL), accessed January 30, 2018, at https://wdl.water.ca.gov.

California Department of Water Resources, 2018b, California Statewide Groundwater Elevation Monitoring (CASGEM) database, accessed January 30, 2018, at https://www.casgem.water.ca.gov.

California Department of Water Resources, 2020, Bulletin 118-Groundwater basins: California Department of Water Resources, accessed November 4, 2020, at https://gis.water.ca.gov/arcgis/rest/services/Geoscientific/i08_B118_CA_GroundwaterBasins/FeatureServer/0.

Cardwell, G.T., 1958, Geology and ground water in the Santa Rosa and Petaluma Valley areas, Sonoma County, California: U.S. Geological Survey Water-Supply Paper 1427, 273 p.

City of Petaluma, 2015, City of Petaluma floodplain management plan, accessed August 16, 2016, at https://storage.googleapis.com/proudcity/petalumaca/uploads/2020/02/2015-Final-Floodplain-Management-Plan-Complete.pdf.

City of Petaluma, 2016, 2015 Urban Water Management Plan, accessed February 16, 2017, at https://storage.googleapis.com/proudcity/petalumaca/uploads/2020/02/FINAL-2015-UWMP-1.pdf.

Davies, E.A., 1986, The stratigraphic and structural relationships of the Miocene and Pliocene formations of the Petaluma valley area: University of California, Berkeley, M.S. thesis, 96 p.

Flint, A.L., and Flint, L.E., 2007, Application of the basin characterization model to estimate in-place recharge and runoff potential in the Basin and Range Carbonate-Rock Aquifer System, White Pine County, Nevada, and Adjacent Areas in Nevada and Utah: U.S. Geological Survey Scientific Investigations Report 2007–5099, 21 p. [Available at https://doi.org/10.3133/sir20075099.]

Ford, E.W., 2007, Geology of Burdell Mountain and implications for long term slip along the east Bay fault system, California: San Francisco, California, San Francisco State University, M.S. thesis, 96 p.

Ford, R.S., 1975, Evaluation of ground water resources: Sonoma County, volume 1: geologic and hydrologic data: California Department of Water Resources Bulletin 118–4, 177 p., 1 plate.

Fox, K.F., Jr., 1983, Tectonic setting of late Miocene, Pliocene, and Pleistocene rocks in part of the Coast Ranges north of San Francisco, California: U.S. Geological Survey Professional Paper 1239, 33 p. [Available at https://doi.org/10.3133/pp1239.]

Fox, K.F., Jr., Fleck, R.J., Curtis, G.H., and Meyer, C.M., 1985, Potassium-argon and fission-track ages of the Sonoma Volcanics in an area north of San Pablo Bay, California: U.S. Geological Survey Miscellaneous Field Studies Map MF 1753, scale 1:250,000.

Goldman, H.B., ed., 1969, Geologic and engineering aspects of San Francisco Bay fill: California Division of Mines and Geology Special Report, v. 97, 130 p.

Graymer, R.W., Brabb, E.E., Jones, D.J., Barnes, J., Nicholson, R.S., and Stamski, R.E., 2007, Geologic map and map database of eastern Sonoma and western Napa Counties, California: U.S. Geological Survey Scientific Investigations Map 2956, scale 1:100,000.

Graymer, R.W., Sarna-Wojcicki, A.M., Walker, J.P., McLaughlin, R.J., and Fleck, R.J., 2002, Controls on timing and amount of right-lateral offset on the East Bay fault system, San Francisco Bay region, California: Geological Society of America Bulletin, v. 114, no. 12, p. 1471–1479. [Available at https://doi.org/10.1130/0016-7606(2002)114%3C1471:COTAAO%3E2.0.CO;2.]

Herbst, C.M., 1982, Evaluation of ground water resources: Sonoma County: Volume 3, Petaluma Valley: California Department of Water Resources Bulletin 118-4, 94 p.

Herbst, C.M., Jacinto, D.M., and McGuire, R.A., 1982, Evaluation of ground water resources, Sonoma County, volume 2: Santa Rosa Plain: California Department of Water Resources Bulletin 118-4, 107 p., 1 plate.

Hitchcock, C.S., and Kelson, K.I., 1998, Assessment of seismogenic sources between the Rodgers Creek and San Andreas faults, northwestern San Francisco Bay region, Sonoma County, California, *in* Zoback, M.L., ed., Proceedings of the first annual northern California earthquake hazards workshop, January 13–14, 2004: U.S. Geological Survey Open-File Report 2004–1424, 50 p.

Isaaks, E.H., and Srivastava, R.M., 1989, An introduction to applied geostatistics: New York, Oxford University Press, 561 p.

Journel, A.G., and Huijbregts, C.J., 1978, Mining geostatistics: New York, Academic Press, 600 p.

Langenheim, V.E., Graymer, R.W., Jachens, R.C., McLaughlin, R.J., Wagner, D.L., and Sweetkind, D.S., 2010, Geophysical framework of the Northern San Francisco Bay region, California: Geosphere, v. 6, no. 5, p. 594–620. [Available at https://doi.org/10.1130/GES00510.1.]

McDonald, S.D., Nichols, D.R., Wright, N.A., and Atwater, B., 1978, Map showing thickness of young bay mud, southern San Francisco Bay, California: U.S. Geological Survey Miscellaneous Field Studies Map MF-976, scale 1:125,000.

McLaughlin, R.J., Sliter, W.V., Sorg, D.H., Russell,P.C., and Sarna-Wojcicki, A.M., 1996, Large-scale right-slip displacement on the East San Francisco Bay Region fault system, California—Implications for location of late Miocene to Pliocene Pacific plate boundary: Tectonics, v. 15, no. 1, p. 1–18. [Available at https://doi.org/10.1029/95TC02347.]

Micheli, E., Flint, L.E., Flint, A.L., Weiss, S., and Kennedy,M., 2012, Downscaling future climate projections to the watershed scale: A north San Francisco Bay case study, San Francisco Estuary and watershed Science v. 10, no. 4. [Available at https://doi.org/10.15447/sfews.2012v10iss4art2.]

Nilsen, T.H., and Clarke, S.H., Jr., 1989, Late Cenozoic basins of northern California: Tectonics, v. 8, no. 6, p. 1137–1158. [Available at https://doi.org/10.1029/TC008i006p01137.]

Powell, C.L., II, Allen, J.R., and Holland, P.J., 2004, Invertebrate paleontology of the Wilson Grove Formation (late Miocene to late Pliocene), Sonoma and Marin counties, California, with some observations on its stratigraphy, thickness, and structure: U.S. Geological Survey Open-File Report 2004–1017, 105 p., 2 plates.

Randolph-Loar, C.E., 2002, Neotectonics of the Rodgers Creek fault, Sonoma County, California: San Francisco, California, San Francisco State University, unpublished M.S. thesis, 94 p.

Ruhl, C.A., and Simpson, M.R., 2005, Computation of discharge using the index-velocity method in tidally affected areas: U.S. Geological Survey Scientific Investigations Report 2005–5004, 31 p. [Available at https://doi.org/10.3133/sir20055004.]

Shepherd, M., 2009, 3-D geocellular modeling, *in* Shepherd, M., ed., Oil field production geology: American Association of Petroleum Geologists Memoir 91, p. 175–188, Published by The American Association of Petroleum Geologists Tulsa, Oklahoma. [Available at https://doi.org/10.1306/13161205M913372.]

Sonoma County, 2006, Sonoma County general plan 2020—Draft Environmental Impact Report, Sonoma County Permit and Resource Management Department, January 2006, accessed July 18, 2016, at https://sonomacounty.ca.gov/PRMD/Planning/Significant-EIRs/#GP2020.

Sonoma Resource Conservation District, 2015, Draft Petaluma watershed enhancement plan, accessed July 19, 2016, at https://sonomarcd.org/wp-content/uploads/2017/06/Petaluma-Watershed-Enhancement-Plan-2015.pdf.

Sweetkind, D.S., and Taylor, E.M., 2010, Digital tabulation of geologic and hydrologic data from water wells in the northern San Francisco Bay region, northern California: U.S. Geological Survey Open-File Report 2010–1063, 125 p. [Available at https://doi.org/10.3133/ofr20101063.]

Sweetkind, D.S., Taylor, E.M., McCabe, C.A., Langenheim,V.E., and McLaughlin, R.J., 2010, Three-dimensional geologic modeling of the Santa Rosa Plain, California: Geosphere, v. 6, no. 3, p. 237–274. [Available at https://doi.org/10.1130/GES00513.1.]

Sweetkind, D.S., 2019, Data release of three-dimensional hydrogeologic framework model of the Petaluma Valley watershed, Sonoma County, California: U.S. Geological Survey data release. [Available at https://doi.org/10.5066/P9NL90P8.]

U.S. Geological Survey, 2016a, USGS 11459150 Petaluma River A Copland Pumping Station A Petaluma CA: U.S. Geological Survey National Water Information System: U.S. Geological Survey web interface, accessed July 18, 2016, at https://doi.org/10.5066/F7P55KJN. [Site information directly accessible at https://nwis.waterdata.usgs.gov/nwis/measurements/?site_no=11459150&agency_cd=USGS&amp.]

U.S. Geological Survey, 2016b, USGS 11459000 Petaluma R A Petaluma CA: U.S. Geological Survey National Water Information System: U.S. Geological Survey web interface, accessed July 18, 2016, at https://doi.org/10.5066/F7P55KJN. [Site information directly accessible at https://waterdata.usgs.gov/ca/nwis/inventory/?site_no=11459000&agency_cd=USGS&amp.]

U.S. Geological Survey, 2016c, USGS 11459300 San Antonio C NR Petaluma CA: U.S. Geological Survey National Water Information System: U.S. Geological Survey web interface, accessed July 18, 2016, at https://doi.org/10.5066/F7P55KJN. [Site information directly accessible at https://nwis.waterdata.usgs.gov/ca/nwis/dv/?referred_module=sw&site_no=11459300.]

U.S. Geological Survey, 2018, USGS 11459150 Petaluma River A Copland Pumping Station A Petaluma CA: U.S. Geological Survey National Water Information System: U.S. Geological Survey web interface, accessed July 26, 2018, at https://doi.org/10.5066/F7P55KJN. [Site information directly accessible at https://waterdata.usgs.gov/ca/nwis/uv/?site_no=11459150.]

Wagner, D.L., Fleck, R.J., Sarna-Wojcicki, A.M., and Deino,A., 2005, Day 1—Golden Gate to southern Sonoma County, Rodgers Creek fault, Burdell Mountain, Donnell Ranch, and southern Sonoma Volcanics, *in* Stevens, C., and Cooper, J., eds., Late Neogene transition from transform to subduction margin east of the San Andreas fault in the wine country of the northern San Francisco Bay area, California: Pacific Section, SEPM (Society for Sedimentary Geology), p. 1–28.

Wagner, D.L., and Gutierrez, C.I., 2010, Geologic map of the Napa 30'x60' quadrangle, California: California Geological Survey Preliminary Geologic Maps, scale 1:100,000, pamphlet, accessed November 9, 2016, at https://ngmdb.usgs.gov/Prodesc/proddesc_94519.htm.

Wagner, D.L., Saucedo, G.J., Clahan, K.B., Fleck, R.J., Langenheim, V.E., McLaughlin, R.J., Sarna-Wojcicki, A.M., Allen, J.R., and Deino, A.L., 2011, Geology, geochronology, and paleogeography of the southern Sonoma volcanic field and adjacent areas, northern San Francisco Bay region, California: Geosphere, v. 7, no. 3, p. 658–683. [Available at https://doi.org/10.1130/GES00626.1.]

Watt, J., Ponce, D., Parsons, T., and Hart, P., 2016, Missing link between the Hayward and Rodgers Creek faults: Science Advances, v. 2, no. 10, 8 p. [Available at https://doi.org/10.1126/sciadv.1601441.]

Weaver, C.E., 1949, Geology of the Coast Ranges immediately north of the San Francisco Bay region, California: Geological Society of America Memoir 35, 242 p. [Available at https://doi.org/10.1130/MEM35-p1.]

West Yost, W., 2004, Technical Memorandum No. 4: Groundwater Feasibility Study, accessed August 4, 2014, at https://cityofpetaluma.net/cdd/pdf/riverfront/West-Groundwater-Feasibility-Study.pdf.

Western Regional Climate Center, 2016, WRCC 046826 Petaluma AP, CA: Western Regional Climate Center, accessed June 26, 2016, at http://wrcc.dri.edu/cgi-bin/cliMAIN.pl?ca6826.

Woolfenden, L.R., and Hevesi, J.A., 2014, Santa Rosa Plain hydrologic model results, chap. E *of* Woolfenden, L.R., and Nishikawa, T., Simulation of groundwater and surface-water resources of the Santa Rosa Plain watershed, Sonoma County, California: U.S. Geological Survey Scientific Investigations Report 2014–5052, p. 151–184.

Wright, T.L., 1992, Field trip guide to Late Cenozoic geology in the North Bay Region: Northern California Geological Society, 151 p. [Available at http://www.ncgeolsoc.org/wp-content/uploads/2018/01/1992-1_Field-Trip-Guide-to-Late-Cenozoic-Geology-in-the-North-Bay-Region.pdf.]

Chapter C. Water Quality of the Petaluma River Watershed, Sonoma County, California

By Nick F. Teague

Introduction

The U.S. Geological Survey (USGS), in cooperation with the Sonoma County Water Agency and the City of Petaluma, used groundwater and surface water-quality to refine the conceptual model of the hydrologic system in the Petaluma valley watershed (PVW, fig. C1). Source, age, and water quality of groundwater were characterized for the PVW using analyses for selected physical properties, inorganic constituents, and stable and radioactive isotopes. Available data were used collaboratively to infer sources of groundwater recharge, groundwater movement, and mixing of groundwater with other water sources. Two possible sources of groundwater impairments in the PVW are saline water and infiltration of high-nitrate water at land surface. One of the goals of this study was to identify the sources and areas where groundwater may be mixing with these sources of impairments. This chapter describes (1) the recharge source and age of groundwater; (2) mixing of groundwater with surface water and other water sources; and (3) the areal, depth-dependent, and temporal variations in groundwater quality. Data used in this characterization were compiled from previous investigations; from databases maintained by the California Department of Public Health (CDPH), the California Department of Water Resources (CDWR), and various public-supply purveyors; and from the analyses of water samples collected from surface-water sites and groundwater wells by the U.S. Geological Survey (USGS) as part of this study. These data represent untreated water samples, which are not equivalent to analyses used for compliance to drinking-water-quality standards. For the purposes of this chapter, specific surface-water sites, springs, and groundwater wells are identified by the abbreviations "SW," "SP," and "W," respectively.

One of the earliest published geohydrologic investigations of the PVW to include water quality was by Cardwell (1958). This study included a limited assessment of water quality based on the analyses of samples from 55 wells and 4 streams, of which 34 analyses were relatively complete for major ions. Cardwell (1958) characterized the quality of groundwater in the northern part of Petaluma Valley groundwater basin as generally satisfactory for most uses based on dissolved solids and hardness concentrations in the range of 250 to 500 milligrams per liter (mg/L) and 40 to 320 mg/L, respectively. However, Cardwell (1958) noted several areas where water was unsatisfactory for use based on high concentrations of chloride. Chloride was cited as a constituent of particular concern in the southern part of Petaluma valley, adjacent to the Petaluma marsh wildlife area (fig. C1), where groundwater was contaminated by intrusion of brackish bay water or unflushed connate water (Cardwell, 1958). The term connate implies that the solute source is older seawater trapped in the geologic formations at the time they were deposited (Hem, 1992). Cardwell (1958) hypothesized that increases in chloride, hardness, and dissolved solids in wells near Petaluma Creek (now referred to as the Petaluma River) were caused by seasonal pumping depressions drawing recharge from the brackish water of the tidal Petaluma River. The Petaluma River (fig. C1), upstream from the tidally influenced reach, was described by Cardwell (1958) as representative of discharging groundwater, but with higher chloride concentrations than in uncontaminated groundwater of the Wilson Grove Formation (fig. C1). Analysis from a sample collected along the lower reach of the Petaluma River indicated considerable mixing of river and San Pablo Bay water (fig. C1; Cardwell, 1958).

In 2000, the California State Water Resources Control Board (SWRCB), USGS, and Lawrence Livermore National Laboratory (LLNL) initiated the Groundwater Ambient Monitoring Assessment (GAMA) Program to assess the quality of ambient groundwater in aquifers used for drinking-water supply and to establish a baseline groundwater-quality monitoring program. The GAMA Program partitioned California into 10 hydrogeologic provinces and 35 study units in these provinces (Belitz and others, 2003). For each study unit, statistical and graphical methods were used to explain relations between water quality and various associative factors, such as well depth, groundwater age, oxidation-reduction (redox) status of the subsurface, and position along a conceptual flow path (Belitz and others, 2003). One such study unit was the north San Francisco Bay (NSF) study unit (not shown), which includes the PVW (Kulongoski and others, 2006, 2010).

In 2004, samples of untreated water were collected from 89 wells in the NSF Study Unit, including 4 wells from the PVW. Analysis of the samples collected from the four wells in the PVW included inorganic and organic constituents (Kulongoski and others, 2006). Inorganic constituents included major and minor elements and nutrients, and organic constituents included volatile organic compounds (VOCs), pesticides and pesticide degradates, and organic wastewater indicators. Stable isotopes (^{18}O, ^{2}H, and ^{13}C) and radioactive isotopes (^{3}H and ^{14}C) were used to characterize sources or ages of groundwater (Kulongoski and others, 2006). Results for the NSF study unit showed that anthropogenic constituents were not detected at concentrations higher than regulatory thresholds, and only a few naturally present constituents (arsenic, radon-222, microbiological contaminants, dissolved solids, iron, manganese, boron, vanadium, and lead) were detected at concentrations above regulatory thresholds (Kulongoski and others, 2006, 2010).

Methods of Sample Collection and Analysis

The methods for the collection and analyses of surface-water and groundwater samples for this study are described in subsequent sections using two categories: (1) historical samples and (2) recent samples. Historical samples were primarily collected prior to 2015 by the CDWR, the CDPH, public-supply purveyors from the City of Petaluma, and the USGS, as part of previous studies (Teague, 2022). Recent samples were collected in 2015 and 2016 by the USGS (Teague, 2022). Methods for historical and recent samples have varied in accordance with different sampling objectives and in response to improvements in sampling protocols and analytical techniques. Sampling protocols and analytical techniques for samples collected and analyzed as part of the GAMA NSF study unit are described by Kulongoski and others (2006, 2010). All non-USGS laboratories used as sources of data in this report have met the requirements of California Code of Regulations Title 22, Division 4, Chapter 19 on the certification of environmental laboratories (Thomson Reuters, 2018a), including successful participation in the California Environmental Laboratory Accreditation Program (ELAP).

Results of chemical analysis of samples from 66 groundwater wells, 3 springs, and 2 surface-water sites are presented in Teague (2022). Data presented in Teague (2022) are the most recent, complete water-quality data for each site and are the data used in most analyses described in this report. In one case, well W48 had an incomplete most recent set of data, and data from the previous sampling effort were used to create the most complete dataset available. In other cases (such as nitrate data for wells W11, W19, W20, W29, W34, W48, W51, W52, W53, W55, W56, W74, and W75; fig. C1; Teague, 2022), more recent data were available for individual constituents; however, the most recent, complete datasets were used to provide the best understanding of current conditions in the PVW. The accuracies of major cation and anion data were evaluated by calculating charge-balance errors. In this report, data with charge-balance errors exceeding 10 percent were not used in interpretations of major-ion data. Data from replicate samples collected as part of this study and previous USGS studies were used to evaluate the accuracy of other constituents analyzed in this report. Constituents are classified for interpretation as high (greater than or equal to the 75th percentile for the dataset), moderate (between the 75th and 25th percentiles for the dataset), or low (less than or equal to the 25th percentile for the dataset), unless otherwise stated.

Time-series data (concentrations over time) for nitrate were evaluated to provide an understanding of temporal trends in water quality in the PVW (Teague, 2022). Wells were chosen from wells listed in Teague (2022) to maximize spatial coverage and to provide the longest periods of record. The majority of the wells evaluated for temporal trends are public-supply wells perforated in the Petaluma Formation and Quaternary mixed unit. The information provided by characterizing these wells may not provide a complete understanding of water-quality changes in the watershed; however, the well-characterization information does provide insight into the changes in the chemistry of groundwater used as public supply.

Historical Sample Collection and Analysis

Water-quality data for groundwater collected from seven wells were reported by CDWR (Teague, 2022). Data from the CDWR presented in this report are from samples that were collected and analyzed following referenced methods of the American Public Health Association (2005) and the U.S. Environmental Protection Agency (1993, 1994). All CDWR samples were analyzed at the California Department of Water Resources Bryte Analytical Laboratory in West Sacramento, California (not shown; Aaron Cuthbert, California Department of Water Resources, written commun., 2017).

Water-quality data for 7 wells presented in this report were reported by the City of Petaluma, and water-quality data for 35 wells and 1 spring were reported by the CDPH (Teague, 2022). Data were obtained from samples that were generally collected, analyzed, or both by consultants or contracted laboratories. Sampling and analyses were completed in accordance with requirements of California Code of Regulations Title 22 (Thomson Reuters, 2018a), by using methods referenced by the American Public Health Association (2005) and the U.S. Environmental Protection Agency (1993, 1994).

Water-quality data for six wells and one spring presented in this report were sampled by the USGS during studies from 2004 to 2012 (Teague, 2022). These data were collected in accordance with the USGS National Field Manual for Collection of Water-Quality Data (U.S. Geological Survey, variously dated). These methods are described in greater detail in the following section.

Recent Sample Collection and Analysis

Water-quality samples were collected as part of this study from 11 wells, 1 spring, and 2 surface-water sites (fig. C1; table C1; Teague, 2022) by the USGS in 2015 and 2016. Samples from wells W1-3, W5, W17-18, W21-22, W42, W72-73 and spring SP1 were collected by the USGS in April 2015 and October 2015 for the analysis of selected inorganic constituents, including major and minor (trace) elements, nutrients, chemical and physical properties (turbidity, dissolved oxygen, pH, specific conductance, temperature, and dissolved solids), and stable (^{18}O, ^{2}H, ^{13}C) and radioactive isotopes (^{3}H and ^{14}C). Samples from surface-water sites SW1 and SW2 were collected by the USGS in May 2016 for the analysis of selected inorganic constituents, including major, minor, and trace elements, nutrients, chemical and physical properties (turbidity, dissolved oxygen, pH, specific conductance, temperature, and dissolved solids), and stable and radioactive isotopes. Samples were collected, treated, and preserved following procedures outlined by the U.S. Geological Survey (variously dated).

Five laboratories managed or contracted by the USGS performed chemical analyses for the PVW study. The USGS National Water-Quality Laboratory (NWQL), in Denver, Colorado, did analyses for inorganic analytes (major ions, trace elements, and nutrients). The following analytical methods were used by the NWQL: major ions were analyzed by inductively coupled plasma with atomic-emission spectrometry (ICP-AES; Fishman and Friedman, 1989; Fishman, 1993; American Public Health Association, 2012); trace elements were analyzed by ICP-AES, inductively coupled plasma with mass spectrometry (ICP-MS), auto-segmented-flow/ion-selective electrode, colorimetry, and automated batch analyzer (Fishman and Friedman, 1989; Fishman, 1993; Struzeski and others, 1996; Garbarino, 1999; Garbarino and others, 2006); and nutrients were analyzed by colorimetry (Fishman, 1993; Patton and Truitt, 2000). The USGS Reston Stable Isotope Laboratory analyzed surface and groundwater samples for ^{2}H and ^{18}O by using a hydrogen-water-equilibration technique (Révész and Coplen, 2008a) and an automated version of the carbon dioxide equilibration technique (Révész and Coplen, 2008b).

Contracted laboratories included the University of Miami Tritium Laboratory in Miami, Florida, and the Woods Hole Oceanographic Institute's National Ocean Sciences Accelerator Mass Spectrometry (NOSAMS) Facility in Woods Hole, Massachusetts. Samples collected for ^{3}H were analyzed at the University of Miami Tritium Laboratory using an electrolytic enrichment with gas proportional counting technique, as described by Ostlund and Dorsey (1975) and the University of Miami Tritium Laboratory (2010). Samples for carbon isotopes (^{14}C and ^{13}C) were analyzed at the NOSAMS facility using accelerator mass spectrometry techniques similar to the methodology described by Fifield (1999).

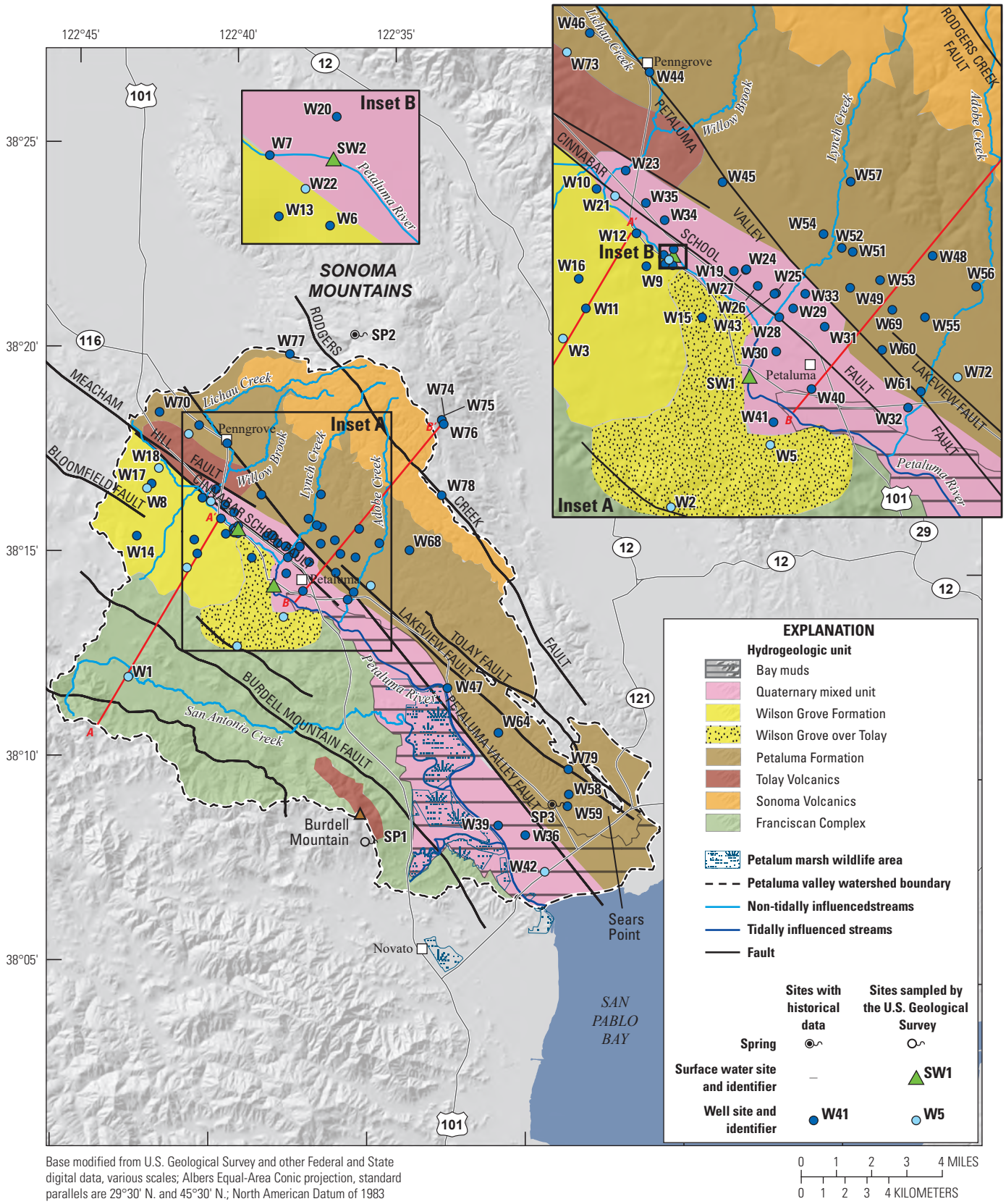

Figure C1. Sample sites in the Petaluma valley watershed, Sonoma County, California, 1974–2016; site information is provided in table C1.

Construction Information for Sampled Wells

Groundwater wells in this the study area span a wide range of depths and perforated (screened) intervals (table C1). Most are production (municipal and domestic) wells that are typically perforated over long intervals (greater than or equal to 100 feet). Perforation information is typically unavailable for older wells; some of these wells could have been constructed in uncased open holes, such that the entire hole is open to the surrounding aquifer units. Perforated intervals for many wells with water-quality data are composed either of a single continuous interval or multiple discrete intervals. For the purposes of this report, wells were categorized in four main classes based on the perforated interval: shallow, deep, mixed-depth, and unknown depth wells (table C1). The well-depth classifications were used to analyze differences in water chemistry between adjacent wells and to identify the hydrogeologic unit sampled by the well. If available, well-completion depth was used to identify the hydrogeologic units for wells with missing perforation data. Data from a total of 79 wells are presented in this report: 12 were shallow, 21 were deep, 20 were mixed depth, and 26 were unknown depth.

Given the spatial distribution of sampled wells and the relatively uniform spatial distribution of sample depths (fig. C2), data are assumed to be representative of the geochemistry of the PVW. Samples collected from wells in the PVW generally represent a single hydrogeologic unit, regardless of screen-interval depth (Donald S. Sweetkind, U.S. Geological Survey, written commun., 2017). Groundwater samples collected from shallow and deep wells in the western part of the PVW primarily characterize the Wilson Grove Formation, but some of the deep wells may penetrate the Franciscan Complex. In the southern part of the PVW, where San Francisco Bay mud deposits overlie deposits of the Quaternary mixed unit, samples collected from shallow wells may represent groundwater from both hydrogeologic units. Wells W74–76 are outside of the PVW boundary and are not shown within a hydrogeologic unit in figures C1 and C2; however, these wells are perforated in the Sonoma Volcanics (Donald S. Sweetkind, U.S. Geological Survey, written commun., 2017).

Table C1. Construction information for selected wells used to collect and compile water-quality data, Petaluma valley watershed, Sonoma County, California.

[3D, three-dimensional; USGS, U.S. Geological Survey; —, no data; CDWR, California Department of Water Resources; CDPH, California Department of Public Health; NA, not available]

Map number (fig. C1)	3D framework formation	Local identifier	USGS station number	State well number	Depth (feet)	Top of screen (feet)	Bottom of screen (feet)	Depth class	Data source
W1	Franciscan	LAGUNA SCHOOL	381158122425601	4N/8W-11N	—	—	—	—	USGS files
W2	Franciscan	HELEN PUTNAM PARK	381248122393101	—	300	160	300	Mixed	USGS[1]
W3	Franciscan	WILSON ELEMENTARY	381441122411101	5N/8W-25R	225	—	—	Shallow	USGS[1]
W4	Tolay/Franciscan	—	—	4N/7W-4F	184	40	184	Shallow	CDWR[2]
W5	Tolay/Franciscan	Nygard Well	381332122380501	4N/7W-4B	—	—	—	—	USGS[1]
W6	Wilson Grove	Cinnabar Theater	—	—	—	—	—	—	CDPH[3]
W7	Wilson Grove	Willowbrook Alehouse	—	—	220	—	—	Mixed	CDPH[3]
W8	Wilson Grove	Liberty School	—	5N/8W-14H1	—	—	—	—	CDPH[3]
W9	Wilson Grove	Cinnabar Elementary	—	5N/7W-20N6	408	270	408	Deep	CDPH[3]
W10	Wilson Grove	KOA Well 1	—	—	—	—	—	—	CDPH[3]
W11	Wilson Grove	Mushroom Farm 1	—	—	560	140	540	Mixed	CDPH[3]
W12	Wilson Grove	Boulevard Heights	—	—	350	250	350	Deep	CDPH[3]
W13	Wilson Grove	Lombardi Deli	—	—	295	140	—	Mixed	CDPH[3]
W14	Wilson Grove	Family Life Center	—	—	300	180	300	Mixed	CDPH[3]
W15	Wilson Grove	S-NSF-H26	381458122390701	5N/7W-29G1	189	—	—	Shallow	USGS[1]
W16	Wilson Grove	—	—	5N/7W-19N	180	130	180	Shallow	CDWR[2]
W17	Wilson Grove	Hart Well	381636122423001	5N/8W-14K	178	136	176	Shallow	USGS[1]
W18	Wilson Grove	Garden Valley Ranch	381706122420901	5N/8W-13D	—	—	—	—	USGS[1]
W19	Mixed	Capri-1	—	5N/7W-21N2	450	90	450	Mixed	CDPH[3]
W20	Mixed	Livestock Auction Yard	—	5N/7W-20	235	65	235	Mixed	CDPH[3]
W21	Mixed	Stony Point Well	381619122402801	5N/7W-28Q	599	318	560	Deep	USGS[1]
W22	Mixed	Kelp Well	381537122393901	5N/7W-20L	260	—	—	—	USGS[1]
W23	Mixed	KOA Well 2	—	—	—	—	—	—	CDPH[3]
W24	Mixed	—	—	5N/7W-21P8	503	331	503	Deep	CDPH[3]
W25	Mixed	Park Place	—	—	314	—	—	—	CDPH[3]
W26	Mixed	Station 9	—	5N/7W-27E	440	180	420	Mixed	CDPH[3]
W27	Mixed	Station 11	—	5N/7W-12N	520	280	500	Deep	CDPH[3]
W28	Mixed	Station 14	—	—	—	—	—	—	CDPH[3]
W29	Mixed	Lucchesi	—	—	450	180	440	Mixed	CDPH[3]
W30	Mixed	S-NSF-VP01	381436122380101	5N/7W-28Q1	64	24	64	Shallow	USGS files

Table C1. Construction information for selected wells used to collect and compile water-quality data, Petaluma valley watershed, Sonoma County, California.—Continued

[3D, three-dimensional; USGS, U.S. Geological Survey; —, no data; CDWR, California Department of Water Resources; CDPH, California Department of Public Health; NA, not available]

Map number (fig. C1)	3D framework formation	Local identifier	USGS station number	State well number	Depth (feet)	Top of screen (feet)	Bottom of screen (feet)	Depth class	Data source
W31	Mixed	#2 McDowell Park	—	—	530	180	520	Mixed	City of Petaluma[4]
W32	Mixed	Casa de Arroyo	—	5N/7W-35F	229	89	229	Shallow	City of Petaluma[4]
W33	Mixed	Miwok well	—	5N/7W-22N	425	305	385	Deep	City of Petaluma[4]
W34	Mixed	Scott Well 5	—	—	680	—	—	Deep	City of Petaluma[4]
W35	Mixed	Stub Street Well	—	—	596	440	554	Deep	City of Petaluma[4]
W36	Mixed	03N06W03C001M	—	3N/6W-3C	—	—	—	—	CDWR[2]
W37	Mixed	03N06W11B001M	—	3N/6W-11L	—	—	—	—	CDWR[2]
W38	Mixed	03N06W11L001M	—	3N/6W-20L	520	328	520	Deep	CDWR[2]
W39	Mixed	04N06W33R001M	—	4N/6W-33R	—	—	—	—	CDWR[2]
W40	Mixed	05N07W34E002M	—	5N/7W-34E	280	—	—	—	CDWR[2]
W41	Mixed	05N07W35H001M	—	5N/7W-35H	542	180	512	Mixed	CDWR[2]
W42	Mixed	SWEDBERG Old Farm #3 Well	380729122293601	3N/6W-11C	400	—	—	Deep	USGS[1]
W43	Mixed	28B1	381515122380401	5N/7W-28B	314	—	—	—	USGS[1]
W44	Petaluma	Nessco Well 2	—	5N/7W-7H3M	460	180	460	Deep	CDPH[3]
W45	Petaluma	Waugh-1	—	5N/7W-9P1	—	—	—	—	CDPH[3]
W46	Petaluma	Green Mill Inn	—	—	—	—	—	—	CDPH[3]
W47	Petaluma	Gilardi Water - 1	—	—	39	19	39	Shallow	CDPH[3]
W48	Petaluma	Adobe Christian Center	—	—	—	—	—	—	CDPH[3]
W49	Petaluma	Condiotti	—	—	360	220	360	Deep	CDPH[3]
W50	Petaluma	Miwok well	—	—	425	305	385	Deep	CDPH[3]
W51	Petaluma	Prince Park South	—	5N/7W-27	500	140	500	Mixed	CDPH[3]
W52	Petaluma	Prince Park North	—	—	480	180	480	Mixed	CDPH[3]
W53	Petaluma	Airport	—	—	607	200	440	Deep	CDPH[3]
W54	Petaluma	Kingsmill	—	—	420	200	400	Deep	CDPH[3]
W55	Petaluma	Cross Creek 2	—	5N/7W-26H	480	220	460	Deep	CDPH[3]
W56	Petaluma	NSFVP-35	381524122350601	5N/7W-24P2	300	85	166	Shallow	USGS[1]
W57	Petaluma	S-NSF-VP12	381633122365901	5N/7W-15K1	280	—	—	—	USGS[1]
W58	Petaluma	Cougar Mountain	—	—	216	116	216	Shallow	CDPH[3]
W59	Petaluma	Black Mountain	—	—	375	70	365	Mixed	CDPH[3]
W60	Petaluma	#1 La Tercera Park	—	—	500	160	420	Mixed	City of Petaluma[4]

Table C1. Construction information for selected wells used to collect and compile water-quality data, Petaluma valley watershed, Sonoma County, California.—Continued

[3D, three-dimensional; USGS, U.S. Geological Survey; —, no data; CDWR, California Department of Water Resources; CDPH, California Department of Public Health; NA, not available]

Map number (fig. C1)	3D framework formation	Local identifier	USGS station number	State well number	Depth (feet)	Top of screen (feet)	Bottom of screen (feet)	Depth class	Data source
W61	Petaluma	#4 Del Oro Park	—	—	500	180	460	Mixed	City of Petaluma[4]
W62	Petaluma	03N05W06C001M	—	3N/5W-6C	250	70	250	Mixed	CDWR[2]
W63	Petaluma	03N06W01Q001M	—	3N/6W-1Q	—	—	—	—	CDWR[2]
W64	Petaluma	04N06W21A001M	—	4N/6W-21A	—	—	—	—	CDWR[2]
W65	Petaluma	04N06W21Q001M	—	4N/6W-21Q	—	—	—	—	CDWR[2]
W66	Petaluma	04N06W27N001M	—	4N/6W-27N	—	—	—	—	CDWR[2]
W67	Petaluma	04N06W27R001M	—	4N/6W-27R	736	—	—	—	CDWR[2]
W68	Petaluma	05N06W30D001M	—	5N/6W-30D	155	65	155	Shallow	CDWR[2]
W69	Petaluma	05N07W26E001M	381507122362001	5N/7W-26E	605	—	—	—	CDWR[2]
W70	Petaluma	05N08W02H001M	—	5N/8W-2H	155	30	150	Shallow	CDWR[2]
W71	Petaluma	06N07W28L001M	382009122382601	6N/7W-28L	921	441	862	Deep	CDWR[2]
W72	Petaluma	Frates Well	381422122352001	5N/7W-36D	502	60	502	Mixed	USGS[1]
W73	Petaluma	Park Well	381757122411401	5N/8W-12A	330	160	330	Mixed	USGS[1]
W74	Sonoma Volcanics	Diamond A - 1	—	—	838	140	838	Mixed	CDPH[3]
W75	Sonoma Volcanics	Diamond A - 2	—	5N/6W-5	740	400	740	Deep	CDPH[3]
W76	Sonoma Volcanics	Diamond A - 3	—	—	559	193	558	Deep	CDPH[3]
W77	Sonoma Volcanics	Tamarack Lane	—	—	910	350	910	Deep	CDPH[3]
W78	Sonoma Volcanics	George Ranch	—	5N/6W-8R1	595	270	550	Deep	CDPH[3]
W79	Sonoma Volcanics	25E1	381000122285601	4N/6W-25E	216	—	—	—	USGS[1]
SP1	Franciscan	TWO BRICK SPRING	380806122351001	—	NA	NA	NA	Spring	USGS[1]
SP2	—	—	382029122355501	—	—	—	—	Spring	USGS[1]
SP3	Petaluma	Potable Spring	—	—	—	—	—	Spring	CDPH[3]
SW1	—	Petaluma R. at Copeland Pump Station	11459150	—	NA	NA	NA	SW	USGS[1]
SW2	—	Petaluma R. at Petaluma, CA	11459000	—	NA	NA	NA	SW	USGS[1]

[1]https://nwis.waterdata.usgs.gov/nwis/qw.

[2]https://wdl.water.ca.gov/waterdatalibrary/WaterQualityDataLib.aspx and https://water.ca.gov/Programs/Groundwater-Management/Wells/Well-Completion-Reports.

[3]https://www.cdph.ca.gov/certlic/drinkingwater/pages/EDTlibrary.aspx.

[4]City of Petaluma, written commun., 2016.

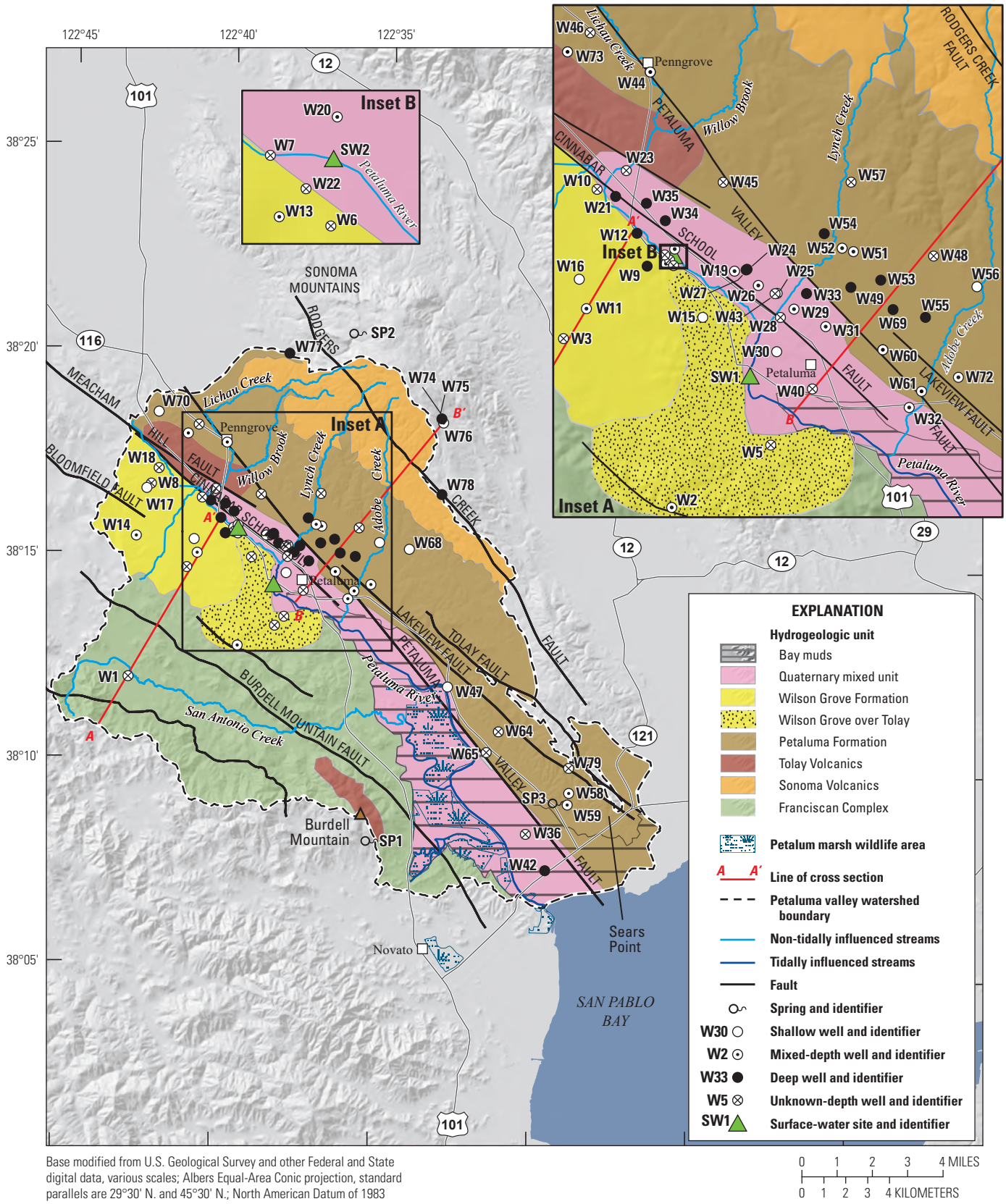

Base modified from U.S. Geological Survey and other Federal and State digital data, various scales; Albers Equal-Area Conic projection, standard parallels are 29°30' N. and 45°30' N.; North American Datum of 1983

Figure C2. Spatial distribution of sampled wells by depth-class with surface-water and spring sampling sites, Petaluma valley watershed, Sonoma County, California; site information is provided in table C1.

Source and Age of Groundwater

Stable (^{18}O, ^{2}H, ^{13}C) and radioactive isotopes (^{3}H and ^{14}C) were used to determine the sources and ages of water in the PVW (table C2). Analyses from samples collected for this study, and selected data from the GAMA NSF study (tables 6 and 7 in appendix B9 of Kulongoski and others, 2010), were used to gain insight into recharge processes and the evolution of water quality in the study area.

Oxygen-18 and Deuterium

The abundance of heavier stable (nonradioactive) isotopes ^{18}O and ^{2}H relative to isotopically lighter oxygen-16 (^{16}O) and hydrogen-1 (^{1}H) can be used to infer the source and evaporative history of water (Clark and Fritz, 1997). Differences in the ratios of $^{18}O/^{16}O$ and $^{2}H/^{1}H$ in samples relative to a standard known as Vienna Standard Mean Ocean Water (VSMOW = 0 per mil) are expressed in delta notation (δ) as per mil (Gat and Gonfiantini, 1981). Analytical precision is generally within about 0.2 and 2 per mil for $\delta^{18}O$ and $\delta^{2}H$, respectively (Coplen, 1994).

The $\delta^{18}O$ and $\delta^{2}H$ compositions of precipitation near coasts cluster along a line known as the global meteoric water line (GMWL) because much of the world's precipitation is derived from the evaporation of seawater (Craig, 1961), such that the relative fractionation of water isotopes is as follows:

$$\delta^{2}H = 8 \times (\delta^{18}O) + 10 \qquad \text{(C1)}$$

Isotopic composition of precipitation shows a general trend from heavier (precipitation having more ^{18}O and ^{2}H than ^{16}O and ^{1}H, respectively, represented by less negative values) to lighter (having less ^{18}O and ^{2}H than ^{16}O and ^{1}H, respectively, represented by more negative values) from the equator to the poles (Gat and Gonfiantini, 1981). Differences also result from fractionation as moist air masses move inland from coastal areas. The concentration of heavier isotopes relative to lighter isotopes decreases because heavier isotopes are preferentially concentrated in the liquid phase, and lighter isotopes are preferentially concentrated in the vapor phase during repeated cycles of evaporation and condensation (Clark and Fritz, 1997). In addition, precipitation that condenses at higher altitudes and at cooler temperatures tends to be isotopically lighter than precipitation that condenses at lower altitudes and warmer temperatures (Muir and Coplen, 1981). Therefore, isotopic ratios can be used to determine similarities or differences in water sources and can be used to help determine groundwater flow paths and mixing.

Ingram and others (1996) used stable-isotopic and salinity data to evaluate the composition and mixing of several surface-water reservoirs in San Pablo Bay and the surrounding region (fig. C1). This work showed a linear response in salinity and the isotopic composition of water in San Pablo Bay (line of best fit on fig. C3), with heavier isotopic ratios correlating with higher salinities. Seasonal variations in isotopic ratios and salinities of water samples in San Pablo Bay are a result of changes in the volume of freshwater inflow to the bay; lower isotopic ratios (more negative) and salinities are coincident with greater inflow during wet climatic periods (Ingram and others, 1996). The isotopic data for samples from San Pablo Bay (Ingram and others, 1996) are used in this report to compare mixing of surface-water and groundwater samples with water from San Pablo Bay.

Stable-isotope data from wells and springs in the PVW plot along the GMWL (fig. C3), indicating that the primary source of the water sampled is recharge of precipitation and movement of groundwater through the aquifer. The $\delta^{18}O$ and $\delta^{2}H$ values for water sampled from wells and springs in the PVW ranged from –7.55 to –5.50 per mil and –52.8 to –35.4 per mil, respectively (table C2). The data from wells and springs in the PVW do not show evidence of evaporation (a less negative shift in $\delta^{18}O$). The tight grouping of the stable-isotope data indicates a similar source of recharge for the wells and springs in the PVW. In a geographic sense, the source of recharge on the western side of the Petaluma River is likely in the Wilson Grove Formation Highlands groundwater basin, and the source of recharge on the eastern side of the river is likely in the Sonoma Mountains (see chapter B). These upland areas, however, are at similar latitudes and altitudes, which would result in similar stable-isotopic compositions. In the PVW, recharge of precipitation to the groundwater system can be from direct infiltration or infiltration of streamflow in the tributaries.

The isotopic ratios for surface-water samples from the Petaluma River (SW1 and SW2) are heavier than samples from groundwater wells (fig. C3), which indicates mixing with San Pablo Bay water that is moved upstream by tidal flow or evaporation. Surface-water samples were collected in 2016, a drought year (U.S. Geological Survey, 2018), so samples may be more strongly influenced by water moving tidally from San Pablo Bay or by evaporation than ones collected during wetter years with higher streamflows. Samples from SW1 and SW2 plot along an evaporative trend line between groundwater in the PVW and San Pablo Bay water sampled during dry climatic periods. These samples likely represent streamflow containing groundwater discharge that has undergone evaporation before discharging to San Pablo Bay. The sample from SW1 (downstream from SW2) plots farther along the evaporative trend line, away from the GMWL, indicating increasing evaporation as water moves downstream (fig. C3). Additionally, the sample from SW1 has a stable-isotopic ratio that plots within the range of relatively saline San Pablo Bay water sampled during dry climatic periods, indicating some possible mixing with tidally moved water from San Pablo Bay (fig. C3; Ingram and others, 1996).

Table C2. Summary of isotopic data for samples from selected surface-water sites and wells in the Petaluma valley watershed, Sonoma County, California, 1988–2016.

[3D, three-dimensional; mm/dd/yyyy, month/day/year; R, below detection level]

Map number (fig. C1)	3D framework formation	Date (mm/dd/yyyy)	Well-depth class	Carbon-14 counting error, water, filtered (percent modern)	Carbon-14, water, filtered (percent modern)	Tritium, water, unfiltered (picocuries per liter)	Delta carbon-13, water unfiltered (per mil)	Delta oxygen-18, water, unfiltered (per mil)	Deuterium/ protium ratio, water, unfiltered (per mil)	Carbon-14 age (years before present)
W1	Franciscan	10/23/2015	Unknown	0.18	82	0.7	–15.67	–5.5	–35.4	1,600
W2	Franciscan	10/20/2015	Mixed	0.06	9	R–0.3	–15.69	–6.6	–42.5	19,600
W3	Franciscan	10/22/2015	Shallow	0.16	67	R–0.6	–18.53	–5.9	–37.7	3,200
W5	Tolay/Franciscan	04/14/2015	Unknown	0.21	98	4.5	–18.47	–.6.0	–38.5	200
W15	Wilson Grove	04/18/2012	Shallow	0.16	53	R–0.0	–16.14	–6.1	–39.3	5,100
W17	Wilson Grove	04/16/2015	Shallow	0.23	110	4.8	–22.39	–6.1	–38.3	0
W18	Wilson Grove	04/14/2015	Unknown	0.09	22	R–0.0	–17.18	–5.8	–36.4	12,200
W21	Mixed	04/16/2015	Deep	0.06	11	R–0.1	–16.09	–6.6	–44.1	17,700
W22	Mixed	04/14/2015	Unknown	0.03	1	R–0.0	–16.71	–7.4	–49.7	34,000
W28	Mixed	06/13/1988	Unknown	—	62	—	—	—	—	—
W30	Mixed	06/18/2012	Shallow	0.32	101	4.0	–17.75	–5.8	–38.4	0
W42	Mixed	04/17/2015	Deep	0.04	2	R–0.1	–17.46	–7.6	–52.8	30,200
W43	Mixed	09/20/2004	Unknown	—	—	8.0	—	–.6.0	–38.5	—
W56	Petaluma	10/18/2004	Shallow	—	—	2.9	—	–5.9	–39.1	—
W57	Petaluma	04/18/2012	Unknown	0.16	57	1.0	–16.47	–6.1	–39.9	4,500
W72	Petaluma	04/15/2015	Mixed	0.18	85	2.7	–18.31	–5.9	–38.3	1,300
W73	Petaluma	04/15/2015	Mixed	0.08	26	0.9	–17.31	–6.4	–42.6	10,900
W79	Sonoma Volcanics	09/28/2004	Unknown	—	—	5.4	—	–6.3	–40.1	—
SP1	Franciscan	10/22/2015	Spring	0.20	99	1.1	–18.40	–6.2	–40.3	100
SP2	—	07/12/2012	Spring	0.26	90	5.0	–17.69	–6.9	–43.4	900
SW1	—	05/04/2016	Surface water	—	—	—	—	–3.5	–25.2	—
SW2	—	05/04/2016	Surface water	—	—	—	—	–4.2	–28.3	—

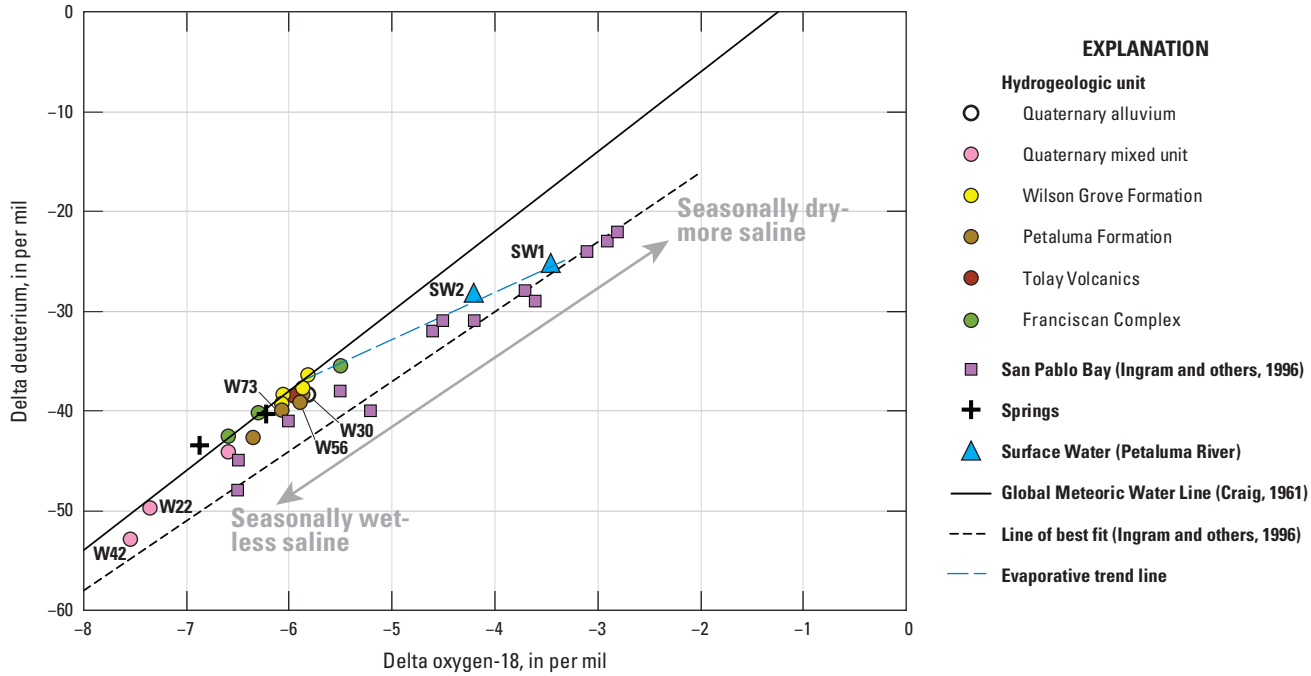

Figure C3. Delta oxygen-18 ($\delta^{18}O$) as a function of delta deuterium ($\delta^{2}H$) in water from wells, springs, and surface-water sites in the Petaluma valley watershed, Sonoma County, California, 2004–16; site information is provided in table C1.

The stable-isotopic data for the wells and springs in the PVW indicate that groundwater discharge is a large source of flow in the Petaluma River during wet climatic periods. The isotopic ratios from samples from groundwater and springs are similar to the ratios of San Pablo Bay water sampled during wetter climatic periods, when greater freshwater input from the Petaluma River enters the bay (fig. C3). Two samples from Quaternary mixed unit wells W22 and W42 have lighter (more negative) values (fig. C3; table C2) that may be indicative of water recharged from a different source or older water that was recharged under different (cooler) climatic conditions (Muir and Coplen, 1981).

Tritium and Carbon

The age of groundwater (time since recharge) was determined using radioactive ^{3}H and ^{14}C isotope data. The ^{3}H isotope is useful for dating recently (post-1952) recharged groundwater, whereas ^{14}C isotope data are useful for determining ages for older, greater than 1,000 years before present (ybp), groundwater; therefore, these data were used together to help constrain the groundwater ages. Ratios of stable ^{13}C to ^{12}C ($\delta^{13}C$) were used to identify any processes that can affect estimates of ^{14}C ages.

Tritium

Tritium is a natural and an anthropogenically generated radioactive isotope of hydrogen (Clark and Fritz, 1997). The half-life of ^{3}H is 12.32 years (Lucas and Unterweger, 2000), and this short half-life is useful for identifying water that has been in the hydrologic cycle about 65 years (post-1952; Clark and Fritz, 1997). Tritium activity is measured in disintegrations per unit of time and is reported in picocuries per liter (pCi/L) in this study. The interaction of cosmic radiation with the upper atmosphere results in the creation of ^{3}H in the atmosphere, which can be measured in precipitation (Lal and Peters, 1967; O'Brien and others, 1991).

Approximately 800 kilograms (kg) of ^{3}H was released as a result of atmospheric testing of thermonuclear weapons during 1952–62, which produced a spike in ^{3}H concentrations in precipitation and in groundwater recharged during that time (Michel, 1976). Atmospheric testing ceased around 1980; by 1990, this anthropogenic source of ^{3}H had been largely washed out of the atmosphere, and concentrations in precipitation had decreased to those close to natural, pre-bomb levels (Clark and Fritz, 1997). Minor amounts of anthropogenic ^{3}H continue to be released to the atmosphere from nuclear power plants and related facilities that process nuclear material (Weiss and others, 1979; United Nations, World Health Organization, 1983). The ^{3}H data can be used in conjunction with data for its daughter product helium-3 (^{3}He) to determine an absolute age; however, this method might not yield reliable ^{3}H-based ages where concentrations of terrigenic helium greatly exceed concentrations derived from thermonuclear ^{3}H (Solomon and Cook, 2000). In the absence of ^{3}He concentrations, ^{3}H data alone were used in this study to interpret qualitative ages of recharge as pre- and post-1950.

Values of ^{3}H in the PVW study area ranged from less than the reporting limit of 0.5 to 8.0 pCi/L (fig. C4; table C2). Based on wells with available well-construction information, ^{3}H was generally detected in samples from shallow or mixed-depth wells that were screened less than 200 feet (ft) below land surface (bls). Samples of water with detections less than the reporting limit were generally from deep wells (greater than 200 ft bls), indicating that regardless of lateral position in the study area, modern (post-1950) water is generally limited to wells screened near land surface. Furthermore, groundwater quality in deep wells is not likely influenced by land-surface activities at time scales of less than about 60 years. The sample from well W43 had the highest ^{3}H concentration. Well W43 is classified as a deep well with a known completion depth of 314 ft bls, but the screened interval is unknown. Based on depth, well W43 may be a mixed-depth well screened near the surface (less than 200 ft bls with a mixture of shallow and mixed-depth water).

Carbon Isotopes

Carbon-14 (^{14}C) is the natural, long-lived (half-life of 5,730 years), radioactive isotope of carbon that can sometimes be used to determine the age of groundwater far beyond the range for ^{3}H. The ^{14}C data are expressed as percent modern carbon (pMC) by comparing ^{14}C activities to the specific activity of National Bureau of Standards oxalic acid; 12.88 disintegrations per minute per gram of carbon from the year 1950 equals 100 pMC (Stuiver and Polach, 1977). The ^{14}C age (residence time) is calculated by the decrease in ^{14}C activity due to radioactive decay since groundwater recharge (Clark and Fritz, 1997). Bombardment of nitrogen atoms by cosmic radiation and thermonuclear testing and nuclear power plants have contributed ^{14}C to the atmosphere, while the burning of fossil fuels during the industrial age has "diluted" the level of ^{14}C (Clark and Fritz, 1997). Atmospheric ^{14}C is present as carbon dioxide (CO_2), which can then be incorporated into various hydrospheric (oceans, lakes, and groundwater) and biospheric (plants and animals) reservoirs. Once these sources of carbon are isolated from the atmosphere, the ^{14}C content in the dissolved carbon steadily decreases.

The isotope ^{14}C that has been isolated from the atmosphere is affected by processes in addition to radioactive decay. Chemical reactions along a groundwater flow path can dilute carbon-14 either by the addition of dissolved inorganic carbon (DIC; that is, carbonate, CO_3, plus bicarbonate, HCO_3) that lacks ^{14}C or by the removal of DIC that contains ^{14}C (Clark and Fritz, 1997). The minerals calcium carbonate ($CaCO_3$) and dolomite ($CaMg(CaCO_3)_2$) were formed long ago, are devoid of ^{14}C, and are often said to contain "dead" carbon (Freeze and Cherry, 1979). The addition of DIC from $CaCO_3$ and $CaMg(CaCO_3)_2$ and the production of DIC from the oxidation of organic matter that is devoid of carbon-14 can dilute the original ^{14}C content to give the appearance of older water. The $\delta^{13}C$ ratios were used in this study as indications of the processes that can affect estimates of residence times. Groundwater can acquire a less negative $\delta^{13}C$ value as it moves along a flow path by exchange of carbon isotopes between CO_3 minerals and DIC (equilibration) and by decomposition (oxidation or mineralization) of organic matter buried in the aquifer (Geyh, 2000). Values of ^{14}C presented in this report are normalized as percent modern carbon. These ^{14}C values have been normalized to a $\delta^{13}C$ value of –25 per mil to account for natural isotopic fractionation; however, stable carbon isotopes also were used to make qualitative inferences about the extent of these processes.

Values of ^{14}C in the PVW ranged from 1.46 to 109.9 pMC (table C2). Based on a half-life of 5,730 years, these values correspond to an uncorrected residence times of 34,000 ybp to greater than modern (Stuiver and Polach, 1977), with a median of about 4,200 ybp. Residence times were the greatest in samples from deep wells along the axis of the PVW where groundwater is at the end of groundwater flow paths (for example, wells W18, W21, and W22 in fig. C4).

Values of $\delta^{13}C$ for samples from wells in the PVW ranged from –22.39 to –15.67 per mil (table C2). Less negative values of $\delta^{13}C$ are generally correlated with older (lower pMC) water (fig. C5). Ranges of $\delta^{13}C$ values for recently recharged groundwater are generally –17 to –16 per mil for unconfined groundwater systems and –13 to –12 per mil for confined groundwater systems (Clark and Fritz, 1997). Values of $\delta^{13}C$ outside of these ranges indicate that the ^{14}C in the samples has been diluted (Geyh, 2000). Values of $\delta^{13}C$ for samples of older water (^{14}C less than 60 pMC; fig. C5) are within the range of groundwater in unconfined groundwater systems because this water infiltrated in areas of the Sonoma Mountains or Wilson Grove Formation Highlands groundwater basin with minimal organic material at land surface. The samples of younger water (^{14}C greater than 60 pMC; fig. C5) are generally lighter (more negative), indicating exchange of carbon from decomposition (oxidation or mineralization) of organic matter buried in the aquifer, because soil CO_2 is biogenic in origin and has a $\delta^{13}C$ value of about –22 per mil (Geyh, 2000). The narrow range of $\delta^{13}C$ values for most of the samples indicate that contribution of carbon from carbonate dissolution is negligible (fig. C5; table C2).

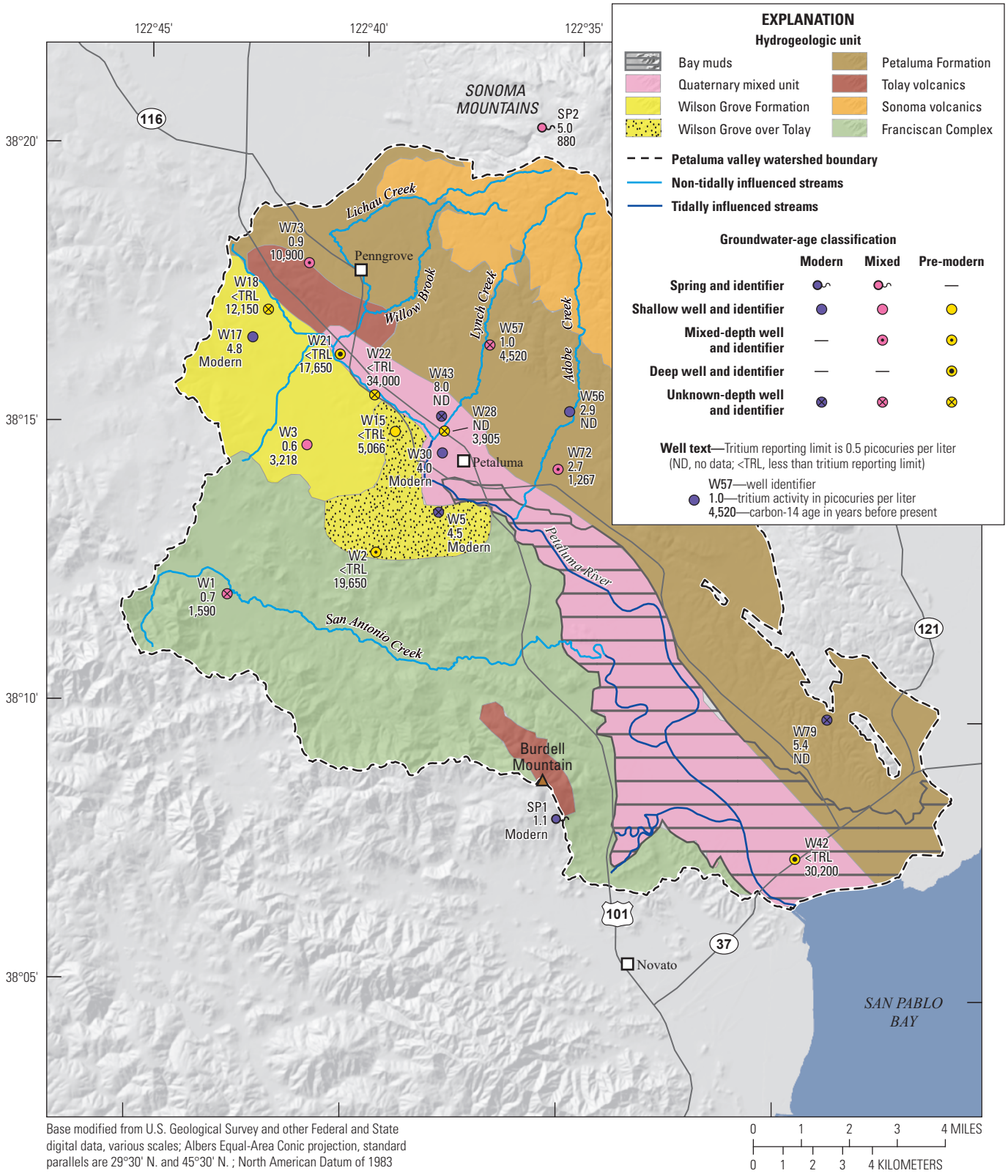

Figure C4. Tritium detections, carbon-14 ages, and age-dating classifications for select wells in the Petaluma valley watershed, Sonoma County, California, 2004–15 (Teague, 2022); site information is provided in table C1.

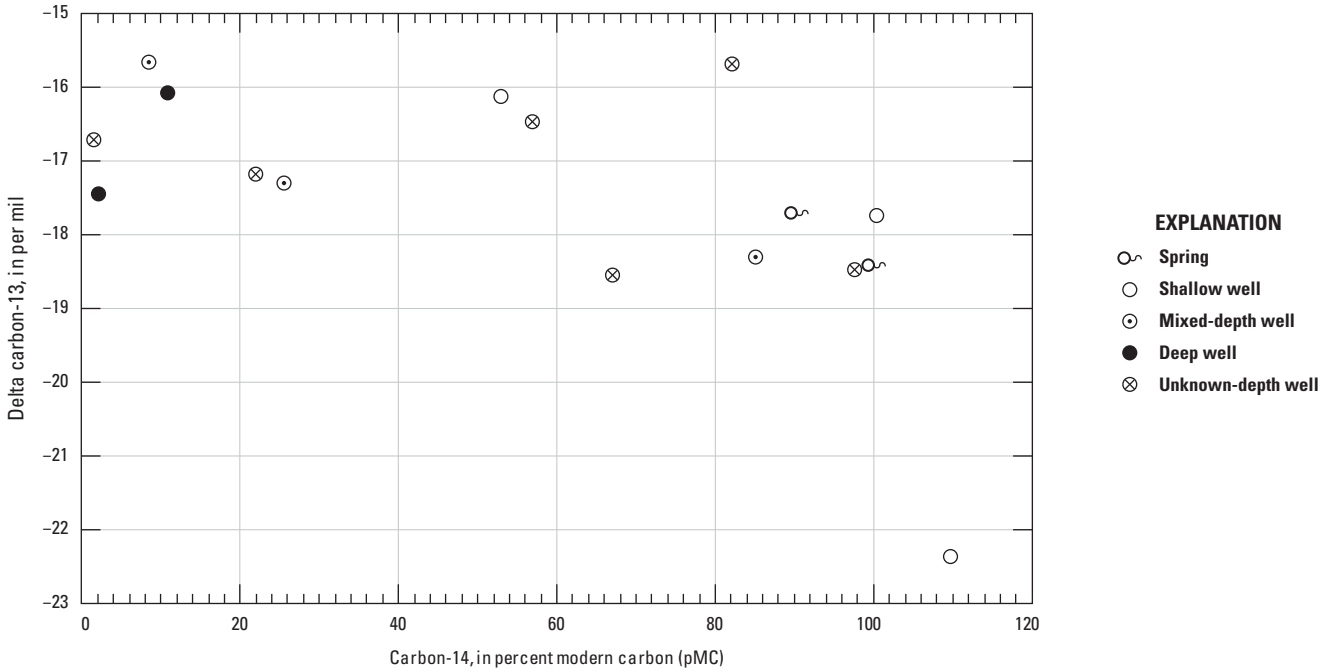

Figure C5. Delta carbon-13 as a function of carbon-14 age for samples from wells in the Petaluma valley watershed, Sonoma County, California, 2004–15 (Teague, 2022); site information is provided in table C1.

Groundwater Age in the Petaluma Valley Watershed

In this study, the age distributions of samples are classified as pre-modern, modern, and mixed (fig. C4). Groundwater samples with ^{3}H activity less than 0.5 pCi/L and ^{14}C less than 90 pMC were designated as pre-modern (recharged before 1950). Groundwater samples with ^{3}H activities greater than 0.5 pCi/L and ^{14}C greater than 90 pMC were designated as modern (recharged after 1950). Samples with pre-modern and modern ages determined from the different isotopes were designated as mixed groundwaters.

In general, the unconfined nature of the groundwater system in the PVW is evident in the groundwater age distributions of water in wells, because wells that are screened near the surface contain modern water that originated as precipitation that recharged at the surface. The groundwater-age data indicate that, regardless of formation, modern (post-1950s) water is in samples from shallow wells and mixed-depth wells screened near land surface (table C2). In general, the groundwater-age data indicate that groundwater sampled from deep wells along the axis of Petaluma valley is pre-modern water (fig. C4).

The ^{3}H and ^{14}C data indicate that wells perforated in the Wilson Grove and Petaluma Formations draw from various water ages and, depending on location, may contain fractions of young water and may be susceptible to influences from the ground surface on time scales of only decades. Samples from shallow wells W15 and W17, perforated in the Wilson Grove Formation, can be classified as pre-modern and modern, respectively (table C2). Water sampled from wells W3 (completed depth of 225 ft bls and unknown perforated interval) and W18 (unknown well construction), also perforated in the Wilson Grove Formation, can be classified as mixed age and pre-modern, respectively (table C2).

Water from wells perforated in the Petaluma Formation with ^{3}H and ^{14}C data can be classified as modern (W56; table C2) or mixed (W57, W72, and W73; table C2), indicating some source of modern water to these wells. The stable-isotope data indicate that the fraction of modern water sampled from wells perforated in the Petaluma Formation originates as direct infiltration of precipitation or infiltration of precipitation-derived streamflow in the many tributaries east of the Petaluma River (fig. C3).

Four wells perforated in the Quaternary mixed unit with ^{3}H and ^{14}C sample data were classified as pre-modern: two deep wells (W21 and W42; table C2) and two wells of unknown screened interval (W22, with a completion depth of 260 ft bls; W28, with unknown perforation depths; tables C1, C2). The ^{14}C ages for wells W22 and W42 were 34,000 and 30,200 ybp, respectively (table C2). Stable-isotope data for these wells were lighter than other samples from the Quaternary mixed unit (fig. C3); therefore, water in these wells was probably recharged under different (cooler) climatic conditions. The apparent ages of tens of thousands of years also indicate long groundwater-residence times. Modern water sampled from well W43, with a completion depth of 314 ft bls (table C1) but with unknown depth classification, indicates that modern water can be a primary source to some wells in the Quaternary mixed unit (table C2). The shallow well perforated in the Quaternary alluvium for which ^{3}H and ^{14}C data were collected (W30) can be classified as modern water (fig. C4; table C2).

Sources of Saline Water

Values of specific conductance (SC) and concentrations of total dissolved solids (TDS) and chloride (Cl) were used to help characterize the sources of saline groundwater in the PVW. Waters are generally classified as salinity-affected when TDS concentrations are greater than 1,000 mg/L (Drever, 1982) or when Cl concentrations are greater than 100 mg/L (Tolman and Poland, 1940; Iwamura, 1980). Farrar and others (2006) used an SC value of 1,000 microsiemens per centimeter (µS/cm) as the threshold for relatively saline water in the adjacent Sonoma Valley groundwater basin. Water-level data indicate that under base-flow conditions, groundwater near sea level can be vulnerable to infiltration of relatively saline water in the PVW through direct infiltration of San Pablo Bay water or tidally influenced Petaluma River water (see chapter B). Another possible source of saline water to groundwater in the study area is connate water (California Department of Water Resources, 1982a). Finally, the concentrations of ions dissolved in groundwater are influenced by water-rock reactions, such as dissolution, precipitation, and ionic exchange, which can increase ionic concentrations through time (Chebotarev, 1955).

Saline water can negatively affect drinking water by creating an undesirable taste and corrosion. Therefore, the State of California has a recommended secondary maximum contaminant level (SMCL) for SC of 900 µS/cm and 250 mg/L for Cl (Thomson Reuters, 2018b). Additionally, although not toxic to humans, Cl presents a toxicity problem for plants (Ayers and Westcot, 1994). Because SC and TDS are measures of ionic concentration (Hem, 1992; California State Water Resources Control Board, 2010), only SC and Cl were used in this report to provide a simple interpretation of the salinity of the samples. For this study, salinity-affected water is defined as water with SC values greater than 1,000 µS/cm and Cl concentrations greater than 100 mg/L. These values are also used as the lower threshold values for high SC and high Cl (Teague, 2022). The SC data presented in Teague (2022) include values measured in the field and in the laboratory. A comparison of field and laboratory SC measurements for each sample showed that relative differences ranged from 0 to 14.2 percent. Given the general similarities between the field and laboratory measurements, in instances where field data were not available, laboratory measurements were used. Specific conductance in groundwater samples evaluated as part of this study ranged from 180 (W78) to 6,120 (W39) µS/cm (Teague, 2022). The concentration of Cl in groundwater samples ranged from 4.6 (W74) to 1,080 (W39) mg/L (Teague, 2022).

For this study, salinity-affected water is defined as water with SC values greater than 1,000 µS/cm and Cl concentrations greater than 100 mg/L. Samples from the surface-water sites SW1 and SW2 had SC values and Cl concentrations exceeding the thresholds for salinity-affected waters (Teague, 2022). Stable-isotope data indicate that saline San Pablo Bay water moved upstream by tidal flow is a primary source of water sampled at SW1 (fig. C3). In contrast, stable-isotope data indicate that the primary source of water at SW2 is evaporated streamflow originating as groundwater (fig. C3). Groundwater discharging to the Petaluma River at SW2 is likely groundwater that has moved from recharge areas along the boundary of the PVW, increasing in ionic concentration as a result of water–rock reactions with aquifer material along the groundwater flow path and thereby increasing the SC value and Cl concentration.

Seven samples from wells W27, W30, W34, W36, W42, W64, and W68 had SC values greater than 1,000 µS/cm and Cl concentrations greater than 100 mg/L (Teague, 2022). These wells are generally deep (W27, W34, and W42) or unknown-depth (W36 and W64) wells located along the axis of the PVW (fig. C6). Because deep wells are not perforated near land surface where tidally influenced river water should infiltrate, high SC and Cl values more likely result from water–rock reactions as groundwater moves from recharge areas to the axis of the PVW. Among deep-well samples with high SC and Cl values, stable isotope and groundwater-age-dating data were only available for water sampled from well W42 (table C2). These data indicate that the source of water to W42 is precipitation that infiltrated in a cooler pre-modern period. Long residence times indicated by the age-dating data would allow for greater water–rock reactions, leading to increased SC and Cl.

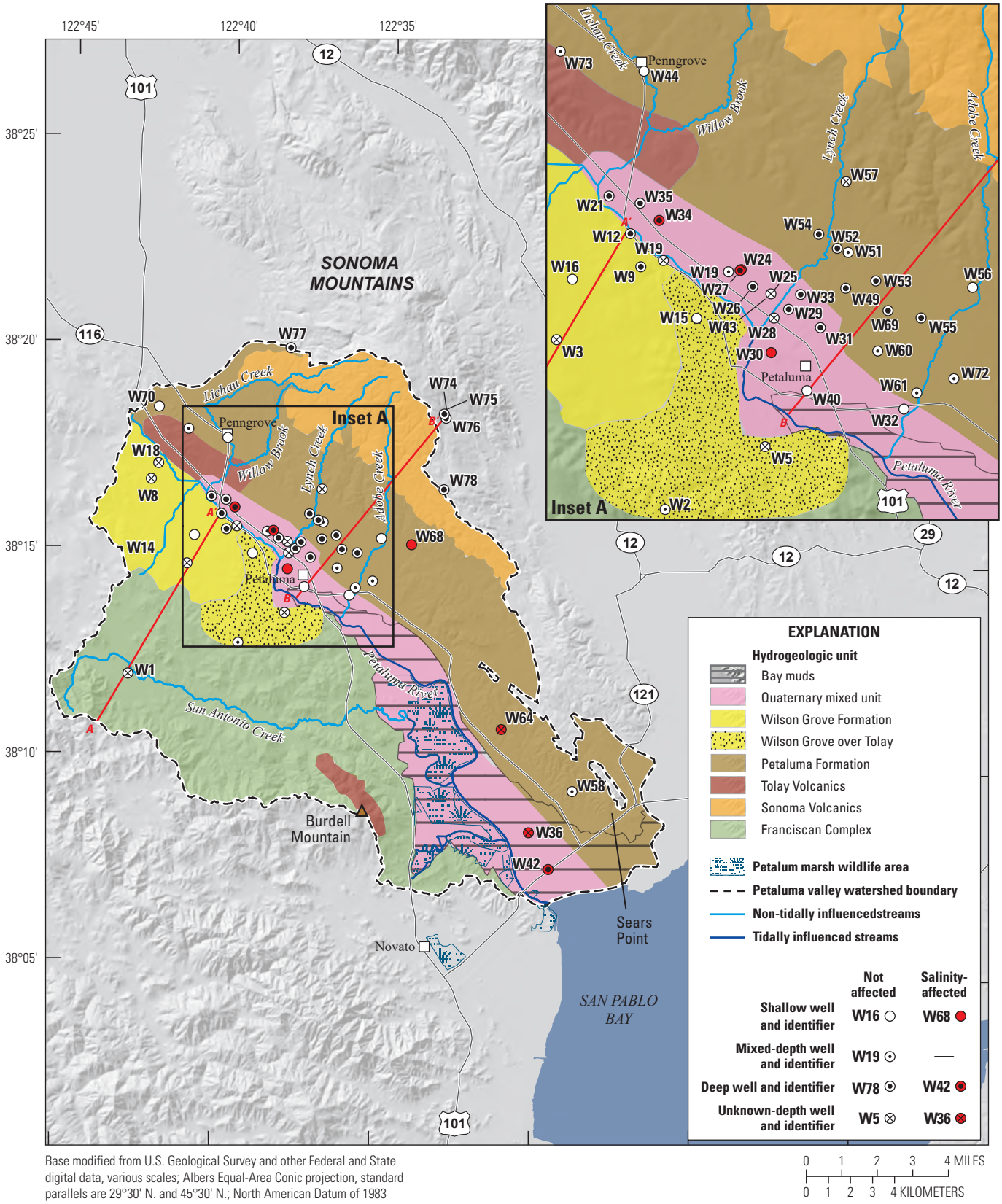

Base modified from U.S. Geological Survey and other Federal and State digital data, various scales; Albers Equal-Area Conic projection, standard parallels are 29°30' N. and 45°30' N.; North American Datum of 1983

Figure C6. Salinity-affected and non-salinity-affected wells in the Petaluma valley watershed, Sonoma County, California, 1974–2015; site information is provided in table C1.

Of the shallow (W30 and W68) wells with SC and Cl values exceeding salinity-affected thresholds, stable isotope and groundwater age-dating data were only available for well W30 (table C2). These data indicate that the recharge source to W30 is modern infiltration of precipitation (fig. C3). Values of SC and Cl exceeding salinity-affected thresholds in samples of modern water from shallow wells indicate that water from land-use activities such as urban runoff or agricultural wastes from irrigation drainage (agricultural return) affect the shallow groundwater.

Chemical Character of Surface Water and Groundwater

The chemistry of water from wells in the PVW is controlled by the chemistry of the recharge water and the water–rock reactions in the aquifer system. Saline water intruding from the tidally influenced reach of the Petaluma River may also alter groundwater chemistry, increase Cl concentrations, and impair the quality of surface water and groundwater. Infiltration of water in areas of agricultural and urban land-use may impair shallow groundwater quality by contributing trace organic compounds, trace elements, and nitrate. In this study, water chemistry was evaluated based on major-ion and nitrate data to determine native groundwater quality and the sources of saline water to wells.

Major-Ion Composition

Generally, the major-ion composition of groundwater is controlled by the natural chemistry of the recharge water, including geochemical reactions in the subsurface, primarily dissolution and precipitation of minerals and anthropogenic factors, such as the disposal of wastewater and agricultural return. The major-ion compositions of surface-water and groundwater samples were characterized by Piper and Stiff diagrams.

A Piper diagram shows the relative contribution of major cations and anions, on a charge-equivalent basis, to the ionic content of the water (Piper, 1944; fig. C7). Percentage scales along the sides of the diagram indicate the percentage of total cations or anions in milliequivalents per liter (meq/L). Cations are shown in the left triangle, anions are shown in the right triangle, and the central diamond integrates the data (fig. C7). Piper diagrams can be used to depict the chemical composition of samples, grouping water types, and determining whether there is simple mixing between chemically different water (Piper, 1944). In this report, the dominant cation and anion species (greater than 50 percent) are used to describe the water type of a water sample; samples that do not have a dominant cation or anion are classified as mixed (fig. C7).

Water samples that are of similar origin or that may have undergone changes in composition resulting from similar chemical processes plot within similar areas in the trilinear diagram (Piper, 1944). For example, as water moves through the aquifer and reacts with the aquifer material, dissolution of $CaCO_3$ increases relative CO_3 and HCO_3 concentrations, and cation exchange of sodium (Na) for calcium (Ca) and magnesium (Mg) in sediments decreases the calcium to sodium ratio in groundwater (Teague, 2022). The evolution of water chemistry as groundwater interacts with intruding saline-mixed seawater follows an initial path of increasing Cl plus sulfate (SO_4) and decreasing HCO_3, followed by further increase in Cl plus SO_4 accompanied by a decrease in Ca to Na (Izbicki and others, 2003). Because major-ion data for San Pablo Bay were unavailable, the endpoint for this relatively saline water–groundwater mixing in the PVW is represented by seawater (fig. C7; Hem, 1992). Water chemistry for the three main hydrogeologic units and the primary recharge areas are described in further detail later in this report.

Stiff diagrams depict the concentrations of major ions in milliequivalents per liter (meq/L) and indicate relative proportions of major ions (Stiff, 1951). Samples represented with similarly shaped diagrams represent groundwater of similar chemical characteristics. Changes in the width of the diagrams indicate differences in the ion concentrations. All Stiff diagrams describe the major cations on the left side—Na at the top, Ca in the middle, and Mg at the bottom—and major anions on the right side—Cl at the top, HCO_3 in the middle, and SO_4 on the bottom (fig. C8).

Areal and depth-related patterns in chemical characteristics for the Petaluma River and water-bearing hydrogeologic units of the PVW are discussed in the next section. Wells are grouped by the hydrogeologic unit in which they are screened and with respect to the three-dimensional framework model described in chapter B. Major-ion data were used to evaluate movement of groundwater from recharge areas to wells from which samples were collected and to evaluate mixing of fresh groundwater with sources of more saline water.

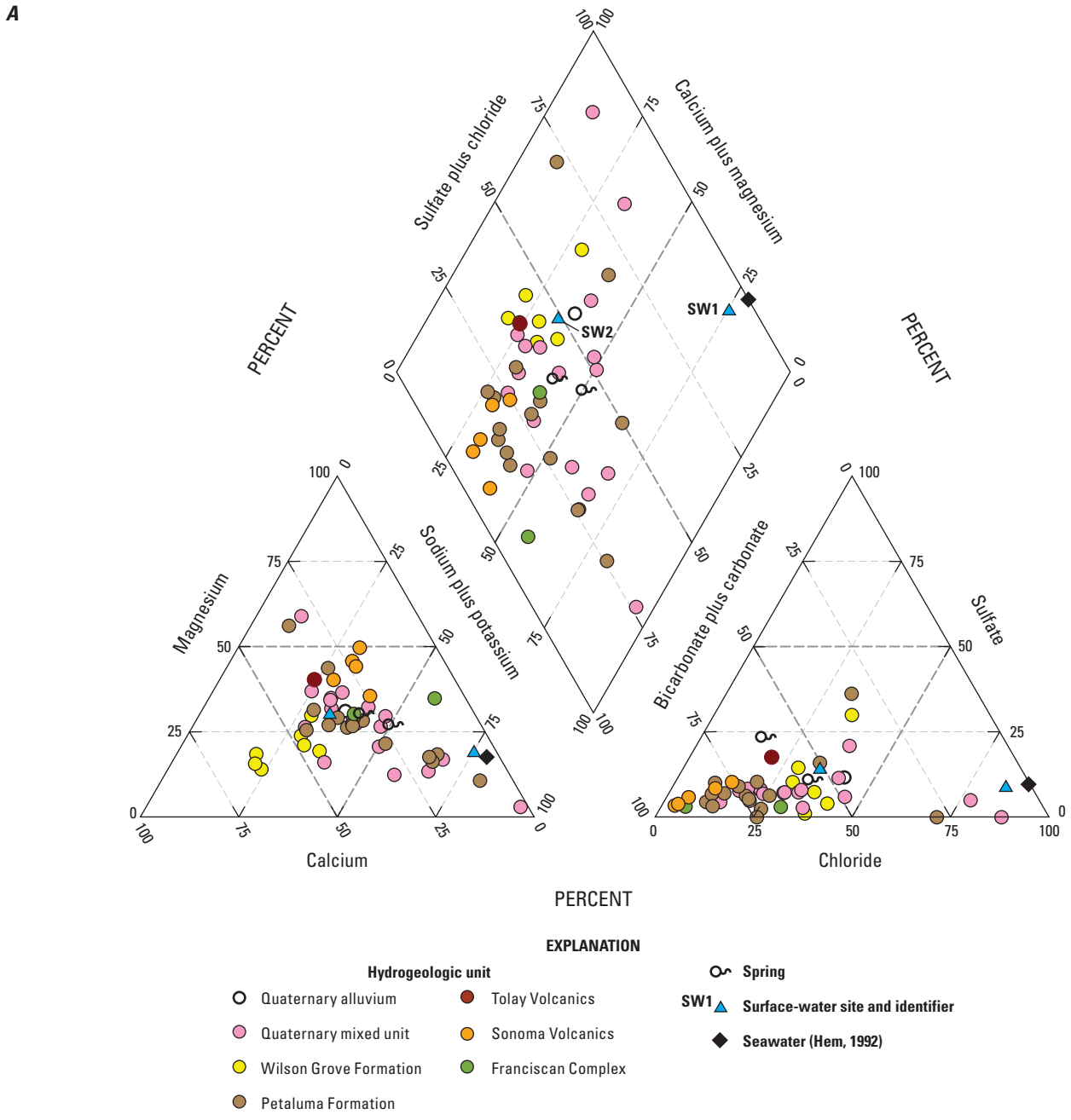

Figure C7. Major-ion composition of the most recent, complete sample from selected surface-water sites, springs, and wells in Sonoma County, California, in the *A*, Petaluma valley watershed; *B*, Wilson Grove Formation; *C*, Petaluma Formation; *D*, Quaternary alluvium and Quaternary mixed unit; and *E*, Franciscan Complex, Tolay Volcanics, and Sonoma Volcanics (Teague, 2022); site information is provided in table C1.

B

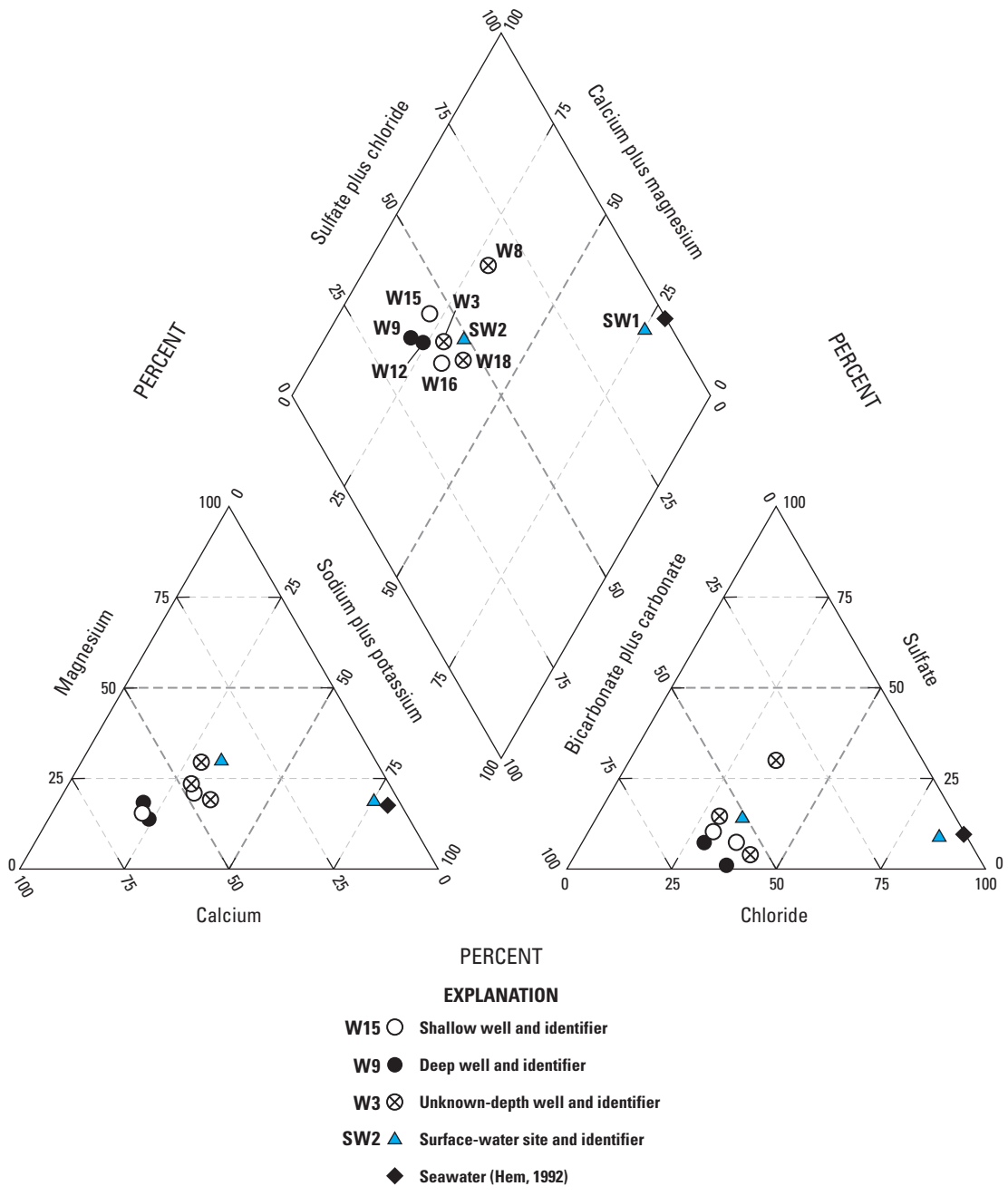

Figure C7.—Continued

C

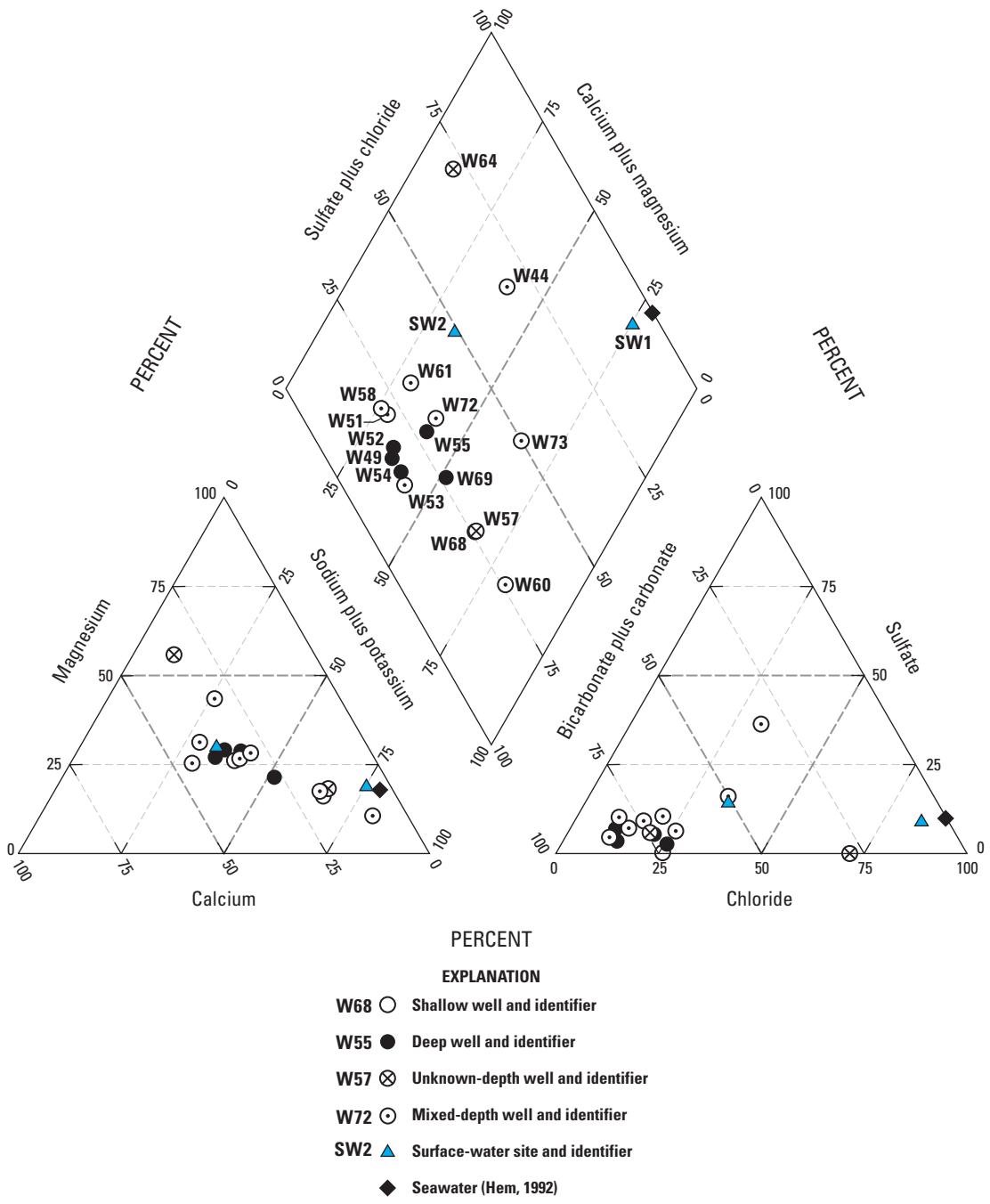

Figure C7.—Continued

D

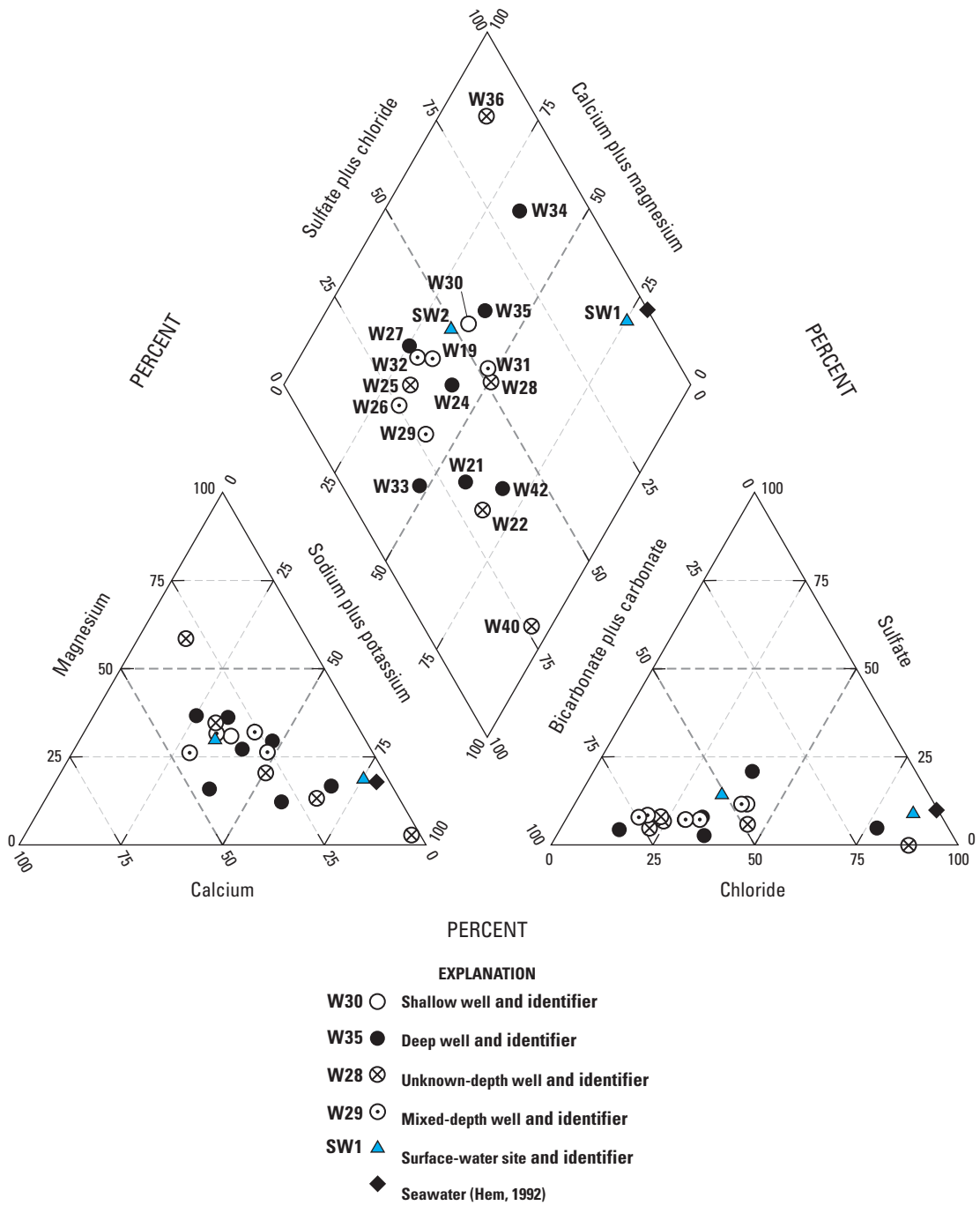

EXPLANATION

W30 ○ **Shallow well and identifier**

W35 ● **Deep well and identifier**

W28 ⊗ **Unknown-depth well and identifier**

W29 ⊙ **Mixed-depth well and identifier**

SW1 ▲ **Surface-water site and identifier**

◆ **Seawater (Hem, 1992)**

Figure C7.—Continued

E

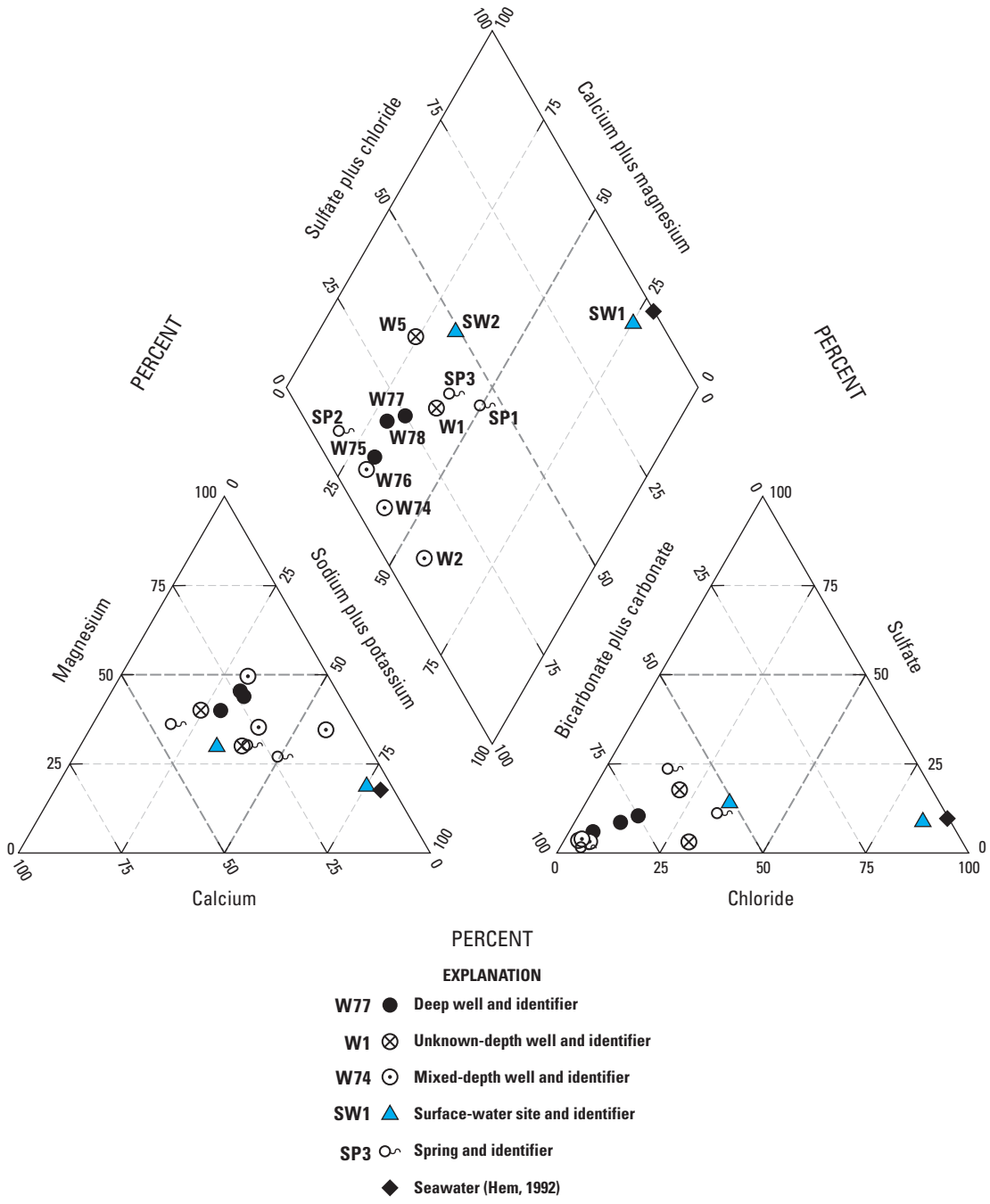

Figure C7.—Continued

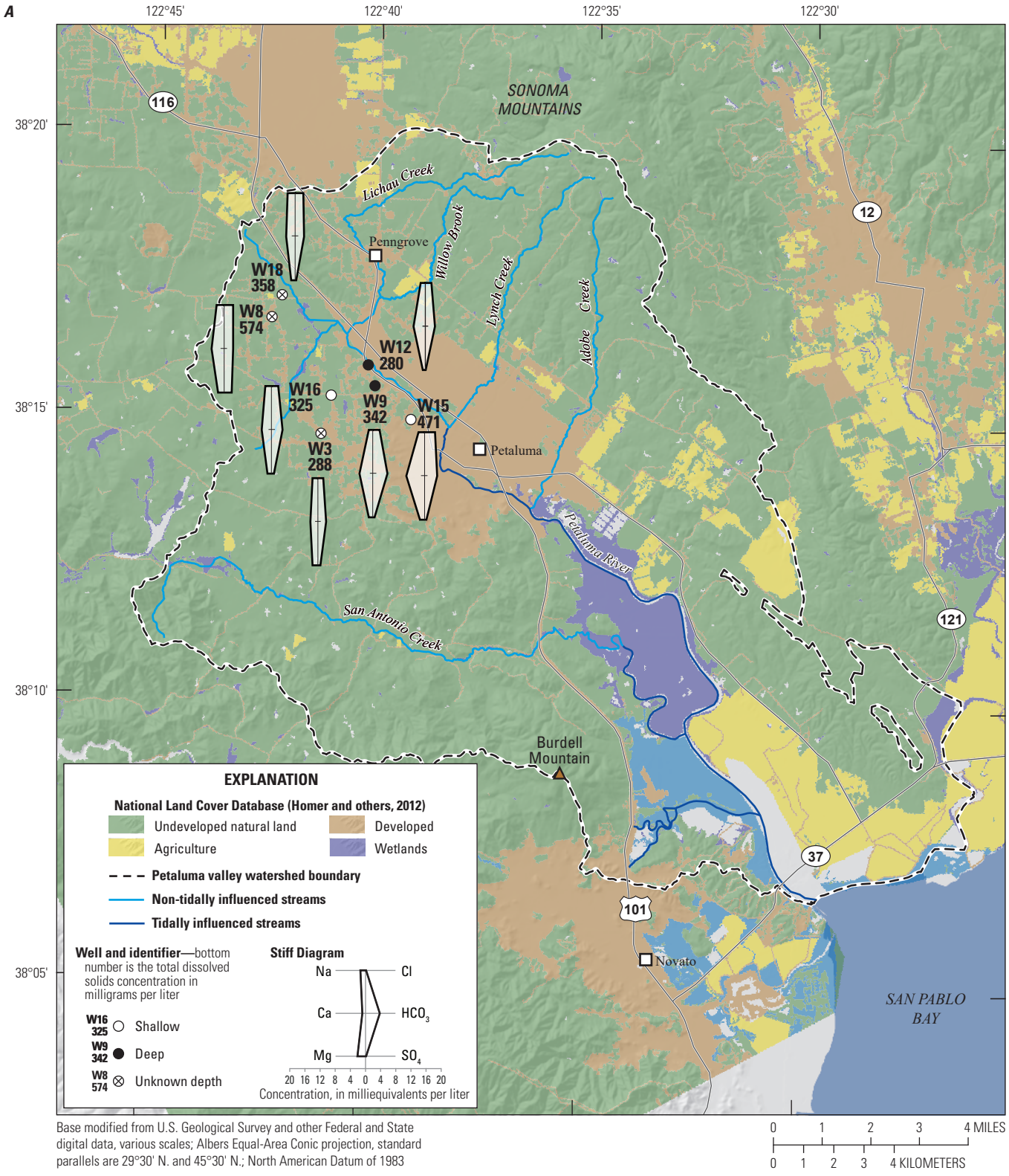

Figure C8. Major-ion composition for selected wells in Sonoma County, California, 1974–2015, perforated in the *A*, Wilson Grove Formation; *B*, Petaluma Formation and Sonoma Volcanics; *C*, Quaternary alluvium and Quaternary mixed unit, and *D*, Sonoma Volcanics, Petaluma valley watershed (Teague, 2022); site information is provided in table C1.

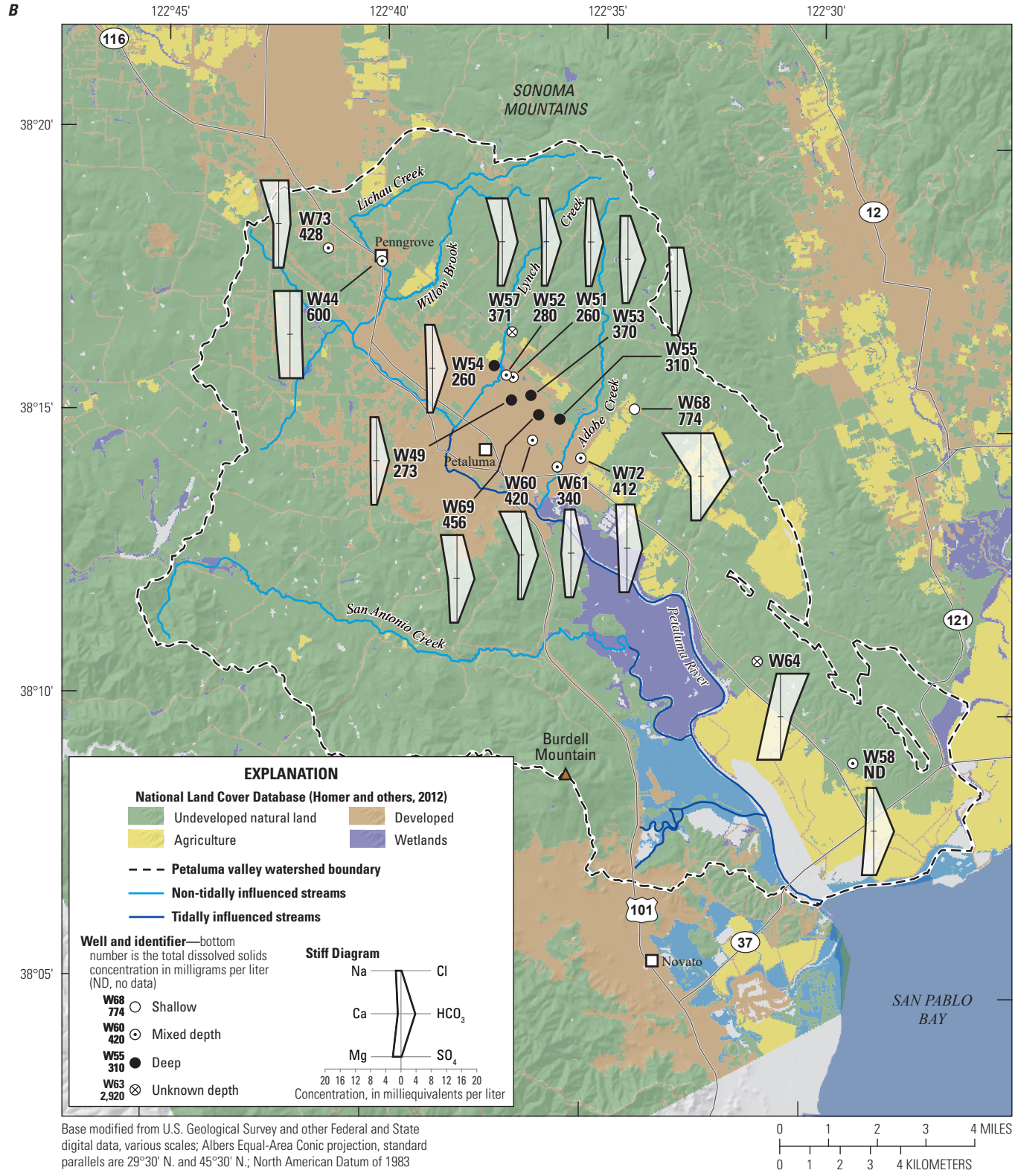

Figure C8.—Continued

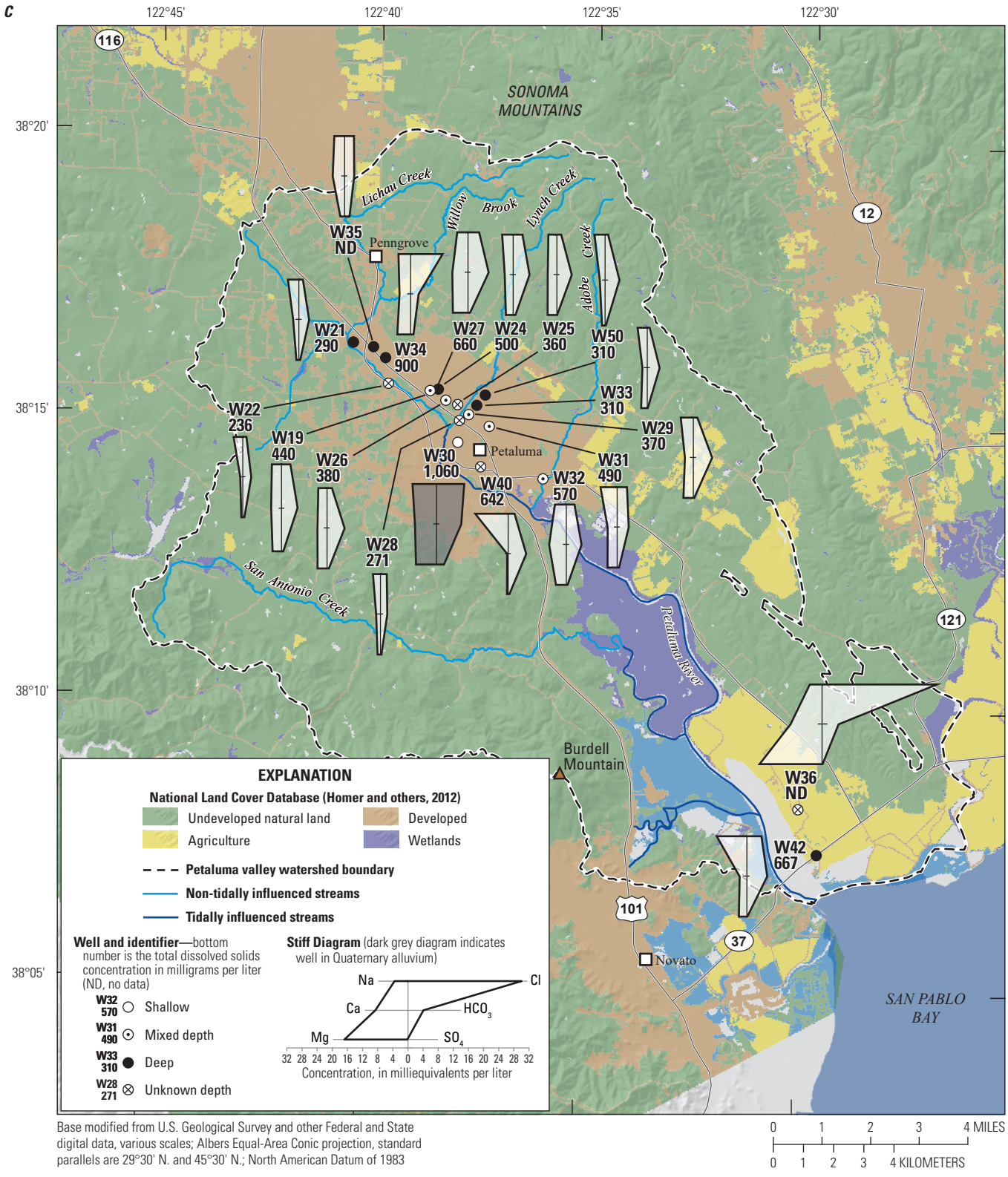

Figure C8.—Continued

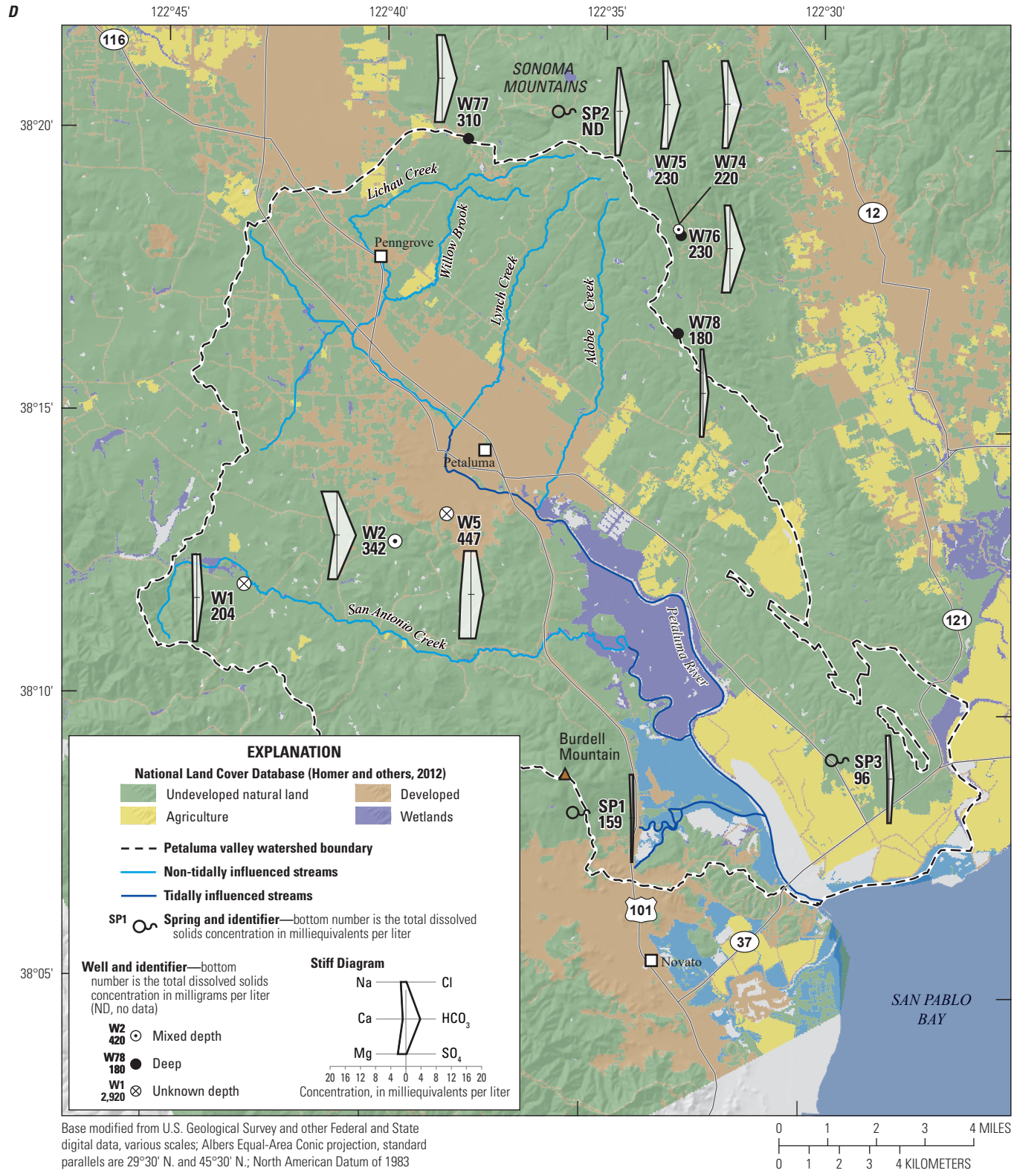

Figure C8.—Continued

Petaluma River

Water from surface-water sites SW1 and SW2 (table C1) is Na-Cl and mixed cation-HCO_3 type water, respectively (fig. C7*A*). The sample from SW1 represents tidally influenced river water indicative of mixing between groundwater and a source of water with an ionic composition similar to seawater—in this case, San Pablo Bay water. The fact that the sample from SW1 plots close to the seawater point indicates that water in the tidally influenced reach of the Petaluma River is mostly made up of San Pablo Bay water mixed with a small amount of groundwater. As discussed in the "Oxygen-18 and Deuterium" section, streamflow in the Petaluma River during warmer climatic periods is composed of groundwater discharging to the river. The absence of groundwater samples plotting on a trajectory toward SW1 indicates that groundwater in the PVW is not mixing with tidally influenced river water (fig. C7*A*). The sample from SW2 had a major-ion composition similar to groundwater samples in the PVW and indicates that the upper reach of the river is dominated by groundwater inputs (fig. C7*A*).

Wilson Grove Formation

Water from wells perforated in the Wilson Grove Formation is generally a mixed cation-HCO_3 or Ca-HCO_3 type water (figs. C7*B*, C8*A*). The tight grouping of data from wells of different locations and depths and the low to moderate TDS (Teague, 2022) type of water throughout the hydrogeologic unit indicate that the groundwater undergoes minor water–rock reactions as it moves through the hydrogeologic unit. As discussed in chapter B of this report, the Wilson Grove Formation is weathered sandstone that is primarily siliceous in composition and resistant to further water–rock reactions with groundwater. The similarity between the general ionic composition of samples from the Wilson Grove Formation and the ionic composition of the sample from SW2 indicate that groundwater from the Wilson Grove Formation is a substantial input to streamflow in the upper reach of the Petaluma River (fig. C7*B*).

Petaluma Formation

The general chemistry of groundwater collected from the Petaluma Formation is variable (figs. C7*C*, C8*B*). The water representative of this formation shows various dominant cation and anion characteristics. As mentioned previously, the groundwater sampled from wells perforated in the Petaluma Formation originates as water recharged in the Sonoma Volcanics, which is a mix of andesitic and rhyolitic rocks (Wagner and others, 2011). Samples from these wells have major-ion compositions characteristic of water flowing through rhyolitic rock (monovalent cations are dominant, and bicarbonate is the most abundant anion; Rosen and Coshell, 1998). Variations in relative proportions of cations and anions in samples from wells perforated in the Petaluma Formation can indicate variations in relative contributions of deep groundwater and variations in the chemistry of water infiltrating from surface-water sources, including the many tributary streams in the area.

Water from wells W49, W51, W52, W53, W54, and W58 is mixed cation-HCO_3 type water (figs. C7*C*, C8*B*). These samples have major-ion compositions similar to water sampled from wells perforated in the Sonoma Volcanics and likely represent groundwater that has moved downgradient from recharge sources in the Sonoma Volcanics (figs. C7*A*, C8*B*, C8*D*). Age-dating data are not available for these wells; however, stable-isotope data indicate that the source of recharge to these wells is infiltration of precipitation (fig. C3). Infiltration can be from direct infiltration at land surface or from infiltration of streamflow. Water from wells W55, W61, and W72 is also mixed cation-HCO_3 type water, but with higher proportions of Cl than the other mixed cation-HCO_3 wells (figs. C7*C*, C8*B*).

Water from wells W57, W60, W68, and W69 is Na-HCO_3 type water, indicating more evolved groundwater than other wells in the Petaluma Formation (figs. C7*C*, C8*B*). Available age-dating data from well W57 indicate these wells have at least some pre-modern groundwater (table C2). Other than well W68, these wells are greater than 200 ft deep (table C1) and may contain greater fractions of older groundwater than other wells perforated in the Petaluma Formation. Well W68 is a shallow well (table C1) that would not be expected to contain evolved groundwater. This well is in an agricultural land-use area (fig. C8*B*), and the chemistry of the groundwater sampled by well W68 may be influenced by irrigation using water pumped from deeper wells that sample more evolved groundwater.

Water from wells W44 and W73 has a greater proportion of Cl and SO_4 than water from other wells in the Petaluma Formation (figs. C7*C*, C8*B*). These wells are in the northern-most part of the Petaluma Formation and do not lie along the same groundwater flow paths as most of the other Petaluma Formation wells (fig. C2). The samples from wells W44 and W73 may represent groundwater that has undergone a different groundwater evolution than groundwater sampled from wells in the central part of the formation (near section B–B' in fig. C2).

Water from well W64 has a greater proportion of Cl than water from other wells in the Petaluma Formation (figs. C7*C*, C8*B*). Well W64 is in the southern-most part of the Petaluma Formation and may also represent groundwater that has undergone a different evolution than groundwater from other wells perforated in the central part of the Petaluma Formation.

Quaternary Alluvium and Quaternary Mixed Unit

Well W30 is the only sampled well perforated in Quaternary alluvium. The general water chemistry of water from well W30 is a mixed cation-mixed anion type water (figs. C7*D*, C8*C*). The major-ion composition of the sample from well W30 is similar to the major-ion composition of SW2, indicating that groundwater in W30 is similar to groundwater discharging to the non-tidally influenced reach of the Petaluma River (fig. C7*D*).

As described in chapter B, the Quaternary mixed unit is a conglomeration of deposits from the Petaluma and Wilson Grove Formations. As such, the general chemistry of groundwater collected from wells perforated in the Quaternary mixed unit is variable (figs. C7*D*, C8*C*) and spans the range of chemistries of samples from the Wilson Grove (figs. C7*B*, C8*A*) and Petaluma (figs. C7*C*, C8*B*) Formations. Samples with mixed cation-HCO_3 type water are generally from deep or mixed-depth wells (W19, W24-27, W29, and W33) upstream from the tidally influenced reach of the Petaluma River and next to the downstream part of Lynch Creek (fig. C2). Based on water-altitude contours (see chapter B, figs. B10*A–C*) and major-ion chemistry (figs. C7*A*, C7*D*, C8*C*), the primary source of water to wells in this area is groundwater moving from the Wilson Grove (figs. C7*B*, C8*A*) and Petaluma (figs. C7*C*, C8*B*) Formations. The similarity in major-ion composition of the samples from wells W19, W24-27, W29, W30, W33, and W35 and the sample from surface-water site SW2 indicate that groundwater from the Quaternary mixed unit and Quaternary alluvium is a substantial input to streamflow in the Petaluma River (fig. C7*D*).

Water from wells W34, W35, and W36 had a greater proportion of Cl than water from other wells perforated in the Quaternary mixed unit (figs. C7*D*, C8*C*). Water samples from wells W34 and W35 are representative of water evolving as it moves from upgradient areas of the northern part of the Petaluma Formation. Wells W34 and W35 are deep wells that are downgradient from well W44 (see chapter B, fig. B11), a well perforated in the Petaluma Formation that had greater Cl and SO_4 concentrations than other wells perforated in the Petaluma Formation. As groundwater moves along the groundwater flow path to the valley axis, the water retains the high-Cl signature because of the conservative nature of Cl. Reducing conditions in the deep aquifer could cause a decrease in SO_4 concentrations. The data for water sampled from wells W34 and W35, however, are insufficient to determine oxidation–reduction conditions (Teague, 2022).

As stated previously (see "Sources of Saline Water"), the groundwater sampled from well W36 (unknown depth) may be representative of groundwater at the end of a groundwater flow path; however, the chemistry of this sample is different than the chemistry of groundwater sampled from well W42 (fig. C7*D*), which is deep groundwater at the end of a groundwater flow path based on stable-isotope and age-dating data (see "Source and Age of Groundwater"). Well W36 is in an agricultural land-use area (fig. C8*C*), and the difference in chemistry of groundwater sampled from W36 and W42 indicates that W36 is perforated near land surface and that agricultural return is influencing the chemistry of groundwater sampled from W36.

Water sampled from wells W21, W22, W40, and W42 is Na-HCO_3 type water (figs. C7*D*, C8*C*). The apparent groundwater ages of water sampled from wells W21, W22, and W42 (deep, unknown depth, and deep, respectively) are pre-modern and are likely indicative of deep groundwater affected by water-rock reactions with aquifer material (table C2). These wells are at the axis of the basin where deep groundwater flow lines would converge, which is an area that would have been a discharge area before groundwater development (fig. C8*C*). The perforated interval for well W40 (completed depth of 280 ft bls) and the age of groundwater in the well are unknown. However, the position of the well along the axis of the valley and the major ion composition indicate that water in W40 has either evolved through ion-exchange processes or other water–rock reactions (figs. C7*D*, C8*C*).

Water from wells W28 and W31 is mixed cation-mixed anion type water (fig. C7*D*). Water in these wells is likely a mixture from various sources, such as recently recharged groundwater and older, evolved groundwater moving from the Petaluma Formation (fig. C7*D*).

Franciscan Complex, Tolay Volcanics, and Sonoma Volcanics

Major-ion data from groundwater sampled from the Franciscan Complex (W1 and W2), Tolay Volcanics (W5), the Sonoma Volcanics (W74-78), and two springs discharging from the Franciscan Complex (SP1 and SP3) are shown in figures C7*E* and C8*D* (table C1). Water from well W1 (unknown-depth), SP1, and SP3 is mixed cation-HCO_3 type water (figs. C7*E*, C8*D*). Relative to well W1, water from well W2 (mixed depth) has a lower Ca concentration, a higher alkalinity value, and is Na-HCO_3 type water (fig. C7*E*; Teague, 2022). As described in chapter B, the Franciscan Complex is not a single hydrogeologic unit; therefore, wells do not always penetrate the same lithology or rock type, and water chemistry can vary among wells. Groundwater sampled from well W5 is a mixed cation-HCO_3 type water and more closely resembles water sampled from surface-water site SW2 than samples from wells perforated in the Franciscan Complex (fig. C7*E*).

The Franciscan Complex and the Tolay Volcanics are not important hydrogeologic units for water supply in the PVW; however, there are areas, especially in the southwestern part of the PVW, where domestic-supply wells extract water solely from these hydrogeologic units. The varying mineralogic nature of the Franciscan Complex and Tolay Volcanics complicates efforts to predict the type of water that is produced from wells in these hydrogeologic units. Water recharged and contained in these hydrogeologic units likely does not influence water in surrounding hydrogeologic units, such as the Wilson Grove and Petaluma Formations, because of the low specific yield of the Franciscan Complex (Cardwell, 1958).

Water from wells perforated in the Sonoma Volcanics (W74-78) is mixed cation-HCO_3 type water (figs. C7*E*, C8*D*). Based on groundwater-level contours, water recharged in the Sonoma Mountains moves into the Petaluma Formation (see chapter B). As stated previously, and as shown in figures C7*A*, C8*B*, and C8*D*, water from wells in the Petaluma Formation near the Sonoma Mountains resembles water from wells in the Sonoma Volcanics, but water in other wells in the Petaluma Formation have different water chemistries caused by groundwater evolution processes or by mixing with water from other sources.

Bay Mud Deposits

Samples were not collected from wells perforated solely in bay mud deposits. Bay mud deposits overlie the Quaternary mixed unit in a large area of the southern part of the study area, including in and around Petaluma marsh. In some areas in the southern part of the watershed, bay mud deposits also overlie the Petaluma Formation (see chapter B, fig. B6). Bay mud deposits may influence water-chemistry in wells in this area by inhibiting direct recharge from precipitation by increasing cation exchange during recharge because of the high percentage of fine-grained material. Additionally, bay mud deposits may contain residual ions (including Cl) from evaporated San Pablo Bay water that can be mobilized by recharged precipitation and transported to the underlying hydrogeologic units. Water collected from well W42 has relatively high SC values, TDS, and Cl concentrations for the study area (fig. C8*C*; Teague, 2022); however, the stable-isotope, age-dating, and major-ion data indicate that a long residence time and water–rock reactions are the primary influences on the chemistry of groundwater from well W42.

Nitrate

Nitrate as nitrogen (NO_3-N) has natural and anthropogenic sources and is one of the most frequently identified contaminants in groundwater (Freeze and Cherry, 1979). Natural sources of NO_3-N include precipitation and decomposition (oxidation or mineralization) of organic material (Hem, 1992). Possible anthropogenic sources of NO_3-N in the PVW include agricultural return, urban runoff, feedlots, dairies, poultry production, fertilizer application, and industrial wastes (California Department of Water Resources, 1982a, b). Concentrations of NO_3-N in drinking water exceeding the EPA maximum contaminant level (MCL) of 10 mg/L are considered detrimental to human health and can result in methemoglobinemia (blue-baby syndrome) in children under 6 months of age (U.S. Environmental Protection Agency, 2018). The Central Coast Regional Water Quality Control Board aquatic-life guideline value for NO_3-N established for aquatic-life beneficial uses is 1.0 mg/L (Worcester and others, 2010).

In 1979, the CDWR was contracted by Sonoma County to investigate NO_3 contamination in wells in the upland area northwest of the City of Petaluma (in the Wilson Grove Formation) because of a 1978–79 case of methemoglobinemia (California Department of Water Resources, 1982b). Three sampling campaigns from 1979 to 1981 showed dissolved NO_3 concentrations exceeding the MCL in 33 to 56 percent of sampled wells (California Department of Water Resources, 1982b). High NO_3 concentrations generally were reported in shallow (less than 200 ft bls) wells, and contamination was attributed to previous poultry and dairy operations (California Department of Water Resources, 1982b).

Nitrate data in Teague (2022) are reported in different units (dissolved NO_3, nitrate plus nitrite, NO_3+NO_2, as nitrogen, N, or NO_3-N) because NO_3 data were obtained from various sources, including the CDWR, SWRCB, and USGS. Values of dissolved NO_3 were converted to units of NO_3-N to simplify the discussion of the NO_3 data (Teague, 2022). Additionally, data were analyzed using the highest reporting limit for the dataset (1.02 mg/L, NO_3 as N); therefore, the data presented in Teague (2022) may not match the data in the original databases. Where NO_3+NO_2 and NO_2 data are available, NO_2 contributes between 0 and 0.32 percent of the nitrogen concentration, indicating minimal contribution. Therefore, for the purposes of this study, it is assumed that NO_3+NO_2 data represent the NO_3-N concentration in the sample. Because most samples were analyzed for dissolved NO_3, NO_3 data were used where NO_3+NO_2 and dissolved NO_3 (as N) data were both available. For this study, NO_3-N concentrations were classified using criteria described in previous reports, including the California GAMA Program report on groundwater in the north San Francisco Bay groundwater basins (high is greater than 10 mg/L, moderate 5–9.9 mg/L, and low is less than 5 mg/L; Kulongoski and others, 2010).

Only 1 of the 60 groundwater samples in this study for which NO_3-N was analyzed had a high NO_3-N concentration (W5, 10.9 mg/L NO_3 as N; figs. C9, C10; Teague, 2022). Additionally, well W5 is south of the area identified as NO_3 affected by CDWR (1982a, b) and may not be related to the same land-surface activities that were responsible for the previous contamination (fig. C10). However, NO_3 contamination was historically detected in shallow (less than 200 ft bls) wells in the Wilson Grove Formation (fig. C10; California Department of Water Resources, 1982b), and the data used for this study are from samples of wells that are generally deeper than 200 ft bls (table C1). The exception is the sample from well W15 (fig. C10), a shallow well with NO_3-N below the reporting limit for this report (Teague, 2022), which is in the NO_3 contamination area as defined by the California Department of Water Resources (1982b).

The absence of high NO_3-N concentrations in groundwater samples for this study indicate that NO_3 contamination has not moved deeper into the aquifer, but these results should not be interpreted as evidence that NO_3 contamination in the shallow part of the Wilson Grove Formation has been resolved. Most of the wells in which NO_3-N concentrations exceed the detection level are in areas of urban (developed) land-use areas, indicating that urban runoff contributes NO_3-N to groundwater in the PVW (fig. C10). A moderate NO_3-N concentration measured in the groundwater sample from well W36, which is in an agricultural land-use area (fig. C10), indicates that agricultural return flow is influencing the chemistry of the water sampled from this well. Agricultural return flow helps explain the differences in water chemistry between wells W36 and W42 (figs. C7*D*, C8*C*). None of the springs had high NO_3-N concentrations (Teague, 2022), and none of the surface-water samples had NO_3-N concentrations that exceeded the central coast aquatic life guideline value of 1.0 mg/L as NO_3-N (Teague, 2022; Worcester and others, 2010).

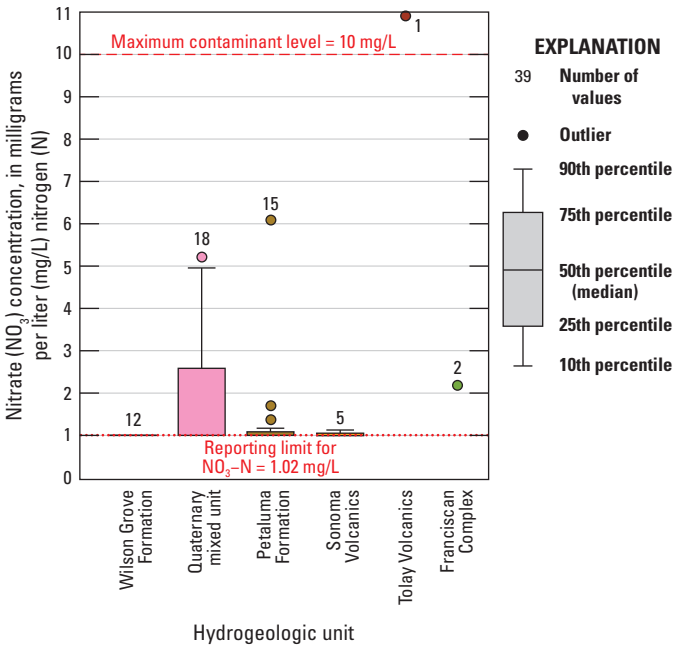

Figure C9. Nitrate data, in milligrams per liter nitrogen, for samples from wells in the Petaluma valley watershed, Sonoma County, California, 1974–2015 (Teague, 2022).

Nitrate concentrations in water from wells perforated in the Sonoma Volcanics and the Franciscan Complex, where anthropogenic contributions were expected to be minimal because of undeveloped land use, ranged from less than the reporting limit for this report of 1.02 mg/L to 2.2 mg/L NO_3-N (fig. C10; Teague, 2022). Nitrate concentrations were generally less in the deep wells of the PVW than in shallow or mixed-depth wells (fig. C11). Low NO_3-N concentrations can be caused by dilution from mixing with low-NO_3-N groundwater or by denitrification. Samples with NO_3-N concentrations exceeding the highest detection limit of 1.02 mg/L were generally from wells in urban and agricultural areas (fig. C10).

Concentrations of NO_3-N measured in samples from wells could vary temporally such that a single groundwater sample does not accurately characterize NO_3-N in the aquifer because the fractions of young, relatively higher NO_3-N water and old, relatively lower NO_3-N water change through time as water levels and pumping rates change. Therefore, data were analyzed for trends in NO_3-N concentration through time to improve the identification of areas where NO_3-N concentrations were increasing or decreasing (fig. C12; Teague, 2022).

Trends in NO_3-N concentration data were identified using the Mann-Kendall method (Helsel and others, 2020) in the R statistical environment (R Core Team, 2021) using the "Kendall" package (McLeod, 2011). Increasing (positive tau values; W48) and decreasing (negative tau values; W26) changes in concentration that were significantly different from zero are trends identified by p-values less than or equal to 0.05 (fig. C12). Increasing NO_3-N concentrations at well W48 were possibly caused by urban or agricultural land use (figs. C10, C12). Well W26 is in an urban land-use area, but decreasing NO_3-N concentrations could be the result of its proximity to natural land (fig. C10). In samples from other wells that exceeded the MCL (W11, W19, W20, W25, W34, W48, W51, W56, and W72; table C1), significant trends in NO_3-N concentrations were not identified (fig. C12).

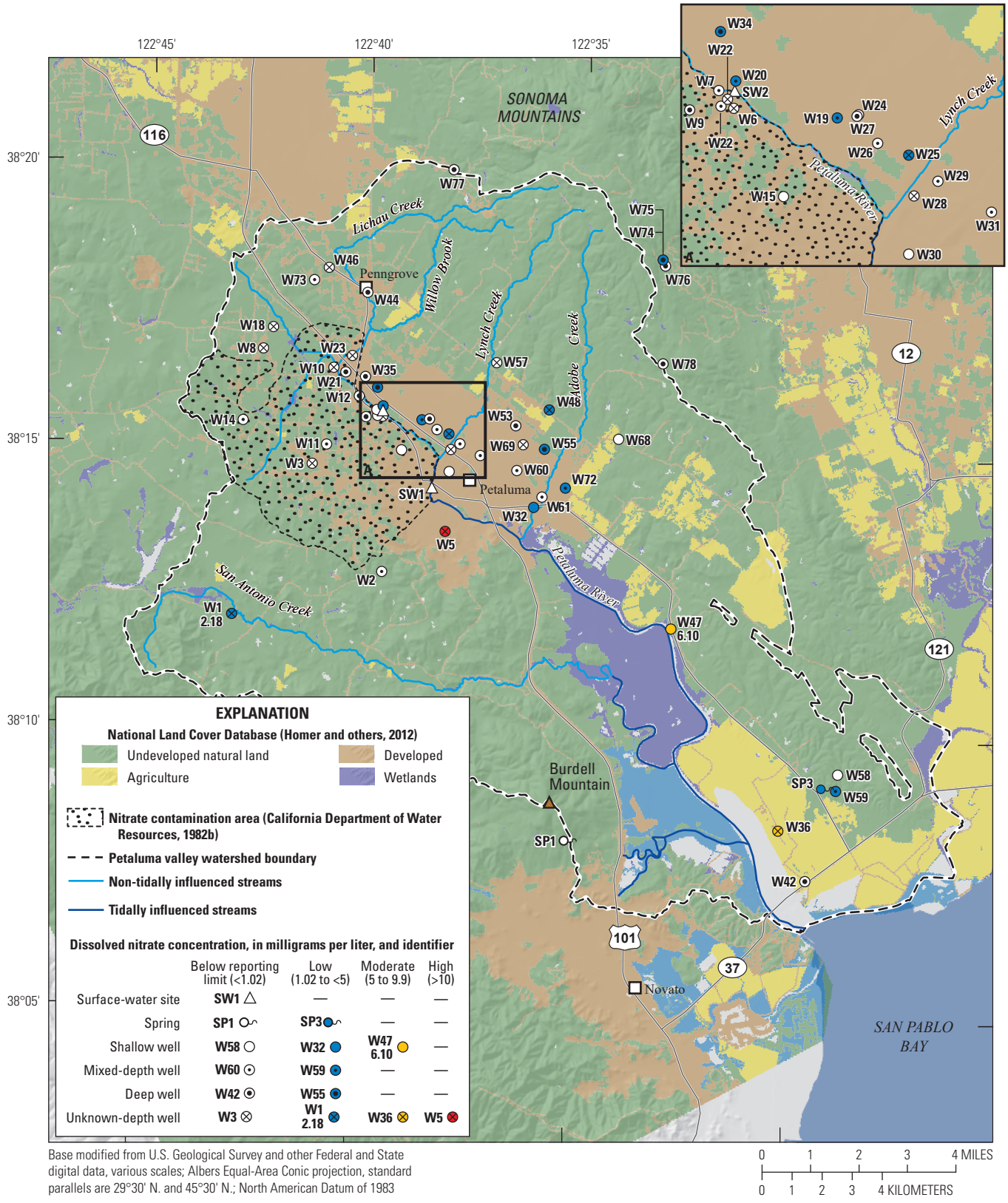

Figure C10. Nitrate concentrations in relation to land-use types (Homer and others, 2012) for samples from the Petaluma valley watershed, Sonoma County, California, 1974–2015 (Teague, 2022); site information is provided in table C1.

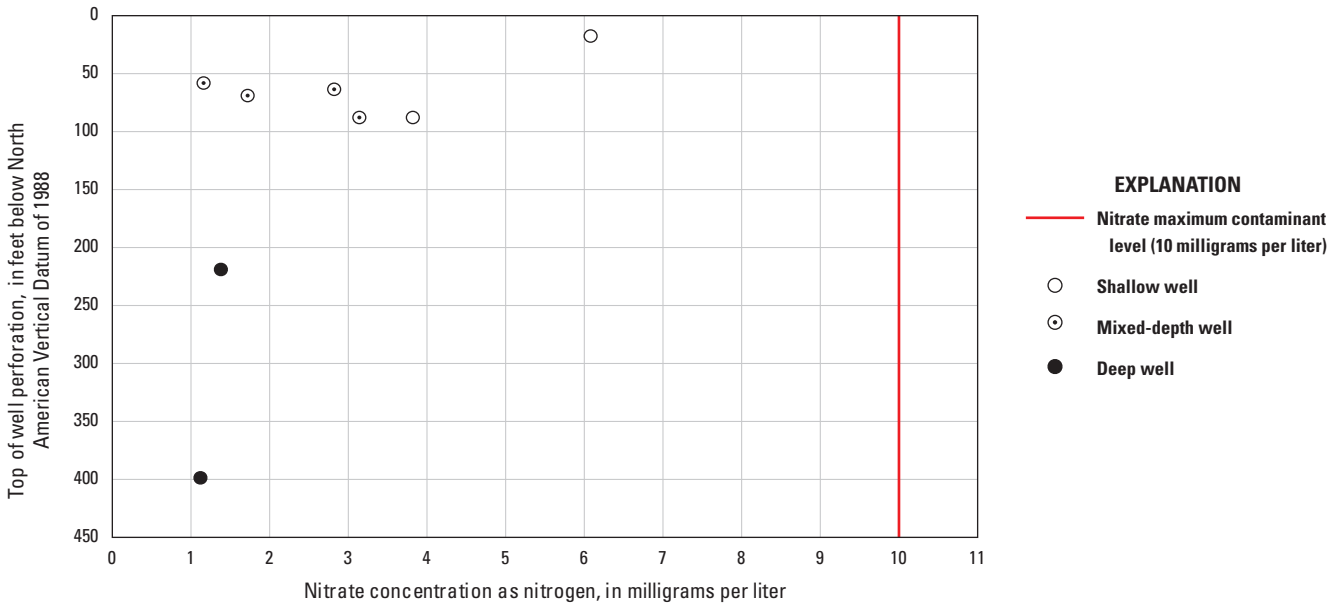

Figure C11. Nitrate data (as nitrogen in mg/L) for wells grouped by depth to the top of the perforated interval for which nitrate concentrations are greater than the reporting limit and well-construction data are available, Petaluma valley watershed, Sonoma County, California, 1974–2015 (Teague, 2022).

Chemical Changes in Groundwater Along Potential Groundwater-Flow Paths

Differences in chemical character of groundwater along a transect of wells across a basin can provide information about groundwater gradients through the basin. Transects may be aligned parallel to the general groundwater gradients along flow paths as inferred from water-level altitude contours. Groundwater flow paths inferred from physical data can be verified and refined using independent groundwater-chemistry data. Previous reports (Cardwell, 1958; California Department of Water Resources, 1982a) and the three-dimensional hydrogeologic framework model presented in chapter B indicate that groundwater flows northeast from the watershed boundaries toward the valley axis on the western side and from the northeast to the southwest on the eastern side. Two transects were selected across the northern PVW to characterize these groundwater flow paths (fig. C2) and selected major-ion concentration data from wells along the transects are presented as vertical profiles (table C3; figs. C13, C14). Wells are plotted along each profile according to their normalized position along the flow path (the distance from the start of the section to the well divided by the distance of the entire section), such that wells with values nearing zero are close to the upgradient end of the flow path, closest to the groundwater basin boundary, and wells with values nearing one are near the downgradient end of the groundwater flow path. Only wells within 2,000 ft of the transect line are included in the analyses described here.

Aquifer and Groundwater Characteristics Along West to East Transect A–A'

Transect A–A' (fig. C2) is aligned from southwest to northeast and follows the groundwater-flow direction indicated by groundwater-level contours (chapter B, fig. B11*A*). The section begins near well W1 in Franciscan Complex, crosses into exposed Wilson Grove Formation, and then ends at the Petaluma River near well W12 (fig. C2). One well is perforated in the Franciscan Complex (W1), and four wells are perforated in the Wilson Grove Formation (W3, W16, W9, and W12; table C3). Water sampled from well W1 had a low TDS concentration (204 mg/L), likely representing natural recharge (fig. C13; table C3). As groundwater flows east toward the Petaluma River, TDS concentrations increased to 342 mg/L (W9) but remained relatively low (fig. C13; table C3). Changes in chemical composition along the section were minimal (fig. C13; table C3) because the Wilson Grove Formation is generally unreactive. The slight decrease in major-ion concentrations between wells W9 and W12 would not be expected from simple rock–water interaction and could be consistent with mixing with a more dilute water source near the presumed discharge area at the axis of the valley (fig. C13; table C3). As previously suggested for wells in the Quaternary mixed unit, groundwater discharge from the convergence of groundwater flow paths would be expected along the axis of the valley under pre-groundwater development conditions. The major-ion data for samples from wells W9 and W12 indicate that groundwater is discharging in the Wilson Grove Formation along the east side of the valley axis.

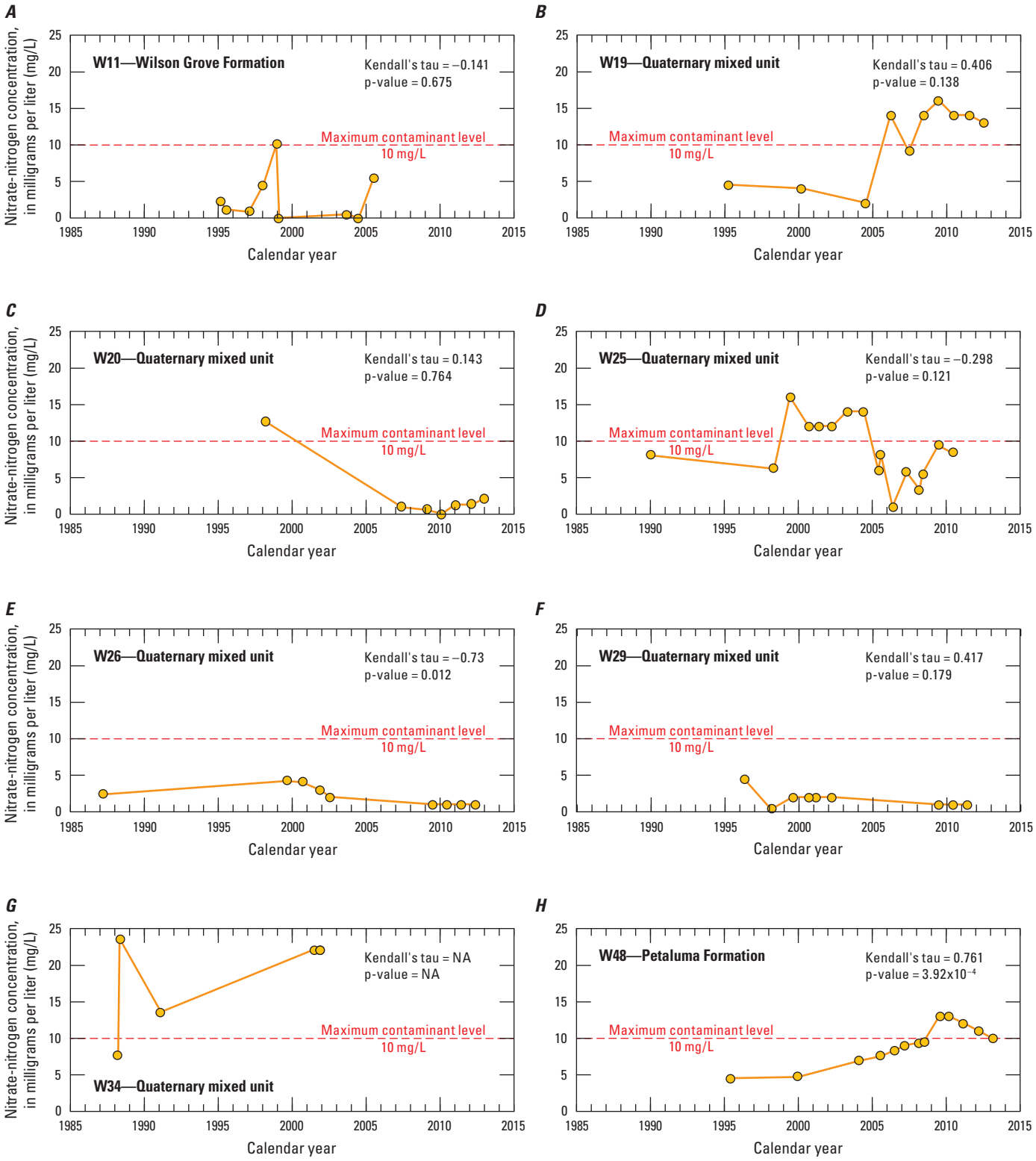

Figure C12. Nitrate-nitrogen concentrations with trend lines, Kendall's tau values, and p-values for selected wells in the Petaluma valley watershed, Sonoma County, California, 1987–2013 (Teague, 2022): *A*, W11, *B*, W19, *C*, W20, *D*, W25, *E*, W26, *F*, W29, *G*, W34, *H*, W48, *I*, W51, *J*, W52, *K*, W53, *L*, W55, *M*, W56, *N*, W72, *O*, W74, *P*, W75 ; site information is provided in table C1.

Figure C12.—Continued

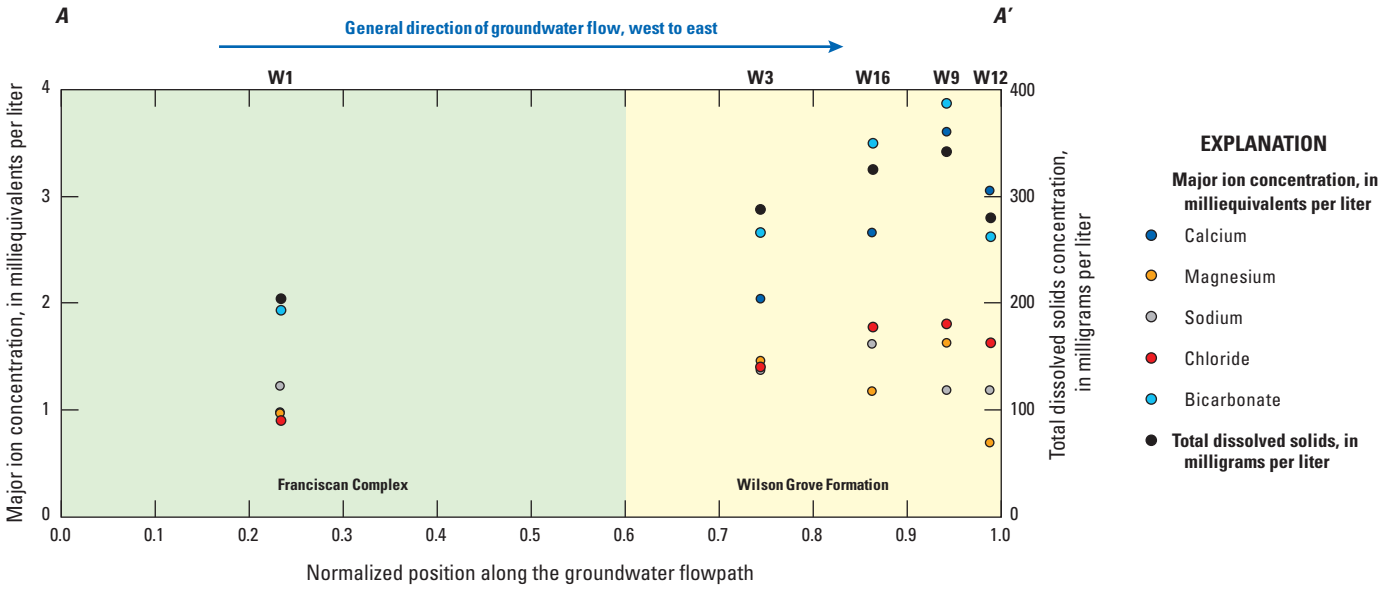

Figure C13. Major-ion composition for select wells along section A–A′ (fig. C2), Petaluma valley watershed, Sonoma County, California (Teague, 2022); site information is provided in table C1.

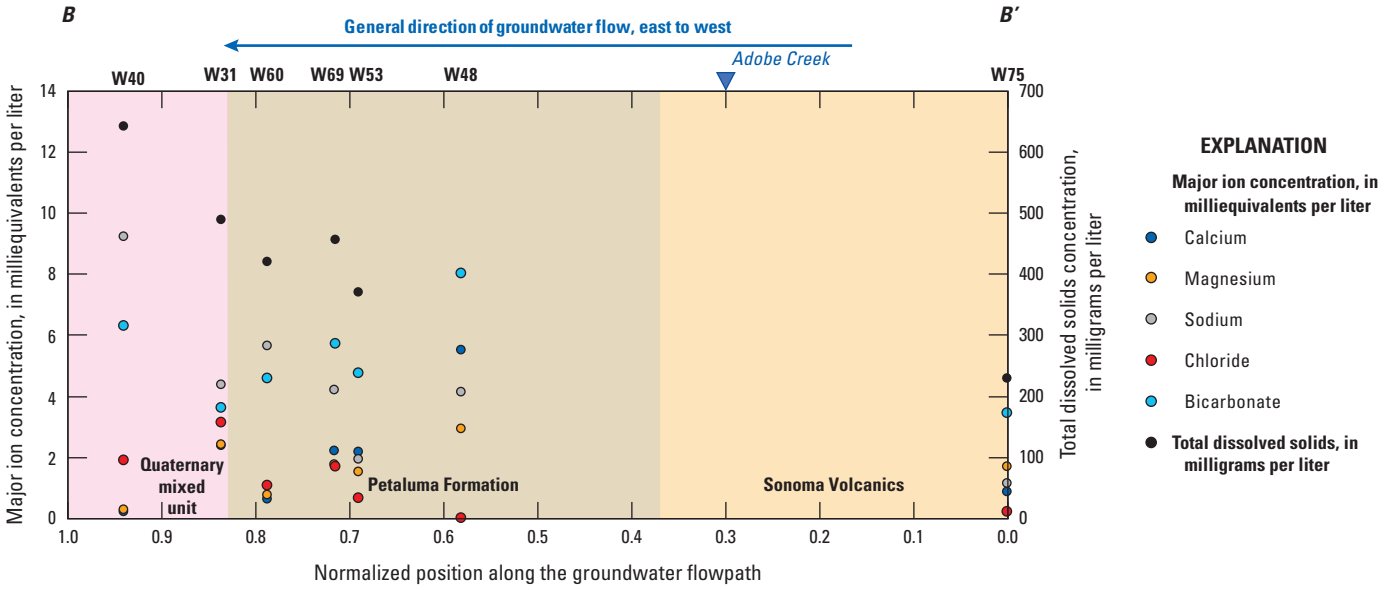

Figure C14. Major-ion composition for select wells along section B–B′ (fig. C2), Petaluma valley watershed, Sonoma County, California (Teague, 2022); site information is provided in table C1.

Table C3. Construction and major-ion data for wells shown in the cross-sections on figures C13 and C14 (Teague, 2022); additional site information is provided in table C1.

[ft bls, feet below land surface; mg/L, milligrams per liter; —, no data]

Map number (fig. C1)	Hydrogeologic unit	Depth of well completion (ft bls)	Depth of top perforation (ft bls)	Depth of bottom perforation (ft bls)	Well-depth classification	Normalized position	Calcium (mg/L)	Magnesium (mg/L)	Sodium (mg/L)	Chloride (mg/L)	Bicarbonate (mg/L)	Total dissolved solids (mg/L)
Section A–A'												
W1	Basement	—	—	—	Unknown	0.23	19.4	[2]11.5	[2]27.9	[2]31.5	[2]118	[2]204
W3	Wilson Grove	225	—	—	Unknown	0.74	40.6	17.4	[2]31.3	[2]48.9	[2]162	[2]288
W16	Wilson Grove	180	130	180	Shallow	0.86	53	14	[2]37	[2]62	213	[2]325
W9	Wilson Grove	408	270	408	Deep	0.94	[1]72	19.4	[2]27	[2]63	236	[2]342
W12	Wilson Grove	350	250	350	Deep	0.99	[1]61	[2]8.2	[2]27	[2]57	[2]160	[2]280
Section B–B'												
W75	Sonoma Volcanics	740	400	740	Deep	0.00	[2]17	20	[2]26	[2]8	210	[2]230
W48	Petaluma	—	—	—	Unknown	0.58	[1]110	[1]35	[1]95	[2]—	[1]490	[2]—
W53	Petaluma	607	200	440	Deep	0.69	43	18	44	[2]23	290	[2]370
W69	Petaluma	605	—	—	Deep	0.72	44	21	[1]96	[2]59	[1]350	456
W60	Petaluma	500	160	420	Mixed	0.79	[2]12	[2]8.9	[1]130	[2]37	280	[2]420
W31	Quaternary mixed unit	530	180	520	Deep	0.84	47	29	[1]100	[1]110	220	490
W40	Quaternary mixed unit	280	—	—	Unknown	0.94	[2]4.2	[2]3.3	[1]212	66	[1]384	[1]642

[1]High concentration.

[2]Low concentration.

In general, the unreactive nature of the Wilson Grove Formation means that groundwater movement is not evident from changes in groundwater chemistry along section A–A'. A non-conservative decrease in major-ion concentration between wells W9 and W12, however, does indicate converging flow paths at the axis of the valley. Although groundwater-age-dating data are unavailable for the wells along section A–A', age-dating data from other wells in the formation (fig. C4) show increasing ages from the PVW boundary to the axis, which is consistent with groundwater movement indicated by groundwater contours presented in chapter B.

Aquifer and Groundwater Characteristics Along Northeast to Southwest Transect B–B'

Transect B–B' is aligned from northeast to southwest and follows the groundwater-flow direction indicated by groundwater-level contours (chapter B, fig. B11*A*). The section begins at well W75 in Sonoma Volcanics, crosses the Petaluma Formation and Quaternary mixed unit, and ends at the Petaluma River near well W40 (fig. C2). During base-flow conditions, the Petaluma River gains water from the confluence with Lichau Creek to just north of the confluence with Lynch Creek, indicating groundwater discharge to the stream channel (chapter B, table B1).

Three wells (W74-76) are perforated in the Sonoma Volcanics (fig. C2) and have similar TDS and major-ion concentrations (Teague, 2022); therefore, the deepest well (W75) was used to represent groundwater in the Sonoma Volcanics (fig. C14; table C3). Water sampled from well W75 had low TDS (230 mg/L) and major-ion concentrations, likely representing natural recharge.

Four wells are perforated in the Petaluma Formation (W48, W53, W69 and W60), and two wells are perforated in the Quaternary mixed unit (W31 and W40). As groundwater moves downgradient from well W75, TDS and major ion concentrations generally increased (fig. C14; table C3), which is consistent with groundwater that has reacted with subsurface material while moving through the aquifer (Chebotarev, 1955; Domenico, 1972). Maximum TDS, HCO_3, and Na concentrations along the section at well W40 are consistent with expected values for the downgradient end of this groundwater flow path (fig. C14).

The groundwater chemistry from samples along transect B–B' show that as groundwater moves from recharge sources in the Sonoma Volcanics toward the axis of the valley, changes in major-ion composition are consistent with groundwater evolution along a flow path. These changes include increases in TDS and HCO_3 and decreases in the Ca to Na ratio. The non-conservative change in Ca and Na concentrations from wells W60 to W31 and W31 to W40 indicate that groundwater sampled from W31 was a mixture of groundwater moving along the groundwater flow path and water from another source, such as modern infiltration.

Summary

The U.S. Geological Survey (USGS), in cooperation with the Sonoma County Water Agency and the City of Petaluma, characterized groundwater chemistry, source, and age for the Petaluma valley watershed (PVW) using analyses for selected physical properties, inorganic constituents, and stable and radioactive isotopes. Stable-isotope data indicated that the primary source of groundwater recharge in the PVW is infiltration of precipitation in the Wilson Grove Formation Highlands groundwater basin and Sonoma Mountains. As groundwater moves from the boundary of the watershed through the major hydrogeologic units toward the axis of the Petaluma valley and the Petaluma River, water-quality changes were caused by chemical reactions between groundwater and aquifer material and by mixing with infiltration of precipitation. Other sources of water include infiltration of agricultural return and urban runoff. Impairments to water-quality included increased specific conductance (SC) values and increased concentrations of chloride (Cl) and nitrate (NO_3-N). In the PVW, the primary source of high SC and Cl groundwater was groundwater evolution through water–rock reactions, and the primary source of high SC and Cl in surface water was the tidal movement of San Pablo Bay into the Petaluma River. Where encountered, high NO_3-N concentrations caused by agricultural return or urban runoff were local, small-scale issues and were limited to wells screened near the land surface.

Study results indicate that water sampled from the tidally influenced reach of the Petaluma River (SW1) contained San Pablo Bay water that has moved upstream by tidal flow mixed with river water that originated as groundwater discharge. This tidally influenced river water had the highest SC values and Cl concentrations measured in the study area. Mixing with San Pablo Bay water was indicated by stable-isotopic and major-ion data. Water sampled from upstream from the tidally influenced reach (SW2) represented a mixture of groundwater inputs from the Wilson Grove Formation and Quaternary mixed unit that had undergone evaporation.

Stable-isotope data for samples from wells in the PVW generally plot along the Global Meteoric Water Line (GMWL), indicating that groundwater in the watershed originated as infiltration of precipitation. Similarities between stable-isotopic composition in groundwater from wells perforated in the Wilson Grove and Petaluma Formations indicate that the source of water for these geographically distinct areas was similar in altitude; based on groundwater-altitude data, the sources of groundwater were the Wilson Grove Formation Highlands groundwater basin to the west and the Sonoma Mountains to the east.

In general, modern (post-1950s) water was in samples from shallow wells and mixed-depth wells screened near land surface, and groundwater sampled from deep wells along the axis of Petaluma valley was pre-modern water. Values of delta carbon-13 ($\delta^{13}C$) for samples of older water, those with carbon-14 (^{14}C) less than 60 percent modern carbon, were within the expected range of recharged groundwater in an unconfined system without sedimentary sources of carbon and indicate that water infiltrated in areas of the Sonoma Mountains or Wilson Grove Formation Highlands groundwater basin where minimal organic material was at land surface. The $\delta^{13}C$ samples of younger water (^{14}C greater than 60 percent modern carbon) were generally lighter (more negative), indicating exchange of carbon from decomposition of organic matter buried in the aquifer. The $\delta^{13}C$ values indicate that contribution of carbon from carbonate dissolution was negligible.

Groundwater in the Wilson Grove Formation underwent little change in water quality moving east from the watershed boundary because of the predominantly siliceous composition of the subsurface material. Instead, groundwater movement from the boundary of the PVW to the axis of the valley was inferred from groundwater ages. Wells perforated in the Wilson Grove Formation near the axis of the PVW have higher concentrations of total dissolved solids (TDS) than wells near the boundary. Groundwater in the Wilson Grove Formation ranged from pre-modern in well W18 of unknown depth (no detectable tritium and carbon-age of 12,000 years before present, or ybp), to a mixture of pre-modern and modern in shallow well W15 (no detectable tritium and a carbon-age of 5,000 ybp), to modern in shallow well W17 (tritium activity equal to 4.8 picocuries per liter and carbon-age of less than 1,000 ybp). Additionally, a non-conservative decrease in major-ion composition between wells W9 and W12 at the axis of the valley indicates a discharge of a deep groundwater source with different chemistry that is caused by converging groundwater flow paths. The groundwater types in wells perforated in the Wilson Grove Formation were tightly grouped and were primarily mixed cation-bicarbonate (HCO_3), or Ca-HCO_3, type water. Similar major-ion compositions in samples from wells perforated in the Wilson Grove Formation and the sample from SW2 indicate that groundwater from the Wilson Grove Formation was a substantial input to streamflow in the upper reach of the Petaluma River. Water quality was generally good in groundwater from wells perforated in the Wilson Grove Formation, with low to moderate SC, total dissolved solids (TDS), Cl, sodium (Na), and calcium (Ca) values indicating a lack of mixing with saline water.

Groundwater chemistry in the eastern part of the Petaluma Formation, near the transition from the Sonoma Volcanics, was similar to that of groundwater in the Sonoma Volcanics, indicating that groundwater moves through the Sonoma Volcanics with minimal changes to chemistry from reactions with the aquifer material before entering the Petaluma Formation. Groundwater moving west through the Sonoma Volcanics and Petaluma Formation undergoes changes in water quality because of mixing with modern water and reactions with aquifer material. The carbon ages and the tritium activities of samples from wells perforated in the Petaluma Formation indicated that groundwater in shallow and mixed-depth wells is a mixture of modern and pre-modern waters, demonstrating pre-modern groundwater mixing with modern water that infiltrated from land surface. As groundwater moves through the Petaluma Formation, to greater depths in the formation and toward the axis of the valley, reactions with aquifer material lead to an increase in SC, TDS, and major-ion concentrations and evolution to Na-HCO_3 type water. Major-ion concentrations in water sampled from a well at the end of the Sonoma Volcanics to Petaluma Formation to Quaternary mixed unit flow path (W40) indicate water–rock reactions that are generally associated with groundwater after long residence times; therefore, this water is representative of the downgradient end of the long groundwater flow path. Groundwater in the northern and southern parts of the PVW was different in composition than other groundwater in the Petaluma Formation. This groundwater moved along a different flow path than the groundwater from wells in the central part of the formation and likely represents a different groundwater evolution.

Groundwater in the Quaternary mixed unit is a mixture of groundwater from the Wilson Grove and Petaluma Formations. Under current conditions, groundwater movement is from the Wilson Grove and Petaluma Formations toward the Quaternary mixed unit. Similar major-ion compositions in samples from wells perforated in the Quaternary mixed unit and the sample from SW2 indicate that groundwater from the Quaternary mixed unit is a large input to streamflow in the upper reach of the Petaluma River.

Groundwater in deep wells perforated in the Quaternary mixed unit is pre-modern and groundwater in the shallow wells is modern. The modern water is a mixture of infiltration of precipitation and infiltration of agricultural return and urban runoff. The major-ion data indicate that pre-modern groundwater in deep wells is a mixture of groundwater from the Wilson Grove and Petaluma Formations, which in some places could be mixing with a deeper, relatively saline source of groundwater. The isotopically light water in wells W22 and W42 indicates the presence of water that infiltrated under a cooler climate, tens of thousands of years before present. Water-chemistry data and groundwater ages greater than 17,000 ybp indicate that water from neighboring wells W21 and W22 may represent the discharging of old groundwater caused by the convergence of long groundwater flow paths at the axis of the valley. A ^{14}C age of 30,000 ybp in deep well W42 is representative of a deep source of older groundwater, and major-ion data indicate water–rock reactions between the groundwater and aquifer material.

Although NO_3-N contamination of groundwater from agricultural land-use has historically been an issue in shallow wells in the Wilson Grove Formation, only one of the samples collected for this study had NO_3-N concentrations exceeding

the MCL. The general absence of high NO_3-N concentrations in groundwater samples for this study demonstrates that NO_3 contamination has not moved deeper into the aquifer. However, this absence of high NO_3-N concentrations should not be interpreted as evidence that NO_3 contamination in the shallow part of the Wilson Grove Formation has been resolved. Concentrations of NO_3-N were generally detected in shallow and mixed-depth wells in urban and agricultural areas. A moderate NO_3-N concentration measured in the groundwater sample from well W36 indicates that agricultural return is influencing the chemistry of the water sampled from some wells in the southern part of the PVW. Significant trends in NO_3-N concentrations were not observed in most of the wells analyzed in this study. Increasing NO_3-N concentrations at well W48 were possibly caused by activities involved with urban or agricultural land use. Decreasing NO_3-N concentrations at well W26 in an urban land-use area could result from its proximity to natural land.

References Cited

American Public Health Association, 2005, Standard methods for the examination of water and wastewater (21st ed.): Washington, D.C., American Water Works Association and Water Pollution Control Federation, 1368 p.

American Public Health Association, 2012, Standard methods for the examination of water and wastewater (22 ed.): Washington, D.C., American Water Works Association and Water Pollution Control Federation, variously paged.

Ayers, R.S., and Westcot, D.W., 1994, Water quality for agriculture, Food and Agriculture Organization of the United Nations: Irrigation and Drainage Paper 29 Rev 1; accessed January 9, 2013, at http://www.fao.org/3/T0234E/T0234E00.htm.

Belitz, K., Dubrovsky, N.M., Burow, K., Jurgens, B., and Johnson, T., 2003, Framework for a ground-water quality monitoring and assessment program for California: U.S. Geological Survey Water-Resources Investigations Report 03–4166, 78 p.

California Department of Water Resources (CDWR), 1982a, Evaluation of ground water resources Sonoma County, volume 3: Petaluma Valley, Bulletin 118-4, June 1982, 89 p.

California Department of Water Resources (CDWR), 1982b, Study of nitrates in ground water: Sonoma County, Petaluma Area, 85 p.

California State Water Resources Control Board, 2010, Groundwater information sheet—Salinity; accessed January 9, 2013, at https://www.waterboards.ca.gov/gama/docs/coc_salinity.pdf.

Cardwell, G.T., 1958, Geology and ground water in Santa Rosa and Petaluma Valley Areas, Sonoma County, California: U.S. Geological Survey Water-Supply Paper 1427, 273 p. [Available at https://pubs.usgs.gov/wsp/1427/report.pdf.]

Chebotarev, I.I., 1955, Metamorphism of natural waters in the crust of weathering—1: Geochimica et Cosmochimica Acta, v. 8, no. 1–2, p. 22–48. [Available at https://doi.org/10.1016/0016-7037(55)90015-6.]

Clark, I., and Fritz, P., 1997, Environmental isotopes in hydrogeology: New York, Lewis Publishers, 328 p.

Coplen, T.B., 1994, Reporting of the stable hydrogen, carbon and oxygen isotopic abundances: Pure and Applied Chemistry, v. 66, no. 2, p. 273–276. [Available at https://doi.org/10.1351/pac199466020273.]

Craig, H., 1961, Isotopic variation in meteoric waters: Science, v. 133, no. 3465, p. 1702–1703. [Available at https://doi.org/10.1126/science.133.3465.1702.]

Domenico, P.A., 1972, Concepts and models in groundwater hydrology: New York, McGraw-Hill.

Drever, J.I., 1982, The geochemistry of natural waters: Englewood Cliffs, New Jersey, Prentice-Hall, 388 p.

Farrar, C.D., Metzger, L.F., Nishikawa, T., Koczot, K.M., Reichard, E.G., and Langenheim, V.E., 2006, Geohydrologic characterization, water-chemistry, and ground-water flow simulation model of the Sonoma Valley area, Sonoma County, California: U.S. Geological Survey Scientific Investigations Report 2006–5092, 167 p.

Fifield, L.K., 1999, Accelerator mass spectrometry and its applications: Reports on Progress in Physics, v. 62, no. 8, p. 1223–1274. [Available at https://doi.org/10.1088/0034-4885/62/8/202.]

Fishman, M.J., 1993, Methods of analysis by the U.S. Geological Survey National Water Quality Laboratory—Determination of inorganic and organic constituents in water and fluvial sediments: U.S. Geological Survey Open-File Report 93–125, 217 p. [Available at https://doi.org/10.3133/ofr93125.]

Fishman, M.J., and Friedman, L.C., 1989, Methods for determination of inorganic substances in water and fluvial sediments: U.S. Geological Techniques of Water-Resources Investigations, book 5, chap. A1, 545 p.

Freeze, R.A., and Cherry, J.A., 1979, Groundwater: Englewood Cliffs, New Jersey, Prentice-Hall, 604 p.

Garbarino, J.R., 1999, Methods of analysis by the U.S. Geological Survey National Water Quality Laboratory—Determination of dissolved arsenic, boron, lithium, selenium, strontium, thallium, and vanadium using inductively coupled plasma-mass spectrometry: U.S. Geological Survey Open-File Report 99–093, 31 p. [Available at https://doi.org/10.3133/ofr9993.]

Garbarino, J.R., Kanagy, L.K., and Cree, M.E., 2006, Determination of elements in natural-water, biota, sediment, and soil samples using collision/reaction cell inductively coupled plasma–mass spectrometry: U.S. Geological Survey Techniques and Methods, book 5, sec. B, chap. 1, 88 p.

Gat, J.R., and Gonfiantini, R., 1981, Stable isotope hydrology, deuterium and oxygen-18 in the water cycle: International Atomic Energy Agency, Technical Reports Series No. 210, 339 p.

Geyh, M.A., 2000, An overview of ^{14}C analysis in groundwater: Radiocarbon, v. 42, no. 1, p. 99–114, accessed June 13, 2016, at https://doi.org/10.1017/S0033822200053078.

Helsel, D.R., Hirsch, R.M., Ryberg, K.R., Archfield, S.A., and Gilroy, E.J., 2020, Statistical methods in water resources: U.S. Geological Survey Techniques and Methods, book 4, chapter A3, 458 p. [Available at https://doi.org/10.3133/tm4A3.]

Hem, J.D., 1992, Study and interpretation of the chemical characteristics of natural water (3d ed.): U.S. Geological Survey Water-Supply Paper 2254, 263 p., 3 plates.

Homer, C.H., Fry, J.A., and Barnes, C.A., 2012, The National Land Cover Database: U.S. Geological Survey Fact Sheet 2012–3020, 4 p.

Ingram, L.B., Conrad, M.E., and Ingle, J.C., 1996, Stable isotope and salinity systematics in estuarine waters and carbonates—San Francisco Bay: Geochimica et Cosmochimica Acta, v. 60, no. 3, p. 455–467. [Available at https://doi.org/10.1016/0016-7037(95)00398-3.]

Iwamura, T.I., 1980, Saltwater intrusion investigation in the Santa Clara County baylands area: California, Santa Clara Valley Water District, 115 p.

Izbicki, J.A., Borchers, J.W., Leighton, D.A., Kulongoski, J.T., Fields, L., Galloway, D.L., and Michel, R.L., 2003, Hydrogeology and geochemistry of aquifers underlying the San Lorenzo and San Leandro areas of the East Bay Plain, Alameda County, California: U.S. Geological Survey Water-Resources Investigations Report 02–4259, 71 p.

Kulongoski, J.T., Belitz, K., and Dawson, B.J., 2006, Ground-water quality data in the north San Francisco Bay hydrologic provinces, California, 2004—Results from the California Ground-water Ambient Monitoring and Assessment (GAMA) program: U.S. Geological Survey Data Series 167, 100 p. [Available at https://doi.org/10.3133/ds167.]

Kulongoski, J.T., Belitz, K., Landon, M.K., and Farrar, C.D., 2010, Status and understanding of groundwater quality in the North San Francisco Bay groundwater basins, 2004: U.S. Geological Survey Scientific Investigations Report 2010–5089, 65 p.

Lal, D., and Peters, B., 1967, Cosmic ray produced radioactivity on the earth—Encyclopedia of Physics: New York, Springer-Verlag, v. 46, p. 407–434.

Lucas, L.L., and Unterweger, M.P., 2000, Comprehensive review and critical evaluation of the half-life of tritium: Journal of Research of the National Institute of Standards and Technology, v. 105, no. 4, p. 541–549. [Available at https://doi.org/10.6028/jres.105.043.]

McLeod, A.I., 2011, Package 'Kendall', version 2.2: Kendall rank correlation and Mann-Kendall trend test, accessed December 1, 2021, at https://cran.r-project.org/web/packages/Kendall/Kendall.pdf.

Michel, R.L., 1976, Tritium inventories of the world oceans and their implications: Nature, v. 263, no. 5573, p. 103–106. [Available at https://doi.org/10.1038/263103a0.]

Muir, K.S., and Coplen, T.B., 1981, Tracing ground-water movement by using the stable isotopes of oxygen and hydrogen, upper Penitencia Creek alluvial fan, Santa Clara Valley, California: U.S. Geological Survey Water-Supply Paper 2075, 18 p.

O'Brien, K., de La Zerda Lerner, A., Shea, M.A., and Smart, D.F., 1991, The production of cosmogenic isotopes in the Earth's atmosphere and their inventories, *in* Sonett, C.P., Giampapa, M.S., Matthews, M.S., eds., The Sun in Time: University of Arizona Press, p. 317–342.

Ostlund, H.G., and Dorsey, H.G., 1975, Rapid electrolytic enrichment of hydrogen gas proportional counting of tritium: International Conference on Low Radioactivity Measurement and Applications, High Tatras, Czechoslovakia, October 1975, Proceedings, 6 p.

Patton, C.J., and Truitt, E.P., 2000, Methods of analysis by the U.S. Geological Survey National Water Quality Laboratory—Determination of ammonium plus organic nitrogen by a Kjeldahl digestion method and an automated photometric finish that includes digest cleanup by gas diffusion: U.S. Geological Survey Open-File Report 00–170, 31 p. [Available at https://doi.org/10.3133/ofr00170.]

Piper, A.M., 1944, A graphic procedure in the geochemical interpretation of water-analyses: American Geophysical Union Transactions, v. 25, no. 6, p. 914–928, https://doi.org/10.1029/TR025i006p00914.

R Core Team,2021, R: A language and environment for statistical computing: R Foundation for Statistical Computing, Vienna, Austria, accessed December 1, 2021, at http://www.Rproject.org/.

Révész, K., and Coplen, T.B., 2008a, Determination of the $\delta(^{2}H/^{1}H)$ of water—RSIL lab code 1574, chap. C1 *of* Révész, K., and Coplen, T.B., eds., Methods of the Reston Stable Isotope Laboratory: U.S. Geological Survey Techniques and Methods 10–C1, 27 p.

Révész, K., and Coplen, T.B., 2008b, Determination of the $\delta(^{18}O/^{16}O)$ of water—RSIL lab code 489, chap. C2 *of* Révész, K., and Coplen, T.B., eds., Methods of the Reston Stable Isotope Laboratory: U.S. Geological Survey Techniques and Methods, 10–C2, 28 p.

Rosen, M.R., and Coshell, L., 1998, Influence of eruptive volcanic lithologies on surface and ground water chemical compositions, Lake Taupo, New Zealand, *in* Arehart, G.B. and Hulston, J.R., eds., Water-rock interaction: Proc. Ninth Int. Symp. On Water–Rock Interaction, Taupo, Balkema, p. 181–184.

Solomon, D.K., and Cook, P.G., 2000, ^{3}H and ^{3}He, chap. 13 *of* Cook, P.G., and Herczeg, A.L., eds., Environmental tracers in subsurface hydrology: Boston, Kluwer Academic Publishers, p. 397–424. [Available at https://doi.org/10.1007/978-1-4615-4557-6_13.]

Stiff, H.A., Jr., 1951, The interpretation of chemical analysis by means of patterns: Journal of Petroleum Technology, v. 3, no. 10, p. 15–3. [Available at https://doi.org/10.2118/951376-G.]

Struzeski, T.M., DeGiacomo, W.J., and Zayhowski, E.J., 1996, Methods of analysis by the U.S. Geological Survey National Water Quality Laboratory-Determination of dis-solved aluminum and boron in water by inductively coupled plasma-atomic emission spectrometry: U.S. Geological Survey Open-File Report 96–149, 17 p.

Stuiver, M., and Polach, H.A., 1977, Discussion reporting of ^{14}C data: Radiocarbon, v. 19, no. 3, p. 355–363. [Available at https://doi.org/10.1017/S0033822200003672.]

Teague, N.F., 2022, Selected chemical and physical properties and inorganic constituents and time-series nitrate in samples from selected wells and/or springs, Petaluma Valley watershed, Sonoma County, California, 1959–2015: U.S. Geological Survey data release. [Available at https://doi.org/10.5066/P9IRYFMB.]

Thomson Reuters, 2018a, Sampling and analysis: California Code of Regulations, Title 22, division 4, chapter 3, Article 6-60321, accessed December 17, 2018, at https://govt.westlaw.com/calregs/Document/IF43ADC30D4B911DE8879F88E8B0DAAAE?viewType=FullText&originationContext=documenttoc&transitionType=CategoryPageItem&contextData=(sc.Default).

Thomson Reuters, 2018b, Secondary maximum contaminant levels and compliance: California Code of Regulations, Title 22, division 4, chapter 15, Article 16-64449, accessed December 17, 2018, at https://govt.westlaw.com/calregs/Document/I2260318DFFF045529B9496276F3A8573?viewType=FullText&originationContext=documenttoc&transitionType=CategoryPageItem&contextData=(sc.Default).

Tolman, C.F., and Poland, J.F., 1940, Ground-water, saltwater infiltration, and ground-surface recession in Santa Clara Valley, Santa Clara County, California: Eos, Transactions of 1940 of the American Geophysical Union, pt. 1, p. 23–35.

United Nations, World Health Organization, 1983, Environmental health criteria for selected radionuclides: Environmental Health Criteria 25. ISBN 92 4 154085 0.

University of Miami Tritium Laboratory, 2010, Tritium procedures and standards: University of Miami Tritium Laboratory, accessed December 13, 2010, at https://tritium.rsmas.miami.edu/analytical-services/procedures-and-standards/tritium/index.html.

U.S. Environmental Protection Agency, 1993, Methods for the determination of inorganic substances in environmental samples: Cincinnati, Ohio, Environmental Monitoring and Support Laboratory, EPA/600/R-93/100.

U.S. Environmental Protection Agency, 1994, Methods for the determination of metals in environmental samples, supplement 1: Cincinnati, Ohio, Environmental Monitoring and Support Laboratory, EPA/600/R-94/111.

U.S. Environmental Protection Agency, 2018, National Primary Drinking Water Regulations: U.S. Environmental Protection Agency Web page, accessed December 14, 2018, at https://www.epa.gov/ground-water-and-drinking-water/national-primary-drinking-water-regulations.

U.S. Geological Survey, variously dated, National field manual for the collection of water-quality data: U.S. Geological Survey Techniques of Water-Resources Investigations, book 9, chaps. A1–A9. [Available at http://pubs.water.usgs.gov/twri9A.]

U.S. Geological Survey, 2018, 2012–2016 California Drought: Historical Perspective, accessed December 14, 2018, at https://ca.water.usgs.gov/california-drought/california-drought-comparisons.html.

Wagner, D.L., Saucedo, G.J., Clahan, K.B., Fleck, R.J., Langenheim, V.E., McLaughlin, R.J., Sarna-Wojcicki, A.M., Allen, J.R., and Deino, A.L., 2011, Geology, geochronology, and paleogeography of the southern Sonoma volcanic field and adjacent areas, northern San Francisco Bay region, California: Geosphere, v. 7, no. 3, p. 658–683. [Available at https://doi.org/10.1130/GES00626.1.]

Weiss, W., Bullacher, J., and Roether, W., 1979, Evidence of pulsed discharges of tritium from nuclear energy installations in Central Europe precipitation in Behaviour of Tritium in the Environment: IAEA-SM-232/18, p. 17–30.

Worcester, K.R., Paradies, D.M., and Adams, M., 2010, Interpreting narrative objectives for biostimulatory substances for California Central Coast waters: Surface Water Ambient Monitoring Program Technical Report, July 2010. [Available at https://www.waterboards.ca.gov/water_issues/programs/swamp/docs/reglrpts/rb3_biostimulation.pdf.]

Chapter D. Petaluma Valley Integrated Hydrologic Model

By Jonathan A. Traum

Introduction

The U.S. Geological Survey (USGS), in cooperation with the Sonoma County Water Agency (SCWA) and the City of Petaluma, developed the Petaluma Valley Integrated Hydrologic Model (PVIHM) to simulate the groundwater-flow system, surface-water flow system, and agricultural and other land-surface processes in the Petaluma valley watershed (PVW). The PVIHM was developed using MODFLOW One Water Hydrologic Flow Model (MODFLOW-OWHM; Hanson and others, 2014) and provides a tool that local water managers, such as the Petaluma Valley Groundwater Sustainability Agency (GSA), SCWA, and the City of Petaluma, can use to evaluate groundwater sustainability through simulation of several hydrologic scenarios. Model-simulated scenarios can evaluate natural changes, such as the hydrologic effects of historical and future climate scenarios. In addition, model simulations can be used to evaluate effects of management actions, such as water conservation; enhanced recharge projects; and the conjunctive use of surface water, recycled water, and groundwater. The PVIHM simulates groundwater altitudes, groundwater storage, and groundwater and surface-water exchange, which are three of the six criteria used to evaluate groundwater sustainability under the Sustainable Groundwater Management Act (SGMA). MODFLOW does not simulate seawater intrusion explicitly; however, boundary flows along San Pablo Bay and the tidally influenced section of the Petaluma River can be used as a proxy for seawater intrusion. Water quality was addressed in chapter C of the report. Land subsidence is not currently an issue in the PVW. This chapter documents the data sources for PVIHM as well as its development, calibration, and results (including water budgets and analyses of simulated groundwater altitude).

Model Data

This section of the report discusses the data that were used in the development of the PVIHM. Several datasets used in the model, including land-surface altitude, soils, and land use, are presented in chapter A of this report. In this chapter, annual periods for model output and annual periods for selected model input datasets are presented as water years (WY). A WY is defined as the period from October 1st to September 30th of the following year and is named for the calendar year in which it ends.

Groundwater Altitude and Streamflow Data

A groundwater-altitude database of values calculated from 1,992 observations of depth to water in wells was compiled for the PVW. The database contains 33 monitoring wells from the California Department of Water Resources (CDWR) Water Data Library (WDL; California Department of Water Resources, 2018a) and 8 monitoring wells from CDWR's California Statewide Groundwater Elevation Monitoring (CASGEM) database (California Department of Water Resources, 2018b). The USGS National Water Information System (NWIS) data are included in the CDWR databases (U.S. Geological Survey, 2018). The locations of the monitoring wells are shown in figure D1, and a list of the wells, along with well-construction and other information, is presented in table D1. The WDL wells are identified with a California State well identification number, whereas the CASGEM wells are identified by a CDWR site code. Data from these monitoring wells were used to estimate initial-groundwater altitudes for the PVIHM and in model calibration, which are described later in this chapter.

Streamflow data are discussed in chapter B, locations of the three streamgages in the PVW are shown in figure D1 and supporting information for the streamgages are presented in table D2. Streamflows were published as daily values (U.S. Geological Survey, 2018); however, for this study, monthly average flows were computed for comparison to the simulated monthly values from the PVIHM for model calibration. These monthly average flows are available on NWIS (U.S. Geological Survey, 2018) using the "Time-series: Monthly statistics" option or in the groundwater model release (Traum, 2022).

Land-Surface Data

Land-surface processes have a substantial effect on the hydrologic conditions of the PVW. Groundwater pumpage for irrigated agriculture lowers groundwater altitudes and could reduce storage. Conversely, inefficient surface-water use from imported or recycled water sources recharges the groundwater system, thereby increasing groundwater altitudes and storage. The datasets discussed in the following sections, including crop data, climate, and water supply and demand, are required for quantifying these potential effects. For simplicity and consistency with MODFLOW-OWHM documentation, land-use types are referred to as "crops" throughout the report, including native vegetation and urban.

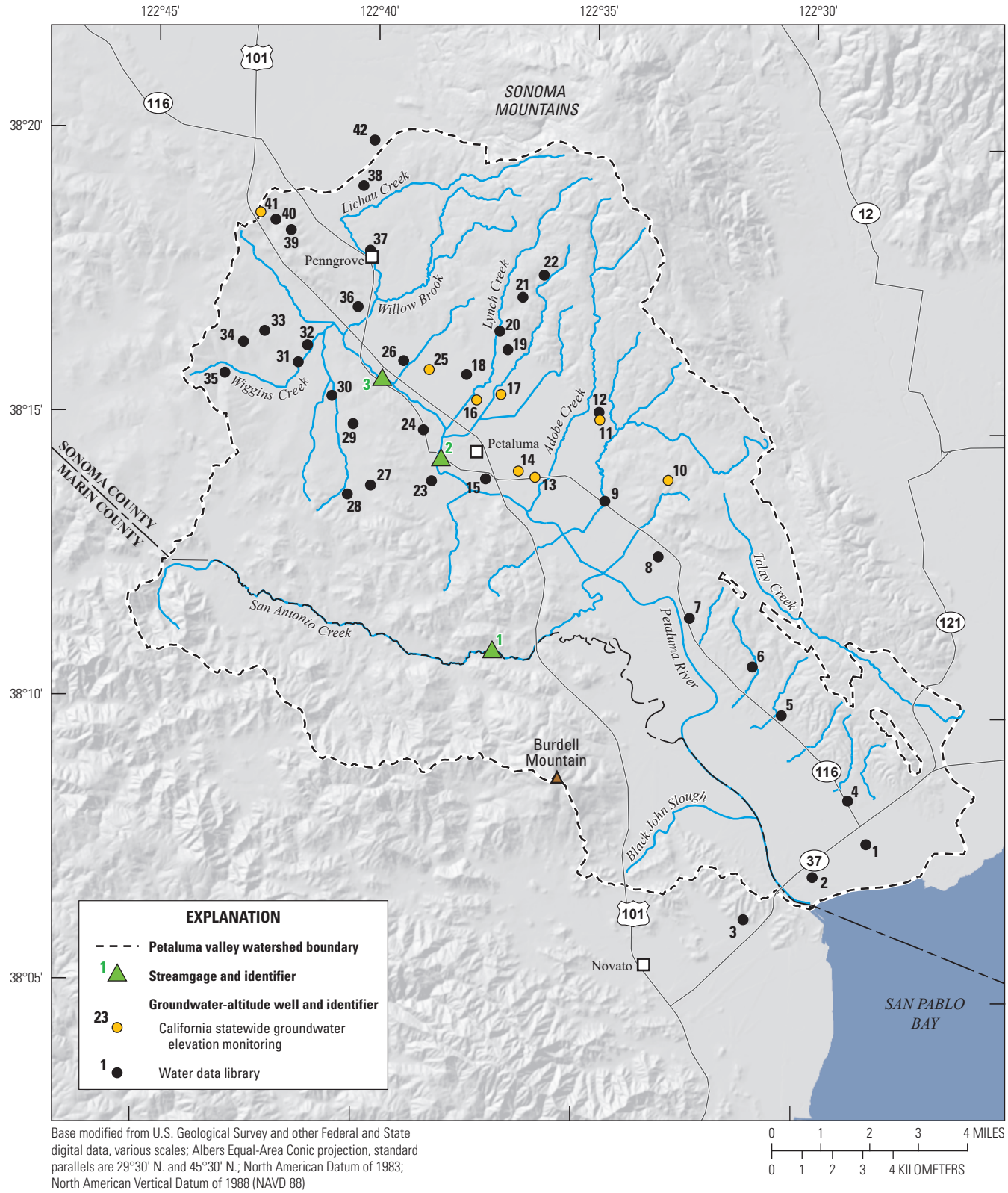

Figure D1. The location of monitoring wells and streamgages in the study area, Petaluma valley watershed, Sonoma County, California (California Department of Water Resources, 2018a, b); site identifiers and information associated with streamgages and wells are provided in table D1.

Table D1. Groundwater-altitude monitoring wells, Petaluma valley watershed, Sonoma County, California.

[Datum is North American Vertical Datum of 1988 (NAVD 88). **Abbreviations**: mm/dd/yyyy, month/day/year; ID, identification; ft, foot; WDL, water data library; CASGEM, California Statewide Groundwater Elevation Monitoring]

Well number (mm/dd/yyyy)	Well ID	Source	Groundwater-level altitude (ft above NAVD 88)	Well depth (ft)	Depth to top of well screen (ft)	Depth to bottom of well screen (ft)	First measurement (mm/dd/yyyy)	Last measurement (mm/dd/yyyy)	Number of measurements
1	3N/6W-01Q001	WDL	4.6	225	—	—	01/25/1950	12/22/2011	61
2	3N/6W-11L001	WDL	3.7	520	328	520	10/23/1990	05/24/1995	9
3	3N/6W-16H001	WDL	12.7	—	—	—	11/29/1973	04/14/2016	59
4	4N/6W-36N001	WDL	20.7	50	30	50	12/01/1989	04/19/1994	8
5	4N/6W-27B001	WDL	52.7	150	—	—	10/13/1980	03/23/1998	34
6	4N/6W-21A001	WDL	157.7	259	220	259	12/01/1989	10/19/2000	23
7	4N/6W-17G001	WDL	12.7	85	60	78	01/19/1990	04/15/1992	25
8	4N/6W-07A001	WDL	42.7	180	140	180	10/13/1980	04/14/2016	53
9	5N/7W-36R001	WDL	21.7	34	—	—	12/01/1989	04/14/2016	108
10	382342N1225525W001	CASGEM	240.0	370	30	370	05/05/2015	05/10/2016	3
11	381503N1223410W001	CASGEM	108.0	429	40	426	01/27/2015	05/10/2016	4
12	5N/7W-25G001	WDL	112.7	426	40	426	12/01/1989	10/15/2014	33
13	381402N1223610W001	CASGEM	18.0	229	89	229	11/07/2012	05/10/2016	9
14	381408N1223633W001	CASGEM	18.0	460	90	460	11/07/2012	05/10/2016	9
15	5N/7W-34L001	WDL	14.7	196	123	163	11/10/1989	03/20/2000	21
16	381522N1223733W001	CASGEM	46.0	425	305	382	11/07/2012	05/10/2016	9
17	381528N1223700W001	CASGEM	58.0	360	220	360	11/07/2012	05/10/2016	9
18	5N/7W-21H001	WDL	67.7	92	47	92	04/10/1990	03/19/1991	3
19	5N/7W-15Q001	WDL	120.7	200	—	—	12/01/1989	07/14/2016	251
20	5N/7W-15K002	WDL	157.7	177	158	177	12/01/1989	04/14/2016	51
21	5N/7W-11N001	WDL	260.8	100	60	100	10/08/1980	04/14/2016	58
22	5N/7W-11F001	WDL	518.8	480	300	450	10/08/1980	04/14/2016	56
23	5N/7W-33M001	WDL	32.7	132	—	—	05/18/1990	05/18/1990	1
24	5N/7W-28M001	WDL	30.7	71	—	—	11/10/1989	03/19/1991	4
25	381553N1223839W001	CASGEM	38.5	562	52	538	11/07/2012	05/10/2016	9
26	5N/7W-20B002	WDL	43.7	158	—	—	12/01/1989	04/14/2016	53
27	5N/7W-31R002	WDL	137.7	95	—	—	10/10/1980	04/14/2016	69
28	5N/7W-31P003	WDL	182.7	244	—	—	11/10/1989	04/14/2016	54
29	5N/7W-30K014	WDL	122.7	185	—	—	11/10/1989	04/14/2016	51

Table D1. Groundwater-altitude monitoring wells, Petaluma valley watershed, Sonoma County, California.—Continued

[Datum is North American Vertical Datum of 1988 (NAVD 88). **Abbreviations**: mm/dd/yyyy, month/day/year; ID, identification; ft, foot; WDL, water data library; CASGEM, California Statewide Groundwater Elevation Monitoring]

Well number (mm/dd/yyyy)	Well ID	Source	Groundwater-level altitude (ft above NAVD 88)	Well depth (ft)	Depth to top of well screen (ft)	Depth to bottom of well screen (ft)	First measurement (mm/dd/yyyy)	Last measurement (mm/dd/yyyy)	Number of measurements
30	5N/7W-19N001	WDL	47.7	180	—	—	01/19/1990	07/14/2016	296
31	5N/8W-24F001	WDL	48.7	340	—	—	11/10/1989	04/23/2008	21
32	5N/8W-13Q001	WDL	42.7	110	—	—	10/13/1980	04/14/2016	67
33	5N/8W-14K002	WDL	172.7	270	—	—	10/14/1980	04/14/2016	68
34	5N/8W-14P001	WDL	167.7	235	—	—	10/13/1980	04/14/2016	55
35	5N/8W-23M001	WDL	122.7	100	—	—	10/10/1980	10/29/2015	51
36	5N/7W-18B001	WDL	81.7	82	58	78	10/13/1980	04/22/2009	48
37	5N/7W-07A001	WDL	67.7	62	35	60	11/09/1989	03/28/2000	21
38	6N/7W-31J001	WDL	135.8	280	45	228	11/09/1989	04/13/2016	42
39	5N/8W-01L002	WDL	282.7	185	165	185	01/21/1976	04/13/2016	75
40	5N/8W-02H001	WDL	162.7	155	30	150	02/03/1976	04/13/2016	74
41	383096N1227098W001	CASGEM	310.0	419	118	418	06/12/2015	05/10/2016	3
[1]42	383315N1226673W001	CASGEM	177.8	—	59	29	11/09/1989	04/13/2016	73

[1]This well was used for estimation general head boundary conditions and not for model calibration.

Table D2. U.S. Geological Survey (USGS) streamgages (U.S. Geological Survey, 2018), Petaluma valley watershed, Sonoma County, California.

[USGS, U.S. Geological Survey; mm/yyyy, month/year; ft^3/s, cubic foot per second]

Streamgage number	USGS station number	USGS station name	Source	First measurement (mm/yyyy)	Last measurement (mm/yyyyy)	Number of measurements[1]	Average flow $(ft^3/s)^{1,4}$	Median flow $(ft^3/s)^{1,4}$	Maximum flow $(ft^3/s)^{1,4}$
1	11459300	San Antonio Creek near Petaluma, California	USGS	08/1975	09/1981	61	17	0.0043	224
2	11459150	Petaluma River at Copland Pumping Station at Petaluma, California[2]	USGS	11/1998	[3]09/2015	215	70	2.7	750
3	11459000	Petaluma River at Petaluma, California	USGS	10/1948	09/1963	180	17	0.058	271

[1]Daily mean flow values were used to compute monthly averages; this table reports average monthly values.

[2]Data are tidally filtered after October 2010.

[3]September 2015 is the end of the model simulation period. The station has data past this date, but they were not included in the analysis.

[4]Incomplete monthly data were used in calculations.

Crop Properties

This section briefly defines and describes the crop-related data used in this study; more detailed definitions are provided in the Farm Process (FMP) documentation (Schmid and others, 2006). Crop-related data include the following:

- Root-zone depths,
- Root-uptake coefficients,
- Crop coefficients,
- Fractions of transpiration and evaporation,
- Irrigation efficiencies,
- Fractions of losses to runoff for precipitation, and
- Fractions of losses to runoff for irrigation.

Root-zone depths were defined for each crop type (table D3) and were used to calculate the groundwater uptake by crops. Root-uptake coefficients represent the relative hydrostatic pressure at which anoxia, optimal growth, and wilting occur for each crop type. Most crops experience anoxia if the roots are inundated for an extended period. Crops such as riparian vegetation have a relative hydrostatic pressure greater than zero for anoxia because they grow even when flooded. Wilting occurs when the water content in the root zone is too low to sustain the crop for an extended period.

A crop coefficient is the ratio of the actual evapotranspiration (ET) for a crop to the reference evapotranspiration (ET_o) and is used as a scaling factor for calculating actual ET from ET_o. Crop coefficients are defined for each crop type and, for this study, were assigned to vary monthly on the basis of the growth stage of the crop (table D4). The fraction of transpiration (FTR) is the proportion of field area covered by each crop type (table D5). The FTR varies monthly on the basis of the growth stage of the crop. For example, a bare field has an FTR of 0.0, whereas a field with a crop canopy covering the entire field has an FTR of 1.0. The fraction of evaporation of irrigation (FEI) is the proportion of the field not covered by the crop canopy that has irrigation water flowing on it (such as an irrigation furrow); FEI values are typically less than or equal to one minus FTR (Schmid and others, 2006; Schmid and Hanson, 2009; Hanson and others, 2014). Even for efficient irrigation systems, however, the FEI can be greater than zero and represent the irrigated area exposed to atmosphere (even if covered by canopy) or other evaporative losses from the application of the irrigation water.

Irrigation efficiency is defined for this study as the ratio of water used by the crop to the water applied to the crop. The fraction of applied water that is in excess of this amount is "lost" to runoff or deep percolation and is equal to 1.0 minus the irrigation efficiency. For example, an irrigation efficiency of 0.7 means that if 100 acre-feet (acre-ft) of irrigation water is applied to the crop, 70 acre-ft is used, and 30 acre-ft becomes runoff or deep percolation. For the PVW, irrigation methods and practices were assumed to be generally similar for the same crop type; thus, irrigation-efficiencies were defined by crop type and held constant through the model simulation period.

The fraction of losses for precipitation is the ratio of excess precipitation water "lost" to runoff compared to percolation. As an example, a fraction of losses for precipitation of 0.8 means that 80 percent of excess precipitation goes to runoff and 20 percent of the excess precipitation goes to percolation. A similar fraction, called the fraction of losses related to irrigation, is the ratio of excess irrigation water "lost" to runoff compared to percolation. The fractions are defined separately for precipitation and irrigation for each crop type and vary between 0.0 and 1.0. A value of 1.0 represents all excess water going to runoff, and a value of 0.0 represents all excess water going to percolation.

Initial values for crop coefficients (KC) were provided by SCWA. These KC values were similar to values used in neighboring study areas such as Sonoma Valley and the Santa Rosa Plain groundwater subbasin (Andrew N. Rich, Sonoma County Water Agency, written commun., June 2020). Initial values for other crop-related datasets were obtained from a previous USGS study (Faunt, 2009). These initial crop-related values were adjusted to account for local climatic conditions in the PVW and modified during the calibration process; the adjusted values are presented in table D4. The urban class was subdivided to differentiate between city–urban and rural–urban land types. Also, for urban classes, the values are only applied to the proportion of the land use that is vegetated, which was assumed to be 25 percent for city–urban and 50 percent for rural–urban.

Water Supply and Demand Data

The major categories of water demand in the study area are agricultural, municipal, rural residential, industrial, and commercial. Agricultural water demand is the largest user of local water and is met using groundwater pumpage, local surface-water supplies, and, as of 1998, recycled water (Leah Walker, City of Petaluma, written commun., 2016). Municipal water demand by the City of Petaluma is met primarily using surface water imported from the Russian River (not shown), but groundwater and recycled water also have been used since 2006 (Leah Walker, City of Petaluma, written commun., 2016). Available data were limited for rural residential, industrial, and commercial water use and water supply, resulting in data gaps. The next section of the report presents and discusses available data and identifies data gaps. Methods used to estimate the missing data required for model development are discussed in the "Model Development" section of this chapter.

Table D3. Crop water-use characteristics used in development of the Petaluma Valley Integrated Hydrologic Model, Petaluma valley watershed, Sonoma County, California (Faunt, 2009).

[ID, identification; ft, foot; PVIHM; Petaluma Valley Integrated Hydrologic Model]

Crop ID	Crop name	Root depth (ft)	Negative hydrostatic-pressure for anoxia (ft)[1]	Negative hydrostatic-pressure optimal high (ft)	Negative hydrostatic-pressure optimal low (ft)	Negative hydrostatic-pressure for wilting (ft)[1]	Irrigation efficiency (percent)	Fraction of excess precipitation torunoff	Fraction of excess irrigation torunoff
1	Citrus and subtropical	3.28	–0.49	–0.98	–19.69	–262.47	82	0.60	0.05
2	Deciduous fruits and nuts	3.28	–0.43	–0.89	–22.77	–291.34	60	0.77	0.05
3	Field crops	3.28	–0.49	–0.98	–98.43	–405.84	68	0.76	0.05
4	Grain and hay crops	3.28	–0.49	–0.98	–170.93	–525.26	74	0.20	0.05
5	Native vegetation	3.28	–0.43	–0.89	–22.77	–410.10	60	0.55	0.00
6	Pasture	3.28	0.03	–0.92	–37.40	–262.47	69	0.20	0.05
7	Riparian vegetation	3.28	1.64	0.43	–27.07	–377.30	60	0.68	0.00
8	Semiagricultural and incidental to agriculture	3.28	–0.25	–0.66	–27.07	–377.30	60	0.69	0.05
9	Truck, nursery, and berry crops	3.28	–0.49	–0.98	–17.88	–262.47	73	0.63	0.05
10	Urban	3.28	–0.43	–0.92	–37.40	–262.47	60	0.79	0.00
11	Vineyards	3.28	–0.49	–0.98	–23.79	–262.47	76	0.28	0.05
12	Rural	3.28	–0.43	–0.89	–22.77	–410.10	60	0.73	0.05

[1]In PVIHM, anoxia and soil-stress losses are turned off for native, riparian, urban, and rural crop types.

Table D4. Crop coefficients used in development of the Petaluma Valley Integrated Hydrologic Model, Petaluma valley watershed, Sonoma County, California.

[Data obtained from Sonoma County Water Agency (Andrew N. Rich, Sonoma County Water Agency, written commun., June 2020). **Abbreviation**: ID, identification]

Crop ID	Crop name	January	February	March	April	May	June	July	August	September	October	November	December
1	Citrus and subtropical	0.75	0.75	0.75	0.75	0.75	0.75	0.75	0.75	0.75	0.75	0.75	0.75
2	Deciduous fruits and nuts	0.75	0.75	0.75	0.75	0.75	0.75	0.90	0.90	0.90	0.80	0.75	0.75
3	Field crops	0.75	0.75	0.75	0.75	0.75	0.90	1.09	0.90	0.75	0.75	0.75	0.75
4	Grain and hay crops	0.75	0.75	0.75	0.75	0.75	0.75	0.75	0.75	0.75	0.75	0.75	0.75
5	Native vegetation	0.75	0.75	0.96	1.09	1.09	1.09	1.09	1.09	1.09	0.75	0.75	0.75
6	Pasture	0.75	0.75	0.75	0.75	0.75	0.75	0.75	0.75	0.75	0.75	0.75	0.75
7	Riparian vegetation	0.95	0.96	1.00	1.03	1.06	1.07	1.07	1.07	1.07	1.07	1.05	0.95
8	Semiagricultural and incidental to agriculture	1.00	1.00	1.00	1.00	1.00	1.00	1.00	1.00	1.00	1.00	1.00	1.00
9	Truck, nursery, and berry crops	1.08	0.75	0.75	0.75	0.77	1.07	1.08	0.75	0.75	0.75	0.77	1.07
10	Urban	0.75	0.75	0.75	0.75	0.75	0.75	0.75	0.75	0.75	0.75	0.75	0.75
11	Vineyards	0.75	0.75	0.75	0.75	0.75	0.75	0.75	0.75	0.75	0.76	0.75	0.75
12	Rural	0.75	0.75	0.96	1.09	1.09	1.09	1.09	1.09	1.09	0.75	0.75	0.75

Agriculture

As stated previously, the primary sources of water for agricultural irrigation are groundwater, surface water, and recycled water. Agricultural demand or agricultural groundwater pumpage data were not available for the PVW, and previous studies have noted that insufficient data exist to estimate agricultural groundwater demand (Herbst, 1982). For this study, land-use information, including crop properties, was used by the PVIHM to estimate agricultural demand and groundwater pumpage needed to meet that demand. This methodology is discussed in the "Model Development" section of this chapter.

Well information, such as locations, screened interval, well radius, and pumping capacity, were available for selected agricultural wells; however, most of the data were unavailable or only available in a format that could not easily be used for this study (non-digitized well logs). To obtain more complete information for the PVW, well-screen intervals were estimated for each township–range section (TRS) using data from the CDWR Online System of Well Completion Reports database (California Department of Water Resources, 2019). This database contains digitized metadata for wells including well depth, top of well screen depth, and bottom of well screen depth. Based on analysis of the database, the average top, middle, and bottom of screen intervals were estimated for each TRS section in the study area. Most of the wells in the study area are screened between 30 and 540 ft below land surface (bls; fig. D2).

The source for estimating the use of local surface-water supplies to meet agricultural demand is the enhanced Water Right Information Management System (eWRIMS), a database managed by the California State Water Resources Control Board that tracks information about water rights in California (California State Water Resources Control Board, 2016). The database provides information about agricultural surface-water use in the PVW from 1959 to present for 140 diverters in the study area. Prior to 2010, however, data for many diverters were not available in the database; therefore, the dataset is considered to be incomplete until 2010.

The eWRIMS database contains many types of data, but the two data types analyzed in this study are "diverted total," which is the amount of water diverted from local streams, and "amount used," which is the amount of water that is applied to the agricultural fields. These values are different because land managers in the study area may divert water from streams to local on-farm storage facilities and then apply diverted water to their fields at a later date. Diverted total ranged from 1,300 acre-ft in WY 2013 to 2,900 acre-ft in WY 2010 (fig. D3). Amount used ranged from 1,300 acre-ft in WY 2011 to 2,100 acre-ft in WY 2010 (fig. D3). Most diversions take place in wet months, such as January and February, when local streams are flowing (fig. D4). In contrast, most surface-water use takes place in the summer months, such as June, July, and August, when crops are growing (fig. D4).

The eWRIMS database also contains details about the location of each diversion. For the purposes of this study, surface water was assumed to be used on land that is near the stream from which the water is diverted and not transferred to another area. When analyzing location data, diversions were spatially assigned to a "subregion" (which are defined and discussed later in the "Subregion Definitions" section of the report), and diversions data were then aggregated by subregion (table D6).

Monthly recycled-water use data from June 1998 through June 2016 were provided by the City of Petaluma (Leah Walker, City of Petaluma, written commun., 2016) and averaged 1,464 acre-feet/year (acre-ft/yr), with a peak monthly use of 540 acre-ft in June 2002 (fig. D5). Location data for parcels that received recycled-water deliveries were provided by the SCWA (fig. D6; Celeste Dodge, Sonoma County Water Agency, written commun., 2018).

City of Petaluma

The City of Petaluma receives most of its water supply from surface water imported from the Russian River, and groundwater pumpage only supplements surface-water supplies to meet peak demands or to provide an emergency backup supply in case of surface-water-supply shortages. Monthly surface-water delivery data to the City of Petaluma were available from July 1996 to December 2015 (fig. D7; Sonoma County Water Agency, 2016). Annual surface-water delivery data from 1959 to 1996 were obtained from a previously published figure (fig. D8; West Yost, 2004). Note that the data in figure D8 are presented by calendar year for consistency between the datasets. The 1959–1996 annual data were converted to monthly data for use in the groundwater-flow model based on monthly ratios from the monthly surface-water delivery data to the City of Petaluma from July 1996 through December 2015.

Monthly surface-water deliveries were lowest in winter months (January and February), when the demand for outdoor water use is low (fig. D7), and highest in summer months (June, July, August), when the demand is high. Total annual surface-water deliveries to the City of Petaluma generally increased from 1959 to the early 2000s, peaking at 11,000 acre-ft in WY 2004 (fig. D8). Surface-water deliveries have generally declined since WY 2004 (fig. D13).

Table D5. Crop fraction of transpiration (FTR) and fraction of evaporation of irrigation (FEI) used in development of the Petaluma Valley Integrated Hydrologic Model, Petaluma valley watershed, Sonoma County, California (Faunt, 2009).

[ID, identification; FTR, fraction of land area where transpiration occurs; FEI, fraction of land where evaporation of irrigation occurs]

Crop ID	Crop name	January		February		March		April	
		FTR	FEI	FTR	FEI	FTR	FEI	FTR	FEI
1	Citrus and subtropical	0.27	0.73	0.27	0.73	0.46	0.14	0.46	0.14
2	Deciduous fruits and nuts	0.10	0.90	0.10	0.90	0.10	0.90	0.50	0.50
3	Field crops	0.01	0.99	0.01	0.99	0.01	0.99	0.15	0.85
4	Grain and hay crops	0.46	0.54	0.92	0.08	0.92	0.08	0.92	0.08
5	Native vegetation	0.28	0.72	0.28	0.72	0.66	0.34	0.66	0.34
6	Pasture	0.18	0.82	0.15	0.85	0.46	0.64	0.91	0.03
7	Riparian vegetation	0.28	0.72	0.28	0.72	0.66	0.34	0.66	0.34
8	Semiagricultural and incidental to agriculture	0.00	1.00	0.00	1.00	0.00	1.00	0.00	1.00
9	Truck, nursery, and berry crops	0.80	0.18	0.80	0.18	0.39	0.61	0.44	0.36
10	Urban	0.25	0.02	0.25	0.02	0.25	0.02	0.25	0.02
11	Vineyards	0.00	0.03	0.00	0.03	0.28	0.22	0.40	0.10
12	Rural	0.27	0.00	0.27	0.00	0.56	0.00	0.56	0.00

The City of Petaluma owns 21 groundwater-production wells (table D7). Table D7 provides information on city wells, including construction date, depth, and screened intervals (modified from West Yost [2004], with input from the SCWA). As of 2015, only 7 of the 21 wells are active, but all 21 wells were used historically to varying degrees. Monthly groundwater-production data by well from January 2000 to December 2015 were provided by the City of Petaluma (Leah Walker, City of Petaluma, written commun., 2016). Monthly total groundwater-production data for the entire City of Petaluma were provided from January 1994 to October 2016 by the city (Leah Walker, City of Petaluma, written commun., October 2017). The annual groundwater production totals for the City of Petaluma wells from 1959 to 1999 were obtained from a figure (West Yost, 2004, fig. D1). These three datasets were combined using the most detailed data available: annual data for entire city from 1960 to 1993, monthly data for entire city from 1994 to 1999, and monthly data by well from 2000 to 2015. These data were then converted to monthly by well, where needed. Annual data from 1960 to 1993 were converted to monthly data on the basis of the monthly average used from the 1994–2015 data. Data for the entire city from 1960 to 1999 were divided evenly among active production wells for each month.

Note that all groundwater-pumpage data provided by the City of Petaluma were based on calendar years. The monthly pumpage from 1994 to 2015 was highly variable, with no pumpage during some periods, such as WY 2004 through WY 2006 (fig. D9). The annual pumpage from WY 1959 to 2015 ranged from none in several years to 1,500 acre-ft in WY 1986 (fig. D10).

The City of Petaluma also uses recycled water to meet demands for urban landscaping, such as irrigation of golf courses and irrigation of turf in city parks and schools. Monthly recycled water use data were provided by the City of Petaluma (fig. D5). Recycled-water use for urban landscaping began in August 2006 and averaged 516 acre-ft/yr from 2006 to 2015 (fig. D5), with a peak monthly use of 170 acre-ft in July 2014 (fig. D5).

Rural Residential, Industrial, and Commercial

Rural residential water use was assumed to be met entirely by groundwater pumpage from domestic wells. As with agricultural wells, data on the quantity of rural residential pumpage were not available, and site information for rural wells was limited. For this study, rural pumpage estimates were provided by SCWA (Andrew N. Rich, Sonoma County Water Agency, written commun., June 2020). The SCWA also estimated that 80 percent of indoor rural water use was returned to the groundwater system as septic seepage.

Data were obtained for calendar year 2016—18 for three industrial users, which the City of Petaluma considers to be the major industrial water users that have wells (Patrick Pulis, City of Petaluma, written commun., 2019). The combined annual pumpage for these three users averaged less than 250 acre-ft/yr. Industrial production data were not available before calendar year 2016, and information about the industrial wells used to pump this water, such as location and perforation intervals, were not available. Finally, data on commercial water use were not available, but commercial water uses were expected to be small and similar to industrial water use.

Table D5. Crop fraction of transpiration (FTR) and fraction of evaporation of irrigation (FEI) used in development of the Petaluma Valley Integrated Hydrologic Model, Petaluma valley watershed, Sonoma County, California (Faunt, 2009). —Continued

[ID, identification; FTR, fraction of land area where transpiration occurs; FEI, fraction of land where evaporation of irrigation occurs]

June		July		August		September		October		November		December	
FTR	FEI	FTR	FEI	FTR	FEI	FTR	FEI	FTR	FEI	FTR	FEI	FTR	FEI
0.46	0.14	0.46	0.14	0.46	0.14	0.46	0.14	0.46	0.14	0.46	0.14	0.46	0.14
0.97	0.03	0.97	0.03	0.97	0.03	0.97	0.03	0.10	0.90	0.10	0.90	0.10	0.90
0.94	0.06	0.94	0.06	0.94	0.06	0.90	0.10	0.01	0.99	0.01	0.99	0.01	0.99
0.00	1.00	0.00	1.00	0.00	1.00	0.00	1.00	0.00	1.00	0.16	0.84	0.35	0.65
0.66	0.34	0.66	0.34	0.66	0.34	0.66	0.34	0.66	0.34	0.66	0.34	0.28	0.72
0.91	0.03	0.96	0.04	0.91	0.03	0.91	0.03	0.46	0.64	0.15	0.85	0.15	0.85
0.66	0.34	0.66	0.34	0.66	0.34	0.66	0.34	0.66	0.34	0.66	0.34	0.28	0.72
0.00	1.00	0.00	1.00	0.00	1.00	0.00	1.00	0.00	1.00	0.00	1.00	0.00	1.00
0.80	0.18	0.80	0.18	0.80	0.18	0.80	0.18	0.80	0.18	0.80	0.18	0.80	0.18
0.25	0.02	0.25	0.02	0.25	0.02	0.25	0.02	0.25	0.02	0.25	0.02	0.25	0.02
0.36	0.14	0.36	0.14	0.36	0.14	0.36	0.14	0.36	0.14	0.36	0.14	0.38	0.12
0.56	0.00	0.56	0.00	0.56	0.00	0.56	0.00	0.56	0.00	0.56	0.00	0.27	0.00

Climate Data

General climate data, including precipitation and temperature, were discussed in chapter A of this report. However, the climate data need to be spatially continuous over the entire PVW for modeling purposes. Spatially varying precipitation and temperature grids were developed from Parameter-elevation Regressions on Independent Slopes Model (PRISM; Daly and others, 2008; PRISM Climate Group, 2013). The PRISM datasets were developed using climate station data interpolated to 2.48-mile (4-kilometer) grid cells for the conterminous United States. These grids were downscaled to 886 ft (270 meters) using the Flint and Flint (2012) method that uses gradient-plus-inverse-distance squared (GIDS) interpolation (Nalder and Wein, 1998), which develops relations between altitude, easting, and northing for each grid cell to spatially downscale the large grids to fine-scale grids. Potential evapotranspiration was calculated using the downscaled PRISM air temperature and a modified Priestley-Taylor equation (Priestley and Taylor, 1972; PRISM Climate Group, 2013).

Based on downscaled PRISM data (PRISM Climate Group, 2013), the 1960 to 2015 annual average precipitation in the PVW was 28.6 in., with annual totals ranging from 11.1 in. (1977) to 56.5 in. (1983; fig. D11). Average annual precipitation varied spatially in the PVW from 23.2 inches per year (in/yr) in the valley to 58.4 in/yr in the eastern hills (fig. D12). Most (90 percent) of the precipitation falls during November to April (fig. D13).

Dry climatic periods were defined in this study as periods when the cumulative departure from the mean precipitation declines, and wet climatic periods were defined as when the cumulative departure from the mean precipitation rises. Dry climatic periods included WYs 1960–66, 1975–77, 1987–94, 2007–09, and 2012–15 (fig. D11). Wet climatic periods included WYs 1967–74, 1978–86, 1995–2006, and 2010–11 (fig. D11).

Monthly varying ET_o datasets for the study area were computed from the PRISM temperature output data using the Hargreaves-Samani equation (Hargreaves and Samani, 1982). Based on the computed data, long-term average annual ET_o in the study area, from WY 1960 to 2015, was 47.0 in., ranging temporally from 45.9 (WY 1964) to 48.9 in. (WY 2015; fig. D14). Spatially, annual average ET_o varies throughout the study area, ranging from 40.2 to 50.0 in/yr (fig. D15). South-facing hills generally have higher ET_o values, north-facing hills generally have lower ET_o values (fig. D15), and 73 percent of ET_o occurs during the growing season between May and October (fig. D13). Irrigation is needed to grow most crops in the study area because average monthly ET_o exceeds average precipitation from April through October (fig. D13), assuming no soil-moisture storage.

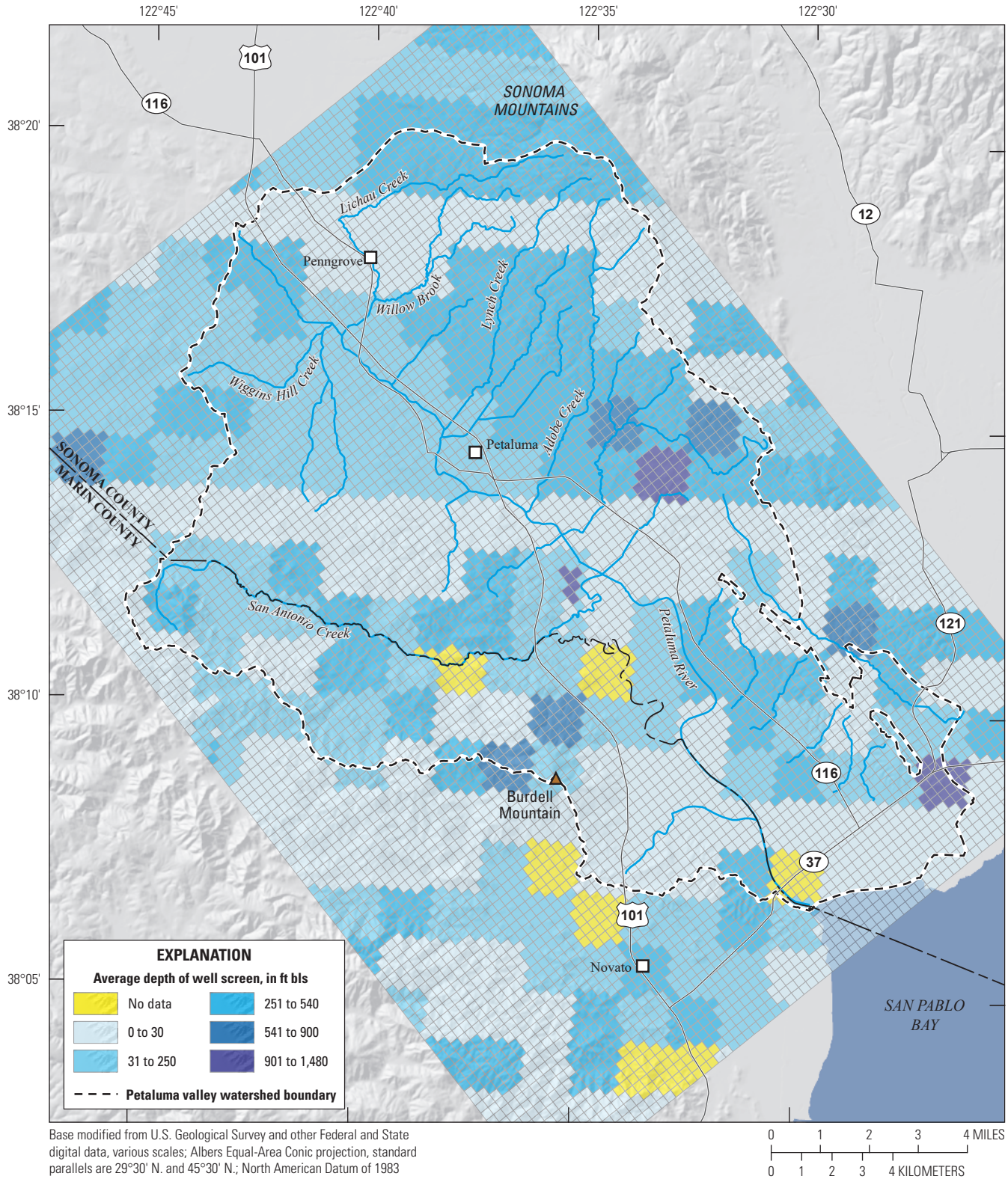

Figure D2. Average well-screen depths, in feet below land surface (ft bls), Petaluma valley watershed, Sonoma County, California; data derived from (California Department of Water Resources, 2019).

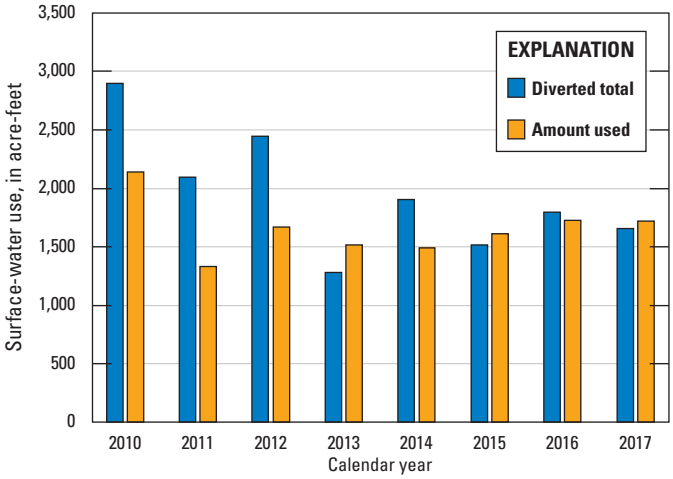

Figure D3. Total annual volume of surface water diverted for agriculture and total annual volume of water used for agriculture from 2010 to 2017 (California State Water Resources Control Board, 2016), Petaluma valley watershed, Sonoma County, California.

Table D6. Agricultural surface-water use by subregion, annual average in acre-feet from water years 2010 to 2017, Petaluma valley watershed, Sonoma County, California.

[acre-ft/yr, acre-foot per year; OGWB, outside of groundwater basin; OWS, outside of watershed]

Subregion	Name	Diverted total (acre-ft/yr)	Amount used (acre-ft/yr)
1	Wilson Grove	18	17
2	Upper Petaluma River	0	0
3	Lynch Creek	25	17
4	Lichau Creek	5	5
5	Lynch Creek OGWB	303	59
6	Upper San Antonio Creek	139	110
7	Upper Petaluma River OGWB	0	1
8	City of Petaluma Wilson Grove	0	0
9	City of Petaluma OGWB	0	0
10	City of Petaluma	0	0
11	Adobe Creek	93	95
12	Adobe Creek OGWB	187	187
13	Lower San Antonio Creek	140	125
14	Upper Petaluma River OGWB 2	8	5
15	Basalt Creek	0	0
16	Lower Petaluma River OGWB	0	0
17	Lower Petaluma River	18	11
18	North Bay Water District	230	245
19	Stage Gulch	55	58
20	Stage Gulch OGWB	7	4
21	Tolay Creek OWS	722	712
Total	—	**1,949**	**1,651**

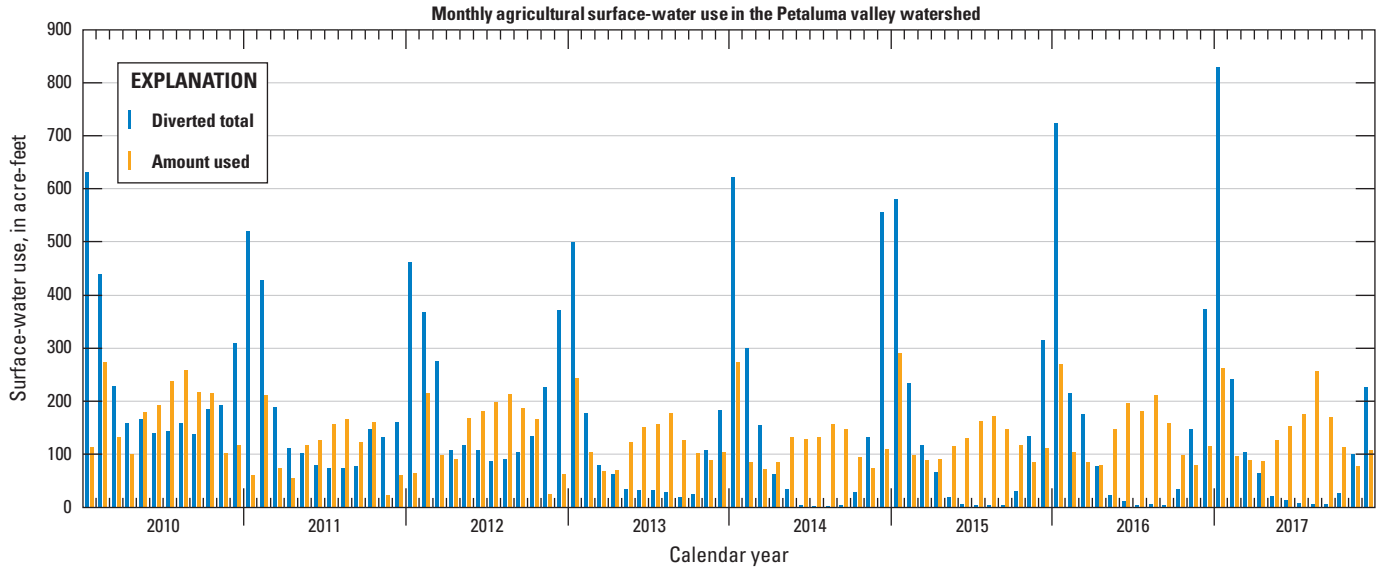

Figure D4. Total monthly volume of water diverted for agriculture and total monthly volume of water used for agriculture from 2010 to 2017 (California State Water Resources Control Board, 2016), Petaluma valley watershed, Sonoma County, California.

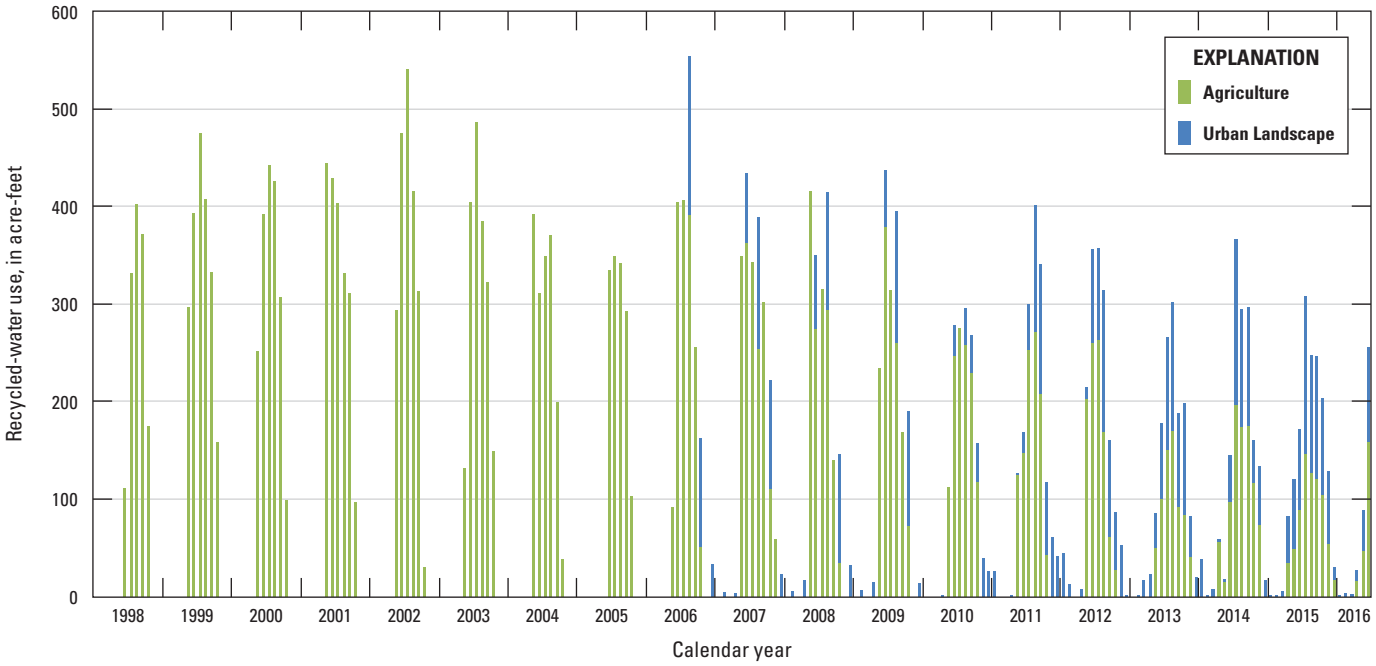

Figure D5. Monthly recycled-water use for agriculture and urban landscape from 1998 through 2015, Petaluma valley watershed, Sonoma County, California.

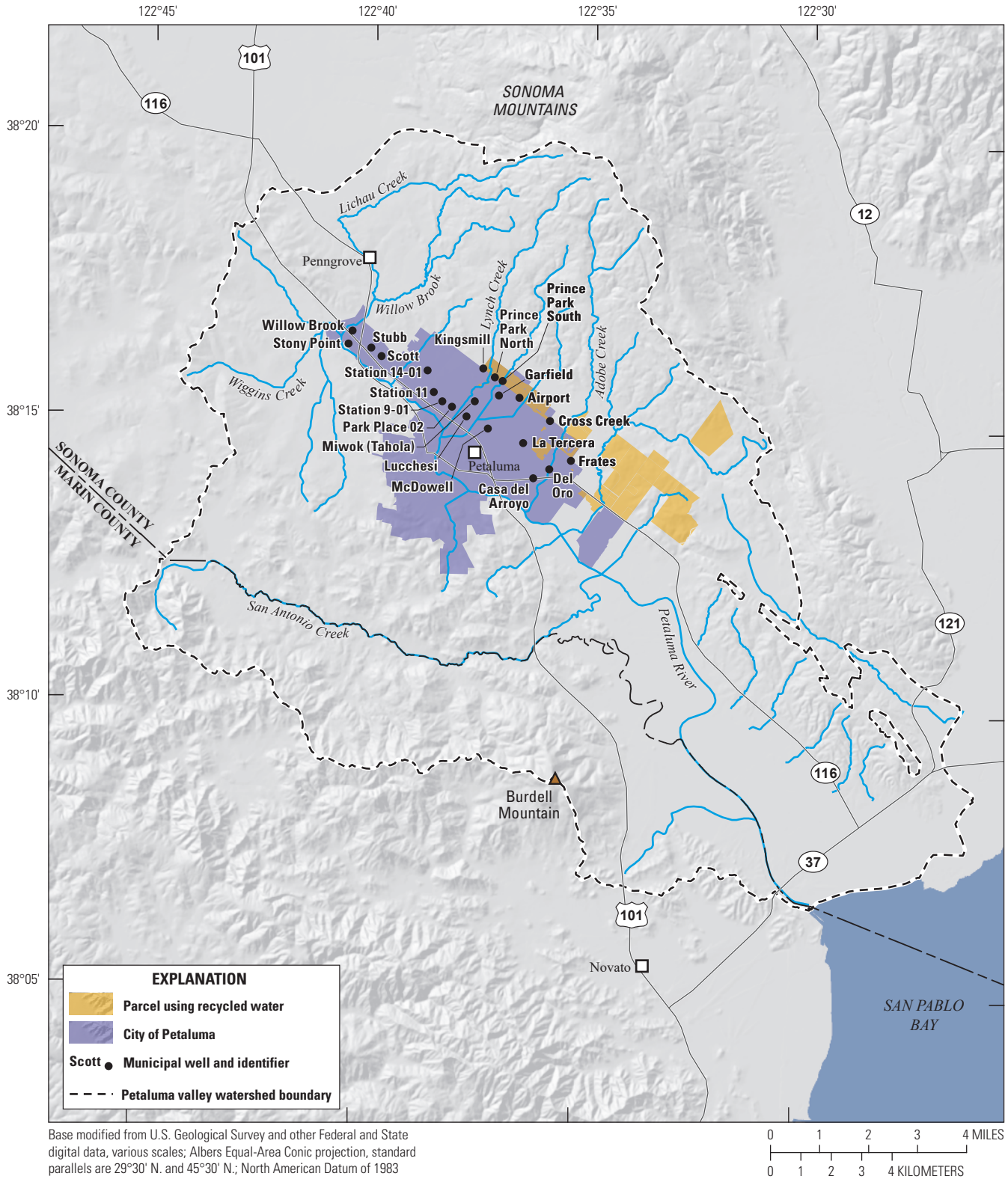

Figure D6. Groundwater-production wells and recycled-water use parcels, Petaluma valley watershed, Sonoma County, California.

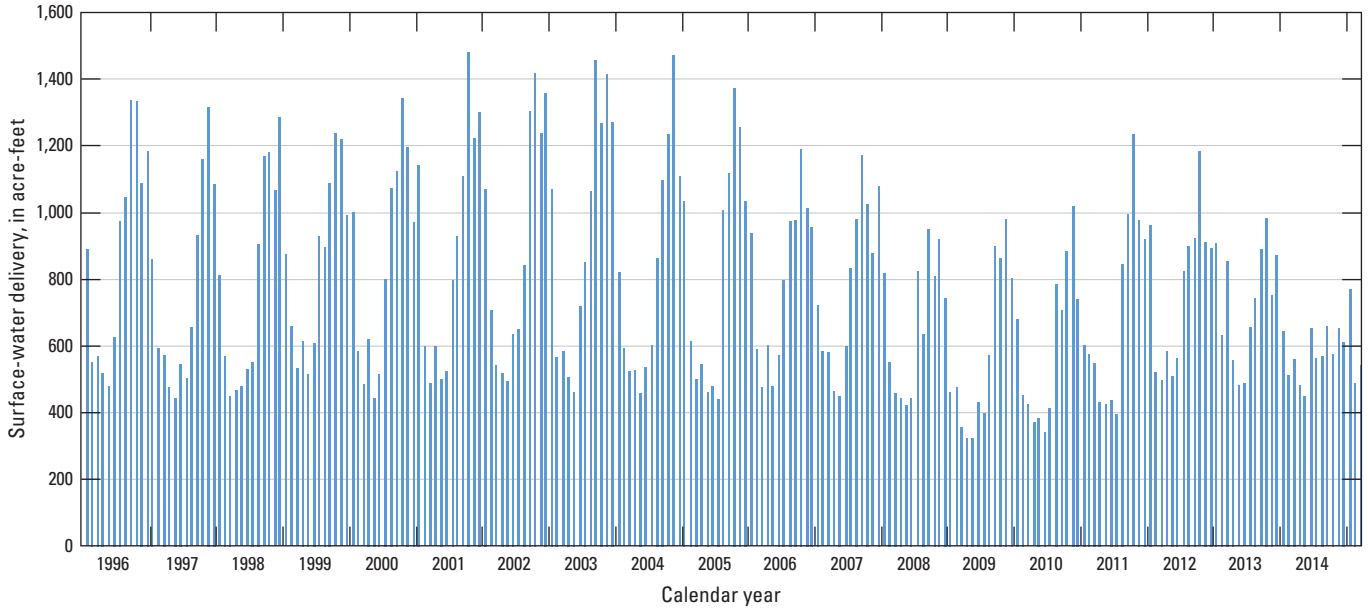

Figure D7. City of Petaluma monthly surface-water deliveries during calendar years 1996–2015, Petaluma valley watershed, Sonoma County, California.

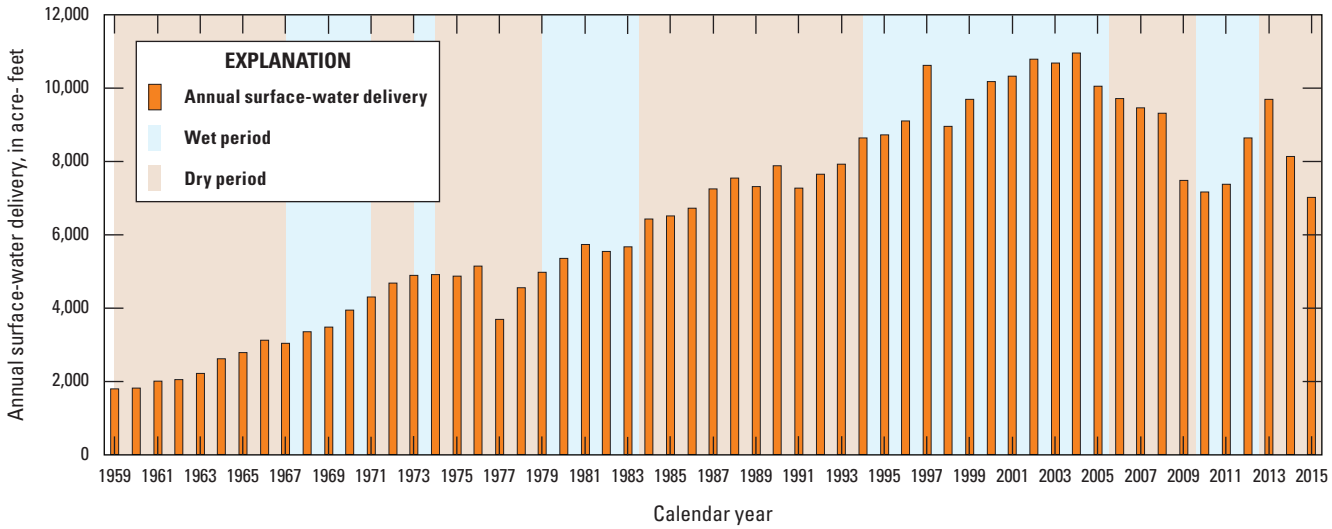

Figure D8. City of Petaluma total annual surface-water deliveries during calendar years 1959–2015, Petaluma valley watershed, Sonoma County, California. Data from 1959 to 1996 obtained from West Yost (2004). Data from 1997 to 2015 obtained from Sonoma County Water Agency (2016).

Table D7. Construction data for City of Petaluma production wells, Petaluma valley watershed, Sonoma County, California.

[in., inches; ft, foot; —, no data]

Well name	Casing diameter (in.)	Well depth (ft)	Top of screen depth (ft)	Bottom of screen depth (ft)	Construction date
Airport Well	10.00	460	220	400	1996
Casa Del Arroyo Well	12.75	232	89	229	1977
Cross Creek Well	10.00	500	330	460	1998
Del Oro Well	10.00	500	—	—	—
Frates Well	10.00	500	60	500	1995
Garfield Well (aka Coniotti)	8.00	360	220	360	1977
Kingsmill Well	10.00	500	200	400	1994
La Tercera Well	10.00	500	—	—	—
Lucchesi Well	10.00	505	180	440	1996
Mcdowell WELL	—	540	—	—	—
Miwok (Tahola) Well	8.00	425	305	385	1997
Park Place Well 02	10.00	440	80	310	1984
Prince Park North Well	8.00	500	180	480	1993
Prince Park South Well	8.00	500	140	500	1993
Scott Well	12.00	680	—	—	1949
Station 11 Well	10.00	550	280	500	1998
Station 14-01 Well	14.00	562	52	538	1957
Station 9-01 Well	10.00	500	180	420	1998
Stony Point Well	12.75	599	318	580	1997
Stubb Well	13.00	598	—	—	—
Willow Brook Well	12.75	409	30	407	1957

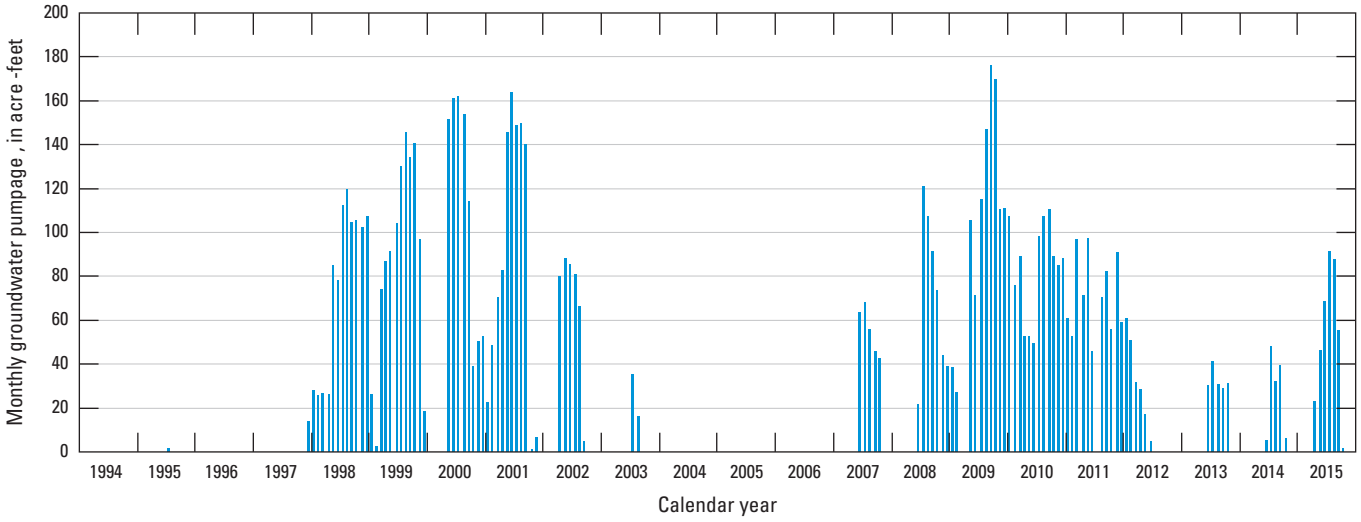

Figure D9. Total monthly groundwater production by City of Petaluma during calendar years 1994–2015, Petaluma valley watershed, Sonoma County, California.

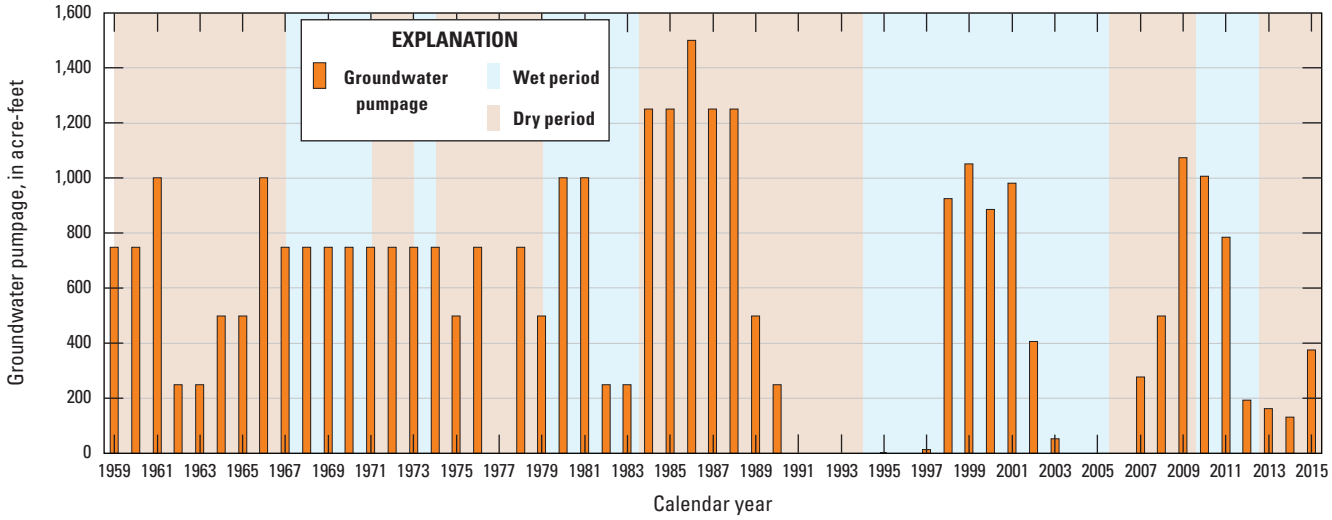

Figure D10. Annual City of Petaluma groundwater production data during calendar years 1959–2015, Petaluma valley watershed, Sonoma County, California.

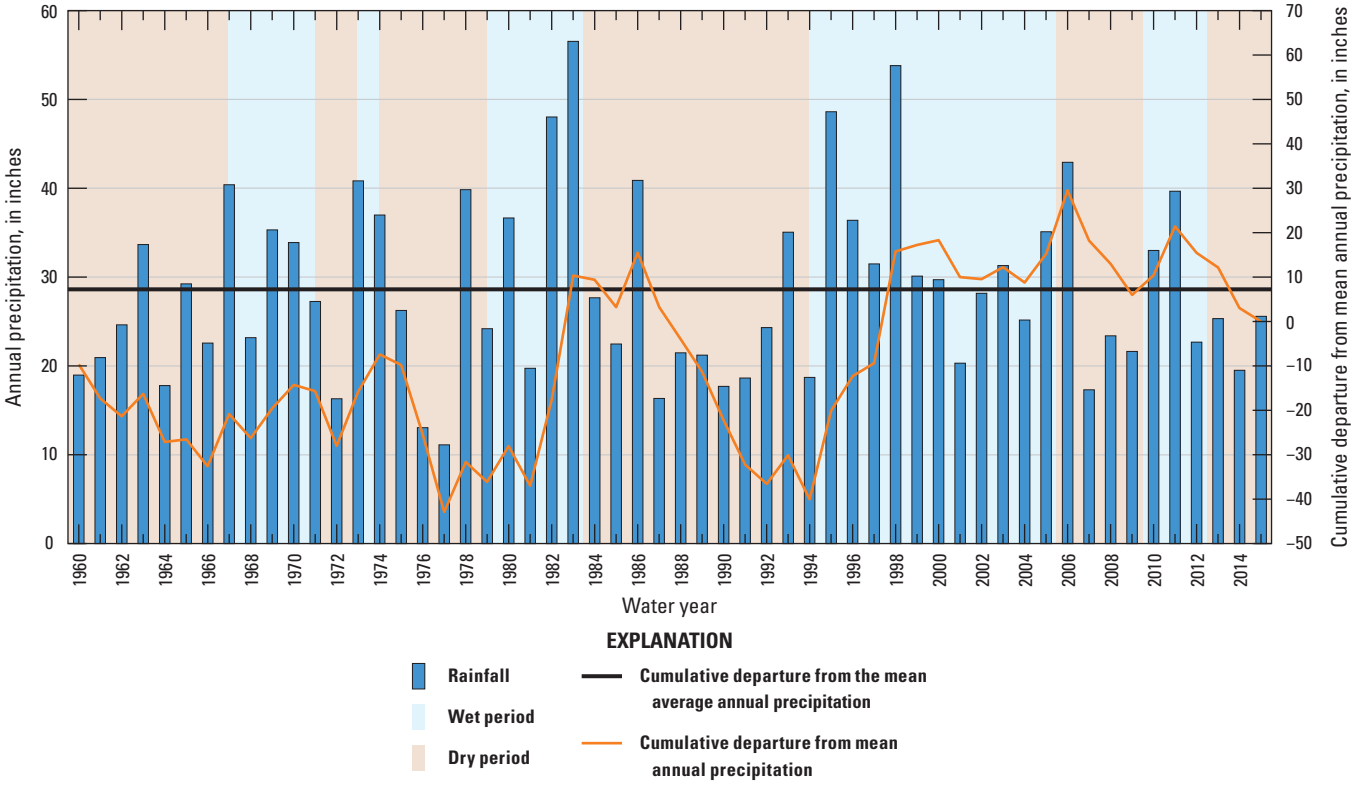

Figure D11. Annual average precipitation, based on downscaled PRISM data (PRISM Climate Group, 2013), spatially averaged over the study area, and the cumulative departure from the average annual precipitation, water years 1960–2015, Petaluma valley watershed, Sonoma County, California.

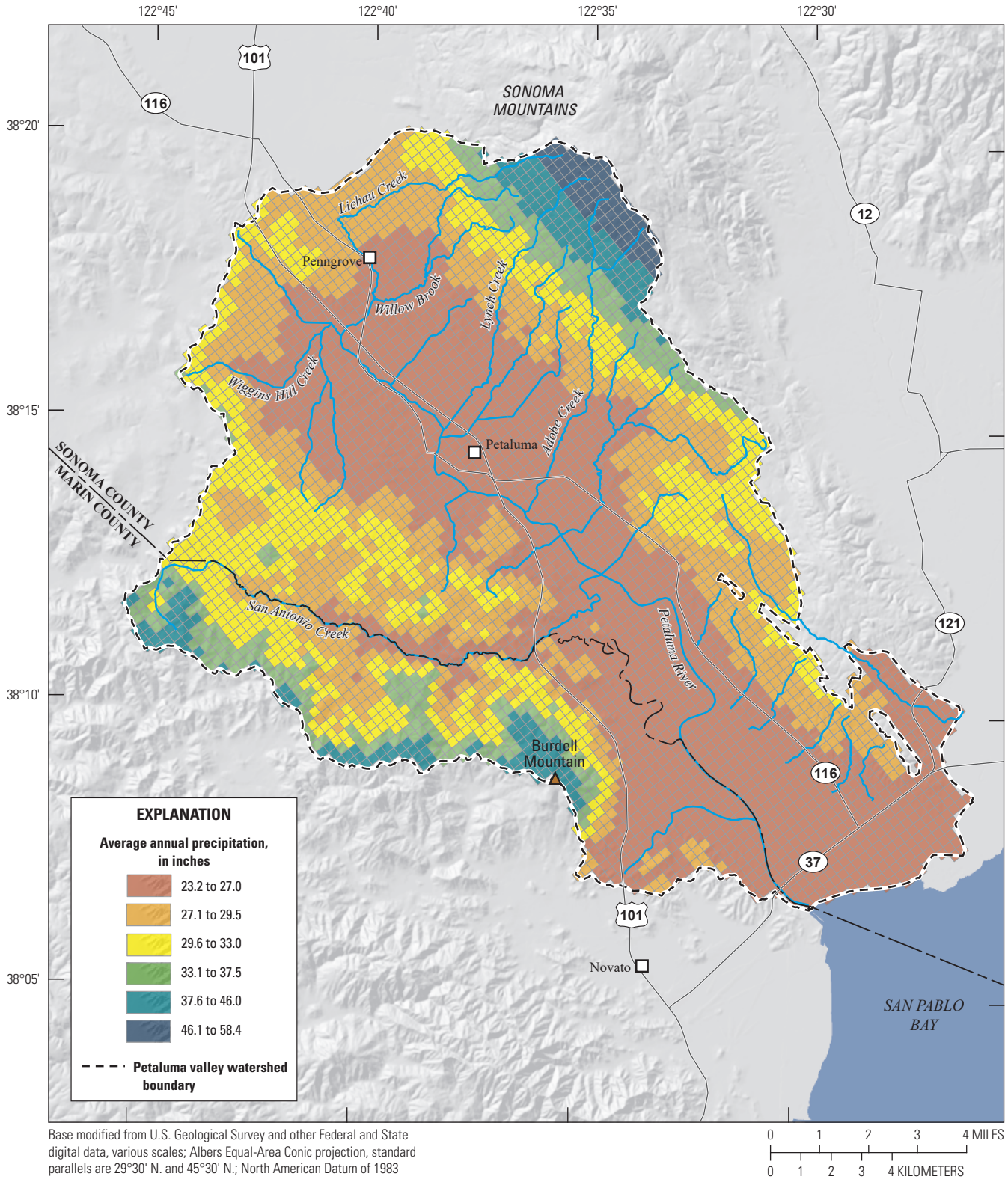

Figure D12. Average annual precipitation during water years 1960–2015, Petaluma valley watershed, Sonoma County, California.

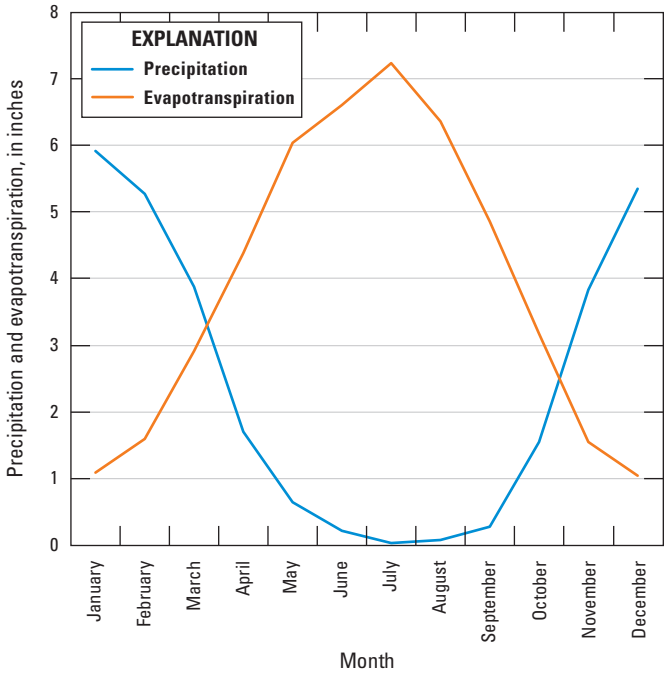

Figure D13. Monthly average precipitation and reference evapotranspiration (ET_0) during water years 1960–2015, Petaluma valley watershed, Sonoma County, California.

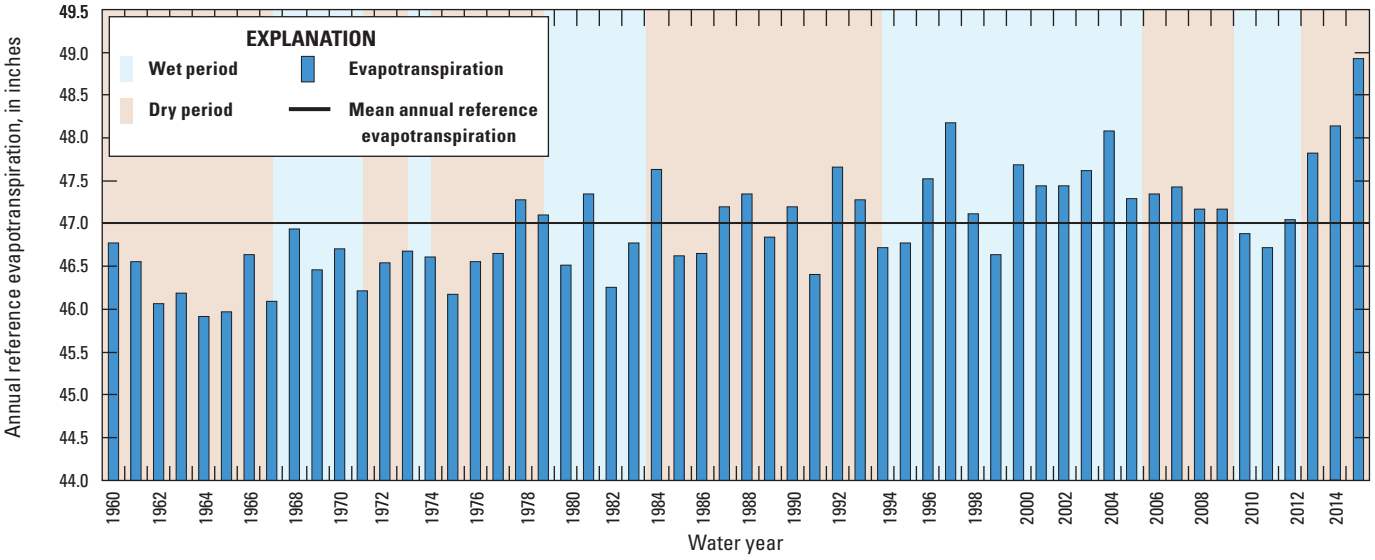

Figure D14. Calculated annual average reference evapotranspiration (ET_0), based on downscaled PRISM data (PRISM Climate Group, 2013), spatially averaged over the study area, water years 1960–2015, Petaluma valley watershed, Sonoma County, California.

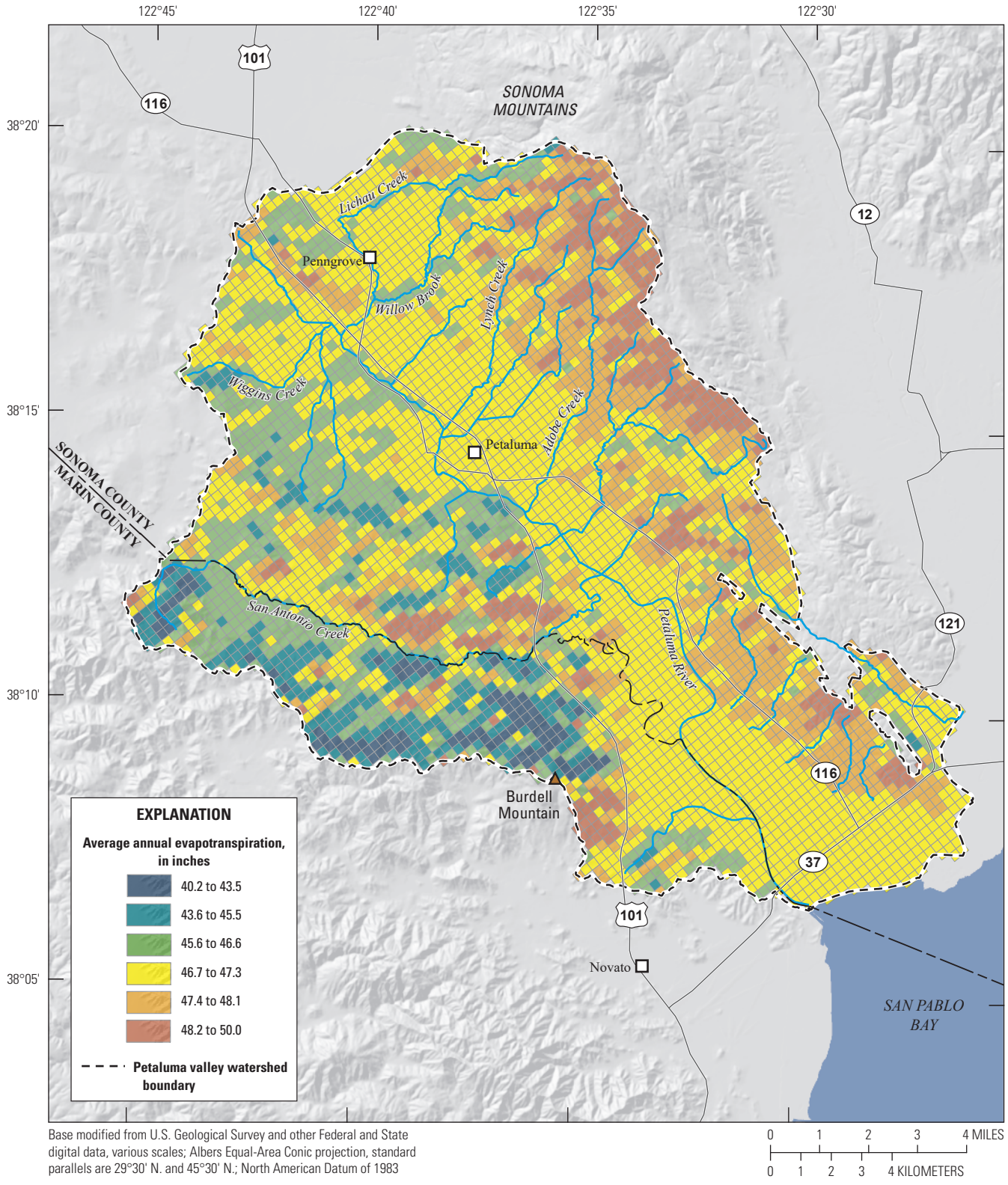

Figure D15. Average annual reference evapotranspiration (ET_o) during water years 1960–2015, Petaluma valley watershed, Sonoma County, California.

Model Development

Groundwater flow, streamflow, and land-surface processes are simulated in the PVIHM using MODFLOW-OWHM (Hanson and others, 2014), which is based on MODFLOW-2005 (Harbaugh, 2005). The list of MODFLOW packages and processes used in the PVIHM is provided in table D8.

The farm process (FMP) was used to simulate the supply and demand components of irrigated agriculture (table D8; Schmid and Hanson, 2009), including estimating pumpage data. The FMP also simulates deep percolation of precipitation and irrigation water and was used to simulate runoff from the ungaged watersheds to the modeled streamflow network (table D8).

The Upstream Weighting Package (UPW; table D8; Niswonger and others, 2011) was used to integrate the geologic framework model described in chapter B with the PVIHM and to specify the aquifer properties, including horizontal hydraulic conductivity (HK) and vertical hydraulic conductivity (VK), specific yield, and specific storage. The Streamflow Routing Package (SFR; table D8; Niswonger and Prudic, 2005) was used to simulate the streamflow in the model and the interaction between these streams and the aquifer system. The Hydmod Package (HYD, table D8; Hanson and Leake, 1999) was used to output data corresponding to observations.

Spatial and Temporal Discretization

The study area is represented by a finite-difference grid containing 108 rows and 77 columns with a grid-cell size of 984 by 984 ft (300 by 300 m), giving each cell an area of 22.2 acres (fig. D16; Seymour and Traum, 2021). The grid is rotated 40 degrees west of north so that the orientation of the grid coincides with the general groundwater-flow direction. Areally, the grid contains a total of 8,316 cells, with 2,427 cells (54,000 acres) representing groundwater flow, streamflow, and land-surface simulation, and 2,017 cells (45,000 acres) representing surface-water and landscape simulation only (fig. D16).

The PVIHM is vertically discretized in five layers based on the geologic-framework model and the well-screen intervals of production wells in the model area. Direct relations between stratigraphic units and model layers were not possible because of the discontinuous nature of the stratigraphic units in the study area. Maps showing the geologic-framework zones in each model layer are provided (fig. D17). Layer 1 extends from land surface to 30 ft bls and represents the shallowest part of the aquifer, where there is no groundwater pumpage. Layer 2 is 220 ft thick and represents the depth where most agricultural and domestic wells and some municipal wells are screened. Layer 3 is 290 ft thick and represents the maximum depth of municipal wells in the study area and the deepest layer where agricultural and domestic pumpage is simulated. Layer 4 is 360 ft thick. Layer 5 extends from 900 ft bls to the top of the Franciscan Complex.

The PVIHM is a transient model with a simulation period from October 1959 to September 2015 (WYs 1960–2015). The 56-year simulation provides a range of climatic conditions from dry to wet, including the WY 1960–66, WY 1975–77, WY 1987–94, WY 2007–09, and WY 2012–15 dry climatic periods and the WY 1967–74, WY 1978–86, WY 1995–2006, and WY 2010–11 wet climatic periods (fig. D2). Data needed for development of the model, including land use and municipal groundwater pumpage and streamflow and groundwater altitudes for model calibration, were available for the WY 1960–2015 period. The simulation period was divided into 672 monthly stress periods, which were further divided into 2 equal-length time steps to aid in numerical convergence. Model outputs (groundwater altitudes, streamflow, and water budgets) were calculated for each time step. Daily streamflow data were averaged to monthly values for the model simulation.

Initial Conditions

Determining initial groundwater altitudes for the study area was difficult because of the lack of available data for groundwater altitudes and pumpage before 1960. A groundwater-altitude map for spring 1951 (Cardwell, 1958; discussed in chapter B) only covered part of the study area. A groundwater-altitude map, based on available data, was constructed to represent initial groundwater altitudes in WY 1960.

The initial groundwater-altitude map was based on selected points from the 1951 groundwater-altitude map and data from groundwater-monitoring wells. Although only one well (3N/6W-01Q01, well 1; table D1; fig. D1) had groundwater-altitude data prior to WY 1960, the first measurement in any well with data prior to WY 1990 was assumed to be representative of WY 1960 conditions because there was no apparent trend in groundwater altitudes. A cutoff date of WY 1990 was selected so that there was an adequate spatial coverage of wells to interpolate a groundwater-altitude surface. Based on this assumption, data from 28 additional wells were available. The WY 1960 groundwater-altitude map was interpolated from the data points and then transferred to the PVIHM grid (fig. D18).

The estimated 1959 groundwater altitudes were specified as the initial groundwater altitudes in all five model layers. A transient simulation was then run without pumpage for 10 years using 120 stress periods, and the simulated groundwater altitudes after 10 years were used in subsequent simulations as initial groundwater altitudes in October 1959. This procedure dissipates any errors or inconsistences in the estimated October 1959 groundwater altitudes (such as areas where groundwater levels may be above land surface) and establishes vertical head gradients between model layers.

Table D8. MODFLOW packages and processes used in the Petaluma Valley Integrated Hydrologic Model, Petaluma valley watershed, Sonoma County, California.

MODFLOW package or process	Abbreviation	Function	Model input data	References
Basic	BAS6	Defining initial conditions and active model layers	Initial groundwater altitudes, active model cells for each layer.	(Harbaugh, 2005)
Discretization	DIS	Defining spatial and temporal discretization	Grid definition, layer definition, simulation period, stress period and time-step length, ground-surface altitude.	(Harbaugh, 2005)
Drain Return Package	DRT	Moves groundwater altitudes above land surface to stream network	Altitude at which groundwater is transferred to streamflow.	(Banta, 2000)
Farm	FMP4	Simulating the water supply and demand for irrigated land	Subregion definition, soil types, precipitation, evapotranspiration, land use, crop types, crop water-use parameters, surface-water deliveries.	(Schmid and Hanson, 2009)
General head Boundary	GHB	Simulating boundary flows into and out of the model area	Groundwater altitude at model boundary, boundary conductance.	(Harbaugh, 2005)
Head Observations	HOB	Defining observed groundwater altitudes used in model calibration	Location of observation wells, dates when observations are available.	(Hill and others, 2000)
Upstream Weighting Package	UPW	Defining the properties or aquifer material	Hydraulic conductivity, specific yield, and specific storage for each class of aquifer material.	(Niswonger and others, 2011)
Hydmod	HYD	Generating time-series model output for calibration wells and streamgages	Location of streamgages and observation wells.	(Hanson and Leake, 1999)
Name	NAM	Defining the names of the input and output files	—	(Harbaugh, 2005)
Multi-Node Well	MNW2	Simulating municipal and domestic wells	Municipal well locations, municipal pumping rates, domestic virtual wells, estimated domestic pumping rates.	(Konikow and others, 2009)
Multiplier	MULT	Scaling aquifer-property values for model calibration	—	(Harbaugh, 2005)
Output Control	OC	Defining when model output is printed	—	(Harbaugh, 2005)
Newton Solver	NWT	Solving the finite difference equations	—	(Niswonger and others, 2011)
Parameter Value	PVAL	Defining model parameters	Model parameters.	(Harbaugh, 2005)
Recharge	RCH	Simulating rural septic return flow	Rural septic seepage estimates.	(Harbaugh, 2005)
Streamflow Routing	SFR2	Simulating streamflow and the groundwater–surface-water interactions	Surface hydrology configuration, streamflow, diversions.	(Niswonger and Prudic, 2005)
Well	WEL	Simulating rural pumpage	Rural pumpage estimates.	(Harbaugh, 2005)
Zone	ZONE	Integrating the geologic model and the flow model	Zones based on geologic model.	(Harbaugh, 2005)

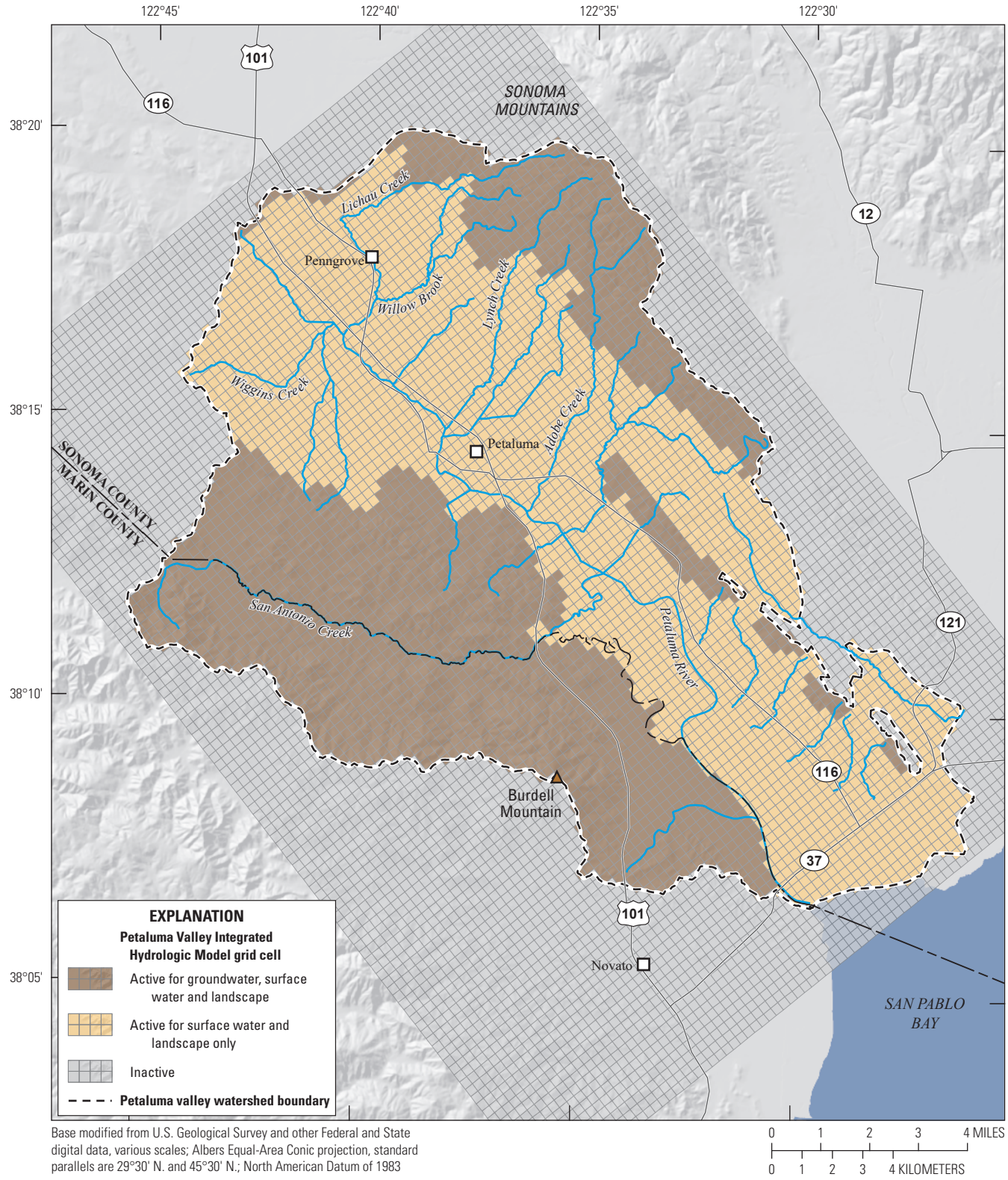

Figure D16. Active and inactive model-grid areas, Petaluma Valley Integrated Hydrologic Model, Petaluma valley watershed, Sonoma County, California.

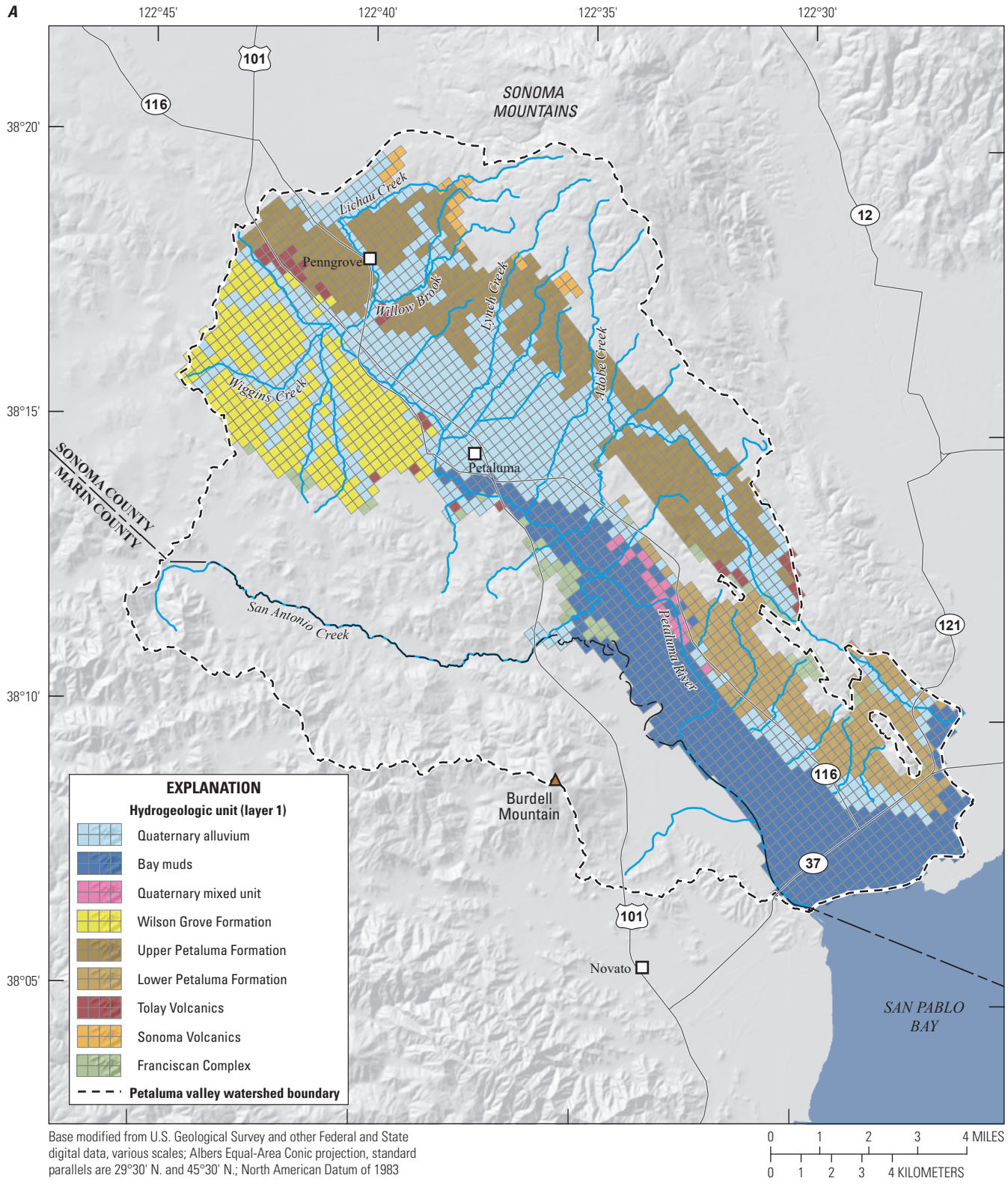

Figure D17. Map showing model zones for the Petaluma Valley Integrated Hydrologic Model for Petaluma valley watershed, Sonoma County, California: *A*, layer 1; *B*, layer 2; *C*, layer 3; *D*, layer 4; and *E*, layer 5.

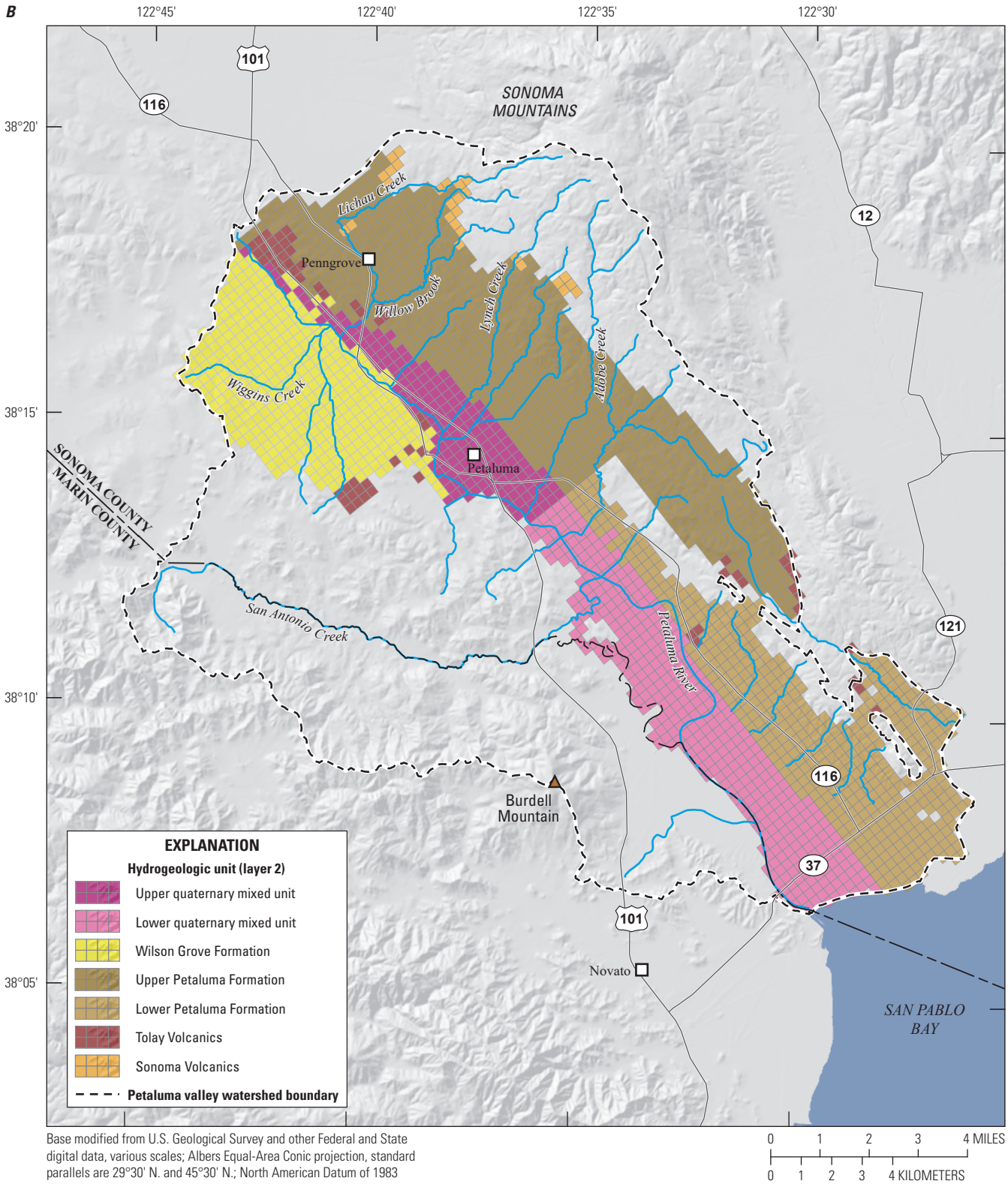

Figure D17.—Continued

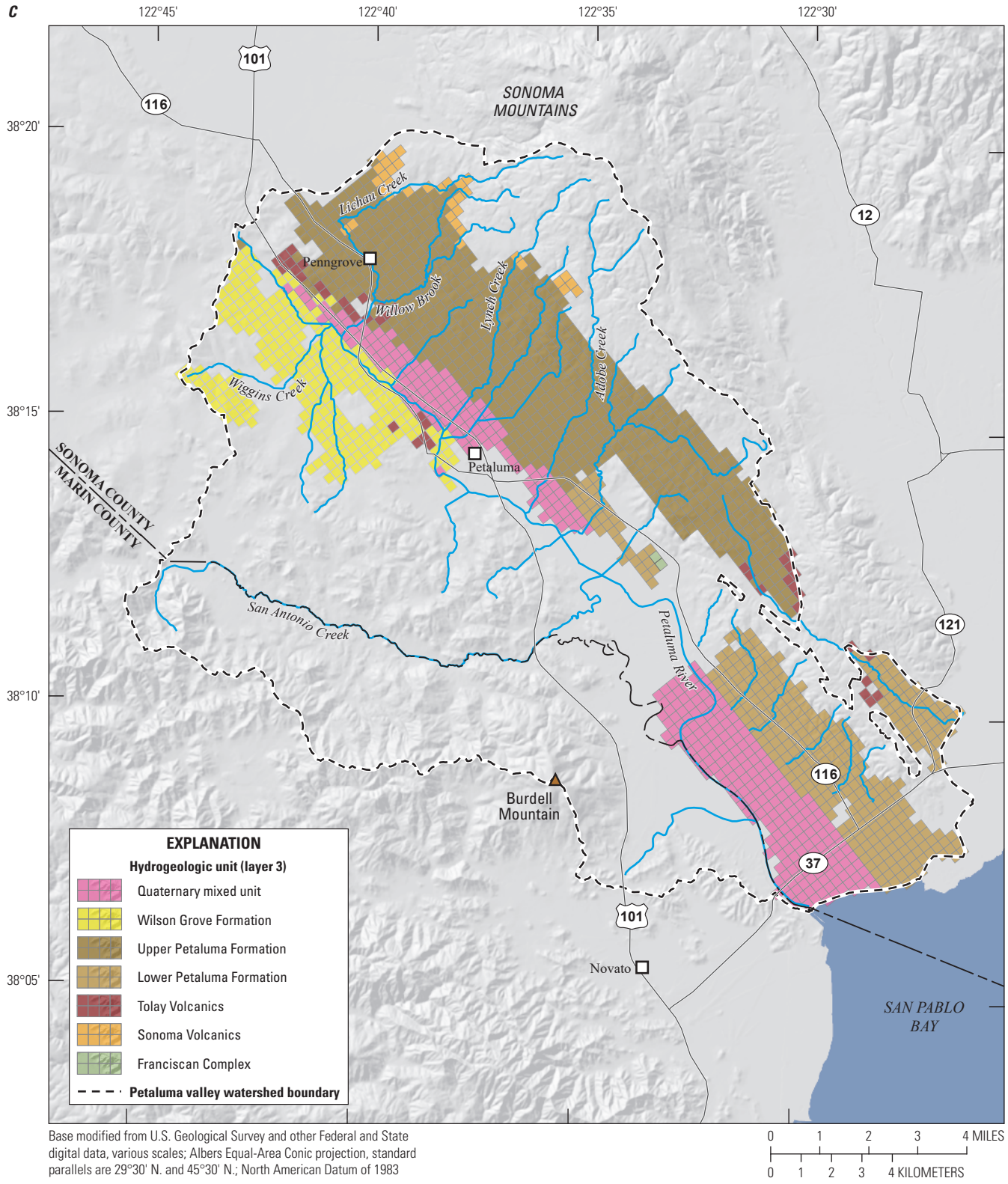

Figure D17.—Continued

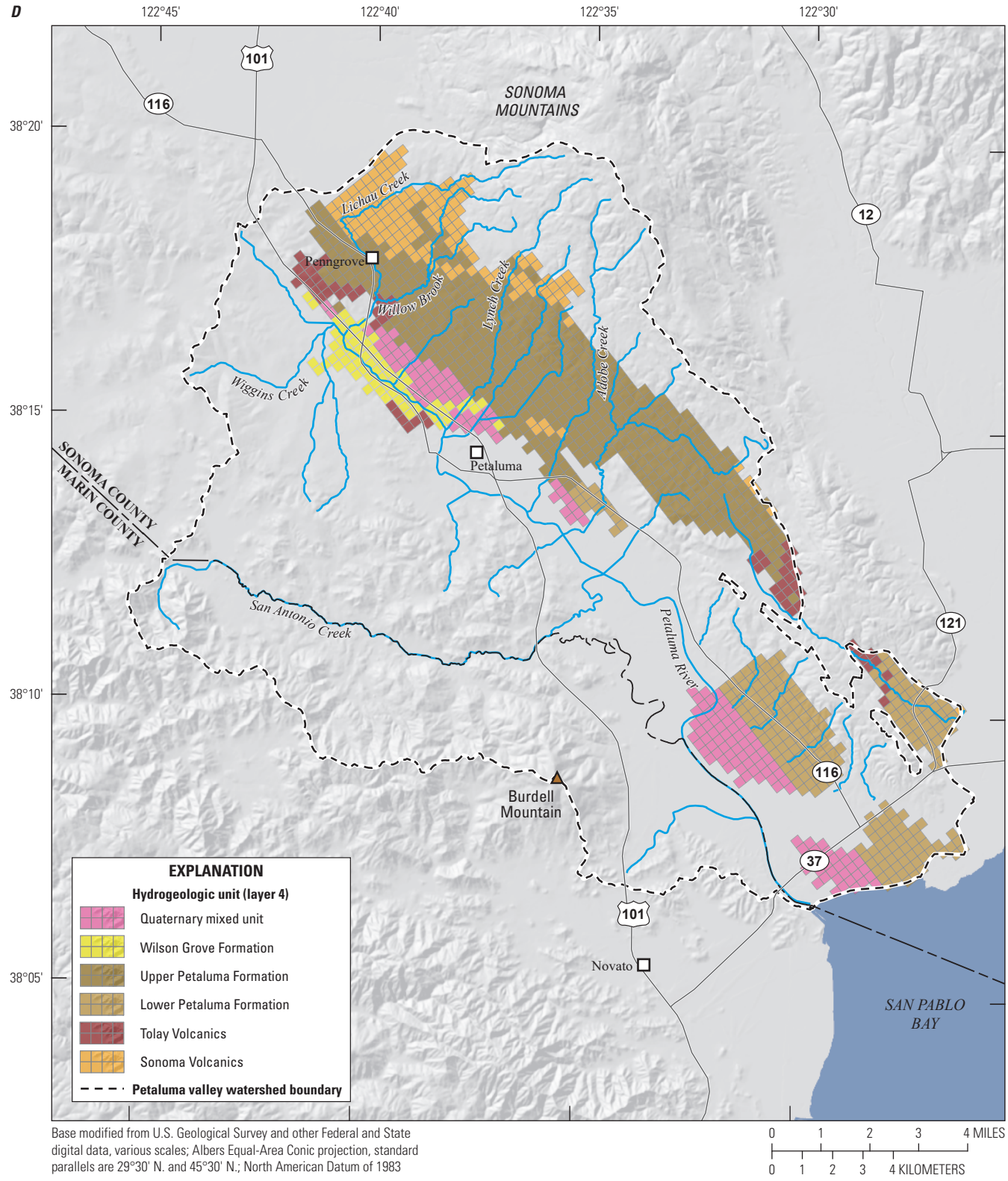

Figure D17.—Continued

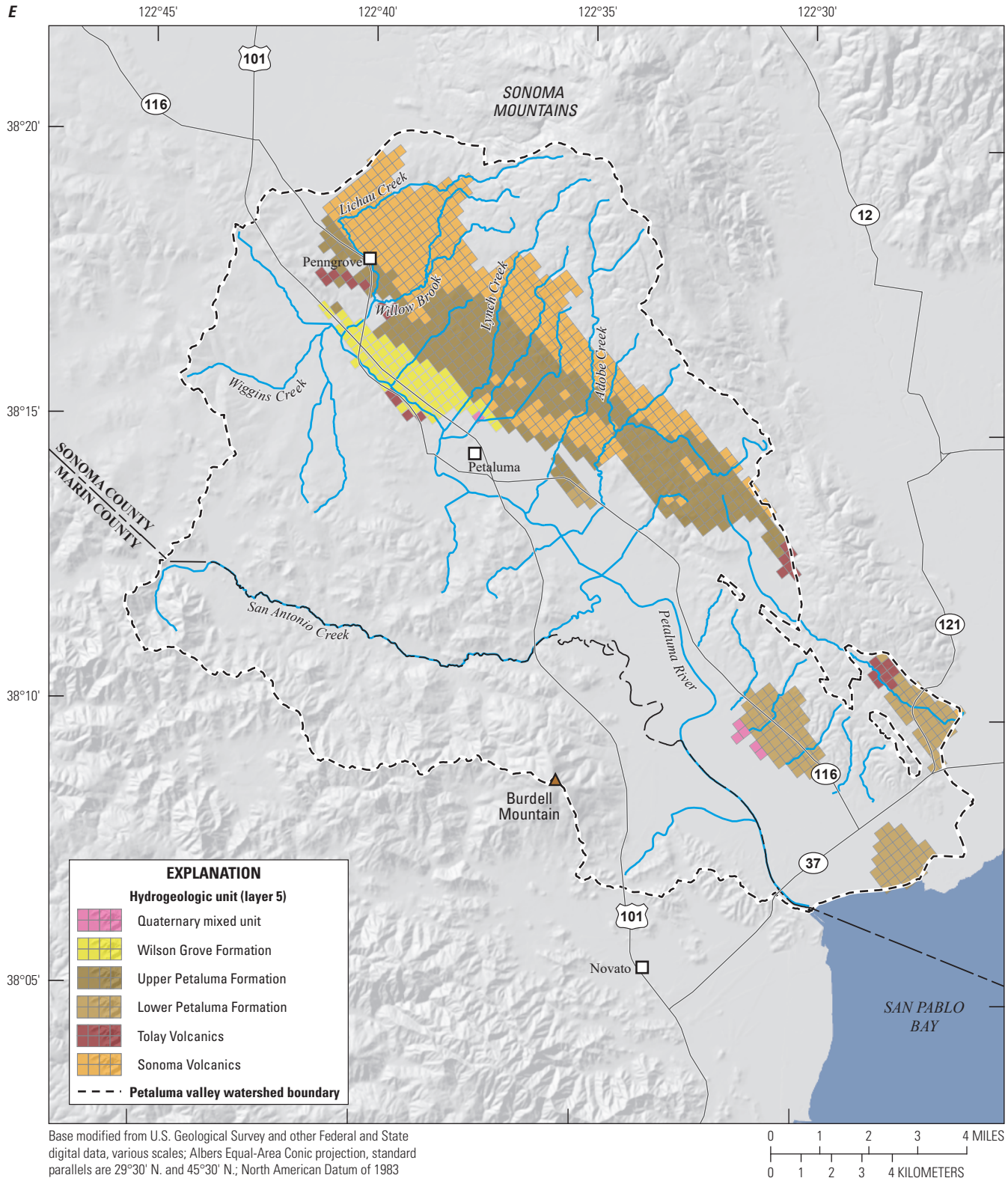

Figure D17.—Continued

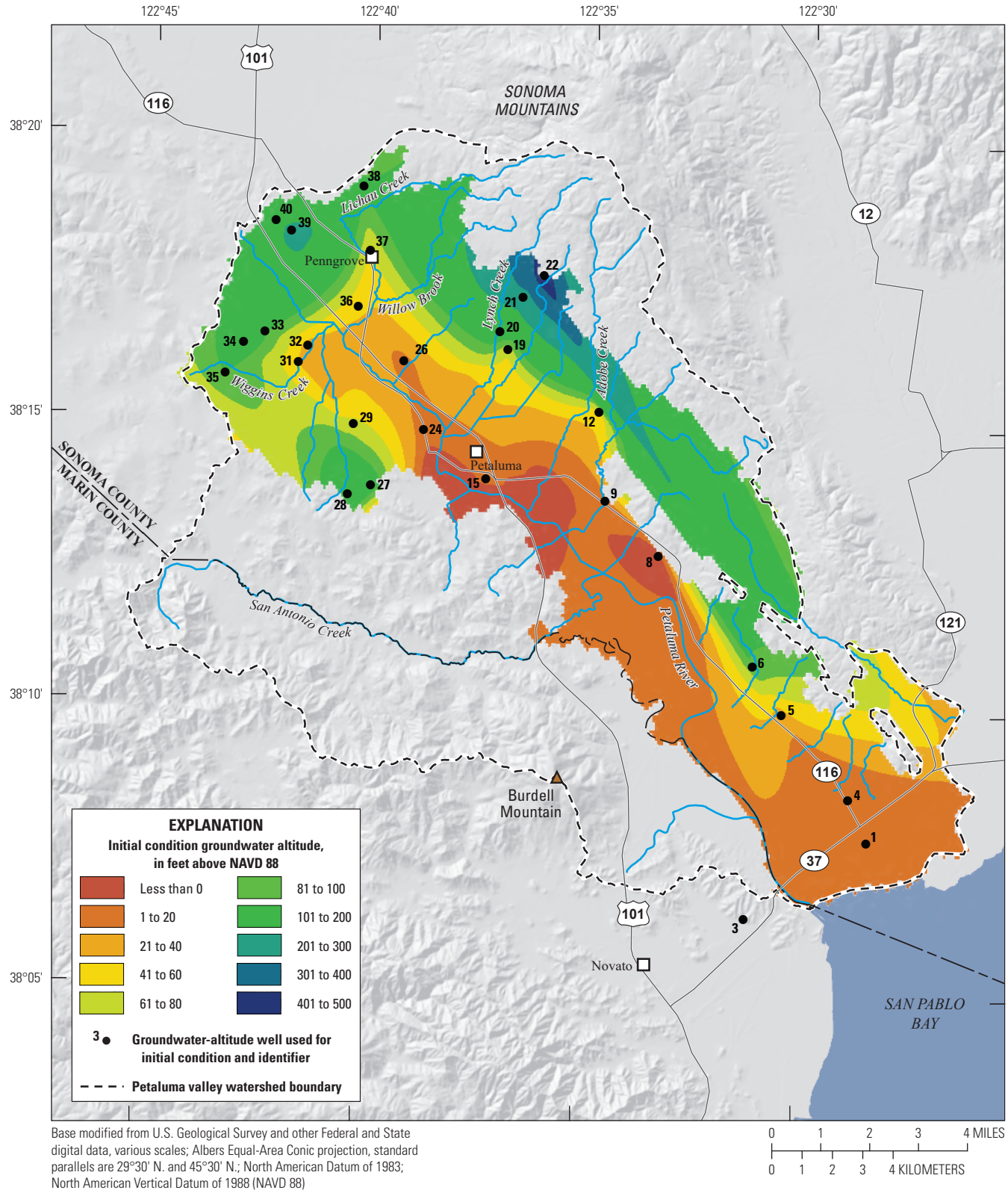

Figure D18. Initial groundwater altitude in feet above North American Vertical Datum of 1988 (NAVD 88) for water year 1960 used in the Petaluma Valley Integrated Hydrologic Model, Petaluma valley watershed, Sonoma County, California (California Department of Water Resources, 2018a; b).

Without performing this procedure, the model was prone to large changes and solver errors in simulated groundwater altitudes and flows during the first several stress periods. After 120 stress periods, simulated groundwater altitude changes were negligible, and inflows and outflows from storage achieved near equilibrium. This procedure was periodically repeated during model calibration as parameter values were adjusted to ensure that the initial groundwater altitudes were consistent with the calibrated parameter values.

Aquifer Properties

The aquifer properties used in the PVIHM include HK, VK, and storage coefficients. Initial values for aquifer properties were determined from previous studies (Herbst, 1982; Woolfenden and Hevesi, 2014) and were adjusted to achieve a good initial fit between measured and simulated groundwater altitudes and flows (table D9).

Aquifer properties were based on the eight hydrogeologic units defined in the geologic framework model described in chapter B (table D9). Each geologic formation has aquifer properties assigned for each of the five layers in the model. For the purposes of assigning aquifer properties, the Petaluma Formation was split into two zones, and the Quaternary mixed unit was split into two zones for model layer 2 (fig. D17*B*). The Quaternary alluvium unit, Wilson Grove Formation, and Quaternary mixed unit are the most permeable formations and were assigned higher initial horizontal hydraulic-conductivity values, with values in model layer 1 ranging from 164 feet per day (ft/d) for the Quaternary alluvium to 23 ft/d for the Wilson Grove Formation. The Petaluma Formation, Tolay Volcanics, Sonoma Volcanics, bay mud deposits, and the Franciscan Complex are less permeable formations and were assigned lower initial horizontal hydraulic-conductivity values (layer 1 value of 3.28 ft/d). Generally, initial hydraulic conductivities were set higher in shallower model layers and lower in deeper model layers to represent more consolidated aquifer maters in deeper aquifer material. The vertical anisotropy parameter (VANI) and horizontal anisotropy parameter (HANI) options are used in the UPW input to simulate vertical hydraulic-conductivity and horizonal anisotropy, respectively. HANI is a unitless scalar that represents the ratio of horizontal hydraulic conductivity along model columns (parallel to the Petaluma River) to hydraulic conductivity along model rows (perpendicular to the valley); a HANI value of greater than 1.0 higher represents a higher horizontal hydraulic conductivity parallel to the flow direction of the Petaluma River. VANI is a unitless scalar that that represents the ratio of horizonal to vertical hydraulic conductivity; a VANI value of greater than 1.0 represents a lower vertical hydraulic conductivity.

Storage properties were also assigned for each hydrogeologic unit and for each model layer. Initial specific storage values were all set to 1.0E–06 ft^{-1} for formations and layers. Specific yield values were assigned to model layers 1 and 2, which were simulated as convertible, and ranged from 5 percent for the Franciscan Complex to 25 percent for the Quaternary alluvium. Parameter values for the hydrogeologic units were modified during calibration as described in the "Model Calibration" section of this chapter.

Several predominantly strike-slip faults in the PVW are described in chapter B, and determining the effects of the faults on the groundwater system can be difficult. These faults were specified in early simulations using the Horizontal Flow Barrier (HFB) Package (Hsieh and Freckleton, 1993). During PVIHM development and calibration, however, faults in the study area were found to have little effect on groundwater flow and were removed in later simulations and the final version of PVIHM. The finding that faults do not influence groundwater altitudes is consistent with previous studies discussed in chapter B.

Boundary Conditions

The PVW aquifer system is hydraulically connected to three neighboring groundwater basins (the Santa Rosa Plain, Sonoma Valley, and Wilson Grove Formation Highlands), the tidally influenced section of the Petaluma River, and San Pablo Bay (fig. D19*A*). In a USGS study of the Santa Rosa Plain, the estimated flow rates between the PVW and the Santa Rosa Plain groundwater subbasin were estimated as less than 50 acre-ft/yr (Woolfenden and Hevesi, 2014). Farrar and others (2006) assumed that there was no underflow between Sonoma Valley and the PVW. Underflows between the PVW and the Wilson Grove Formation Highlands groundwater basin and between the PVW and San Pablo Bay have not been estimated. All other boundaries are classified as no-flow boundaries. No-flow conditions were assumed for the Sonoma Valley boundary based on a groundwater-flow model of Sonoma Valley (Andrew N. Rich, Sonoma County Water Agency, written commun., 2017).

Head-dependent boundary conditions were assigned using the General-Head Boundary (GHB) Package (Harbaugh, 2005) along boundaries with the Santa Rosa Plain, Sonoma Valley, and Wilson Grove Formation Highlands groundwater basins, the tidally influenced section of the Petaluma River, and San Pablo Bay (fig. D19*A*). The direction and magnitude of underflow was computed from the simulated hydraulic-head gradient and the conductance value of aquifer materials assigned to the boundary. The conductance values were estimated during model calibration and were adjusted to increase or decrease underflow to improve matches to observed groundwater altitudes.

Table D9. Initial aquifer properties used in the Petaluma Valley Integrated Hydrologic Model, Petaluma valley watershed, Sonoma County, California.

[Data obtained from ranges of values used in Herbst (1982) and Woolfenden and Hevesi (2014). **Abbreviations**: HK, horizontal hydraulic conductivity; ft/d, foot per day; SY, specific yield; SS, specific storage; VK, vertical hydraulic conductivity; 1/ft, one per foot; —, no data]

Stratigraphic unit	Layer 1					Layer 2				
	HK flow (ft/d)	HK non-flow (ft/d)	VK (ft/d)	SY (unitless)	SS (1/ft)	HK flow (ft/d)	HK non-flow (ft/d)	VK (ft/d)	SY (unitless)	SS (1/ft)
Quaternary alluvium	164.04	164.04	3.28	0.25	1.0E–06	—	—	—	—	—
Bay mud	9.84	3.28	3.28	0.15	1.0E–06	—	—	—	—	—
Lower quaternary mixed unit	—	—	—	—	—	229.66	22.97	3.28	0.20	1.0E–06
Upper quaternary mixed unit	45.93	22.97	3.28	0.20	1.0E–06	229.66	22.97	3.28	0.20	1.0E–06
Wilson Grove Formation	22.97	22.97	3.28	0.10	1.0E–06	22.97	22.97	3.28	0.10	1.0E–06
Upper Petaluma Formation	32.81	3.28	3.28	0.20	1.0E–06	0.66	0.33	0.33	0.20	1.0E–06
Lower Petaluma Formation	32.81	3.28	3.28	0.20	1.0E–06	3.28	0.33	0.33	0.20	1.0E–06
Sonoma Volcanics	3.28	3.28	3.28	0.20	1.0E–06	0.33	0.33	0.33	0.20	1.0E–06
Tolay Volcanics	3.28	3.28	3.28	0.20	1.0E–06	0.33	0.33	0.33	0.20	1.0E–06
Bedrock	3.28	3.28	3.28	0.05	1.0E–06	—	—	—	—	—

Groundwater altitudes were not available directly along the Wilson Grove Formation highlands (WGFH) boundary. Woolfenden (2014) used Santa Rosa Plain (SRP) boundary heads that ranged spatially from 85 to 131 ft; however, these data did not vary with time. Annual and sub-annual groundwater-altitude data were provided by CDWR and USGS and were used to estimate the boundary heads more accurately along the WGFH and SRP boundaries. The monitoring wells used to estimate the temporally and spatially varying groundwater altitudes along the SRP and WGFH GHB are shown in figure D19*B*. The monitoring wells were chosen on the basis of proximity to the GHB model cells and temporal data coverage. The GHB cells that were closest in distance and altitude to the monitoring wells were referred to as primary-data GHB cells (fig. D19*B*) and were assigned those groundwater altitudes either directly or with a linear offset; the final groundwater altitudes were set as part of the model calibration. Missing groundwater altitudes for stress periods between discrete measurements were estimated using linear interpolation. Missing groundwater altitudes from 1959 to the first groundwater-altitude observation and from the last groundwater-altitude observation to 2015 were extrapolated using the long-term trend (slope) of the measured groundwater altitudes.

Groundwater altitudes for the nonprimary-data GHB cells (fig. D19*B*) were estimated based on proximity and relative altitudes to the primary-data GHB cells (chapter B, fig. B11; City of Petaluma, 2016). Groundwater altitudes for the nonprimary-data WGFH GHB cells were estimated using linear interpolation between primary-data GHB cells associated with wells 40 and 35 or were set equal to a single value spatially to maintain zero slope (fig. D19*B*). The two blocks of WGFH GHB cells that were set equal to a single groundwater-altitude value were allowed to fluctuate temporally based on primary-data GHB cells. Specifically, the northern block was near the boundary with the SRP and fluctuated according to the primary-data SRP GHB cell associated with well 40, whereas the southern block fluctuated according to the primary-data WGFH GHB cell associated with well 35. Groundwater altitudes for the nonprimary-data SRP GHB cells located between primary-data SRP GHB cells were associated with wells 40 and 42 (fig. D19*B*) and were estimated using linear interpolation. The groundwater altitudes for the nonprimary-data SRP GHB cells located between the SRP GHB cell associated with well 40 and the northern block of zero-slope WGFH GHB cells were estimated using linear interpolation between the primary-data GHB cell and the block of zero-slope groundwater altitudes. The monitoring wells used to estimate GHB groundwater altitudes (wells 35, 40, and 42) were perforated in model layers 1 and 2 (table D1). After missing groundwater-altitude data were estimated temporally and spatially, estimated groundwater altitudes were assigned to any model layer that was not perforated by the well.

Table D9. Initial aquifer properties used in the Petaluma Valley Integrated Hydrologic Model, Petaluma valley watershed, Sonoma County, California. —Continued

[Data obtained from ranges of values used in Herbst (1982) and Woolfenden and Hevesi (2014). **Abbreviations**: HK, horizontal hydraulic conductivity; ft/d, foot per day; SY, specific yield; SS, specific storage; VK, vertical hydraulic conductivity; 1/ft, one per foot; —, no data]

Layer 3				Layer 4				Layer 5			
HK flow (ft/d)	HK non-flow (ft/d)	VK (ft/d)	SS (1/ft)	HK flow (ft/d)	HK non-flow (ft/d)	VK (ft/d)	SS (1/ft)	HK flow (ft/d)	HK non-flow (ft/d)	VK (ft/d)	SS (1/ft)
—	—	—	—	—	—	—	—	—	—	—	—
—	—	—	—	—	—	—	—	—	—	—	—
—	—	—	—	—	—	—	—	—	—	—	—
3.28	3.28	3.28	1.0E–06	3.28	3.28	3.28	1.0E–06	3.28	3.28	3.28	1.0E–06
3.28	3.28	3.28	1.0E–06	3.28	3.28	3.28	1.0E–06	3.28	3.28	3.28	1.0E–06
3.28	0.33	0.33	1.0E–06	3.28	0.33	0.33	1.0E–06	3.28	0.33	0.33	1.0E–06
3.28	0.33	0.33	1.0E–06	3.28	0.33	0.33	1.0E–06	3.28	0.33	0.33	1.0E–06
0.33	0.33	0.33	1.0E–06	0.33	0.33	0.33	1.0E–06	0.33	0.33	0.33	1.0E–06
0.33	0.33	0.33	1.0E–06	0.33	0.33	0.33	1.0E–06	0.33	0.33	0.33	1.0E–06
0.16	0.16	0.03	1.0E–06	—	—	—	—	—	—	—	—

The tidally influenced part of the Petaluma River, its tributaries, and Tolay Creek as well as for the San Pablo Bay boundary were represented as a GHB (fig. D19*A*). To determine the tidally influenced cells along the streams, a high-resolution DEM that encompasses the study area was used (Fregoso and others, 2017). The bathymetry data in this DEM were compared with the mean high water (MHW) of 5.68 feet in San Pablo Bay at the mouth of the Petaluma River (Mak and others, 2016). Any stream cell with a bathymetry altitude below 5.68 feet was set as a tidally influenced cell. The mean tide level (MTL) in San Pablo Bay at the mouth of the Petaluma River was 3.39 feet (Mak and others, 2016), and this value was specified as the general head for the tidally influenced stream cells and the San Pablo Bay boundary cells. Although San Pablo Bay water is saline, an equivalent freshwater head was not calculated because the head difference due to density is small. These boundary heads were also assumed to be constant during model calibration. Both assumptions can be modified if additional data become available in the future as the heads are setup using the TABFILE feature in the GHB Package. San Pablo Bay and the tidally influenced stream boundary conditions were applied to layer 2 of the model.

Groundwater Recharge

The primary source of groundwater recharge (or inflows) to the PVIHM is percolation of precipitation. Other inflows include irrigation-return flow, infiltration from streams, septic-tank discharge, underflow from adjacent groundwater basins, and excess water applied to irrigated land (irrigation-return flow) during the growing season. Percolation of precipitation and irrigation-return flow were simulated by the FMP as described in the "Simulation of Land-Surface Processes" section of this chapter. Leakage from streams to the aquifer system was simulated by the SFR as described in the "Simulation of Surface Water" section of this chapter. Septic-tank discharge was assumed to be negligible and is not addressed in the model.

Groundwater Discharge

Groundwater discharges (or outflows) from the PVIHM as municipal, rural-residential, and agricultural pumpage, root uptake of shallow groundwater, groundwater discharge to streams, and underflow through model boundaries. Municipal pumpage was simulated using the Multi-Node Well (MNW2) Package (Konikow and others, 2009) because many municipal wells were perforated across more than one model layer. Rural-residential pumpage was simulated using the Well Package (WEL; Harbaugh, 2005). Agricultural pumpage were estimated using the FMP and simulated using FMP wells. In PVIHM, all FMP wells that pump were assumed to be perforated in a single model layer and were not linked with MNW2 wells. Other pumpage, such as industrial and commercial pumpage, was not simulated in PVIHM because the amount pumped, as based on analysis of limited available data, was determined to be negligible.

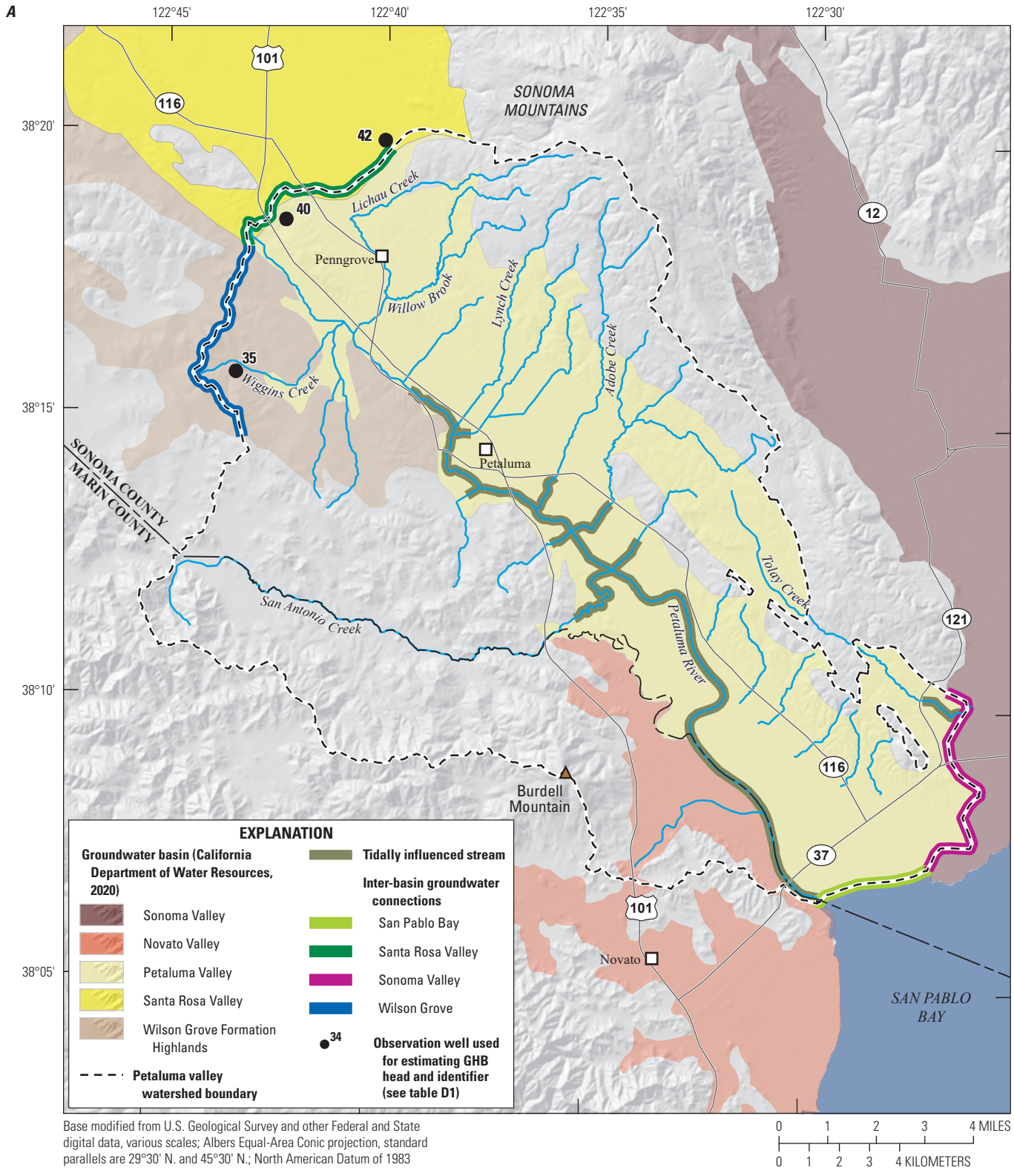

Figure D19. Boundary conditions simulated in the Petaluma Valley Integrated Hydrologic Model, Petaluma valley watershed, California: *A*, all boundary conditions; *B*, northern general-head boundary (GHB); groundwater basins are from (California Department of Water Resources, 2020; see table D1).

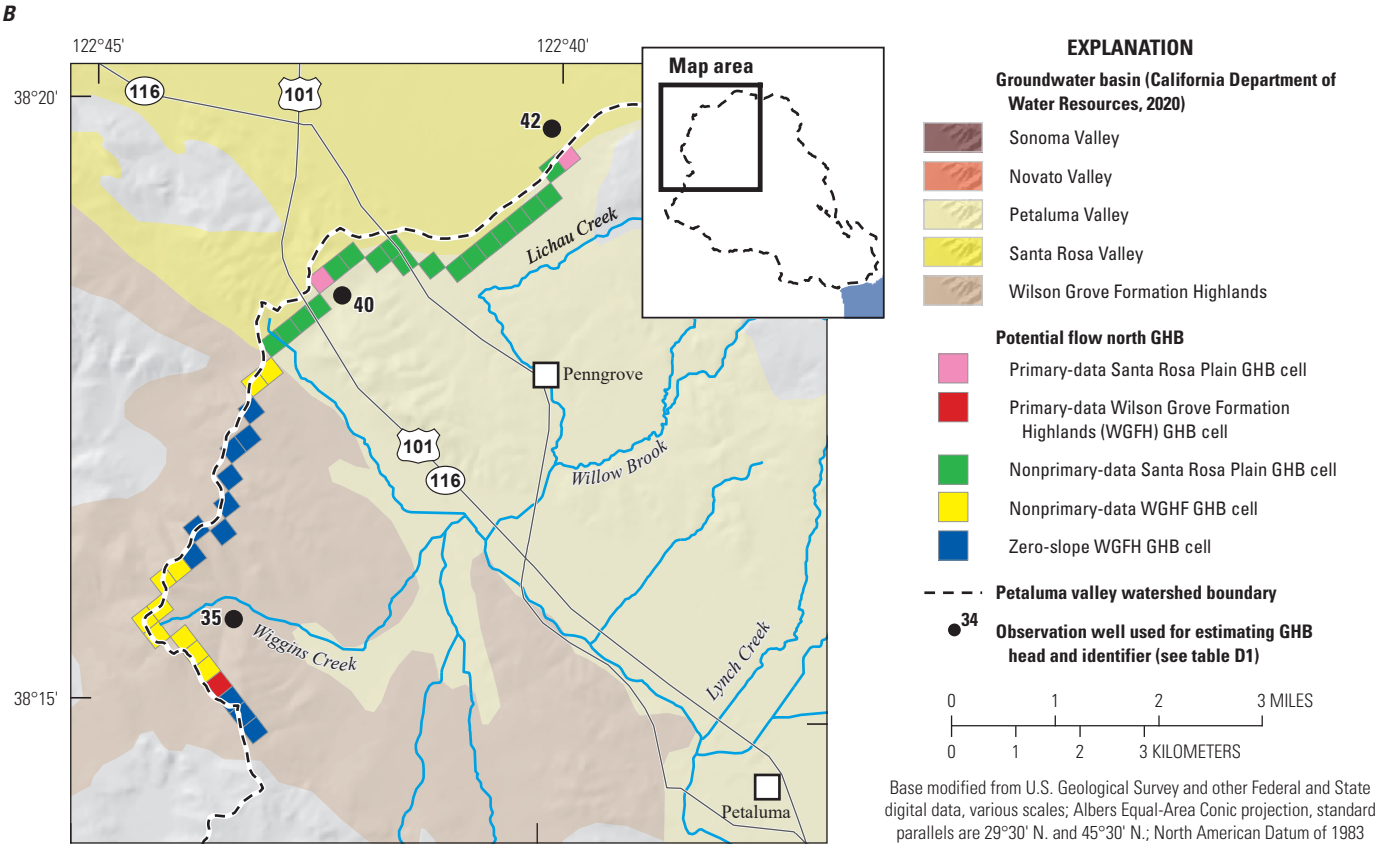

Figure D19.—Continued

Municipal Pumpage

Locations of municipal wells, well properties, and pumpage rates were presented previously in the "Water Supply and Demand Data" section of this chapter. These datasets were used to generate the MNW2 input file. Gaps in the well-construction data, including well radius and the top and bottom of the screened interval (table D7), needed to be estimated. The diameter of the McDowell well was not reported; therefore, the casing diameter was assumed to equal 10 in. The bottom altitude of the well-screen was estimated by the well depth if construction data were not available (Del Oro, La Tercera, McDowell, Scott, and Stubb wells, table D7). The top altitude of the well-screen was assumed to be 30 ft bls if construction data were not available (Del Oro, La Tercera, McDowell, Scott, and Stubb wells). The well-construction date was used to determine when wells were active for the purpose of spatially distributing pumpage to wells before pumpage data by well were available (before 2000). Construction dates were missing for four wells: Stubb, McDowell, La Tercera, and Del Oro wells (table D7). Pumpage from the Stubb well was simulated during the entire model period before WY 2000 because well logs indicated the well had a large radius (13 in.), and older wells typically have larger radii because of different technology and drilling practices used at the time. The other three wells were assumed to begin pumpage in WY 2001 because they were labeled "under construction" in previous reports (West Yost, 2004).

The SKIN option in MNW2 was used to account for head losses adjacent to and within the borehole and well screen. The SKIN option requires values for the hydraulic conductivity and radius of the well skin; skin radius is defined as the radius to the outer limit of formation damage around the well borehole. However, skin radius and hydraulic conductivity data were not available. Therefore, skin radius was assumed to be twice the well radius, and the hydraulic conductivity of the skin was equal to twice the hydraulic conductivity of the aquifer.

The next step in generating the MNW2 file was to estimate a complete monthly pumpage record by well for WY 1960 through 2015. From WY 2000 to 2015, monthly pumpage records were available by well, and these data were used directly. From WY 1994 to 1999, monthly total pumpage records were available for the City of Petaluma wells; however, spatial data describing the distribution of pumpage were not available. From WY 1960 to 1993, only total annual pumpage for the city wells was available. Annual pumpage data for the WY 1960–93 period was distributed among 12 months by computing the average percentage of annual pumpage in each month from WY 1994 to 2015 and applying monthly percentages to WY 1960–93 annual pumpage data (table D10).

Next, to distribute the monthly pumpage data to each well, each active well was assumed to be pumped equally each month. The well construction date was used to determine the year when a well became active. This assumption is generally poor because data from WY 2000 to 2015 indicate that the relative pumpage by well was variable; however, this was the only method available given the lack of other data.

Rural and Agricultural Pumpage

Data concerning the location and properties of the agricultural pumpage wells were not available for the PVW; therefore, a virtual pumped well was placed in each model cell representing an irrigated crop. These wells were assigned a single model layer from layer 1 to layer 3 (fig. D20) on the basis of analysis of the well-screen data in CDWR Online System of Well Completion Reports database (California Department of Water Resources, 2019), which is discussed earlier. A total of 2,411 virtual agricultural wells were represented in the PVIHM, but only 318 of these wells were active for groundwater pumpage according to the 2012 land use (California Department of Water Resources, 2016). These inactive wells could be included in future scenarios to simulate different pumping distributions with minimal setup and changes to model inputs. The pumpage rates for the virtual-agricultural wells were computed by the FMP on the basis of the supply and demand water balance for irrigated agriculture, as described in the "Simulation of Land-Surface Processes" section of this chapter.

Rural-residential pumpage was simulated in the PVIHM by using the Well Package (WEL). A WEL file was provided by SCWA (Andrew N. Rich, Sonoma County Water Agency, written commun., June 2020) and is available in the groundwater model release (Traum, 2022). The pumpage in the WEL Package (Harbaugh, 2005) file used a virtual well screened in a single model layer for each cell (fig. D21). The SCWA also provided a Recharge Package (RCH, Harbaugh, 2005; Andrew N. Rich, Sonoma County Water Agency, written commun., June 2020) to simulate the portion of indoor rural water use returned to the groundwater system as septic seepage, which is also available in the groundwater model release (Traum, 2022).

Table D10. Percentages used to distribute annual municipal-pumpage data during water years 1960–1993 to monthly records, Petaluma valley watershed, Sonoma County, California.

Month	Percentage of pumpage per month
January	4.6
February	4.5
March	5.5
April	7.3
May	9.9
June	11.7
July	13.4
August	12.8
September	10.7
October	8.5
November	5.9
December	5.0

Other Forms of Discharge

Root uptake and evaporation of shallow groundwater were simulated as a sink of groundwater discharge, and this process is especially important in the Petaluma marsh (chapter A, fig. A1), where depth to the water table is generally shallow. This process was simulated by the FMP, as described in the "Simulation of Land-Surface Processes" section of this chapter. The exchange of surface water and groundwater can be both a groundwater source and sink in the PVW. This process is simulated by the SFR (Niswonger and Prudic, 2005) and described in the "Simulation of Surface Water" section of this chapter. The Drain Return Flow (DRT1) Package (Banta, 2000) was used in the PVIHM to prevent simulation conditions where groundwater altitudes were above land surface. Drain levels were set to land surface for all model cells and for all times with an artificially high conductance value. Using a feature in MODFLOW-OWHM, water removed from the groundwater system by these drains was added to the surface-water network. For the purposes of reporting model results, water removed from the groundwater system using DRT1 was recorded as the "rejected recharge" term in the groundwater budget.

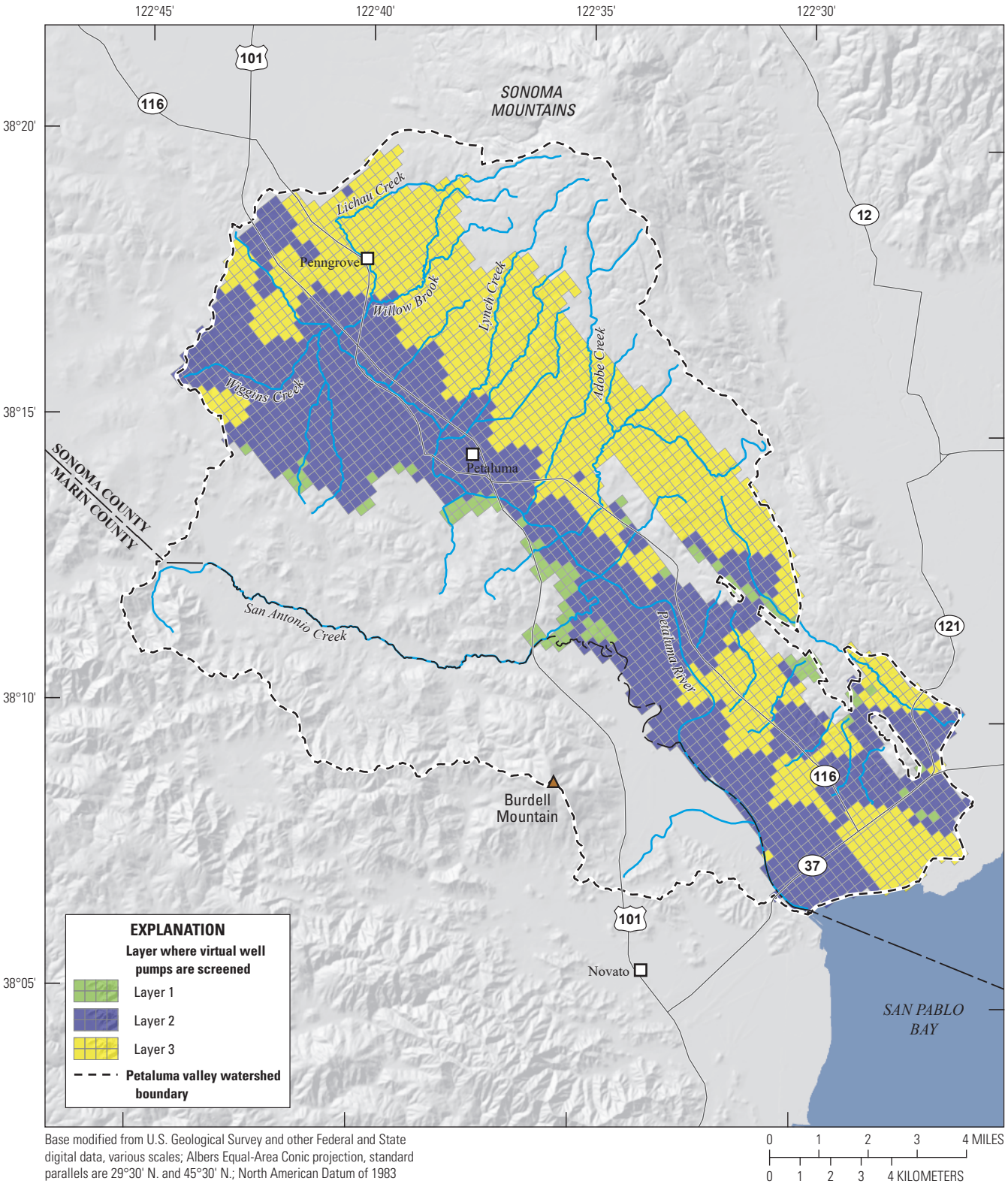

Figure D20. Layers where agricultural wells are screened, Petaluma valley watershed, Sonoma County, California.

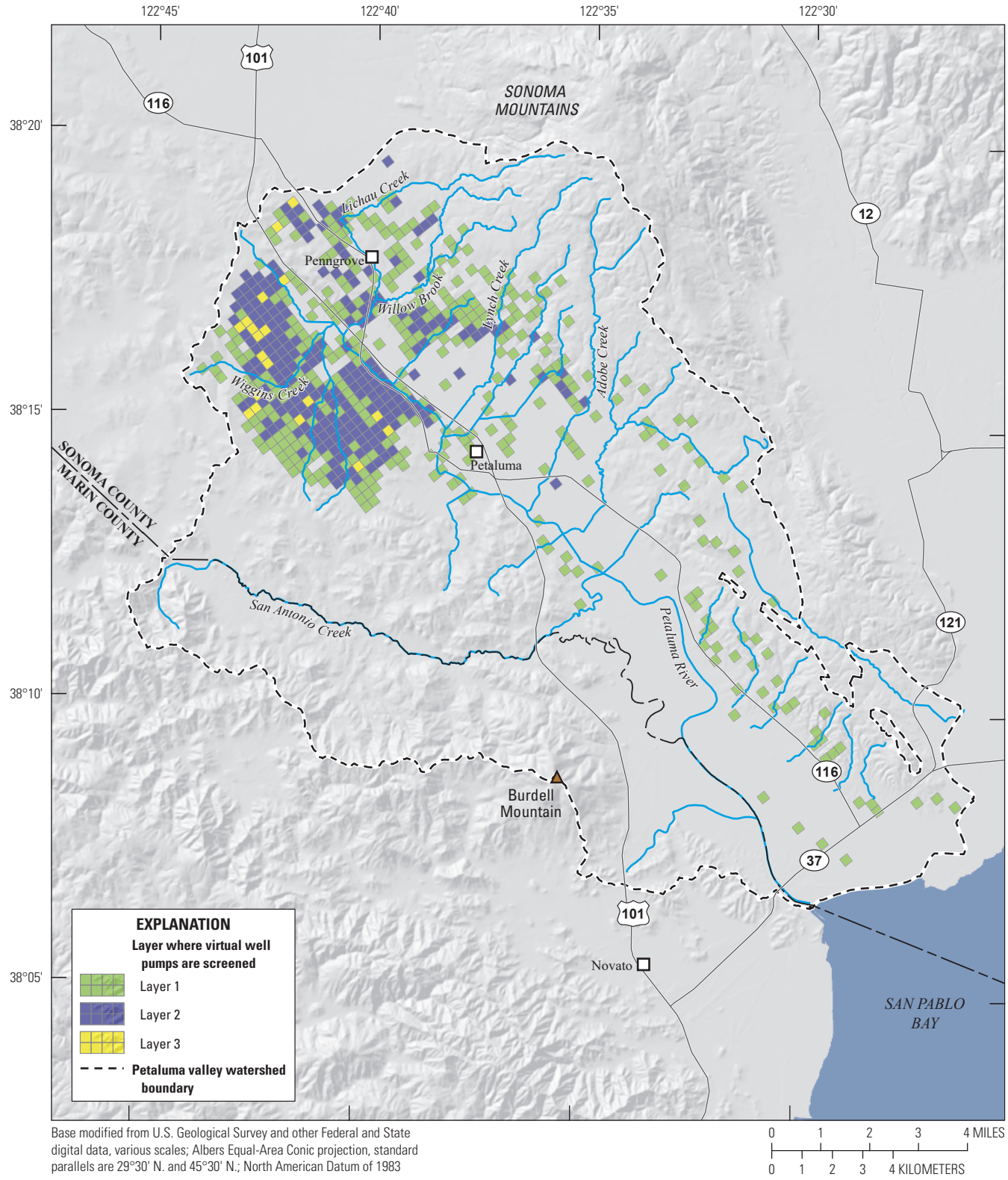

Figure D21. Layers where rural wells are screened, Petaluma valley watershed, Sonoma County, California.

Simulation of Land-Surface Processes

The FMP (Schmid and others, 2006; Schmid and Hanson, 2009; Hanson and others, 2014) was used to simulate the water supply and demand components of agriculture, rural residential outdoor use met by precipitation, and native vegetation. This report provides an overview of how the FMP functions with regard to those components used for the PVIHM. A comprehensive description of the FMP, including its theoretical and mathematical underpinnings, can be found in the FMP documentation (Schmid and others, 2006; Schmid and Hanson, 2009; Hanson and others, 2014).

For the purposes of this report and to be consistent with FMP terminology, any inflow from the land-surface system is considered a supply, and any outflow from the landscape-surface system is considered a demand. Water-supply components include precipitation, root uptake of shallow groundwater, and irrigation from surface-water and groundwater sources. Water-demand components include plant ET, runoff of precipitation and irrigation water, and percolation to groundwater. Although runoff and percolation may not typically be regarded as a demand, they are part of the total outflow "side" of the water-balance supply and demand equation. In addition, for areas that do not have irrigated crops (such as native vegetation), ET and other outflows are referred to as demands.

Ground-surface altitudes were used by the FMP to route runoff from precipitation and irrigation to the simulated streams and to estimate ET of shallow groundwater. Soils data were used to define the capillary-fringe depth and other parameters that influenced transpiration from groundwater. The remaining FMP datasets are discussed in the remainder of this subsection of the report.

Subregion Definitions

The PVIHM was subdivided into 21 subregions (table D11; fig. D22) to improve simulation of water supply and demand in the PVW. Subregions were defined primarily on the basis of the Petaluma River sub-watersheds because the dominant land use in the study area was native vegetation, and vegetated lands were the main source of surface-water runoff and groundwater recharge in the study area. In addition, subregions were segregated to represent the Petaluma Valley and the Wilson Grove Formation Highlands groundwater basins, the City of Petaluma, and the North Bay Water District. North Bay Water District does not actually provide any water service but was included as a subregion to add flexibility to the model for simulating any future conditions that might include North Bay Water District operations. Defining subregions in this way allowed for different combinations of subregions to represent areas of interest when processing model outputs. For example, subregions 8, 9, and 10 make up the City of Petaluma, and subregions 2, 3, 4, 10, 11, 17, 18, 19, and 21 cover the Petaluma Valley groundwater basin (fig. D22).

Surface-Water and Recycled Delivery

Surface-water and recycled-water data were previously discussed in the "Agriculture" section of the "Water Supply and Demand Data" section of this report. Diversion locations for surface water and locations of parcels that use recycled water were overlaid with the subregions to determine the water-supply deliveries to each subregion. Recycled water in PVIHM was simulated as non-routed deliveries.

Because of the mismatch in timing between when diversions take place and when they are used, the FMP is not able to directly simulate the surface-water diversions from local streams for agricultural use. Water is typically diverted in winter months and then stored in on-farm storage ponds prior to irrigation deliveries in summer months. The storage of irrigation water and the delay between diversion and application of water cannot be simulated in the current version of MODFLOW-OHWM. Other MODFLOW packages, such as the Lake Package (LAK; Merritt and Konikow, 2000), could be used to simulate the storage ponds but do not currently have linkages with the FMP and the SFR Packages.

To overcome this mismatch in timing, surface-water diversions from streams are instead sent to a dummy subregion, which essentially exports water the out of the model. This dummy subregion is set in row 1, column 1 of the model, with an artificial land use set to pasture, and a large "added demand" to ensure that all surface water is actually diverted. Surface water is then imported back to the PVIHM using non-routed deliveries. Importing the water ensures that the amount of water that the subregions receive matches the delivery data, even if simulated streamflow is not sufficient in summer months.

This limitation in the FMP, and assumptions used, should not affect simulation results because volumes of streamflow are typically several orders of magnitude larger than volumes of irrigation diversions. For example, based on the eWRIMS data, the largest total monthly diversion was 633 acre-ft in January 2010 (California State Water Resources Control Board, 2016). During January 2010, the average streamflow in the Petaluma River (USGS streamgage 11459150; U.S. Geological Survey, 2018) was 375 ft^3/s (for the days with available data from January 18 through January 31), which converts to 23,000 acre-feet per month, which is 36 times to the amount diverted.

Table D11. Descriptions of the Petaluma Valley Integrated Hydrologic Model subregions (see fig. D22 for locations), Petaluma valley watershed, Sonoma County, California.

[OGWB, outside of groundwater basin; OWS, outside of watershed]

Subregion number	Subregion name	Simulated area (acres)	Active for groundwater simulation	Description
1	Wilson Grove	6,900	Yes	Union of the upper Petaluma sub-watershed and the Wilson Grove Formation Highlands groundwater basin. Northwest of the City of Petaluma.
2	Upper Petaluma River	1,800	Yes	Union of the upper Petaluma sub-watershed and the Petaluma Valley groundwater basin. Northwest of the City of Petaluma.
3	Lynch Creek	6,000	Yes	Union of the Lynch Creek sub-watershed and the Petaluma Valley groundwater basin.
4	Lichau Creek	4,600	Yes	Union of the upper Petaluma sub-watershed and the Petaluma Valley groundwater basin. Northwest of the City of Petaluma. Lichau Creek flows through it.
5	Lynch Creek OGWB	4,900	No	Part of the Lynch Creek sub-watershed that lies outside the Petaluma Valley groundwater basin.
6	Upper San Antonio Creek	9,400	No	Upper San Antonio Creek sub-watershed.
7	Upper Petaluma River OGWB	1,100	No	Part of the upper Petaluma sub-watershed that lies outside the Wilson Grove Formation Highlands groundwater basin. West of the City of Petaluma.
8	City of Petaluma Wilson Grove	600	Yes	Union of the City of Petaluma and the Wilson Grove Formation Highlands groundwater basin.
9	City of Petaluma OGWB	1,500	No	Part of the City of Petaluma that lies outside the Petaluma Valley groundwater basin.
10	City of Petaluma	7,200	Yes	Union of City of Petaluma and the Petaluma Valley Groundwater Basin.
11	Adobe Creek	3,600	Yes	Union of the Adobe Creek sub-watershed and the Petaluma Valley groundwater basin.
12	Adobe Creek OGWB	5,400	No	Part of the Adobe Creek sub-watershed that lies outside the Petaluma Valley groundwater basin.
13	Lower San Antonio Creek	10,100	No	Lower San Antonio Creek sub-watershed.
14	Upper Petaluma River OGWB 2	2,300	No	Part of the upper Petaluma sub-watershed that lies outside the Petaluma Valley groundwater basin. South of the City of Petaluma.
15	Basalt Creek	5,100	No	Basalt Creek sub-watershed.
16	Lower Petaluma River OGWB	3,500	No	Part of the lower Petaluma sub-watershed that lies outside the Petaluma Valley groundwater basin.
17	Lower Petaluma River	5,800	Yes	Union of the upper Petaluma sub-watershed and the Petaluma Valley groundwater basin. Northwest of the North Bay Water District and southeast of the City of Petaluma.
18	North Bay Water District	11,000	Yes	North Bay Water District boundary.
19	Stage Gulch	3,400	Yes	Union of Stage Gulch sub-watershed and the Petaluma Valley groundwater basin. Outside of the North Bay Water District.
20	Stage Gulch OGWB	1,100	No	Part of the Stage Gulch sub-watershed that lies outside the Petaluma Valley groundwater basin.
21	Tolay Creek OWS	3,400	Yes	Part of the Petaluma groundwater basin that lies outside of the Petaluma valley watershed.

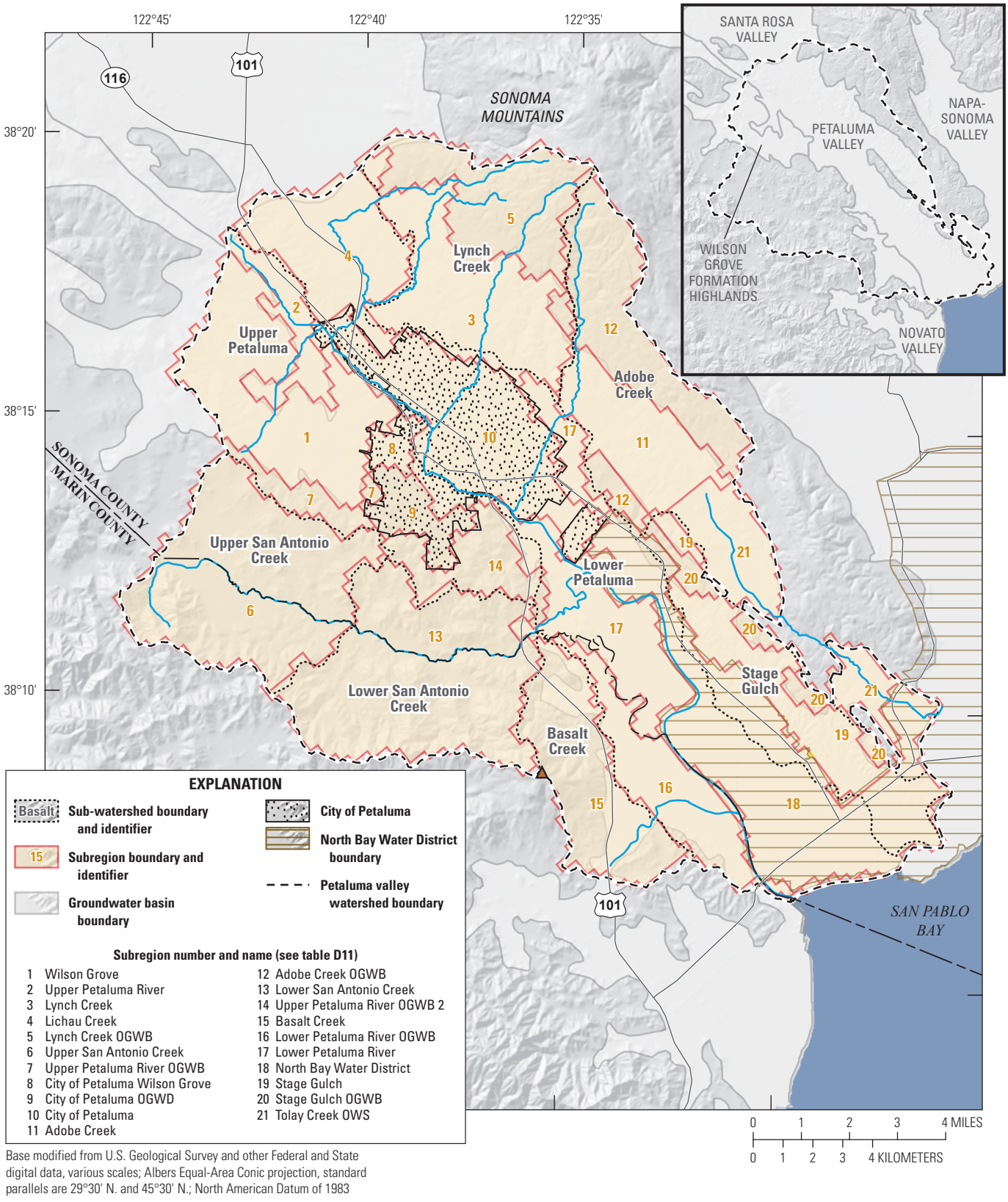

Base modified from U.S. Geological Survey and other Federal and State digital data, various scales; Albers Equal-Area Conic projection, standard parallels are 29°30' N. and 45°30' N.; North American Datum of 1983

Figure D22. Petaluma Valley Integrated Hydrologic Model subregions and boundaries of features used to define the subregions, Petaluma valley watershed, Sonoma County, California; OGWB, outside of groundwater basin; OWS, outside of watershed. Additional information about subregions is provided in table D11.

Water Supply and Demand Calculation

A strength of the FMP is that it allows for the estimation of agricultural groundwater pumpage, which is an unknown in the PVW, using known or estimable parameters. This section briefly describes how agricultural groundwater pumpage is calculated in MODFLOW-OWHM. The reader should refer to the MODFLOW-OWHM report (Hanson and others, 2014) for a complete description of the calculation of water supply and demand. The water demand computed by the FMP for each model cell that contains vegetation (agriculture, rural, native, urban landscaping) is a function of the crop type and the crop parameters that were discussed previously (table D3). The calculation of water demand from these variables involves many calculations and is beyond the scope of this report. Water is supplied to crops in the following order: precipitation, root uptake from shallow groundwater, surface-water irrigation (including recycled water), and groundwater pumpage. The groundwater pumpage term is calculated in order to match the water demand of the crop. If demand is met by the first three sources (precipitation, root uptake, and surface water), then groundwater pumpage is not used. If met by the first two sources (precipitation and root uptake), then surface-water supply is not used.

For non-irrigated crops and native vegetation, water demand is met by precipitation and root uptake. If all demand is unmet, crop ET is automatically lowered to meet available supply using the deficit irrigation option in the FMP. This reduction in crop ET simulates the stresses on the crop and the eventual wilting and dying off caused by the lack of water.

The following are a few examples to clarify how the demand and supply calculation is made:

- Example 1: An irrigated area has a calculated demand of 100 acre-ft. An area of 40 acre-ft is met by precipitation; 10 acre-ft is met by root uptake; and 20 acre-ft is met by surface water. The FMP calculates that 30 acre-ft of groundwater pumpage is required in order to meet irrigation demand.

- Example 2: An irrigated area has a calculated demand of 100 acre-ft. An area of 80 acre-ft is met by precipitation, and 10 acre-ft is met by root uptake. There is 20 acre-ft of surface water available, but only 10 acre-ft is used, and the remaining 10 acre-ft is not used. No groundwater pumpage is needed.

- Example 3: A non-irrigated area has a calculated demand of 100 acre-ft. An area of 40 acre-ft is met by precipitation, and 10 acre-ft is met by root uptake. Other water supply is not possible, so the FMP will reduce the demand to 50-acre-ft using the deficit irrigation method.

The FMP sums of all groundwater pumpage for each cell by subregion and then distributes that pumpage to the agricultural wells in the subregion (previously described in the "Rural and Agricultural Pumpage" section). Using the virtual well method to simulate agricultural wells results in underestimation of local drawdowns near actual irrigation wells. Conversely, this approach tends to overestimate local drawdowns in areas distant from actual irrigation wells. In order to somewhat compensate for this limitation, the FMP "PRORATE By Capacity" option was used, which divides agricultural well pumpage in a model subregion using a ratio of total well capacity rather than distributing the pumpage evenly to each well (which is the FMP "default" method). Using this method allows for greater pumpage in areas where land use or groundwater altitudes indicate that additional pumpage could be needed.

Land-use survey data (presented in chapter A; California Department of Water Resources, 2016) were used to identify which areas were irrigated and which areas were non-irrigated. The land-use datasets contain three possible irrigation attributes, which are "i" for irrigated, "n" for non-irrigated, and "*" for not defined (fig. D23). Based on guidance from the SCWA (Andrew N. Rich, Sonoma County Water Agency, written commun., April 2020), a PVIHM cell was considered to be irrigated if most of the cell area overlays land-use parcels with the "irrigated" attribute. Any virtual agricultural wells in non-irrigated cells had capacities set to 0 so that they would not pump. Land-use survey data from 2012 (California Department of Water Resources, 2016) also were used to identify areas that only use groundwater and areas that only receive surface water (fig. D24). These data were considered when determining the distribution of agricultural pumpage. The land-use survey data also were used to identify areas that use reclaimed (recycled) water, and these data were used in conjunction with data provided by the SCWA (fig. D11) to determine locations for simulating recycled water use. Virtual agricultural wells in cells that received only surface water or recycled water had well capacities set to zero so that they would not pump. The "NOCIRNOQ" flag was also utilized in the FMP, which inactivates pumping at virtual wells in a cell that has no irrigation requirement.

Simulation of Surface Water

Streamflow and exchange of groundwater and surface water is simulated in the PVIHM for the Petaluma River, San Antonio Creek, and other tributaries (including Lichau Creek, Willow Brook, Lynch Creek, Adobe Creek, and Black John Slough; fig. D1) using the SFR Package. Tolay Creek (fig. D1) overlies a part of the Petaluma Valley groundwater basin and was also included in the model even though Tolay Creek flows into the Sonoma Creek watershed (not shown). The SFR Package was used to track streamflow through the stream network by routing the flow downstream through a series of stream reaches. Flow in each reach can be increased or decreased based on the interaction of surface water and groundwater or can be increased from runoff of precipitation or irrigation water, as calculated by the FMP.

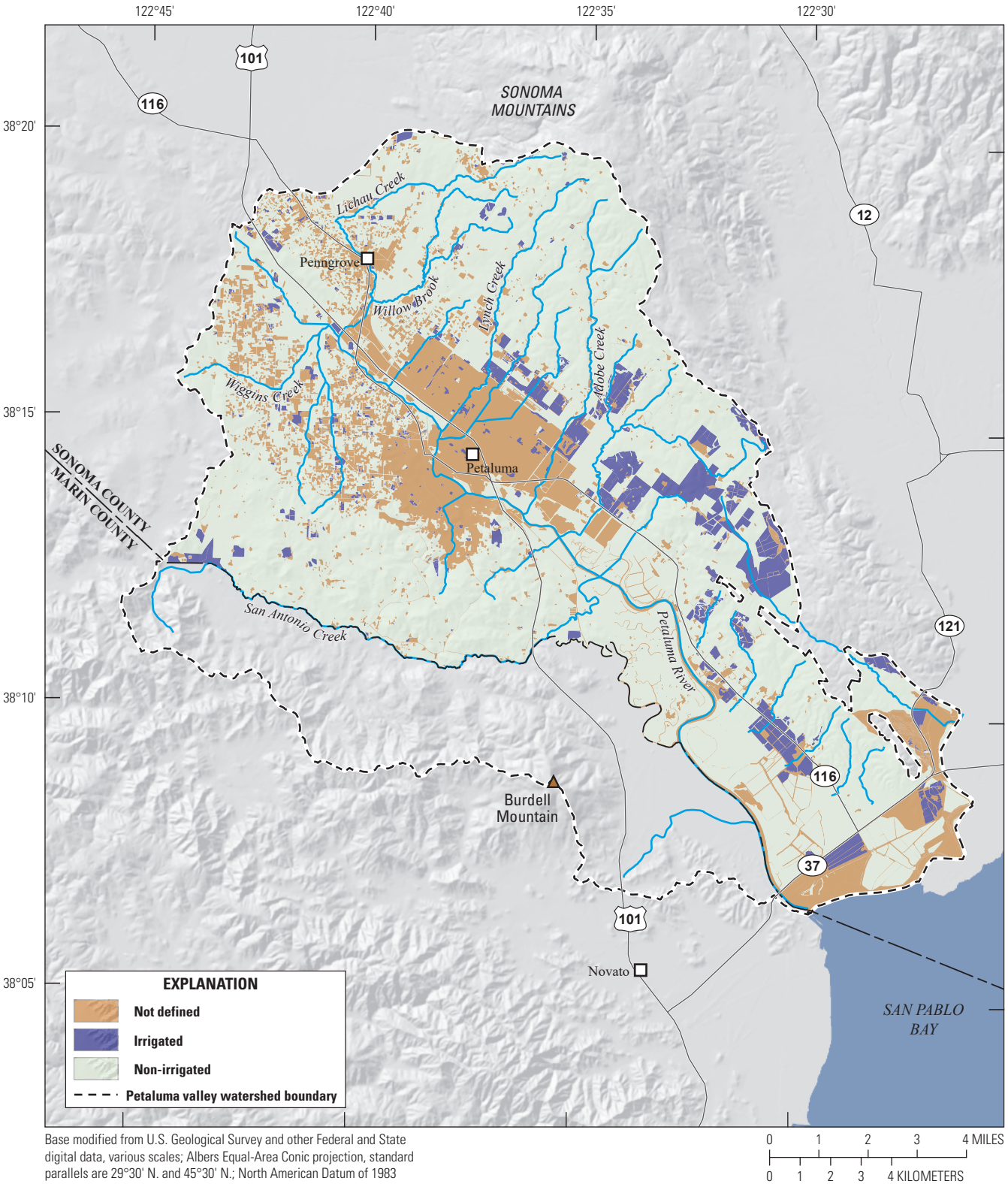

Figure D23. Areas irrigated and non-irrigated, based on 2012 land-use survey data (California Department of Water Resources, 2016), Petaluma valley watershed, Sonoma County, California.

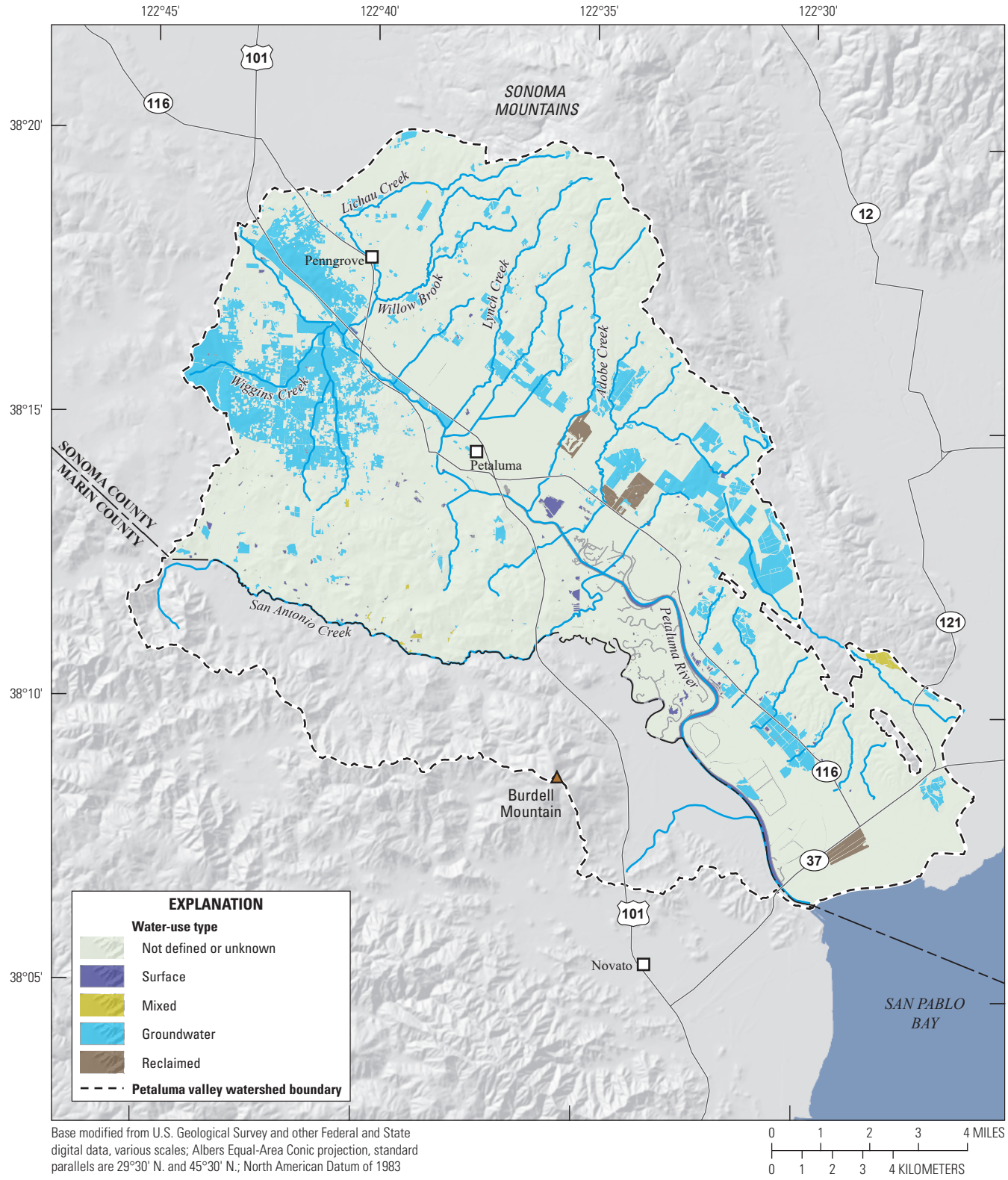

Figure D24. Areas using groundwater, surface water, and reclaimed water, based on land-use surveys completed in 2012 (California Department of Water Resources, 2016), Petaluma valley watershed, Sonoma County, California.

The stream network was represented by 746 stream reaches that were grouped into 111 stream segments (represented by same-colored cells in fig. D25). Each stream segment had similar hydrologic characteristics, such as streambed slope and streambed hydraulic conductivity. Streambed altitudes were estimated from ground-surface altitude data and were assumed to be between 0 and 16.4 ft below the surrounding land surface, which is generally consistent with limited field observations. Generally, higher flow streams were assumed to have deeper streambeds; however, the streambed altitude was modified during calibration to help match groundwater altitudes near streams. Streambed altitudes were modified where necessary to ensure a downstream gradient. The streambed thickness was assumed to be 3.28 ft. The stream width was assumed to range between 3.28 and 32.8 ft, increasing from upstream to downstream.

The streambed hydraulic conductivity was set to zero where the river was simulated using the GHB Package to avoid double counting of stream seepage in the tidally influenced part of the Petaluma River. This part of the river receives runoff and tributary flow and is included in the network so that a simulated amount of streamflow leaving the model into San Pablo Bay can be calculated. The upper segments that are outside of the active groundwater area also have their streambed hydraulic conductivity set to zero because groundwater–surface-water interaction is not possible. Streambed hydraulic-conductivity values for the remaining stream segments were assigned initial values of 0.5 to 100 ft/d; final values were estimated during model calibration.

Simulation of Streamflow

The upper sections of the stream network did not include any streamgages; therefore, streamflow was estimated using the FMP. Surface-water runoff was routed to the SFR stream network using the "fully routed" routine in the FMP. Under the fully routed routine, surface-water runoff generated within a subregion is routed to all stream reaches in that same subregion. Streamflow exited the PVIHM at the farthest downstream segment on the Petaluma River (segment 108, reach 14 in fig. D25) and on the farthest downstream segment of Tolay Creek (segment 98, reach 10 in fig. D25). Streamflow also exited the model from several small unnamed streams that flow from the hills east of Petaluma marsh because flow from these streams does not reach the Petaluma River (segment 86, reach 2; segment 93, reach 3; segment 59, reach 6; segment 90, reach 3; segment 89, reach 3; and segment 88, reach 2; fig. D25).

Diversions for agriculture are simulated in the streamflow routing package. The diversion locations are estimated from the eWRIMS database (California State Water Resources Control Board, 2016). These diversions were aggregated into 37 diversion locations in the model. As previously discussed, because of a mismatch in the timing of diversions and timing of water use, this diverted water is not directly sent to the FMP for use. Instead, the water is sent to a dummy subregion where it is exported out of the model. The water is then imported back into the model using a non-routed delivery.

Exchange of Surface Water and Groundwater

Stream depths in each stream reach were computed by the SFR Package using Manning's equation as applied to a wide rectangular channel. Stream stages (equal to stream depth plus streambed altitude) were then used to calculate the vertical hydraulic gradient between the stream reach and each model cell underlying the stream. If the stream stage was above the simulated groundwater altitude in the cell (positive hydraulic gradient), streamflow infiltrated into the groundwater system (losing reach). Conversely, if the stream stage was below the simulated groundwater altitude in the cell (negative hydraulic gradient), groundwater discharged to the stream (gaining reach).

The magnitude of streamflow gain or loss is determined by the magnitude of the hydraulic gradient and the streambed conductance. Streambed conductance is based on the length of the stream in the cell, streambed thickness, stream width, and streambed hydraulic conductivity. The stream length in each cell was calculated by overlaying the stream network with the model grid using Geographic Information Systems (GIS) software.

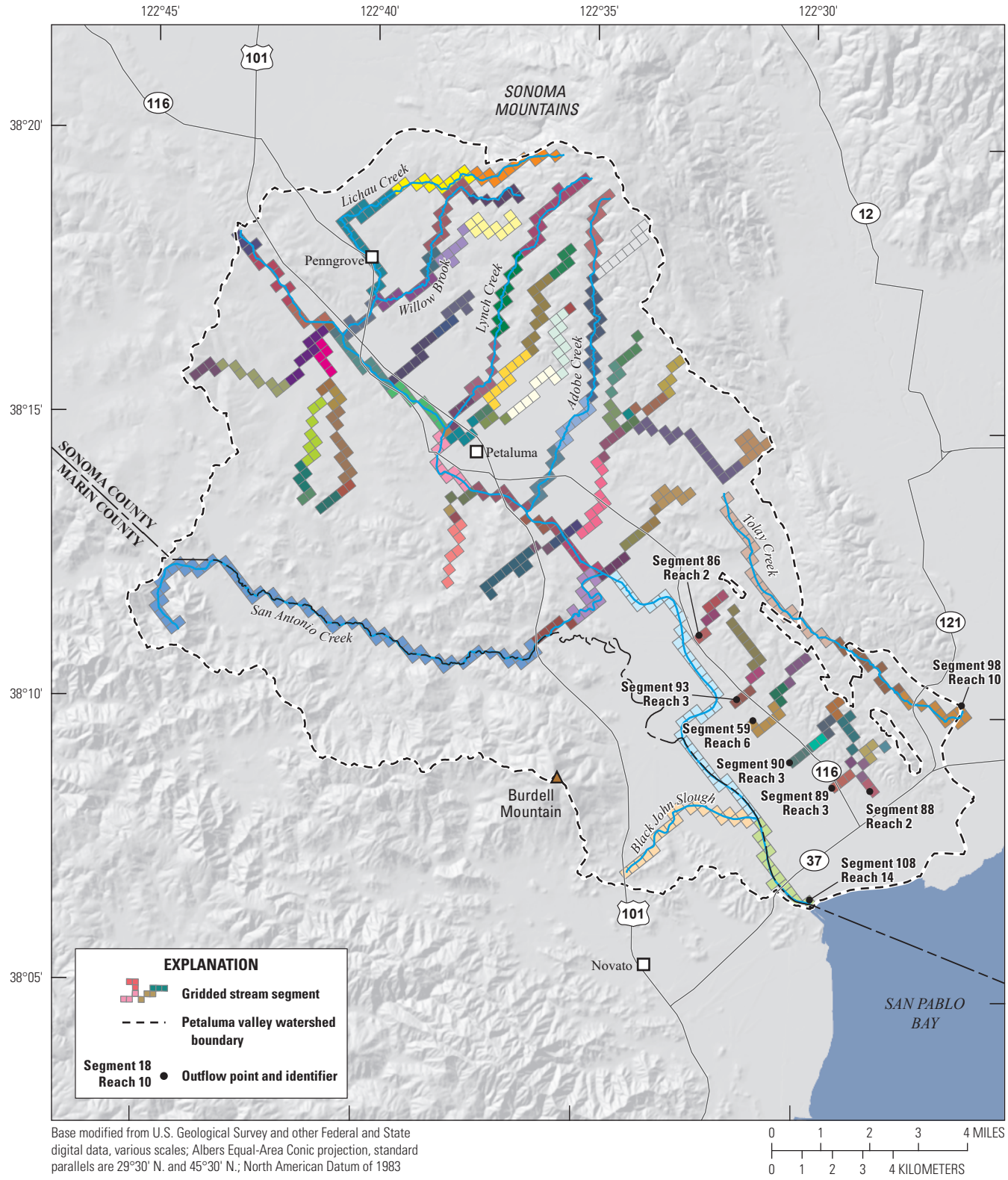

Figure D25. Petaluma Valley Integrated Hydrologic Model simulated streamflow network, Petaluma valley watershed, Sonoma County, California.

Model Calibration

The PVIHM was calibrated to a historical set of observed data (groundwater altitudes and streamflow) that were known and measurable at discrete locations with a degree of uncertainty that was based principally on measurement error. The distribution and values of model parameters (such as hydraulic conductivity) are unknown and can be constrained to a range of reasonable values based on these measurements and estimates from previous investigations. The goal of calibrating the PVIHM was to develop a hydrologically reasonable and representative model that provided a good match to observed historical values for simulations of past and potential future aquifer-system responses to natural and imposed hydrologic stresses.

Calibration Data

Observed groundwater-altitude and streamflow data were used to calibrate the PVIHM. Historical data from 41 groundwater monitoring wells (table D1; fig. D1), totaling 1,673 observations, were used in the final calibration process. For the calibration purposes, groundwater-altitude observations were treated as independent measurements; however, observations at the same well likely were correlated.

Simulated groundwater altitudes at observation points were interpolated from simulated groundwater altitudes for model layers intercepted by the well-screen interval using the Observation Package (OBS; Hill and others, 2000). For wells with missing screen-interval data, the top of the screen was assumed to be 30 ft bls, and the bottom of the screen was equal to the well depth. Generally, this assumption results in screen lengths that are larger than a normal well and that intersect many model layers. The assumption may also lead to the underestimation of vertical gradients and a misestimation of vertical hydraulic conductivity because groundwater pumpage is spread out over multiple model layers.

Data from three streamgages (U.S. Geological Survey, 2018) were also used in model calibration (table D2; fig. D1; Traum, 2022). These data included 242 monthly average streamflows during the simulated period as follows, which taken from HYD Package output (Hanson and Leake, 1999):

- Petaluma River at Petaluma, Calif., 11459000: 48 observations between October 1959 and September 1963; streamgage data were available back to October 1948, before the model simulation begins.
- Petaluma River at Copland Pumping Station at Petaluma, Calif.,11459150: 120 observations between November 1998 and September 2015; streamgage data are available after the model simulation-period ends.
- San Antonio Creek near Petaluma, Calif., 11459300: 74 observations between August 1975 and September 1981.

Observed streamflows were compared with monthly simulated flows for the corresponding segments and reaches defined in the SFR Package. Streamflow observations were treated as independent observations; however, some observations likely are correlated.

Calibration Process

The process of model calibration involves the comparison of model output with observed conditions and adjustment of model parameters within reasonable ranges until simulated conditions adequately replicate observed conditions. Prior to calibration, all model parameters were assigned initial values based on previous studies (Herbst, 1982; Woolfenden and Hevesi, 2014), expert knowledge, and preliminary hand-calibrated model runs to achieve a good initial fit with calibration objectives.

Calibration of the PVIHM was accomplished in a semi-automated manner by using the public-domain model-independent parameter-estimation program, BeoPEST (Doherty, 2016). BeoPEST is a version of PEST, a serial parameter-estimation program, that allows execution of parallel model runs on multiple computers, greatly shortening the runtime for the calibration process. BeoPEST also uses a parallelized search method to determine an optimal parameter upgrade vector for each PEST iteration.

Parameter estimation was completed using a regularization method that uses prior-information equations and applies a penalty if parameter values deviate from specified values (similar to Tikhonov regularization; Doherty, 2016). The use of regularization helps avoid the estimation of spurious parameter values and ensures that calibrated parameter values remain within a reasonable range. Regularization also adds stability to the calibration process because parameters that are insensitive to observations do not change values during each PEST iteration (Doherty and others, 2010). In other words, these parameters are now most sensitive to their regularized value. The regularization value used in the prior-information equation was initially set based on expert knowledge but was adjusted during calibration if the parameter value that actually calibrated the model began deviating from the regularized value. The weighting of the prior-information equations was adjusted during model calibration through expert judgement to ensure the influence on parameter values from the prior information was commensurate with the influence of the groundwater altitude and streamflow observations on the parameter values.

BeoPEST was used to identify the parameter set that minimizes the sum of the squared deviations between observed and simulated values (referred to as the "objective function") calculated as follows (Doherty, 2016):

$$\Phi = \sum_{m} ((h_m^{sim} - h_m^{obs}) * w_m)^2 \quad \text{(D1)}$$

where

Φ is the objective function PEST is trying to minimize,

h_m^{obs} is the m^{th} observed value of observation (note that this includes observations of groundwater altitude, streamflow, and prior information),

h_m^{sim} is the m^{th} simulated value corresponding to observation,

w_m is the weight of the m^{th} observation, and

m is the total number of observations.

A residual is defined here as the simulated value minus the observed value ($h_m^{sim} - h_m^{obs}$). A negative residual indicates that the model is underestimating the observed value, and a positive residual indicates that the model is overestimating the observed value.

Parameters Estimated

Several BeoPEST runs were required to achieve the final calibration of PVIHM. Part of the semi-automated approach to calibration involved manually adjusting the estimated parameters. Adjustable parameters were added or removed during the calibration process after reviewing the results of the previous PEST runs. Also, other manual changes were made to model parameters that were not considered in the PEST calibration parameter set.

For the final BeoPEST run, 268 model parameters were estimated for the PVIHM and included the following:

- HK along rows (in this case, perpendicular to the valley) by hydrogeologic unit and by layer (table D9)—35 parameters.
- Ratio of HK along columns to hydraulic conductivity along rows (HANI; in this case, along the axis of the valley) by hydrogeologic unit and by layer (table D9)—35 parameters.
- Vertical hydraulic conductivity (VK) (as VANI) by hydrogeologic unit and by layer (table D9)—35 parameters.
- Specific yield (by hydrogeologic for layer 1 and 2; table D9)—16 parameters.
- Specific storage (by hydrogeologic unit and by layer; table D9)—35 parameters.
- General-head boundary conductance—four estimable parameters (Wilson Grove Formation Highlands groundwater basin boundary, Santa Rosa Plain groundwater basin boundary, San Pablo Bay boundary, and tidally influenced part of the Petaluma River) and three fixed parameters.
- Streambed hydraulic conductivity (by segment)—80 estimable parameters, 31 fixed parameters.
- Irrigation-runoff coefficient (one global multiplier)—1 parameter.
- Irrigation efficiency (one global multiplier)—1 parameter.
- Crop coefficients (per crop, tied by month)—12 estimable parameters, 132 tied parameters.
- Precipitation runoff coefficient (per crop)—12 estimable parameters.

Observation Weights

In the PEST calibration process, observation weights were assigned for streamflows and groundwater altitudes. The first purpose of observation weights was to account for differences in measurement types. A typical streamflow observation magnitude in PVIHM is 392,000 cubic yards per day (300,000 cubic meters per day), and a typical groundwater altitude is 98.4 ft (30 meters; note that all MODFLOW-OHHM simulations for this study used metric units). Weights were assigned to streamflows so that the contribution to the objective function was roughly 10-times greater for groundwater altitudes than for streamflow. This higher relative weighting for groundwater altitudes reflects the primary parameter-estimation goal for the model to match groundwater altitudes. Higher relative weighting also accounts for unit discrepancies and the fact that streamflow observations tend to have greater measurement error (and thus should be weighted lower). The second purpose of observation weights was to make the weighted residuals for streamflow observations be roughly equal for high flow and low flow observations. Weighting high and low streamflows residuals equally ensures that parameters controlling high and low flows influence model calibration. High flows are driven primarily by precipitation runoff, whereas low flows typically are driven by irrigation runoff and groundwater and surface-water exchange. Also, in hydrologic model calibration, weights should be set at a level that is commensurate with the level of measurement noise, and higher streamflows tend to have higher measurement noise than lower streamflows. The third purpose of observation weights was to balance the total contribution to the calibration objective function from each well and ensure that PEST does not just match groundwater altitudes at wells with many observations. Wells with

many observations (such as wells 30 or 19) had individual observations given a smaller weight. Wells with fewer observations, such as all the CASGEM wells, had individual observation given a greater weight.

As discussed previously, weights on prior information were adjusted as needed during calibration to ensure the prior information neither dominated nor failed to influence the objective function. After all final weights were set, groundwater-altitude residuals represented 95 percent of the objective function, streamflow residuals represented 5 percent of the objective function, and prior information represented 0.06 percent of the objective function. These relative contributions to the objective function insured that the model was well calibrated to groundwater-altitude observations (which is the primary objective of the model). The prior-information component, although small, was sufficient to ensure that parameters did not deviate too far from the regularized value.

Calibration Results

Calibration of the PVIHM using the procedure described in this chapter resulted in a set of reasonable parameter estimates (tables D12–D15). Maps of final, calibrated aquifer parameters are provided for each layer of horizontal hydraulic conductivity values in the direction of flow parallel to the axis of the river valley (fig. D26), horizontal hydraulic conductivity values perpendicular to river valley axis (fig. D27), and vertical hydraulic conductivity values (fig. D28).

Generally, final calibrated parameter values were consistent with the geologic framework of the model and within the range of values expected on the basis of previous studies (Herbst, 1982). Estimated parameters were also similar to values estimated in studies in nearby basins, such as the Santa Rosa Plain (Woolfenden and Hevesi, 2014) and Sonoma Valley (Farrar and others, 2006), with similar geologic formations.

One area where calibrated parameters values differed from what was initially expected is in the Petaluma marsh area (chapter A, fig. A1), which includes the bay muds (layer 1) and Quaternary mixed (lower; layer 2). Initially, the HK values were expected to be low in this area because of fine-grained deposits. Low HK values in that area, however, resulted in simulated groundwater altitudes in areas upstream from the Petaluma marsh that were too high. Observed groundwater altitudes only increased from about 0 ft at San Pablo Bay to about 10 ft at the south end of the City of Petaluma, and these groundwater altitudes are consistent with a high HK value between these two areas. These higher HK values may be representative of ancestral Petaluma River channel deposits. In conjunction with higher HK values, layer 2 was also made thicker under the Petaluma marsh area (by lowering the altitude of the Franciscan Complex) compared to the initial geologic framework model to increase the overall conductance of the aquifer. The depth of the Franciscan Complex in this area is uncertain because of a lack of drillers' logs to provide control data.

In model layer 1, artificially high hydraulic-conductivity values (horizontal and vertical) were used for cells that underlay the SFR network (figs. D26–D28), which is generally considered a good modeling practice when using the SFR Package (R.G. Niswonger, U.S. Geological Survey, written commun., 2019). These high hydraulic-conductivity values helped stabilize the model and ensured that the groundwater and surface-water exchange was controlled by the streambed conductivity and not limited by the aquifer conductance.

Model Fit to Observations of Groundwater Altitudes

The histogram of residuals was examined to quantify the model fit between the simulated groundwater altitudes and measured groundwater altitudes for all 1,643 observations at the 41 calibration-target wells (table D1; fig. D29). Residuals generally indicated that the simulated groundwater altitudes matched the groundwater altitudes reasonably well. About 55 percent of simulated values were within 10 ft of the observed values, and about 78 percent of simulated values were within 20 ft. Residuals ranged from –39 to 88 ft, had a mean of 5.0 ft, an absolute mean of 12.7 ft, a standard error of 17.1 ft, and a skewness of 0.90. Ideally, the mean residual value would be 0; therefore, the mean value of 5.0 ft indicated that the model generally overestimated the observed groundwater altitudes.

Given the scale of the PVIHM, these statistics indicated that simulated groundwater altitudes reasonably matched the observed groundwater altitudes. Generally, a regional hydrologic model is considered to be more accurate when it matches higher observed groundwater altitudes in a hydrograph rather than matching lower observed groundwater altitudes because many seasonal low observations are affected by local pumping conditions that often cannot be captured by a regional-scale model. Also, the residual histogram does not reflect the weighting by the number of observations. If the number of observations is included in the residual analysis (see eq. D1), then the mean weighted residual equals 0.31 ft.

The relation between the simulated groundwater altitudes and observed groundwater altitudes is shown in figure D30. If the PVIHM simulated the observed groundwater altitudes perfectly, then all points would lie on the 1:1 line shown in figure D30. Points that plot above and below the 1:1 line indicate calibration-data points where the PVIHM overestimated or underestimated the observed groundwater altitudes, respectively.

Table D12. Petaluma Valley Integrated Hydrologic Model (Traum, 2022) calibrated groundwater parameter values, Petaluma valley watershed, Sonoma County, California.

[ft/d, foot per day; VANI, vertical anisotropy parameter; HANI, horizontal anisotropy parameter; 1/ft, one per foot]

Parameter name	Parameter type	Formation	Final estimated value	Units
		Layer 1		
hk_q1	Hydraulic conductivity	Alluvium	3.16E+01	ft/d
hk_mud1	Hydraulic conductivity	Bay mud	3.28E+01	ft/d
hk_mix1	Hydraulic conductivity	Quaternary mixed unit	7.18E+01	ft/d
hk_wil1	Hydraulic conductivity	Wilson Grove	2.60E+01	ft/d
hk_pet1	Hydraulic conductivity	Petaluma (upper)	7.24E+00	ft/d
hk_petl1	Hydraulic conductivity	Petaluma (lower)	1.15E+01	ft/d
hk_son1	Hydraulic conductivity	Sonoma Volcanics	1.64E+01	ft/d
hk_tol1	Hydraulic conductivity	Tolay Volcanics	2.32E+00	ft/d
hk_bed1	Hydraulic conductivity	Bedrock	6.56E–01	ft/d
vk_q1	VANI	Alluvium	4.75E+01	Unitless
vk_mud1	VANI	Bay mud	3.55E+00	Unitless
vk_mix1	VANI	Quaternary mixed unit	1.40E+01	Unitless
vk_wil1	VANI	Wilson Grove	1.00E+00	Unitless
vk_pet1	VANI	Petaluma (upper)	1.71E+00	Unitless
vk_petl1	VANI	Petaluma (lower)	1.27E+00	Unitless
vk_son1	VANI	Sonoma Volcanics	1.10E+00	Unitless
vk_tol1	VANI	Tolay Volcanics	1.92E+00	Unitless
vk_bed1	VANI	Bedrock	1.00E+00	Unitless
hani_q1	HANI	Alluvium	1.10E+00	Unitless
hani_mud1	HANI	Bay mud	4.40E+00	Unitless
hani_mix1	HANI	Quaternary mixed unit	3.12E+00	Unitless
hani_wil1	HANI	Wilson Grove	1.00E+00	Unitless
hani_pet1	HANI	Petaluma (upper)	2.56E+00	Unitless
hani_petl1	HANI	Petaluma (lower)	4.21E+00	Unitless
hani_son1	HANI	Sonoma Volcanics	1.75E+00	Unitless
hani_tol1	HANI	Tolay Volcanics	9.39E+00	Unitless
hani_bed1	HANI	Bedrock	1.00E+00	Unitless
sy_q1	Specific yield	Alluvium	2.52E–01	Unitless
sy_mud1	Specific yield	Bay mud	1.92E–01	Unitless
sy_mix1	Specific yield	Quaternary mixed unit	1.52E–01	Unitless
sy_wil1	Specific yield	Wilson Grove	1.09E–01	Unitless
sy_pet1	Specific yield	Petaluma (upper)	1.50E–01	Unitless
sy_petl1	Specific yield	Petaluma (lower)	2.29E–01	Unitless
sy_son1	Specific yield	Sonoma Volcanics	1.50E–01	Unitless
sy_tol1	Specific yield	Tolay Volcanics	1.50E–01	Unitless
sy_bed1	Specific yield	Bedrock	2.00E–02	Unitless
ss_q1	Specific storage	Alluvium	3.05E–07	1/ft
ss_mud1	Specific storage	Bay mud	5.77E–07	1/ft
ss_mix1	Specific storage	Quaternary mixed unit	2.11E–06	1/ft
ss_wil1	Specific storage	Wilson Grove	1.85E–06	1/ft

Table D12. Petaluma Valley Integrated Hydrologic Model (Traum, 2022) calibrated groundwater parameter values, Petaluma valley watershed, Sonoma County, California.—Continued

[ft/d, foot per day; VANI, vertical anisotropy parameter; HANI, horizontal anisotropy parameter; 1/ft, one per foot]

Parameter name	Parameter type	Formation	Final estimated value	Units
		Layer 1—Continued		
ss_pet1	Specific storage	Petaluma (upper)	6.44E–06	1/ft
ss_petl1	Specific storage	Petaluma (lower)	1.47E–06	1/ft
ss_son1	Specific storage	Sonoma Volcanics	4.96E–07	1/ft
ss_tol1	Specific storage	Tolay Volcanics	3.93E–07	1/ft
ss_bed1	Specific storage	Bedrock	3.46E–07	1/ft
		Layer 2		
hk_mud2	Hydraulic conductivity	Quaternary mixed (lower)	4.49E+01	ft/d
hk_mix2	Hydraulic conductivity	Quaternary mixed (upper)	4.59E+00	ft/d
hk_wil2	Hydraulic conductivity	Wilson Grove	4.59E+00	ft/d
hk_pet2	Hydraulic conductivity	Petaluma (upper)	3.53E–01	ft/d
hk_petl2	Hydraulic conductivity	Petaluma (lower)	2.25E–01	ft/d
hk_son2	Hydraulic conductivity	Sonoma Volcanics	4.28E–01	ft/d
hk_tol2	Hydraulic conductivity	Tolay Volcanics	1.29E–01	ft/d
vk_mud2	VANI	Quaternary mixed (lower)	3.77E+00	Unitless
vk_mix2	VANI	Quaternary mixed (upper)	4.20E+00	Unitless
vk_wil2	VANI	Wilson Grove	3.41E+00	Unitless
vk_pet2	VANI	Petaluma (upper)	3.00E+00	Unitless
vk_petl2	VANI	Petaluma (lower)	1.09E+00	Unitless
vk_son2	VANI	Sonoma Volcanics	1.00E+00	Unitless
vk_tol2	VANI	Tolay Volcanics	1.12E+00	Unitless
hani_mud2	HANI	Quaternary mixed (lower)	1.00E+01	Unitless
hani_mix2	HANI	Quaternary mixed (upper)	1.00E+01	Unitless
hani_wil2	HANI	Wilson Grove	1.49E+00	Unitless
hani_pet2	HANI	Petaluma (upper)	3.79E+00	Unitless
hani_petl2	HANI	Petaluma (lower)	7.69E+00	Unitless
hani_son2	HANI	Sonoma Volcanics	4.42E+00	Unitless
hani_tol2	HANI	Tolay Volcanics	2.40E+00	Unitless
sy_mud2	Specific yield	Quaternary mixed (lower)	2.00E–01	Unitless
sy_mix2	Specific yield	Quaternary mixed (upper)	1.99E–01	Unitless
sy_wil2	Specific yield	Wilson Grove	5.00E–02	Unitless
sy_pet2	Specific yield	Petaluma (upper)	2.36E–01	Unitless
sy_petl2	Specific yield	Petaluma (lower)	1.76E–01	Unitless
sy_son2	Specific yield	Sonoma Volcanics	1.50E–01	Unitless
sy_tol2	Specific yield	Tolay Volcanics	1.50E–01	Unitless
ss_mud2	Specific storage	Quaternary mixed (lower)	2.08E–06	1/ft
ss_mix2	Specific storage	Quaternary mixed (upper)	4.01E–07	1/ft
ss_wil2	Specific storage	Wilson Grove	6.41E–07	1/ft
ss_pet2	Specific storage	Petaluma (upper)	3.95E–07	1/ft
ss_petl2	Specific storage	Petaluma (lower)	3.05E–07	1/ft
ss_son2	Specific storage	Sonoma Volcanics	1.80E–05	1/ft

Table D12. Petaluma Valley Integrated Hydrologic Model (Traum, 2022) calibrated groundwater parameter values, Petaluma valley watershed, Sonoma County, California.—Continued

[ft/d, foot per day; VANI, vertical anisotropy parameter; HANI, horizontal anisotropy parameter; 1/ft, one per foot]

Parameter name	Parameter type	Formation	Final estimated value	Units
		Layer 2—Continued		
ss_tol2	Specific storage	Tolay Volcanics	3.05E–07	1/ft
		Layer 3		
hk_mix3	Hydraulic conductivity	Quaternary mixed unit	6.56E–01	ft/d
hk_wil3	Hydraulic conductivity	Wilson Grove	1.64E+01	ft/d
hk_pet3	Hydraulic conductivity	Petaluma (upper)	8.20E–02	ft/d
hk_petl3	Hydraulic conductivity	Petaluma (lower)	1.97E–01	ft/d
hk_son3	Hydraulic conductivity	Sonoma Volcanics	1.26E+00	ft/d
hk_tol3	Hydraulic conductivity	Tolay Volcanics	8.20E–02	ft/d
hk_bed3	Hydraulic conductivity	Bedrock	1.31E–01	ft/d
vk_mix3	VANI	Quaternary mixed unit	2.00E+00	Unitless
vk_wil3	VANI	Wilson Grove	1.95E+00	Unitless
vk_pet3	VANI	Petaluma (upper)	1.03E+00	Unitless
vk_petl3	VANI	Petaluma (lower)	1.00E+00	Unitless
vk_son3	VANI	Sonoma Volcanics	1.07E+00	Unitless
vk_tol3	VANI	Tolay Volcanics	1.73E+00	Unitless
vk_bed3	VANI	Bedrock	3.48E+00	Unitless
hani_mix3	HANI	Quaternary mixed unit	1.01E+00	Unitless
hani_wil3	HANI	Wilson Grove	1.00E+01	Unitless
hani_pet3	HANI	Petaluma (upper)	1.45E+00	Unitless
hani_petl3	HANI	Petaluma (lower)	5.87E+00	Unitless
hani_son3	HANI	Sonoma Volcanics	2.32E+00	Unitless
hani_tol3	HANI	Tolay Volcanics	1.00E+00	Unitless
hani_bed3	HANI	Bedrock	1.04E+00	Unitless
ss_mix3	Specific storage	Quaternary mixed unit	1.39E–06	1/ft
ss_wil3	Specific storage	Wilson Grove	3.76E–07	1/ft
ss_pet3	Specific storage	Petaluma (upper)	5.93E–07	1/ft
ss_petl3	Specific storage	Petaluma (lower)	5.55E–06	1/ft
ss_son3	Specific storage	Sonoma Volcanics	2.53E–05	1/ft
ss_tol3	Specific storage	Tolay Volcanics	2.24E–06	1/ft
ss_bed3	Specific storage	Bedrock	1.52E–06	1/ft
		Layer 4		
hk_mix4	Hydraulic conductivity	Quaternary mixed unit	6.56E–01	ft/d
hk_wil4	Hydraulic conductivity	Wilson Grove	7.71E–01	ft/d
hk_pet4	Hydraulic conductivity	Petaluma (upper)	8.20E–02	ft/d
hk_petl4	Hydraulic conductivity	Petaluma (lower)	9.95E–01	ft/d
hk_son4	Hydraulic conductivity	Sonoma Volcanics	2.31E–01	ft/d
hk_tol4	Hydraulic conductivity	Tolay Volcanics	1.30E–01	ft/d
vk_mix4	VANI	Quaternary mixed unit	1.00E+00	Unitless
vk_wil4	VANI	Wilson Grove	2.00E+00	Unitless
vk_pet4	VANI	Petaluma (upper)	2.00E+00	Unitless

Table D12. Petaluma Valley Integrated Hydrologic Model (Traum, 2022) calibrated groundwater parameter values, Petaluma valley watershed, Sonoma County, California.—Continued

[ft/d, foot per day; VANI, vertical anisotropy parameter; HANI, horizontal anisotropy parameter; 1/ft, one per foot]

Parameter name	Parameter type	Formation	Final estimated value	Units
		Layer 4—Continued		
vk_petl4	VANI	Petaluma (lower)	1.02E+00	Unitless
vk_son4	VANI	Sonoma Volcanics	1.15E+00	Unitless
vk_tol4	VANI	Tolay Volcanics	2.00E+00	Unitless
hani_mix4	HANI	Quaternary mixed unit	1.00E+00	Unitless
hani_wil4	HANI	Wilson Grove	1.05E+00	Unitless
hani_pet4	HANI	Petaluma (upper)	1.31E+00	Unitless
hani_petl4	HANI	Petaluma (lower)	1.07E+00	Unitless
hani_son4	HANI	Sonoma Volcanics	1.17E+00	Unitless
hani_tol4	HANI	Tolay Volcanics	1.23E+00	Unitless
ss_mix4	Specific storage	Quaternary mixed unit	1.00E–06	1/ft
ss_wil4	Specific storage	Wilson Grove	8.69E–07	1/ft
ss_pet4	Specific storage	Petaluma (upper)	5.94E–07	1/ft
ss_petl4	Specific storage	Petaluma (lower)	1.05E–05	1/ft
ss_son4	Specific storage	Sonoma Volcanics	1.03E–06	1/ft
ss_tol4	Specific storage	Tolay Volcanics	1.12E–05	1/ft
		Layer 5		
hk_mix5	Hydraulic conductivity	Quaternary mixed unit	2.06E+00	ft/d
hk_wil5	Hydraulic conductivity	Wilson Grove	6.56E–01	ft/d
hk_pet5	Hydraulic conductivity	Petaluma (upper)	9.42E–01	ft/d
hk_petl5	Hydraulic conductivity	Petaluma (lower)	5.73E–01	ft/d
hk_son5	Hydraulic conductivity	Sonoma Volcanics	1.41E+00	ft/d
hk_tol5	Hydraulic conductivity	Tolay Volcanics	2.29E–01	ft/d
vk_mix5	VANI	Quaternary mixed unit	1.09E+00	Unitless
vk_wil5	VANI	Wilson Grove	1.00E+00	Unitless
vk_pet5	VANI	Petaluma (upper)	2.00E+00	Unitless
vk_petl5	VANI	Petaluma (lower)	1.00E+00	Unitless
vk_son5	VANI	Sonoma Volcanics	1.96E+00	Unitless
vk_tol5	VANI	Tolay Volcanics	1.02E+00	Unitless
hani_mix5	HANI	Quaternary mixed unit	1.31E+00	Unitless
hani_wil5	HANI	Wilson Grove	5.04E+00	Unitless
hani_pet5	HANI	Petaluma (upper)	1.00E+00	Unitless
hani_petl5	HANI	Petaluma (lower)	9.99E+00	Unitless
hani_son5	HANI	Sonoma Volcanics	1.00E+01	Unitless
hani_tol5	HANI	Tolay Volcanics	1.12E+00	Unitless
ss_mix5	Specific storage	Quaternary mixed unit	3.71E–07	1/ft
ss_wil5	Specific storage	Wilson Grove	5.07E–07	1/ft
ss_pet5	Specific storage	Petaluma (upper)	5.77E–06	1/ft
ss_petl5	Specific storage	Petaluma (lower)	2.05E–05	1/ft
ss_son5	Specific storage	Sonoma Volcanics	5.17E–07	1/ft
ss_tol5	Specific storage	Tolay Volcanics	2.18E–06	1/ft

Table D13. Petaluma Valley Integrated Hydrologic Model (Traum, 2022) calibrated general-head boundary (GHB) parameter values, Petaluma valley watershed, Sonoma County, California.

[ghb, general head boundary; ft²/d, square foot per day]

Parameter name	GHB conductance area	Final estimated conductance (ft²/d)
ghb_river	Tidally influenced part of the Petaluma River simulated as GHB	5.74E+05
ghb_bay	San Pablo Bay	5.44E+06
ghb_sonoma[1]	Sonoma Valley groundwater basin	0.00E+00
ghb_santa	Santa Rosa Plain	4.25E+03
ghb_wilson	Wilson Grove Formation Highlands	1.84E+05
ghb_marsh[2]	Petaluma Marsh	0.00E+00
ghb_low[2]	Cells with low altitudes	0.00E+00

[1]Parameter value fixed at zero is assumed to be no flow.

[2]Parameter value fixed at zero is legacy parameter not used in model.

Table D14. Petaluma Valley Integrated Hydrologic Model (Traum, 2022) calibrated streamflow-routing (SFR) parameter values, Petaluma valley watershed, Sonoma County, California.

[ID, identification; SFR, streamflow routing; ft/d, foot per day]

Parameter name	Segment name	SFR segment ID	Final estimated value (ft/d)
[1]sfr_ado1	Adobe Creek 1	8	0.00E+00
[1]sfr_blah	Black John Slough	96	0.00E+00
[1]sfr_che1	Cherry Creek 1	9	0.00E+00
[1]sfr_dav1	Davis Creek 1	11	0.00E+00
[1]sfr_ead1	E. Adobe Creek 1	3	0.00E+00
[1]sfr_ewa1	E. Washington Creek 1	19	0.00E+00
[1]sfr_ell1	Ellis Creek 1	13	0.00E+00
[1]sfr_ell6	Ellis Creek 6	105	0.00E+00
[1]sfr_gre1	Gregory Creek 1	10	0.00E+00
[1]sfr_lic1	Lichau Creek 1	4	0.00E+00
[1]sfr_lyn1	Lynch Creek 1	2	0.00E+00
[1]sfr_mar1	Marin Creek 1	22	0.00E+00
[1]sfr_mda1	Marsh drainage A 1	39	0.00E+00
[1]sfr_mdc1	Marsh drainage C 1	18	0.00E+00
[1]sfr_mdf1	Marsh drainage F 1	25	0.00E+00
[2]sfr_pt10	Petaluma River 10	110	0.00E+00
[2]sfr_pt11	Petaluma River 11	108	0.00E+00
[2]sfr_pt8	Petaluma River 8	111	0.00E+00
[2]sfr_pt9	Petaluma River 9	109	0.00E+00
[1]sfr_san1	San Antonio Creek 1	5	0.00E+00
[1]sfr_san3	San Antonio Creek 3	104	0.00E+00
[1]sfr_sr1	SR 14 Creek 1	14	0.00E+00
[1]sfr_sr3	SR 14 Creek 3	100	0.00E+00
[1]sfr_tho1	Thompson Creek 1	37	0.00E+00
[1]sfr_tho4	Thompson Creek 4	91	0.00E+00
[1]sfr_wac1	W. Adobe Creek 1	1	0.00E+00
[1]sfr_was1	Washington Creek 1	7	0.00E+00
[1]sfr_whe2	Wheat Creek 2	42	0.00E+00
[1]sfr_whe4	Wheat Creek 4	107	0.00E+00
[1]sfr_wib1	Willow Brook 1	6	0.00E+00
[1]sfr_wil1	Wilson Creek 1	23	0.00E+00
sfr_ado4	Adobe Creek 4	85	5.75E+00
sfr_cor3	Corona Creek 3	73	2.48E+00
sfr_ewa4	E. Washington Creek 4	74	1.57E+00
sfr_ell5	Ellis Creek 5	75	6.56E+00
sfr_lib3	Liberty Creek 3	84	1.96E+00
sfr_lic4	Lichau Creek 4	79	2.53E+00
sfr_lyn4	Lynch Creek 4	77	1.54E+00
sfr_mar4	Marine Creek 4	82	7.18E–01
sfr_mar5	Marine Creek 5	87	1.66E+00

Table D14. Petaluma Valley Integrated Hydrologic Model (Traum, 2022) calibrated streamflow-routing (SFR) parameter values, Petaluma valley watershed, Sonoma County, California.—Continued

[ID, identification; SFR, streamflow routing; ft/d, foot per day]

Parameter name	Segment name	SFR segment ID	Final estimated value (ft/d)
sfr_mda4	Marsh drainage A 4	88	2.35E+00
sfr_mdb3	Marsh drainage B 3	89	2.75E+00
sfr_mdc4	Marsh drainage C 4	90	7.04E–01
sfr_mdd3	Marsh drainage D 3	59	1.86E+00
sfr_mde3	Marsh drainage E 3	93	2.92E+00
sfr_mdf4	Marsh drainage F 4	86	1.19E+00
sfr_pt1	Petaluma River 1	95	4.81E+00
sfr_pt2	Petaluma River 2	76	7.50E–01
sfr_pt3	Petaluma River 3	97	8.51E–01
sfr_pt4	Petaluma River 4	101	1.82E+00
sfr_pt5	Petaluma River 5	102	1.64E+00
sfr_pt6	Petaluma River 6	103	1.15E+00
sfr_pt7	Petaluma River 7	106	1.14E+00
sfr_sr2	SR 14 Creek 2	83	1.45E+00
sfr_tho3	Thompson Creek 3	70	1.95E+00
sfr_tol3	Tolay Creek 3	98	1.05E+00
sfr_was4	Washington Creek 4	78	1.75E+00
sfr_was5	Washington Creek 5	92	9.05E–01
sfr_whe3	Wheat Creek 3	71	8.87E–01
sfr_wig4	Wiggens Creek 4	94	1.87E+00
sfr_wig3	Wiggins Creek 3	81	3.11E+00
sfr_wil4	Wilson Creek 4	80	1.06E+00
sfr_san2	San Antonio Creek 2	99	2.66E+00
sfr_ado3	Adobe Creek 3	47	5.48E+01
sfr_che3	Cherry Creek 3	61	4.07E+01
sfr_cor2	Corona Creek 2	66	2.11E+01
sfr_dav3	Davis Creek 3	56	3.52E+01
sfr_ewa3	E. Washington Creek 3	58	2.76E+01
sfr_ell3	Ellis Creek 3	52	1.28E+01
sfr_ell4	Ellis Creek 4	65	4.29E+01
sfr_gre3	Gregory Creek 3	53	5.41E+01
sfr_lib2	Liberty Creek 2	55	2.49E+01
sfr_lic3	Lichau Creek 3	50	2.59E+01
sfr_lyn3	Lynch Creek 3	60	3.42E+01
sfr_mar3	Marine Creek 3	63	5.48E+01
sfr_mda3	Marsh drainage A 3	44	5.47E+01
sfr_mdb2	Marsh drainage B 2	49	3.65E+01
sfr_mdc3	Marsh drainage C 3	45	4.24E+01
sfr_mdd2	Marsh drainage D 2	51	3.82E+01
sfr_mde2	Marsh drainage E 2	72	5.47E+01
sfr_mdf3	Marsh drainage F 3	68	5.48E+01
sfr_tol2	Tolay Creek 2	57	2.42E+01
sfr_was3	Washington Creek 3	46	4.21E+01
sfr_wig2	Wiggins Creek 2	67	1.18E+01
sfr_wib3	Willow Brook 3	54	1.83E+01
sfr_wib4	Willow Brook 4	69	4.39E+01
sfr_wil3	Wilson Creek 3	64	1.56E+01
sfr_tho2	Thompson Creek 2	62	2.13E+01
sfr_ado2	Adobe Creek 2	28	1.65E+02
sfr_che2	Cherry Creek 2	34	2.51E+02
sfr_cor1	Corona Creek 1	48	2.15E+02
sfr_dav2	Davis Creek 2	29	2.14E+02
sfr_ewa2	E. Washington Creek 2	20	2.00E+02
sfr_ell2	Ellis Creek 2	36	1.69E+02
sfr_gre2	Gregory Creek 2	24	1.91E+02
sfr_lib1	Liberty Creek 1	30	3.40E+01
sfr_lic2	Lichau Creek 2	12	4.47E+02
sfr_lyn2	Lynch Creek 2	16	4.07E+02
sfr_mar2	Marine Creek 2	43	2.49E+02
sfr_mda2	Marsh drainage A 2	40	3.24E+02
sfr_mdb1	Marsh drainage B 1	32	4.01E+02
sfr_mdc2	Marsh drainage C 2	41	2.18E+02
sfr_mdd1	Marsh drainage D 1	26	1.75E+02
sfr_mde1	Marsh drainage E 1	31	1.64E+02
sfr_mdf2	Marsh drainage F 2	35	4.92E+02
sfr_tol1	Tolay Creek 1	38	2.21E+02
sfr_was2	Washington Creek 2	15	4.92E+02
sfr_whe1	Wheat Creek 1	27	3.10E+02
sfr_wig1	Wiggins Creek 1	21	3.00E+02
sfr_wib2	Willow Brook 2	17	4.92E+02
sfr_wil2	Wilson Creek 2	33	1.70E+02

[1]These segments are outside of the active groundwater area so no groundwater and surface-water interaction is possible—parameter value fixed at 0.

[2]These segments are the tidally influenced part of the Petaluma River—parameter value fixed at 0 because the general head boundary accounts for the groundwater and surface-water interaction.

Observation wells were divided among six groups to evaluate the fit between the simulated and observed groundwater altitudes, with each group having similar groundwater-altitude magnitudes and trends. The six groups

Table D15. Petaluma Valley Integrated Hydrologic Model (Traum, 2022) calibrated FMP parameter values, Petaluma valley watershed, Sonoma County, California.

[N/A, not applicable]

Parameter name	Parameter type	Month	Crop	Final estimated value (unitless)
irrig_run	Irrigation runoff multiplier	N/A	N/A	3.82E–01
ie	Irrigation efficiency multiplier	N/A	N/A	8.33E–01
kc-1-1	Crop coefficient	January	Citrus	4.93E–01
kc-1-2	Crop coefficient	January	Orchard	1.08E–01
kc-1-3	Crop coefficient	January	Field	1.57E–01
kc-1-4	Crop coefficient	January	Grain	5.97E–01
kc-1-5	Crop coefficient	January	Native	1.10E+00
kc-1-6	Crop coefficient	January	Pasture	1.10E+00
kc-1-7	Crop coefficient	January	Riparian	1.10E+00
kc-1-8	Crop coefficient	January	SemiAg	3.75E–01
kc-1-9	Crop coefficient	January	Truck	1.55E–01
kc-1-10	Crop coefficient	January	Urban	9.85E–01
kc-1-11	Crop coefficient	January	Vineyards	9.72E–02
kc-1-12	Crop coefficient	January	Rural	8.00E–01
[1]kc-2-1	Crop coefficient	February	Citrus	5.40E–01
[1]kc-2-2	Crop coefficient	February	Orchard	1.08E–01
[1]kc-2-3	Crop coefficient	February	Field	1.57E–01
[1]kc-2-4	Crop coefficient	February	Grain	1.12E+00
[1]kc-2-5	Crop coefficient	February	Native	1.10E+00
[1]kc-2-6	Crop coefficient	February	Pasture	1.10E+00
[1]kc-2-7	Crop coefficient	February	Riparian	1.10E+00
[1]kc-2-8	Crop coefficient	February	SemiAg	4.90E–01
[1]kc-2-9	Crop coefficient	February	Truck	2.96E–01
[1]kc-2-10	Crop coefficient	February	Urban	9.85E–01
[1]kc-2-11	Crop coefficient	February	Vineyards	1.69E–01
[1]kc-2-12	Crop coefficient	February	Rural	8.00E–01
[1]kc-3-1	Crop coefficient	March	Citrus	6.16E–01
[1]kc-3-2	Crop coefficient	March	Orchard	1.08E–01
[1]kc-3-3	Crop coefficient	March	Field	1.04E–01
[1]kc-3-4	Crop coefficient	March	Grain	1.27E+00
[1]kc-3-5	Crop coefficient	March	Native	1.10E+00
[1]kc-3-6	Crop coefficient	March	Pasture	1.10E+00
[1]kc-3-7	Crop coefficient	March	Riparian	1.10E+00
[1]kc-3-8	Crop coefficient	March	SemiAg	5.29E–01
[1]kc-3-9	Crop coefficient	March	Truck	4.23E–01
[1]kc-3-10	Crop coefficient	March	Urban	9.85E–01
[1]kc-3-11	Crop coefficient	March	Vineyards	4.77E–01
[1]kc-3-12	Crop coefficient	March	Rural	8.00E–01
[1]kc-4-1	Crop coefficient	April	Citrus	6.16E–01
[1]kc-4-2	Crop coefficient	April	Orchard	1.08E–01
[1]kc-4-3	Crop coefficient	April	Field	3.50E–01

Table D15. Petaluma Valley Integrated Hydrologic Model (Traum, 2022) calibrated FMP parameter values, Petaluma valley watershed, Sonoma County, California.—Continued

[N/A, not applicable]

Parameter name	Parameter type	Month	Crop	Final estimated value (unitless)
[1]kc-4-4	Crop coefficient	April	Grain	1.27E+00
[1]kc-4-5	Crop coefficient	April	Native	1.10E+00
[1]kc-4-6	Crop coefficient	April	Pasture	1.10E+00
[1]kc-4-7	Crop coefficient	April	Riparian	1.10E+00
[1]kc-4-8	Crop coefficient	April	SemiAg	5.96E–01
[1]kc-4-9	Crop coefficient	April	Truck	7.19E–01
[1]kc-4-10	Crop coefficient	April	Urban	9.85E–01
[1]kc-4-11	Crop coefficient	April	Vineyards	3.77E–01
[1]kc-4-12	Crop coefficient	April	Rural	8.00E–01
[1]kc-5-1	Crop coefficient	May	Citrus	6.16E–01
[1]kc-5-2	Crop coefficient	May	Orchard	2.95E–01
[1]kc-5-3	Crop coefficient	May	Field	7.56E–01
[1]kc-5-4	Crop coefficient	May	Grain	9.44E–01
[1]kc-5-5	Crop coefficient	May	Native	1.10E+00
[1]kc-5-6	Crop coefficient	May	Pasture	1.10E+00
[1]kc-5-7	Crop coefficient	May	Riparian	1.10E+00
[1]kc-5-8	Crop coefficient	May	SemiAg	7.11E–01
[1]kc-5-9	Crop coefficient	May	Truck	1.06E+00
[1]kc-5-10	Crop coefficient	May	Urban	9.85E–01
[1]kc-5-11	Crop coefficient	May	Vineyards	3.40E–01
[1]kc-5-12	Crop coefficient	May	Rural	8.00E–01
[1]kc-6-1	Crop coefficient	June	Citrus	6.16E–01
[1]kc-6-2	Crop coefficient	June	Orchard	3.93E–01
[1]kc-6-3	Crop coefficient	June	Field	1.03E+00
[1]kc-6-4	Crop coefficient	June	Grain	1.80E–01
[1]kc-6-5	Crop coefficient	June	Native	1.10E+00
[1]kc-6-6	Crop coefficient	June	Pasture	1.10E+00
[1]kc-6-7	Crop coefficient	June	Riparian	1.10E+00
[1]kc-6-8	Crop coefficient	June	SemiAg	6.73E–01
[1]kc-6-9	Crop coefficient	June	Truck	1.10E+00
[1]kc-6-10	Crop coefficient	June	Urban	9.85E–01
[1]kc-6-11	Crop coefficient	June	Vineyards	5.23E–01
[1]kc-6-12	Crop coefficient	June	Rural	8.00E–01
[1]kc-7-1	Crop coefficient	July	Citrus	6.16E–01
[1]kc-7-2	Crop coefficient	July	Orchard	4.92E–01
[1]kc-7-3	Crop coefficient	July	Field	9.07E–01
[1]kc-7-4	Crop coefficient	July	Grain	1.80E–01
[1]kc-7-5	Crop coefficient	July	Native	1.10E+00
[1]kc-7-6	Crop coefficient	July	Pasture	1.10E+00
[1]kc-7-7	Crop coefficient	July	Riparian	1.10E+00
[1]kc-7-8	Crop coefficient	July	SemiAg	6.73E–01

Table D15. Petaluma Valley Integrated Hydrologic Model (Traum, 2022) calibrated FMP parameter values, Petaluma valley watershed, Sonoma County, California.—Continued

[N/A, not applicable]

Parameter name	Parameter type	Month	Crop	Final estimated value (unitless)
[1]kc-7-9	Crop coefficient	July	Truck	1.10E+00
[1]kc-7-10	Crop coefficient	July	Urban	9.85E–01
[1]kc-7-11	Crop coefficient	July	Vineyards	5.63E–01
[1]kc-7-12	Crop coefficient	July	Rural	8.00E–01
[1]kc-8-1	Crop coefficient	August	Citrus	6.16E–01
[1]kc-8-2	Crop coefficient	August	Orchard	5.90E–01
[1]kc-8-3	Crop coefficient	August	Field	1.51E–01
[1]kc-8-4	Crop coefficient	August	Grain	1.80E–01
[1]kc-8-5	Crop coefficient	August	Native	1.10E+00
[1]kc-8-6	Crop coefficient	August	Pasture	1.10E+00
[1]kc-8-7	Crop coefficient	August	Riparian	1.10E+00
[1]kc-8-8	Crop coefficient	August	SemiAg	5.09E–01
[1]kc-8-9	Crop coefficient	August	Truck	1.06E+00
[1]kc-8-10	Crop coefficient	August	Urban	9.85E–01
[1]kc-8-11	Crop coefficient	August	Vineyards	3.96E–01
[1]kc-8-12	Crop coefficient	August	Rural	8.00E–01
[1]kc-9-1	Crop coefficient	September	Citrus	6.16E–01
[1]kc-9-2	Crop coefficient	September	Orchard	5.90E–01
[1]kc-9-3	Crop coefficient	September	Field	1.57E–01
[1]kc-9-4	Crop coefficient	September	Grain	1.80E–01
[1]kc-9-5	Crop coefficient	September	Native	1.10E+00
[1]kc-9-6	Crop coefficient	September	Pasture	1.10E+00
[1]kc-9-7	Crop coefficient	September	Riparian	1.10E+00
[1]kc-9-8	Crop coefficient	September	SemiAg	3.27E–01
[1]kc-9-9	Crop coefficient	September	Truck	6.34E–01
[1]kc-9-10	Crop coefficient	September	Urban	9.85E–01
[1]kc-9-11	Crop coefficient	September	Vineyards	3.76E–01
[1]kc-9-12	Crop coefficient	September	Rural	8.00E–01
[1]kc-10-1	Crop coefficient	October	Citrus	6.16E–01
[1]kc-10-2	Crop coefficient	October	Orchard	1.08E–01
[1]kc-10-3	Crop coefficient	October	Field	1.57E–01
[1]kc-10-4	Crop coefficient	October	Grain	1.80E–01
[1]kc-10-5	Crop coefficient	October	Native	1.10E+00
[1]kc-10-6	Crop coefficient	October	Pasture	1.10E+00
[1]kc-10-7	Crop coefficient	October	Riparian	1.10E+00
[1]kc-10-8	Crop coefficient	October	SemiAg	2.59E–01
[1]kc-10-9	Crop coefficient	October	Truck	1.55E–01
[1]kc-10-10	Crop coefficient	October	Urban	9.85E–01
[1]kc-10-11	Crop coefficient	October	Vineyards	2.80E–01
[1]kc-10-12	Crop coefficient	October	Rural	8.00E–01
[1]kc-11-1	Crop coefficient	November	Citrus	6.16E–01

Table D15. Petaluma Valley Integrated Hydrologic Model (Traum, 2022) calibrated FMP parameter values, Petaluma valley watershed, Sonoma County, California.—Continued

[N/A, not applicable]

Parameter name	Parameter type	Month	Crop	Final estimated value (unitless)
[1]kc-11-2	Crop coefficient	November	Orchard	1.08E–01
[1]kc-11-3	Crop coefficient	November	Field	1.57E–01
[1]kc-11-4	Crop coefficient	November	Grain	1.80E–01
[1]kc-11-5	Crop coefficient	November	Native	1.10E+00
[1]kc-11-6	Crop coefficient	November	Pasture	1.10E+00
[1]kc-11-7	Crop coefficient	November	Riparian	1.10E+00
[1]kc-11-8	Crop coefficient	November	SemiAg	2.59E–01
[1]kc-11-9	Crop coefficient	November	Truck	1.55E–01
[1]kc-11-10	Crop coefficient	November	Urban	9.85E–01
[1]kc-11-11	Crop coefficient	November	Vineyards	9.72E–02
[1]kc-11-12	Crop coefficient	November	Rural	8.00E–01
[1]kc-12-1	Crop coefficient	December	Citrus	5.31E–01
[1]kc-12-2	Crop coefficient	December	Orchard	1.08E–01
[1]kc-12-3	Crop coefficient	December	Field	1.57E–01
[1]kc-12-4	Crop coefficient	December	Grain	2.71E–01
[1]kc-12-5	Crop coefficient	December	Native	1.10E+00
[1]kc-12-6	Crop coefficient	December	Pasture	1.06E+00
[1]kc-12-7	Crop coefficient	December	Riparian	1.10E+00
[1]kc-12-8	Crop coefficient	December	SemiAg	2.98E–01
[1]kc-12-9	Crop coefficient	December	Truck	1.55E–01
[1]kc-12-10	Crop coefficient	December	Urban	9.85E–01
[1]kc-12-11	Crop coefficient	December	Vineyards	9.72E–02
[1]kc-12-12	Crop coefficient	December	Rural	7.73E–01
p_run_citrus	Precipitation runoff coefficient	N/A	Citrus	5.52E–01
p_run_orchar	Precipitation runoff coefficient	N/A	Orchard	8.07E–01
p_run_field	Precipitation runoff coefficient	N/A	Field	8.27E–01
p_run_grain	Precipitation runoff coefficient	N/A	Grain	2.91E–01
p_run_native	Precipitation runoff coefficient	N/A	Native	5.39E–01
p_run_pastur	Precipitation runoff coefficient	N/A	Pasture	2.00E–01
p_run_ripari	Precipitation runoff coefficient	N/A	Riparian	6.35E–01
p_run_semiag	Precipitation runoff coefficient	N/A	SemiAg	5.96E–01
p_run_truck	Precipitation runoff coefficient	N/A	Truck	7.30E–01
p_run_urban	Precipitation runoff coefficient	N/A	Urban	7.05E–01
p_run_vineya	Precipitation runoff coefficient	N/A	Vineyards	2.57E–01
p_run_rural	Precipitation runoff coefficient	N/A	Rural	6.85E–01

[1]These parameters are tied to same crop type in January and are not directly estimated.

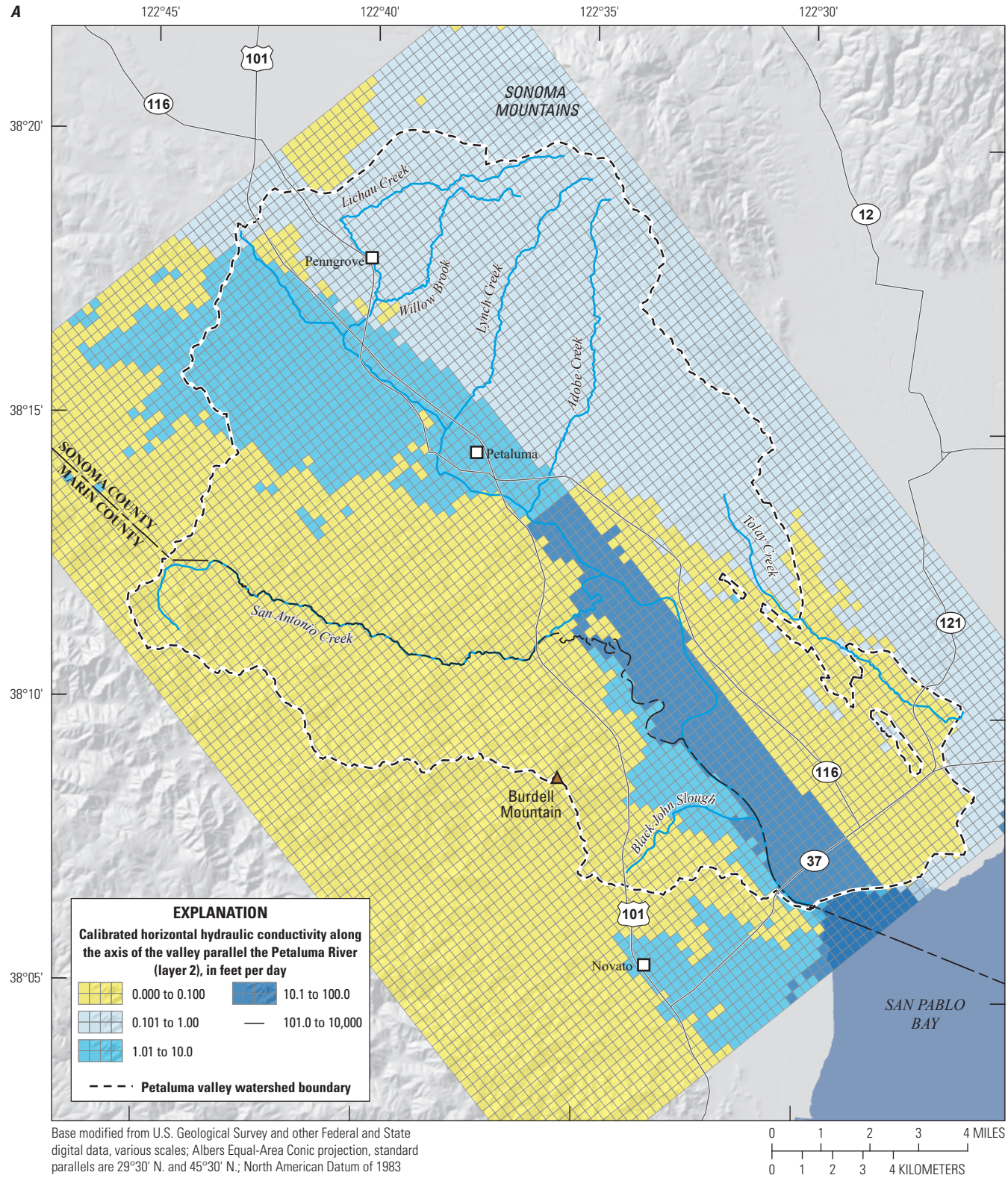

Figure D26. Calibrated horizontal hydraulic conductivity values along the axis of the valley parallel the Petaluma River for the Petaluma Valley Integrated Hydrologic Model (Traum, 2022), Petaluma valley watershed, Sonoma County, California: *A*, model layer 1; *B*, model layer 2; *C*, model layer 3; *D*, model layer 4; *E*, model layer 5.

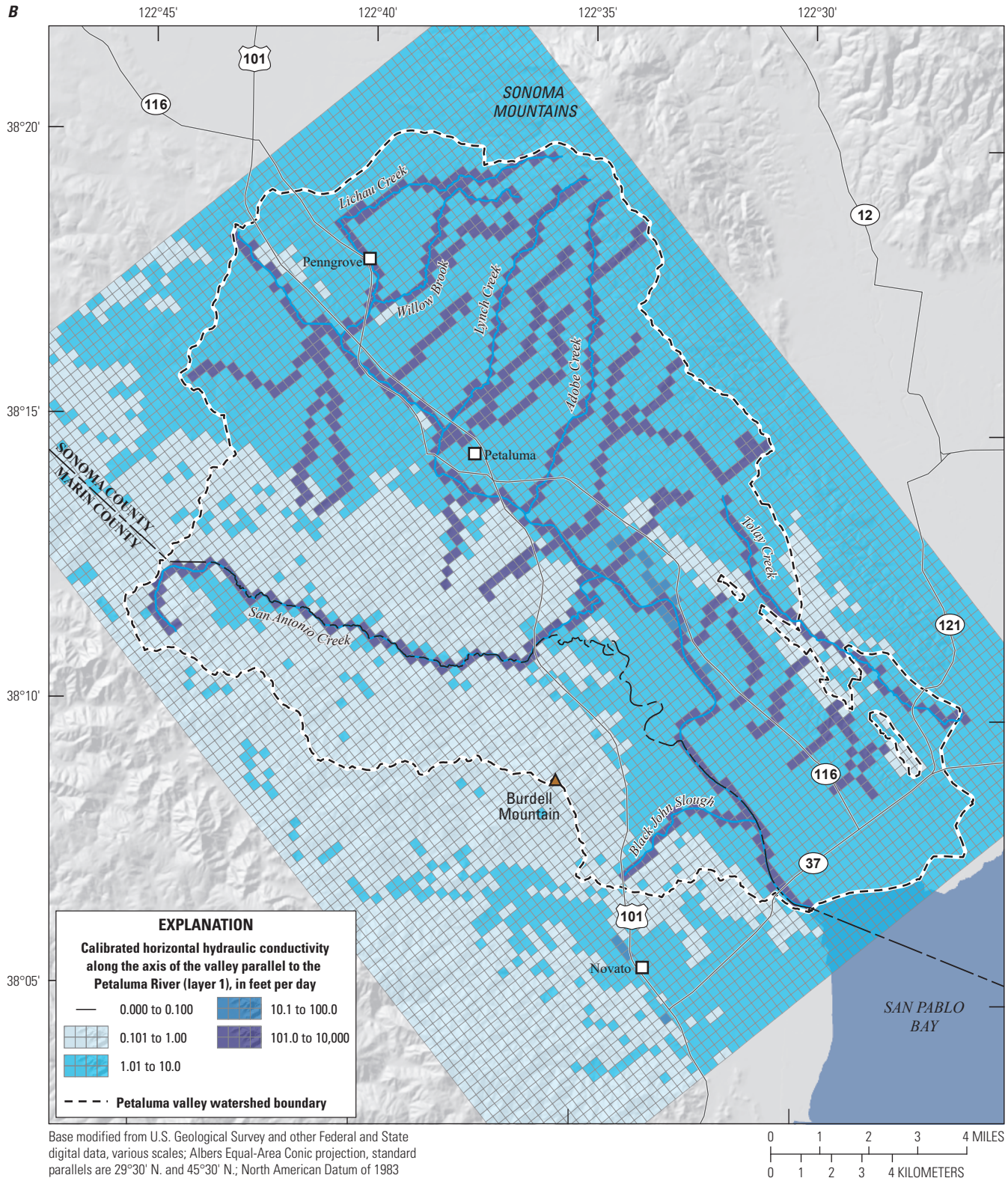

Figure D26.—Continued

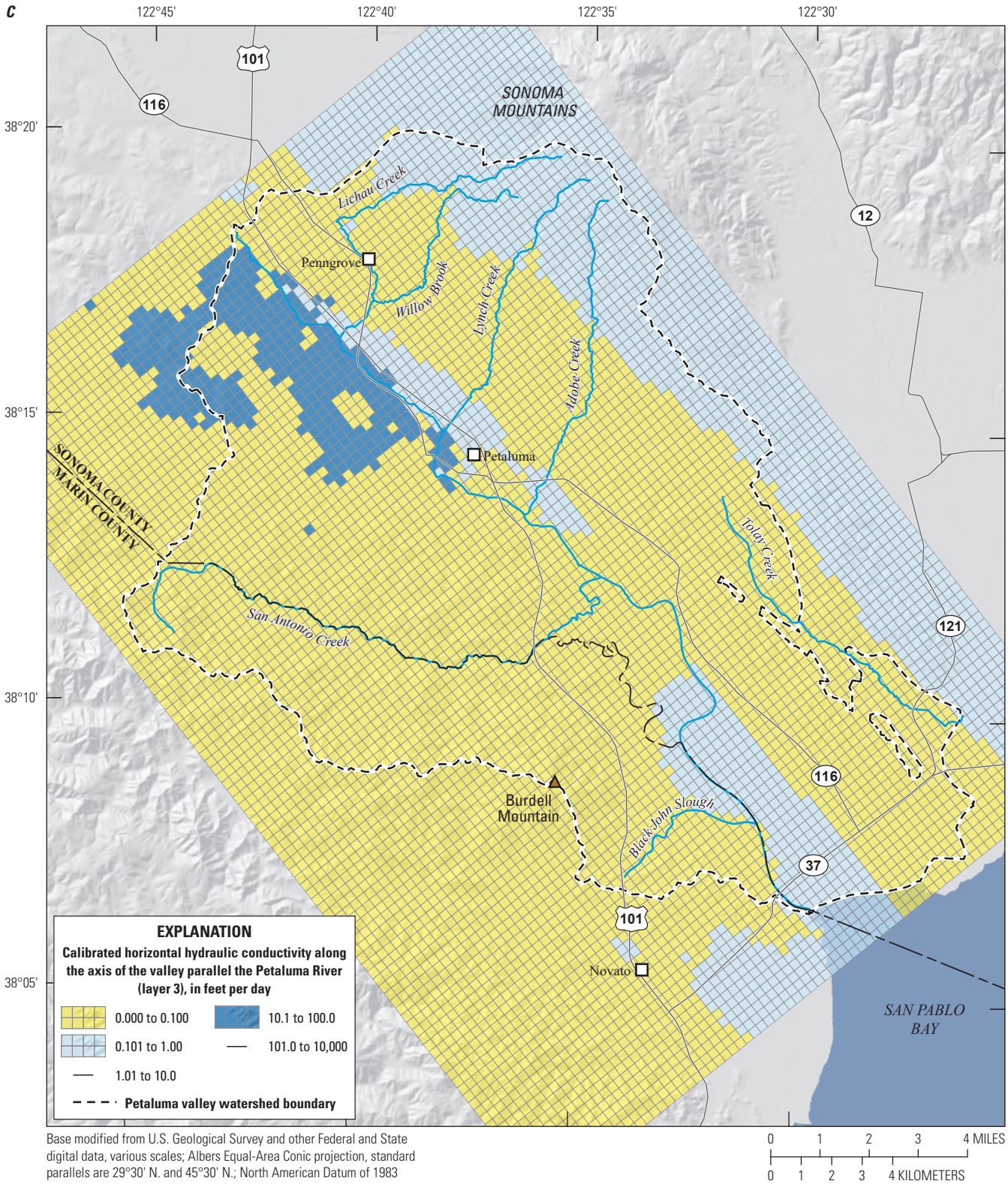

Figure D26.—Continued

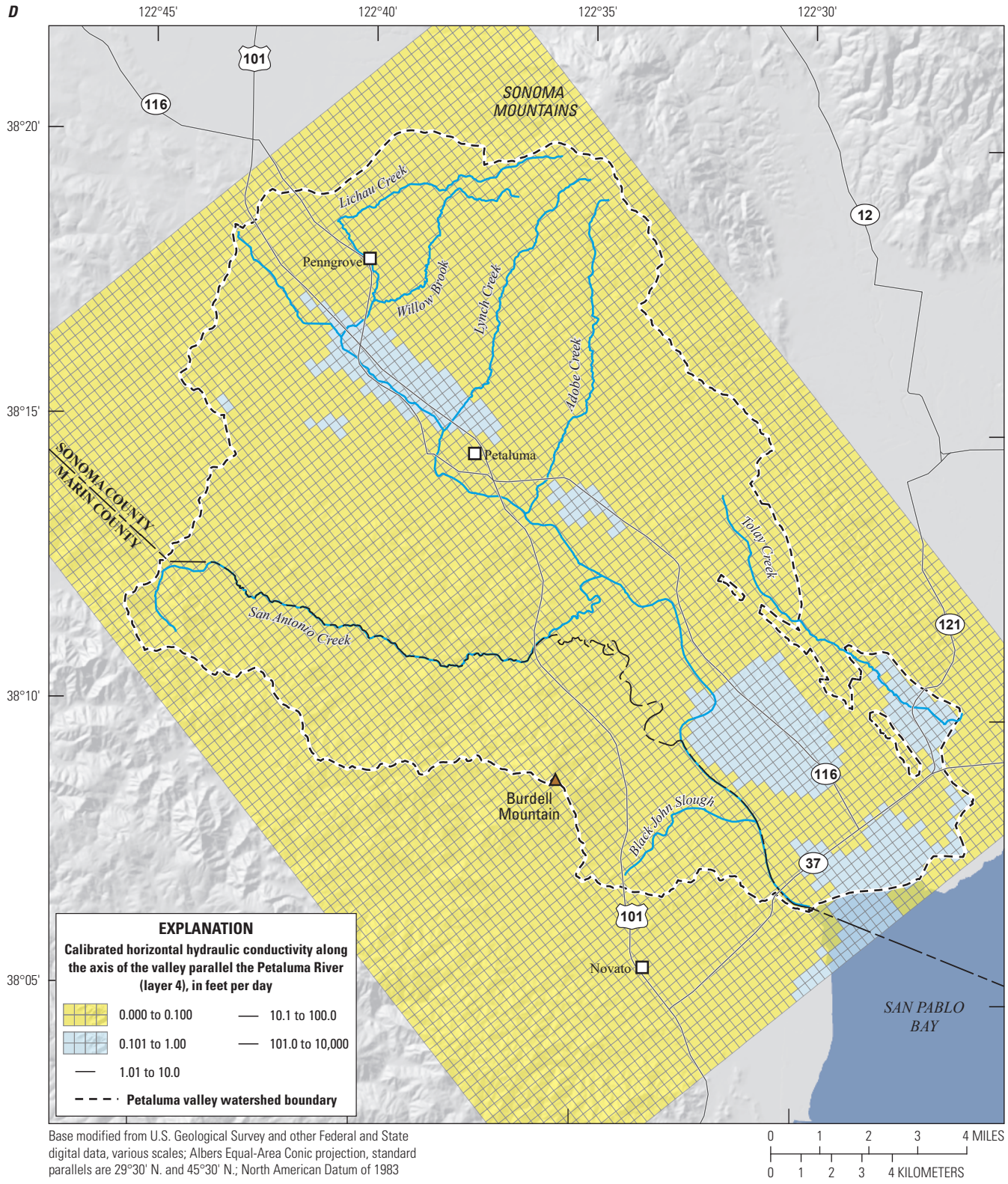

Figure D26.—Continued

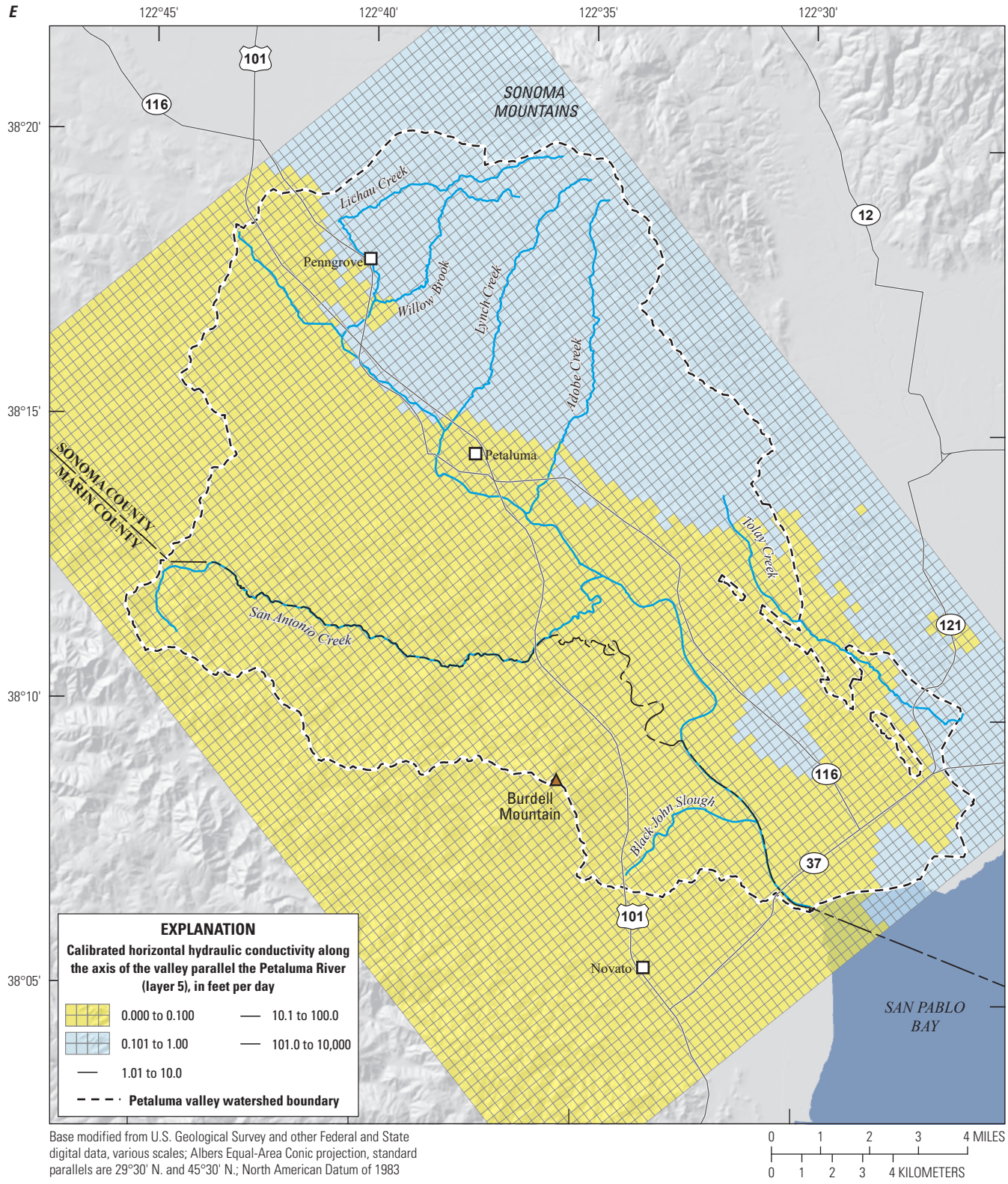

Figure D26.—Continued

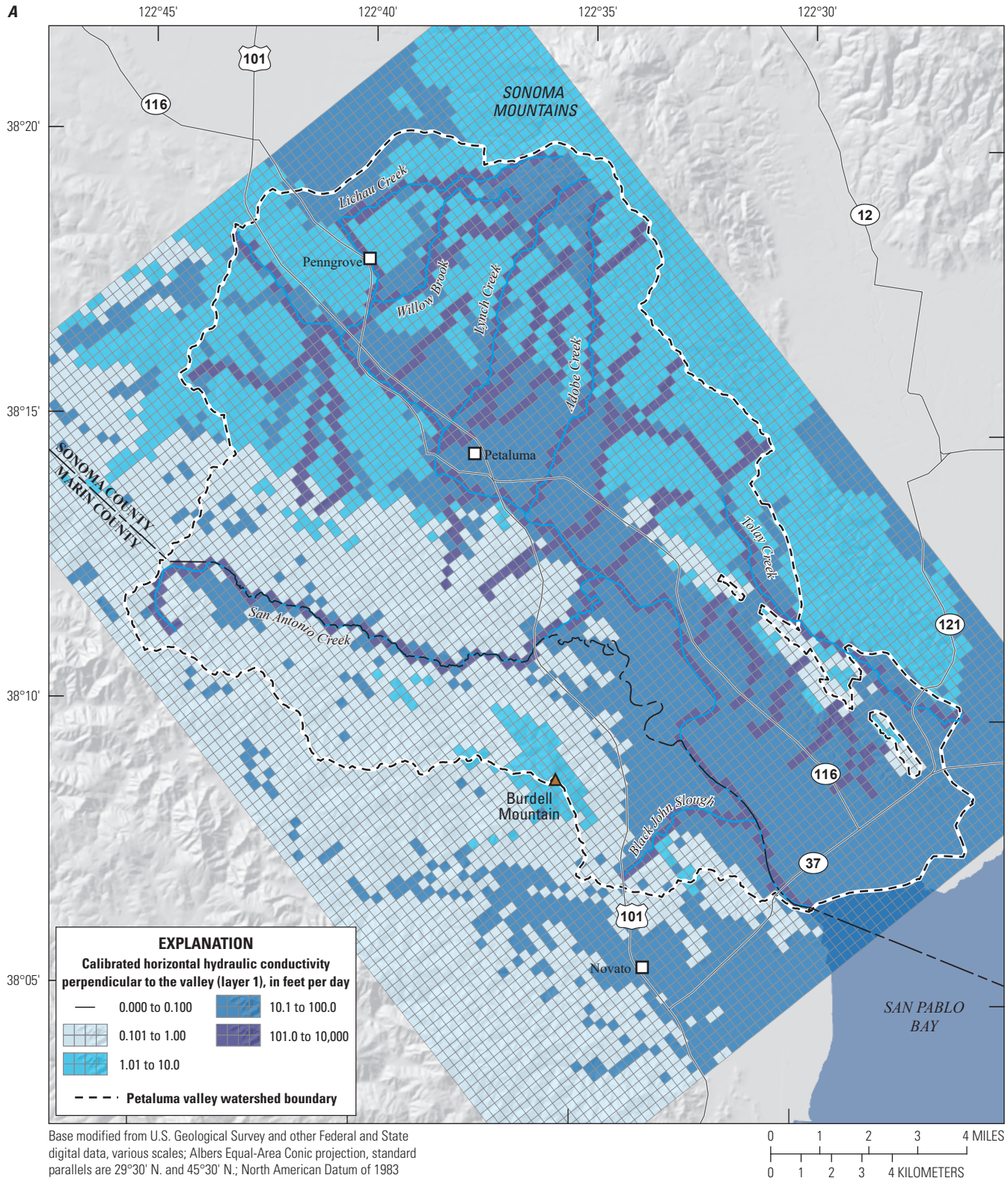

Figure D27. Calibrated horizontal hydraulic conductivity values perpendicular to the valley axis for the Petaluma Valley Integrated Hydrologic Model (Traum, 2022), Petaluma valley watershed, Sonoma County, California: *A*, model layer 1; *B*, model layer 2; *C*, model layer 3, *D*, model layer 4 and *E*, model layer 5.

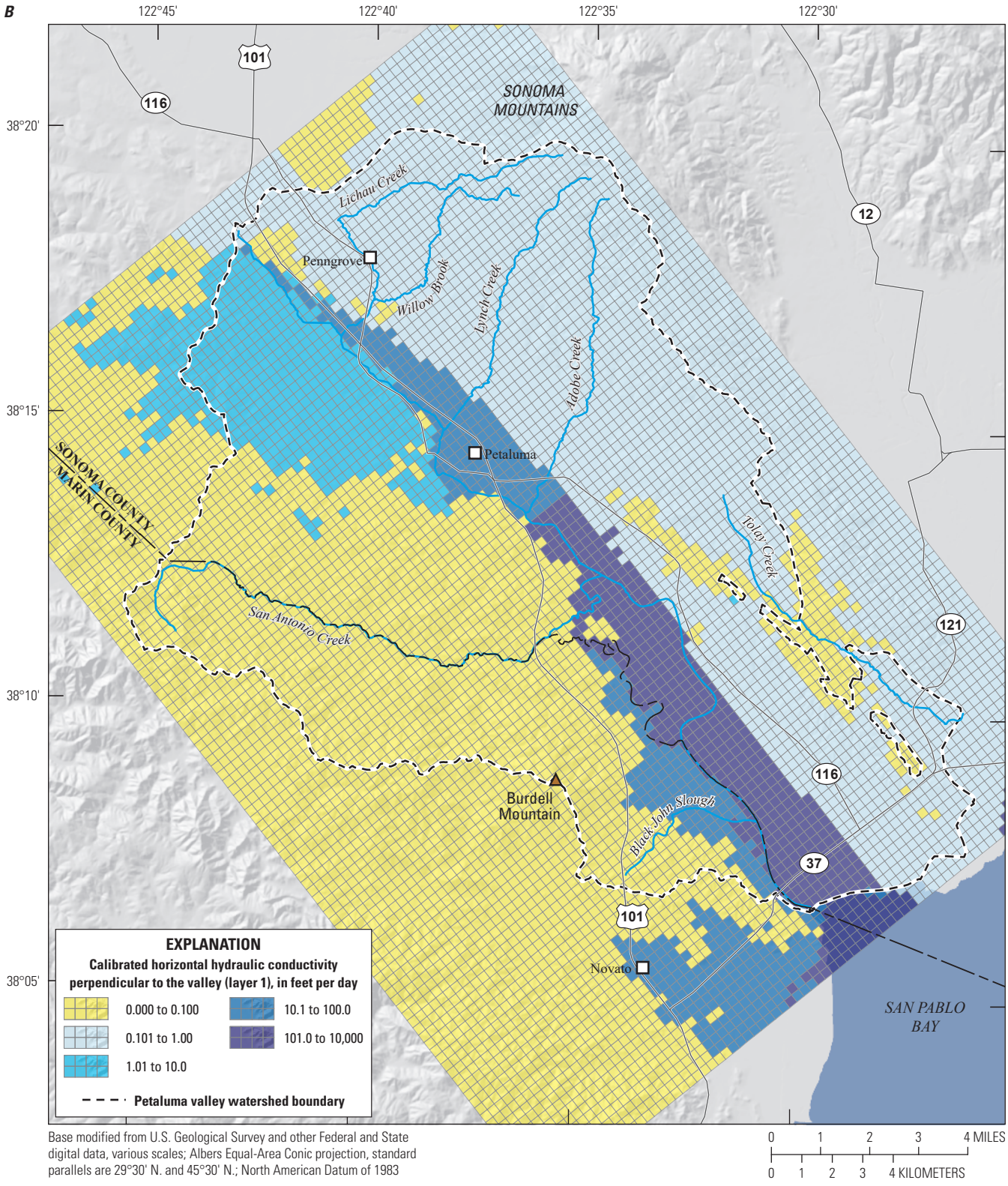

Figure D27.—Continued

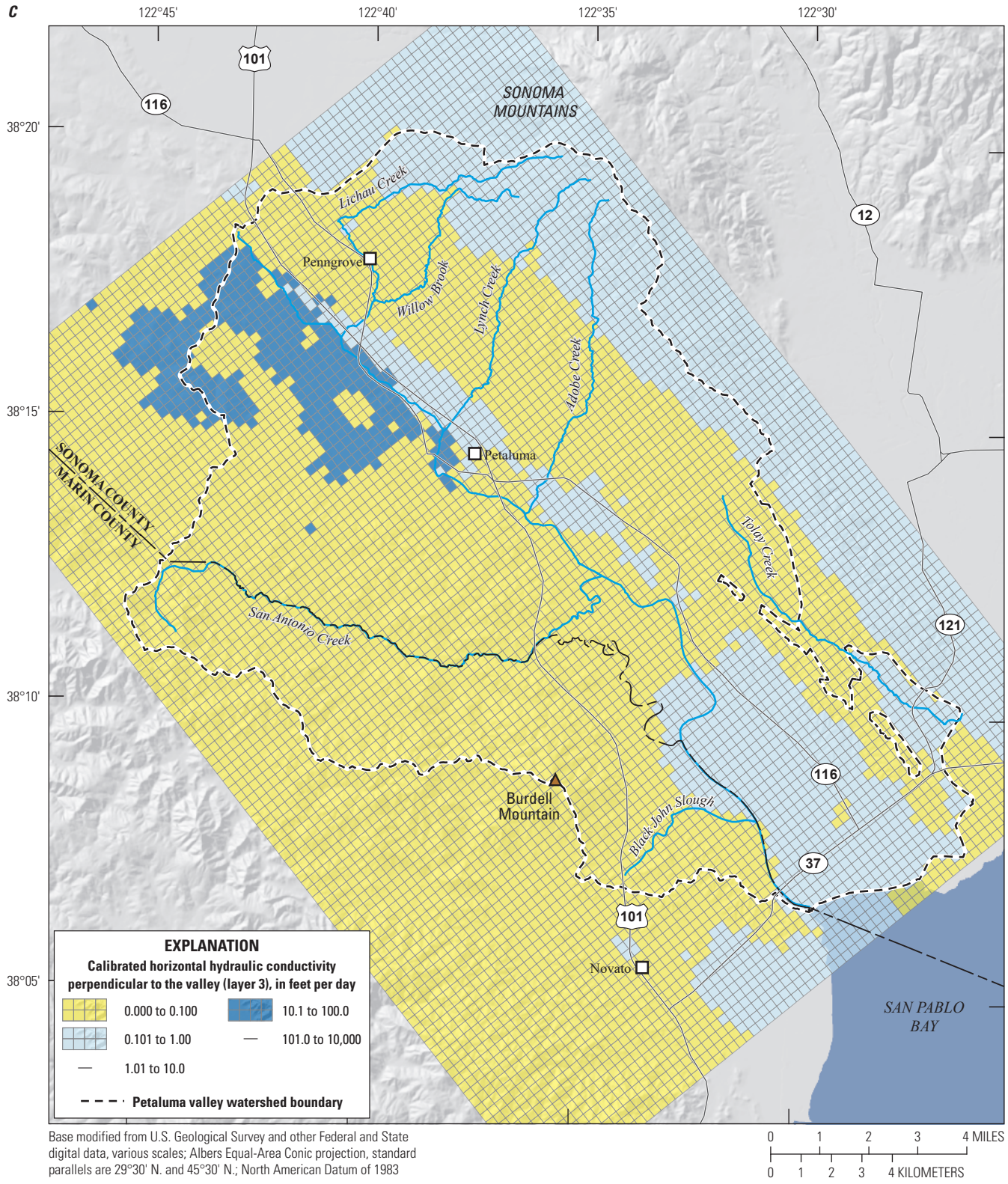

Figure D27.—Continued

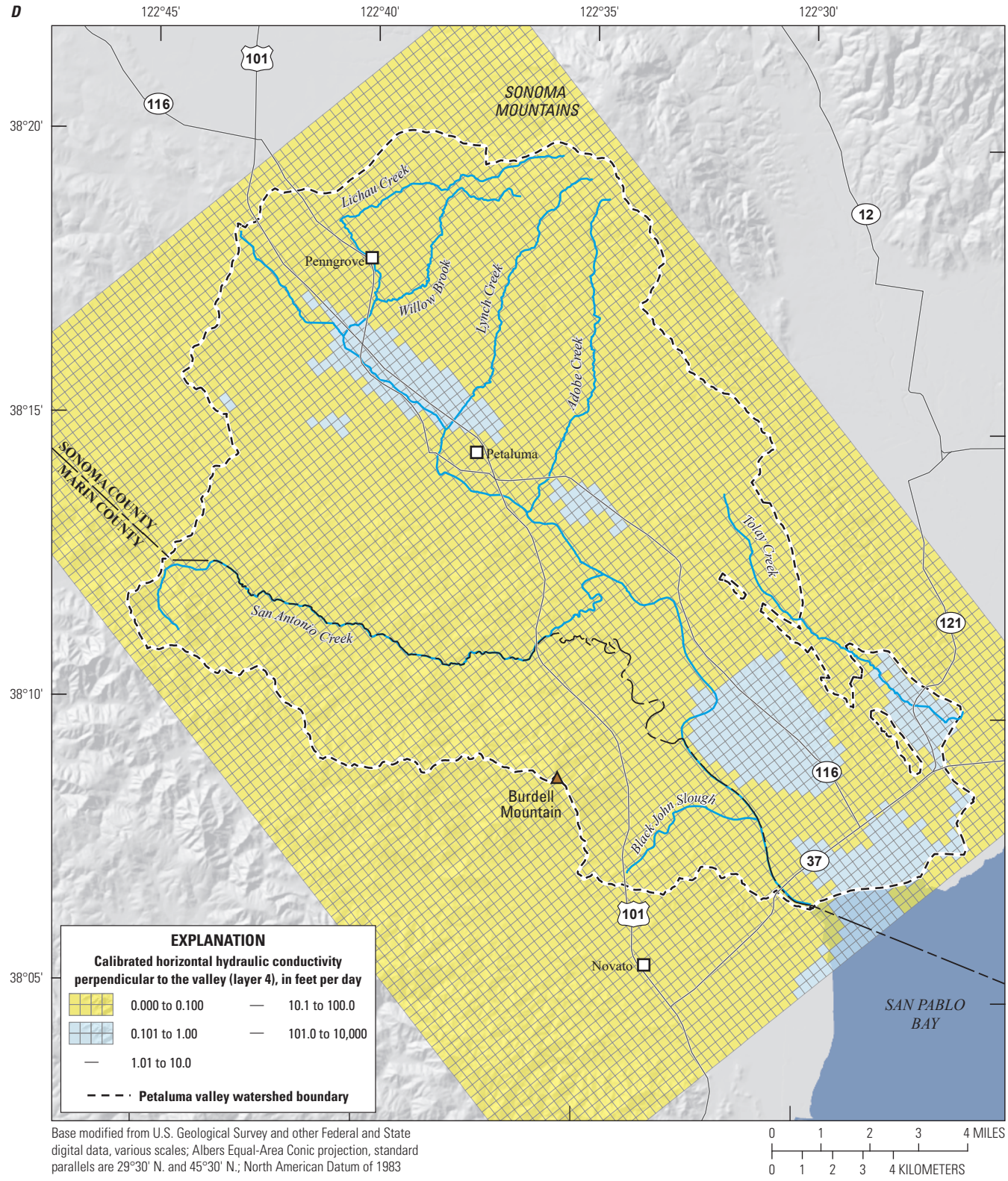

Figure D27.—Continued

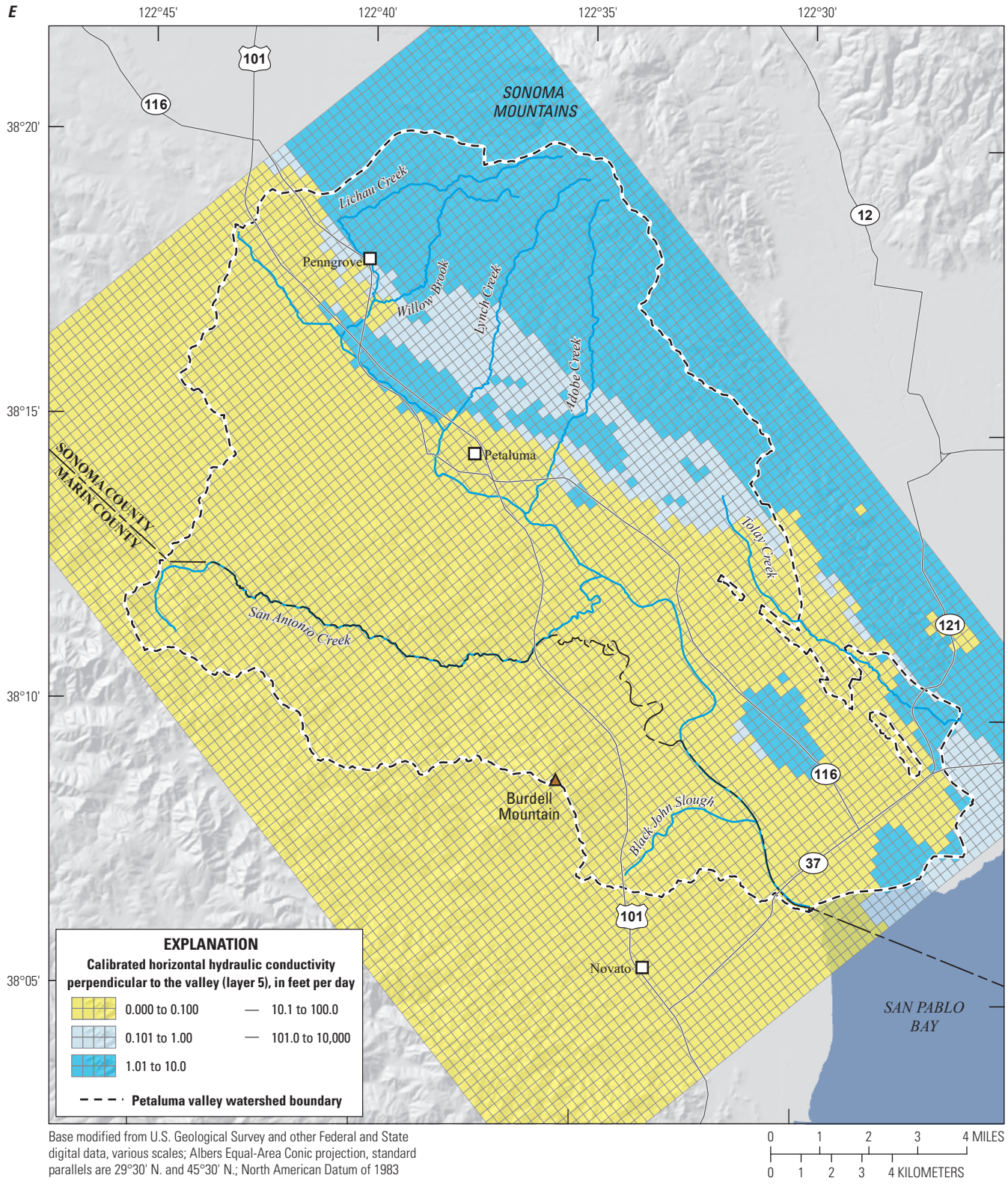

Figure D27.—Continued

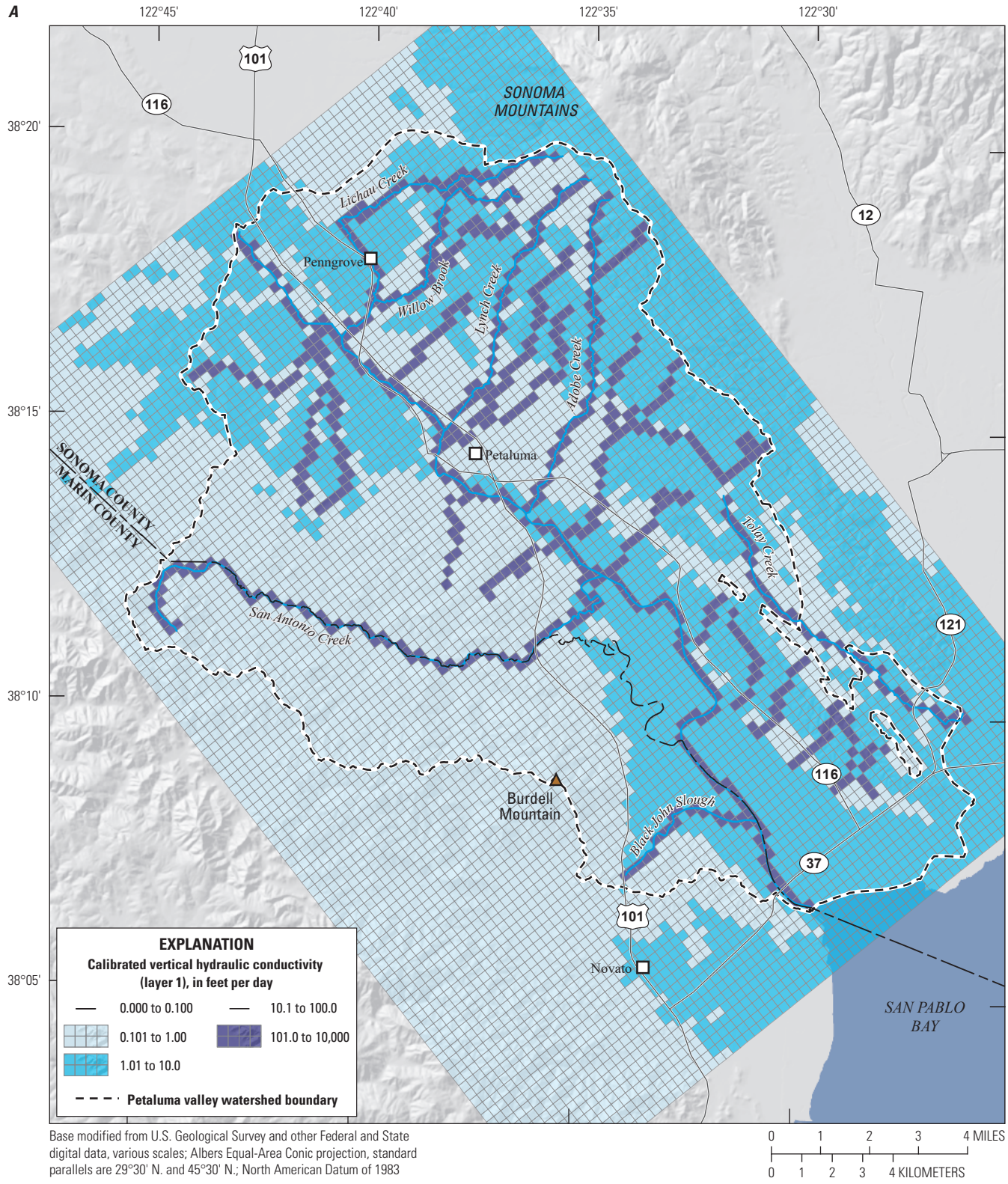

Figure D28. Calibrated vertical hydraulic conductivity values for the Petaluma Valley Integrated Hydrologic Model, Petaluma valley watershed (Traum, 2022), Sonoma County, California: *A*, model layer 1; *B*, model layer 2; *C*, model layer 3; *D*, model layer 4; and *E*, model layer 5.

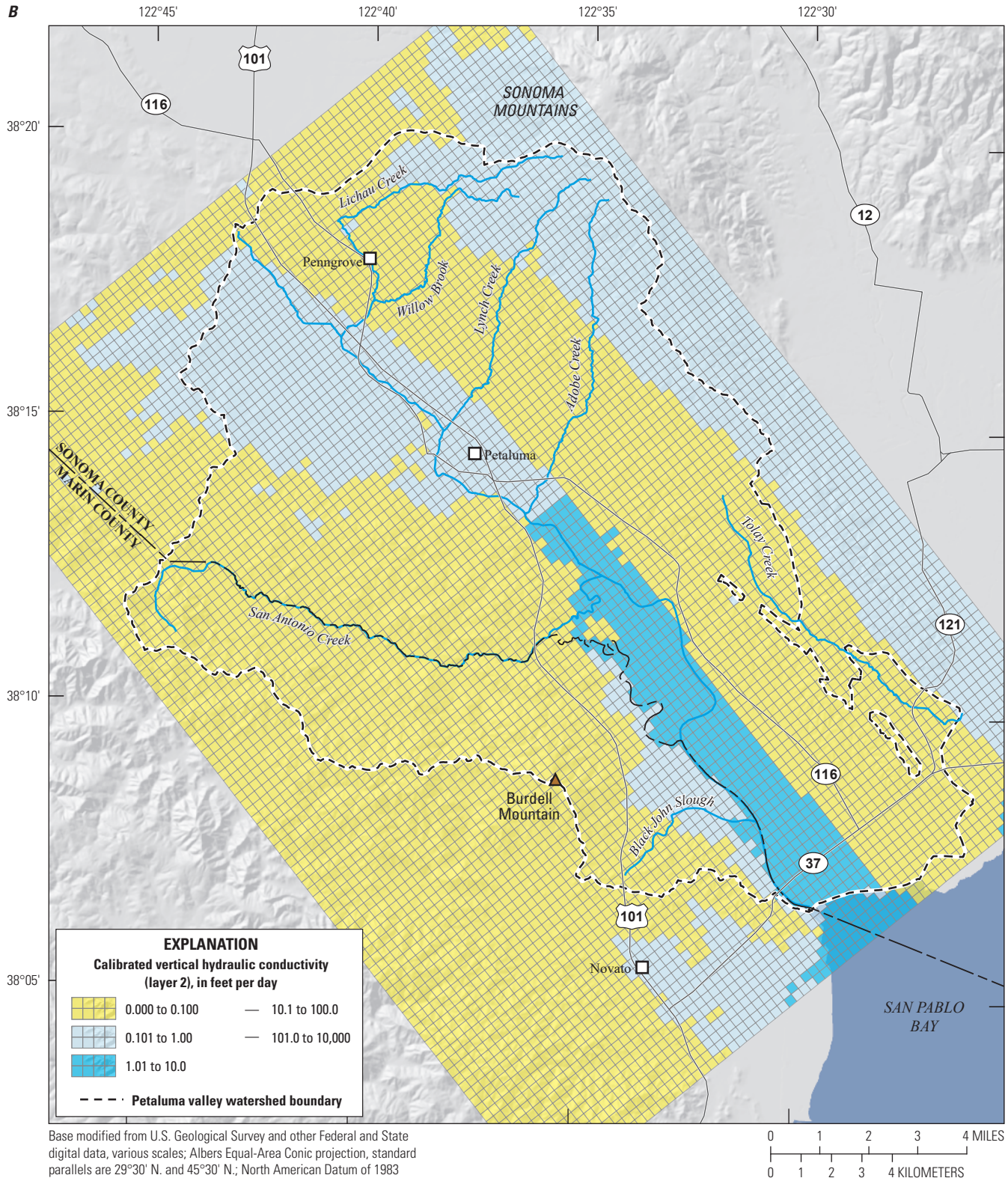

Figure D28.—Continued

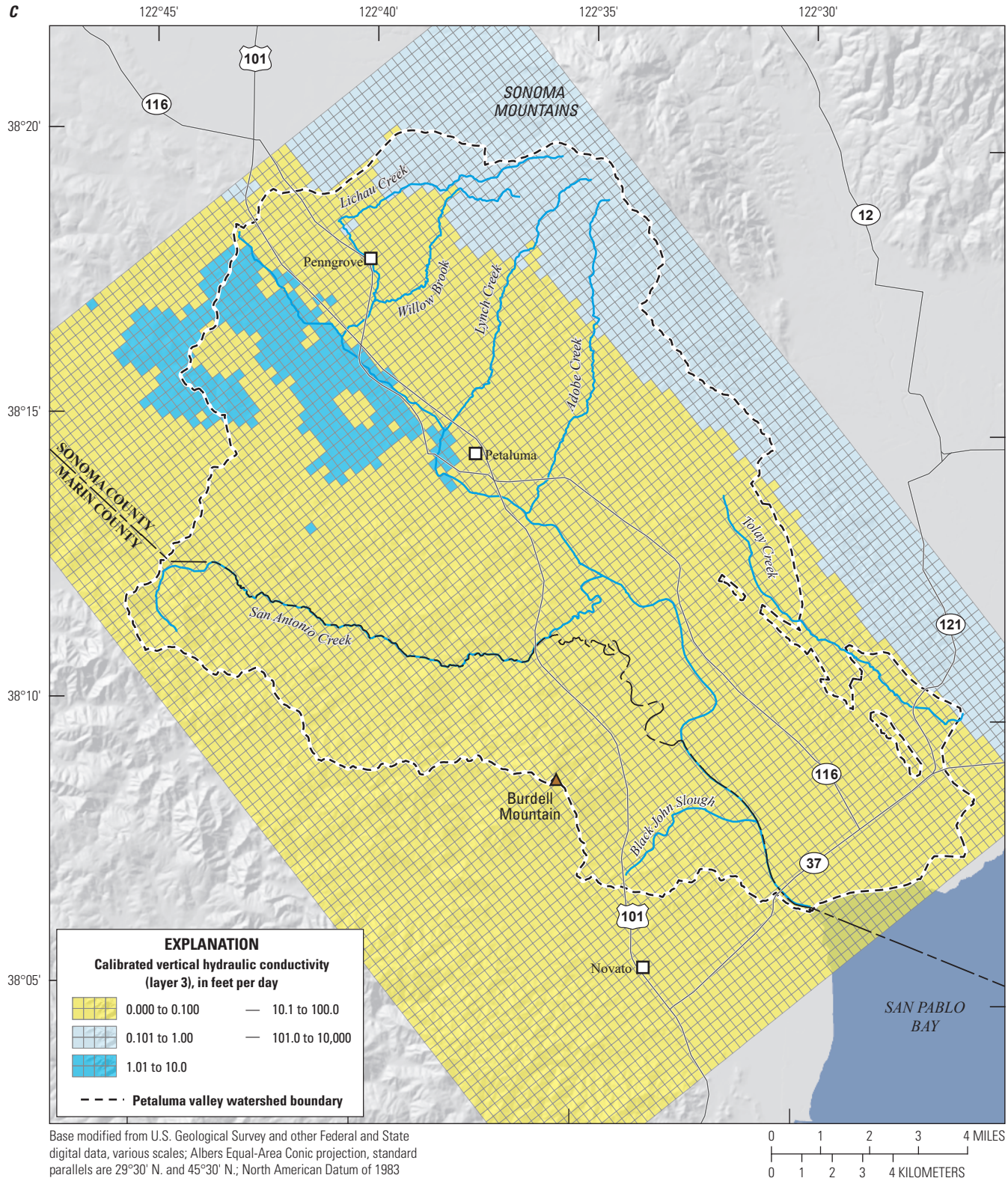

Figure D28.—Continued

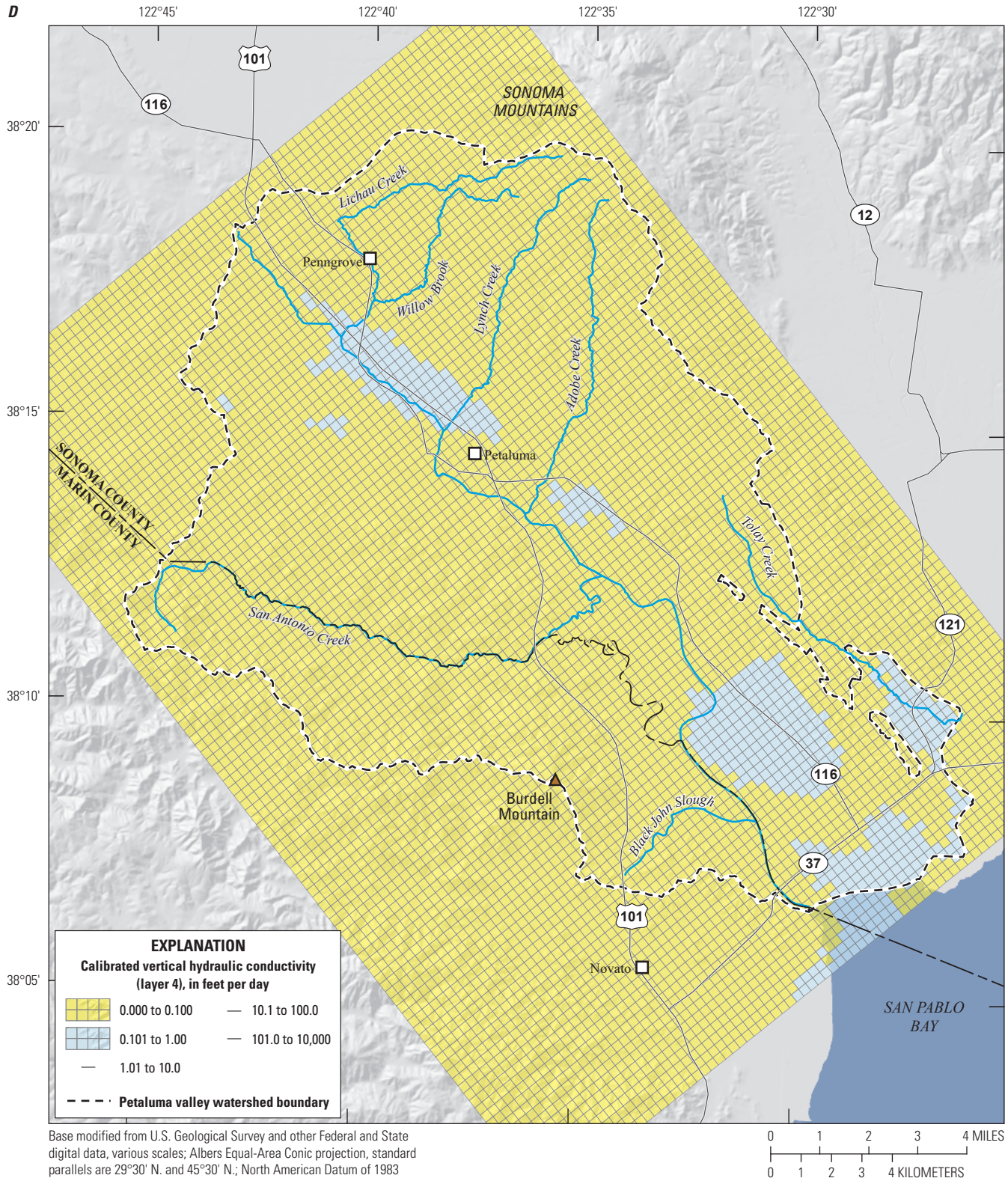

Figure D28.—Continued

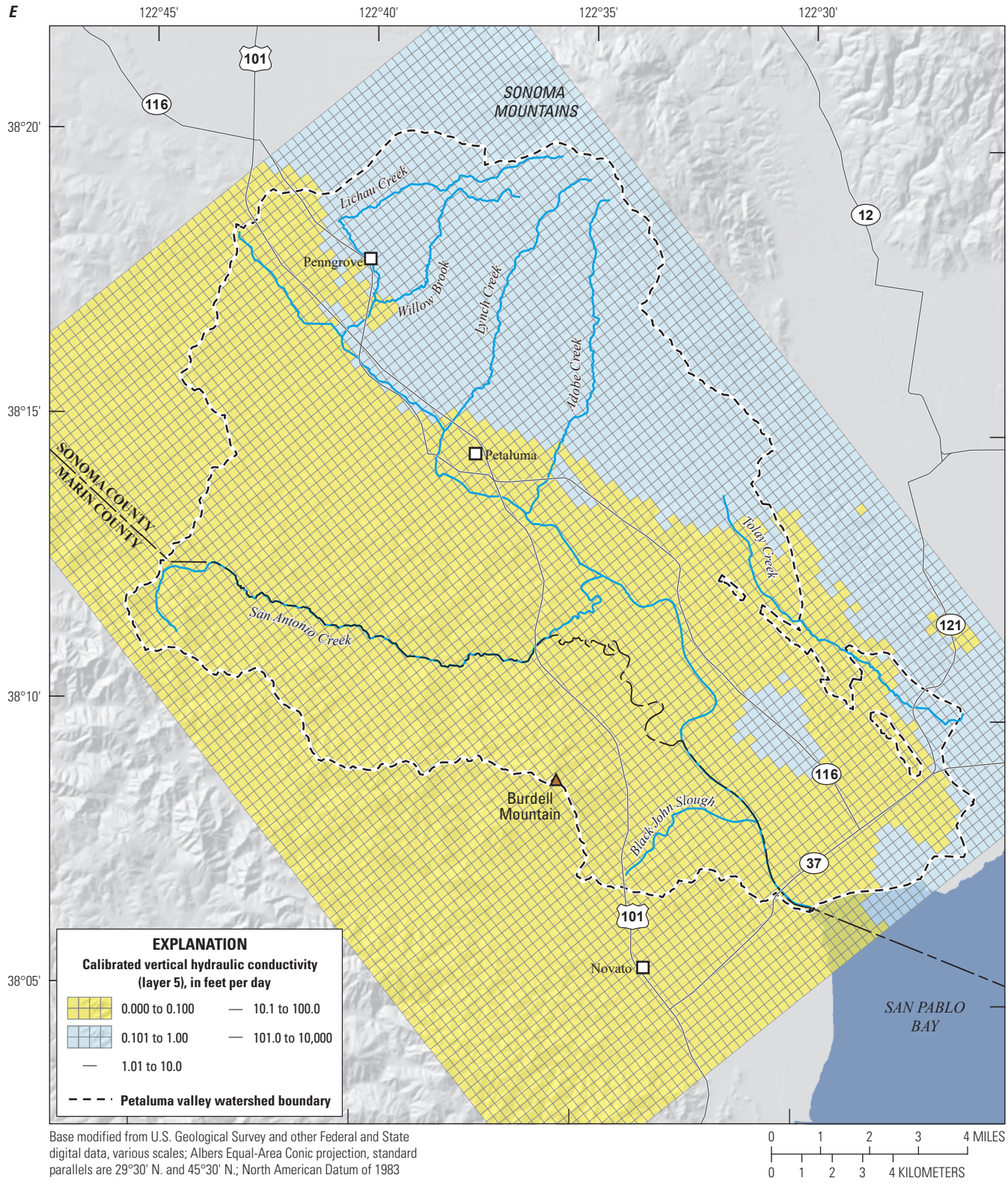

Figure D28.—Continued

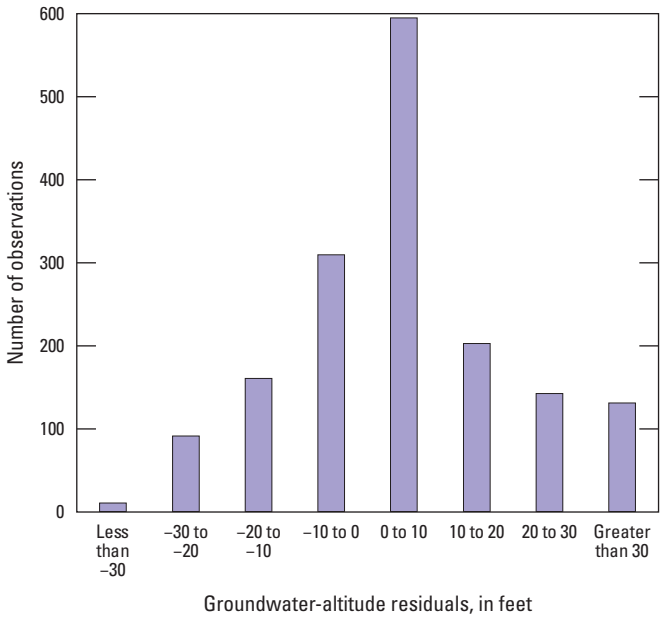

Figure D29. Histogram of groundwater-level residuals for the Petaluma Valley Integrated Hydrologic Model, Petaluma valley watershed, Sonoma County, California.

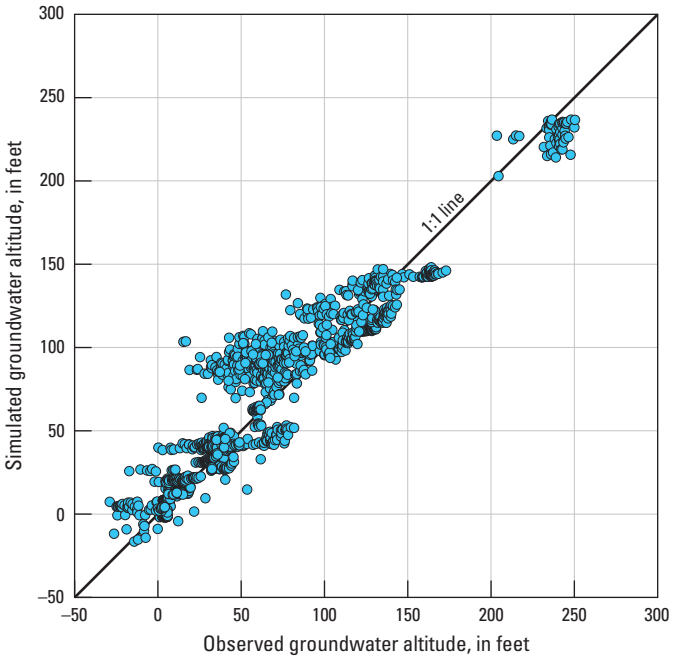

Figure D30. Observed groundwater levels compared with simulated groundwater levels for the Petaluma Valley Integrated Hydrologic Model, Petaluma valley watershed, Sonoma County, California.

are shown in figure D30 and described here:

- Group 1: Petaluma marsh area (wells 1, 2, 3, 4),
- Group 2: Hills east of Petaluma marsh (wells 5, 6, 7, 8, 9),
- Group 3: City of Petaluma (wells 13, 14, 15, 16, 17, 18, 23, 24, 25, 26),
- Group 4: Hills east of City of Petaluma (wells 10, 11, 12, 19, 20, 21, 22),
- Group 5: Wilson Grove (wells 27, 28, 29, 30, 31, 32, 33, 34, 35), and
- Group 6: Penngrove area (wells 36, 37, 38, 39, 40, 41).

Observations are color coded by group on figure D30. Most of the points were close to the 1:1 line, indicating a good model fit.

Residuals were evaluated for spatial bias that can indicate local processes are not being simulated correctly. Spatial plots of average residuals for each observation well indicate that spatial bias was generally minimal in the residuals (fig. D31). For example, groundwater altitudes were overestimated for well 13, but the average residual for nearby wells 14 and 15 was less than 5 ft (figs. D1, D31). Similarly, groundwater altitudes were overestimated for well 40, but underestimated for nearby wells 39 and 41 (figs. D1, D31).

Simulated Streamflow

A histogram of residuals was examined to quantify the model fit between the simulated and observed streamflows for all 242 observations at the 3 streamgages (fig. D32). About 70 percent of simulated values were within 50 cubic feet per second (ft^3/s) of the observed values, and about 84 percent of simulated values were within 100 ft^3/s. The residuals ranged from –642 to 166 ft^3/s and had a mean of –11.7 ft^3/s, an absolute mean of 49.0 ft^3/s, a standard error of 91.2 ft^3/s, and a skewness of –3.52. The mean of –11.7 ft^3/s indicates that, on average, the model is slightly underestimating streamflow. A standard deviation of 91.2 ft^3/s, however, indicates large variability between simulated and observed streamflows. The relation between observed and simulated streamflows and the 1:1 correlation line are shown in figure D33. The results indicated that the model generally overestimated low (less than 100 ft^3/s) streamflows and underestimated high (greater than 100 ft^3/s) streamflows. Specifically, streamflow was overestimated at streamgages 11459150 and 11459300 and poorly estimated at streamgage 11459150 (fig. D33).

Hydrographs comparing the simulated and observed streamflows at the three calibration streamgages are shown in figure D34. The PVIHM simulated values (Traum, 2022) closely matched the observed streamflows at the San Antonio Creek streamgage (11459300; fig. D34*A*; U.S. Geological Survey, 2018). This streamgage was

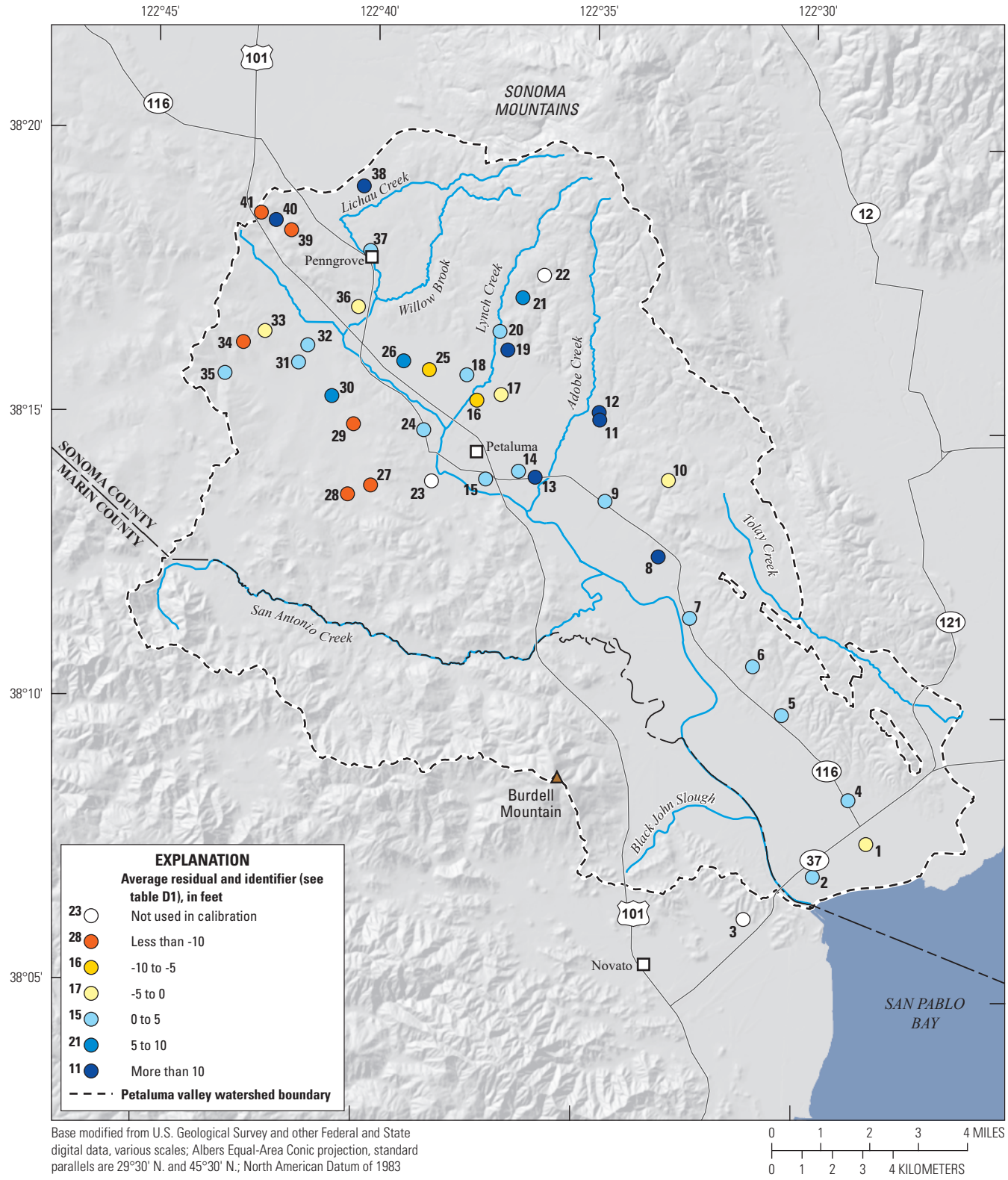

Figure D31. Average residual groundwater altitude for observation wells from the Petaluma Valley Integrated Hydrologic Model for the entire simulation period (water year 1960–2015), Petaluma valley watershed, Sonoma County, California.

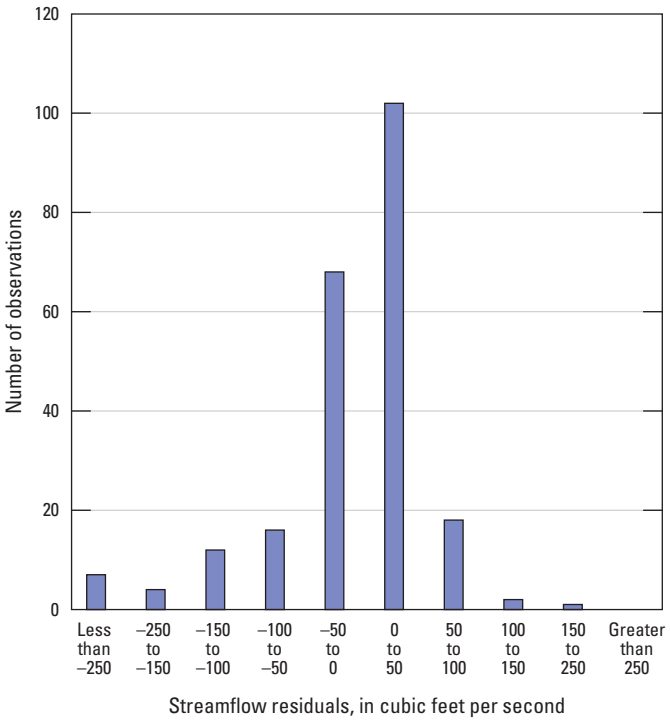

Figure D32. Histogram of streamflow residuals for the Petaluma Valley Integrated Hydrologic Model, Petaluma valley watershed, Sonoma County, California.

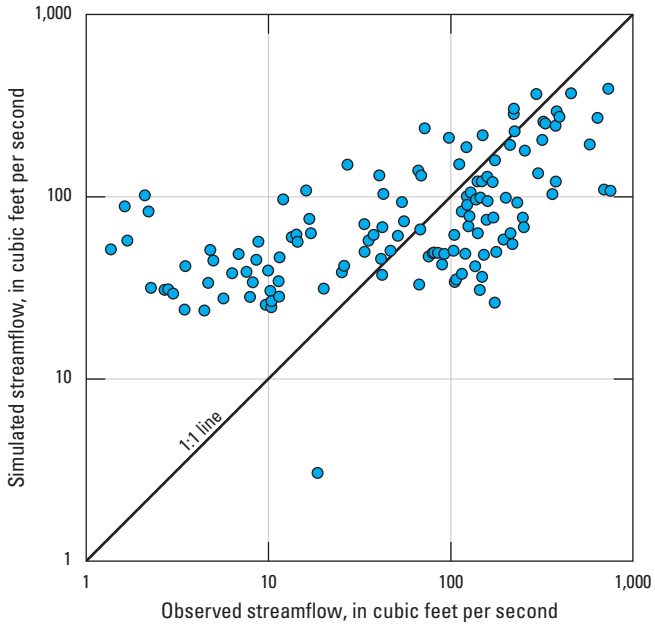

Figure D33. Observed streamflows from U.S. Geological Survey streamgages 11459000, 11459150, and 11459300 (U.S. Geological Survey, 2018) compared with simulated streamflows from the Petaluma Valley Integrated Hydrologic Model (Traum, 2022), Petaluma valley watershed, Sonoma County, California.

outside of the active model area for groundwater simulation; therefore, simulated flows only included runoff accumulated from excess precipitation and irrigation. For the Petaluma River streamgages (1459000 and 11459150), the PVIHM matched the seasonal variability in streamflow; however, the PVIHM generally overestimated low flows by simulating a base flow on the Petaluma River of about 20 ft^3/s for streamgage 1459000 (fig. D34*B*) and 30 ft^3/s for 11459150 (fig. D34*C*); observed streamflows were less than 20 ft^3/s. The PVIHM also underestimated peak flows over about 300 ft^3/s at streamgage 11459150. The model fit for streamflow was relatively poor compared to the fit for groundwater; however, given the temporal and spatial scale of the PVIHM and the statistics presented here, the model fit indicated that overall average streamflow for all observation is reasonably matched with an average observed of 71.1 ft^3/s compared to an average simulated value of 59.4 ft^3/s.

There are several reasons the model did not accurately estimate streamflow. There were no streamgages in the upper reaches of streams. If streamgages were present, streamflow data could have been used directly as input data or been used to improve estimates of inflows to the stream network. Also, the Petaluma River is generally a runoff-dominated system, and all runoff data were estimated in the model. In model areas where groundwater flow is not simulated, all excess precipitation immediately enters the stream network as runoff rather than being stored and flowing out over time as base flow. As a result, there is a mismatch in timing between precipitation and streamflow, although some of the mismatch is likely smoothed by monthly stress periods. Base flow becomes an important component of streamflow during summer months, and groundwater altitudes in the City of Petaluma area were generally overestimated by about 5–10 ft, which can explain why simulated base flows were higher than observed base flows. Also as previously discussed, the main focus of the calibration was groundwater-altitude observations, and streamflow observations were weighted relatively lower than groundwater observations.

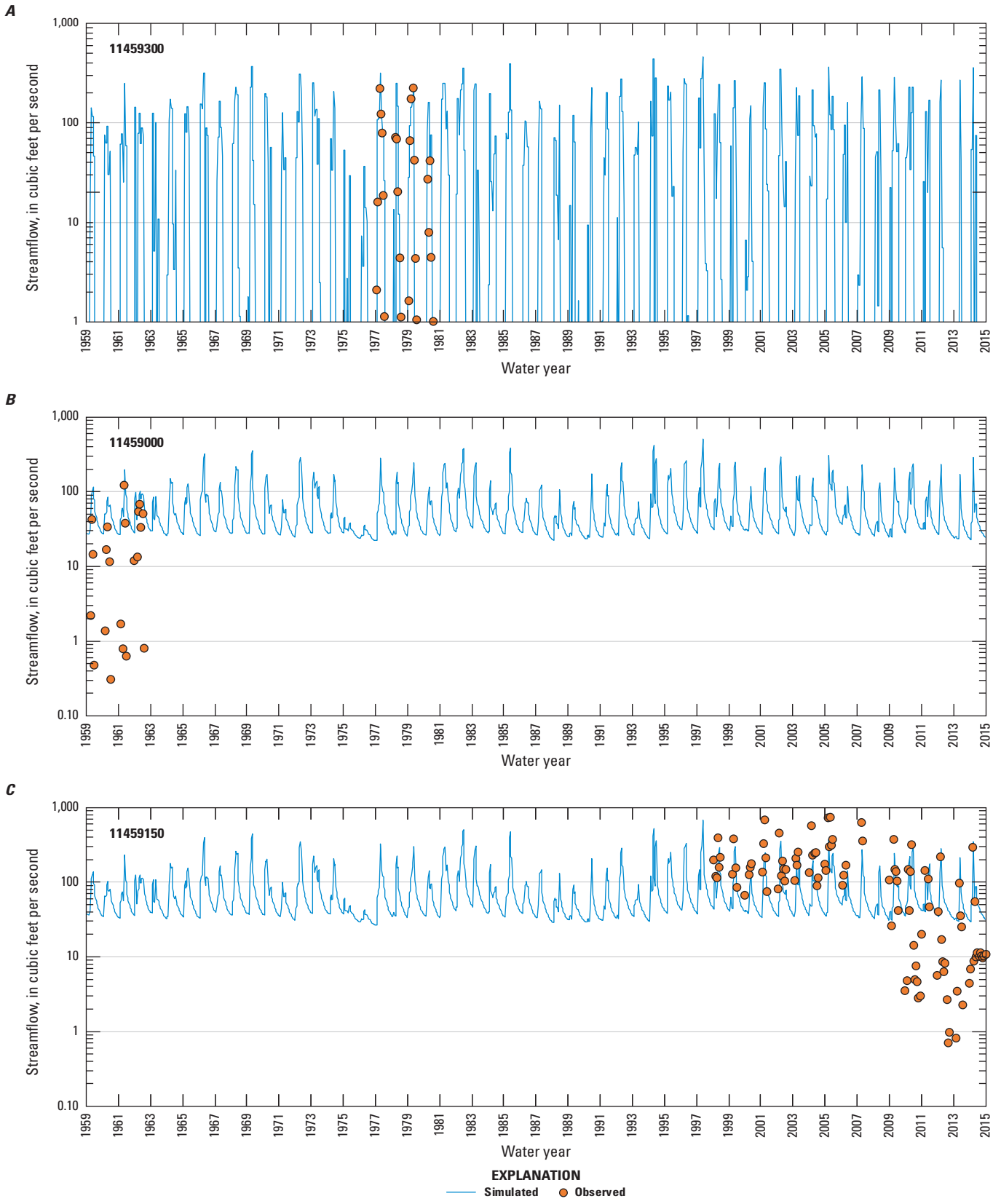

Figure D34. Streamflow hydrographs comparing simulated (Traum, 2022) and observed streamflows (U.S. Geological Survey, 2018), Petaluma Valley Integrated Hydrologic Model, Petaluma valley watershed, Sonoma County, California for three streamgages: *A*, San Antonio Creek (11459300); *B*, Petaluma River (1459000); *C*, Petaluma River (11459150).

Correlation Coefficient

The correlation coefficient (R) is a measure of model fit that explains how well the trends in the simulated values match the trends of the observed values. R is defined as follows (Doherty, 2016):

$$R = \frac{\sum_m \left(w_m \cdot h_m^{obs} - \overline{h}^{obs}\right) \cdot \left(w_m \cdot h_m^{sim} - \overline{h}^{sim}\right)}{\sqrt{\sum_m (w_m \cdot h_m^{obs} - \overline{h}^{obs})^2 \cdot \sum_m (w_m \cdot h_m^{sim} - \overline{h}^{sim})^2}} \quad \text{(D2)}$$

where

R is the correlation coefficient,
h_m^{obs} is the value of observation m (note that this includes observations of groundwater altitude, streamflow, and prior information),
$\overline{h}^{obs}$ is the mean of the weighted observed values,
h_m^{sim} is the simulated value corresponding to observation m,
$\overline{h}^{sim}$ is the mean of the weighted simulated values, and
W_m is the weight of the m^{th} observation.

Generally, a value of R greater than 0.9 indicates that the fit between the simulated and observed trends is acceptable (Hill and Tiedeman, 2007). The R value for all the data used to calibrate the PVIHM was 0.998, indicating an acceptable fit between simulated and observed trends.

Parameter Sensitivity

Quantifying the parameter sensitivity to simulated results is an important step in judging the performance of a complex hydrologic model (Hill and Tiedeman, 2007). A sensitivity analysis was performed on the model parameters to test the robustness of the estimated parameter values. The sensitivity of each parameter is a measure of how much the simulated values (each corresponding to an observation) change with respect to a change in the parameter value. Parameter sensitivities indicate which parameters can be estimated using the available data and give a sense of the tolerance within which model parameters can vary without substantially changing the model calibration. More sensitive parameters can only change a small amount before the model is out of calibration, whereas less sensitive parameters can change a large amount. Some parameters are more sensitive to the prior information than to the simulated values and have their final calibrated values determined mostly by the prior-information constraint. The sensitivity analysis also delineates the parameters that are well estimated and that influence the simulation results.

The final, calibrated parameters represent the set of parameters that minimized the sum of the squared residuals between each observed and simulated value, including the prior-information constraints placed on the parameters. In a complex hydrologic model, however, the calibrated parameter set can be varied by large amounts and generate similar model results with a similar objective function value (Anderson and others, 2015). The final, calibrated parameter set can be viewed as a single set of parameters from an entire range of parameter sets that also could calibrate the model; this is known as nonuniqueness.

The composite sensitivity of a model parameter is defined by the following equation (Doherty, 2016):

$$S_n = \frac{\sqrt{\sum_m (J_{mn} * w_m)^2}}{z} \quad \text{(D3)}$$

where

S_n is the composite sensitivity of the n^{th} parameter,
J_{mn} is the change in the simulated value for the m^{th} observation with respect to a change in the n^{th} parameter value (the m-by-n matrix of all these changes is known as the Jacobian matrix),
w_m is the weight of the m^{th} observation (same as used during calibration),
z is the normalization factor (set to the number of observations by PEST),
n is the number of parameters, and
m is the number of observations.

Multiplying the composite sensitivity by the parameter value (P_n) results in the relative composite sensitivity, which allows for a better comparison of composite sensitivities for parameters of different magnitudes. Figure D35 shows the composite sensitivity of the 25 most sensitive parameters ranked in order from the most to the least sensitive.

The results indicate that the most sensitive parameters are the crop coefficients for several irrigated crops (grain, orchards, and vineyards), which affect water demand and groundwater pumpage. The precipitation runoff and crop coefficients for pasture, grain, and native vegetation were also highly sensitive parameters. These parameters control how much excess precipitation there is on native lands (crop coefficient) and how much of this excess precipitation runs off compared to percolating (precipitation runoff coefficient). The irrigation efficiency multiplier, which affects the water demand for crops (and thus groundwater pumpage) in the PVIHM, is also a sensitive parameter.

Among the aquifer parameters, the hydraulic-conductivity-related parameters (HK, HANI, and VANI) for the Petaluma Formation were highly sensitive in many model layers (fig. D35). The high sensitivity is likely a result of the many observation wells within the Petaluma Formation. In addition, many observation wells are down gradient from the Petaluma Formation, which affects groundwater altitudes in the rest of the model. Other sensitive aquifer parameters either contain many calibration wells, such as the hydraulic conductivity of layer 2 in the Wilson Grove Formation, or they affect the gradient in the model.

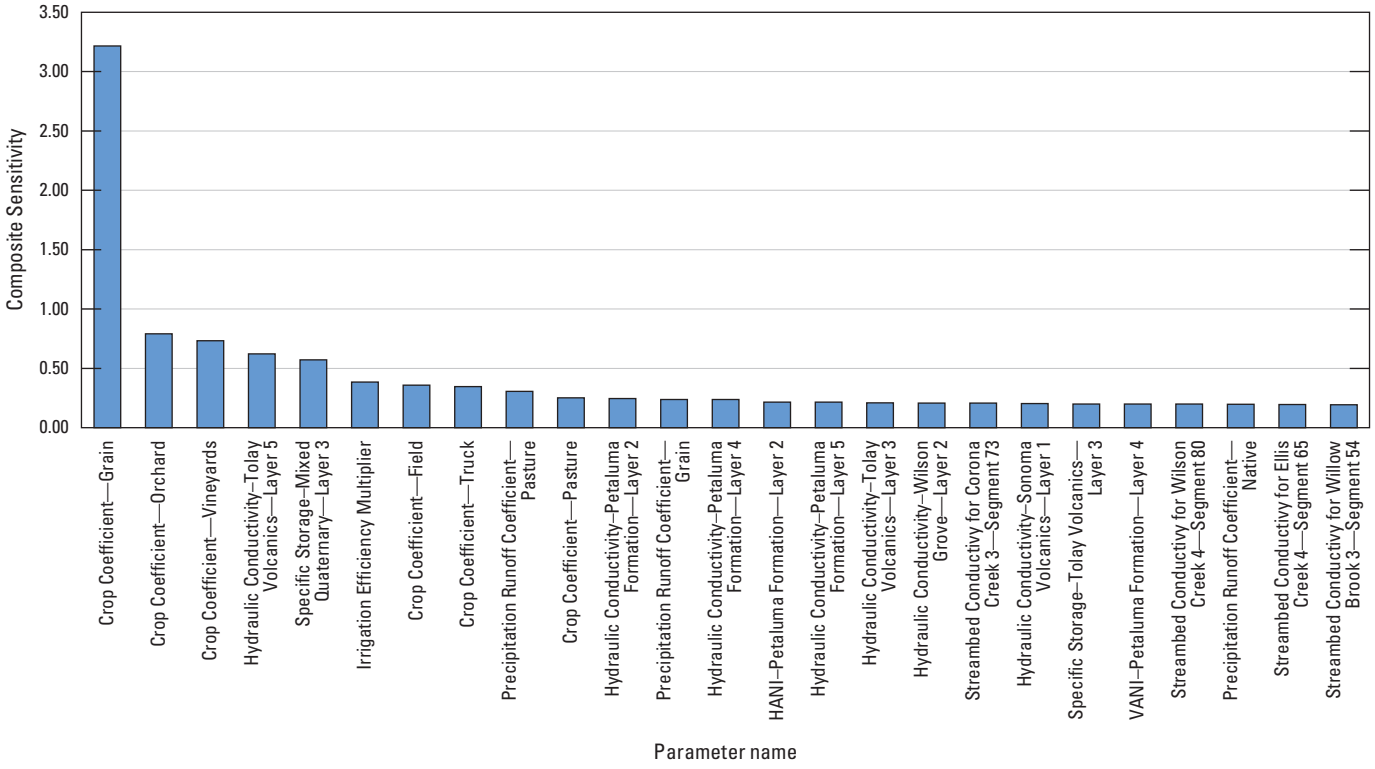

Figure D35. Relative composite sensitivities of the 25 most sensitive parameters of Petaluma Valley Integrated Hydrologic Model parameters, Petaluma valley watershed, Sonoma County, California. Calibrated parameter values are located in tables D12–D15. HAVI, horizontal anisotropy parameter; VANI, vertical anisotropy parameter.

There are limitations to the presented analyses that must be discussed. First, computations of the PVIHM sensitivities assume that simulated values vary linearly with changes in parameter values. In reality, model sensitivity may increase because of non-linear responses of the model to changes in parameter values. Second, the sensitivity analysis only measures the variability of the simulated values that correspond to observations. One of the main purposes of PVIHM is to provide a tool that can be used to evaluate groundwater sustainability indicators that support a future SGMA groundwater-sustainability plan. These groundwater sustainability indictors include model outputs, such as groundwater and surface-water interaction, change in groundwater storage, and boundary flow at the San Pablo Bay boundary (an indication of possible seawater intrusion). Model outputs, such as groundwater recharge and agricultural pumpage, are also important to the SGMA planning process. Model observations do not correspond to these indicators, however, and some parameters may be insensitive to the observations of groundwater altitude and streamflow but sensitive to the SGMA-related model outputs. The sensitivity of the calibrated parameter values to these model outputs is beyond the scope of this report but can be explored in a predictive uncertainty analysis.

Model Results

Model results presented in this section include simulated water budgets for groundwater, land surface, and streamflow; simulated groundwater-altitude hydrographs; and simulated groundwater-altitude maps. Model output was temporally available for every time step and spatially available for each subregion (land surface) or for each model cell (groundwater and streamflow). Spatial and temporal averaging of model results were used to document model results in this chapter.

Simulated Water Budgets

Presented water budgets include groundwater (or zone), the land-surface (or water-use), and streamflow budgets. The key components for each of these water budgets are shown and defined in table D16. Some budget components are reported in more than one budget (such as agricultural groundwater pumpage), and slight differences in values are possible for the same component in different budgets because of rounding. Positive values indicate inflows to the budgeted system, and negative values indicate outflows from the budgeted system. As an example, "root uptake" in the groundwater budget is negative because the crops are removing groundwater from the aquifer system; however, "root uptake" in the land-surface budget is positive because water is being added (supplied) to the land-surface system.

Groundwater Budget

The groundwater budget provides information regarding the simulated balance of flows into and out of the aquifer system. This section presents three methods of summarizing the groundwater budget: (1) as average annual values for the entire simulation period (fig. D36), (2) as annual totals from WY 1960 to 2015 (fig. D37), and (3) as average annual values by subregion for the entire simulation period (table D17) and for the last years of the simulation period (table D18).

Table D16. Simulated water-budget components for the Petaluma Valley Integrated Hydrologic Model, Petaluma valley watershed, Sonoma County, California.

Budget component	Description
	Groundwater budget
Upland boundary flow	General head boundary flow from the Wilson Grove and Santa Rosa Plain.
Bay boundary flow	General head boundary flow from San Pablo Bay and the tidally influenced part of the Petaluma River.
Stream seepage[1]	Groundwater gain from the stream network.
Stream discharge[1]	Groundwater loss to the steam network.
Agricultural pumpage	Groundwater pumpage to meet demand of irrigated crops.
Rural pumpage	Groundwater pumpage to meet demand of rural indoor and outdoor water use.
Municipal pumpage	Groundwater pumpage at City of Petaluma municipal wells.
Percolation[2]	Percolation of precipitation or irrigation water from the land surface into the groundwater system.
Root uptake[2]	Uptake of shallow groundwater by crops into the land surface system.
Inter-region flow	Net subsurface flow from one subregion to another.
Change in storage	Difference between all groundwater recharge and groundwater discharge sources.
	Land surface budget
Precipitation	Rainfall on the land surface.
Root uptake[2]	Uptake of shallow groundwater by crops to the land-surface system.
Surface water	Delivery of surface water (includes recycled water).
Agricultural pumpage	Groundwater pumpage to meet demand of irrigated crops.
Rural pumpage	Groundwater pumpage to meet demand of rural indoor and outdoor water use.
Evapotranspiration	Water moved from the land surface to the air by evaporation from the soil and transpiration from crops.
Runoff	Drainage of water from the land surface to the stream system.
Percolation[2]	Percolation of precipitation or irrigation water from the land surface to the groundwater system.
	Streamflow budget
Runoff	Drainage of water from the land surface to the stream system.
Net stream seepage	Groundwater loss to the steam network minus groundwater gain from the stream network.
Petaluma River outflow	Flow out of the model from the Petaluma River.
Tolay Creek outflow	Flow out of the model from Tolay Creek.
Marsh drainage outflow	Flow out of the model from several small unnamed streams that flow directly to Petaluma marsh.

[1]Net stream seepage is the sum of steam seepage and stream discharge.

[2]Net percolation is the difference between percolation and root uptake.

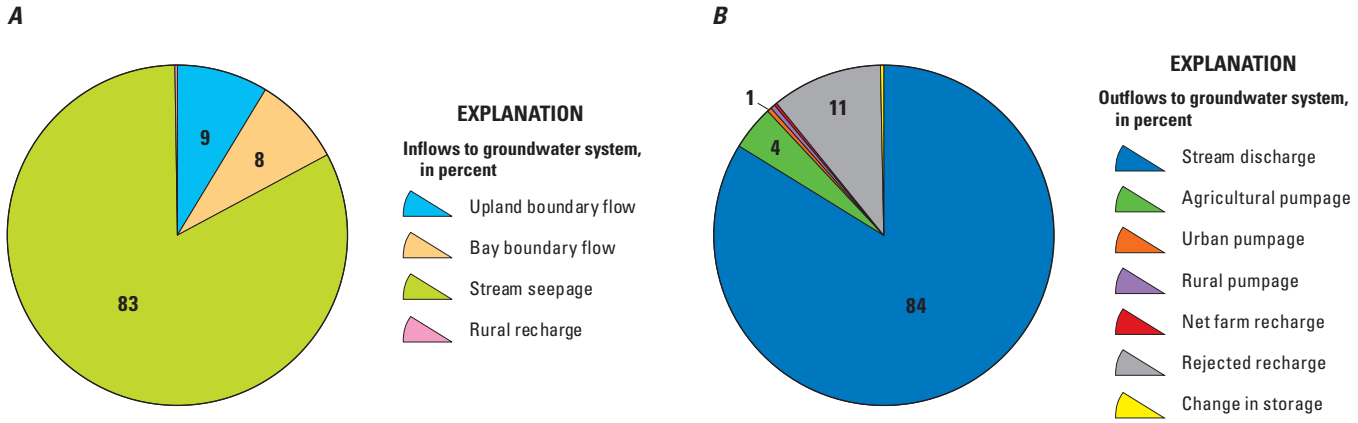

Figure D36. Average annual groundwater-budget components for water years 1960–2015, Petaluma Valley Integrated Hydrologic Model (Traum, 2022), Petaluma valley watershed, Sonoma County, California: *A*, inflows; *B*, outflows.

The average annual groundwater budget for the entire simulation period (fig. D36) can be used to understand the long-term averages for each budget component. The average annual water budget indicated that stream seepage to groundwater is the predominant inflow to the groundwater system (83 percent, fig. D36*A*). Other sources of inflow include upland boundary flow (9 percent) and San Pablo Bay boundary flow (8 percent). Groundwater discharge to streams is the predominant outflow from the groundwater system (84 percent, fig. D36*B*). Other sources of outflow include water sent to the stream network to prevent simulation of groundwater altitudes above land surface (rejected recharge; 11 percent) and agricultural groundwater pumpage (4 percent). Urban pumpage, rural pumpage, and net farm recharge account for less than 1 percent each of total groundwater outflow. Average annual change in storage during the simulation period was less than 1 percent (399 acre-ft/yr) of the total groundwater outflows.

The average annual totals of the groundwater budget (fig. D37) can be used to understand how the components of the groundwater budget change through time during the simulation period. Many of the groundwater-budget components, such as percolation, depend on climate. For example, percolation was highest in WY 1982 (an extremely wet year) and WY 1978 (a wet year after multiple dry years); in contrast, percolation was lowest in WY 1976 and 1977 (dry years). Other components, such as agricultural pumpage, are more complex because they depend on a variety of factors. Agricultural pumpage depends on precipitation because more pumpage is required during dry years as a result of decreased precipitation and associated surface-water deliveries. Agricultural pumpage also depends on other factors, however, such as land use and other crop-related variables. For example, during WY 1987 (a dry year), pumpage was triple that of WY 1983 (a wet year), and land use did not change substantially between the 1979 and 1986 surveys. Therefore, other factors contributed to the pumpage differences in these years, such as the difference in water availability during dry and wet years. Finally, increases in agricultural pumpage in later years (WY 2000–15 average of 8,000 acre-ft/yr; table D18) compared to the entire model period (WY 1960–2015 average of 5,400 acre-ft/yr; table D17) can likely be attributed to an increase in irrigated land acreage in the last 15 years compared to historical land use (chapter A, figs. A6–A10).

Figure D37 shows the time-varying cumulative change in aquifer storage. Although the long-term change in storage was nearly zero (average loss in storage of 400 acre-ft/yr), individual years showed large variation in storage gains and losses related primarily to climate variability. The largest gain in storage was in WY 1978 (20,100 acre-ft gain), a wet year following an extremely dry period. Other years with large gains in groundwater storage include WYs 1995, 1982, 1973, and 1998. The largest decline in storage was in WY 1976 (18,700 acre-ft loss), a dry year. Other years with large depletions of groundwater storage include WYs 2007, 1977, 1984, and 1964.

Table D17 shows the average annual groundwater-budget components by subregion. Groundwater discharge to streams (-107,500 acre-ft/yr), however, and stream seepage to the groundwater system (105,300 acre-ft/yr) make up the largest inflows and outflows for the groundwater system, respectively. The results show that the model-wide net stream seepage to groundwater was -2,300 acre-ft/yr (indicating that on average the groundwater system is discharging water to the stream network). Other sources of groundwater inflow are upland boundary flow (11,000 acre-ft/yr), inflow from the tidally influenced portion of the Petaluma River and San Pablo Bay (10,800 acre-ft/yr), and percolation of precipitation and irrigation water (23,000 acre-ft/yr). Other sources of groundwater outflow are root uptake of shallow groundwater (23,300 acre-ft/yr), agriculture pumpage (5,400 acre-ft/yr), rural pumpage (500 acre-ft/yr), municipal pumpage (500 acre-ft/yr).

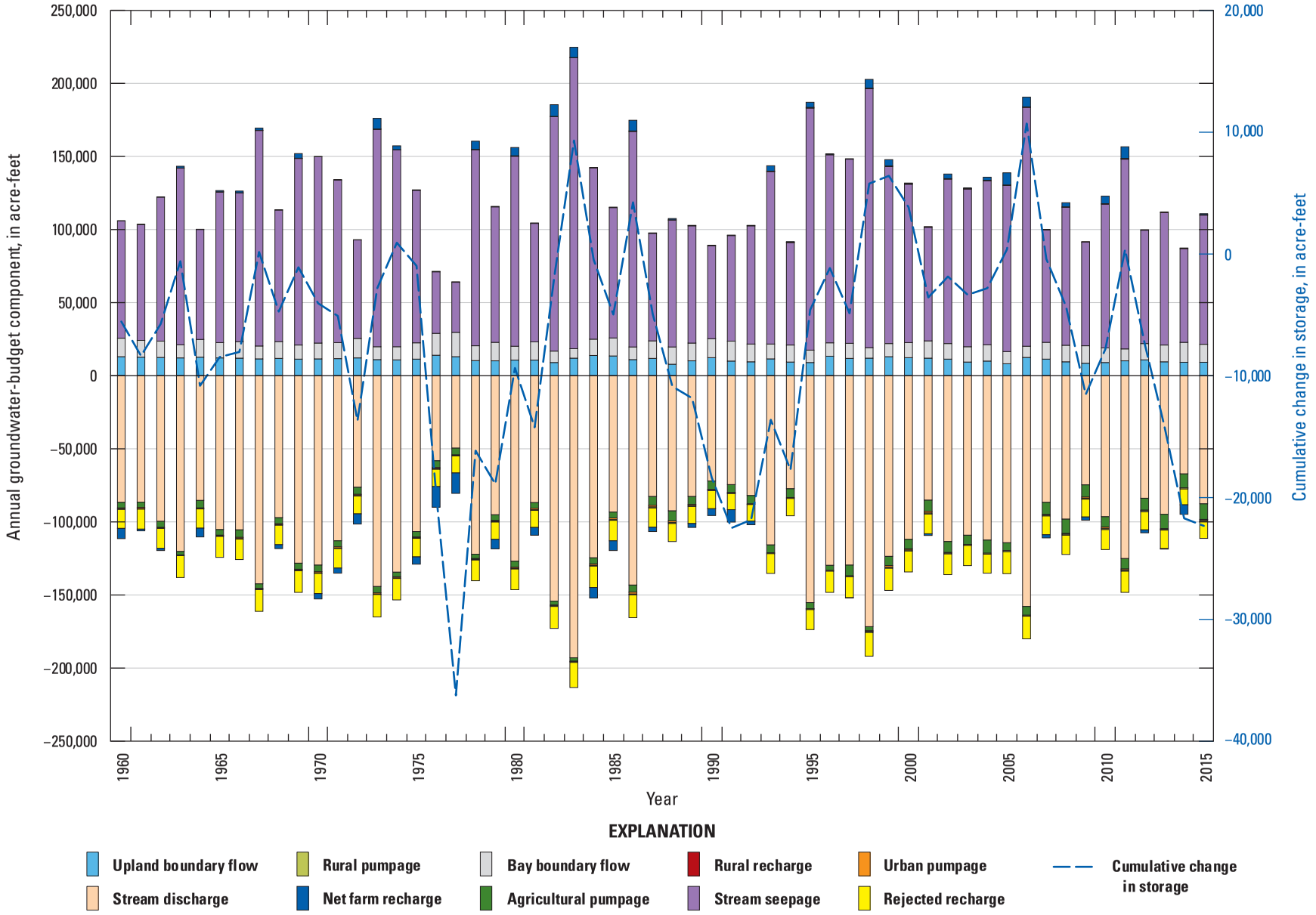

Figure D37. Annual total groundwater inflows and outflows and cumulative change in storage, water years 1960–2015, Petaluma Valley Integrated Hydrologic Model (Traum, 2022), Petaluma valley watershed, Sonoma County, California.

Table D17. Petaluma Valley Integrated Hydrologic Model (Traum, 2022) average annual groundwater budget in acre-feet per year by subregion for water years 1960–2015, Petaluma valley watershed, Sonoma County, California.

[OWS, outside of watershed]

Sub-region	Name	Upland boundary flow	Bay boundary flow	Stream seepage	Stream discharge	Agricultural pumpage	Urban pumpage	Rural pumpage	Rural recharge	Net percolation	Rejected recharge	Inter-region flow	Change in storage
1	Wilson Grove	11,300	0	10,300	–10,700	–200	0	–300	200	1,300	–2,000	–10,000	0
2	Upper Petaluma River	–100	0	2,000	–9,600	0	0	0	0	300	–100	7,400	0
3	Lynch Creek	–300	0	24,900	–15,100	–700	0	–100	0	2,400	–100	–11,100	–100
4	Lichau Creek	200	0	5,600	–9,900	–200	0	0	0	1,400	0	2,900	–100
8	City of Petaluma Wilson Grove	0	–200	0	–100	–200	0	0	0	200	0	300	0
10	City of Petaluma	0	–6,100	8,400	–14,900	–1,100	–500	–100	0	1,500	0	12,900	0
11	Adobe Creek	0	0	21,500	–18,700	–1,000	0	0	0	1,500	0	–3,400	0
17	Lower Petaluma River	0	4,400	3,800	–2,200	–700	0	0	0	–3,800	0	–1,400	0
18	North Bay Water District	0	12,700	8,300	–9,900	–400	0	0	0	–7,100	–11,400	7,700	0
19	Stage Gulch	0	0	6,200	–2,800	–100	0	0	0	800	0	–4,200	0
21	Tolay Creek OWS	0	0	14,100	–13,500	–900	0	0	0	1,200	0	–1,000	–100
Total[1]	—	11,000	10,800	105,300	–107,500	–5,400	–500	–500	300	–300	–13,500	0	–400

[1]Total may not equal the sum of each subregion due to rounding.

Table D18. Petaluma Valley Integrated Hydrologic Model (Traum, 2022) average annual groundwater budget in acre-feet per year by subregion for water years 2000–2015, Petaluma valley watershed, Sonoma County, California.

[OWS, outside of watershed]

Sub-region	Name	Upland boundary flow	Bay boundary flow	Stream seepage	Stream discharge	Agricultural pumpage	Urban pumpage	Rural pumpage	Rural recharge	Net farm recharge	Rejected recharge	Inter-region flow	Change in storage
1	Wilson Grove	9,500	0	9,500	–9,500	–300	0	–400	300	1,400	–1,200	–9,400	–200
2	Upper Petaluma River	–100	0	1,900	–8,900	–100	0	0	0	400	0	6,800	–100
3	Lynch Creek	–100	0	22,500	–13,300	–1,000	0	–100	0	2,300	–100	–10,900	–500
4	Lichau Creek	800	0	5,600	–10,200	–300	0	0	0	1,200	–100	2,700	–300
8	City of Petaluma Wilson Grove	0	–200	0	–100	–200	0	0	0	200	0	300	0
10	City of Petaluma	0	–6,000	8,000	–14,500	–300	–400	–100	0	700	0	12,400	–100
11	Adobe Creek	0	0	20,500	–17,600	–2,300	0	0	0	2,200	0	–3,000	–100
17	Lower Petaluma River	0	4,600	3,700	–2,200	–700	–100	0	0	–3,900	0	–1,400	0
18	North Bay Water District	0	12,400	8,500	–10,100	–600	0	0	0	–5,700	–11,900	7,300	–100
19	Stage Gulch	0	0	5,800	–2,500	–200	0	0	0	800	0	–4,000	–100
21	Tolay Creek OWS	0	0	13,100	–12,400	–2,100	0	0	0	1,900	0	–900	–400
Total[1]	—	10,100	10,700	99,200	–101,200	–8,000	–400	–700	400	1,500	–13,300	0	–1,800

[1]Total may not equal the sum of each subregion due to rounding.

Many subregions (such as 3, 11, and 19), however, showed large average gains to the groundwater system from the stream. Net percolation (representing the difference between percolation and root uptake) was positive throughout the model, except in subregions 17 and 18, where groundwater altitudes in the Petaluma marsh were generally near land surface and root uptake caused negative net-percolation values. The Wilson Grove Formation Highlands groundwater basin contributes most of the upland boundary inflow to the model area (subregion 1 upland boundary inflow of 11,300 acre-ft/yr). The San Pablo Bay boundary flow for subregion 18 (12,700 acre-ft/yr) indicates an inflow of groundwater for the bay. Farther inland, however, in subregion 10 (City of Petaluma), bay boundary flow was negative (-6,100 acre-ft/yr), which indicates an outflow of groundwater to tidally influenced parts of the Petaluma River and its tributaries and indicates that infiltration of saline water that far inland is not likely. Net inflows from San Pablo Bay and tidally influenced parts of the Petaluma River varied monthly and by wet and dry periods.

Land-Surface Budget

The land-surface budget provides information about the water demand of crops and other plants in the study area and the various water supplies that meet this demand. This section presents four approaches to summarizing the land-surface budget: total annual values (fig. D38), average monthly values (fig. D39), average annual values by subregion (tables D19, D20), and average annual values by crop (tables D21, D22).

The total annual land-surface budget for the PVW from WY 1960 to 2015 can be used to understand the annually varying components of the land-surface budget (fig. D38). Many of the land-surface-budget components depend on precipitation, which was the primary water source for the study area. Percolation ranged from 7,100 acre-ft/yr in dry conditions (WY 1977) to 34,000 acre-ft/yr in wet conditions (WY 1983).

The monthly average land-surface budget for the PVW can be used to understand the seasonal components of the land-surface budget (fig. D39). From October to May, precipitation is the major source of water supply. Excess precipitation that is not used by ET becomes either runoff or percolation, with most becoming runoff, based on the relatively high fractions of precipitation to runoff (see "fraction of excess precipitation to runoff" in table D3). During the growing season, root uptake and agricultural pumpage become more important sources of water supply and are the major water sources in July to August. From May to September, most supply that is not consumed by ET because of inefficient irrigation becomes percolation, based on low fractions of irrigation to runoff (see "fraction of excess irrigation to runoff" in table D3). Evapotranspiration is also reduced during summer months (when compared to potential ET) because non-irrigated crops and native and riparian vegetation wilt from a lack of water. Surface-water delivery is not a large source of supply in any month.

The annual average land-surface budget (from WYs1960 to 2015) for each subregion can be used to understand the spatial distribution of supply and demand (table D19). For example, only subregions that are active for groundwater simulation (subregions 1, 2, 3, 4, 8, 10, 11, 17, 18, 19, and 21) can use agricultural pumpage to meet supply and generate percolation to groundwater. Most of the agricultural pumpage is from subregions 3, 10, and 21. Groundwater is taken up by plants in subregions that overlie the Petaluma marsh and that have generally shallow water tables (subregions 10, 17, and 18), where root update is a major form of groundwater discharge (supply to the land-surface budget) from the study area. In more recent periods, agricultural pumpage increased from 5,400 to 8,000 acre-ft/yr (tables D19, D20), likely as a result of an increase in irrigated-land acreage in the past 15 years compared to historical land use. Surface-water delivery has also increased from 800 to 1,800 acre-ft/yr (tables D19, D20) because of the increased use of recycled water for agriculture.

The annual average land-surface budget (from WYs 1960 to 2015) for each crop can be used to understand how much each crop type contributes to the different supply and demand components of the land-surface budget (table D21). For example, most of the runoff in the PVW (94,900 acre-ft/yr) is from native land use (table D21). Most of the demand in the PVW (3,500 acre-ft/yr) is from grain crops, which make up the majority of the irrigated area in the study area (table D21). In more recent periods, demand from pasture has increased from 2,000 to 5,500 acre-ft/yr, and demand from vineyards has increased from 300 to 1,100 acre-ft/yr, due to an increase in irrigated area for both crops (tables D21, D22).

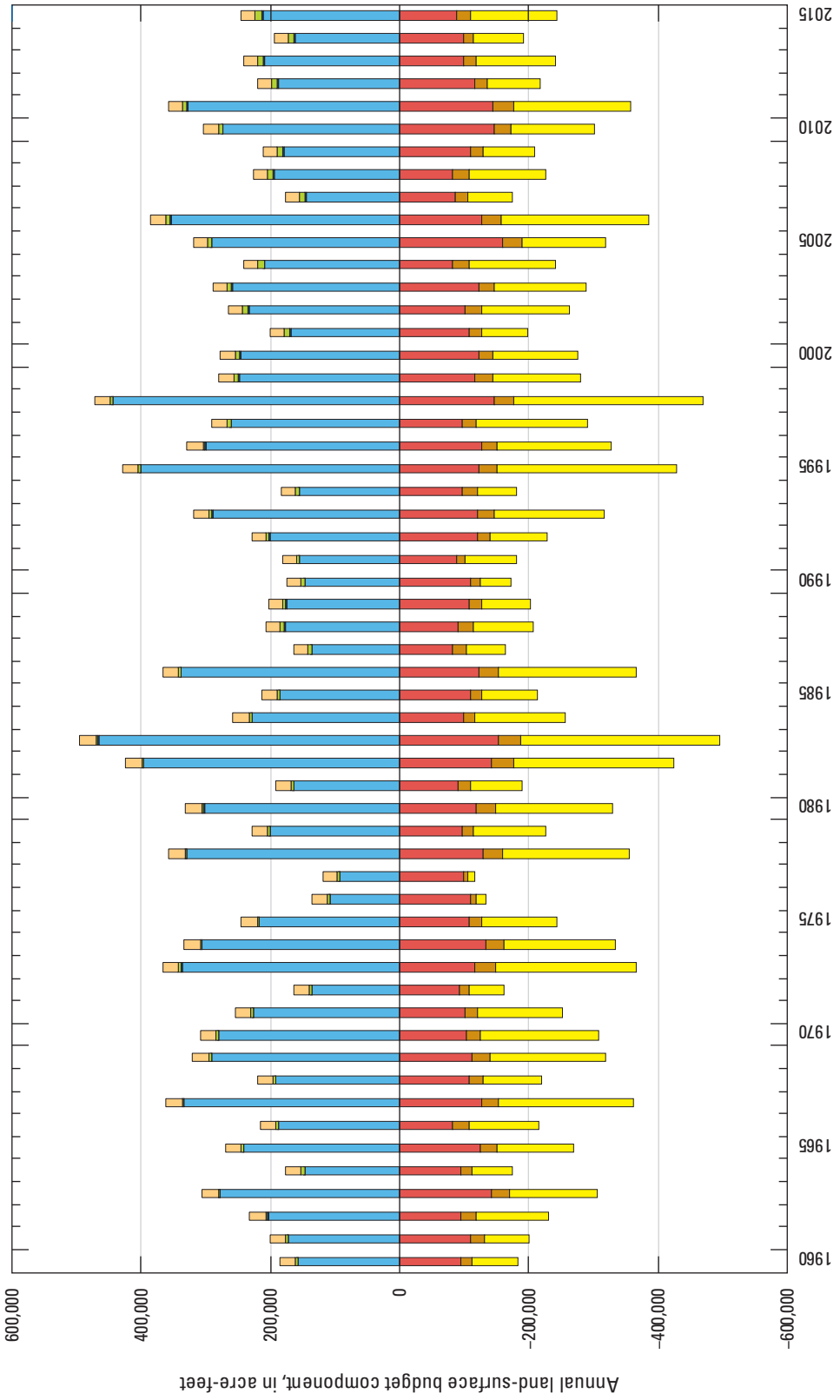

Figure D38. Annual total land-surface budget, water years 1960–2015, Petaluma Valley Integrated Hydrologic Model (Traum, 2022), Petaluma valley watershed, Sonoma County, California.

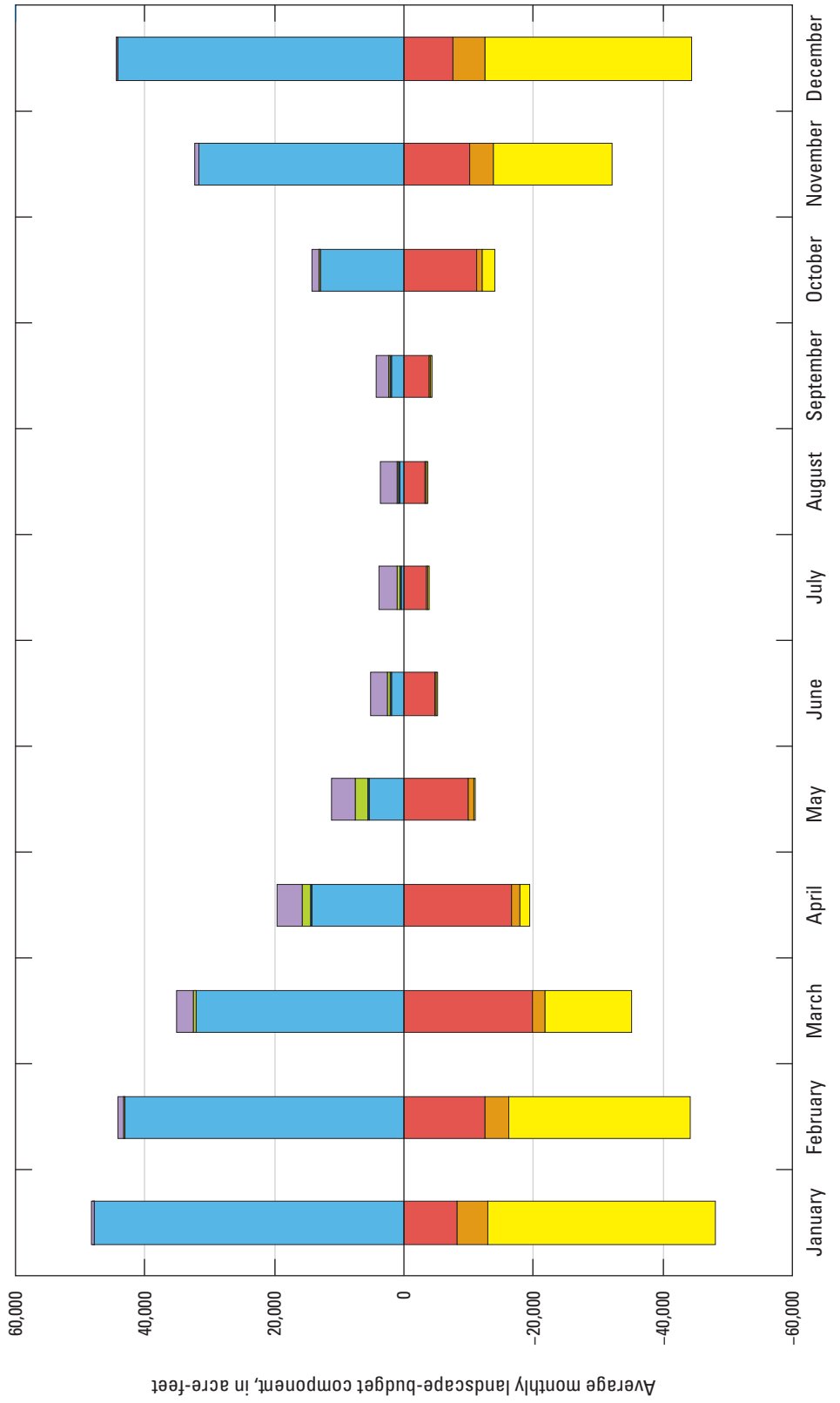

Figure D39. Monthly average land-surface budget, water years 1960–2015, Petaluma Valley Integrated Hydrologic Model (Traum, 2022), Petaluma valley watershed, Sonoma County, California.

Table D19. Petaluma Valley Integrated Hydrologic Model (Traum, 2022) average annual values of land-surface budget by subregion for water years 1960–2015, Petaluma valley watershed, Sonoma County, California.

[acre-ft/yr, acre-feet per year; OGWB, outside of groundwater basin; OWS, outside of watershed]

Subregion	Name	Area (acres)	Supply (acre-ft/yr)				Demand (acre-ft/yr)		
			Precipitation	Surface water	Agricultural pumpage	Root uptake	Evapotranspiration	Percolation	Runoff
[1]1	Wilson Grove	6,916	15,800	0	200	900	6,800	2,200	7,800
[1]2	Upper Petaluma River	1,757	3,900	0	0	400	2,000	800	1,600
[1]3	Lynch Creek	5,960	13,600	0	700	300	5,900	2,600	6,000
[1]4	Lichau Creek	4,604	10,500	0	200	200	4,000	1,600	5,300
5	Lynch Creek OGWB	4,893	14,800	0	0	0	5,300	0	9,600
6	Upper San Antonio Creek	9,385	24,500	0	0	0	9,400	0	15,000
7	Upper Petaluma River OGWB	1,134	2,800	0	0	0	1,100	0	1,700
[1]8	City of Petaluma Wilson Grove	623	1,300	0	200	0	500	200	700
9	City of Petaluma OGWB	1,490	3,300	0	0	0	1,100	0	2,200
[1]10	City of Petaluma	7,206	15,000	100	1,100	1,300	6,900	2,700	7,800
[1]11	Adobe Creek	3,625	8,500	200	1,000	300	4,200	1,700	3,900
12	Adobe Creek OGWB	5,449	16,600	0	0	0	6,000	0	10,600
13	Lower San Antonio Creek	10,141	26,100	0	0	0	9,900	0	16,200
14	Lower Petaluma River OGWB	2,268	5,200	0	0	0	2,100	0	3,100
15	Basalt Creek	5,093	12,300	0	0	0	4,800	0	7,500
16	Bay Mud OGWB	3,536	7,600	0	0	0	3,200	0	4,400
[1]17	Lower Petaluma River	5,849	12,300	100	700	6,200	10,700	2,300	6,300
[1]18	North Bay Water District	10,964	23,200	100	400	13,100	19,200	6,100	11,500
[1]19	Stage Gulch	3,380	7,700	0	100	300	3,500	1,000	3,600
20	Stage Gulch OGWB	1,134	2,700	0	0	0	1,100	0	1,600
[1]21	Tolay Creek OWS	3,425	8,100	300	900	500	4,000	1,700	4,000
Total[2]	—	98,832	235,900	800	5,400	23,300	112,000	23,000	130,500

[1]Groundwater simulation is active.

[2]Total may not equal the sum of each subregion due to rounding.

Table D20. Petaluma Valley Integrated Hydrologic Model (Traum, 2022) average annual land-surface budget by subregion for water years 2000–2015, Petaluma valley watershed, Sonoma County, California.

[acre-ft/yr, acre-feet per year; OGWB, outside of groundwater basin; OWS, outside of watershed]

Sub-region	Name	Area (acres)	Supply (acre-ft/yr)				Demand (acre-ft/yr)		
			Precipitation	Surface water	Agricultural pumpage	Root uptake	Evapotranspiration	Percolation	Runoff
[1]1	Wilson Grove	6,916	15,400	0	300	700	6,700	2,100	7,700
[1]2	Upper Petaluma River	1,757	3,800	0	100	300	1,900	700	1,600
[1]3	Lynch Creek	5,960	12,900	0	1,000	300	6,000	2,600	5,600
[1]4	Lichau Creek	4,604	10,000	0	300	300	4,000	1,400	5,100
5	Lynch Creek OGWB	4,893	14,000	0	0	0	5,400	0	8,600
6	Upper San Antonio Creek	9,385	24,000	0	0	0	9,600	0	14,400
7	Upper Petaluma River OGWB	1,134	2,800	0	0	0	1,100	0	1,600
[1]8	City of Petaluma Wilson Grove	623	1,300	0	200	0	600	200	700
9	City of Petaluma OGWB	1,490	3,200	0	0	0	1,100	0	2,000
[1]10	City of Petaluma	7,206	14,200	300	300	1,200	6,400	1,900	7,700
[1]11	Adobe Creek	3,625	7,900	500	2,300	300	5,100	2,500	3,400
12	Adobe Creek OGWB	5,449	15,500	0	0	0	6,100	0	9,400
13	Lower San Antonio Creek	10,141	25,800	0	0	0	10,200	0	15,600
14	Lower Petaluma River OGWB	2,268	5,100	0	0	0	2,200	0	2,900
15	Basalt Creek	5,093	12,100	0	0	0	4,900	0	7,200
16	Bay Mud OGWB	3,536	7,300	0	0	0	3,100	0	4,100
[1]17	Lower Petaluma River	5,849	11,800	400	700	6,200	10,900	2,200	5,900
[1]18	North Bay Water District	10,964	22,200	200	600	12,200	18,100	6,400	10,700
[1]19	Stage Gulch	3,380	7,400	0	200	300	3,500	1,100	3,300
20	Stage Gulch OGWB	1,134	2,600	0	0	0	1,100	0	1,400
[1]21	Tolay Creek OWS	3,425	7,700	400	2,100	500	4,800	2,400	3,500
Total[2]	—	98,832	227,000	1,800	8,000	22,100	112,800	23,600	122,600

[1]Shading indicates groundwater simulation is active.

[2]Total may not equal the sum of each subregion due to rounding.

Table D21. Petaluma Valley Integrated Hydrologic Model (Traum, 2022) average annual land-surface budget by crop for water years 2000–2015, Petaluma valley watershed, Sonoma County, California.

[ID, identification; acre-ft/yr, acre-foot per year]

Crop name	Crop ID	Total area (acres)	Irrigated area (acres)	Precipitation (acre-ft/yr)	Root uptake (acre-ft/yr)	Demand (acre-ft/yr)	Evapotranspiration (acre-ft/yr)	Deep percolation (acre-ft/yr)	Runoff[1] (acre-ft/yr)
Bare land	0	6,682	0	14,200	100	0	4,000	1,200	4,900
Citrus	1	140	0	400	0	0	100	0	300
Orchard	2	68	8	200	0	0	0	0	100
Field	3	226	170	500	100	200	300	100	400
Grain	4	11,245	2,916	24,300	5,900	3,500	13,800	8,700	11,300
Native	5	68,152	0	169,800	7,500	0	74,000	8,400	94,900
Pasture	6	1,004	378	2,300	500	2,000	2,500	1,200	1,000
Riparian	7	6,408	0	13,500	8,700	0	13,000	1,600	7,500
SemiAg	8	1,217	74	2,700	0	0	700	500	1,600
Truck	9	163	63	400	100	200	300	100	300
Urban	10	1,831	0	3,900	100	0	1,700	300	2,000
Vineyards	11	506	382	1,100	0	300	400	500	600
Rural	12	1,189	0	2,700	200	0	1,100	300	1,500
Total[2]	—	98,832	3,992	235,900	23,300	6,200	112,000	23,000	126,200

[1]Includes rejected recharge by the Drain Return package, so this number is different from what is shown in the land-surface budget (table D19).

[2]Total may not equal the sum of each crop due to rounding.

Table D22. Petaluma Valley Integrated Hydrologic Model (Traum, 2022) average annual land-surface budget by crop for water years 2000–2015, Petaluma valley watershed, Sonoma County, California.

[ID, identification; acre-ft/yr, acre-foot per year]

Crop name	Crop ID	Total area (acres)	Irrigated area (acres)	Precipitation (acre-ft/yr)	Root uptake (acre-ft/yr)	Demand (acre-ft/yr)	Evapotranspiration (acre-ft/yr)	Deep percolation (acre-ft/yr)	Runoff[1] (acre-ft/yr)
Bare land	0	9,288	0	19,100	100	0	5,700	1,600	6,300
Citrus	1	156	0	400	0	0	100	0	300
Orchard	2	72	28	200	0	100	0	0	100
Field	3	183	117	400	100	200	200	100	300
Grain	4	11,748	2,179	24,400	7,000	2,400	14,300	8,300	11,200
Native	5	60,842	0	148,300	3,700	0	65,100	5,900	80,900
Pasture	6	2,007	1,090	4,400	400	5,500	5,400	3,100	1,800
Riparian	7	7,867	0	15,900	10,200	0	15,700	1,800	8,700
SemiAg	8	1,017	56	2,200	100	0	600	400	1,300
Truck	9	239	172	500	200	600	600	300	300
Urban	10	2,722	0	5,600	100	0	2,500	400	2,800
Vineyards	11	1,590	1,273	3,300	100	1,100	1,400	1,500	1,600
Rural	12	1,123	0	2,400	200	0	1,000	200	1,300
Total[2]	—	98,854	4,915	227,000	22,100	9,800	112,800	23,600	117,000

[1]Includes rejected recharge by the Drain Return package, so this number is different from what is shown in the land-surface budget (table D20).

[2]Total may not equal the sum of each crop due to rounding.

Streamflow Budget

The streamflow budget provides information about the inflows and outflows to the stream network in the study area. The streamflow budget for the Petaluma River is presented as annual totals from WYs 1960 to 2015 in figure D40. Values greater than zero (runoff to the river and net stream seepage from groundwater) indicate inflows, primarily to the Petaluma River, and values less than zero indicate outflows from the stream system. In general, runoff to streams was the predominant source of water to the river, with an average runoff of 200 ft^3/s, a minimum runoff of 31 ft^3/s in WY 1977 (a dry year), and a maximum runoff of 450 ft^3/s in WY 1983 (a wet year; fig. D40). Net stream seepage from groundwater averaged 3.0 ft^3/s, with a maximum of 22 ft^3/s in WY 1976 and a minimum of –17 ft^3/s in WY 1978. The negative net stream seepage in WY 1978 indicates a stream loss to the groundwater system and was likely caused by low groundwater altitudes from the WY 1976–77 drought. Most (88 percent) of the stream outflow to San Pablo Bay was through the Petaluma River (average of 180 ft^3/s). The remaining outflows were from Tolay Creek (7.7 ft^3/s, or 4 percent) and from unnamed drainages (14 ft^3/s, or 7 percent) that drain directly into the Petaluma marsh. Diversions from the stream for agricultural use accounted for less than 1 percent of outflows (1.2 ft^3/s average).

Simulated Groundwater Altitude, Flow, and Movement

Simulated groundwater altitudes are presented as groundwater-altitude maps to show the spatial extent of simulated groundwater altitude for selected dates and selected model layers. Simulated groundwater altitudes are presented at the 41 calibration wells (table D1) to show the temporal change in groundwater altitudes as comparing groundwater altitudes in different model layers at a specific point as well. Simulated groundwater and surface-water-exchange maps are presented to show reaches of the Petaluma River and its tributaries that are gaining water from or losing water to the groundwater system.

Simulated Groundwater Altitude Maps

Maps showing simulated groundwater altitudes were developed for the end of the simulation (September 2015, fig. D41), dry conditions (October 1977, fig. D42), and wet conditions (April 1983, fig. D43). October was selected to show simulated groundwater altitudes for dry conditions because groundwater altitudes are generally lower in early fall months because summer groundwater pumpage during the growing season has ended but seasonal precipitation typically has not started. April was selected to show simulated groundwater altitudes for wet conditions because groundwater altitudes are generally higher in later spring months after recharge from precipitation and before groundwater pumpage resumes in summer months.

Figures D41–D43 show observed groundwater altitudes at wells used to calibrate the model. The observed groundwater altitudes shown on the maps correspond with the model layer in which the wells are screened. Generally, observed groundwater altitudes also correspond with the month and year for which the simulated groundwater altitudes are shown. In some cases, however, observed groundwater altitudes might represent simulated data that are expected to have similar simulated groundwater altitudes. For example, an observation from March of 1983 in model layer 2 would be shown on the April 1983 map (fig. D43*B*) if that well was only sampled in March of 1983 (but not in April). The maps show that simulated groundwater altitudes generally match well with observed groundwater altitudes.

Simulated groundwater altitudes for September 2015 indicate that the general direction of groundwater flow was from the uplands toward the center axis of the valley and then south-southeast along the center axis of the valley toward San Pablo Bay (fig. D41), which agrees with interpretations from analysis of non-model results. In model layer 1, simulated groundwater altitudes ranged from 505 ft above the North American Vertical Datum of 1988 (NAVD 88) where Lichau Creek enters the groundwater basin to 4 ft below NAVD 88 near San Pablo Bay. Negative groundwater altitudes near San Pablo Bay are caused by evapotranspiration of shallow groundwater in Petaluma marsh and induced a net boundary inflow from San Pablo Bay of 12,274 acre-ft in 2015. Groundwater altitudes are generally similar in all model layers; however, local differences exist (fig. D41). For example, minimum simulated groundwater altitudes in model layer 3 are 19 ft below NAVD 88. Lower groundwater altitudes compared to layer 1 are caused by groundwater pumpage at wells screened in layer 2 and layer 3.

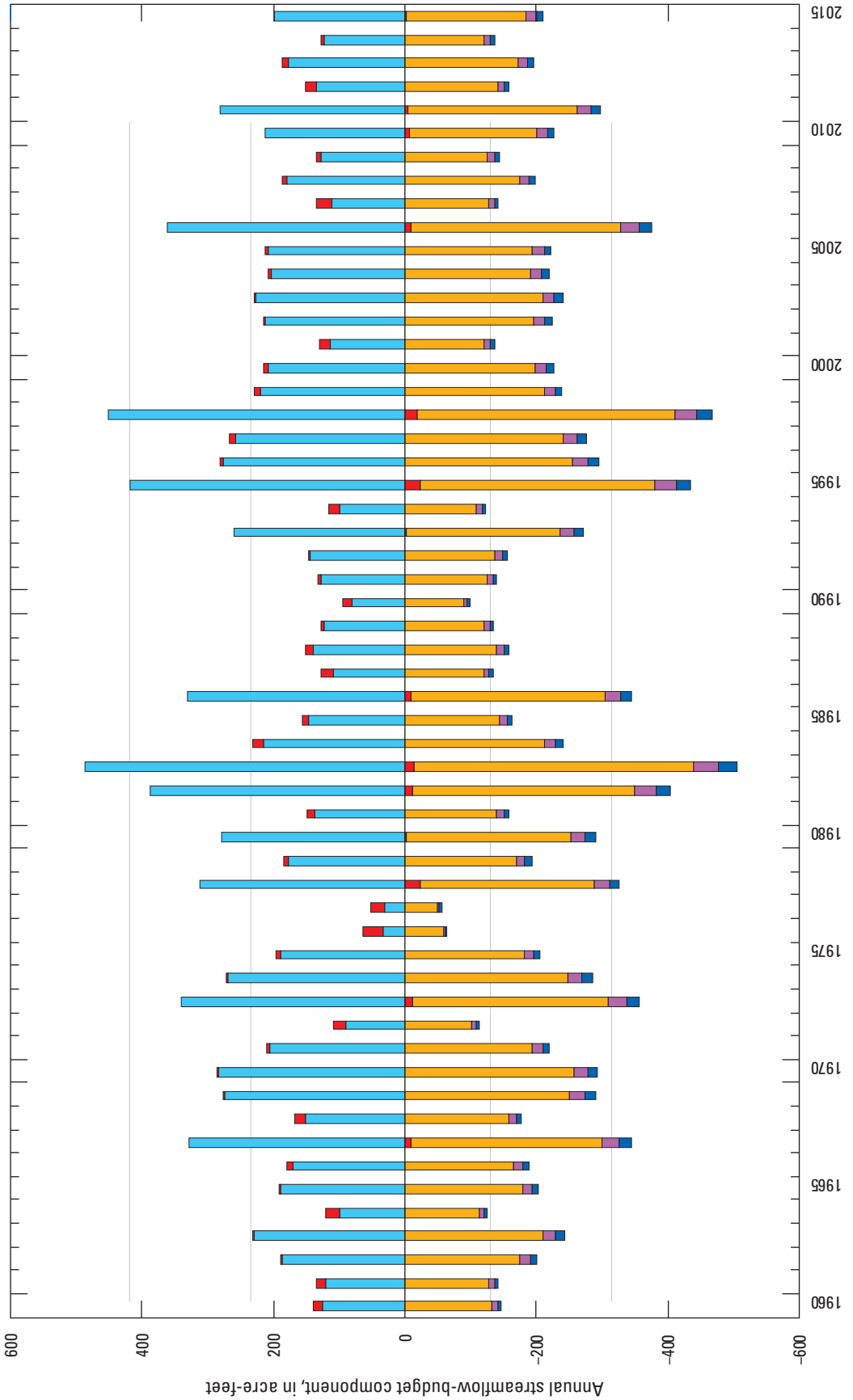

Figure D40. Annual total streamflow budget for the Petaluma Valley Integrated Hydrologic Model (Traum, 2022), water years 1960–2015, Petaluma valley watershed, Sonoma County, California.

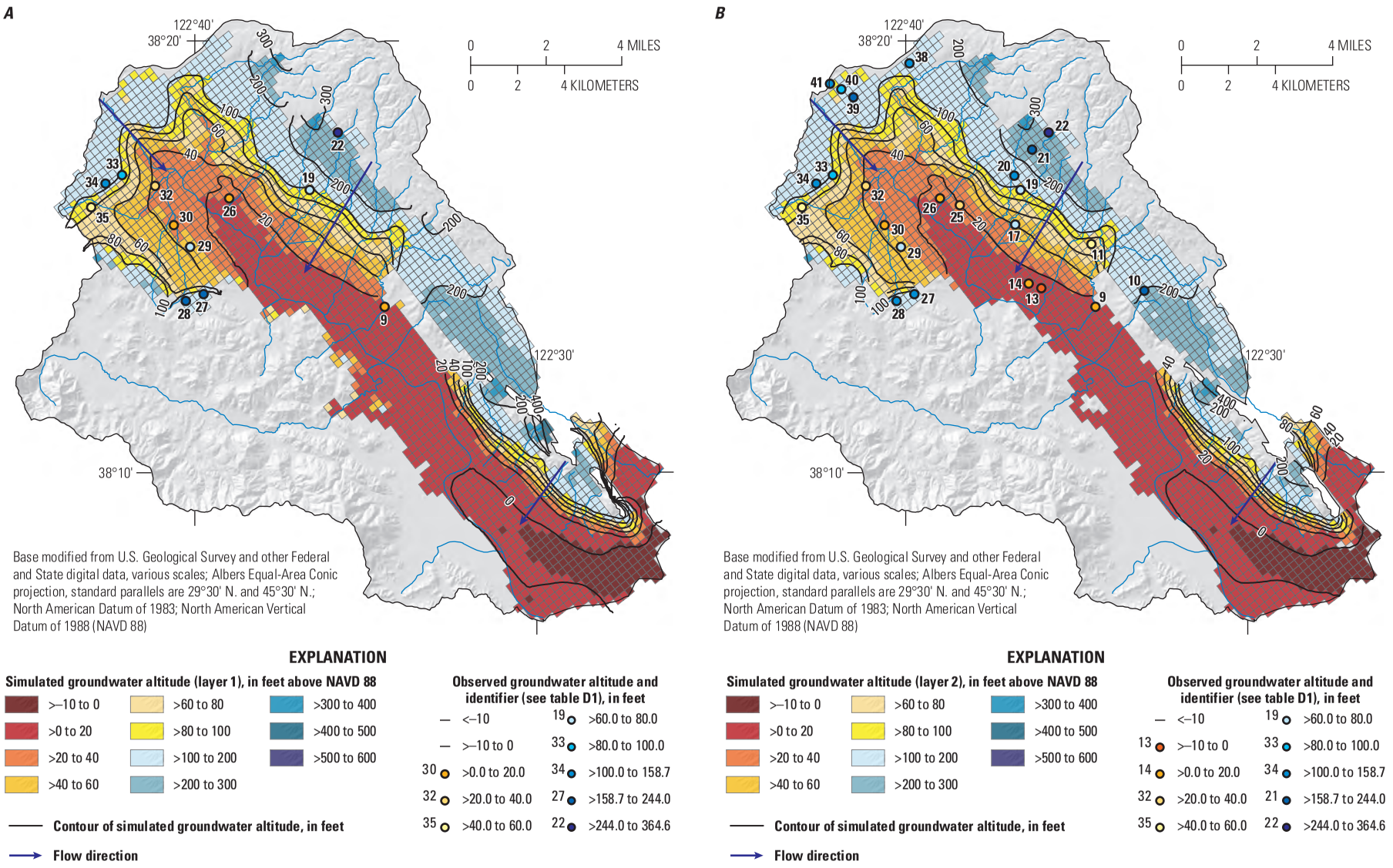

Figure D41. Simulated groundwater altitude in feet above North American Vertical Datum of 1988 (NAVD 88) at the end of the simulation (September 2015), the Petaluma Valley Integrated Hydrologic Model, Petaluma valley watershed, Sonoma County, California (Traum, 2022): *A*, model layer 1; *B*, model layer 2; *C*, model layer 3; *D*, model layer 4; *E*, model layer 5.

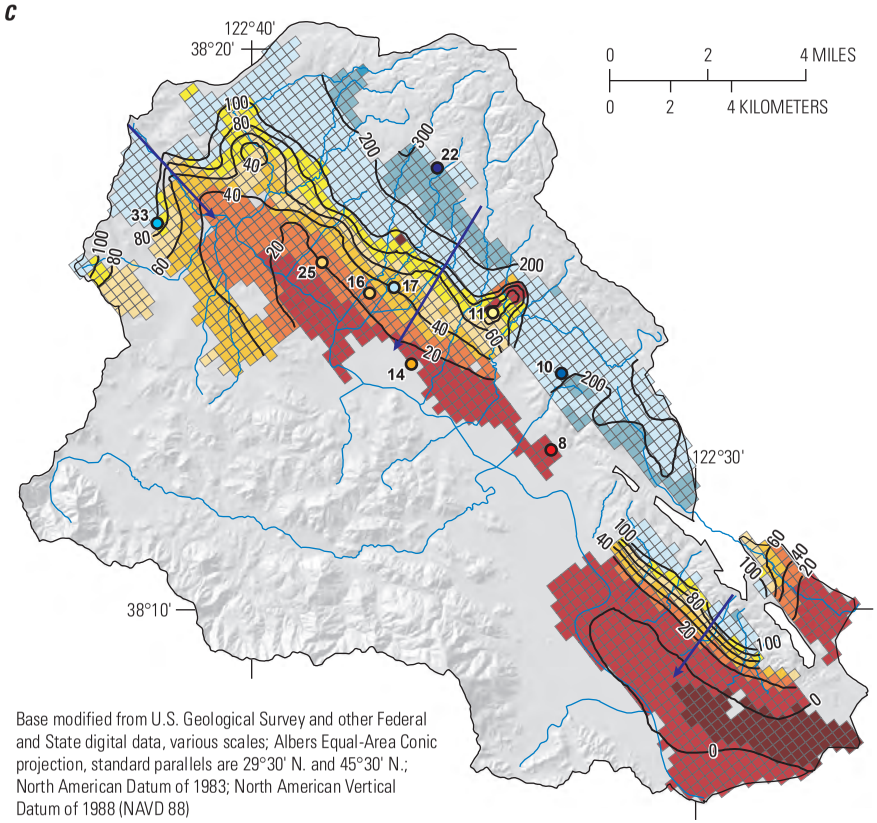

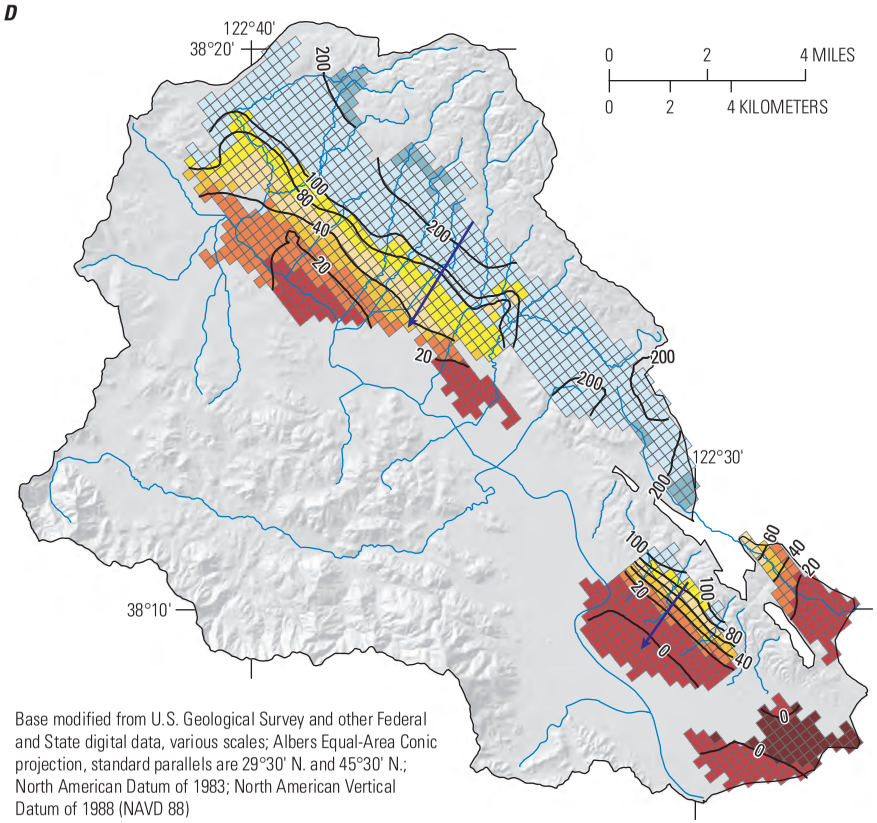

Figure D41.—Continued

E

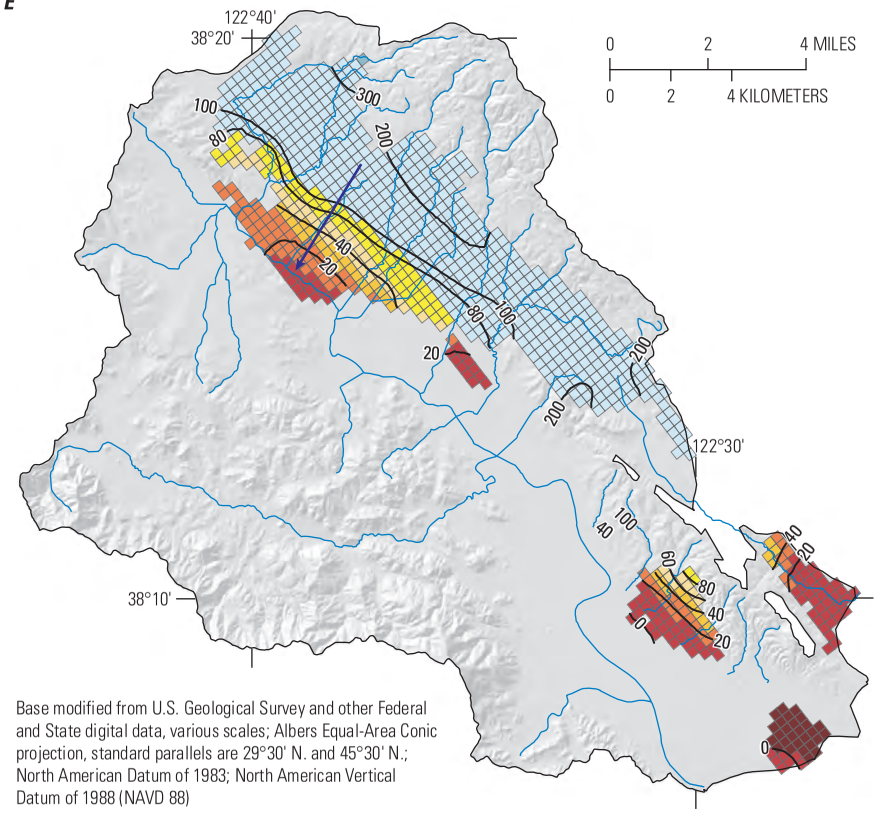

Base modified from U.S. Geological Survey and other Federal and State digital data, various scales; Albers Equal-Area Conic projection, standard parallels are 29°30' N. and 45°30' N.; North American Datum of 1983; North American Vertical Datum of 1988 (NAVD 88)

EXPLANATION

Simulated groundwater altitude (layer 5), in feet above NAVD 88

>–10 to 0	>60 to 80	>300 to 400
>0 to 20	>80 to 100	>400 to 500
>20 to 40	>100 to 200	>500 to 600
>40 to 60	>200 to 300	

Contour of simulated groundwater altitude, in feet

Flow direction

Figure D41.—Continued

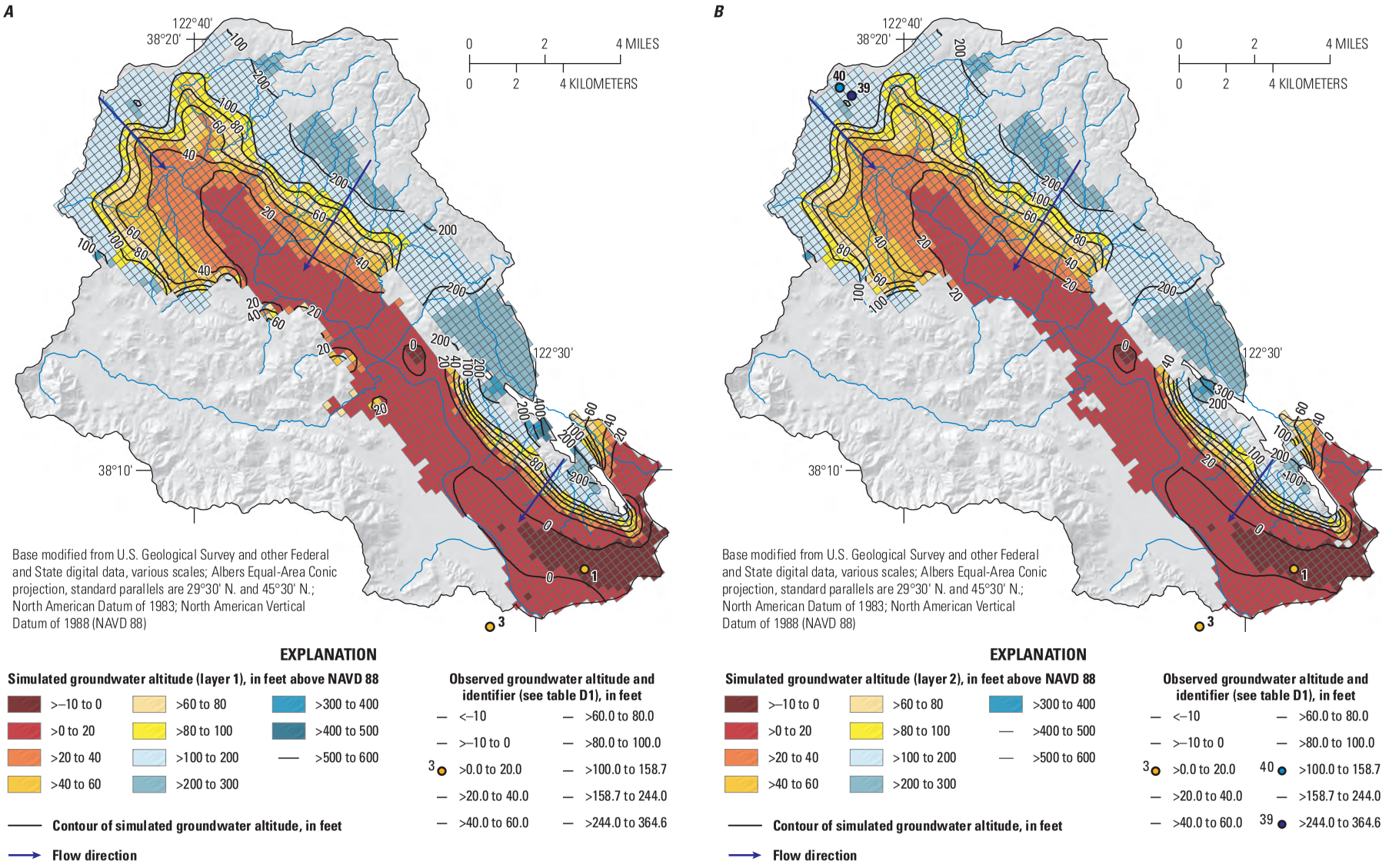

Figure D42. Simulated groundwater altitude for dry conditions (October 1977), Petaluma Valley Integrated Hydrologic Model, Petaluma valley watershed, Sonoma County, California: *A*, model layer 1; *B*, model layer 2; *C*, model layer 3; *D*, model layer 4; *E*, model layer 5.

C

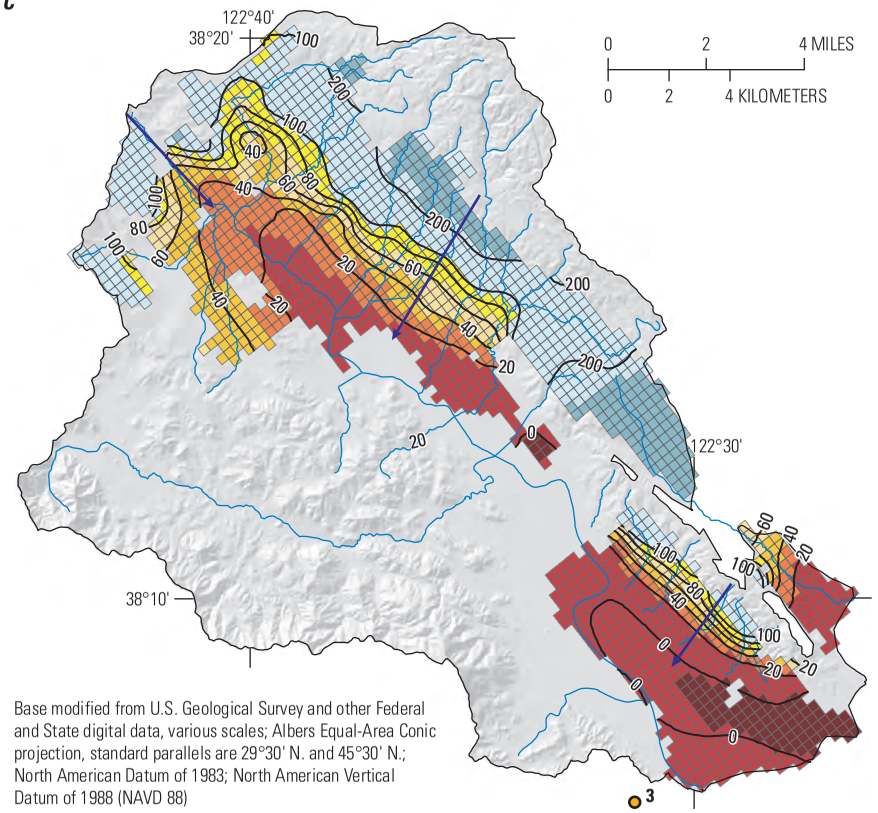

Base modified from U.S. Geological Survey and other Federal and State digital data, various scales; Albers Equal-Area Conic projection, standard parallels are 29°30' N. and 45°30' N.; North American Datum of 1983; North American Vertical Datum of 1988 (NAVD 88)

EXPLANATION

Simulated groundwater altitude (layer 3), in feet above NAVD 88

- >–10 to 0
- >0 to 20
- >20 to 40
- >40 to 60
- >60 to 80
- >80 to 100
- >100 to 200
- >200 to 300
- >300 to 400
- >400 to 500
- >500 to 600

Contour of simulated groundwater altitude, in feet

Flow direction

Observed groundwater altitude and identifier (see table D1), in feet

- <–10
- >–10 to 0
- 3 >0.0 to 20.0
- >20.0 to 40.0
- >40.0 to 60.0
- >60.0 to 80.0
- >80.0 to 100.0
- >100.0 to 158.7
- >158.7 to 244.0
- >244.0 to 364.6

D

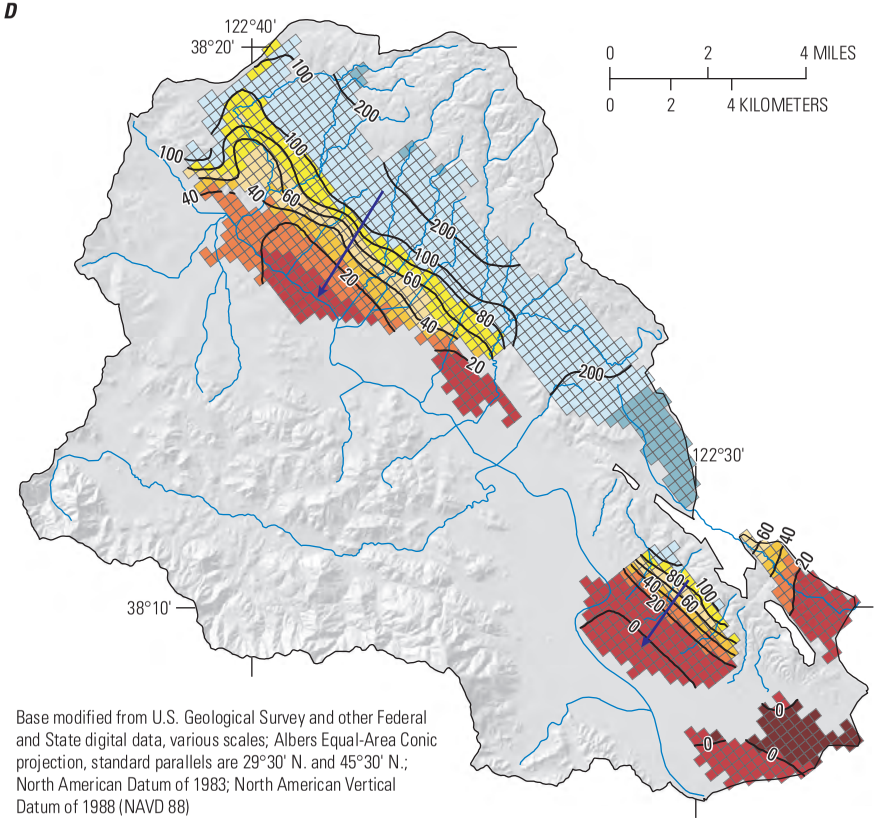

Base modified from U.S. Geological Survey and other Federal and State digital data, various scales; Albers Equal-Area Conic projection, standard parallels are 29°30' N. and 45°30' N.; North American Datum of 1983; North American Vertical Datum of 1988 (NAVD 88)

EXPLANATION

Simulated groundwater altitude (layer 4), in feet above NAVD 88

- >–10 to 0
- >0 to 20
- >20 to 40
- >40 to 60
- >60 to 80
- >80 to 100
- >100 to 200
- >200 to 300
- >300 to 400
- >400 to 500
- >500 to 600

Contour of simulated groundwater altitude, in feet

Flow direction

Figure D42.—Continued

E

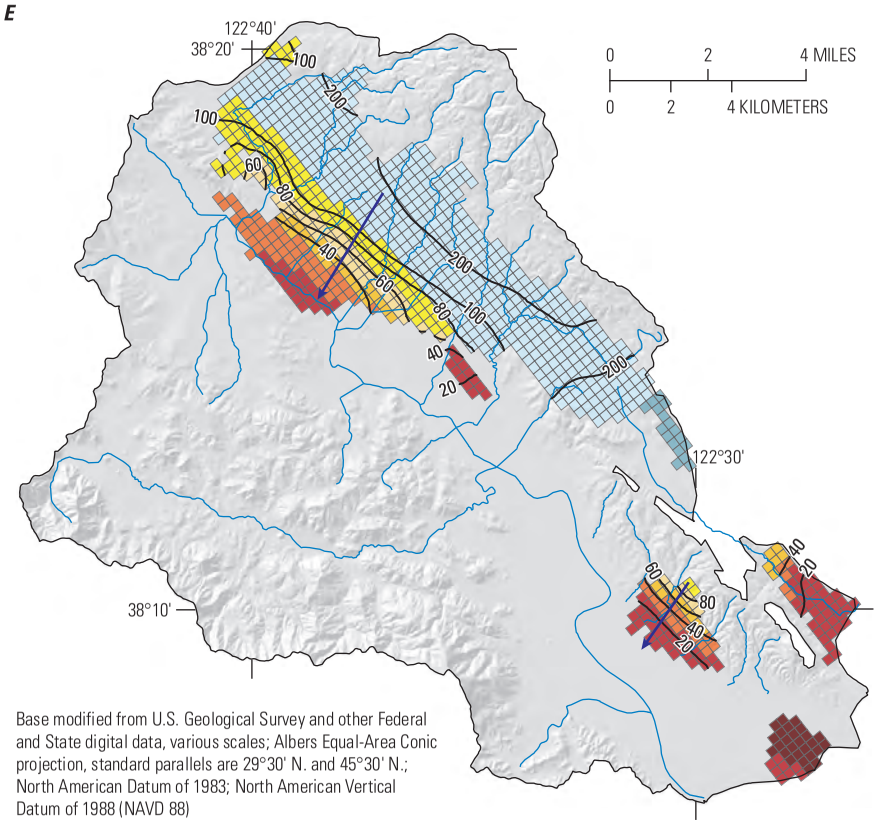

Base modified from U.S. Geological Survey and other Federal and State digital data, various scales; Albers Equal-Area Conic projection, standard parallels are 29°30' N. and 45°30' N.; North American Datum of 1983; North American Vertical Datum of 1988 (NAVD 88)

EXPLANATION

Simulated groundwater altitude (layer 5), in feet above NAVD 88

>–10 to 0	>60 to 80	>300 to 400
>0 to 20	>80 to 100	>400 to 500
>20 to 40	>100 to 200	>500 to 600
>40 to 60	>200 to 300	

Contour of simulated groundwater altitude, in feet

Flow direction

Figure D42.—Continued

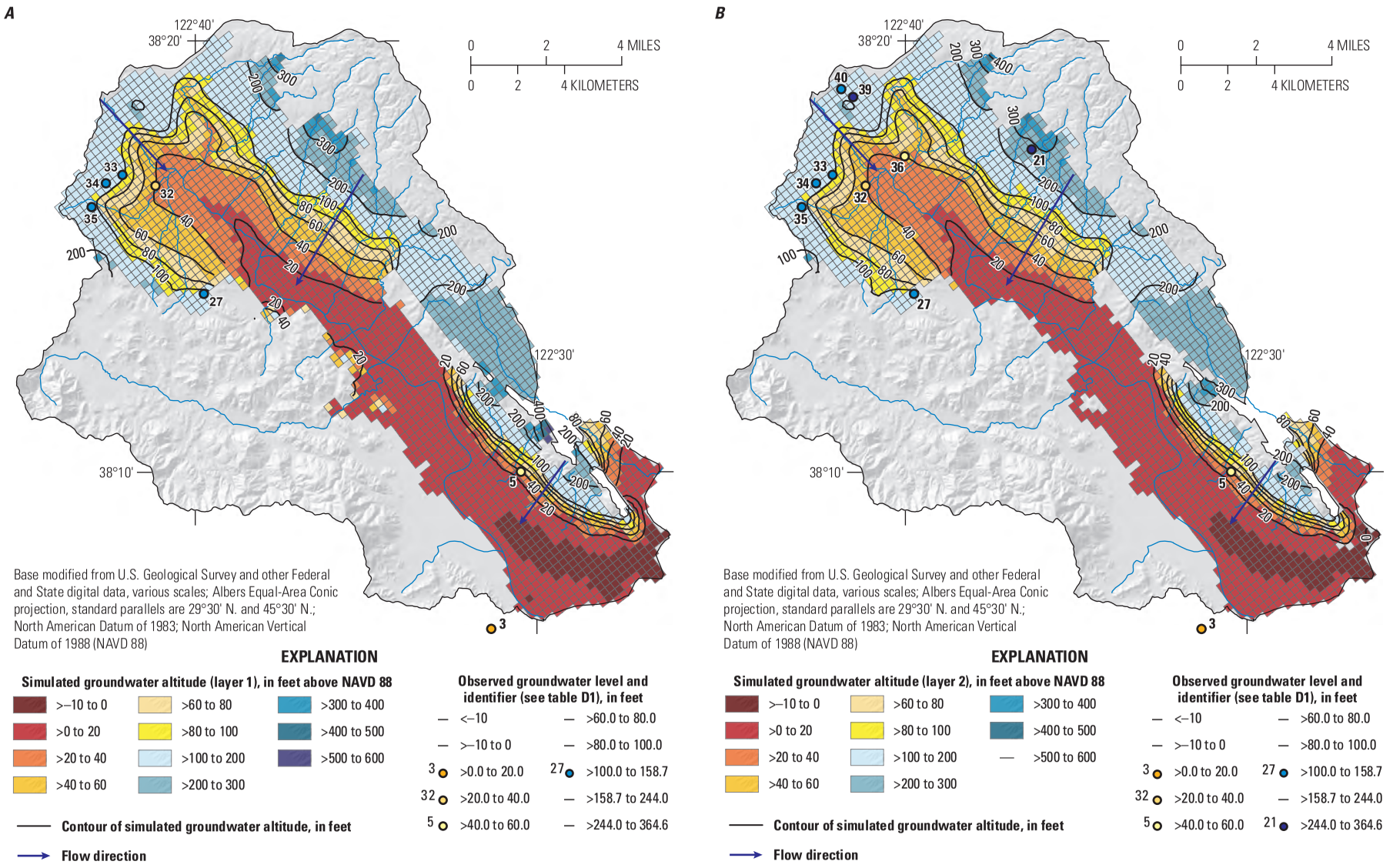

Figure D43. Simulated groundwater altitude for wet conditions (April 1983), Petaluma Valley Integrated Hydrologic Model, Petaluma valley watershed, Sonoma County, California: *A*, model layer 1; *B*, model layer 2; *C*, model layer 3; *D*, model layer 4; *E*, model layer 5.

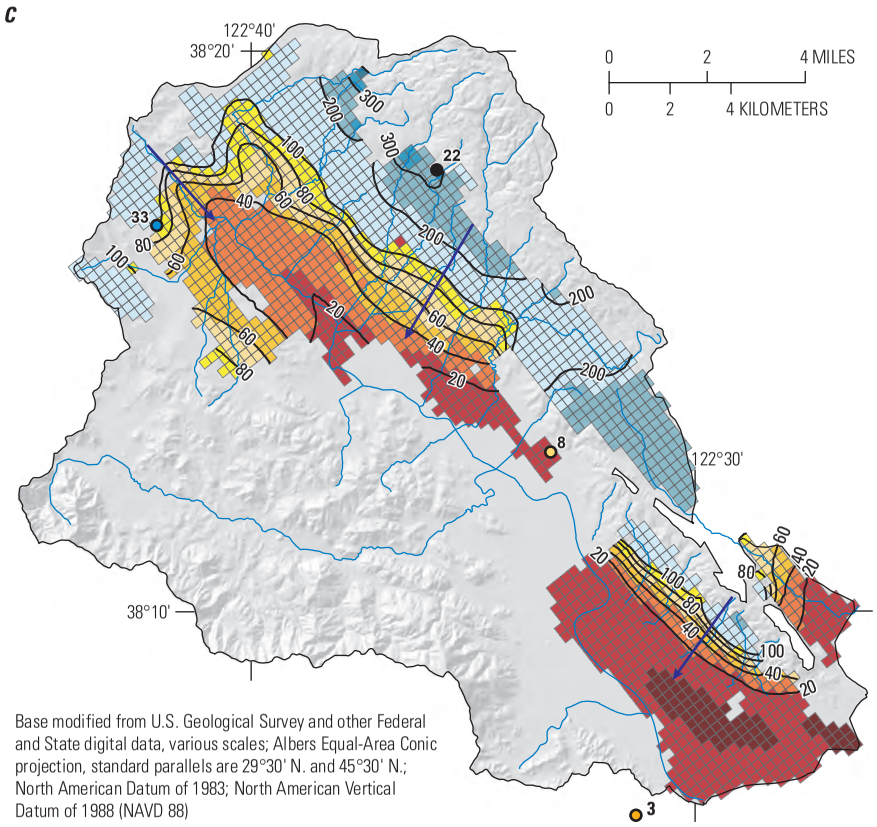

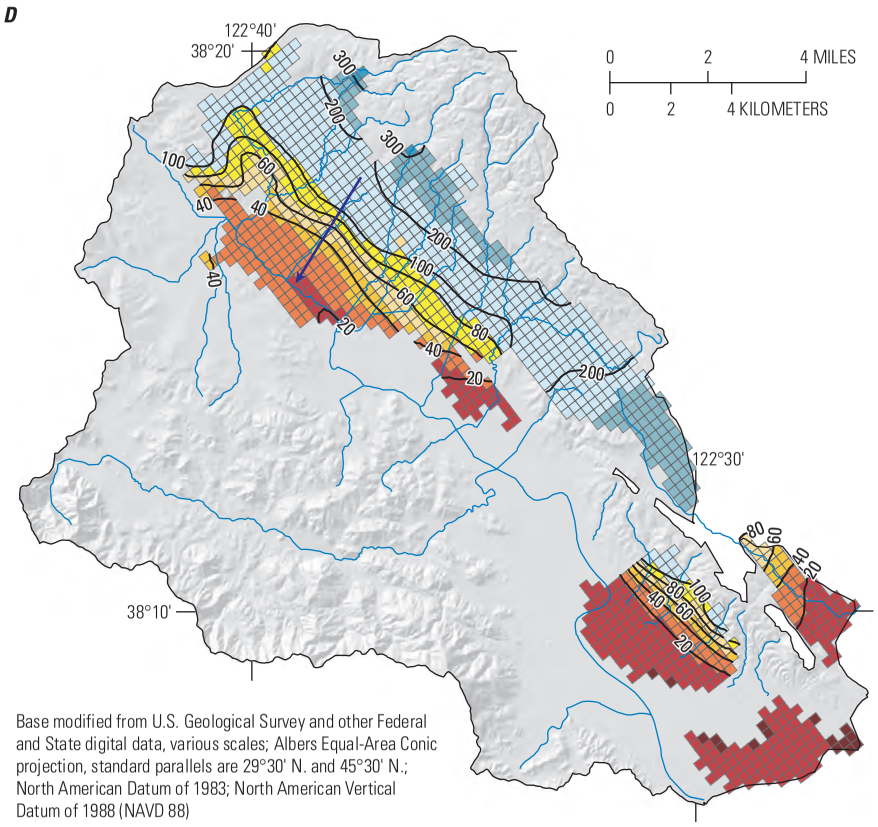

Figure D43.—Continued

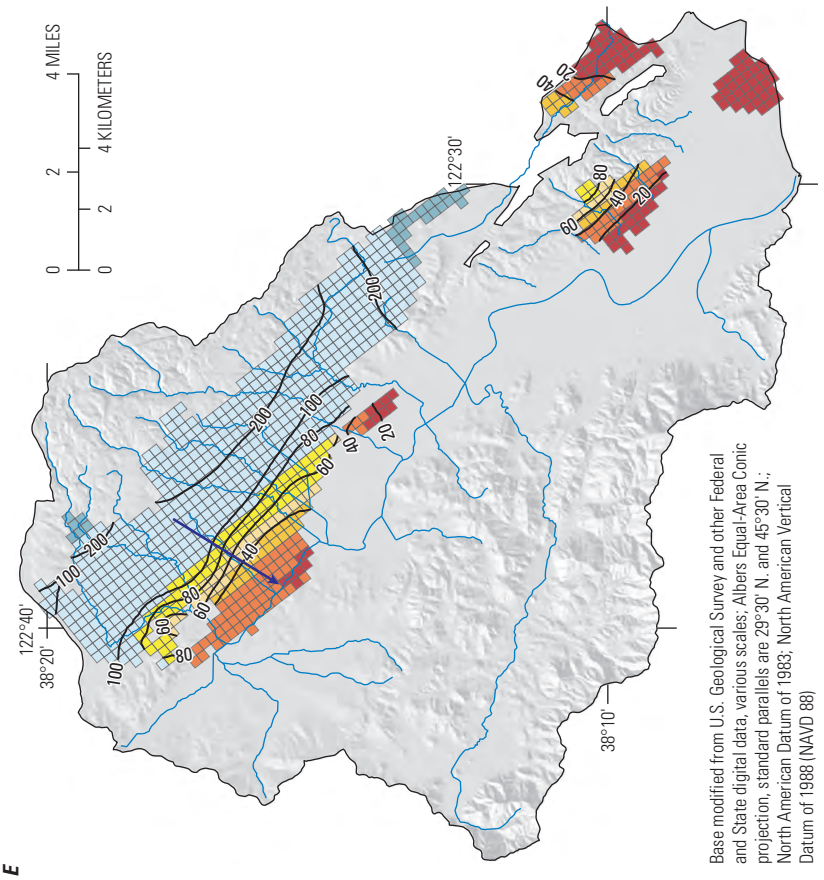

Figure D43.—Continued

Simulated groundwater altitudes in October 1977 (fig. D42) represent extremely dry conditions for the PVW after 2 years of record dry conditions in WYs 1976 and 1977. The general direction of groundwater flow was unchanged compared with the September 2015 results, and simulated groundwater altitudes in layer 1 ranged from 499 ft above NAVD 88 to 5 ft below NAVD 88. Simulated groundwater altitudes from WY 1977 were generally a few feet lower than simulated groundwater altitudes from WY 2015. Lower groundwater altitudes in WY 1977 resulted a net boundary inflow from San Pablo Bay of 16,647 acre-ft, more than 4,000 acre-ft than inflow during WY 2015. However, groundwater altitudes were much lower in WY 2015 in other areas, such as near the Wilson Grove and Santa Rosa Plain boundaries, because of lower GHB heads in WY 2015 compared to WY 1977. Also, localized areas in the hills east of the City of Petaluma had lower simulated groundwater altitudes because of increased groundwater pumpage from an increase in irrigated acreage in WY 2015 compared to WY 1977. Localized pumping effects were especially pronounced in model layers 2 and 3.

Simulated groundwater altitudes in April 1983 (fig. D43) represented extremely wet conditions for the PVW after the record wet winter of WY 1983. The general direction of groundwater flow was unchanged compared with the WY 2015 results, but there was a generally steeper hydraulic gradient toward the Petaluma River in the lower section of the model. Simulated groundwater altitudes in model layer 1 ranged from 516 ft above NAVD 88 to 4 ft below NAVD 88 (fig. D43). April 1983 simulated groundwater altitudes were higher than September 2015 by an average of 7 ft. Groundwater altitudes were lower throughout the entire model area, except in the northeast corner of the model, where local boundary conditions resulted in higher groundwater altitudes in WY 2015, which is consistent with observed long-term trends at nearby calibration well 38 (fig. D44*F*).

Simulated Groundwater Altitude Hydrographs

Hydrographs comparing the simulated groundwater altitudes (Traum, 2022) with observed groundwater altitudes (California Department of Water Resources, 2018a; California Department of Water Resources, 2018b) for all 41 calibration wells (previously shown in fig. D1) are presented in figure D44. The simulated groundwater altitudes are shown only for model layers in which the wells were screened. As discussed in the "Model Fit to Observations of Groundwater Altitudes" section, the observation wells were assembled in six groups, with each group having similar groundwater-altitude magnitudes and trends (fig. D30).

Group 1 contains calibration wells 1–4 in the Petaluma marsh area (figs. D1, D44*A*). Observed groundwater altitudes in this area were generally within 5 ft of NAVD 88. Observed groundwater altitudes varied seasonally by about 5 ft, and long-term gains or declines in groundwater altitudes were not observed. Simulated groundwater altitudes closely matched with the observed groundwater altitudes at all calibration wells in this area. Simulated groundwater altitudes were constrained by the San Pablo Bay GHB, the Petaluma River, and the ET of shallow groundwater in the Petaluma marsh are. Wells 1 and 2 are about 1.25 miles (mi) apart and are perforated in layers 1 and 2 and in layer 3, respectively. Simulated results indicate that well 2 groundwater altitudes were about 2 ft higher than those in well 1 (fig. D44*A*), although observed data indicate that well 1 groundwater altitudes were about 3 ft higher than those in well 2. Wells 2 and 4 are about 1.75 mi apart and are perforated in layers 3 and 2, respectively. Simulated results indicate that well 2 groundwater altitudes were about 3 ft lower than those in well 4 (fig. D44*A*), although the observed data indicate that the two wells had similar groundwater altitudes.

Group 2 contains calibration wells 5–9 in the hills east of the Petaluma marsh area (figs. D1, D44*B*). Observed groundwater altitudes in this area are highly variable, ranging from –65 ft (below NAVD 88) in well 8 to 104 ft (above NAVD 88) in well 6. Observed groundwater altitudes at some wells show declines during dry periods in the early 1990s, with some declining by over 100 ft compared to altitudes in the mid-1980s. At all wells, however, groundwater altitudes recovered at the end of dry periods, and long-term declines in groundwater altitudes were not observed. Simulated groundwater altitudes generally matched the trends in the observed data. However, declines in simulated groundwater altitudes did not reach the same magnitude as observed declines. Wells 7 and 8 are the only two wells in this group that are in close proximity to each other (about 1.4 mi), and these wells are perforated in different model layers (figs. D1, D44*B*). Specifically, well 7 is perforated in layer 2, and well 8 is perforated in layer 3. Simulated groundwater altitudes in well 7 were, on average, about 7 ft higher than those in well 8, although the observed data indicated a greater difference in groundwater altitudes (fig. D44*B*).

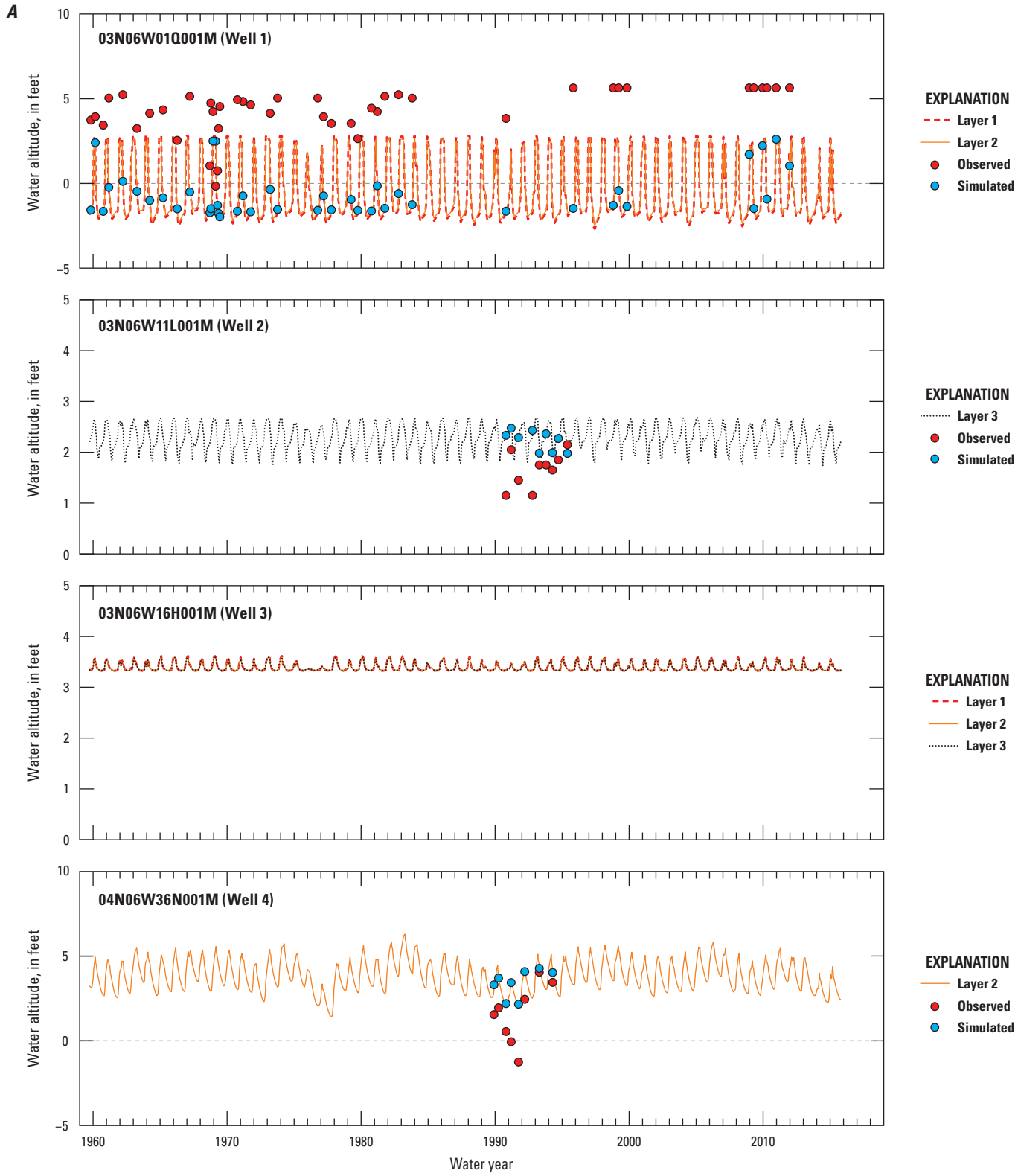

Figure D44. Simulated (Traum, 2022) and observed (California Department of Water Resources, 2018a, b) groundwater altitudes above or below the North American Vertical Datum of 1988 (NAVD 88) for Petaluma Valley Integrated Hydrologic Model calibration wells, Petaluma Valley Integrated Hydrologic Model, Petaluma valley watershed, Sonoma County, California: *A*, group 1; *B*, group 2; *C*, group 3; *D*, group 4; *E*, group 5; *F*, group 6; groups are identified in the "Model Fit to Observations of Groundwater Altitudes" section of this report and in figure D30.

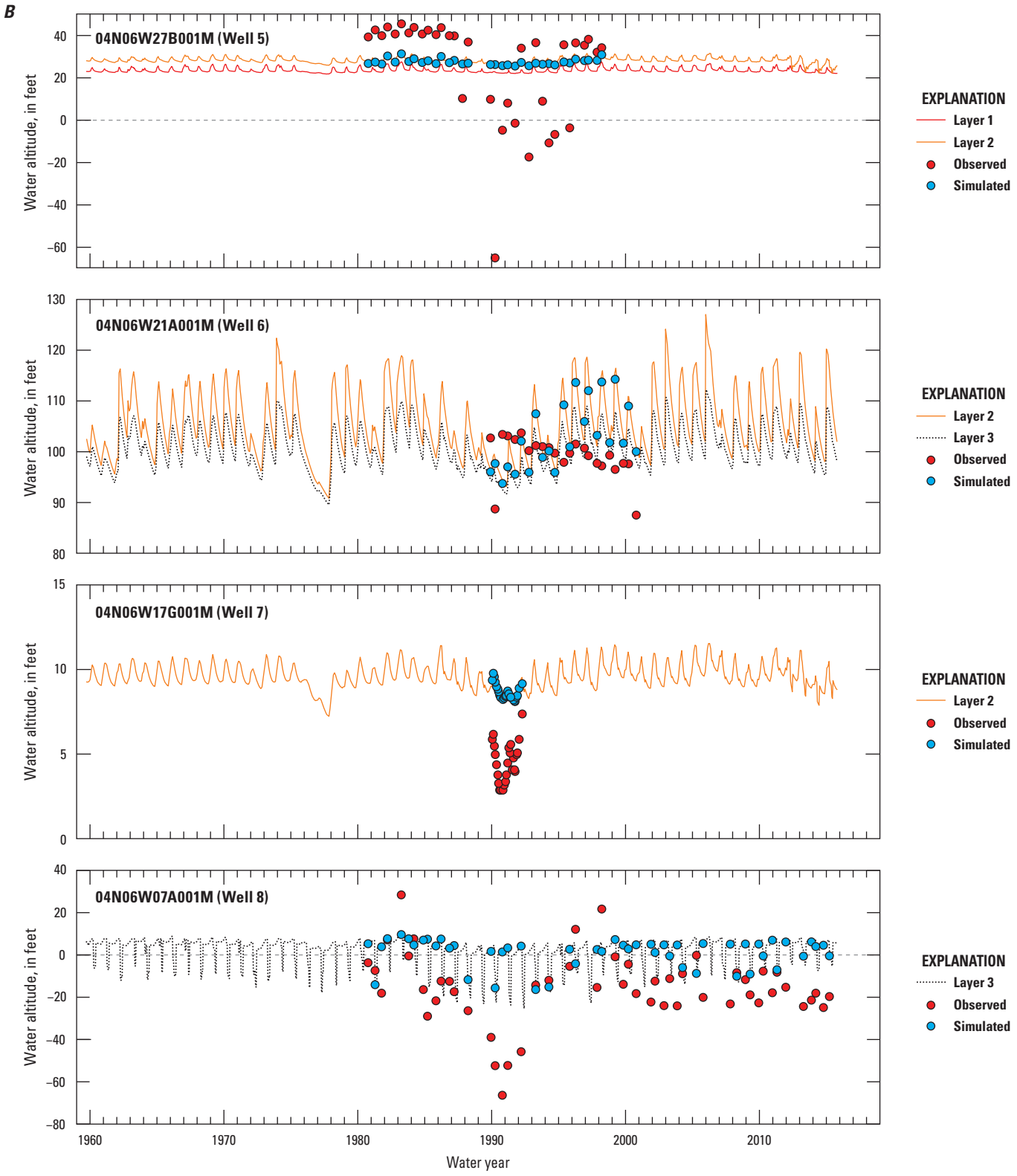

Figure D44.—Continued

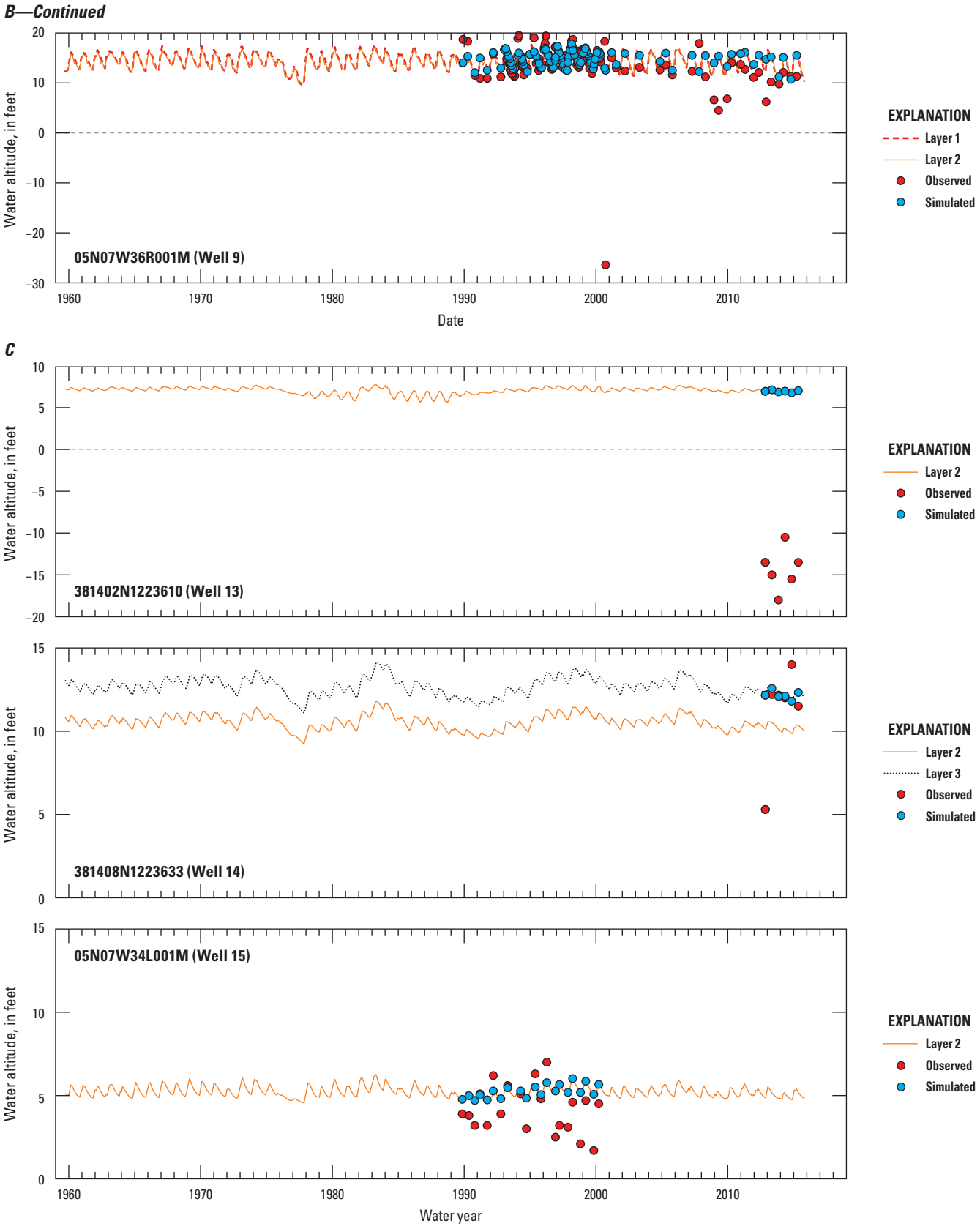

Figure D44.—Continued

C—Continued

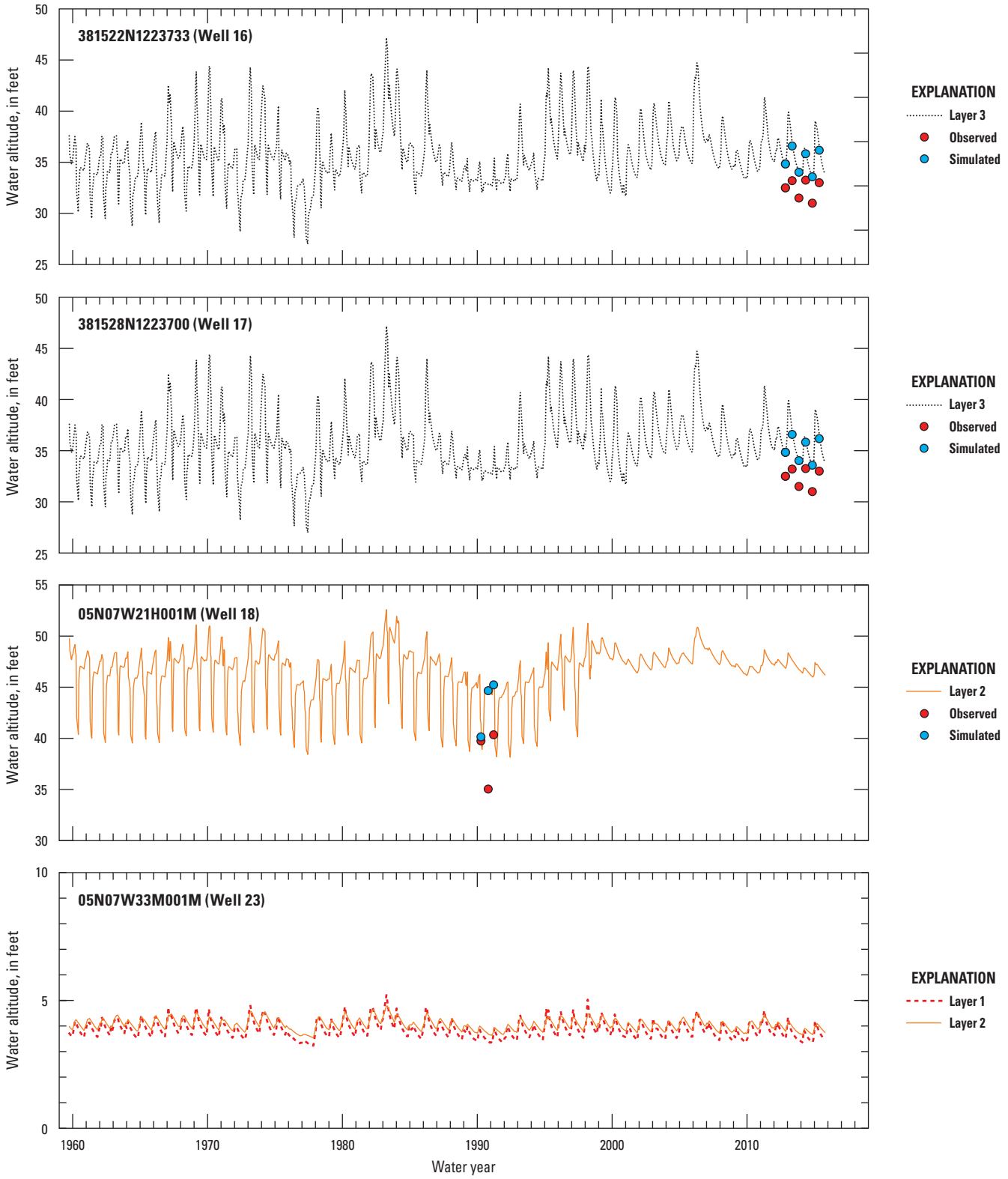

Figure D44.—Continued

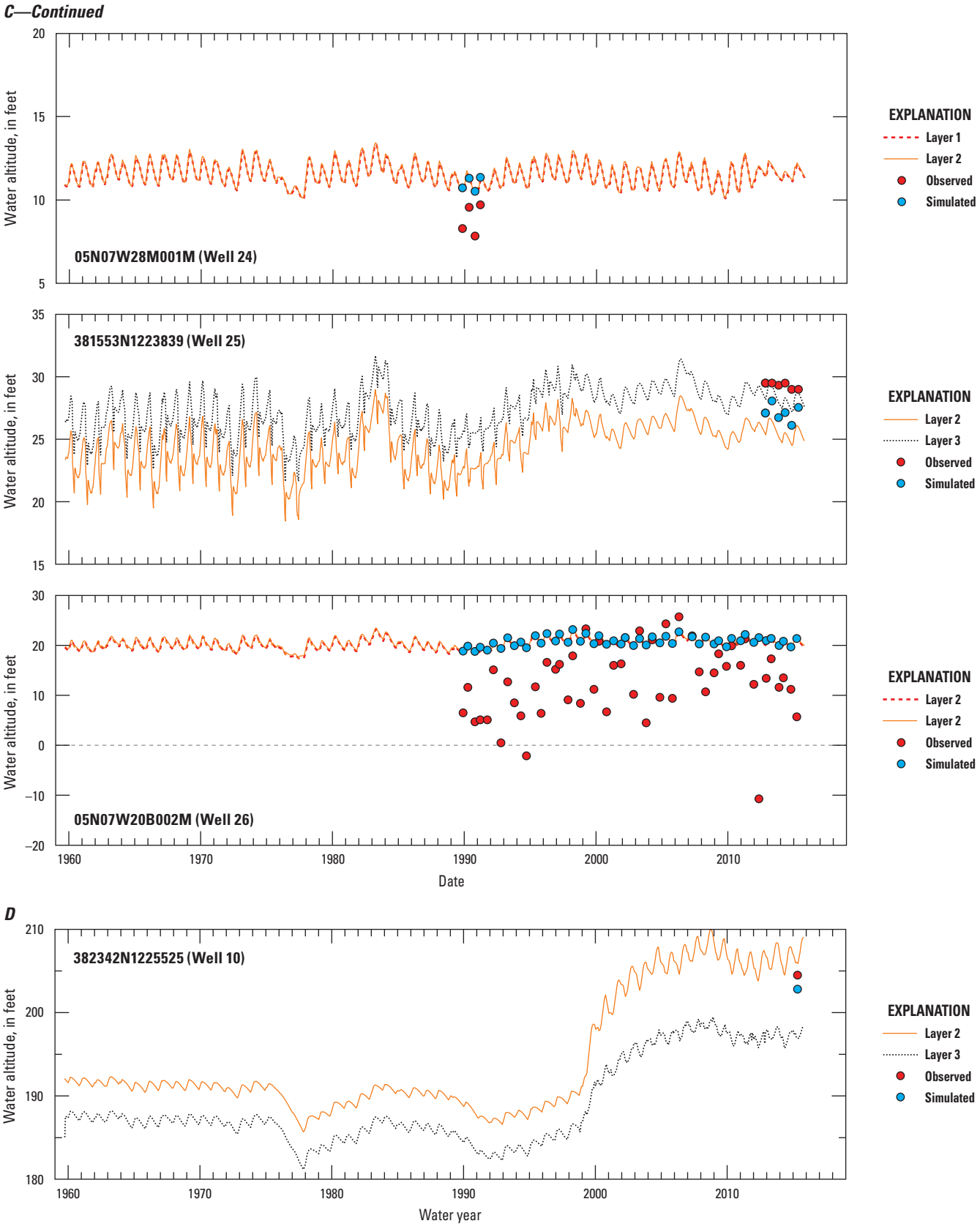

Figure D44.—Continued

D—Continued

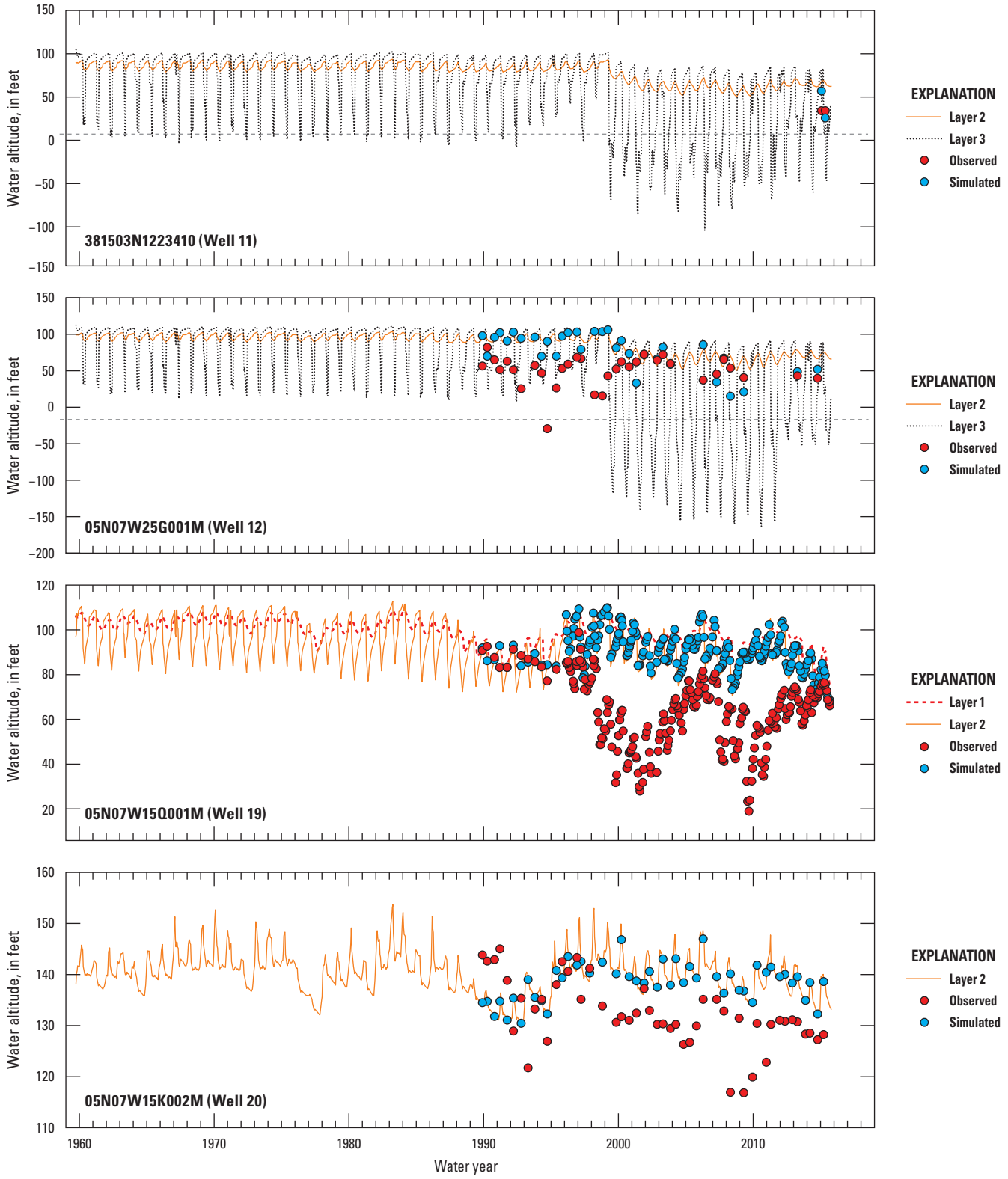

Figure D44.—Continued

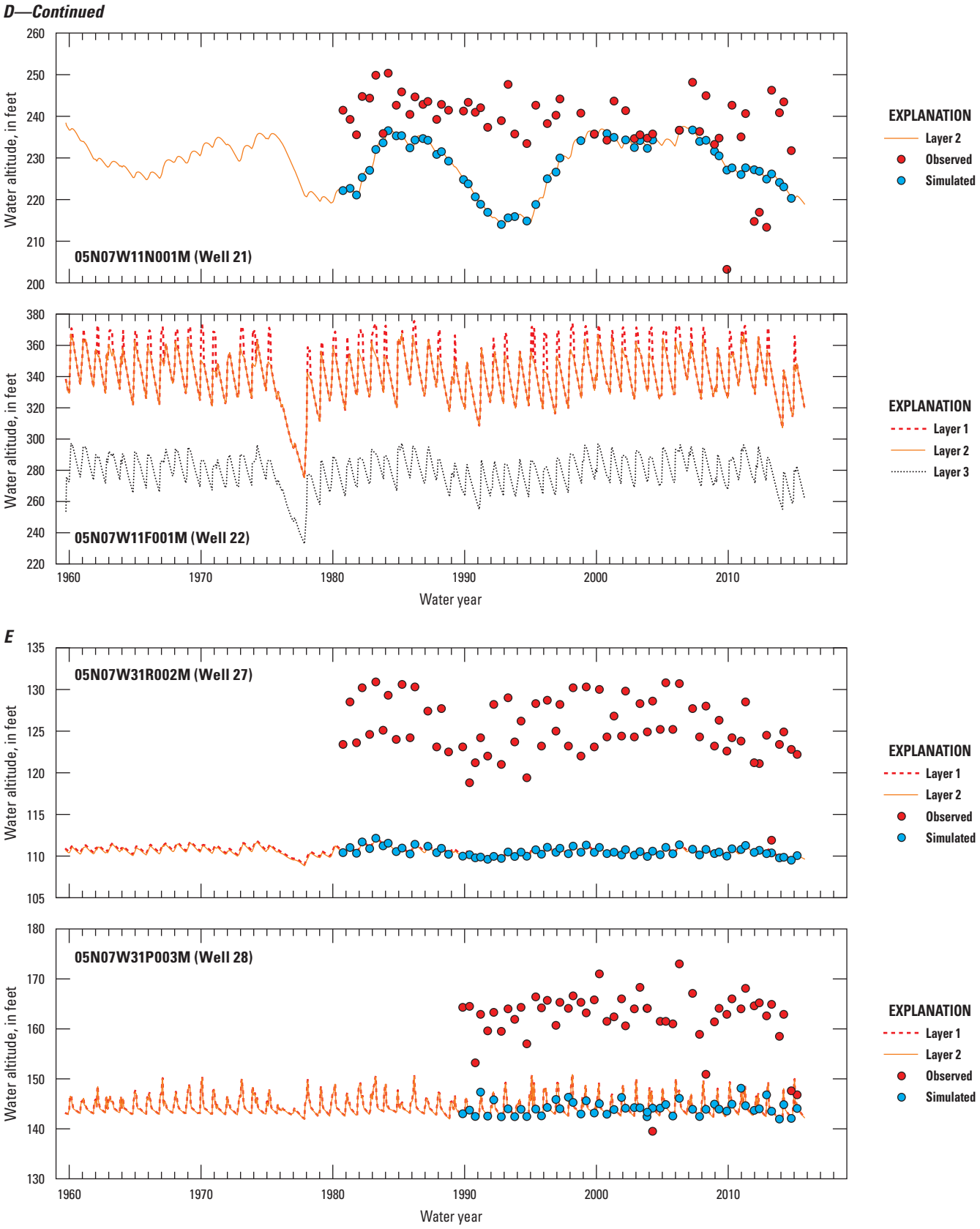

Figure D44.—Continued

E—Continued

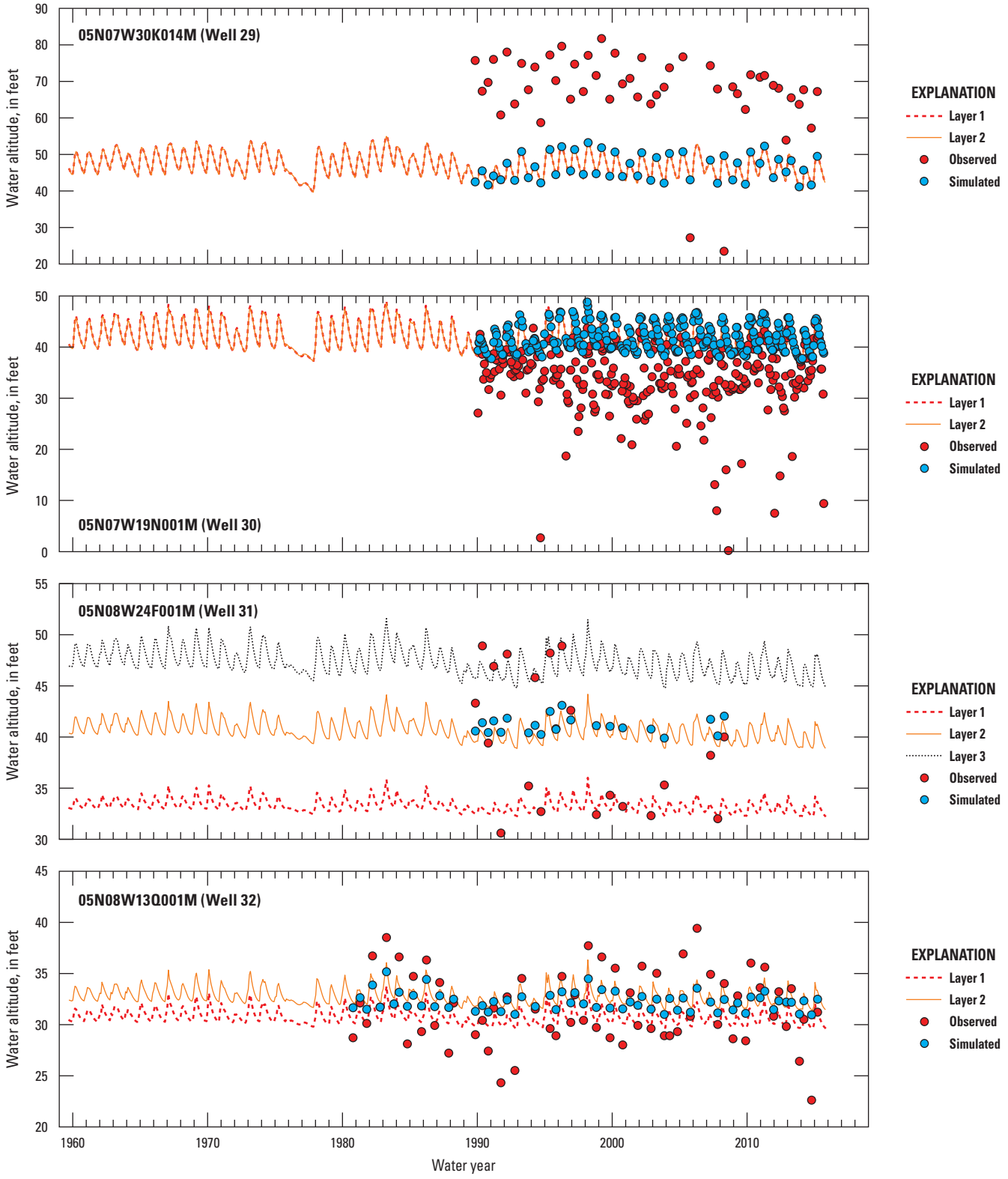

Figure D44.—Continued

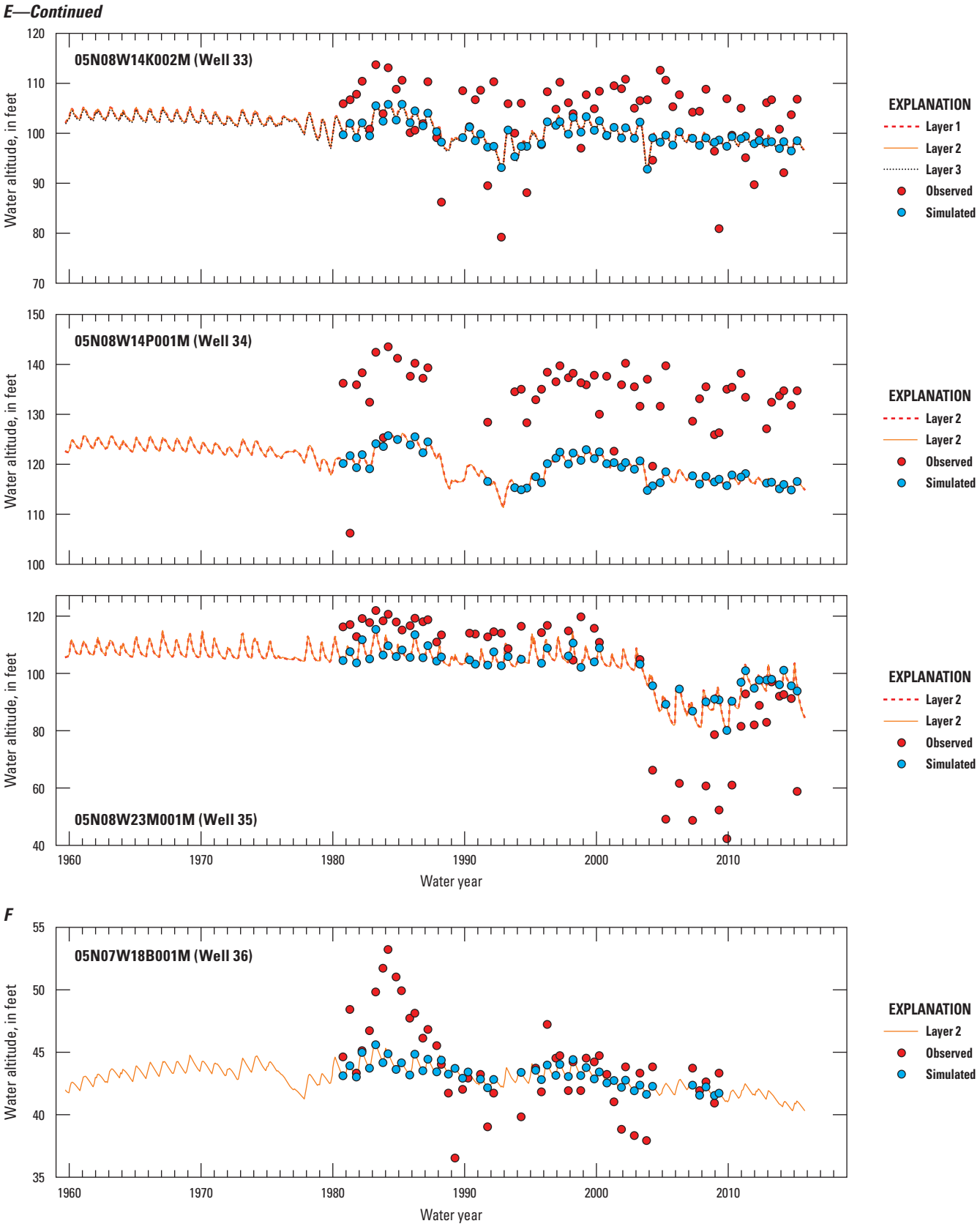

Figure D44.—Continued

F—Continued

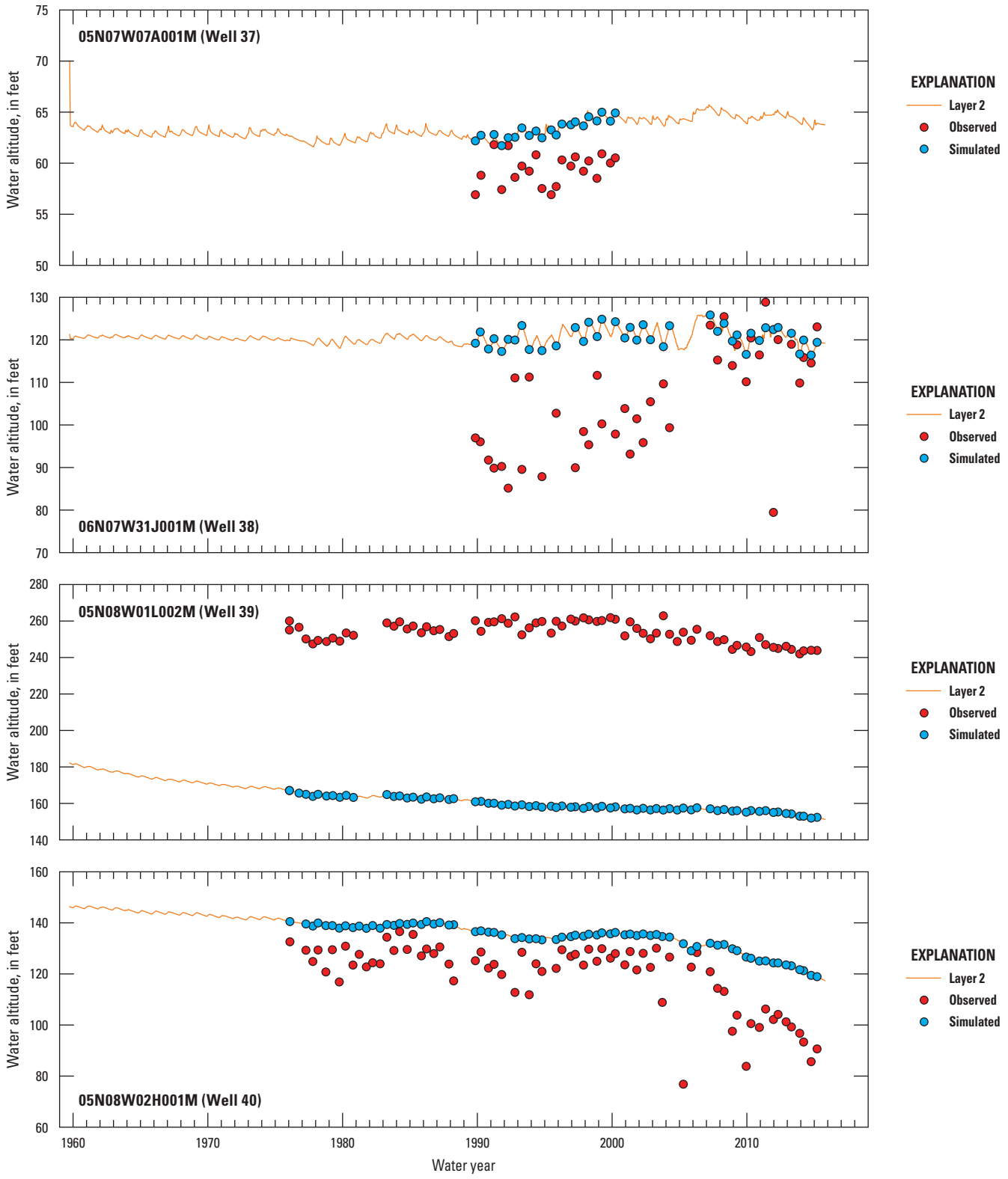

Figure D44.—Continued

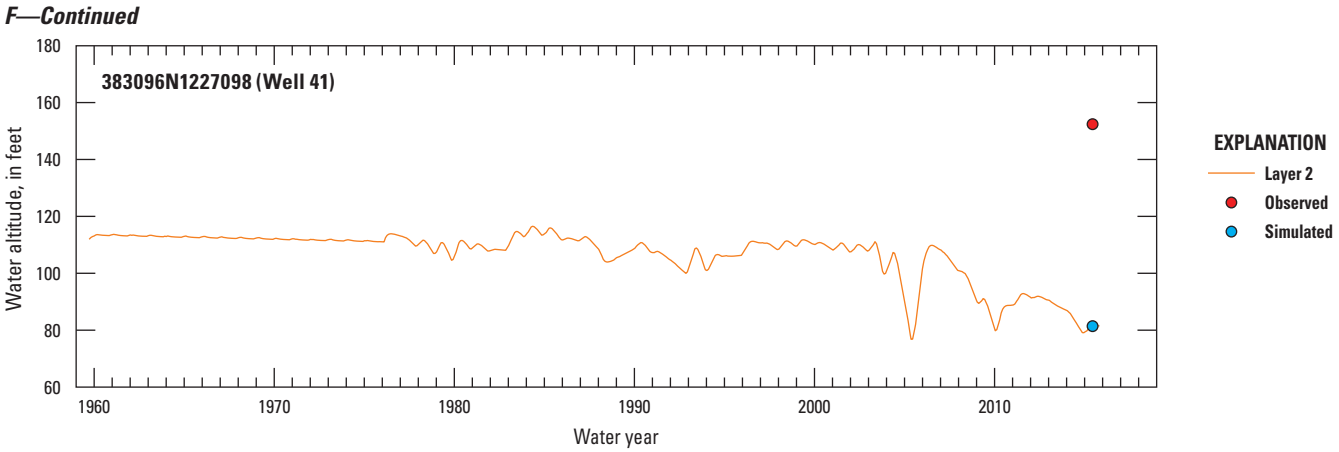

Figure D44.—Continued

Group 3 contains calibration wells 13–18 and 23–26 in the City of Petaluma (figs. D1, D44*C*). Observed groundwater altitudes in the City of Petaluma varied from –17 ft (below NAVD 88) at the south side of the city (well 13) to 62 ft (above NAVD 88) at the north east side of the city (well 17). In general, determining long-term trends in observed groundwater altitudes was difficult in this area because most wells only had observed data for a few years. The wells with longer-term records (wells 15 and 26; fig. D44*C*) show generally steady long-term groundwater altitudes with a seasonal fluctuation of between 5 and 20 ft. Simulated groundwater altitudes generally matched well with observed data in the group 3 wells. In some areas, matching simulated groundwater altitudes with all observed groundwater altitudes was not possible because of wells close together (both horizontally and with similar vertical screened intervals) having drastically different observed groundwater altitudes. For example, the model overestimated groundwater altitudes at well 13 by about 20 ft but estimated groundwater altitudes within 5 ft at wells 14 and 15. Similarly, the model overestimated groundwater altitudes and underestimated seasonal fluctuations at well 26 but underestimated groundwater altitudes and overestimated seasonal fluctuations at nearby well 25. Wells 16 and 18 are the only two wells in group 3 that are close to each other (about 0.5 mi) and are perforated in different model layers (figs. D1, D44*C*); however, Lynch Creek lies between the wells, which may contribute to observed differences. Well 16 is perforated in layer 3, and well 18 is perforated in layer 2. Simulated groundwater altitudes in well 16 averaged about 10 ft lower than in well 18 and generally agreed with observed groundwater-altitude data (fig. D44*C*).

Group 4 contains calibration wells 10–12 and 19–22 in the hills east of the City of Petaluma that generally overlie the Petaluma Formation (figs. D1, D44*D*). Observed groundwater altitudes generally increase as land-surface altitudes increase, from 19 ft (well 19) to 506 ft (well 22) above NAVD 88. Observed groundwater altitudes in this area are highly variable; for example, at well 19, observed groundwater altitudes declined by almost 80 ft during dry periods. There are also data from many wells in this area that demonstrate a long-term decline in groundwater altitudes of about 10 to 20 ft (for example, wells 20 and 21). Simulated groundwater altitudes generally match observed groundwater altitudes at all calibration wells in this area, and groundwater altitudes increase as land surface increases. Groundwater-altitude values had large variations in response to dry periods at wells 19 and 12. Group 4 does not have wells in close proximity to each other that are perforated in different layers. Therefore, an analysis of the vertical differences in simulated groundwater altitude cannot be done.

Group 5 contains calibration wells 27–35 in the Wilson Grove area (figs. D1, D44*E*). Observed groundwater altitudes in this area generally followed the land-surface altitude profile, ranging from 173 ft (above NAVD 88) at higher altitude wells (well 28) to 0 ft (NAVD 88) at lower altitude wells (well 30). Observed groundwater altitudes in this area varied seasonally by about 20 ft at most wells. Long-term groundwater altitudes in this area were generally stable. However, well 35 shows a substantial decline in groundwater altitudes in the early 2000s; some recovery has taken place, but groundwater altitudes in well 35 are still lower than historical conditions. Simulated groundwater altitudes generally matched with observations in this area; however, the model tends to underestimate groundwater altitudes at higher altitude wells (wells 27–29 and 34). At lower altitude wells, simulated groundwater altitudes matched with observed seasonal water-altitude highs but did not simulate the same magnitude of seasonal variations (wells 30–32). Simulated values at well 35 were probably influenced by the Wilson Grove GHB. The simulated vertical gradients in some of the group 5 wells was upward, with deeper layers having simulated groundwater altitudes 10 to 15 ft higher than shallower layers (well 31). Wells 31 and 32 are the only two wells in group 5 that are near each other (about 0.3 mi) and are perforated in different model layers (figs. D1, D44*E*). Well 31 is perforated in layers 1–3,

and well 32 is perforated in layers 1 and 2. The difference between the observed data for wells 31 and 32 was about 10 feet. Likewise, the difference between simulated results between well 31 and well 32 was about 10 feet. Therefore, the simulated groundwater gradient between these two wells matches the observed data.

Group 6 contains calibration wells 36–41 in the Penngrove area (figs. D1, D44*F*). Observed groundwater altitudes in this area ranged from 36 ft (well 36) to 262 ft (well 39) above NAVD 88. Observed groundwater altitudes in this area were variable, with well 41 demonstrating declining groundwater altitudes during the last 15 years and well 38 demonstrating increasing groundwater altitudes. Simulated groundwater altitudes generally approximated observed data in this area. However, simulated groundwater altitudes could not match all observed groundwater altitudes because some wells were close together but had observed groundwater altitudes that differed substantially. For example, well 39 had observed groundwater altitudes of around 250 ft and well 40 had observed groundwater altitudes of around 120 ft, which is a gradient of 130 ft over less than 0.5 mi. Simulated groundwater altitudes underestimated the magnitude of this gradient, with simulated groundwater altitudes of between 150 and 180 ft at well 39 and simulated groundwater altitudes of between 120 and 150 ft at well 40. Simulated values did not match the increasing groundwater altitudes observed at well 38; however, this trend was seen in the simulated groundwater altitudes at nearby well 37 (where observed data were not available after WY 2000). All the wells in group 6 are perforated in layer 2 (fig. D44*F*); therefore, an analysis of the vertical differences in simulated groundwater altitudes between model layer cannot be done.

Simulated Exchange of Groundwater and Surface Water

Reaches of the Petaluma River and its tributaries that are gaining water from and losing water to the groundwater system can be identified on a streamflow-network map (fig. D45). Much spatial variably was observed during the model simulation period (WYs 1960–2015), with many stream segments having both gaining and losing reaches (fig. D45*A*). However, streams generally tended to have a net loss to groundwater in upper reaches and a net gain from groundwater in lower reaches. In major tributaries to the Petaluma River, such as Lichau Creek, Willow Brook, Lynch Creek, Adobe Creek, and Wiggins Creek, most higher altitude reaches lost water to the groundwater system and most lower altitude reaches gained water from the groundwater system. Most reaches of the Petaluma River gained water from the groundwater system. These data agree with previously shown groundwater-budget data (table D17), which show the average annual net stream seepage (which is defined as stream seepage plus stream discharge in table D17) is positive for the higher altitude subregions (such as #3 Lynch Creek, #11 Adobe Creek, and #19 Stage Gulch) and negative for lower altitude subregions (such as #2 Upper Petaluma River and #10 City of Petaluma). In general, simulated gaining and losing stream reach results were consistent with observed conditions that were discussed in chapter B of this report.

In dry conditions (WY 1977), more individual stream reaches lose water to groundwater system (fig. D45*B*), likely because of overall lower groundwater altitudes. However, the stream system gained a net total of 15,376 acre-ft from the groundwater system in WY 1977 (fig. D37) compared to an average annual stream gain from groundwater of only 2,253 acre-ft for the entire simulation period (table D17). Even though there were fewer gaining reaches in WY 1977 compared to the average annual value, reaches that did gain water from the groundwater system had a much larger magnitude of gain, which is likely a result of lower flow rates in the stream system.

In wet conditions (WY 1983), more individual steam reaches gained water from groundwater system (fig. D45*C*), likely because of overall higher groundwater altitudes. Although there were more reaches gaining water in WY 1983, the overall net annual seepage was reduced to –5,808 acre-ft (fig. D37), with the negative value indicating a net loss to the stream system (gain in groundwater system). Furthermore, reaches that did lose water to the groundwater system had a much larger magnitude of loss because of much higher flow rates in the stream system.

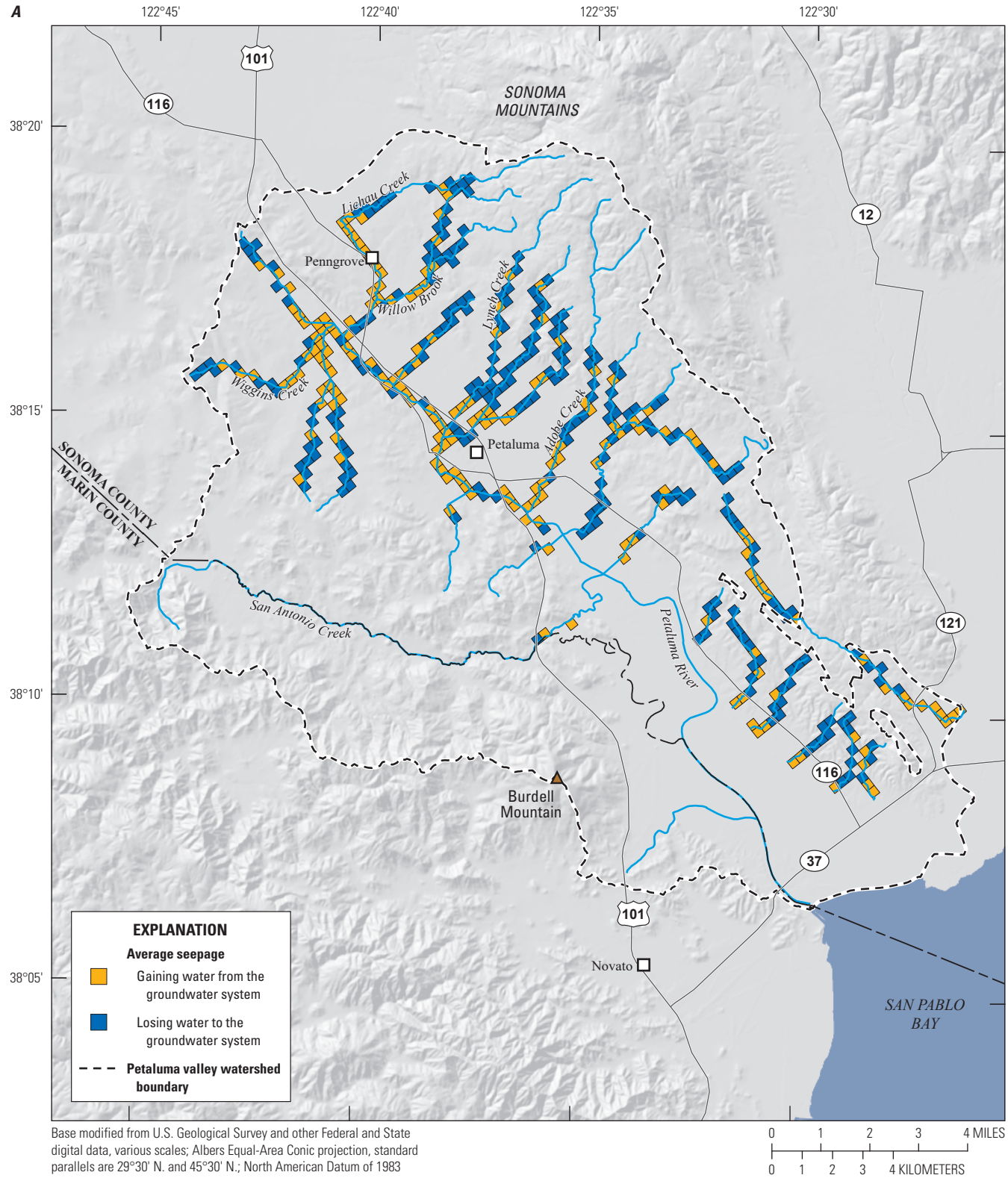

Figure D45. Simulated streamflow-network reaches that gain water from the groundwater system and lose water to the groundwater system (Traum, 2022), Petaluma Valley Integrated Hydrologic Model, Petaluma valley watershed, Sonoma County, California, for *A*, average of entire simulation period, water year (WY) 1960 to WY 2015; *B*, WY 1977; *C*, WY 1983.

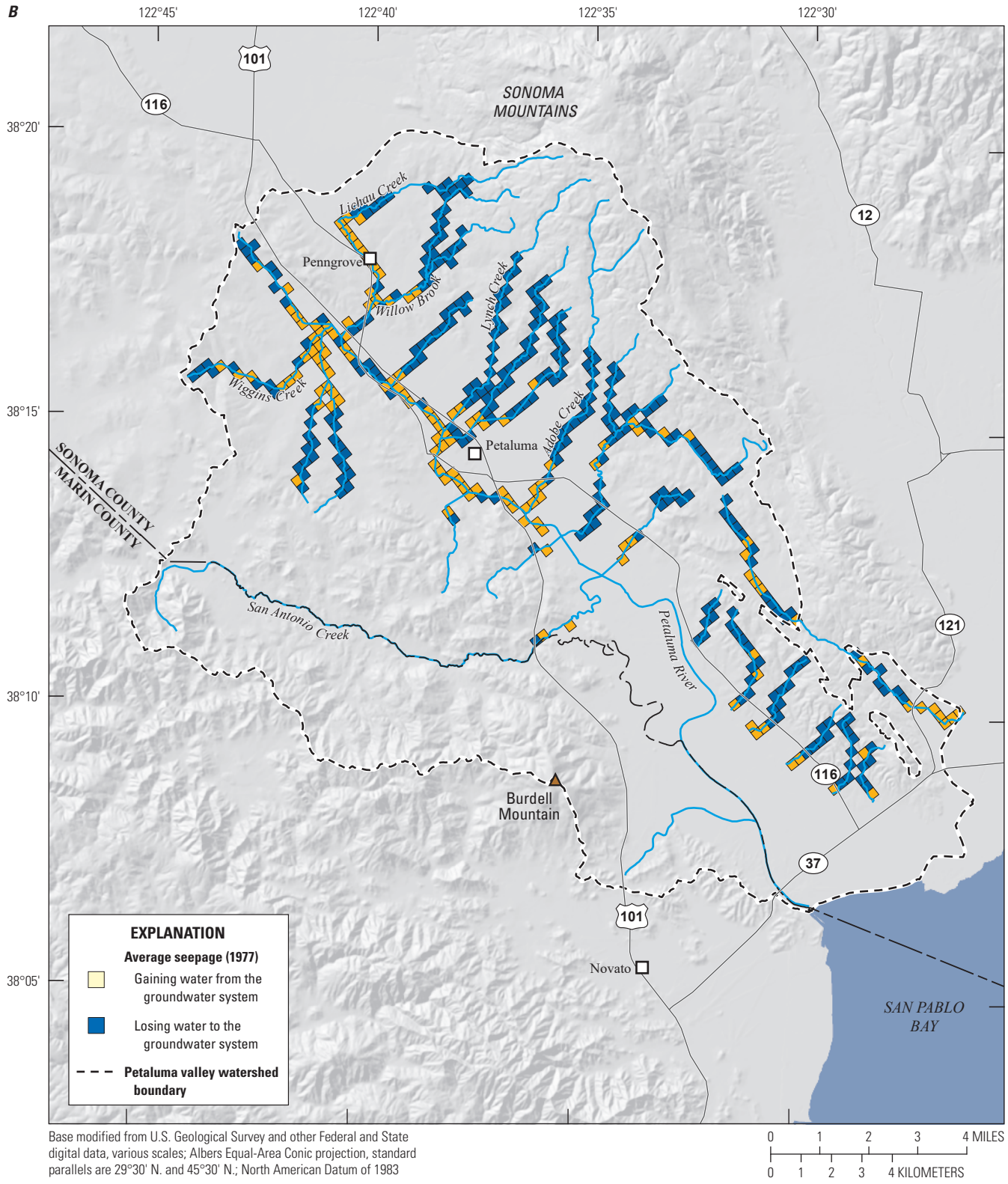

Figure D45.—Continued

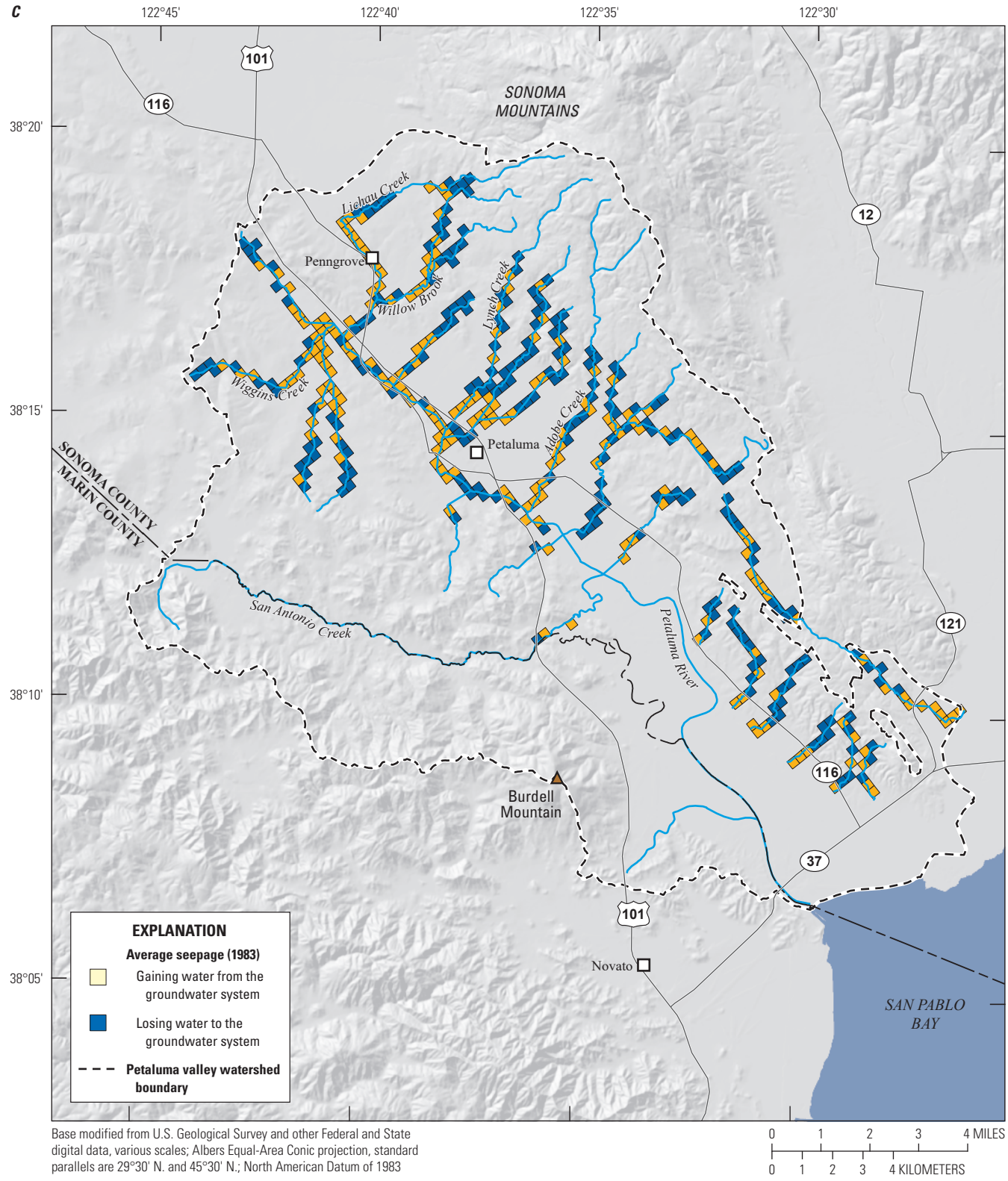

Figure D45.—Continued

Model Data Gaps, Limitations, and Appropriate Use

The PVIHM is an approximate mathematical representation of the physical conditions in the PVW. These approximations and associated assumptions contribute to the inability of the model to fully replicate the historical observations at all locations at all times. These limitations must be fully understood when using PVIHM to evaluate the hydrologic effects of water-management alternatives or for other purposes.

The PVIHM represents the physical system by using a series of mathematical approximations across time and space. The physical system is inherently complex and mostly unknown because very little actual data were available to describe the system. For example, all available geologic information only represents a small part of the study area (where well-bore data were located), and we can only assume or interpret the geology between these data points. A complete mathematical model of the system cannot be developed without introducing certain simplifying assumptions. As with most numerical groundwater models, the PVIHM solves for average conditions within each model cell; cells in the PVIHM are 984 ft by 984 ft, laterally. Therefore, the PVIHM is best at simulating hydrologic responses on a regional scale rather than for evaluating effects for smaller areas, such as the parcel-level scale. The PVIHM also assumes that pumpage and recharge remain constant during each stress period (month). Thus, the PVIHM would not be suited for simulating processes on a shorter time scale, such as daily timing of agricultural pumpage or the timing of recharge after a rain event (hours to days).

The input data used in the PVIHM represent the best information available at the time of the study, and assumptions were made during the model-development process to deal with missing data. For example, agricultural pumpage data and percolation of precipitation and irrigation return-flow are unknown and were estimated using the FMP, and estimates depend on limited available data (tables D3, D4). For example, limited local crop-related data (such as irrigation efficiencies and crop coefficients) were available. Therefore, crop model datasets were largely based on widely used values for the State of California (Faunt, 2009) or for the entire world (Allen and others, 1998) and were modified during calibration.

Groundwater-production data and the spatial distribution of pumpage for the City of Petaluma were limited prior to 2000 (Leah Walker, City of Petaluma, written commun., October 2017), and only annual pumpage totals were available prior to 1994 (West Yost, 2004). Agricultural pumpage data were estimated on the basis of land-use data, which were only available at five points during the simulation period (1959, 1979, 1986, 1999, and 2012), as discussed in chapter A. Rural-pumpage data was estimated using an analysis done by SCWA (WEL Package file in groundwater model release; Traum, 2022). Agriculture and rural-residential pumpage were simulated using virtual wells because data about the location and properties of the agriculture and rural-residential wells were not available. Limited historical data for which parcels were irrigated or not and which parcels used groundwater compared to surface water were available.

Boundary-head values used to simulate the general-head boundary conditions for the PVIHM were estimated from an extremely limited set of data. Therefore, care should be exercised when using the PVIHM to estimate the hydrologic effects of projects that may result in a large change in the general-head boundary flows.

Complete data on the agricultural use of surface water were only available for use in the model from WYs 2010 to 2015, and assumptions were made regarding the location, timing, and quantity of local surface-water supplies used to meet agricultural demands before WY 2010. Agricultural surface-water deliveries were simulated using non-routed deliveries rather than diverting them from the streamflow network because of the mismatch in timing between local surface-water availability and surface-water application to fields and because of the inability of the FMP to simulate on-farm storage.

The accuracy of the model depends on the spatial and temporal availability of observation data. The model was calibrated using observed groundwater altitude and streamflow data (U.S. Geological Survey, 2018); however, observed data were not available for all locations and for all periods. Based on these limitations, the PVIHM is best at estimating hydraulic responses to management actions in areas where the observation data were available and where simulated values matched observations reasonably well. Also, observed data were not available for calibration of many components of the PVIHM water budgets that could be important for planning purposes, such as groundwater recharge from precipitation and percolation, agricultural pumpage, groundwater and surface-water exchange, change in groundwater storage, and flow to and from San Pablo Bay. Model results indicated an average net outflow to San Pablo Bay of about 500 acre-ft/yr, but in some years this flow reverses, indicating possible seawater intrusion. A predictive uncertainty analysis could be used to determine whether budget components are sensitive to the estimated parameter values and could provide information about the uncertainty of these model outputs before relying on simulated values to make planning decisions; however, a predictive uncertainty analysis is beyond the scope of the study described in this report.

Summary and Conclusions

The Petaluma Valley Integrated Hydrologic Model (PVIHM) was developed by the U.S. Geological Survey (USGS), in cooperation with the Sonoma County Water Agency and the City of Petaluma. The PVIHM simulates the 99,000-acre Petaluma valley watershed and includes 54,000 acres where groundwater flow is active. The model simulates 56 years of historical hydrology (water years 1960–2015) that includes a range of wet and dry climatic conditions. The model incorporates data collected as part of this study, such as the updated hydrogeology, as well as other datasets from local (Sonoma County Water Agency and City of Petaluma), State, and Federal sources. Other datasets include land-surface altitude; land-use and crop-related data; water supply and demand; groundwater altitudes; streamflows; and climate, soil, and aquifer properties.

The PVIHM is an integrated hydrologic model that simulates groundwater-flow, surface-water flow, and land-surface process systems in a single model using MODFLOW-OWHM. The MODFLOW FMP was used to simulate land-surface processes, including precipitation, surface-water delivery, groundwater pumpage, plant uptake of shallow groundwater, evapotranspiration, on-farm efficiencies, precipitation and irrigation runoff, and percolation to groundwater. The MODFLOW Streamflow Routing (SFR) Package was used to simulate the streamflow in the Petaluma River and its tributaries and to simulate groundwater and surface-water exchange. The MODFLOW Upstream Weighting (UPW) Package incorporated the updated geologic-framework model to represent the multi-layered aquifer system. Groundwater production to meet municipal demands was simulated using the Multi-Node Well (MNW2) Package. The model simulated boundary flows with adjacent groundwater basins, San Pablo Bay, and the tidally influenced section of the Petaluma River using the General-Head Boundary (GHB) Package.

The model was calibrated using observed groundwater altitudes from 41 groundwater monitoring wells and measured streamflow data from 3 USGS streamgages. The simulated groundwater altitudes reasonably matched the observed groundwater altitudes given the scale of the PVIHM; on average, simulated groundwater altitudes slightly overestimated observed groundwater altitudes. The model calibration of streamflow was generally poor compared to groundwater altitudes, overestimating low streamflows and underestimating high streamflows. Model parameters were calibrated in a semi-automated manner using the BeoPEST software. Final calibrated parameter values were consistent with the geologic framework of the model and within the range of values expected based on previous studies and local knowledge. A parameter-sensitivity analysis was performed to evaluate the robustness of the calibrated parameter values. Overall, results of the sensitivity analysis indicated that the model was most sensitive to crop parameters, such as irrigation efficiencies, precipitation–runoff coefficients, and crop coefficients. Hydraulic conductivities in the major hydrogeologic formations (such as the Petaluma and Wilson Grove Formations and the Quaternary alluvium) were also highly sensitive. The relative lack of sensitivity among other model parameters indicates that final calibrated values were determined mostly by the use of prior information in the calibration process.

The model generated monthly water budgets for water use, groundwater flow, and streamflow for water years 1960–2015. Model results were used to generate simulated groundwater altitude hydrographs, simulated streamflow hydrographs, and maps of simulated groundwater altitude. Model results indicated that long-term, simulated groundwater altitudes were generally stable, especially for observation wells in the City of Petaluma and Wilson Grove groups (groups are identified in the "Model Fit to Observations of Groundwater Altitudes" section of this report and in fig. D30). Locally, simulated groundwater altitudes varied up to 20 feet (ft) because of seasonal groundwater production and showed decline during multi-year periods of drought, but these declines have historically been followed by recovery during wet periods.

During the water years 1960–2015 simulation period, the average annual change in storage was –400 acre-feet per year (acre-ft/yr) for the entire study area, which was less than 1 percent of the total groundwater inflows to the system. The average annual net stream seepage of –2,200 acre-ft/yr indicated a gain in streamflow from groundwater. The average annual net inflow from the tidally influenced part of the Petaluma River and San Pablo Bay of 11,000 acre-ft/yr indicated possible infiltration of saline water (which was hypothesized in chapter C). However, the more inland areas of the tidally influenced part of the Petaluma River indicated a net outflow to the bay.

Limitations of the PVIHM must be understood before using the PVIHM to make water-management decisions. Some components of the land-surface, groundwater, and streamflow budgets were estimated externally from the model (such as agricultural surface-water delivery before 2010 or the temporal and spatial distribution of municipal pumpage before 1994). Other budget components were estimated in the model by the FMP (such as net recharge, agricultural pumpage, runoff to streams, and rural pumpage) using limited available input data. The model was calibrated against measured groundwater-altitude and streamflow data and was not calibrated against any of the simulated flow components of the groundwater budget, including net recharge, boundary inflows and outflows, agricultural pumpage, and net stream seepage. Results of model calibrations demonstrated that simulated groundwater altitudes and streamflows could closely match observed groundwater altitude and streamflow data while simulating a wide range of values of the groundwater flow components. For example, the model was found to be relatively insensitive to GHB conductance values simulated in the model; therefore, prior-information constraints on these parameters were largely responsible for controlling the relative

magnitudes of boundary flow into and out of the study area. Although beyond the scope of this project, a more robust predictive uncertainty analysis could improve understanding of the uncertainty in simulated groundwater-budget terms.

The PVIHM provides a tool for local stakeholders to evaluate hydrologic effects related to water-management strategies, such as conjunctive use. Model scenarios can be developed to simulate future conditions under various hydrologic and water-management conditions. The PVIHM is a tool that can be used to evaluate future groundwater sustainability to support the development of a Groundwater Sustainability Plan (GSP) and to analyze Sustainable Groundwater Management Act related questions.

References Cited

Allen, R.G., Pereira, L.S., Raes, D., and Smith, M., 1998, Crop evapotranspiration—Guidelines for computing crop water requirements—FAO Irrigation and drainage paper 56: Rome, FAO - Food and Agriculture Organization of the United Nations, 300 p.

Anderson, M.P., Woessner, W.W., and Hunt, R.J., 2015, Applied groundwater modeling—Simulation of flow and advective transport (2d ed.): Academic Press, 630 p.

Banta, E.R., 2000, MODFLOW-2000, The U.S. Geological Survey modular ground-water model; documentation of packages for simulating evapotranspiration with a segmented function (ETS1) and drains with return flow (DRT1): U.S. Geological Survey Open-File Report 00–466, 127 p. [Available at https://doi.org/10.3133/ofr00466.]

California Department of Water Resources, 2016, California Land and Water Use—Land Use Surveys, accessed July 18, 2016, at https://water.ca.gov/programs/water-use-and-efficiency/land-and-water-use/land-use-surveys.

California Department of Water Resources, 2018a, California Water Data Library (WDL), accessed January 30, 2018, at https://wdl.water.ca.gov.

California Department of Water Resources, 2018b, California Statewide Groundwater Elevation Monitoring (CASGEM) database, accessed January 30, 2018, at https://www.casgem.water.ca.gov.

California Department of Water Resources, 2019, Online System of Well Completion Reports database, California Department of Water Resources, accessed June 25, 2019, at https://water.ca.gov/Programs/Groundwater-Management/Wells/Well-Completion-Reports.

California Department of Water Resources, 2020, Bulletin 118-Groundwater basins: California Department of Water Resources, accessed November 4, 2020, at https://gis.water.ca.gov/arcgis/rest/services/Geoscientific/i08_B118_CA_GroundwaterBasins/FeatureServer/0.

California State Water Resources Control Board, 2016, Electronic Water Rights Information Management System (eWRIMS), accessed July 12, 2016, at https://www.waterboards.ca.gov/waterrights/water_issues/programs/ewrims/index.html.

Cardwell, G.T., 1958, Geology and ground water in the Santa Rosa and Petaluma Valley areas, Sonoma County, California: U.S. Geological Survey Water-Supply Paper 1427, 273 p.

City of Petaluma, 2016, 2015 Urban Water Management Plan, accessed February 16, 2017, at https://storage.googleapis.com/proudcity/petalumaca/uploads/2020/02/FINAL-2015-UWMP-1.pdf.

Daly, C., Halbleib, M., Smith, J.I., Gibson, W.P., Doggett, M.K., Taylor, G.H., Curtis, J., and Pasteris, P.P., 2008, Physiographically sensitive mapping of climatological temperature and precipitation across the conterminous United States: International Journal of Climatology, a Journal of the Royal Meteorological Society, v. 28, no. 15, p. 2031–2064. [Available at https://doi.org/10.1002/joc.1688.]

Doherty, J., 2016, PEST model-independent parameter estimation user manual (6th ed.): Watermark Numerical Computing, variously paged, https://pesthomepage.org/downloads.

Doherty, J.E., Fienen, M.N., and Hunt, R.J., 2010, Approaches to highly parameterized inversion—Pilot-point theory, guidelines, and research directions: U.S. Geological Survey Scientific Investigations Report 2010–5168, 36 p.

Farrar, C.D., Metzger, L.F., Nishikawa, T., Koczot, K.M., Reichard, E.G., and Langenheim, V.E., 2006, Geohydrologic characterization, water-chemistry, and ground-water flow simulation model of the Sonoma Valley area, Sonoma County, California: U.S. Geological Survey Scientific Investigations Report 2006–5092, 167 p.

Faunt, C.C., ed., 2009, Groundwater availability of the Central Valley aquifer, California: U.S. Geological Survey Professional Paper 1766, 225 p. [Available at https://doi.org/10.3133/pp1766.]

Fregoso, T.A., Wang, R-F, Alteljevich, E., and Jaffe, B.E., 2017, San Francisco Bay-Delta bathymetric/topographic digital elevation model (DEM): U.S. Geological Survey data release. [Available at https://doi.org/10.5066/F7GH9G27.]

Flint, L.E., and Flint, A.L., 2012, Downscaling future climate scenarios to fine scales for hydrologic and ecological modeling and analysis: Ecological Processes, v. 1, no. 2, 15 p. [Available at https://doi.org/10.1186/2192-1709-1-2.]

Hanson, R.T., Boyce, S.E., Schmid, W., Hughes, J.D., Mehl, S.M., Leake, S.A., Maddock, T., III, and Niswonger, R.G., 2014, One-Water Hydrologic Flow Model (MODFLOW-OWHM): U.S. Geological Survey Techniques and Methods 6–A51, 120 p. [Available at https://doi.org/10.3133/tm6A51.]

Hanson, R.T., Leake, S.A., 1999, Documentation for HYDMOD; a program for extracting and processing time-series data from the U.S. Geological Survey's modular three-dimensional finite-difference ground-water flow model, U.S. Geological Ofen-File Report 98-564, 57 p. [Available at https://pubs.er.usgs.gov/publication/ofr98564.]

Harbaugh, A.W., 2005, MODFLOW-2005, the U.S. Geological Survey modular ground-water model—The ground-water flow process: U.S. Geological Survey Techniques and Methods book 6, chap. A16, variously paged.

Hargreaves, G.H., and Samani, Z.A., 1982, Estimating potential evapotranspiration: Journal of the Irrigation and Drainage Division, v. 108, no. 3, p. 225–230. [Available at https://doi.org/10.1061/JRCEA4.0001390.]

Herbst, C.M., 1982, Evaluation of ground water resources, Sonoma County, volume 3: Petaluma Valley, California Department of Water Resources, Bulletin 118-4, 94 p.

Hill, M.C., and Tiedeman, C.R., 2007, Effective groundwater model calibration—With analysis of data, sensitivities, predictions, and uncertainty: Hoboken, N.J., John Wiley and Sons, Inc., 480 p. [Available at https://doi.org/10.1002/0470041080.]

Hill, M.C., Banta, E.R., Harbaugh, A.W., and Anderman, E.R., 2000, MODFLOW-2000, the U.S. Geological Survey modular ground-water model; user guide to the observation, sensitivity, and parameter-estimation processes and three post-processing programs: U.S. Geological Survey Open-File Report 2000–184, 209 p. [Available at https://doi.org/10.3133/ofr00184.]

Hsieh, P.A., and Freckleton, J.R., 1993, Documentation of a computer program to simulate horizontal-flow barriers using the U.S. Geological Survey modular three- dimensional finite-difference ground-water flow model: U.S. Geological Survey Open-File Report 92–477, 32 p.

Konikow, L.F., Hornberger, G.Z., Halford, K.J., and Hanson, R.T., 2009, Revised multi-node well (MNW2) package for MODFLOW ground-water flow model: U.S. Geological Survey Techniques and Methods 6–A30, 67 p. [Available at https://doi.org/10.3133/tm6A30.]

Mak, M., Harris, E., Lightner, M., Vandever, J., and May, K., 2016, San Francisco Bay tidal datums and extreme tides study, Final report, February 2016, 140 p.

Merritt, M.L., and Konikow, L.F., 2000, Documentation of a computer program to simulate lake-aquifer interaction using the MODFLOW ground-water flow model and the MOC3D solute-transport model: U.S. Geological Survey Water-Resources Investigations Report 00–4167, 146 p.

Nalder, I.A., and Wein, R.W., 1998, Spatial interpolation of climatic normals—Test of a new method in the Canadian boreal forest: Agricultural and Forest Meteorology, v. 92, no. 4, p. 211–225. [Available at https://doi.org/10.1016/S0168-1923(98)00102-6.]

Niswonger, R.G., and Prudic, D.E., 2005, Documentation of the Streamflow-Routing (SFR) Package to include unsaturated flow beneath streams—A modification to SFR1: U.S. Geological Survey Techniques and Methods, book 6, chap. A13, 50 p.

Niswonger, R.G., Panday, S., and Ibaraki, M., 2011, MODFLOW-NWT, A Newton formulation for MODFLOW-2005: U.S. Geological Survey Techniques and Methods 6–A37, 44 p. [Available at https://doi.org/10.3133/tm6A37.]

PRISM Climate Group, 2013, 30-year normals: PRISM Climate Group database, Oregon State University, accessed February 16, 2017, at https://prism.oregonstate.edu/.

Priestley, C.H.B., and Taylor, R.J., 1972, On the assessment of surface heat flux and evaporation using large-scale parameters: Monthly Weather Review, v. 100, no. 2, p. 81–92, [Available at https://doi.org/10.1175/1520-0493(1972)100%3C0081:OTAOSH%3E2.3.CO;2.]

Schmid, W., and Hanson, R.T., 2009, The Farm Process Version 2 (FMP2) for MODFLOW-2005—Modifications and upgrades to FMP1: U.S. Geological Survey Techniques and Methods 6–A32, 102 p. [Available at https://doi.org/10.3133/tm6A32.]

Schmid, W., Hanson, R.T., Maddock, T., III, and Leake, S.A., 2006, User guide for the farm process (FMP1) for the U.S. Geological Survey's modular three-dimensional finite-difference ground-water flow model, MODFLOW-2000: U.S. Geological Survey Techniques and Methods 6–A17, 127 p. [Available at https://doi.org/10.3133/tm6A17.]

Seymour, W.A., and Traum, J.A., 2021, Petaluma model GIS data: U.S. Geological Survey data release. [Available at https://doi.org/10.5066/P9IQDHIT.]

Sonoma County Water Agency, 2016, Water Delivery Data, accessed February 23, 2016, at https://www.sonomawater.org/water-delivery-data.

Traum, J.A., 2022, MODFLOW-OWHM used to characterize the flow system of the Petaluma River Watershed, Sonoma County, California: U.S. Geological Survey data release. [Available at https://doi.org/10.5066/P965IDQZ.]

U.S. Geological Survey, 2018, USGS water data for the Nation: U.S. Geological Survey National Water Information System database, accessed January 30, 2018, at https://doi.org/10.5066/F7P55KJN.

West Yost, 2004, Technical Memorandum No. 4: Groundwater Feasibility Study, accessed August 4, 2014, at https://cityofpetaluma.net/cdd/pdf/riverfront/West-Groundwater-Feasibility-Study.pdf.

Woolfenden, L.R., 2014, Groundwater-component model, chap. C *of* Woolfenden, L.R. and Nishikawa, T., eds., Simulation of groundwater and surface-water resources of the Santa Rosa Plain watershed, Sonoma County, California: U.S. Geological Survey Scientific Investigations Report 2014–5052, p. 21–54. [Available at https://doi.org/10.3133/sir20145052.]

Woolfenden, L.R., and Hevesi, J.A., 2014, Santa Rosa Plain hydrologic model results, chap. E *of* Woolfenden, L.R. and Nishikawa, T., eds., Simulation of groundwater and surface-water resources of the Santa Rosa Plain watershed, Sonoma County, California: U.S. Geological Survey Scientific Investigations Report 2014–5052, p. 151–184. [Available at https://doi.org/10.3133/sir20145052.]

For more information concerning the research in this report, contact the

Director, California Water Science Center
U.S. Geological Survey
6000 J Street, Placer Hall
Sacramento, California 95819
https://www.usgs.gov/centers/ca-water/

Publishing support provided by the U.S. Geological Survey
Science Publishing Network, Sacramento Publishing Service Center

ISSN 2328-0328 (online)
https://doi.org/10.3133/sir20225009